The Hipparcos and Tycho Catalogues

SP–1200
June 1997

The Hipparcos and Tycho Catalogues

Astrometric and Photometric Star Catalogues

derived from the

ESA Hipparcos Space Astrometry Mission

A Collaboration Between

the European Space Agency

and

the FAST, NDAC, TDAC and INCA Consortia

and the Hipparcos Industrial Consortium led by

Matra Marconi Space

and

Alenia Spazio

European Space Agency
Agence spatiale européenne

Cover illustration: an impression of selected stars in their true positions around the Sun, as determined by Hipparcos, and viewed from a distant vantage point. Inset: sky map of the mean observation epoch of stars in the Hipparcos Catalogue, relative to J1991.25, in ecliptic coordinates.

Published by:	ESA Publications Division, c/o ESTEC, Noordwijk, The Netherlands
Scientific Coordination:	M.A.C. Perryman, ESA Space Science Department and the Hipparcos Science Team
Composition:	Volume 1: M.A.C. Perryman Volume 2: K.S. O'Flaherty Volume 3: F. van Leeuwen, L. Lindegren & F. Mignard Volume 4: U. Bastian & E. Høg Volumes 5–11: Hans Schrijver Volume 12: Michel Grenon Volume 13: Michel Grenon (charts) & Hans Schrijver (tables) Volumes 14–16: Roger W. Sinnott Volume 17: Hans Schrijver & W. O'Mullane Typeset using TEX (by D.E. Knuth) and dvips (by T. Rokicki) in Monotype Plantin (Adobe) and Frutiger (URW)
Film Production:	Volumes 1–4: ESA Publications Division, ESTEC, Noordwijk, The Netherlands Volumes 5–13: Imprimerie Louis-Jean, Gap, France Volumes 14–16: Sky Publishing Corporation, Cambridge, Massachusetts, USA
ASCII CD-ROMs:	Swets & Zeitlinger B.V., Lisse, The Netherlands
Publications Management:	B. Battrick & H. Wapstra
Cover Design:	C. Haakman
©1997	European Space Agency ISSN 0379–6566 ISBN 92–9092–399-7 (Volumes 1–17)
Price:	650 Dfl ($400) (17 volumes) 165 Dfl ($100) (Volumes 1 & 17 only)

Volume 1

Introduction and Guide to the Data

Contents

Volume 1: Part 1. The Hipparcos and Tycho Catalogues

Volume 1: Part 2. Description of Catalogues and Annexes

Volume 1: Part 3. Properties of the Catalogues

Volume 1: Appendices

Contents of Volumes 2–17

Preface

The Hipparcos astrometry mission was accepted within the European Space Agency's scientific programme in 1980. The Hipparcos satellite was designed and constructed under ESA responsibility by a European industrial consortium led by Matra Marconi Space (France) and Alenia Spazio (Italy), and launched by Ariane 4 on 8 August 1989. High-quality scientific data were acquired between November 1989 and March 1993, and communications with the satellite were terminated on 15 August 1993. All of the scientific goals motivating the mission's adoption in 1980 were surpassed.

The products of the Hipparcos mission are two major astrometric catalogues, the Hipparcos Catalogue (of 118 218 stars) and the Tycho Catalogue (of more than one million stars), both derived from instruments on board the Hipparcos satellite. The global data analysis tasks, proceeding from nearly 1000 Gbit of raw satellite data to the final catalogues, was a lengthy and complex process, and was undertaken by the NDAC and FAST Consortia, together responsible for the production of the Hipparcos Catalogue, and the Tycho Consortium, responsible for the production of the Tycho Catalogue. A fourth scientific consortium, the INCA Consortium, was responsible for the construction of the Hipparcos observing programme, compiling the best-available data for the selected stars before launch into the Hipparcos Input Catalogue. The production of the Hipparcos and Tycho Catalogues marks the formal end of the involvement in the mission by the European Space Agency and the four scientific consortia.

Each of the catalogues includes a large quantity of very high quality astrometric and photometric data, as well as annexes featuring variability and double/multiple star data. In the case of the Hipparcos Catalogue, the principal parts are provided in both printed and machine-readable form. In the case of the Tycho Catalogue, results are provided in machine-readable form only. Although in general only the final reduced and calibrated astrometric and photometric data are provided, some auxiliary files containing results from intermediate stages of the data processing, of relevance for the more-specialised user, have also been retained for publication.

The printed volumes include both a description of the Hipparcos and Tycho Catalogues and associated annexes, a description of the satellite operational phase, a description of the corresponding data analysis tasks, and the appropriate subsets of the final data. Machine-readable versions of the catalogues are provided in two forms: the definitive mission products are released as a set of ASCII files on a series of CD-ROMs, which contain all of the printed catalogue information as well as some additional data. A distinct CD-ROM product, *Celestia 2000*, contains the principal astrometric and photometric data, in compressed form, along with specific interrogation software.

Considerable emphasis has been placed on presenting a unique set of fully reduced and calibrated astrometric and photometric parameters. An almost conflicting requirement has been to make the final results available promptly. The Hipparcos and Tycho Catalogues have been finalised, documented, and archived within three years of the termination of the satellite operations, and the compilers trust that deviations from a perfect product may be viewed in this context.

M.A.C. Perryman, ESA Project Scientist
E. Høg, Tycho Consortium
J. Kovalevsky, FAST Consortium
L. Lindegren, NDAC Consortium
C. Turon, INCA Consortium

Summary of the Hipparcos and Tycho Catalogues

Measurement period	1989.85–1993.21
Catalogue epoch	J1991.25
Reference system	ICRS
Coincidence with respect to ICRS (all 3 axes)	±0.6 mas
Proper motion deviation from inertial (all 3 axes)	±0.25 mas/yr
Hipparcos Catalogue:	
Number of entries	118 218
Entries with associated astrometry	117 955
Entries with associated photometry	118 204
Mean sky density	~ 3 per square degree
Limiting magnitude	V ~ 12.4 mag
Completeness	Up to V = 7.3 – 9.0 mag
Median precision of positions, J1991.25 ($Hp < 9$ mag)	0.77/0.64 mas (RA/dec)
Median precision of parallaxes ($Hp < 9$ mag)	0.97 mas
Median precision of proper motions ($Hp < 9$ mag)	0.88/0.74 mas/yr (RA/dec)
10 per cent (each of the five parameters) better than	0.47–0.66 mas
Distance determined to better than 10 per cent ($\sigma_\pi/\pi < 0.1$)	20853
Distance determined to better than 20 per cent ($\sigma_\pi/\pi < 0.2$)	49399
Inferred ratio of external errors to standard errors	~ 1.0 – 1.2
Estimated systematic errors in astrometry	< 0.1 mas
Total number of independent astrometric abscissae	~ 3.6×10^6
Median photometric precision (Hp, for $Hp < 9$ mag)	0.0015 mag
Mean number of photometric observations per star	110
Total number of Hp photometric measurements	~ 13×10^6
Number of entries variable or possibly variable	11597 (8237 new)
Periodic variables	2712 (970 new)
Cepheid type	273 (2 new)
RR Lyrae type	186 (9 new)
δ Scuti and SX Phoenicis type	108 (35 new)
Eclipsing binaries (e.g. EA, EB, EW,..)	917 (343 new)
Other types (e.g. M, SR, RV Tau,..)	1238 (576 new)
Non-periodic and unsolved (e.g. RCrB, γ Cas, Z And)	5542 (4145 new)
Not investigated (including micro-variables)	3343 (3122 new)
Number of solved or suspected double/multiple systems	23882
Systems with component data (annex part C)	12195 (2996 new)
Orbital systems (annex part O)	235
Astrometric binaries (annex parts G and V)	2910
Suspected non-single (including annex part X)	8542
Tycho Catalogue:	
Number of entries (including 6301 HIP only)	1 058 332
Mean sky density	~ 25 per square degree
Limiting magnitude	V_T ~ 11.5 mag
Completeness	V_T ~ 10.5 mag
Median astrometric precision (all stars), J1991.25	25 mas
Median astrometric precision ($V_T < 9$ mag), J1991.25	7 mas
Inferred ratio of external errors to standard errors	~ 1.0 – 1.5
Systematic errors in astrometry	< 1 mas
Mean number of astrometric and photometric observations per star	130
Total number of astrometric and photometric observations	~ 130×10^6
Median photometric precision (all stars): B_T, V_T, $B_T - V_T$	0.07, 0.06, 0.10 mag
Median photometric precision ($V_T < 9$ mag): B_T, V_T, $B_T - V_T$	0.014, 0.012, 0.019 mag

Scientific Involvement in the Hipparcos Mission

The Hipparcos observing programme was based upon a single, uniquely-defined Input Catalogue. Compiled at the Observatoire de Paris, Meudon, the preparation of this catalogue involved the collaboration of a large number of ESA Member State scientists—for the detailed assessment of existing astrometric and photometric data, for the extensive compilation of ground-based observations necessary to bring the observing catalogue to the quality required for the satellite observations and data analyses, and for the iterative selection of programme stars made by simulating the satellite observations. While the INCA Consortium Leader was responsible for the Hipparcos Input Catalogue compilation as a whole, various 'task leaders' were responsible for the various subsets of the work. The Consortium included institutes from Belgium, Denmark, France, Germany, The Netherlands, Spain, Switzerland, the U.K., and the U.S.A.

The data analysis tasks were substantial, and the entire organisation of the preparation and execution of the work was complex. The leaders of the three Consortia were assisted by Executive Committees comprising the 'task leaders' responsible for the various disciplines and data processing stages and, where appropriate, by evaluation or software maintenance groups. The work of each Consortium was 'monitored' by a Steering Committee with representatives of each participating country.

Within the NDAC Consortium, the data analysis was performed in the countries which developed the respective software elements—that is, in Denmark, Sweden, and in the U.K., with the individual participating institutes responsible for their own software quality, data interfaces, and data management.

Within the FAST Consortium, all of the integrated software was run within the CNES (Toulouse) computing centre; substantial elements of the integrated software also ran within the Consortium's First-Look Facility at SRON (Utrecht). The software elements of the scientific data processing package were developed within participating institutes in France, Germany, Italy, and The Netherlands. Acceptance tests were run before and after software integration, and the responsible institutes participated closely in the evaluation of results during execution.

The Tycho Consortium relied on some software elements and results of the data processing within NDAC and FAST (in particular, the satellite attitude for TDAC was derived by the NDAC Consortium within Denmark, based upon the first analysis steps carried out in U.K.). The data processing activities specific to the Tycho Catalogue construction were carried out at institutes within Denmark, France, and Germany.

Extensive cross-checking of the intermediate data processing stages was carried out where the expertise and resources permitted. Thus, the one-dimensional 'great-circle' results from FAST and NDAC were intercompared at the Geodetic Institute in Delft, where the relevant FAST software was developed; the precise reconstructed satellite attitude data from both Consortia were intercompared and evaluated at CSS (Torino) where the software for the first stages of the FAST data treatment were developed and coded. Other major intercomparison exercises were carried out at various institutes.

All results, including intermediate catalogues, were compiled in a centralised data base at SRON (Utrecht) where final verification was undertaken.

The scientific activities related to the project were coordinated by the ESA Project Scientist, supported by the Hipparcos Science Team.

FAST: ◆
Asiago
Bari
Bologna
Delft
Firenze
Frascati
Grasse
Haystack (U.S.A.)
Heidelberg
Leiden
Marseille
Milano
Paris
Pasadena (U.S.A.)
Torino
Tououse
Utrecht

NDAC: ⌘
Cambridge
Cardiff
Copenhagen
Dorking
Lund

TDAC: ●
Asiago
Baltimore (U.S.A.)
Cambridge
Chilton
Copenhagen
Geneve
Grasse
Groningen
Heidelberg
Leiden
London
Lund
Paris
Strasbourg
Torino
Tubingen
Washington (U.S.A.)

INCA: ◘
Barcelona
Besancon
Bonn
Bordeaux
Btorfelde
Bruxelles
Cambridge
Cambridge (U.S.A.)
Geneve
Hamburg
Heidelberg
Lausanne
Leiden
Liege
Marseille
Montpellier
Paris
San Fernando
Strasbourg
Texas (U.S.A.)

ESA / Industry: ⊠
ESA/ESTEC
ESA/ESOC
Toulouse (Matra)
Torino (Alenia)

Location of scientific institutes participating in Hipparcos
(irrespective of level of contribution)
ESA-ESTEC, ESA-ESOC and the main industrial contractors are also indicated

The Hipparcos and Tycho Catalogues

resulting from the
European Space Agency's Hipparcos Space Astrometry Mission
have been prepared by:

The NDAC Consortium
under the leadership of
L. Lindegren
Consortium Leader (1990–97)
Lund Observatory
Lund, Sweden
[formerly E. Høg (1982–90)]

The FAST Consortium
under the leadership of
J. Kovalevsky
Consortium Leader (1982–97)
Observatoire de la Côte d'Azur
Grasse, France

for the Hipparcos Catalogue and associated annexes

and

The Tycho Consortium
under the leadership of
E. Høg
Consortium Leader (1983–97)
Copenhagen University Observatory
Copenhagen, Denmark

for the Tycho Catalogue and associated annexes

based on

The Hipparcos Input Catalogue
compiled by
The INCA Consortium
under the leadership of
C. Turon
Consortium Leader (1982–94)
Observatoire de Paris-Meudon
France

and

data from the ESA Hipparcos satellite, operated in orbit 1989–93
acquired under the scientific responsibility of
M.A.C. Perryman
ESA Hipparcos Project Scientist (1981–97)
Space Science Department
European Space Agency, Noordwijk
The Netherlands

Scientific coordination of the Hipparcos project has been led by

M.A.C. Perryman
ESA Hipparcos Project Scientist (1981–97)
European Space Agency, Noordwijk
The Netherlands

and

The Hipparcos Science Team (1981–97 unless otherwise noted):

U. Bastian	Astronomisches Rechen-Institut, Heidelberg, Germany (from 1993)
P.L. Bernacca	Astrophysical Observatory, Asiago, Italy (from 1989)
M. Crézé	Observatoire de Strasbourg, France (from 1983)
F. Donati	Centro di Studi Sui Sistemi, Torino, Italy
M. Grenon	Observatoire de Genève, Switzerland (from 1982)
M. Grewing	Astronomisches Institut, Tübingen, Germany (from 1983)
E. Høg	Copenhagen University Observatory, Denmark
J. Kovalevsky	Observatoire de la Côte d'Azur/CERGA, Grasse, France
F. van Leeuwen	Royal Greenwich Observatory, Cambridge, U.K. (from 1986)
L. Lindegren	Lund Observatory, Sweden
H. van der Marel	Delft University of Technology, The Netherlands (from 1987)
F. Mignard	Observatoire de la Côte d'Azur/CERGA, Grasse, France (from 1991)
C.A. Murray	Royal Greenwich Observatory, Herstmonceux, U.K.
M.A.C. Perryman	European Space Agency, The Netherlands *(Chairman)*
R.S. Le Poole	University of Leiden, The Netherlands
H. Schrijver	SRON, Utrecht, The Netherlands (from 1990)
C. Turon	Observatoire de Paris-Meudon, France

The Hipparcos Science Team, whose composition changed slightly during the lifetime of the Hipparcos project, advised ESA on all scientific aspects of the mission, and held responsibility for the overall scientific conduct of the Hipparcos project, through to the completion and distribution of the final catalogues. Previous members of the Science Team during the satellite design and development phase were P. Brosche (1982), C. Coleman (1981–82), A.M. Cruise (1983–86), D.T. van Daalen (1986), C. Jaschek (1981), M. Saisse (1981), H.G. Walter (1981), C.G. Wynne (1981–84).

The FAST Consortium

France:

M.T. Dumoulin†, J. Falin, J.L. Falin, M. Frœschlé, F. Gazengel, F. Genova, A. Guerry, D. Hestroffer, C. Huc, J. Kovalevsky *(Consortium Leader)*, P. Lacroute†, J.F. Lestrade, C. Martin, F. Mignard, B. Morando†, J.L. Pieplu, G. Serieys, M. Vadel

A. Bec-Borsenberger*, E. Bois*, A. Budowski*, B. Chausserie-Laprée*, S. Daillet*, J. Dupic*, J.Y. Le Gall*, M.H. Gomez*, V. Roman*, C. Taieb*, A. Vargas*, M. Villenave*

Germany:

H.H. Bernstein, C. Dettbarn, R. Hering, H. Lenhardt, S. Röser, H.G. Walter, R. Wielen

U. Bastian*, W. Fricke†

Italy:

M. Badiali, P.L. Bernacca, L. Borriello, B. Bucciarelli, E. Canuto, D. Cardini, F. Donati, A. Emanuele, B. Fassino, M.G. Lattanzi, F.P. Murgolo, R. Pannunzio, G. Prezioso, G. Sechi, A. Spagna

M. Amoretti*, P. Belforte*, D. Bertani*, B. Betti*, D. Carlucci*, M. Cetica*, W. Delaney*, I.I. Galligani*, M. Gonano*, D. Iorio-Fili*, F. Migliaccio*, F. Sansò*, M.G. Schirone*, T. Tommasini*, V. Zappala*

The Netherlands:

W.N. Brouw, H. van der Marel, R.S. Le Poole, H. Schrijver

D.T. van Daalen*, F.A. van den Heuvel*, P.J. de Jonge*, T.M. Kamperman*, J.J. Kok†, G.J. Wiersma*

United States of America:

D.L. Jones, R.B. Phillips, R.A. Preston

* former member, or not active during the data reductions † deceased

The NDAC Consortium

Denmark:
E. Høg, C.S. Petersen

G.K. Andreasen*, P.C. Hansen*, N. Lund*, K. Poder*

Sweden:
L. Lindegren *(Consortium Leader)*, S. Söderhjelm

United Kingdom:
D.W. Evans, F. van Leeuwen, C.A. Murray,
M.J. Penston, N. Ramamani

J.R. Allington-Smith*, S.A. Cowling*, A.M. Cruise*,
N. Elton*, M.A.J. Snijders*, G. Whitfield*

* former member, or not active during the data reductions

The Tycho Consortium

Denmark:
C. Fabricius, E. Høg *(Consortium Leader)*, V.V. Makarov, H. Pedersen, C.S. Petersen

G.K. Andreasen*, P.C. Hansen*, N. Lund*, A.B. Saust*, M. Yoshizawa*

France:
D. Egret, J.L. Halbwachs, J. Kovalevsky, C. Turon

P. Didelon*

Germany:
G. Bässgen, U. Bastian, M. Grewing, V. Großmann,
H. Mauder, D. Scales, P. Schwekendiek, M.A.J. Snijders, K. Wagner, A. Wicenec

Italy:
P.L. Bernacca, F. Donati

The Netherlands:
M.A.C. Perryman

P.R. Wesselius*

Sweden:
L. Lindegren

Switzerland:
M. Grenon

United Kingdom:
F. van Leeuwen

A. Butchins*, D. McNally*, B. Stewart*

United States of America:
B. McLean

J.L. Russell*

* former member, or not active during the data reductions

The INCA Consortium

Belgium:
J. Dommanget, O. Nys

P. Lampens, J. Manfroid

Denmark:
L. Helmer

France:
F. Arenou, A. Bec-Borsenberger, M. Chareton, M. Crézé, F. Crifo, D. Egret, A. Gómez, M.O. Mennessier, D. Morin, L. Prévot, Y. Réquième, M. Rousseau, C. Turon *(Consortium Leader)*

J.E. Arlot, A. Baglin, D. Barthés, M.O. Baylac, J. Delhaye, J.M. Mazurier, E. Oblak, J.P. Périé, M. Rapaport, A. Sellier

Germany:
H. Jahreiß,

P. Brosche, C. Dettbarn, M. Erbach, W. Fricke†, T. Lederle, H.-J. Tucholke, C. de Vegt

The Netherlands:
M.A.C. Perryman

J. Lub, R.S. Le Poole

Spain:
F. Figueras, C. Jordi, L. Quijano, J. Torra

Switzerland:
M. Grenon, J.C. Mermilliod, B. Nicolet

M. Burnet, M. Mermilliod, B. Pernier

United Kingdom:
A.N. Argue

L.V. Morrison, C.A. Murray

United States of America:
P.D. Hemenway, J.A. Mattei

[A complete membership list of the consortium is given in the Hipparcos Input Catalogue, ESA SP–1136, 1992]

† deceased

The Scientific Proposals Selection Committee

(for determining the scientific objectives of the observing programme, 1982–88)

A. Blaauw *(Chairman)*, J. Dommanget, W. Gliese†, M. Hack,
E.P.J. van den Heuvel, C. Jaschek, J. Lequeux, P.O. Lindblad,
A. Maeder, P.E. Nissen, B.E.J. Pagel, A. Renzini,
C. de Vegt, P.A. Wayman, R. Wielen

† deceased

Contributors by Subject: Hipparcos Data Analysis

Image Dissector Tube and
Star Mapper Data Processing
Leaders: F. van Leeuwen (NDAC) & F. Donati (FAST)
E. Canuto, B. Fassino, C.A. Murray

Instrument Calibration
Leaders: J. Kovalevsky, H. Schrijver & F. van Leeuwen
D.W. Evans, J.L. Falin, M.J. Penston

Attitude Determination
Leaders: F. Donati (FAST) & F. van Leeuwen (NDAC)
E. Canuto, M.J. Penston, G. Sechi

Great-Circle Reductions
Leaders: H. van der Marel (FAST) & C.S. Petersen (NDAC)
J.L. Falin

Sphere Solution in FAST
Leader: M. Frœschlé
B. Bucciarelli, M.G. Lattanzi

Astrometric Parameter Determination in FAST
Leaders: H.G. Walter & R. Hering
H.H. Bernstein, C. Dettbarn, J.L. Falin,
M. Frœschlé, H. Lenhardt, F. Mignard

Sphere Solution and
Astrometric Parameter Determination in NDAC
Leader: L. Lindegren
S. Söderhjelm

...continued

Hipparcos Data Analysis (cont.)

Double & Multiple Star Reductions
Leaders: S. Söderhjelm (NDAC) & F. Mignard (FAST)
M. Badiali, P.L. Bernacca, H.H. Bernstein, L. Borriello, D. Cardini,
A. Emanuele, J.L. Falin, F. Gazengel, J. Kovalevsky,
L. Lindegren, C. Martin, R. Pannunzio, G. Prezioso, A. Spagna

Photometric Reductions
Leaders: F. Mignard (FAST) & F. van Leeuwen (NDAC)
D.W. Evans, J.L. Falin, M. Grenon

Operational Software System in NDAC
Leaders: F. van Leeuwen & C.S. Petersen
D.W. Evans, M.J. Penston, S. Söderhjelm

Operational Software System in FAST
Leaders: J.L. Pieplu, J. Kovalevsky & J.L. Falin
E. Canuto, R. Hering, C. Huc, J.J. Kok†, F.P. Murgolo
A. Guerry, J. Dupic, M. Villenave

† deceased

Contributors by Subject: Tycho Data Analysis

Signal Prediction
Leader: U. Bastian
P. Schwekendiek

Signal Detection and Estimation
Leader: A. Wicenec
G. Bässgen

Tycho Input Catalogue Revision
Leader: J.L. Halbwachs
G. Bässgen, U. Bastian, P. Schwekendiek, A. Wicenec

Signal Identification
Leader: K. Wagner
A. Wicenec, P. Schwekendiek

Astrometric Reductions
Leaders: E. Høg & V.V. Makarov
C. Fabricius, H. Pedersen

Photometric Reductions
Leaders: V. Großmann & J.L. Halbwachs
A. Wicenec

Catalogue Production
Leader: E. Høg
D. Egret, C. Fabricius, V. Großmann, V.V. Makarov, A. Wicenec

Scientific Working Groups

Double Star Working Group
Leader: F. Mignard

S. Söderhjelm & L. Lindegren

M. Badiali, H.H. Bernstein, J. Dommanget°, P. Lampens°, R. Pannunzio

Photometry Working Group
Leader: D.W. Evans

F. Mignard & F. van Leeuwen

M. Grenon°, V. Großmann

Variable Star Working Group
Leaders: F. van Leeuwen & M. Grenon°

L. Eyer*, J.A. Mattei°, M.J. Penston

Astrometric Results Merging Working Group
Leader: F. Arenou°

C.A. Murray

M. Frœschlé, F. Mignard, L. Lindegren

Reference Frame Working Group
Leaders: J. Kovalevsky & L. Lindegren

P. Hemenway°, K.J. Johnston*, V. Kislyuk*,
J.F. Lestrade, L.V. Morrison°, I. Platais*, S. Röser,
E. Schilbach*, H.-J. Tucholke°, C. de Vegt°, J. Vondrak*

Documentation Working Group
Leader: M.A.C. Perryman

E. Høg, J. Kovalevsky, F. van Leeuwen, L. Lindegren,
F. Mignard, H. Schrijver, C. Turon°

° INCA Consortium * not a formal member of a Hipparcos scientific consortium

Catalogue Production and Publication

The Hipparcos Catalogue (Volumes 5–9)
Leaders: L. Lindegren & J. Kovalevsky
J.L. Falin, M. Frœschlé, M. Grenon, F. van Leeuwen
F. Mignard, M.A.C. Perryman, H. Schrijver

The Tycho Catalogue
Leader: E. Høg
G. Bässgen, U. Bastian, D. Egret, C. Fabricius,
V. Großmann, J.L. Halbwachs, V.V. Makarov,
P. Schwekendiek, K. Wagner, A. Wicenec

Double and Multiple Systems Annex (Volume 10)
Leaders: S. Söderhjelm, L. Lindegren & F. Mignard
F. Arenou°, M. Badiali, H.H. Bernstein, J. Kovalevsky,
C. Martin, R. Pannunzio, R. Wielen

Solar System Observations (Volume 10)
Leaders: D. Hestroffer & B. Morando†
U. Bastian, E. Høg, J. Kovalevsky, L. Lindegren,
V.V. Makarov, F. Mignard, C.A. Murray

Variability Annex (Volume 11)
Leaders: F. van Leeuwen & M. Grenon°
D.W Evans, L. Eyer*, M.J. Penston
M.B. van Leeuwen-Toczko*, S. Meara*, C. Waelkens*, I. Zegelaar*
N.N. Samus*, M.S. Frolov*, O.V. Durlevich*, E.V. Kazarovets*

Light Curves (Volume 12)
Leaders: M. Grenon° & F. van Leeuwen
D.W Evans, L. Eyer*, G. Foster*, J.A. Mattei°, M.J. Penston

Identification Charts (Volume 13)
Leader: M. Grenon°
D. Mégevand*, L. Weber*

Millennium Star Atlas (Volumes 14–16)
Leaders: R.W. Sinnott* & M.A.C. Perryman
H. Schrijver, E. Høg
E.T. Mentall*, R.T. Fienberg*, G. Dinderman*, S.M. MacGillivray*, L.J. Robinson*

...continued

° INCA Consortium † deceased
* not a formal member of a Hipparcos scientific consortium

Catalogue Production and Publication (cont.)

Hipparcos Catalogue: Epoch Photometry Annex
Leaders: D.W. Evans & F. Mignard
M. Grenon°, F. van Leeuwen

Tycho Catalogue: Epoch Photometry Annex
Leader: V. Großmann
A. Wicenec, G. Bässgen, U. Bastian,
J.L. Halbwachs, V.V. Makarov, K. Wagner

Hipparcos Intermediate Astrometry
Leaders: F. Arenou° & C.A. Murray
J.L. Falin, M. Frœschlé, L. Lindegren, F. Mignard

Hipparcos Transit Data
Leaders: S. Söderhjelm & L. Lindegren

ASCII CD-ROM Organisation
Leaders: H. Schrijver & M.A.C. Perryman
K.S. O'Flaherty*, W. O'Mullane*

***Celestia 2000* CD-ROM**
Leaders: D. Priou* & C. Turon°
M.A.C. Perryman, E. Høg, L. Lindegren,
U. Bastian, D. Morin°, H. Schrijver

Results Data Base and Catalogue Unification
Leader: H. Schrijver

Printed Catalogue: Layout and Production
Leaders: H. Schrijver & M.A.C. Perryman

Star Identification Tables (Volume 13)
Leader: H. Schrijver
D. Morin°

Statistical Properties (Section 3)
Leader: H. Schrijver
J.L. Falin, L. Lindegren, F. Mignard
C. Fabricius, V.V. Makarov

° INCA Consortium * not a formal member of a Hipparcos scientific consortium

Catalogue and Annex Descriptions and Formats

Leader: M.A.C. Perryman
U. Bastian, E. Høg, F. van Leeuwen, L. Lindegren,
F. Mignard, H. Schrijver, C. Turon

Technical and Industrial Involvement

The ESA Hipparcos Project Team

(management of the satellite development and operations by ESA-ESTEC since 1981)

L. Emiliani (Project Manager, 1980–84)
H. Hassan (Project Manager, 1984–89)
M.A.C. Perryman (Project Manager, 1990–93)

Section Heads (at Flight Acceptance Review):
K. Clausen (spacecraft), K. van Katwijk (payload),
O. Pace (integration), M. Schuyer (system analysis)

T. Batut, K.D. Bock, R. Bonnefoy, H.A. Eggel, A. Errington,
H.K. Fiebrich, P. Gleadle, J. van der Ha (ESOC), L. Hansson, K. Hühn,
D. Huthoff, E. Jäkel, G. Jung, B. Kroese, T. van der Laan,
H. Laue (ESOC), W. Liebrandt, P.N. Morgan, G. Ratier, S. Schroeder†,
M. Setzke, M.J. Smith, S. Vaghi, R.D. Wills, D.R. Wotton

The ESOC Mission Operations Team

(operation of the Hipparcos satellite in orbit by ESA-ESOC)

Operations & Mission Analysis:
D. Heger, H. Nye
M. McCaig, J. Nolan, O. Ojanguren, C. Sollazzo
R. Leroux, M. Monaldi, E. Schambion, P. Vogt

Mission Analysis:
J. van der Ha, H.-H. Klinkrad

Flight Dynamics:
A. Schütz
A. Batten, P. Davies, A. McDonald, S. Retbøll
P. de Broeck†, P. Kristiansen

Software Support:
N. Head
J. Allan, R. Blake, J. Harborne, M. Keenan, C. Spanholtz

[A complete list of the ESOC Mission Operations Team is given in Volume 2]

† deceased

The Hipparcos Industrial Development Team

(for industrial development of the Hipparcos satellite)

Matra Marconi Space, Toulouse, France
(Satellite Prime Contractor and Payload Development)

C. Guionnet, Project Manager: 1982–85
M. Bouffard, Project Manager: 1985–90

Assistant Project Managers (at Flight Acceptance Review):
M. Le Moine (system), G. Fade (payload), R. Giralt (integration),
J. Tisserant (project control), M. Siguier (product assurance), G. Martin (contracts)

J.J. Arnoux, I. Asseman, A. Bader, G. Bajard, J.J. Bertier, C. Biscans,
E. Bonnes, C. Bousquet, L. Brett, B. Calvel, J.P. Camus, C. Cantone,
S. Carthade, G. Chenut, M. Comet-Barthe, H. Costard, C. Dagras,
D. Dubet, M. Duran, A.M. Florentin, M. Fruit, J.P. Gardelle, V. Gardes,
B. Gonzalez, F.X. Guerre, M. Hervieux, P. Hollier, N. Iche, G. Laffaye,
A. Le Nenaon, J.P. Noel, C. Page, D. Pawlak, G. Planche, J.M. Pochet,
P. Ranzoli, J.P. Roujas, I. Rouvière, J.M. Rupil, K. Soukhavong, G. Soulat,
P. Temporelli, E. Truelle, D. Valat, E. Zeis, D. Zeller

Alenia Spazio, Torino, Italy
(Co-Prime Contractor: Spacecraft Procurement
and Satellite Assembly, Integration & Test)

B. Strim, Project Manager

Assistant Project Managers:
G. Finocchiaro (spacecraft procurement), W. Cugno (integration and test),
S. Rota (project control), G. Giusiano (product assurance),
C. Fea (contracts)

B. Bonafede, M. Braida, P. Baù, M. Bonato, M. Bianco,
G. Bria Berter, M. Casale, M. Cernicchiaro, M. Curletti, A. De Biasi,
G. De Bernardi, G. Fimognari, F. Frittella, E. Giorgio, G. Giulianelli,
C. Godoli, G. Morsillo, L. Matteotti, A. Marotta, M. Marchi,
G. Marocco, M. Mottica, C. Ostorero, A. Pavarani, O. Piersanti,
A. Polirpo, G. Patti, F. Pradotto, V. Roberto, S. Rustichelli,
F. Raineri, A. Regis, P. Rossotto, P. Santoro, P. Strada,
M. Teghille, R. Tosini, L. Terrasi, R. Veneri, D. Vettorato

Payload Industrial Sub-Contractors:

Carl Zeiss, Oberkochen, Germany
Spherical and Folding Mirrors, Relay Optics
W. Egle

CASA, Madrid, Spain
Payload External Baffles
J. Larrauri

CSEM, Neuchatel, Switzerland
Modulating Grid
M. Roulet

Dornier Satellitensysteme, Friedrichshafen, Germany
Mechanism Drive Electronics & Thermal Control Electronics
W. Wlaka

IAL, Liège, Belgium
Optical Ground Support Equipment and Payload Calibration
C. Jamar

LAS, Marseille, France
Optical Performance and Alignment
M. Saisse, J.-Y. Le Gall

Matra Marconi Space, Velizy, France
Optical Filters
D. Laroche

Matra Marconi Space, Velizy, France
Payload Structure
J.-P. Allard

Oerlikon-Contraves, Zurich, Switzerland
Flip-Flop Mechanisms
M. Gygax

REOSC, St Pierre du Perray, France
Beam Combiner
R. Geyl

SRON, Utrecht, The Netherlands
Detection Subsystem
R. Hoekstra

TPD-TNO, Delft, The Netherlands
Refocusing Assembly, Grid Calibration, Straylight Analysis
M. Hammerschlag†, H.J. van Agthoven

† deceased

Spacecraft Industrial Sub-Contractors (at Subsystem Level):

British Aerospace, Bristol, United Kingdom
Electrical Power and Harness
R.H.W. Fox

Daimler-Benz Aerospace (formerly MBB-ERNO), Bremen, Germany
Structure and Reaction Control
J. Thaeter

Fokker Space and Systems, Leiden, The Netherlands
Solar Arrays
C.W. Claassens

Fokker Space and Systems, Leiden, The Netherlands
Thermal Control
T. Olievierse

Matra Marconi Space, Velizy, France
Attitude and Orbit Control
R. Cau

Saab-Ericsson Space, Gotenborg, Sweden
Data Handling and Telecommunications
B. Lind

SEP - Société Européenne de Propulsion, Moissy, France
Apogee Boost Motor
W. Asad

Software Industrial Sub-Contractors:

CAPTEC, Dublin, Ireland
In-Orbit Payload Calibration
F. Kennedy

Logica UK, London, United Kingdom
Accuracy Assessment
P.E. Davies

Section 1.1

Introduction to the Hipparcos and Tycho Catalogues

1.1. Introduction to the Hipparcos and Tycho Catalogues

1.1.1. Overview of the Hipparcos Mission

The Hipparcos mission was the first space experiment dedicated to astrometry, and was accepted within the ESA scientific programme in 1980. The primary objective of the mission was the determination of accurate astrometric data—positions, annual proper motions and absolute trigonometric parallaxes, at levels of some 2 milliarcsec—for about 100 000 stars.

The Hipparcos Catalogue, the primary result of the observations and reductions of the satellite-acquired data, contains 118 218 entries with median astrometric precision of around 1 milliarcsec, and specific results for double and multiple systems. In 1982 the Hipparcos mission was extended to include the transmission, and subsequent reduction, of data from the satellite's star mapper. As a result the Tycho Catalogue, of slightly more than 1 000 000 objects, has been constructed in parallel with the construction of the Hipparcos Catalogue, and has a median astrometric precision of 7 milliarcsec for $V < 9$ mag, and 25 milliarcsec at $V = 10 - 11$ mag. The majority of stars contained in the Hipparcos Catalogue are also contained in the Tycho Catalogue. The complete stellar content of both catalogues is mapped in Volumes 14–16.

Accurate broad-band photometry at an average of some 110 epochs was acquired for all objects in the Hipparcos Catalogue, and two-colour photometry for nearly all objects in the Tycho Catalogue. The precision of median Hipparcos magnitudes, for constant stars, is in the range $0.0004-0.007$ mag (over the interval $2-12$ mag) with corresponding individual transit errors in the range $0.003-0.05$ mag. The typical precisions, at around 8 mag, are around 0.0015 mag on the median, and 0.011 mag on the individual errors. The precision of mean Tycho magnitudes is typically 0.012 mag for $V < 9$ mag, and around 0.06 mag for fainter stars.

The Hipparcos and Tycho Catalogues are based on data that were acquired and reduced in different ways, resulting in data content and astrometric and photometric accuracies which reflect these differences. Each catalogue comprises accurate astrometry, combined with fully calibrated photometry; the Hipparcos Catalogue comprises milliarcsec positions, parallaxes, and proper motions, while the Tycho Catalogue also provides homogeneous positions and proper motions in the Hipparcos reference frame, and parallaxes, although of lower precision than the Hipparcos Catalogue.

The results are available for immediate astrophysical application: in particular, the positions and proper motions are on a common, rigid, and quasi-inertial reference system, and the parallaxes are absolute. Formal astrometric standard errors, and correlations between the parameters, are provided, with the former believed to be a close representation of the true external errors. The positions and proper motions are on the same system as the extragalactic reference system defined by the IAU based on the directions to compact radio sources. Systematic errors in positions, parallaxes, and annual proper motions are believed to be below one or two tenths of a milliarcsec in the case of the Hipparcos Catalogue.

Observations of solar system objects, made either by the Hipparcos main mission or as part of the Tycho observations, have been treated separately, and are published independently from the stellar observations. Details are given in Section 2.7.

Satellite operational principle: The optical telescope on-board the satellite measured the signal from stars crossing the instrument's fields of view, modulated by a one-dimensional grid in the focal surface. The satellite attitude was monitored by a separate 'star mapper' detection chain. Two fields of view, about 1 degree square, and separated by about 58° on the sky, were superimposed in the focal surface. As the satellite scanned the sky in a complex series of precessing great circles, maintaining a constant inclination to the Sun's direction, a continuous pattern of one-dimensional measurements was built up. In the data reduction process, these measurements were brought together into a common system of astrometric parameters of all stars observed repeatedly over the operational lifetime. The principles of the satellite operation, and the corresponding data reductions, are described in Volumes 2–4.

Observations leading to the Hipparcos Catalogue: Data processed to form the Hipparcos Catalogue were based on observations using the 'main mission' detection system, described more fully in Volume 2. A detailed description of the theory and construction of the Hipparcos Catalogue is given in Volume 3.

The operation of the relevant instrument was such that 'programme' stars were observed individually, and had to be carefully selected in advance of the satellite launch. The limiting magnitude of individual observations, combined with the overall observing time available to a scanning satellite, meant that the set of stars observed comprises some 60 000 objects complete to about 7.3–9 mag depending on galactic latitude and spectral type, with the remainder representing a dedicated (and incomplete) sampling of objects down to a limiting magnitude of about 12 mag. The stellar density of the catalogue is roughly constant at about 3 stars per square degree, and the observing programme constituted a list of stars optimised in terms of satellite operations, requirements for an astrometric reference frame, and scientific importance of individually selected stars. The list of stars observed by the satellite was compiled and fixed before launch, and is referred to as the 'Hipparcos Input Catalogue'.

Each Hipparcos Catalogue entry (the term 'entry' is used to draw attention to the fact that many entries are themselves double or multiple) was observed at some 100–150 or so distinct epochs (i.e. crossings of the telescope's fields of view) throughout the three-year operational period, corresponding to some 25–60 distinct scanning configurations. The latter is more relevant to the resulting quality of the astrometric and multiple star solutions than the number of individual observations: it is significantly smaller because of the slow precession of the satellite's scanning motion. The precise epochs and pattern of observations, and the resulting astrometric accuracies, depended on the position of the object on the sky and its relationship with the ecliptic-based 'scanning law'. The astrometric data processing collected all of the observations and, for single objects, derived five astrometric parameters per object: the two positional components, the two proper motion components, and the trigonometric parallax. A rigorous estimate of the standard errors and correlation coefficients was derived at the same time.

Many catalogue entries were known *a priori* to be, or subsequently found to be, double or multiple. For such systems, including astrometric binaries, more than five parameters per object were used to characterise the astrometry. Disentangling of the components was possible in many cases, the instrument having also been optimised for the detection and classification of double systems. Nevertheless, results for double or multiple systems were more complex to derive, and more intricate to present in any uniform manner. The results depend upon the sky coordinates (and hence scanning geometry) and the

separation, magnitude difference, multiplicity, component variability, and the presence of non-linear photocentric motion. The interplay of all these aspects sometimes made it difficult to specify a unique interpretation of the observations, especially for large magnitude differences between components. Handling of the resulting uncertainties, and resolving discrepancies with respect to existing ground-based observations, has been a major challenge within the timescale set for the catalogue production.

Results from the photometric analysis of the same data entering the astrometric catalogue yielded a precise, calibrated, photoelectric magnitude at each of the observed epochs, in a broad-band photometric system (referred to as Hp) for objects observed by the main mission. The Hipparcos Catalogue includes median magnitudes and related statistical indicators characterising the variability of the entries.

The reduced data from these observations together constitute the Hipparcos Catalogue. Annexes contain information on double and multiple stars (the Double and Multiple Systems Annex, itself divided into five parts), calibrated photometry at each epoch of observation (referred to as the Hipparcos Catalogue Epoch Photometry Annex), derived information on photometric variability (the Variability Annex), observations of solar system objects, and certain intermediate astrometric data defined at the level of the individual 'reference great circles' traced out by the scanning motion.

Observations leading to the Tycho Catalogue: Data processed to form the Tycho Catalogue were based on observations using the 'star mapper' detection system, described more fully in Volume 2. A detailed description of the theory and construction of the Tycho Catalogue is given in Volume 4.

The satellite's star mapper provided a continuous estimate of the satellite's attitude, necessary to direct the main mission observations. In parallel, this star mapper provided a continuous stream of data which resulted in a second catalogue of astrometric and photometric data for slightly more than one million objects—including 97 per cent of the entries in the Hipparcos Catalogue. This is referred to as the 'Tycho experiment'. Although of lower astrometric quality than the Hipparcos Catalogue, the resulting Tycho Catalogue provides astrometry in the same reference system: positions and proper motions are given in a quasi-inertial reference frame, parallaxes are absolute, and systematic errors are believed to be below about one milliarcsec.

The Tycho astrometric data are complemented by two-colour photometric data, referred to as Tycho magnitudes, B_T and V_T, and closely approximating B and V in the Johnson UBV system. The Tycho Catalogue has a limiting magnitude of about $B_T = 12.2$ mag and $V_T = 11.5$ mag for stars of typical colour index $(B - V) = 0.7$ mag, and is largely complete to a limit of about $V_T = 10.5$ mag. Due to the lower astrometric precision of the Tycho Catalogue, results for double and multiple stars are not presented as a comprehensive annex of double star data. Resolved objects are presented as distinct Tycho Catalogue entries, while suspected double systems are flagged accordingly. Similarly, the lower photometric precision means that it has not been considered appropriate to provide 'epoch photometry' for all entries—the Tycho Catalogue Epoch Photometry Annex contains a subset of the Tycho Catalogue entries selected amongst bright stars, photometric standards, and candidate variables.

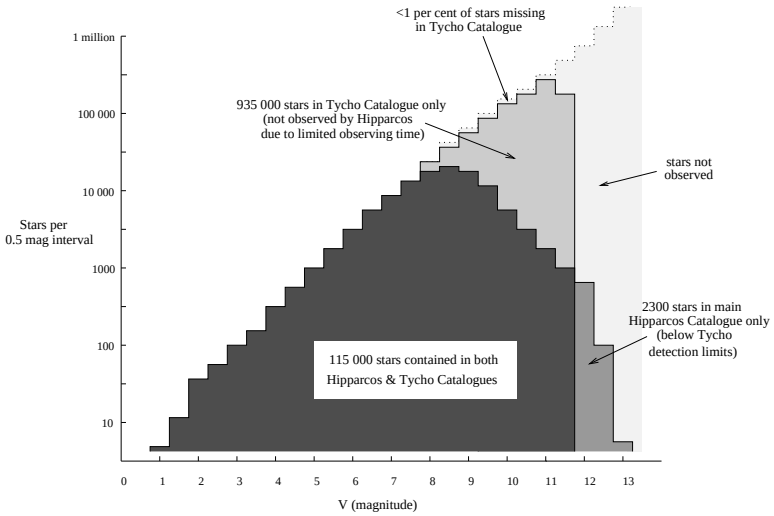

Figure 1.1.1. *The overlap and completeness of the 118 218 entries of the main Hipparcos Catalogue and the Tycho Catalogue. The former is largely complete to around $V = 7.3 - 9$ mag, depending on galactic latitude and spectral type. Other stars, with a roughly constant density over the celestial sphere, are included down to the observability limit at around $V = 12.5$ mag. The Tycho Catalogue is largely complete to around $V = 10.5$ mag, and contains objects down to the limit of the Tycho observations, at around $V = 11 - 11.5$ mag. Consequently, most Hipparcos entries are contained in the Tycho Catalogue, except for some 2300 entries below the Tycho detection threshold.*

The relationship between the Hipparcos and Tycho Catalogues: The completeness and overlap of the Hipparcos and Tycho Catalogues are illustrated in Figure 1.1.1. Only 6301 components contained in the Hipparcos Catalogue, corresponding to the faintest 2300 entries plus a small number of brighter stars, were not observed by Tycho. Objects contained in the Hipparcos Catalogue, including the components contained in Part C of the Double and Multiple Systems Annex, are cross-referenced in the Tycho Catalogue.

The Hipparcos Catalogue contains 118 218 entries corresponding to 129 332 stellar components, including those in the Part C of the Double and Multiple Systems Annex. 123 031 of these were observed by Tycho, and contained in 117 130 entries of the Tycho Catalogue, with small separation double systems merged into one 'star' when observed by Tycho (there are 5895 affected entries with two Hipparcos components, and 3 entries with three components). The remaining 6301 Hipparcos components not observed by Tycho are of three kinds: 4484 components (amongst which are the faintest 2300 Hipparcos entries) too faint to be observed by Tycho ($Hp > 11$ mag); 1247 probably disturbed by other stars; and 570 missed by Tycho for various other reasons. These 'missing' stars have been included in the Tycho Catalogue, with a flag referring to the Hipparcos Catalogue. A total of 1 052 031 entries were successfully observed by Tycho. It follows that 934 901 entries in the Tycho Catalogue are not contained in the Hipparcos Catalogue (not including the 263 Hipparcos entries without astrometry among the 118 218 entries in the Hipparcos Catalogue). The completeness of the Tycho Catalogue compared with entries in the main Hipparcos Catalogue with $Hp < 11$ mag is approximately 99 per cent.

For objects observed by both the main mission and Tycho, Tycho adds little or no astrometric weight. However, the Tycho astrometric results for objects not observed by the main detector are extensive, and are provided within the same astrometric reference frame as for the Hipparcos Catalogue. Tycho provides two-colour photometry for nearly all objects in the Tycho Catalogue, including entries from the Hipparcos Catalogue above the limit of detectability of Tycho.

1.1.2. Catalogues and Documentation before Satellite Launch

The following material summarises the status of the Hipparcos mission before launch:

- a comprehensive pre-launch description of the Hipparcos mission, given in the three-volume ESA Special Publication ESA SP–1111, including an overview of the satellite and its planned operations (Volume I), a detailed description of the preparation of the 'Hipparcos Input Catalogue' (Volume II), and the methods foreseen for the data reductions (Volume III);

- the Hipparcos Input Catalogue, constructed pre-launch, and published in printed form in March 1992 (ESA SP–1136, Volumes 1–7). It is also available, in machine-readable form, from the CDS (Strasbourg). It was released on a specifically created CD-ROM with dedicated interrogation software in August 1994;

- the Tycho Input Catalogue of three million stars, compiled pre-launch, and available in machine-readable form from the CDS (Strasbourg).

The Hipparcos Input Catalogue: In the case of the Hipparcos Catalogue, the Hipparcos Input Catalogue was necessary for the conduct of the observations—for the object selection, for the detector pointing, and (based on the magnitude) for the observing time allocation.

The Hipparcos Input Catalogue contained the list of stars and solar system objects constituting the detailed satellite observing programme. It represented a compilation of ground-based data necessary for the definition and execution of the optimised scientific observing programme, along with additional information of astronomical or astrophysical value. The published Hipparcos Input Catalogue (ESA SP–1136) consisted of Volumes 1–5 comprising the main catalogue, including principal cross-identifications, Volume 6 providing information on double and multiple stars, and Volume 7 providing identification charts.

Each entry was identified by its Hipparcos Input Catalogue (HIC) identifier. The same numbering system is strictly adhered to in the final catalogue, so that the Hipparcos Catalogue (HIP) number is the same as the HIC number for any given entry. Components of multiple systems which have been treated as a single target for the satellite observations, and entries previously considered as single objects but discovered to be double or multiple, are flagged accordingly, and treated separately in an annex.

Although the HIC and HIP identifers with the same running number refer to the same object, the HIC identifier is strictly identified with the pre-launch catalogue compilation (and corresponding ground-based data), while the HIP identifier is strictly identified with the final mission products based on the satellite data.

The Tycho Input Catalogue: While the Tycho observations themselves were not based on an *a priori* observing list, and a starting catalogue was not strictly necessary for the conduct of the observations, the Tycho Catalogue construction was greatly facilitated by the availability of a list of objects, rather complete to limits beyond the Tycho detection threshold, and with coordinates accurate to about 1 arcsec. This list constituted the 'Tycho Input Catalogue'. The Tycho data analysis resulted in the Tycho Catalogue of approximately one million stars, referred to by their TYC identifiers.

1.1.3. The Hipparcos and Tycho Catalogues and Products

The products of the mission are as follows:

- the present collection of 16 printed volumes, describing the contents of the final Hipparcos and Tycho Catalogues, the satellite performance and data reduction procedures, and the printed part of the Hipparcos Catalogue;
- the Hipparcos Catalogue, deposited with the CDS (Strasbourg), and released on CD-ROMs in ASCII format. These accompany the printed catalogue as Volume 17. In addition to the data in the printed catalogue, the machine-readable version includes the complete photometric and double/multiple star annexes, certain cross-identifications, and additional files containing results from intermediate stages of the astrometric data processing;
- the Tycho Catalogue, deposited with the CDS (Strasbourg), and also released on CD-ROMs in ASCII format. In addition, the ASCII CD-ROMs include a Tycho Epoch Photometry Annex, providing the individual photometric observations for a selection of the Tycho Catalogue stars. These also accompany the printed Hipparcos catalogue as Volume 17. A larger selection of the individual photometric observations, called Tycho Epoch Photometry Annex B and comprising about half of all Tycho stars, will also be deposited with the CDS, but not distributed with the printed catalogue. There is no printed version of the Tycho Catalogue;
- the Hipparcos and Tycho Catalogues, released on a specifically created CD-ROM with a compressed data format, and with dedicated interrogation software designed for specific computer platforms. This is referred to collectively as the *Celestia 2000* package, to distinguish it from the primary (ASCII) CD-ROM data products. Specific target platforms and specific interrogation facilities mean that this product will have a limited lifetime, but is intended nevertheless to make the Hipparcos and Tycho Catalogues more easily accessible to users in the short term.

The final data products were generated as illustrated in Figure 1.1.2.

Hipparcos and Tycho Catalogue numbering system: The Hipparcos Catalogue entries are referred to by their HIP running number, and the Tycho Catalogue entries by their TYC (3-component) running number. The HIP running number is the same as the HIC (Hipparcos Input Catalogue) number for a given entry. The TYC number is derived from the numbers assigned to stars in the Hubble Space Telescope's Guide Star Catalog (B. Lasker *et al.*, 1990, *Astronomical Journal*, 99, 2019); entries resolved into two or more components as part of the Tycho data processing were allocated new numbers consistent with this numbering scheme. The HIP and TYC acronyms are registered for the Hipparcos and Tycho Catalogues respectively within the Centre de Données astronomiques de Strasbourg (CDS).

Content of the Hipparcos Catalogue: While the stellar content of the Hipparcos Input Catalogue and the final Hipparcos Catalogue is nominally the same, the catalogues are of very different nature. The Hipparcos Input Catalogue is a compilation of observational catalogues or *ad hoc* observations, while the Hipparcos Catalogue resulting from the satellite observations is a primary observational catalogue.

The same general layout of the printed versions of both the Hipparcos Input Catalogue and the final Hipparcos Catalogue was adopted to allow the data contents of both catalogues to be consulted in parallel with relative ease.

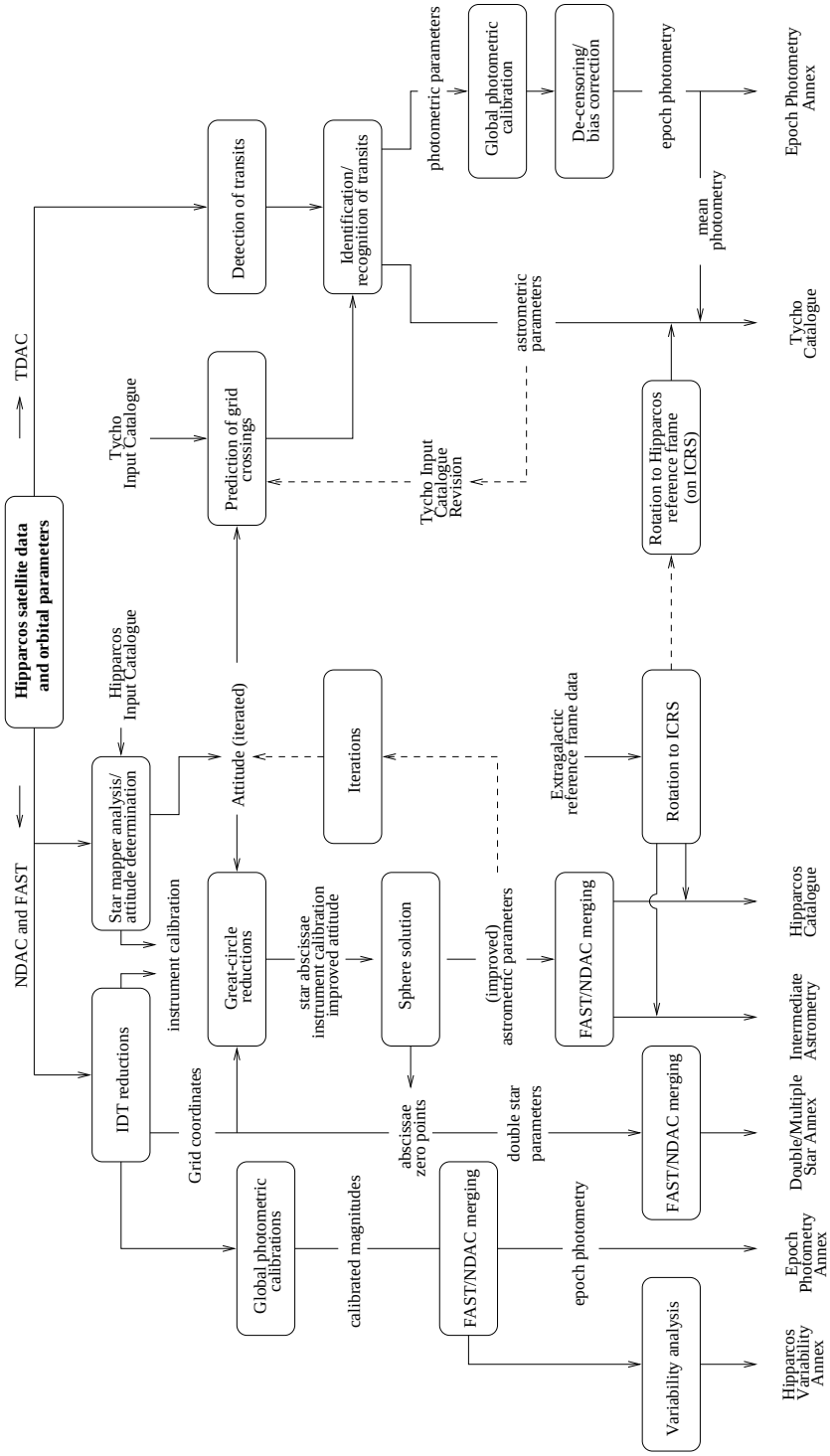

Figure 1.1.2. *The relationship between the input data, the data processing, and the final products.*

The Hipparcos Catalogue contains primary data obtained directly from the satellite observations, with few other data included. A clear distinction has thus been maintained between the Hipparcos data, and complementary data acquired from ground-based observations or from other data bases (which may be expected to change with time).

The astrometric and photometric data contained in the Hipparcos Input Catalogue are largely superseded (but, especially in the case of the photometric data, not completely so) by the values given in the final Hipparcos Catalogue. Cross-identifications and certain other auxiliary data (in particular the radial velocity, spectral type, variability type, and multiplicity data) provided in the Hipparcos Input Catalogue apply equally to the final Hipparcos Catalogue.

Content of the Tycho Catalogue: Because the Hipparcos Catalogue is incomplete down to its observability limit, and because this observability limit is itself slightly fainter than the Tycho Catalogue observability limit, there are a (relatively small) number of stars in the Hipparcos Catalogue not contained within the Tycho Catalogue. Conversely, since the Tycho Catalogue is rather complete down to its observability limit, most of the Hipparcos Catalogue stars are contained within the Tycho Catalogue.

For objects contained in both catalogues, the Hipparcos Catalogue invariably provides astrometric data, multiplicity information, and photometric and variability information all of a higher precision than corresponding data from the Tycho Catalogue. The two-colour Tycho Catalogue photometry nevertheless represents independent photometric information for such objects.

The considerable similarities between the two final catalogues have led to a high degree of congruence imposed on the Hipparcos and Tycho Catalogue formats. Many of the fields of the printed and machine-readable versions apply to the two catalogues in both precise format and meaning.

Content of *Celestia 2000*: In addition to the data in the printed Hipparcos Catalogue, *Celestia 2000* also includes: (a) the Tycho astrometry and mean photometry; (b) auxiliary files containing non-Hipparcos data, extracted principally from an updated version of the Hipparcos Input Catalogue, considered sufficiently extensive or sufficiently important for basic astrophysical interpretation of the Hipparcos data (including cross-identifications to other catalogues, spectral types, radial velocities, and identification charts); (c) interrogation software for accessing and extracting data from the *Celestia 2000* CD-ROM.

1.1.4. How to Use the Hipparcos and Tycho Catalogues

Table 1.1.1 gives a summary of the various data products, and indicates which of the products are provided within the printed, ASCII, or *Celestia 2000* media.

Some of the data—for example, photometry, colour indices, etc.—are 'distributed' amongst the various data products. Figure 1.1.3 provides an overview of the main categories of astrometric and photometric data provided in either of the Hipparcos or Tycho Catalogues, and indicates where a description of the data is given, and where the data are to be found. It complements Table 1.1.1.

Table 1.1.1. The location of the various data sets

Information	Description (Section) (Volume 1)	Printed Catalogue (Vols 1–16)	CD-ROMs ASCII (Vol. 17)	CD-ROMs *Celestia 2000*
Introduction and Guide to the Data		√ (1)	√	–
The Hipparcos Satellite Operations		√ (2)	√	–
Construction of the Hipparcos Catalogue		√ (3)	√	–
Construction of the Tycho Catalogue		√ (4)	√	–
The Hipparcos Catalogue[a]	2.1	√ (5–9)	√	√
The Tycho Catalogue[b]	2.2	–	√	√
Hipparcos Double & Multiple Systems Annex[c]	2.3	√ (10)	√	√
„ (supplementary details)[d]	2.3	–	√	–
Hipparcos Variability Annex[e]	2.4	√ (11)	√	√
Hipparcos Light Curves[f]	2.4	√ (12)	√	√
Hipparcos Epoch Photometry Annex[g]	2.5	–	√	–
Tycho Epoch Photometry Annex[h]	2.6	–	‡	–
Solar system objects[i]	2.7	√ (10)	√	–
Hipparcos intermediate astrometry[j]	2.8	–	√	–
Hipparcos transit files[k]	2.9	–	‡	–
Identification charts[l]	2.10	√ (13)	√	√
Identification tables	2.10	√ (13)	√	√
Star atlas (with Sky Publishing Corporation)		√ (14–16)	–	–
Hipparcos Input Catalogue data[m]		–	‡	‡
Interrogation software[n]		–	√	√

‡ subset of data only

(a) astrometry (Hipparcos), mean photometry (Hipparcos and Tycho), and summary double star data
(b) astrometry and mean photometry from Tycho
(c) includes configuration charts for each double or multiple system
(d) supplementary double/multiple star parameters, including correlation coefficients
(e) parameters derived from analysis of the Hipparcos epoch photometry (periodic and unsolved)
(f) light curves or folded light curves constructed from the Hipparcos epoch photometry
(g) 'epoch photometry' for all Hipparcos entries, i.e. photometric data at each epoch of observation
(h) 'epoch photometry' for specific Tycho entries, i.e. photometric data at each epoch of observation
(i) includes observations from both Hipparcos and Tycho
(j) astrometric data (Hipparcos) at the level of the reference great circles
(k) astrometric data (Hipparcos) at the level of the transit files (subset of stars)
(l) charts for faint stars and/or stars in clusters
(m) relevant (sometimes updated) parameters, including cross-identifiers to major catalogues
(n) C code record extraction (ASCII); menu-driven platform-dependent (*Celestia 2000*)

Table 1.1.2 lists the identifiers that are used for fields in the printed or machine-readable files. The corresponding file names are given in Section 2.11.2.

Figures 1.1.4(a,b) give an extract of the main Hipparcos Catalogue, with a summary of the meaning of the fields included.

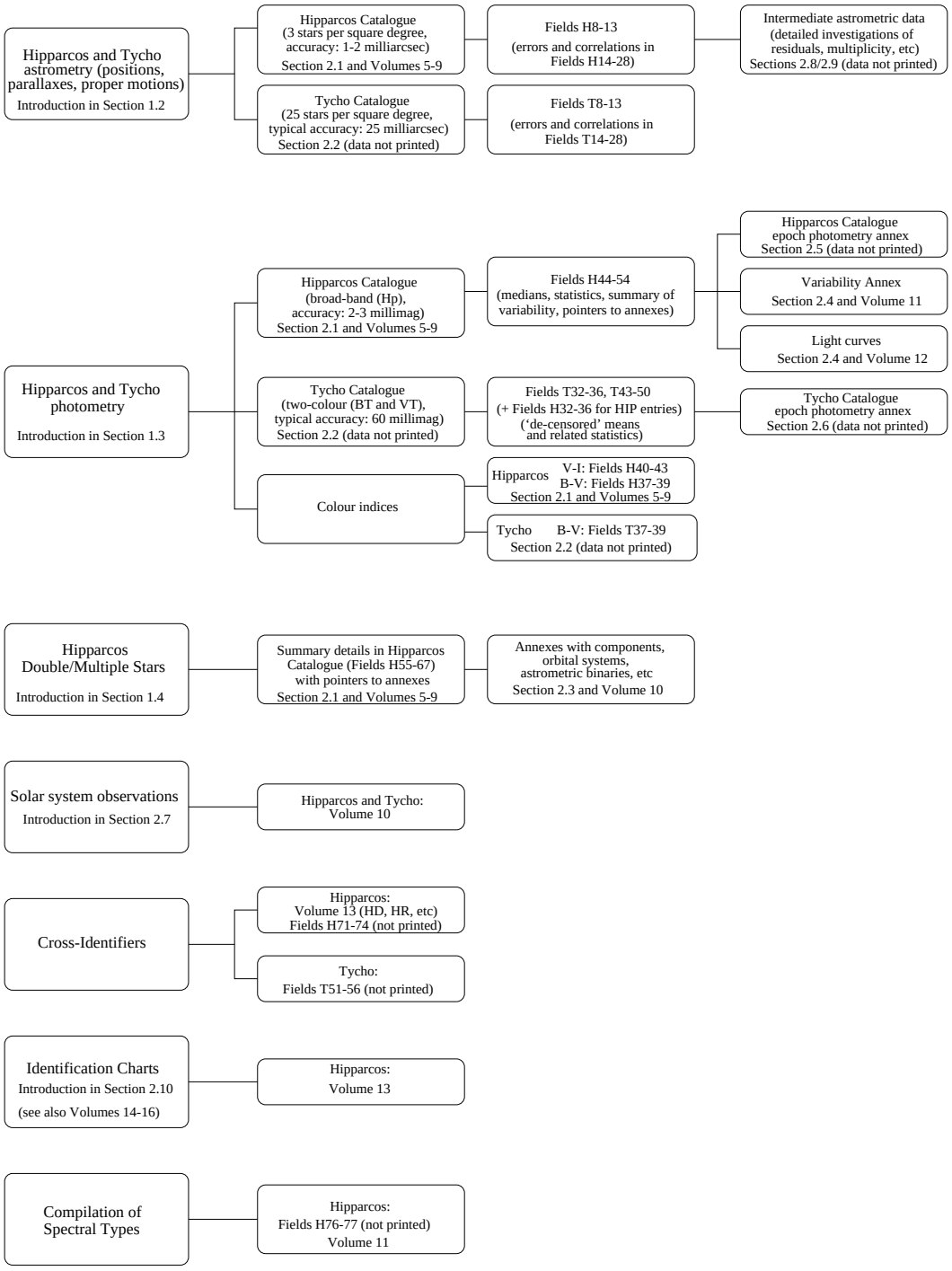

Figure 1.1.3. *The contents of the Hipparcos and Tycho Catalogues, and where to find the data.*

Table 1.1.2. Identifiers for fields in the printed or machine-readable files (listed alphabetically)

Id.	Data Content	Description	Printed Volume(s)
DC	Hipparcos Double & Multiple Systems Annex: components	2.3	10
DG	Hipparcos Double & Multiple Systems Annex: accelerations	2.3	10
DO	Hipparcos Double & Multiple Systems Annex: orbits	2.3	10
DV	Hipparcos Double & Multiple Systems Annex: variability	2.3	10
DX	Hipparcos Double & Multiple Systems Annex: stochastic	2.3	10
H	Hipparcos Catalogue	2.1	5–9
HH	Hipparcos Epoch Photometry Annex: header record	2.5	–
HHE	Hipparcos Epoch Photometry Annex Extension: header record	2.5	–
HT	Hipparcos Epoch Photometry Annex: transit record	2.5	–
HTE	Hipparcos Epoch Photometry Annex Extension: transit record	2.5	–
IA	Hipparcos Intermediate Astrometry: abscissa	2.8	–
IH	Hipparcos Intermediate Astrometry: header	2.8	–
IR	Hipparcos Intermediate Astrometry: reference data	2.8	–
JH	Hipparcos Transit Data: header record	2.9	–
JP	Hipparcos Transit Data: pointing record	2.9	–
JT	Hipparcos Transit Data: transit record	2.9	–
P	Hipparcos Variability Annex: periodic variables	2.4	11
SHA	Solar System Objects: Hipparcos astrometry	2.7	10
SHP	Solar System Objects: Hipparcos photometry	2.7	10
ST	Solar System Objects: Tycho astrometry and photometry	2.7	10
T	Tycho Catalogue	2.2	–
TH	Tycho Epoch Photometry Annex: header record	2.6	–
TT	Tycho Epoch Photometry Annex: transit record	2.6	–
U	Hipparcos Variability Annex: unsolved variables	2.4	11

$19^h\ 11^m\ 39^s$ - $19^h\ 12^m\ 46^s$ **1896**
94301 - 94400

HIP identifier (same as HIC identifier); * implies that the entry is out of order with respect to its right ascension.

Proximity flag: derived from nearby HIP or TYC entries; indicates that caution is needed in using it as an astrometric reference.

Sexagesimal identifier: provided 'for information' and derived from the definitive position. Epoch is J1991.25. Reference system is ICRS.

Johnson V magnitude, variability flag, and source of magnitude. These provide an indication of magnitude and possible variability, derived from information given in other fields.

The Hipparcos position, at epoch J1991.25, within the ICRS reference system. General considerations related to the astrometric parameters are given in Section 1.2. Derivation of positions at different epochs (within ICRS) is considered in Section 1.5. Positions, and the other astrometric parameters, were derived from a merging of the data from the two consortia. Intermediate data are described in Sections 2.8–2.9.

If the entry is double, the flag indicates whether the astrometric data in these (and subsequent) fields refer to a component or photocentre, or (rarely) the centre of mass for an orbital system.

The Hipparcos parallax in milliarcsec (negative values arise from measurement errors).

The Hipparcos proper motion, at epoch J1991.25, in milliarcsec per year, both components expressed in great-circle measure.

The standard errors of the five primary astrometric parameters: position, parallax, and proper motion components, respectively.

The correlation coefficients between the five astrometric parameters.

Statistical indicators of the quality of the astrometric solution: percentage of data rejected from the final astrometric model, and resulting (gaussianised) goodness-of-fit, respectively.

Checksum. See Section 2.11.3.

Number HIP 1 2	Descriptor: epoch J1991.25 RA h m s 3	Dec ±° ′ ″ 4	V mag 5 6 7	Position: epoch J1991.25 (ICRS) α deg 8	δ deg 9 10	Par. π mas 11	Proper Motion $\mu_{\alpha*}$ mas/yr 12	μ_δ 13	Standard Errors α* mas 14	δ 15	π mas 16	$\mu_{\alpha*}$ mas/yr 17	μ_δ 18	Astrometric Correlations (%) 19 20 21 22 23 24 25 26 27 28	Soln F1 29	F2 30
94301	19 11 39.93	+19 25 54.2	9.32 H	287.916 356 71	+19.431 710 10	4.36	10.76	12.29	0.88	1.03	1.47	1.11	1.55	+39 −15 −32 − 7 −16 +22 − 8 + 8 −24 +29	3	−0.08
94302	19 11 40.52	+56 51 32.7	5.13 H	287.918 837 62	+56.859 095 94	9.57	48.09	48.00	0.44	0.45	0.47	0.51	0.61	− 1 + 8 + 3 +17 + 2 − 5 + 1 +16 −11 + 3	1	0.76
94303	19 11 41.74	−33 42 31.2	10.70 G	287.923 923 90	−33.708 672 65	5.45	3.45	−18.20	2.44	1.16	2.39	4.06	1.96	+ 0 −16 −18 +26 +34 −17 + 2 −45 +30 −47	0	0.43
+94304	19 11 41.95	−81 24 46.5	7.60 H	287.924 807 49	−81.412 923 39	9.72	19.40	35.91	0.54	0.59	0.70	0.64	0.76	− 6 −23 + 5 + 0 −10 − 1 − 8 +13 − 5 −12	0	0.32
+94305	19 11 41.93	+09 57 06.2	8.44 H	287.924 721 08	+09.951 709 33	3.77	1.11	−8.82	1.12	0.77	1.28	1.25	0.86	−14 −12 −19 −26 +26 −28 +16 −39 +37 −22	0	−0.29
94306 H	19 11 43.52	+17 53 01.0	8.20 G	287.931 328 93	+17.883 612 16 A	0.57	1.30	−7.00	1.31	1.17	1.58	1.83	1.60	+13 − 9 −15 +55 − 9 +15 −15 +20 −11 −10	2	0.37
94307	19 11 44.21	−47 11 16.7	9.66 H	287.934 207 13	−47.187 963 08 A	7.43	−13.75	−8.22	1.96	1.51	1.91	2.56	1.94	+39 −14 −18 −11 −19 + 3 −23 −51 +12 +41	1	−0.02
94308	19 11 45.03	+26 14 57.6	7.80 H	287.937 607 07	+26.249 326 14 A	8.34	2.81	−5.67	0.67	0.85	1.09	0.72	0.93	−13 −17 + 1 +23 + 6 − 5 + 8 + 0 − 3 −10	2	2.19
94309	19 11 45.35	−19 11 21.6	8.15 2 H	287.938 964 02	−19.189 330 69	5.84	7.06	11.43	0.89	0.55	0.99	1.05	0.67	+ 8 −14 − 3 − 6 −11 +20 −12 −43 −14 − 3	0	0.92
94310 H	19 11 45.76	−53 19 22.0	8.90 H	287.940 663 10	−53.322 766 02 A	15.39	58.23	−37.78	2.31	2.49	2.32	2.74	1.81	+26 − 8 −14 + 3 −11 −24 −28 −44 − 8 + 5	1	0.68
94311	19 11 46.01	+31 17 00.5	5.93 1 H	287.941 712 76	+31.283 463 60	3.33	−3.17	−3.16	0.38	0.44	0.55	0.45	0.55	−11 − 8 −16 + 4 +11 − 2 +11 + 9 +13 −14	0	−1.63
94312	19 11 46.35	−31 07 45.8	12.40 2 H	287.943 111 87	−31.129 399 09	−3.74	20.08	−2.68	6.76	3.24	7.41	7.76	5.90	+16 −35 +12 + 2 −15 −10 −22 −55 +18 +16	7	1.13
94313	19 11 46.62	+18 05 16.2	7.62 H	287.944 262 91	+18.087 820 96	7.12	−7.18	−8.16	0.61	0.59	0.86	0.93	0.86	+12 −11 −15 +43 −11 +20 −15 +20 + 1 −15	0	−1.57
94314	19 11 47.24	+12 52 16.1	9.27 H	287.946 850 59	+12.871 136 27	3.33	0.47	3.99	1.06	0.99	1.44	1.07	0.98	+ 2 −28 −22 −26 + 2 +20 + 6 −31 + 5 + 3	3	−0.40
94315	19 11 47.60	+13 54 33.3	8.78 H	287.948 314 45	+13.909 261 07	3.87	0.97	−9.12	0.71	0.76	1.12	0.81	0.87	+27 −11 −15 +10 −29 +15 −30 −14 + 4 +20	2	0.74
94316	19 11 49.77	+05 22 38.3	7.92 H	287.957 367 84	+05.377 298 93	3.08	22.82	12.21	0.93	0.72	1.15	1.05	0.73	+12 −14 − 1 −30 −15 −23 −16 −41 + 7 −14	0	−1.10
94317	19 11 50.06	+08 42 39.3	11.25 H	287.958 570 84	+08.710 903 69 B	1.33	0.85	−5.84	43.82	28.65	3.89	4.57	2.98	+ 3 − 9 − 1 − 1 + 0 − 4 − 2 − 3 +24 + 4	1	−0.07
94318	19 11 50.30	−70 48 24.4	9.36 H	287.959 564 33	−70.806 778 51	0.28	7.80	−1.98	0.57	0.87	1.26	0.75	1.00	−20 −14 − 3 +18 −10 −13 −11 + 6 + 7 −30	2	−1.03
94319	19 11 50.57	+08 42 18.7	9.97 H	287.960 712 17	+08.705 205 93 A	1.33	0.85	−5.84	4.62	3.06	3.89	4.57	2.98	+ 6 − 6 −16 −27 + 1 − 4 − 1 −30 +24 + 4	1	−0.07
94320	19 11 52.19	−20 22 51.2	8.36 H	287.967 456 19	−20.380 887 80	2.72	−7.04	−2.58	0.98	0.56	1.08	1.29	0.75	− 8 − 3 − 3 +15 − 4 +34 − 7 −32 −17 −21	2	0.19
94321	19 11 53.34	+14 34 56.1	8.05 H	287.972 257 05	+14.582 240 63	2.50	2.58	−10.03	0.60	0.60	0.95	0.66	0.69	+31 −17 − 4 +23 −22 +11 −26 − 8 + 4 +22	0	−0.22
94322	19 11 53.36	−44 34 13.0	10.15 H	287.972 335 96	−44.570 291 03	8.48	−35.58	−113.22	1.59	1.01	1.82	1.79	1.29	+16 −41 −12 −26 +18 + 7 +17 −41 + 5 +13	0	0.70
94323	19 11 54.96	−14 35 04.4	7.04 G	287.979 014 50	−14.584 562 45	2.94	51.08	6.06	0.79	0.50	0.94	0.88	0.58	+18 −32 −10 −11 − 5 +36 − 5 −33 + 2 + 6	0	−1.39
94324	19 11 56.51	+43 53 25.9	8.01 H	287.985 457 13	+43.890 524 95	2.65	2.14	−0.79	0.58	0.61	0.66	0.59	0.79	− 3 + 8 − 3 +13 +23 − 1 +28 +18 +10 + 5	3	−0.57
94325	19 11 56.86	−46 08 40.5	8.02 H	287.986 899 66	−46.144 583 06	3.79	−20.68	−11.91	1.12	0.85	1.43	1.62	1.17	+17 − 2 −37 −36 +21 −36 + 8 −54 +30 − 4	0	0.42
94326	19 11 57.30	−39 30 00.9	8.80 H	287.988 748 43	−39.500 242 33	21.37	88.74	−102.48	1.29	0.79	1.45	2.11	1.07	+ 1 −12 −24 +15 +30 −42 + 5 −36 +35 −41	0	0.47
94327	19 11 57.47	+22 07 22.7	9.08 H	287.989 449 37	+22.122 962 72	−0.44	1.77	1.33	0.74	0.89	1.24	1.01	1.06	+23 −13 + 0 +20 + 12 +17 + 8 +11 +22 +29	0	0.79
94328	19 12 00.32	+39 25 14.6	7.50 H	288.001 317 95	+39.420 706 01	5.17	9.15	11.53	0.52	0.53	0.63	0.61	0.68	− 2 + 4 − 3 +15 + 9 −12 +10 +16 − 4 + 2	0	0.63
94329	19 12 00.48	−30 16 13.1	10.43 H	288.001 992 90	−30.270 310 50	2.51	7.08	−1.70	2.25	1.24	2.81	3.71	1.91	+19 −22 − 3 − 6 + 0 −54 −20 −61 +20 −20	4	0.09
94330	19 12 02.85	+07 55 46.8	9.84 H	288.011 858 21	+07.929 663 91	0.48	−1.60	−4.90	1.33	0.98	1.61	1.46	1.14	+24 −36 −24 − 4 + 2 + 3 − 9 −24 +21 − 9	2	0.47
94331 H	19 12 03.28	+02 37 21.4	6.94 H	288.013 660 99	+02.622 616 58 +	4.35	−3.30	−10.44	1.28	0.77	1.07	1.02	0.82	+ 6 −24 − 2 −19 + 4 − 2 + 3 −27 + 8 +13	1	0.22
94332	19 12 03.94	−31 12 21.3	9.12 G	288.016 434 70	−31.205 927 04	5.42	0.89	−12.97	1.60	0.74	1.65	1.84	1.17	+10 −40 − 4 + 6 + 3 −15 −15 −51 +17 −14	0	0.16
94333	19 12 04.19	−23 44 25.8	8.02 G	288.017 461 98	−23.740 509 91	−0.07	−1.82	−8.31	1.04	0.54	0.99	1.32	0.81	−31 − 4 −11 −30 +33 − 7 +30 −57 +18 −39	0	−0.43
+94334	19 12 04.87	−43 55 27.2	10.19 G	288.020 286 12	−43.924 228 35	4.36	5.06	−5.76	1.61	1.17	1.98	2.13	1.54	+ 9 −16 −20 −23 +29 −14 +21 −49 +19 − 5	0	−1.25
+94335	19 12 04.86	+46 19 26.5	9.35 2 H	288.020 260 65	+46.324 018 65	7.69	−0.82	45.43	0.75	0.71	0.89	0.88	0.75	+ 5 −19 +18 + 5 + 8 −17 +16 −14 −19 +28	3	−0.87
+94336 H	19 12 05.22	+49 51 15.3	5.85 G	288.021 731 47	+49.854 238 07 A	40.16	−205.02	624.33	0.99	0.92	0.83	0.97	0.89	− 1 −24 +12 +12 + 3 − 3 + 5 + 1 + 3 +10	7	1.21
+94337	19 12 05.10	+69 42 28.5	9.00 H	288.021 240 72	+69.707 914 48	5.81	8.31	8.77	0.65	0.58	0.65	0.77	0.69	+10 −19 − 1 + 9 + 3 − 6 + 2 + 4 + 0 +12	0	−0.44
94338 H	19 12 05.81	−21 55 41.7	7.83 H	288.024 221 48	−21.928 241 09 A	3.42	5.85	−5.95	1.98	1.09	1.87	1.80	1.31	+ 1 − 1 −10 − 4 − 7 + 4 + 1 −34 +25 + 35	2	0.23
94339	19 12 06.30	−50 14 38.2	8.02 H	288.026 262 65	−50.243 956 33	0.81	15.62	−34.94	0.84	0.60	0.94	1.13	0.66	− 2 −18 − 8 − 3 +20 + 7 +15 −33 − 6 −15	0	−0.03
94340	19 12 06.47	−28 29 05.8	9.49 H	288.026 951 21	−28.484 941 29	12.86	−18.38	−87.28	1.98	0.76	2.02	1.95	1.09	+ 0 −63 − 4 + 7 +12 −15 − 8 −50 +14 −27	2	1.25
94341	19 12 08.15	+24 07 48.2	11.22 G	288.033 953 64	+24.130 060 36	29.35	−119.82	−197.53	1.78	2.07	3.13	2.33	2.56	− 8 −12 − 3 −22 − 8 + 2 − 9 −23 +12 + 0	0	
94342	19 12 08.38	+36 09 46.4	8.78 H	288.034 905 56	+36.162 886 37	3.01	1.84	−2.13	0.63	0.69	0.82	0.71	0.79	− 8 + 8 −11 +13 +17 −18 +16 +10 − 2 − 7	1	−0.02
94343	19 12 09.52	+41 50 15.5	8.20 H	288.039 675 39	+41.837 647 01	5.79	17.57	−15.61	0.63	0.64	0.76	0.67	0.88	− 9 −28 + 4 − 6 + 2 + 6 + 3 +26 + 4 −13	0	−1.19
+94344	19 12 09.78	−37 34 59.1	6.55 G	288.040 738 35	−37.583 090 57	2.37	5.47	−5.95	0.83	0.47	0.85	1.09	0.60	+ 1 −32 + 8 +26 − 1 + 1 − 10 −35 −11 −21	0	1.30
+94345	19 12 09.72	−16 25 49.4	8.02 G	288.040 497 17	−16.430 379 03	6.76	−15.54	−45.00	0.92	0.56	1.00	0.98	0.64	+ 1 −26 − 6 − 6 + 2 + 8 + 3 −33 + 7 + 5	0	0.09
94346	19 12 11.12	+57 40 15.6	7.04 1 G	288.046 334 48	+57.670 989 03	50.00	217.75	408.26	0.51	0.51	0.54	0.54	0.60	+ 6 − 9 +11 +20 +11 − 4 +15 + 6 −12 +21	0	0.55
94347	19 12 11.15	−83 29 00.2	7.26 H	288.046 443 34	−83.483 386 75	22.25	136.95	−128.05	1.50	1.61	1.94	1.71	2.02	−10 −17 + 3 − 5 + 0 + 0 + 1 −15 −10 −14	0	
94348	19 12 13.20	−52 14 33.0	9.96 G	288.054 985 34	−52.242 501 53	2.68	−2.29	−12.40	1.62	1.47	1.70	2.22	1.72	+53 + 1 +11 −45 −45 −17 −45 −73 −18 +48	2	−0.11
94349	19 12 13.55	+02 53 15.6	11.09 G	288.056 468 21	+02.887 668 13 +	98.56	1789.15	−520.07	2.06	1.88	2.66	2.72	2.00	− 3 −26 +26 − 7 +25 +18 + 0 − 5 + 5 + 5 +21	2	2.14
94350 H	19 12 14.80	+32 15 09.9	7.37 G	288.061 662 66	+32.252 758 91 A	3.02	2.01	1.67	0.67	0.71	0.84	0.74	0.78	+ 0 + 0 − 1 +27 + 6 − 4 + 5 + 4 +25 + 3	1	−0.06
94351	19 12 15.71	+47 22 30.0	6.54 H	288.065 444 51	+47.374 992 51	1.33	3.69	−1.21	0.52	0.46	0.57	0.62	0.51	+ 0 + 3 − 9 −16 + 8 −10 + 6 −11 +10 +21	4	−1.61
94352	19 12 15.99	+48 08 00.6	8.56 H	288.066 627 50	+48.133 493 55	4.26	−2.06	18.08	0.72	0.68	0.77	0.82	0.78	+10 −10 −15 −39 + 1 + 3 − 3 −17 +16 +21	3	−0.63
94353	19 12 16.99	−51 48 43.6	8.42 G	288.070 803 02	−51.812 117 63	4.00	1.34	−27.03	0.99	0.82	1.17	1.30	0.92	+19 + 2 +24 −22 −11 −22 − 8 −59 −39 +27	0	−1.19
94354	19 12 17.40	+41 14 16.0	7.08 2 H	288.072 500 66	+41.237 772 32	3.35	1.13	−16.63	0.48	0.50	0.58	0.50	0.64	−12 + 5 − 9 + 4 + 4 − 9 + 4 +25 − 1 −11	0	0.06
94355 H	19 12 18.64	+21 13 29.0	8.24 H	288.077 652 63	+21.224 732 22 +	0.77	0.48	−6.14	1.15	1.26	1.18	0.98	1.03	+39 −15 + 0 − 1 − 3 − 1 − 3 + 0 + 2 +29	1	0.06
94356	19 12 19.25	−35 56 30.4	10.00 G	288.080 222 33	−35.941 771 55	2.03	−6.86	−7.04	1.49	0.85	1.59	2.08	1.15	+ 8 −28 −13 +23 + 8 −21 −14 −39 +17 −28	0	−0.28
94357	19 12 19.47	+09 19 22.5	9.56 H	288.081 110 16	+09.322 929 29	1.46	5.19	−7.98	1.36	1.12	1.75	1.62	1.09	+ 1 −18 −17 −34 +15 −22 + 4 −44 +24 − 6	2	−0.11
94358	19 12 19.73	−08 56 09.5	9.19 H	288.082 227 00	−08.935 968 51	0.97	−2.34	−5.21	0.98	0.63	1.17	1.16	0.77	+15 −11 − 7 − 4 + 8 +29 + 9 −17 +13 +11	0	−2.30
94359	19 12 21.44	+53 56 52.2	9.32 H	288.089 345 97	+53.947 831 10	2.77	−26.40	−35.28	0.92	0.81	0.89	1.00	1.12	− 9 −20 +12 −37 + 8 − 2 + 7 −18 − 2 +12	0	1.68
94360	19 12 22.49	−34 27 47.3	8.63 G	288.093 724 04	−34.463 089 92	0.06	5.89	−3.93	1.13	0.80	1.38	1.34	1.13	+40 −28 −20 +10 +26 −24 + 3 + 5 +28 +60	4	1.34
94361	19 12 22.61	+73 53 32.3	7.26 2 H	288.094 217 13	+73.892 314 23	2.79	−1.50	16.17	0.52	0.48	0.53	0.59	0.52	− 4 −17 +15 − 1 +13 − 3 +13 − 6 + 1 + 9	0	−0.29
94362	19 12 22.79	+20 30 44.7	9.19 H	288.094 939 81	+20.512 404 48	2.71	−5.15	−2.49	0.71	0.82	1.23	0.82	1.13	+24 −30 − 3 −12 − 7 + 3 − 2 + 6 −16 +23	0	−0.32
94363 H	19 12 23.60	+30 20 51.9	7.65 G	288.098 342 26	+30.347 763 71 A	0.72	2.37	−5.26	0.97	1.09	1.28	1.01	1.32	−20 −12 − 6 + 9 +11 − 7 +11 −12 − 3 −26	7	2.02
94364 T	19 12 23.67	−04 27 28.9	11.77 H	288.098 618 54	−04.458 039 89	4.21	−25.71	−21.46	5.51	3.43	6.21	7.62	5.74	+36 −11 +10 +14 +11 +28 + 8 + 2 +20 +42	9	0.25
94365	19 12 24.12	−51 40 20.0	7.06 H	288.100 511 57	−51.825 553 37	2.80	0.85	−20.68	0.78	0.65	0.89	0.69	0.69	+30 + 5 +11 −26 +17 −18 −26 −62 −33 +28	0	0.47
94366	19 12 24.36	+36 10 55.9	6.95 H	288.101 491 96	+36.182 204 82	3.03	5.86	9.59	0.43	0.52	0.60	0.49	0.64	− 9 + 8 −12 − 5 +13 −19 +13 +16 − 1 −12	0	−0.82
94367 H	19 12 25.20	−33 03 43.8	8.00 G	288.104 996 81	−33.062 169 41 A	15.43	−44.84	33.68	2.11	1.58	1.92	2.34	1.44	+15 − 4 −33 − 2 +22 −26 + 7 −38 +42 −28	2	−0.07
94368	19 12 25.55	−55 52 06.1	11.31 G	288.106 440 51	−55.868 371 87	50.04	−278.15	−169.46	2.03	1.69	2.72	2.32	2.25	+45 −26 −17 +10 −41 + 1 −34 −44 + 4 +60	2	3.20
94369	19 12 26.83	+19 12 30.7	8.99 H	288.111 806 31	+19.208 530 80	1.95	6.66	3.50	0.83	0.82	1.28	1.17	1.27	+29 + 0 −23 +28 − 2 +29 + 2 +20 − 7 +15	0	0.01
94370	19 12 27.42	−05 24 51.9	8.06 G	288.114 244 00	−05.414 414 46	19.04	−9.66	−52.48	0.87	0.61	1.07	0.95	0.73	+24 −25 −21 −23 + 1 +22 + 5 −25 + 9 +17	0	0.18
94371	19 12 27.46	+16 51 02.2	7.94 H	288.114 402 11	+16.850 597 96	21.72	115.83	−175.06	0.76	0.99	1.04	0.98	1.06	+25 −10 −34 + 0 + 1 +19 + 3 + 3 − 2 +14	4	0.42
94372	19 12 28.02	−21 55 41.7	6.39 H	288.116 746 70	−21.658 327 64	3.13	31.83	−22.34	0.74	0.37	0.77	0.73	0.49	+17 −33 + 1 − 6 + 6 +18 +14 −37 + 0 − 1	3	−2.03
94373	19 12 28.47	+18 00 06.8	7.45 H	288.118 608 34	+18.001 900 61	6.00	4.16	15.93	0.58	0.55	0.83	0.86	0.86	+21 −23 −15 +37 − 5 +12 −10 +17 + 6 + 0	1	−0.72
94374	19 12 28.72	−36 35 04.7	8.77 2 H	288.119 657 17	−36.584 632 13	0.75	16.69	−12.42	1.20	0.71	1.30	1.52	0.89	+18 −31 − 9 +21 + 4 −15 −12 −35 +12 −10	0	1.36
94375	19 12 28.98	+23 27 33.6	8.07 H	288.120 749 74	+23.459 331 35	2.38	−1.38	−3.10	0.48	0.58	0.93	0.58	0.68	−27 − 9 − 7 −16 − 7 + 7 − 8 −12 +13 −14	0	0.96
94376	19 12 33.15	+67 39 40.7	3.07 G	288.138 145 81	+67.661 316 95	32.54	94.49	92.30	0.47	0.41	0.46	0.47	0.45	−12 −20 + 6 −18 +20 + 5 +18 − 4 + 6 + 6	3	2.22
94377 H	19 12 34.45	+18 50 47.2	6.73 2 G	288.143 556 04	+18.846 448 22 A	3.85	2.18	−11.64	1.08	1.02	1.29	1.31	1.07	+ 25 − 1 −25 +17 −10 +20 −11 − 2 − 3 + 6	2	1.07
94378	19 12 34.54	−37 31 26.4	7.15 H	288.143 924 90	−37.523 997 61	3.41	−0.68	−16.01	0.86	0.49	0.91	1.04	0.60	− 4 −38 +14 +21 − 1 + 5 − 3 −32 −14 −14	0	1.71
94379	19 12 34.74	−58 54 08.3	9.20 G	288.144 742 16	−58.902 302 60	6.76	37.92	−13.60	1.00	0.70	1.41	1.35	1.15	+ 7 −10 −13 +22 −13 + 4 − 7 −13 +21 +34	0	2.34
94380	19 12 35.87	+12 52 58.2	9.56 H	288.149 464 20	+12.882 829 64	2.15	−6.15	−0.52	1.14	1.02	1.54	1.18	1.07	+ 6 −15 −12 −12 + 5 +32 +10 −11 − 5 + 2	0	−0.13
94381	19 12 36.18	+16 18 18.5	9.18 G	288.150 751 85	+16.305 138 12	4.39	−13.76	5.02	0.97	0.96	1.41	1.18	1.43	+33 + 1 + 0 − 3 − 14 +33 −17 −19 + 5 +35	0	−0.13
94382	19 12 36.72	+21 33 16.4	6.02 H	288.153 018 33	+21.554 560 41	3.24	14.51	4.79	0.42	0.45	0.64	0.53	0.54	+24 −20 −19 + 0 + 2 +10 + 1 − 2 +13 +26	1	−0.58
94383	19 12 37.00	+06 02 22.3	7.46 G	288.154 177 08	+06.039 537 20	4.58	−1.00	−15.20	0.83	0.60	0.92	0.88	0.61	+28 −23 −10 −17 −17 −14 −23 −32 +17 − 1	0	−1.06
94384	19 12 40.25	−06 27 31.6	9.12 2 H	288.167 726 91	−06.458 791 64	1.20	0.05	−4.39	0.99	0.71	1.20	1.21	0.89	+ 6 −14 −10 −13 + 9 + 6 + 7 −23 − 3 −21	2	−1.36
94385	19 12 40.70	−07 56 22.2	5.35 1 H	288.169 598 61	−07.939 500 77	2.68	12.69	−7.06	0.73	0.45	0.80	0.72	0.47	− 9 −15 −20 −36 +30 − 2 +26 −39 +24 −11	0	−0.04
94386	19 12 42.17	+13 22 59.8	8.42 H	288.175 728 28	+13.383 287 96	2.86	2.94	−14.74	0.88	0.80	1.10	1.06	0.87	− 9 − 6 −11 − 2 + 3 + 5 + 4 −26 +10 − 2	2	0.15
94387 H	19 12 42.40	+24 34 36.4	8.11 H	288.176 686 96	+24.576 782 06 +	13.40	68.25	−5.55	1.73	2.60	1.26	0.92	1.05	−22 +10 −20 −28 + 2 −10 + 2 −19 +17 −12	1	1.98
94388	19 12 42.82	+39 29 50.3	8.28 G	288.178 403 91	+39.497 310 83	2.68	2.09	−0.88	0.59	0.57	0.69	0.69	0.75	− 3 − 1 − 2 +25 + 5 − 2 + 6 +21 −11 + 3	0	−1.57
94389	19 12 43.00	−25 40 09.7	8.57 H	288.179 156 87	−25.669 362 17	16.93	1.89	−13.72	1.25	0.65	1.17	1.34	0.86	−32 −12 −10 −21 +32 − 4 +35 −43 +16 −22	0	0.48
94390	19 12 43.85	−11 33 01.3	7.61 H	288.182 728 38	−11.550 350 58	2.42	35.76	4.16	0.79	0.45	0.99	1.00	0.72	+24 −33 − 8 −15 + 6 +36 +11 −19 − 3 + 7	0	1.81
94391	19 12 43.92	−33 51 13.8	7.79 H	288.183 007 37	−33.853 846 93	12.07	51.61	−149.66	1.38	0.64	1.42	2.37	1.04	+24 −16 −27 +37 +41 −29 −17 −58 +36 −53	0	2.55
94392	19 12 44.11	−42 04 52.5	10.50 G	288.183 778 24	−42.081 253 89	1.25	−11.50	−16.16	2.09	1.37	2.18	2.14	1.48	+47 −55 −26 + 4 −14 − 7 −28 −47 + 6 +12	0	0.28
94393	19 12 44.13	−33 50 46.2	7.26 H	288.183 860 83	−33.846 168 20	2.19	−4.25	−8.00	1.28	0.60	1.28	2.28	0.99	+15 −17 −23 +30 +45 −26 − 9 −58 +32 −58	0	0.87
94394	19 12 44.16	−19 14 06.9	8.14 H	288.184 019 56	−19.235 245 95	13.96	−119.59	−124.36	0.87	0.50	0.98	1.00	0.68	+ 4 +20 − 5 − 8 −11 +26 − 4 −35 −39 − 8 +11	0	−1.40
94395	19 12 44.56	+08 36 37.9	7.76 H	288.185 658 11	+08.610 514 29	4.66	6.44	−0.33	0.88	0.57	1.04	0.83	0.60	− 2 −40 −10 −20 + 3 + 5 − 6 −27 +20 −23	0	−1.18
94396	19 12 44.97	+18 48 44.5	10.16 H	288.187 389 57	+18.812 349 74	17.22	113.91	166.28	1.25	1.38	1.85	1.71	2.03	+47 −13 − 1 +29 +10 +19 +10 +36 + 8 + 21	0	−1.27
94397	19 12 45.52	−24 29 14.0	7.57 H	288.189 668 63	−24.487 218 52	6.11	30.36	−15.43	1.16	0.56	1.00	1.61	0.89	−46 + 2 −11 −33 +48 + 6 +44 −64 +11 −61	0	−1.76
94398 T	19 12 46.10	−50 29 10.7	6.12 G	288.192 072 29	−50.486 317 35	7.13	44.73	−42.12	0.66	0.48	0.76	0.83	0.46	+ 8 −31 −25 − 4 +18 + 6 +11 −34 − 4 −19	0	−2.21
94399	19 12 46.27	−24 54 22.5	8.87 H	288.192 798 54	−24.906 254 58	5.34	29.10	5.56	1.37	0.72	1.27	3.03	1.40	−44 −32 +16 −39 +59 +34 + 39 −73 −21 −79	0	−0.74
94400	19 12 46.67	−58 15 58.4	7.80 H	288.194 475 33	−58.266 214 06	5.76	−20.38	−80.06	0.74	0.56	1.08	0.96	0.87	− 4 −22 − 6 +39 − 2 − 4 + 6 +15 + 4 +33	0	−0.40

61858 22554

Figure 1.1.4(a). *Summary interpretation of the left-hand pages of the Hipparcos Catalogue*

1897 **287°.916 - 288°.194**

94301 - 94400

No.	Tycho Magnitudes					Colour Indices			Magnitude (Hp)				Variability (Hp)				Multiplicity Data									Misc
HIP	B_T	σ	V_T	σ		B–V	σ		V–I	σ		Hp	σ	s	N	Max	Min	P		CCDM		Flags	AB	θ	ρ	σ_ρ	ΔHp	σ	Flags
	mag	mag	mag	mag		mag	mag		mag	mag		mag	mag	mag		mag	mag	days						″	″		mag	mag	
31	32	33	34	35	36	37	38	39	40	41	42-3	44	45	46	47 48	49	50	51	52-4	55	56-7	58-61	62	63	64	65	66	67	68-70
94301	9.612	0.015	9.360	0.018		0.240	0.022	T	0.27	0.03	L	9.3896	0.0019	0.021	145	9.35	9.44					1							
94302	6.422	0.004	5.246	0.002		1.008	0.003	T	0.98	0.00	L	5.2950	0.0007	0.005	100	5.29	5.30					1							S
94303	11.176	0.075	10.652	0.083		0.710	0.020	G	0.76	0.02	H	10.8155	0.0029	0.031	84	10.76	10.86		C			1							G
94304	8.029	0.008	7.629	0.008		0.391	0.009	T	0.46	0.01	L	7.6877	0.0011	0.013	128	7.66	7.71					1							S
94305	9.070	0.014	8.530	0.013		0.506	0.017	T	0.58	0.02	L	8.5541	0.0025	0.019	86	8.52	8.59					1							
94306	8.420	0.012	8.159	0.013	A	0.108	0.140	G	0.22	0.03	L +	8.1913	0.0018	0.015	112 +	8.17	8.22		C	19117+1753	I 1	2 C B	AB	84	1.949	0.039	3.51	0.15	
94307	10.216	0.032	9.665	0.031	A	0.522	0.033	T	0.59	0.04	L	9.7764	0.0142	0.022	85 A	9.75	9.81		C	19117−4711	I 1	2 C D	AB	152	13.901	0.063	3.37	0.32	D
94308	8.070	0.007	7.733	0.008	A	−0.016	0.009	G	0.01	0.01	H	7.8045	0.0066	0.029	196 A	7.76	7.86		D	19118+2615	I 1	2 C A	AB	23	15.113	0.013	2.48	0.06	S
94309	9.187	0.014	8.246	0.011		0.817	0.014	T	0.84	0.01	L	8.2891	0.0026	0.023	107	8.25	8.33		U 2	19118−1911	I 1	1							
94310	9.749	0.024	9.027	0.020	+	0.649	0.023	T	0.71	0.02	L +	9.0311	0.0033	0.024	76 +	8.99	9.07		D	19118−5319	I 1	2 C A	AB	182	0.438	0.007	1.33	0.04	
94311	5.851	0.003	5.924	0.003		−0.062	0.004	T	−0.04	0.00	L	5.9180	0.0013	0.012	130	5.90	5.93		U 2			1							S
94312											T	12.5469	0.0137	0.141	104	12.06	12.73		U			1 S							D
94313	8.052	0.008	7.667	0.008		0.411	0.001	G	0.48	0.00	H	7.7107	0.0018	0.015	145	7.69	7.74					1							S
94314	10.824	0.046	9.432	0.024		1.177	0.041	T	1.14	0.04	L	9.4339	0.0038	0.022	74	9.38	9.48					1							G
94315	9.010	0.013	8.814	0.016		0.187	0.019	T	0.21	0.02	L	8.8400	0.0017	0.016	115	8.81	8.88		C			1							
94316	9.425	0.018	8.067	0.011		1.150	0.017	T	1.11	0.01	L	8.0831	0.0014	0.011	68	8.06	8.11		C			1							
94317	11.916	0.165	10.806	0.092	B	0.957	0.147	T	0.94	0.11	L	11.4548	0.1277		B				D	19118+0842	I 2	1 C F D							D
94318	9.350	0.010	9.343	0.013		0.007	0.014	T	0.03	0.01	L	9.3715	0.0018	0.026	237	9.32	9.43					1							
94319	10.517	0.044	9.985	0.046	A	0.499	0.058	T	0.57	0.06	L	10.0790	0.0445	0.041	77 A	9.94	10.13		D	19118+0842	I 2	1 C P D							G D
94320	9.764	0.022	8.501	0.013		1.076	0.020	T	1.04	0.02	L	8.5268	0.0021	0.016	93	8.49	8.56					1							
94321	8.014	0.007	8.049	0.009		−0.027	0.010	T	−0.01	0.01	L	8.0475	0.0013	0.013	135	8.03	8.06		C			1							
94322	11.184	0.061	10.276	0.046		0.791	0.059	T	0.82	0.04	L	10.2922	0.0038	0.027	99	10.25	10.35		C			1							G
94323	8.890	0.015	7.176	0.007		1.431	0.013	T	1.48	0.02	A	7.1618	0.0012	0.008	82	7.15	7.17					1							S
94324	8.021	0.007	8.006	0.008		0.019	0.010	T	0.04	0.01	L	8.0282	0.0015	0.011	121	8.01	8.05		C			1							S
94325	9.607	0.019	8.160	0.011		1.220	0.017	T	1.18	0.02	L	8.1787	0.0024	0.016	87	8.16	8.21					1							S
94326	9.631	0.036	8.886	0.030		0.667	0.036	T	0.73	0.03	L	8.9326	0.0022	0.016	72	8.91	8.96		C			1							
94327	9.328	0.015	9.138	0.018		0.182	0.022	T	0.20	0.03	L	9.1415	0.0023	0.026	134	9.10	9.19		C			1							
94328	7.578	0.007	7.510	0.007		0.068	0.009	T	0.08	0.01	L	7.5329	0.0011	0.011	120	7.51	7.55					1 S							S
94329	11.618	0.094	10.512	0.053		1.050	0.020	G	1.02	0.02	H	10.5970	0.0040	0.029	109	10.53	10.63					1							G
94330	10.129	0.028	9.816	0.032		0.297	0.040	T	0.34	0.05	L	9.9123	0.0022	0.018	76	9.88	9.95		C			1							G
94331	7.064	0.005	6.955	0.006	+	0.102	0.003	G	0.12	0.00	R +	6.9845	0.0015	0.010	76 +	6.97	7.01		D	19121+0237	I 1	2 C A	BA	184	0.248	0.003	0.48	0.05	S
94332	9.791	0.022	9.178	0.020		0.574	0.020	G	0.65	0.02	H	9.2481	0.0016	0.020	115	9.20	9.28					1 S							
94333	7.987	0.007	8.033	0.009		−0.018	0.015	G	0.00	0.01	H	8.0220	0.0010	0.010	118	8.01	8.05		C			1							S
94334	10.707	0.037	10.165	0.035		0.481	0.005	G	0.55	0.01	H	10.3138	0.0026	0.031	105	10.26	10.38					1							G
94335	10.016	0.025	9.395	0.022		0.574	0.025	T	0.65	0.02	L	9.4722	0.0034	0.045	101	9.43	9.67	2.18	P 1 A			1							
94336	7.294	0.007	6.569	0.006	A	0.666	0.006	G	0.73	0.01	R +	5.9819	0.0008	0.009	109 +	5.97	6.00		D	19121+4951	I 1	2 C A	AB	208	7.648	0.003	0.15	0.01	S
94337	9.348	0.016	9.038	0.017		0.337	0.015	G	0.39	0.02	H	9.0852	0.0010	0.015	116	9.06	9.12		D			1							
94338	9.375	0.014	7.994	0.008	A	1.000	0.495	G	1.09	0.05	L +	7.9990	0.0012	0.012	128 +	7.98	8.02		D	19121−2156	I 1	2 C B	AB	330	7.565	0.049	3.71	0.32	
94339	9.899	0.027	8.183	0.012		1.440	0.001	G	1.44	0.00	H	8.1295	0.0013	0.012	90	8.11	8.15		C			1							
94340	10.424	0.031	9.576	0.024		0.760	0.020	G	0.80	0.02	H	9.6322	0.0022	0.021	104	9.60	9.67		C			1							
94341						1.410	0.020	G	1.70	0.05	I	11.3476	0.0041	0.054	193	11.25	11.43					1 X							G
94342	8.764	0.011	8.785	0.014		−0.015	0.016	T	0.01	0.01	L	8.7802	0.0015	0.016	131	8.75	8.82					1							
94343	8.541	0.010	8.232	0.011		0.296	0.003	G	0.34	0.00	H	8.2745	0.0018	0.015	110	8.25	8.30					1							
94344	7.821	0.007	6.682	0.006		1.016	0.000	G	0.99	0.00	H	6.7166	0.0008	0.007	83	6.71	6.73		C			1							S
94345	8.711	0.011	8.089	0.010		0.596	0.015	G	0.67	0.01	H	8.1352	0.0010	0.012	93	8.12	8.17		D			1							S
94346	8.037	0.008	7.118	0.007		0.804	0.009	G	0.84	0.01	H	7.1762	0.0020	0.018	100	7.15	7.21		U 2 C			1							S
94347	7.767	0.006	7.310	0.006		0.444	0.007	T	0.51	0.01	L	7.3587	0.0010	0.013	133	7.34	7.38					1 X							S
94348	11.973	0.139	10.101	0.042		1.490	0.015	G	1.49	0.02	A	10.1047	0.0027	0.021	71	10.07	10.14		C			1							G
94349						1.542	0.051	G	2.58	0.02	A	11.1029	0.0033	0.038	75	11.04	11.16		D	19122+0253	I 1	1 O							G D
94350	7.458	0.006	7.433	0.008	A	0.050	0.015	G	0.03	0.01	L +	7.4321	0.0009	0.011	133 +	7.42	7.45		D	19122+3215	I 1	2 C A	AB	147	1.083	0.016	3.25	0.08	S
94351	7.839	0.007	6.643	0.005		1.024	0.007	T	1.00	0.01	L	6.7040	0.0012	0.008	104	6.69	6.72			19123+4723	I 1	1							S
94352	9.958	0.025	8.663	0.014		1.101	0.022	T	1.06	0.02	L	8.7285	0.0012	0.015	113	8.70	8.76		C			1							
94353	9.016	0.016	8.440	0.015		0.480	0.015	G	0.55	0.02	H	8.5508	0.0024	0.016	79	8.52	8.58		C	19124−5148	I 2	1							
94354	9.160	0.013	7.307	0.006		1.573	0.012	T	2.41	0.03	O	7.1127	0.0042	0.043	124	7.05	7.18		U 2			1 S							S
94355	8.400	0.009	8.252	0.010	+	0.142	0.012	T	0.16	0.01	L +	8.2949	0.0018	0.017	133 +	8.26	8.32		D	19123+2113	I 1	2 C A	AB	113	0.208	0.003	0.27	0.10	S
94356	9.810	0.026	9.968	0.044		−0.130	0.015	G	−0.12	0.02	H	9.9743	0.0035	0.027	100	9.92	10.03		C			1							G
94357	9.943	0.027	9.540	0.029		0.381	0.037	T	0.45	0.04	L	9.6543	0.0030	0.024	78	9.62	9.69					1							G
94358	9.361	0.014	9.211	0.017		0.144	0.021	T	0.16	0.02	L	9.2413	0.0022	0.015	109	9.21	9.27					1							
94359	10.720	0.045	9.432	0.024		1.096	0.040	T	1.06	0.04	L	9.4890	0.0018	0.021	102	9.46	9.53		C			1							
94360	10.143	0.033	8.695	0.018		1.160	0.218	G	1.52	0.11	S	8.6798	0.0019	0.017	80	8.64	8.71		R	19124−0428	I 2	1							
94361	9.438	0.017	7.495	0.007		1.647	0.015	T	2.44	0.04	O	7.2945	0.0044	0.042	115	7.24	7.37		U 2			1 S							S
94362	9.663	0.014	9.225	0.014		0.413	0.018	T	0.48	0.02	A	9.2841	0.0021	0.026	157	9.23	9.32					1							
94363	7.603	0.007	7.591	0.011	+	0.010	0.015	G	0.03	0.01	H +	7.6636	0.0014	0.013	140 +	7.64	7.70		D	19124+3021	I 1	2 C A	AB	317	9.953	0.005	1.18	0.02	S
94364											T	11.9080	0.0159	0.144	76	11.37	12.09		D	19124−0428	I 2	1 S							
94365	9.023	0.018	7.231	0.009		1.480	0.015	G	1.44	0.03	L	7.1933	0.0026	0.014	78	7.17	7.22			19124−5148	I 2	1							S
94366	6.912	0.005	6.947	0.006		−0.027	0.007	T	−0.01	0.01	L	6.9487	0.0007	0.008	127	6.94	6.97		C			1							S
94367	8.729	0.011	8.080	0.010	+	0.588	0.015	G	0.66	0.01	H +	8.1128	0.0015	0.014	116 +	8.09	8.13		D	19124−3304	I 1	2 C B	AB	23	0.387	0.002	0.10	0.02	S
94368						1.450	0.020	G	1.95	0.02	A	11.3845	0.0056	0.044	107	11.29	11.45		C			1							G
94369	9.121	0.012	9.027	0.014		0.092	0.017	T	0.10	0.02	L	9.0312	0.0020	0.022	145	9.00	9.08					1							
94370	8.714	0.011	8.128	0.010		0.561	0.015	G	0.63	0.01	H	8.1716	0.0012	0.011	91	8.16	8.20		C			1							
94371	8.866	0.014	8.023	0.011		0.760	0.000	G	0.80	0.00	H	8.0810	0.0020	0.013	84	8.06	8.10			19126+1651	I 2	1 G							D
94372	7.844	0.006	6.519	0.004		1.129	0.001	G	1.09	0.00	H	6.5564	0.0007	0.007	124	6.55	6.57		C			1							S
94373	7.926	0.008	7.500	0.006		0.402	0.009	T	0.47	0.01	L	7.5454	0.0011	0.010	146	7.53	7.56		C			1							S
94374	10.953	0.054	9.046	0.019		1.583	0.045	T	1.60	0.05	L	8.8884	0.0035	0.025	97	8.85	8.94		U 2			1 S							
94375	8.379	0.006	8.092	0.006		0.273	0.008	T	0.31	0.01	L	8.1399	0.0013	0.016	241	8.11	8.17					1							
94376	4.362	0.002	3.188	0.002		0.990	0.018	G	0.94	0.03	C	3.2296	0.0005	0.004	110	3.22	3.24			19126+6740	I 1	1							S
94377	6.707	0.006	6.729	0.007	+	−0.010	0.000	G	0.01	0.00	H +	6.7103	0.0024	0.017	89 +	6.69	6.75		U 2	19126+1651	I 2	2 C A	AB	137	0.664	0.002	0.83	0.01	S P
94378	7.246	0.006	7.149	0.007		0.087	0.008	T	0.10	0.01	L	7.1818	0.0009	0.007	89	7.17	7.19					1							S
94379	9.745	0.019	9.237	0.013		0.493	0.014	T	0.57	0.02	H	9.3006	0.0026	0.020	115	9.26	9.34					1							
94380	9.888	0.027	9.567	0.030		0.305	0.038	T	0.35	0.05	L	9.6386	0.0036	0.027	72	9.58	9.69					1							G
94381	9.677	0.023	9.185	0.022		0.420	0.013	G	0.49	0.01	H	9.2760	0.0030	0.015	72	9.25	9.31		C			1							
94382	6.102	0.003	6.025	0.003		0.069	0.004	T	0.08	0.00	L	6.0510	0.0006	0.006	138	6.04	6.06		C			1							S
94383	8.231	0.012	7.537	0.010		0.640	0.013	T	0.70	0.01	L	7.5784	0.0014	0.012	74	7.56	7.60		C			1							S
94384	9.476	0.018	8.149	0.019		0.391	0.007	G	0.46	0.01	H	9.2115	0.0041	0.041	93	9.16	9.28		U 2			1							
94385	5.475	0.002	5.371	0.002		0.094	0.003	T	0.11	0.00	L	5.3864	0.0009	0.011	101	5.36	5.40		U 2			1							S
94386	9.799	0.026	8.523	0.016		1.086	0.024	T	1.05	0.02	L	8.5866	0.0018	0.017	77	8.56	8.62		C			1							
94387	8.784	0.009	8.217	0.008	+	0.530	0.011	T	0.60	0.01	L +	8.2268	0.0014	0.018	185 +	8.20	8.27		D	19127+2435	I 1	2 C A	AF	100	0.203	0.009	1.07	0.26	
94388	8.195	0.009	8.296	0.012		−0.070	0.010	G	−0.05	0.01	H	8.2753	0.0012	0.013	127	8.26	8.30					1							
94389	9.276	0.014	8.648	0.013		0.579	0.014	T	0.65	0.01	L	8.6930	0.0022	0.019	105	8.66	8.73					1							
94390	9.026	0.011	7.739	0.007		1.095	0.010	T	1.06	0.01	L	7.7785	0.0009	0.010	140	7.76	7.81					1							
94391	8.232	0.012	7.801	0.013							T	7.8394	0.0013	0.015	107	7.81	7.87		D	19127−3351	I 2	1 S							S
94392	11.141	0.066	10.553	0.060		0.516	0.020	G	0.59	0.02	H	10.6713	0.0054	0.037	73	10.62	10.72					1							G
94393	7.249	0.011	7.353	0.015		0.362	0.071	G	0.42	0.08	R	7.3481	0.0013	0.012	106	7.33	7.36		D	19127−3351	I 2	1 S							S
94394	8.780	0.010	8.221	0.010		0.528	0.010	T	0.60	0.01	L	8.2596	0.0014	0.014	114	8.24	8.29		C			1							
94395	7.944	0.007	7.788	0.010		0.150	0.011	T	0.17	0.01	L	7.8187	0.0014	0.011	79	7.80	7.84		C			1							S
94396	11.242	0.048	10.243	0.033		0.873	0.043	T	0.88	0.03	L	10.3145	0.0032	0.038	173	10.23	10.38		C			1							G
94397	7.631	0.006	7.578	0.008		0.048	0.009	T	0.06	0.01	L	7.5913	0.0010	0.009	115	7.58	7.61		C			1							S
94398	7.349	0.006	6.224	0.003		0.954	0.006	G	0.94	0.00	H	6.2771	0.0009	0.008	94	6.27	6.29		C	19128−5029	I 1	1							S
94399	9.259	0.016	8.907	0.017		0.342	0.021	T	0.40	0.03	L	8.9556	0.0017	0.013	100	8.93	8.98		C			1							
94400	8.965	0.011	7.911	0.008		0.915	0.010	T	0.91	0.01	L	7.9591	0.0012	0.012	130	7.94	7.98		C			1							S
																											04540	41532	

HIP identifier, as Field 1. Field T31 gives the cross-identification between HIP and TYC for Tycho Catalogue entries.

Photometry from Tycho Catalogue: mean magnitudes, corrected for 'censored' data. Entries without Tycho photometry are blank.

Johnson B-V colour index, from Tycho photometry (transformed using spectral type) or from ground if Tycho photometry was unavailable or imprecise. Values do not necessarily correspond to B-V given for the same entry in the Tycho Catalogue.

Cousins' V-I colour index and related information, from various sources.

Median Hipparcos magnitude in the broad-band Hp system, derived from the Hipparcos Epoch Photometry Annex, described in Section 2.5.

Magnitudes at maximum and minimum luminosity (in Hp) derived from the 5th and 95th percentiles of the epoch photometry. Period (truncated precision) and type of variability are given for identified variables.

1–2 in Field H53 points to tabular data for periodic and unsolved variables (see Section 2.4 and Volume 11) giving further details of the variability, variable star name, period and epoch, references to literature, etc. A–C in Field H54 points to the light curves (Volume 12).

CCDM number assigned to double or multiple systems (either previously, or from Hipparcos). Also given are the origin of the CCDM identifier, and the number of catalogue entries with the same CCDM number.

Classification of the double or multiple star solution, and pointers to relevant sections of the Double and Multiple Systems Annex.

Summary of the astrometric and photometric parameters of a double system, when the Hipparcos observations resolve the system into precisely two components.

Flags indicating 'survey' star, identification chart, or note on the entry: the note flag may point to notes at the end of Volumes 5–9, or for double and multiple systems (Volume 10) or for variables (Volume 11).

Checksum. See Section 2.11.3.

Figure 1.1.4(b). *Summary interpretation of the right-hand pages of the Hipparcos Catalogue*

Section 1.2

Astrometric Data

1.2. Astrometric Data

This section provides a framework for the interpretation of the astrometric data given in the Hipparcos and Tycho Catalogues. It explains the coordinate system, time scales and units used in the Catalogues, and in particular their relations to the standard astronomical reference systems. The precise definition of the astrometric parameters requires the introduction of several auxiliary concepts which are covered in the last two subsections.

Additional information relevant for the practical use of the astrometric data is found in Section 1.5. This includes the transformations to ecliptic and galactic coordinates and to arbitrary epochs; the calculation of space coordinates and velocities; and the propagation of errors in these transformations.

1.2.1. The Astrometric Parameters Determined by Hipparcos

The basic astrometric data in the Hipparcos and Tycho Catalogues include directions (positions), specified by celestial coordinates, their rate of change (proper motions), and trigonometric parallaxes. This is the first observational catalogue to contain parallaxes in addition to positions and proper motions for all stars in the observing programme.

The positions and proper motions are given within the International Celestial Reference System (ICRS), which is consistent with the conventional equatorial system for the mean equinox and equator of J2000, previously realised by the FK5 Catalogue (see Section 1.2.2). The timing of events is consistently based on the terrestrial time-scale, TT (see Section 1.2.3).

The standard astrometric model for a single star (Section 1.2.8) assumes uniform rectilinear space motion relative to the solar system barycentre. At some reference epoch, T_0, the motion is then described by the following six parameters:

- barycentric coordinate direction; this is specified as right ascension, α, and declination, δ;
- annual parallax, π, from which the coordinate distance is $(\sin\pi)^{-1}$ astronomical units;
- rate of change of the barycentric coordinate direction expressed as proper motion components $\mu_{\alpha*} = \mu_\alpha \cos\delta$ and μ_δ, in angular measure per unit time;
- radial (i.e. line of sight) velocity, V_R, in linear measure per unit time.

The radial velocity is normally obtained from spectroscopic observations. The remaining parameters, referred to as the ‘five astrometric parameters’, are determined from analysis of the Hipparcos observations and are given for almost all stars in the catalogue.

The six parameters listed above refer, in principle, to the reference epoch T_0. The propagation of the parameters and their covariances to arbitrary epochs is treated in Section 1.5. Normally only the changes in α and δ, due to the proper motion, are appreciable. In rigorous treatment the time-dependence of all six parameters must however be explicitly considered (see Section 1.5.5). In such cases their values at the catalogue epoch T_0 are denoted α_0, δ_0, π_0, $\mu_{\alpha*0}$, $\mu_{\delta 0}$ and $V_{\mathrm{R}0}$.

The system of units used for these data is as follows (see Sections 1.2.3 and 1.2.5):

- for α and δ when expressed as full angles: degrees (deg);
- for differential coordinates such as $\Delta\alpha* = \Delta\alpha \cos\delta$ and $\Delta\delta$: milliarcsec (mas);
- for π: milliarcsec (mas);
- for $\mu_{\alpha*}$ and μ_δ: milliarcsec per Julian year (mas yr^{-1});
- for V_{R}: km s^{-1}.

Stellar distances are measured in parsec. To sufficient approximation, the distance in parsec is given by $1000/\pi$, where π is expressed in mas.

The common reference epoch used throughout the catalogue is $T_0 = \mathrm{J1991.25(TT)}$ (see Section 1.2.6).

The standard astrometric model, using the five astrometric parameters, was found to be adequate for the majority of the stars, including the components of most resolved double and multiple stars. For several thousand apparently single stars, however, the standard model did not give an acceptable fit to the observations. These are probably binary stars, in which the centre of light describes a curved path on the sky due to the orbital motions of the components around their common centre of mass. For such 'astrometric binaries' additional parameters had to be introduced to describe the motion in accordance with the observations. In most cases a good empirical fit was obtained by including one or two additional terms in the Taylor expansion of the variation of the barycentric coordinate direction with time. In a few hundred cases even this was not sufficient, and Keplerian elements (sometimes partially based on existing ground-based data) were introduced to describe the orbital motion of the photocentre. These extended solutions are also given in the Double and Multiple Systems Annex.

When comparing the Hipparcos and Tycho Catalogues with previous astrometric catalogues, the following points are noted:

- positions and proper motions are given for the catalogue epoch, T_0 = J1991.25(TT), which is close to the central epoch of observations (the distinction between the epoch which specifies the equinox and equator of a coordinate system, typically B1950 or J2000, and the epoch at which the star passed through the given position, should be noted);

- the International Celestial Reference System (ICRS), as represented by the Hipparcos and Tycho Catalogues, replaces the FK5 system as the practical definition of celestial coordinates in the optical region. The construction of the ICRS (see Section 1.2.2) ensures that no discontinuity larger than the uncertainty of the FK5 system occurs in the transition from FK5 (mean equinox and equator J2000) to ICRS. Thus, from the viewpoint of optical astrometry, the Hipparcos and Tycho Catalogues can be regarded as an extension and improvement of the J2000(FK5) system, retaining approximately the global orientation of that system but without its regional errors. However, it should be noted that the Hipparcos and Tycho Catalogues have *not* been tied to the FK5 system, but to the ICRS through the extragalactic radio frame (see Volume 3, Chapter 18). The relation between the ICRS(Hipparcos) reference frame and the J2000(FK5) system is further discussed in Section 1.5.7;

- providing positions within the ICRS means that they are consistent with present knowledge of the (extragalactic) radio reference system. Providing proper motions within the ICRS means that they are consistent with the best present realisations of a quasi-inertial reference system (i.e. non-rotating with respect to distant galaxies);

- since parallax is explicitly derived in the data reduction, the directions represented by the right ascension and declination at epoch T_0 are strictly barycentric. In previous astrometric catalogues, the unknown displacement due to parallax for each observation perturbed the final catalogue positions;

- at the accuracy achieved by Hipparcos, general relativity effects cannot be ignored. In the relativistic framework, the observed directions are *proper directions* referred to the Lorentzian frame moving with the observer. In order to relate the observed directions at different epochs and of different objects to a simple geometrical model of the stars and their motions, the 'local' effects of the moving observer (stellar aberration) and space curvature (gravitational light deflection by the Sun) are removed by transforming the proper directions to *coordinate directions* corresponding to the coordinate differences between the object and observer, expressed in the (solar system) barycentric coordinate system;

- stellar aberration has been computed from the barycentric motion of the satellite, using the full relativistic formula and combining the geocentric satellite velocities accurate to about 0.2 m s^{-1}, determined by the ground stations, with the appropriate ephemeris (see Section 1.2.4) for the barycentric motion of the Earth. Gravitational light deflection has been computed in the heliocentric metric, assuming spherical symmetry. The treatment of aberration is consistent with the IAU (1984) recommendation that the total barycentric velocity of the Earth should be used; prior to that date the elliptic component of velocity, which changes very slowly with time, was conventionally ignored;

- the proper motions are instantaneous rates of change of the barycentric coordinates at the epoch T_0. For stars with large parallax, large proper motion, and large radial velocity, the apparent acceleration of coordinates due to perspective effects may be significant. These can be calculated on the assumption of uniform space motion relative to the barycentre, and have been accounted for, in the case of the few most significantly affected stars, in reducing the individual observations to T_0, as described in Section 1.2.8;

- still assuming uniform barycentric motion, star positions and proper motions, within the fixed quasi-inertial reference frame of ICRS, can be calculated for arbitrary epochs, using the catalogue data and, where appropriate, taking into account the perspective accelerations. Procedures for this, and the corresponding propagation of uncertainties, are discussed in Section 1.5;

- while ground-based proper motions are typically obtained by comparing positional catalogues having an epoch difference of 20 to 50 years, the Hipparcos proper motions are determined using a temporal baseline of only a few years. The ground-based values thus give the mean motion over several decades, while the Hipparcos proper motions are, by comparison, quasi-instantaneous. This is of no consequence as long as the motions are uniform, which is a valid assumption at least for the single stars. However, many apparently single stars are in reality double, and the actual motions of the individual components or of the photocentre of the double star may be significantly non-uniform. For such objects there may be a discrepancy between the space and ground-based proper motions which is not attributable to random errors or differences of the reference frames. More extreme cases of non-uniform motion become noticeable already during the few years of the Hipparcos mission and require the extended solutions given in the Double and Multiple Systems Annex.

1.2.2. The Hipparcos Reference Frame

The positions given in the Hipparcos and Tycho Catalogues effectively define a grid of celestial coordinates (α, δ) for the epoch J1991.25. By means of the proper motions also given in the catalogues, this grid can be extended forward and backward in time to arbitrary epochs (albeit with an uncertainty that increases with the epoch difference). The positions and proper motions thus define a specific coordinate system on the sky, accessible in optical wavelengths at any epoch: the Hipparcos Reference Frame.

The Hipparcos and Tycho Catalogues have been constructed in such a way that the Hipparcos Reference Frame coincides, to within limits set by observational uncertainties, with the International Celestial Reference System (ICRS). The ICRS is practically defined by the adopted positions of several hundred extragalactic radio sources.

Construction of the ICRS: In 1995, the IAU Working Group on Reference Frames identified the celestial reference system of the International Earth Rotation Service (IERS) as the next official IAU celestial reference system under the name of 'International Celestial Reference System' (ICRS). The definition of the ICRS complies with the 1991 IAU recommendations on reference frames. The axes of the system are realised with an accuracy of ±30 μas. Their directions are consistent with those of the FK5 system (mean equinox and equator J2000) within the uncertainty of the latter (±50–80 mas; E.F. Arias, P. Charlot, M. Feissel & J.-F. Lestrade, 1995, *Astronomy & Astrophysics*, 303, 604), and their tie to the best current realisation of the FK5 dynamical reference system is within ±3 mas (W.M. Folkner, P. Charlot, M.H. Finger, J.G. Williams, O.J. Sovers, X X Newhall & E.M. Standish, Jr., 1994, *Astronomy & Astrophysics*, 287, 279).

In October 1995, the IAU Working Group on Reference Frames released the ICRS coordinates of some 250 extragalactic objects (out of some 600 that are monitored), constituting the International Celestial Reference Frame (ICRF). The accuracy of the coordinates of more than half of the sources is better than ±0.47 mas. In the future, the IERS will continue to monitor the sources, issuing appropriate updates, while keeping the reference coordinates unchanged.

In order to align the Hipparcos Reference Frame with the ICRS it is necessary to find objects whose positions and/or proper motions can be referred to both systems. Unfortunately, none of the extragalactic objects defining the ICRS is bright enough at optical wavelengths for direct observation by Hipparcos. Therefore, the linking of the two systems was made *a posteriori* through auxiliary ground-based observations, as described in detail in Volume 3, Chapter 18. The estimated uncertainty of the link corresponds to a standard error of 0.6 mas in the alignment of the axes at the catalogue epoch J1991.25, and 0.25 mas yr^{-1} in the rate of rotation of one system with respect to the other. Since the ICRS is defined by means of extragalactic sources, the Hipparcos and Tycho proper motions are quasi-inertial to within ±0.25 mas yr^{-1}.

Thus, within the uncertainties quoted above, the Hipparcos and Tycho Catalogues represent the extension to optical wavelengths of the extragalactic reference system as realised by the International Celestial Reference Frame (ICRF). In the catalogues, the positions and proper motions are thus specified as referring to the ICRS.

Traditionally, astrometric catalogues have been referred to the mean equinox and equator of some standard epoch such as B1950 or J2000. This practice was in principle based on the *dynamical* definition of a reference system in terms of two fundamental planes, the mean equatorial plane (given by the Earth's rotation after elimination of nutation terms) and the ecliptic plane. The intersection of the two planes defines the mean equinox as the origin of right ascension. The two planes are not inertially fixed, but move slowly due to luni-solar and planetary precession. In order to define a fixed (inertial) reference system it was necessary to specify a certain date E at which to 'freeze' the fundamental planes, and hence set the reference axes

for the celestial coordinates. The latter are then said to refer to the mean equinox and equator of E (say, J2000). Transformation of coordinates between reference systems of different equinoxes E_1, E_2 is equivalent to correcting the positions for the accumulated precession between the two dates E_1 and E_2. This process is dependent on a dynamical theory of precession and the observationally determined constants of the theory.

With the adoption of the ICRS and a purely conventional definition of celestial coordinates (through a list of adopted source positions), the mean equatorial plane and the ecliptic have lost their fundamental significance for the celestial reference system. Consequently it is not meaningful to speak of the 'equator' or 'equinox' of the ICRS, except possibly as (inappropriate) designations of the origins of α and δ in that system. In particular, no specific date is associated with the origin of α in ICRS, although it is close to the mean dynamical equinox of J2000.

The positions and proper motions in the Hipparcos Catalogue define a reference frame which is likely to be accurate, on a global scale, to about 0.1 mas (at J1991.25) and 0.1 mas yr^{-1}. Due to the large number of stars, the potential level of definition might even be a factor 10 better than these numbers, although current techniques do not allow any assessment on that accuracy level. Intrinsically, therefore, the Hipparcos Reference Frame is considerably better defined than its link to the extragalactic ICRS. Once fixed through the Hipparcos Catalogue, the Hipparcos Reference Frame will have its own independent existence as one particular realisation of the ICRS; for many years, it is likely to remain the best realisation of the ICRS in the optical domain.

1.2.3. Time Scales

The time scale used in the Hipparcos and Tycho Catalogues (for both the astrometric and the photometric data) is Terrestrial Time (TT). The practical realisation of this scale is through International Atomic Time (TAI). The basic unit of TAI and TT is the SI second, and the offset between them is conventionally 32.184 s (with deviations, attributable to the physical defects of atomic time standards, probably between the limits ± 10 μs), so that the realisation of TT in terms of TAI is taken to be:

$$\mathrm{TT(TAI)} = \mathrm{TAI} + 32.184\ \mathrm{s} \qquad [1.2.1]$$

For details of the choice and definition of time scales, see the *Explanatory Supplement to the Astronomical Almanac*, 1992, University Science Books, P.K. Seidelmann (ed.).

Relativistic effects and relativistic timescales: The rate of an atomic clock depends on the gravitational potential and its motion with respect to other clocks; thus the timescale entering the equations of motion (and its relationship with TAI) depends on the coordinate system to which the equations refer. Since 1984 *The Astronomical Almanac* referred to two such timescales: Terrestrial Dynamical Time (TDT) used for geocentric ephemerides, and Barycentric Dynamical Time (TDB) used for ephemerides referred to the solar system barycentre. TDT differs from TAI by a constant offset, which was chosen to give continuity with ephemeris time. TDB and TDT differ by small periodic terms (arising from the transverse Doppler effect and gravitational red-shift experienced by the observer) that depend on the form of the relativistic theory being used: the difference includes an annual sinusoidal term of approximately 1.66 ms amplitude, planetary terms contributing up to about 20 μs, and lunar and diurnal terms contributing up to about 2 μs.

In 1991 the IAU adopted resolutions introducing new timescales which all have units of measurement consistent with the unit of time, the SI second. Terrestrial Time (TT) is the time reference for apparent geocentric ephemerides, and can be considered as equivalent to TDT. Barycentric Coordinate Time (TCB) is the coordinate time for a coordinate system with origin at the solar system barycentre. Because of relativistic transformations TDB, and therefore TT, differ in rate from TCB by approximately 49 seconds per century.

The relationships between TT, TAI and UTC: For civil and legal purposes it is necessary to have a time scale which approximates the diurnal rotation of the Earth relative to the Sun. Historically this has been known as Universal Time, but because the Earth's angular spin rate is variable, the Universal Time scale is non-uniform with respect to TAI. The civil time scale, which has been available through broadcast time signals since 1972, is known as Co-ordinated Universal Time (UTC), and differs from TAI by an integer number of seconds—it is adjusted, when judged necessary by the International Earth Rotation Service (IERS), by adding a 'leap' second at midnight on December 31, or on June 30. The transformations between the various time scales during the Hipparcos mission are given in Table 1.2.1.

Table 1.2.1. Relationship between time scales during the mission

Start interval (UTC)	End interval (UTC)	TAI–UTC (s)	TT–UTC (s)
Launch (1989 Aug 8)	1990 Jan 1 0^h	24	56.184
1990 Jan 1 0^h	1991 Jan 1 0^h	25	57.184
1991 Jan 1 0^h	1992 Jul 1 0^h	26	58.184
1992 Jul 1 0^h	end of observations	27	59.184

Tables giving the correspondences between TT (preceded by ephemeris time), TAI (since 1955), and UTC, can be found in the yearly reports of IERS as well as in the major astronomical almanacs.

1.2.4. Fundamental Constants

For the Hipparcos reductions the former IAU (1976) system of astronomical constants has been adopted, with the exception of certain planetary masses entering the Earth ephemeris. This affects primarily the position and velocity of the solar system barycentre relative to the Sun, which enter, respectively, in the computation of barycentric directions and stellar aberration.

The ephemeris for the Earth used formulae provided by the Bureau des Longitudes based on VSOP 82 (P. Bretagnon, 1982, *Astron. Astrophys.*, 114, 278) and ELP 2000 (M. Chapront-Touzé & J. Chapront, 1983, *Astron. Astrophys.*, 124, 50). Although there are small differences in certain of the constants used by the Bureau des Longitudes ephemeris and the JPL ephemeris DE200 (for example in the mass of Pluto and in the obliquity of the ecliptic) VSOP 82 was fitted to DE200 rather than directly to observations, so that the basis for the Earth ephemeris is essentially DE200. Differences between the respective ephemerides are of the order of a few mm/s in velocity, and correspondingly small in position, differences which are entirely negligible (< 0.01 mas) in the calculation of stellar aberration and parallax.

The numerical values or sources of data used in the data reductions are given in Table 1.2.2. The unit of time is the SI second, or the Julian Year when this is more convenient. The speed of light enters mainly in the computation of stellar aberration. The astronomical unit is the basis for the definition of parallax. The heliocentric and geocentric gravitational constants are used to compute the gravitational light bending by the Sun and the Earth. The obliquity of the ecliptic has no direct significance for the data reductions, but is used as a conventional value to transform between the equatorial and ecliptic systems. The Earth ephemeris is relevant for the calculation of aberration and parallax.

Table 1.2.2. Physical and astronomical constants used for the data reductions

Symbol	Meaning/Application	Value
	Unit of time	SI second as realised on the geoid
	Time scale	Terrestrial Time (TT)
Julian Year	Proper motion unit (mas yr^{-1})	$365.25 \times 86\,400$ s (exactly)
c	Speed of light	299 792 458 m s^{-1} (exactly)
A	Astronomical unit	(499.004 782 s)×c (exactly)
		$= 1.495\,978\,701 \times 10^{11}$ m (A_m)
		= 1000 mas pc (A_p)
		= 4.740 470 446 km yr s^{-1} (A_v)
		$= 9.777\,922\,181 \times 10^{8}$ mas km yr s^{-1} (A_z)
GS	Heliocentric gravitational constant	$1.327\,124\,38 \times 10^{20}$ m^{3}s^{-2}
GE	Geocentric gravitational constant	$3.986\,005 \times 10^{14}$ m^{3}s^{-2}
ϵ	Obliquity of ecliptic (J2000.0)	23° 26′ 21.448″ (exactly)
		$= 23\overset{\circ}{.}439\,291\,111\,1\ldots$
	Earth ephemeris	VSOP 82/ELP 2000

Note: The astronomical unit A appears in all formulae relating linear measures to the parallax. Depending on the context and the units used, it is represented by a variety of numerical values, as indicated in the table. The appropriate numerical value in a given formula can always be ascertained from the units, but for clarity the specific designations A_m, A_p, A_v or A_z may also be used.

1.2.5. Conventions for Angular Coordinates

As explained in Section 1.2.2, astrometric data in the Hipparcos and Tycho Catalogues are referred to the International Celestial Reference System (ICRS), and are given for the mean catalogue epoch T_0 = J1991.25(TT). With the choice of the ICRS, the angular coordinates to be used are the equatorial ones: right ascension (α) and declination (δ). Note, however, that the observations and, as a consequence, the error properties of the resulting catalogue have a strong dependence on, and a strong symmetry when expressed in, ecliptic latitude.

The proper motion is the rate of change of the position. As such it may be defined as the time derivative of the positional coordinates, $\mu_\alpha \equiv \mathrm{d}\alpha/\mathrm{d}t$ and $\mu_\delta \equiv \mathrm{d}\delta/\mathrm{d}t$. However, for the proper motion component in right ascension, the quantity tabulated in the catalogues is $\mu_{\alpha*} \equiv (\mathrm{d}\alpha/\mathrm{d}t)\cos\delta$. The factor $\cos\delta$ (signified by the asterisk in $\mu_{\alpha*}$) converts the proper motion in α to great-circle measure, making it directly comparable to μ_δ and to the proper motion components of other stars. For instance, the total proper motion (length of the proper motion vector) is given by $\mu = (\mu_{\alpha*}^2 + \mu_\delta^2)^{1/2}$, and the position angle θ of the proper motion vector is defined through $\mu_{\alpha*} = \mu\sin\theta$, $\mu_\delta = \mu\cos\theta$.

The standard errors in position are similarly expressed in great-circle measure: $\sigma_{\alpha*} \equiv$ (standard error in α) $\times \cos\delta = \sigma_\alpha \cos\delta$, $\sigma_\delta \equiv$ (standard error in δ). As a result, the quoted error is the true positional uncertainty on the sky; the resulting figures show no systematic increase with increasing declination. Thus, for a star with $\delta = 80°$, a typical error in right ascension is $\sigma_{\alpha*} = 1$ milliarcsec, while $\sigma_\alpha = 6$ milliarcsec.

The standard errors in proper motion refer to the uncertainties in the great-circle measures $\mu_{\alpha*}$ and μ_δ; they are designated $\sigma_{\mu_{\alpha*}}$ and σ_{μ_δ}.

For a more rigorous definition of the standard errors, and especially for their propagation to other epochs, it is convenient to introduce local rectangular coordinates (ξ, η) in the vicinity of the star; see Section 1.2.9.

In stellar catalogues, right ascension and declination have conventionally been given in sexagesimal units, with the right ascension angle expressed as time (i.e. h m s for α and $\pm$° ′ ″ for δ). This is widely recognised as inconvenient for computation, and the publication of the Hipparcos and Tycho Catalogues offered an ideal opportunity to establish an alternative practice. The options for the choice of angular unit included the radian, degree, and arcsec. The choice must also consider the related units for the proper motions, the parallax, and the standard errors. It has been decided to use degrees, and decimal parts of the degree, for all celestial coordinates, and milliarcsec (1 mas = 0.001 arcsec) for the standard errors, parallax and annual proper motions.

It would clearly have been computationally convenient to express all astrometric parameters in the same units, particularly for applications involving updating of positions and for the computation of covariances. Since the use of the arcsec for parallax and annual proper motion components is convenient and well-established, and since the standard errors of the astrometric parameters are generally small numbers of milliarcsec, the milliarcsec has been adopted as the unit for all astrometric errors, as well as for parallaxes and annual proper motions. The contrasting use of (decimal) degrees for positions was considered as an acceptable compromise. While the consistent use of radians, nanoradians, or milliarcsec might have been considered as scientifically more desirable, such deviation from accepted astronomical practice was not considered to be justifiable.

Approximate right ascension and declination are nevertheless given for each object, for identification purposes, in the conventional sexagesimal units (h m s, $\pm$° ′ ″). By including these sexagesimal positions with truncated precision, possible confusion as to which quantities constitute the definitive Hipparcos and Tycho Catalogue positions should be avoided.

The astrometric parameters, as well as the other observational quantities in the catalogues, are given with a sufficient number of decimals to ensure that the rounding errors introduced by the finite number of decimals are much smaller than the observational uncertainties, even for the most accurate data. As a result, less accurate data may be given with several non-significant decimals. The right ascension, for example, is always given to eight decimal places (corresponding to a maximum rounding error of $0.018 \cos\delta$ mas), although fewer decimals would in principle suffice near the poles or for the less precise positions. For many purposes, especially statistical and graphical uses of the data, the rather high numerical resolution is a distinct advantage.

1.2.6. Conventions for Epochs

Time enters in the Hipparcos and Tycho Catalogues at several levels: for the standard epoch of the coordinate system, for the epochs of the individual astrometric observations; for the epoch of the published reference positions; for the unit of time for the proper motions; for the epochs, and sometimes the time dependence, in the description of double and multiple stars; and for the timing of the Hipparcos and Tycho photometric observations. For all except the photometric observations, the practical unit is the Julian year (of exactly 365.25 days or 31 557 600 s). For the propagation of stellar astrometric positions to different epochs the subtleties of the precise time-scales employed may, generally, be ignored.

This is not the case for the timing of individual photometric observations which are provided in the Hipparcos and Tycho Epoch Photometry Annexes. An internal precision of 0.01 s is achieved, although preserving such precision is not warranted in view of the

uncertainty of the photometric measurements. The observation time is given in the catalogues to 10^{-5} day, or to about one second. At this level, the precise time scale has to be specified. Adopting the TT scale for the photometric, as well as astrometric, results means that the epoch photometry is also presented on a continuous time scale (i.e. without the timing discontinuities present in UTC). Users of the epoch photometry must note the potentially significant difference between the TT and UTC time scales.

Epochs relevant to astrometry in the Hipparcos and Tycho Catalogues are expressed in years and decimal fractions of a year. Observations of solar system objects are given in terms of Julian Date (JD). The epochs in the Hipparcos and Tycho Epoch Photometry Annexes (the compilations of epoch photometry) have been corrected to the solar system barycentre by the application of light-time corresponding to the projected coordinate distance from the satellite to the barycentre, and are expressed in terms of Barycentric Julian Date, BJD(TT). This accords with the procedure widely adopted by photometrists to avoid yearly phasing of light curves. (It should be noted that this is not the same as expressing the observation epochs in barycentric coordinate time, TCB.) An offset of 2 440 000.0 days has been introduced in order to conserve space, again following a widely used convention. All Julian Dates in the Hipparcos context are in the time-scale TT, and denoted JD(TT). Some confusion in the use of Julian Dates from the literature may arise because they may be given (in the literature) either in TT or UTC, without explicit specification. It should be carefully noted that Modified Julian Date (i.e. JD−2 400 000.5) is not used in the context of the Hipparcos or Tycho Catalogues.

The standard epoch of the fundamental astronomical coordinate system J2000 corresponds to JD 2 451 545.0 terrestrial time (TT), and to the calendar date 2000 January 1, $12^{\rm h}$ = 2000 January 1.5(TT).

Epoch definitions are based on the Julian year of 365.25 days. Thus the Julian epoch Jyyyy.yy corresponds to:

$$\mathrm{JD} = 2\,451\,545.0 + (\mathrm{yyyy.yy} - 2000.0) \times 365.25 \qquad [1.2.2]$$

In particular, the adopted catalogue epoch for the Hipparcos and Tycho Catalogues is:

$$T_0 = \mathrm{J1991.25(TT)} = \mathrm{JD\ 2\,448\,349.0625(TT)} \qquad [1.2.3]$$

which is a good approximation to the mean central epoch of the observations.

Note that the adopted catalogue epoch contrasts with the standard epoch J2000 used, for example, for the Hipparcos Input Catalogue compilation. This is simply a consequence of the fact that the Hipparcos and Tycho Catalogues are observational catalogues spanning the measurement interval 1989–93.

In principle, the mean observational epochs for the individual stars could have been explicitly included in the catalogue, and the associated standard errors referred to that epoch. This would have minimised the numerical values of the tabulated positional standard errors, as well as the correlations between the position and proper motion components. However, because the astrometric parameters are derived from one-dimensional measurements (scans) across an object, with an irregular distribution both in time and position angle, the mean observational epoch is in general different in the two coordinates. This non-uniqueness of the definition of the mean observational epoch and the additional complexity in handling the individual epochs have prevented the adoption of this approach. Instead, a single common catalogue epoch has been used. The complete information on the mean observational epochs is still preserved, as explained in Section 1.2.7, in the standard errors and correlations, both of which are referred to the catalogue epoch J1991.25(TT).

1.2.7. Variance-Covariance Data and Correlations

Although the catalogue gives the first positional coordinate as right ascension, the quantity actually determined is $\Delta\alpha\cos\delta$, where $\Delta\alpha$ is a correction to an initial value, α_0. Similarly, $\Delta\delta$ is a correction to an initial value of declination, δ_0. The five variables, estimated by a weighted least-squares method, are therefore:

$$\begin{aligned} a_1 &= \Delta\alpha* \equiv \Delta\alpha\cos\delta \\ a_2 &= \Delta\delta \\ a_3 &= \pi \\ a_4 &= \mu_{\alpha*} \equiv \mu_\alpha\cos\delta \\ a_5 &= \mu_\delta \end{aligned} \qquad [1.2.4]$$

In the context of least-squares estimation, all information on the quality of the estimated values $a_i^{\rm est}$ is contained in the 5×5 variance-covariance matrix with elements $c_{ij} = \mathrm{E}[(a_i^{\rm est}-a_i^{\rm true})(a_j^{\rm est}-a_j^{\rm true})]$ $(=c_{ji})$; $i,j=1,\ldots,5$. However, the physical significance of the covariances is made more transparent by giving separately the standard errors, σ_i, of the estimated parameters and the correlation coefficients, ρ_{ij} $(=\rho_{ji})$. The elements of the variance-covariance matrix can be reconstructed from the standard errors and correlations by:

$$c_{ii}=\sigma_i^2\,, \quad c_{ij}=\rho_{ij}\sigma_i\sigma_j \qquad [1.2.5]$$

In the catalogues, the correlation coefficients are given in the order ρ_{21}, ρ_{31}, ρ_{32}, ρ_{41}, ..., ρ_{54} and are designated $\rho^{\delta}_{\alpha*}$, $\rho^{\pi}_{\alpha*}$, ρ^{π}_{δ}, $\rho^{\mu_{\alpha*}}_{\alpha*}$, ..., $\rho^{\mu_\delta}_{\mu_{\alpha*}}$. This sequence corresponds to the triangular part of the correlation matrix below the main diagonal, taken in row-wise order (or the upper-triangular part taken in column-wise order).

The use of the asterisk notation is not strictly required in the correlations, since the correlation coefficient is the same between (say) α and δ, as between $\alpha\cos\delta$ and δ (with $\cos\delta$ considered a fixed factor). Nevertheless, it has been retained for uniformity.

Correlation coefficients are consistently provided, when appropriate, throughout the astrometric parts of the Hipparcos and Tycho Catalogues. For the Hipparcos Catalogue, only the 10 correlation coefficients among the five standard astrometric parameters are given in the printed catalogue, while the machine-readable version gives the full set of correlation coefficients also for the more complex solutions of double and multiple systems. Correlations are provided in order to allow the standard errors of transformed quantities to be correctly estimated (see Section 1.5).

The correlation coefficients and standard errors also implicitly define the mean observational epoch for an individual object. This is in general different depending on which positional coordinate is considered; for instance, it is different in right ascension and declination, while still other mean epochs are found in galactic longitude and latitude. For a particular coordinate axis the mean observational epoch may be defined as the epoch of zero correlation between the components of position and proper motion in that coordinate; this epoch also minimises the standard error in the position coordinate. With F*n* referring to fields H*n* or T*n* of the Hipparcos and Tycho Catalogues respectively, the mean observational epoch in right ascension is given by:

$$\mathrm{J1991.25}-\rho^{\mu_{\alpha*}}_{\alpha*}\times\frac{\sigma_{\alpha*}}{\sigma_{\mu_{\alpha*}}}=\mathrm{J1991.25}-\mathrm{F22}\times\frac{\mathrm{F14}}{\mathrm{F17}} \qquad [1.2.6]$$

at which epoch the standard error in right ascension is:

$$\sigma_{\alpha*}\sqrt{1-(\rho^{\mu_{\alpha*}}_{\alpha*})^2}=\mathrm{F14}\times\sqrt{1-\mathrm{F22}\times\mathrm{F22}} \qquad [1.2.7]$$

The mean epoch in declination is given by:

$$\mathrm{J1991.25} - \rho_{\delta}^{\mu_\delta} \times \frac{\sigma_\delta}{\sigma_{\mu_\delta}} = \mathrm{J1991.25} - \mathrm{F26} \times \frac{\mathrm{F15}}{\mathrm{F18}} \qquad [1.2.8]$$

at which epoch the standard error in declination is:

$$\sigma_\delta \sqrt{1 - (\rho_{\delta}^{\mu_\delta})^2} = \mathrm{F15} \times \sqrt{1 - \mathrm{F26} \times \mathrm{F26}} \qquad [1.2.9]$$

If an 'effective epoch' for individual objects is required, it may be defined as the epoch minimising the sum of the variances of the two positional coordinates (this definition is invariant with respect to the choice of coordinate system); it is given by:

$$\mathrm{J1991.25} - \frac{\rho_{\alpha*}^{\mu_{\alpha*}} \sigma_{\alpha*} \sigma_{\mu_{\alpha*}} + \rho_{\delta}^{\mu_\delta} \sigma_\delta \sigma_{\mu_\delta}}{\sigma_{\mu_{\alpha*}}^2 + \sigma_{\mu_\delta}^2} = \mathrm{J1991.25} - \frac{\mathrm{F22} \times \mathrm{F14} \times \mathrm{F17} + \mathrm{F26} \times \mathrm{F15} \times \mathrm{F18}}{\mathrm{F17} \times \mathrm{F17} + \mathrm{F18} \times \mathrm{F18}} \qquad [1.2.10]$$

The effective epoch always falls between the epochs given by Equations 1.2.6 and 1.2.8. The standard errors in right ascension and declination at the effective epoch are slightly larger than the values given by Equations 1.2.7 and 1.2.9.

Observation epochs determined according to these precepts must be interpreted with caution for 'non-standard' solutions, such as certain orbital systems, or secondary components of 'two-pointing' entries fixed with respect to the primary (with large positional errors and small errors in proper motion) where the calculated mean epochs may even lie outside of the observation interval [1989.845, 1993.207].

1.2.8. The Standard Model of Stellar Motion

The five astrometric parameters given in the Hipparcos and Tycho Catalogues describe the instantaneous motion of the star relative to the solar system barycentre, in a plane perpendicular to the line of sight. The sixth parameter needed to completely specify the space motion is the radial velocity, normally determined by spectroscopic means. The physical model underlying this description is that the stars move through space with constant velocity vector. This section reviews the formulae needed to calculate the positions of the stars for arbitrary epochs according to this 'standard' model of stellar motion, which is the basis for the main astrometric reduction of the Hipparcos data.

In reality the space velocity may vary because of perturbations from a companion star, planets, or the gravity field of other stars; ultimately, the curvatures of the galactic orbits of the star and of the Sun must be taken into account when extrapolating to sufficiently distant epochs. Except for the perturbations by close companions, these effects can generally be ignored in the computation of stellar positions over time spans of a century or less, even at the precision level of Hipparcos. Uniform space motion thus remains the standard model for the majority of stars in the Hipparcos Catalogue. The perturbations by close companions, when significant, are covered by the special solutions of type G and O in the Double and Multiple Systems Annex; see Section 2.3.

The five astrometric parameters, as given in the catalogues, refer to the common epoch T_0 = J1991.25(TT). Since the parameters change with time, subscript $_0$ will be used, when necessary, to denote their values as given in the catalogues. In particular, the barycentric direction towards the star at the epoch T_0 is specified by the celestial coordinates α_0, δ_0 given in Fields H8 and H9 of the Hipparcos Catalogue, or Fields T8 and T9 in the Tycho Catalogue. Equivalently, this direction may be expressed as a unit vector $\mathbf{r}_0$, whose rectangular equatorial coordinates are given by:

$$\mathbf{r}_0 = \begin{pmatrix} \cos\delta_0 \cos\alpha_0 \\ \cos\delta_0 \sin\alpha_0 \\ \sin\delta_0 \end{pmatrix} \qquad [1.2.11]$$

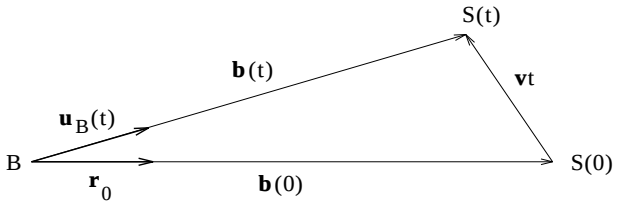

Figure 1.2.1. *Definition of the barycentric coordinate direction* $\mathbf{u}_B(t)$ *to a star moving with uniform space velocity* $\mathbf{v}$ *relative to the solar system barycentre B.* $S(0)$, $S(t)$ *are the positions of the star at times* 0 *and* t.

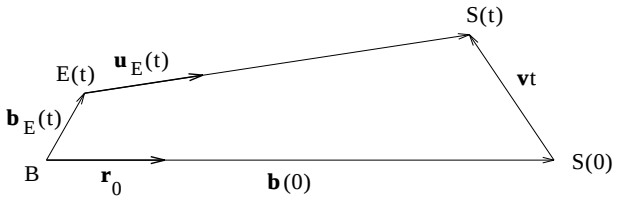

Figure 1.2.2. *Definition of the topocentric coordinate direction* $\mathbf{u}_E(t)$. $\mathbf{b}_E(t)$ *= barycentric vector to the observer at* $E(t)$*; other designations as in Figure 1.2.1.*

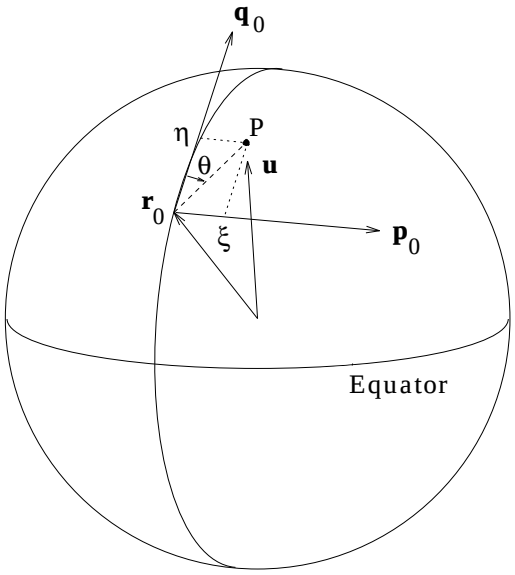

Figure 1.2.3. *Definition of local plane coordinates* (ξ, η) *in the tangent plane at* $\mathbf{r}_0$. *The orthogonal unit vectors* $\mathbf{p}_0$ *and* $\mathbf{q}_0$*, which span the tangent plane, are oriented in the local directions of* $+\alpha$ *and* $+\delta$ *at* $\mathbf{r}_0$*, respectively. P is the projection of unit vector* $\mathbf{u}$ *in the tangent plane,* ξ *and* η *its rectangular coordinates with respect to* $\mathbf{p}_0$ *and* $\mathbf{q}_0$. *The position angle* θ *of* $\mathbf{u}$ *with respect to* $\mathbf{r}_0$ *is indicated.*

The standard model is a prescription for calculating the celestial position (direction) at the arbitrary epoch $T = T_0 + t$.

Two cases are considered: the calculation of the *barycentric* direction (as seen from the solar system barycentre), and of the *topocentric* direction (as seen from an arbitrary location such as a point on the Earth). The two directions differ by the parallactic displacement of the star.

Note that all directions discussed in this section are *coordinate directions* corresponding to the coordinate differences between the source and observer in the barycentric coordinate frame. The transformation of coordinate directions to observed (proper) directions is discussed in Volume 3, Chapter 12; see also, for example, C.A. Murray, 1983, *Vectorial Astrometry*, Bristol, and the annual issues of *The Astronomical Almanac*, Section B. Furthermore, light-time effects are ignored here, i.e. no distinction is made between the time of light emission at the object and the time of light reception by the observer; both are designated T (or t) as if the speed of light were infinite. It can be shown that the errors introduced by this approximation are negligible as far as the modelling of the coordinate direction as a function of time is concerned: even in an extreme case such as Barnard's star, the errors are smaller than those caused by neglecting the curvature of its galactic orbit. See also the note after Equation 1.2.20.

The barycentric coordinate direction: In the standard model the barycentric vector to the star is given by:

$$\mathbf{b}(t) = \mathbf{b}(0) + \mathbf{v}t \qquad [1.2.12]$$

where $\mathbf{b}(0) = \mathbf{r}_0 A/\pi_0$ is the barycentric position at the catalogue epoch and $\mathbf{v}$ the constant space velocity (Figure 1.2.1). Using angular brackets to denote vector normalisation, the barycentric direction is given by the unit vector $\mathbf{u}_B(t) = \langle\, \mathbf{b}(0) + \mathbf{v}t \,\rangle$. This expression is unsuitable for calculation because of the appearance of the parallax in the denominator. A more convenient form is:

$$\mathbf{u}_B(t) = \langle\, \mathbf{r}_0 + \mathbf{v}(\pi_0/A)t \,\rangle \qquad [1.2.13]$$

where the normalisation factor is very close to unity.

The proper motion vector is the time derivative of the unit vector $\mathbf{u}_B(t)$. From its equatorial components at epoch T_0, $\mu_{\alpha*0}$ and $\mu_{\delta 0}$, the proper motion vector is calculated as:

$$\boldsymbol{\mu}_0 = \mathbf{p}_0\mu_{\alpha*0} + \mathbf{q}_0\mu_{\delta 0} \qquad [1.2.14]$$

where $\mathbf{p}_0$ and $\mathbf{q}_0$ are the unit vectors in the directions of increasing α and δ at $\mathbf{r}_0$ (see Figure 1.2.3):

$$\mathbf{p}_0 = \begin{pmatrix} -\sin\alpha_0 \\ \cos\alpha_0 \\ 0 \end{pmatrix} \qquad \mathbf{q}_0 = \begin{pmatrix} -\sin\delta_0\cos\alpha_0 \\ -\sin\delta_0\sin\alpha_0 \\ \cos\delta_0 \end{pmatrix} \qquad [1.2.15]$$

The orthogonal vector triad $[\,\mathbf{p}_0\ \mathbf{q}_0\ \mathbf{r}_0\,]$ is known as the *normal triad* at $\mathbf{r}_0$ relative to the equatorial system, and is important for the definition of differential quantities such as the proper motion components, the standard errors in position, or the local plane coordinates defined in Section 1.2.9. The normal triad should be regarded as a fixed set of coordinate axes completely defined by the given values of α_0 and δ_0; it is thus unaffected, for instance, by the observational uncertainty of these angles.

The tangential vectors at $\mathbf{r}_0$ relative to the equatorial system can be written as $\mathbf{p}_0 = \langle \mathbf{z}\times\mathbf{r}_0 \rangle$ and $\mathbf{q}_0 = \mathbf{r}_0\times\mathbf{p}_0$, where $\mathbf{z}$ is equatorial polar direction (towards $\delta = +90°$). In equatorial rectangular coordinates, where $\mathbf{z} = (0\ 0\ 1)'$ and $\mathbf{r}_0$ is given by Equation 1.2.11, evaluation of these expressions gives Equation 1.2.15. Other

coordinate systems, e.g. the ecliptic and galactic systems, have different normal triads at $\mathbf{r}_0$ corresponding to their polar directions (see Section 1.5.3).

Writing the space velocity as $\mathbf{v} = \boldsymbol{\mu}_0 A/\pi_0 + \mathbf{r}_0 V_{R0}$, Equation 1.2.13 becomes:

$$\mathbf{u}_B(t) = \langle\, \mathbf{r}_0 + (\mathbf{p}_0\mu_{\alpha*0} + \mathbf{q}_0\mu_{\delta 0} + \mathbf{r}_0\zeta_0)t \,\rangle = \langle\, \mathbf{r}_0(1 + \zeta_0 t) + \boldsymbol{\mu}_0 t \,\rangle \qquad [1.2.16]$$

where:

$$\zeta_0 = V_{R0}\pi_0/A \qquad [1.2.17]$$

is the relative change in distance per year.

It is seen from Equation 1.2.16 that $\mu_{\alpha*0}$, $\mu_{\delta 0}$ and ζ_0 are the components of the space velocity, scaled by the inverse distance at epoch T_0, along the vectors of the normal triad at $\mathbf{r}_0$. The quantity ζ_0 is therefore the equivalent, in the radial direction, to the proper motion in the tangential direction, and is statistically of a similar size when expressed in the corresponding unit. With V_{R0} expressed in [km s^{-1}], π_0 in [mas], and A in [km yr s^{-1}] (= A_V in Table 1.2.2), Equation 1.2.17 gives ζ_0 in [mas yr^{-1}]. Using A expressed in [mas km yr s^{-1}] (= A_Z in Table 1.2.2) gives ζ_0 in [yr^{-1}], appropriate for calculating the factor $(1 + \zeta_0 t)$ in Equation 1.2.16.

The topocentric coordinate direction: The coordinate difference between the object and the observer is given by the vector $\mathbf{b}(0) + \mathbf{v}t - \mathbf{b}_E(t)$, where $\mathbf{b}_E$ is the barycentric position of the observer (Figure 1.2.2). The topocentric direction is therefore given by the unit vector:

$$\mathbf{u}_E(t) = \langle\, \mathbf{r}_0(1 + \zeta_0 t) + \boldsymbol{\mu}_0 t - \mathbf{b}_E(t)\pi_0/A \,\rangle \qquad [1.2.18]$$

where, again, the normalising factor is very close to unity.

For Earth-bound applications of the Hipparcos and Tycho Catalogues it is sufficient to consider a geocentric observer. In that case $\mathbf{b}_E(t)/A$ may be taken directly from a barycentric equatorial ephemeris of the Earth, such as given in Section B of *The Astronomical Almanac*.

Equations 1.2.14 to 1.2.17 allow the barycentric direction to be calculated in terms of the six parameters α_0, δ_0, π_0, $\mu_{\alpha*0}$, $\mu_{\delta 0}$ and V_{R0}. The topocentric direction is similarly obtained by using Equation 1.2.18 instead of Equation 1.2.16. Either direction may be converted to celestial coordinates $\alpha(t)$, $\delta(t)$ using the component form of the unit vector:

$$\mathbf{u}(t) = \begin{pmatrix} \cos\delta(t)\cos\alpha(t) \\ \cos\delta(t)\sin\alpha(t) \\ \sin\delta(t) \end{pmatrix} \qquad [1.2.19]$$

It should be noted that many applications of the catalogue data, such as the further transformation into 'proper' directions for comparison with observations, is best done using vector calculus, in which case $\alpha(t)$, $\delta(t)$ are usually never explicitly needed.

Secular or perspective acceleration: The ζ_0 introduced by Equation 1.2.17 is the relative change in distance per unit time. The factor $(1+\zeta_0 t)$ appearing in the normalising factors of Equations 1.2.16 and 1.2.18 thus accounts for the perspective diminishing of the proper motion of a receding object. This is known as the 'secular' or 'perspective' acceleration of the star. It is important to note that it is a purely geometrical effect which does not correspond to any physical action on the star.

Table 1.2.3. Radial velocities used for the correction of perspective acceleration

HIP	V_R (km s^{-1})	HIP	V_R (km s^{-1})
439	+22.9	71681	−18.1
3829	−38.0	71683	−26.2
5336	−98.1	74234	+308.0
15510	+86.7	74235	+294.3
19849	−42.7	86990	−115.0
24186	+245.5	87937	−111.0
26857	+105.6	99461	−129.8
54035	−84.3	104214	−64.8
54211	+68.8	104217	−64.3
57939	−99.1	108870	−40.4
70890	−16.0		

The radial velocity of HIP 3829 has been adjusted from the observed value of +15 km s^{-1} to account for gravitational redshift and pressure shift (note that the value used for the data reductions is significantly different from the value given in the Hipparcos Input Catalogue).

The accumulated effect on the position is approximately given by $\zeta_0 \mu_0 t^2$. It is thus proportional to $\pi \times \mu \times V_R$ and practically negligible except for some nearby, high proper motion stars with large radial velocity. For the purpose of the Hipparcos data reductions, available ground-based radial velocity estimates for particularly critical objects were used as given in Table 1.2.3. In all other cases, V_R was assumed to be zero. The sample in Table 1.2.3 contains all Hipparcos stars with available radial velocities, for which the predicted accumulated effect over two years exceeds 0.1 mas.

Computation of transverse motions: The component of the stellar space velocity tangent to the line of sight, V_T, is traditionally calculated as:

$$V_T = \frac{A_v \mu}{\pi} \qquad [1.2.20]$$

where $A_v = 4.740\,47\ldots$ equals the astronomical unit, expressed in [km yr s^{-1}] (see Table 1.2.2). Many textbooks give slightly different values for A_v, usually because they assume the (now obsolete) tropical year as time unit for the proper motions.

Equation 1.2.20 is consistent with the standard model of stellar motions, in that it neglects the light-time effects. As mentioned before, this is an acceptable approximation for the modelling of the apparent motions of stars over historical time spans. However, light-time effects are not necessarily negligible for the calculation of the transverse velocity. In principle, the space velocity should be defined as $\mathbf{v} = \mathrm{d}\mathbf{b}/\mathrm{d}t^*$, where $t^* = t - b/c$ is the time of light emission at the star. Since $\mathrm{d}t^*/\mathrm{d}t = 1 - V_R/c$, it follows that the correct expression for the space velocity, in terms of the observed proper motion and radial velocity, is:

$$\mathbf{v} = (\boldsymbol{\mu} A/\pi + \mathbf{r}_0 V_R)(1 - V_R/c)^{-1} \qquad [1.2.21]$$

The expression for V_T, Equation 1.2.20, should thus in principle be amended to include the Doppler factor $k = (1 - V_R/c)^{-1}$. While the omission of this factor has drastic consequences for the interpretation of relativistic motions (for example, as superluminal expansion), it causes only a very small error on the calculated space velocities of galactic stars and there is generally no harm in using Equation 1.2.20 as it stands. (Equation 1.2.21 assumes that V_R is defined as the rate of change in coordinate distance per unit of t. Depending on the formula used to convert the observed redshift to a velocity, this may or may not be true.) The calculation of space coordinates and velocities is more extensively treated in Section 1.5.6.

1.2.9. Use of Local Plane Coordinates

While the use of vector calculus is generally to be recommended for rigorous computation of celestial directions, there are circumstances where small changes in the directions are best described differentially with respect to some reference direction. A typical example is the use of separation and position angle to characterise the relative positions of the components in a double or multiple star, or the definition of orbital parameters for binaries.

The classical method to express such positional offsets is by means of direct differences in the celestial coordinates. In the equatorial system these are typically denoted $\Delta\alpha \cos\delta$ and $\Delta\delta$, where the $\cos\delta$ factor is introduced to make the arc measures comparable in the two coordinates.

Quantities like $\Delta\alpha \cos\delta$ and $\Delta\delta$, while perfectly serviceable in many situations, suffer from a certain ambiguity or lack of rigour which make them unsuitable for general computation. Unpleasant or unforeseen things could happen especially when used for stars close to the celestial poles. These disadvantages can be eliminated by adopting a precise definition of offset coordinates. Among several possible choices, the one adopted presently appears eminently suitable for propagating positions according to the standard model described in the previous section. It corresponds closely to the use of 'standard coordinates' in photographic astrometry. In order to avoid association with the less well-defined $\Delta\alpha \cos\delta$ and $\Delta\delta$, a specific notation (ξ, η) is introduced for the offset coordinates according to this definition.

The offset coordinates (ξ, η) are defined as rectangular coordinates in the tangent plane at the fixed reference point $\mathbf{r}_0$, with ξ and η increasing respectively in the directions of the vectors $\mathbf{p}_0$ and $\mathbf{q}_0$ (Figure 1.2.3). The normal triad $[\,\mathbf{p}_0\ \mathbf{q}_0\ \mathbf{r}_0\,]$, and hence the offset coordinate system, is completely defined by the barycentric celestial coordinates α_0 and δ_0 at the catalogue epoch T_0; its equatorial components are given by Equations 1.2.11 and 1.2.15.

For the arbitrary direction $\mathbf{u}$ the offset coordinates are calculated as:

$$\begin{aligned} \xi &= \frac{\mathbf{p}_0' \mathbf{u}}{\mathbf{r}_0' \mathbf{u}} \\ \eta &= \frac{\mathbf{q}_0' \mathbf{u}}{\mathbf{r}_0' \mathbf{u}} \end{aligned} \qquad [1.2.22]$$

where the prime ($'$) denotes scalar product, or the transpose of the column matrix representing the vector. Note that Equation 1.2.22 does not require that $\mathbf{u}$ is of unit length. Conversely, the direction may be calculated from the offset coordinates as:

$$\mathbf{u} = \langle\, \mathbf{r}_0 + \mathbf{p}_0 \xi + \mathbf{q}_0 \eta \,\rangle \qquad [1.2.23]$$

An alternative way to express the offset position is by means of polar coordinates ϱ (separation) and θ (position angle), as used for instance for double stars. The exact relation between the two representations is given by:

$$\begin{aligned} \xi &= \tan\varrho \sin\theta \\ \eta &= \tan\varrho \cos\theta \end{aligned} \qquad [1.2.24]$$

Inserting Equation 1.2.16 in 1.2.22 gives a particularly simple expression for the offset coordinates of the barycentric position according to the standard model:

$$\begin{aligned} \xi_{\rm B}(t) &= \frac{\mu_{\alpha*0}t}{1+\zeta_0 t} \\ \eta_{\rm B}(t) &= \frac{\mu_{\delta 0}t}{1+\zeta_0 t} \end{aligned} \qquad [1.2.25]$$

As seen from the barycentre, the star moves in a straight line in the (ξ, η) plane. To the extent that $\zeta_0 t$ can be neglected the motion is, moreover, linear in time. For the topocentric direction the offset coordinates become:

$$\begin{aligned} \xi_{\rm E}(t) &= \frac{\mu_{\alpha*0}t - \mathbf{p}_0'\mathbf{b}_{\rm E}(t)\pi_0/A}{1+\zeta_0 t - \mathbf{r}_0'\mathbf{b}_{\rm E}(t)\pi_0/A} \\ \eta_{\rm E}(t) &= \frac{\mu_{\delta 0}t - \mathbf{q}_0'\mathbf{b}_{\rm E}(t)\pi_0/A}{1+\zeta_0 t - \mathbf{r}_0'\mathbf{b}_{\rm E}(t)\pi_0/A} \end{aligned} \qquad [1.2.26]$$

To the accuracy of the Hipparcos data the last term in the denominators of Equation 1.2.26 can always be ignored.

In Parts G, O and V of the Double and Multiple Systems Annex (Section 2.3) the non-linear motions of the photocentres of unresolved binaries are expressed relative to a fiducial point moving according to the standard model in Section 1.2.8, with astrometric parameters as given in the main catalogue (and assuming $\zeta_0 = 0$ except for the stars in Table 1.2.3). See Equations 2.3.1, 2.3.5, and 2.3.9. The offset coordinates of the fiducial point are denoted $\xi_{\rm s}(t)$ and $\eta_{\rm s}(t)$ and may be calculated from Equation 1.2.25 or 1.2.26 depending on whether barycentric or topocentric positions are required.

Section 1.3

Photometric Data, Magnitudes, and Variability

1.3. Photometric Data, Magnitudes and Variability

1.3.1. Hipparcos (Main Mission) Photometry: Single Stars

An introduction to the Hipparcos observations has been given in Section 1.1.1. The astrometric results contained in the Hipparcos Catalogue were derived from observations made at different epochs as the satellite scanned the celestial sphere. The modulated signal was measured by a photon-counting image dissector tube device. Whilst the phase of the modulated signal provided the astrometric information, its mean level and amplitude contained information on the intensity of the observed objects.

Both the mean level (dc component) and the amplitude (ac component) were used to produce fully calibrated magnitudes for each object at each epoch of observation. The dc component is the more powerful and precise measurement of the two, but is affected by background. The ac component is insensitive to the background level, but influenced by duplicity. The photometric data presented in the main Hipparcos Catalogue and in the Hipparcos Epoch Photometry Annex have been derived from the dc component. Corresponding results for the ac component can be found in the Hipparcos Epoch Photometry Annex Extension.

The Hipparcos main instrument observed in a broad-band system in order to optimise the astrometric signal. This system is referred to as Hp and is specific to the Hipparcos configuration (Figure 1.3.1). The photometry obtained with such a broad-band system is limited in its astrophysical content compared to multi-colour photoelectric photometry. The precision of each observation is, however, high.

The main mission photometric data were reduced using a selection of 22 000 standard stars. This list included some stars which could not be strictly regarded as photometric standards, in particular among the very red stars—these stars were nevertheless necessary for the control of the calibration parameters for stars with extremely red colour indices. An initial selection was made on the basis of ground-based photometry, using standard stars identified in the Hipparcos Input Catalogue. The final standard star list incorporates some new standard stars, while some stars from the initial selection were classified as variable on the basis of the Hipparcos measurements and subsequently rejected as standards.

The resulting collection of epoch photometry comprises a total of 13 000 000 observations, an average of some 110 observations for each of the 118 000 programme stars. While significant variations in the number of observations occurred, primarily related to the object's ecliptic latitude, the Hipparcos Epoch Photometry represents the largest compilation of high-precision, multi-epoch photometry acquired to date. It consequently defines a uniform all-sky photometric system, unaffected by seasonal and hemisphere-related influences.

The epoch photometry can be affected by a difference between the Cousins' $(V-I)_{\rm C}$ colour used in the reductions and the actual colour of the star, due to the ageing of the optical chain and the resulting changes in the passband. Section 1.3.4 includes a description of how the epoch photometry can be corrected for such colour errors.

1.3.2. Hipparcos (Main Mission) Photometry: Double Stars

The Hipparcos photometry for double and multiple stars had to be treated with particular care. The image dissector tube detector had an instantaneous field of view of about 30 arcsec diameter, attenuation starting at about 5 arcsec from the centre. For double stars with separations between 5 and 20 arcsec one or both of the components was therefore inevitably positioned where the attenuation of the instantaneous field of view changed rapidly. Observed intensities were therefore very sensitive to the exact pointing of the instantaneous field of view with respect to the stellar images. This was of importance in particular when the two components of a double star were of similar brightness. In many such cases the resulting photometric data were unreliable, and were accordingly flagged.

A total of 5803 entries for double stars had their dc magnitudes corrected for the effects of measuring off-centre in the instantaneous field of view, and for the presence of another component within the same instantaneous field of view. They are among 12 961 entries which can be recognised from the component flag in the first header record of the epoch photometry data file: if not blank, the star is a double star and significant corrections may have been applied. The largest corrections were made for stars with component flag 'B', followed by those with component flag 'A'. Corrections made for stars with component flag '*' were generally very small. All stars with the component flag set have the correction that was applied given in the header records of the Hipparcos Epoch Photometry Annex file. As ac magnitudes were not corrected, these stars should be excluded from investigations involving comparisons between ac and dc magnitudes. This section describes the corrections that were applied to double star photometry.

Every object in the Hipparcos Input Catalogue had its own target position, used by the satellite to point the sensitive area of the image dissector tube detector. For single stars this was simply the direction of the star. Double stars with separations below 10 arcsec were observed as a single catalogue entry, with the target position being either at the photocentre or at the geometric centre of the two components. Components of double stars with wider separations were considered as separate potential targets although not all components of such systems were necessarily included in the Hipparcos Input Catalogue. The pointing of the detector's instantaneous field of view had an associated uncertainty of a few arcsec, unimportant for single stars except for the very brightest. However, for double or multiple stars with at least one component near the steep slope of the detector's response profile, these uncertainties were important.

The typical situation is illustrated in Figure 1.4.1 of Section 1.4, and the detector's response profile is given in Table 1.4.1. The response was characterised by a flat region of about 5 arcsec in diameter (attenuation ≤ 0.01 mag) followed by a slow decline in sensitivity up to 11 arcsec (attenuation ~ 0.1 mag), and finally a sharp increase in attenuation at larger distances.

During the observations of a double star with a separation between 5 and 35 arcsec, pointing at the primary, the secondary was not always on the central part of the detector's profile and could consequently appear dimmed. The total intensity as measured by the instrument was therefore smaller than the true intensity. The photometric results for such double stars have been corrected for this effect, in the computation of both the combined magnitudes and the component magnitudes.

For the simplest case with the detector pointing at the primary, the intensity ratio between the primary and secondary is given by:

$$r = \frac{I_2}{I_1} = 10^{-0.4\,\Delta m} \qquad [1.3.1]$$

where Δm is the magnitude difference between the two components, and I_1, I_2 the corresponding intensities. For the instrumental magnitude difference, $\widetilde{\Delta m} = \Delta m + \psi(\varrho)$ where ϱ is the component separation, and $\psi(\varrho)$ is the attenuation profile expressed in magnitudes. This yields the instrumental intensity ratio:

$$\tilde{r} = \frac{\tilde{I}_2}{I_1} = 10^{-0.4\,\widetilde{\Delta m}} \qquad [1.3.2]$$

The combined true intensity is given by:

$$I = I_1 + I_2 = I_1(1 + r) \qquad [1.3.3]$$

while the measured quantity was:

$$\tilde{I} = I_1 + \tilde{I}_2 = I_1(1 + \tilde{r}) \qquad [1.3.4]$$

From which:

$$Hp = \tilde{H}p + 2.5 \log \frac{1 + \tilde{r}}{1 + r} \qquad [1.3.5]$$

and:

$$H_1 = \tilde{H}p + 2.5 \log(1 + \tilde{r}) \qquad [1.3.6]$$

$$H_2 = \tilde{H}p + 2.5 \log(1 + \tilde{r}) - 2.5 \log r \qquad [1.3.7]$$

where Hp is the true combined magnitude, $\tilde{H}p$ the observed value and H_1, H_2 the true magnitudes of the two components. Similar expressions apply for a pointing at the geometric centre, where simultaneous allowance is made for the attenuation of the primary and secondary components.

A correction has been applied to all the transits of the Hipparcos Epoch Photometry Annex of the double stars included in Part C of the Double and Multiple System Annex in order to derive the combined magnitude Hp, and the magnitudes of the components. No correction was applied to double stars not resolved by Hipparcos, and as a consequence no information is given for the component flag in Field HH2. The magnitude of the components of the triple and quadruple stars have been corrected by adapting Equations 1.3.5–1.3.7 to more than two components, but only for the summary photometric information given in the Double and Multiple Systems Annex. The errors on ϱ and Δm have been propagated and added quadratically to the estimated standard error of the Hp magnitude of the transits and to that of the median $\overline{Hp}$.

The corrections were computed in a uniform way assuming a pointing at the brighter component for each single-pointing system and at the brighter or fainter component for every two pointing system. While this is not perfectly rigorous for a system with the pointing at the geometric centre, the median of the resulting error is less than 1 millimagnitude over the 760 such systems and reaches a level of 0.02 mag only for about 10 systems with separation close to 10 arcsec and with components of nearly equal brightness. The choice made was motivated by the need to have a correction that was easily reversible. More detailed corrections were not justified, considering this error in comparison with other uncertainties affecting the photometry of the double stars, such as the typical standard error of Δm of several hundredths of mag, the unknown variability of the components, the fact that the colour has been taken as some mean colour for the system and, for systems with large separation, the instability of the signal due to pointing offset.

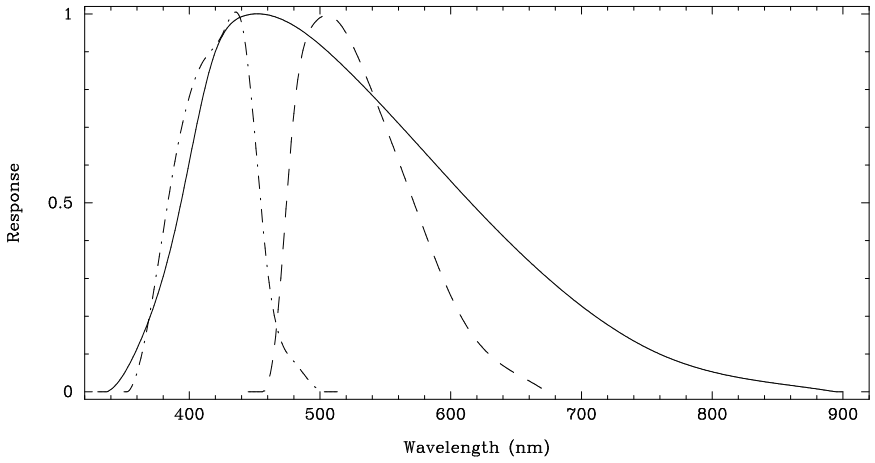

Figure 1.3.1. *The Hipparcos (Hp, solid line) and Tycho (B_T, dot-dash line, and V_T, long-dash line) photometric systems.*

Table 1.3.1. The Hp, V_T and B_T passbands as a function of wavelength (in nm).

λ	B_T	V_T	Hp	λ	B_T	V_T	Hp	λ	V_T	Hp	λ	Hp
330	0.000	0.000	0.000	475	0.101	0.530	0.979	620	0.135	0.483	765	0.092
335	0.000	0.000	0.000	480	0.080	0.737	0.969	625	0.114	0.465	770	0.085
340	0.000	0.000	0.006	485	0.059	0.870	0.958	630	0.097	0.447	775	0.079
345	0.000	0.000	0.023	490	0.036	0.940	0.946	635	0.082	0.429	780	0.073
350	0.000	0.000	0.047	495	0.016	0.973	0.933	640	0.069	0.412	785	0.067
355	0.014	0.000	0.078	500	0.003	0.990	0.919	645	0.058	0.395	790	0.062
360	0.058	0.000	0.114	505	0.000	0.996	0.903	650	0.047	0.378	795	0.057
365	0.123	0.000	0.154	510	0.000	0.991	0.888	655	0.038	0.361	800	0.053
370	0.206	0.000	0.198	515	0.000	0.975	0.871	660	0.028	0.345	805	0.049
375	0.305	0.000	0.248	520	0.000	0.949	0.855	665	0.018	0.329	810	0.045
380	0.416	0.000	0.305	525	0.000	0.916	0.838	670	0.008	0.314	815	0.041
385	0.530	0.000	0.369	530	0.000	0.878	0.820	675	0.000	0.298	820	0.038
390	0.636	0.000	0.442	535	0.000	0.837	0.803	680	0.000	0.283	825	0.035
395	0.724	0.000	0.523	540	0.000	0.794	0.785	685	0.000	0.269	830	0.032
400	0.787	0.000	0.608	545	0.000	0.749	0.766	690	0.000	0.254	835	0.029
405	0.830	0.000	0.694	550	0.000	0.704	0.748	695	0.000	0.241	840	0.026
410	0.861	0.000	0.774	555	0.000	0.658	0.729	700	0.000	0.227	845	0.024
415	0.889	0.000	0.845	560	0.000	0.612	0.710	705	0.000	0.214	850	0.022
420	0.920	0.000	0.901	565	0.000	0.565	0.691	710	0.000	0.201	855	0.019
425	0.953	0.000	0.941	570	0.000	0.518	0.672	715	0.000	0.189	860	0.017
430	0.982	0.000	0.967	575	0.000	0.471	0.653	720	0.000	0.177	865	0.015
435	1.002	0.000	0.984	580	0.000	0.424	0.634	725	0.000	0.166	870	0.012
440	0.976	0.000	0.993	585	0.000	0.379	0.615	730	0.000	0.155	875	0.010
445	0.861	0.000	0.998	590	0.000	0.335	0.596	735	0.000	0.144	880	0.007
450	0.685	0.000	1.000	595	0.000	0.293	0.577	740	0.000	0.134	885	0.005
455	0.489	0.000	1.000	600	0.000	0.254	0.558	745	0.000	0.125	890	0.002
460	0.317	0.022	0.998	605	0.000	0.218	0.539	750	0.000	0.116	895	0.000
465	0.202	0.115	0.993	610	0.000	0.186	0.520	755	0.000	0.108	900	0.000
470	0.136	0.301	0.987	615	0.000	0.159	0.502	760	0.000	0.100		

1.3.3. Tycho (Star Mapper) Photometry

In addition to the broad-band photometric observations acquired by the Hipparcos (main mission) detector, the star mapper data (which were processed independently and constitute the Tycho Catalogue) yielded two-colour photometric data, also at many different epochs. These two-colour observations correspond rather closely to (and can be approximately transformed into) the Johnson B and V magnitudes. The Tycho magnitude systems are referred to as B_T and V_T respectively. The spectral transmission (Figure 1.3.1 and Table 1.3.1) has been inferred from observations of photometric standard stars (updated with respect to ground-based calibrations of the instrument). The Tycho photometric data were reduced using standard stars which were initially selected on the basis of ground-based photometric standards identified in the Tycho Input Catalogue. The final standard star list included new standards, as well as the rejection of objects subsequently identified as variable.

The number of Tycho observations for each star is not given explicitly in the printed Hipparcos Catalogue. It is about 130 on average, dependent on ecliptic latitude as a result of the scanning law, and roughly 20–30 per cent larger than the number of Hipparcos photometric measurements of the same star (this number is given in the main catalogue). The larger number of observations of a given star by Tycho arises from the fact that, while the star mapper slits were only 40 arcmin in length, compared with the main field of view width of 54 arcmin, there were two slit groups.

The Tycho observations have a different spatial resolution compared with the Hipparcos observations—Tycho was able to distinguish directly components in double or multiple systems with separations $\varrho > 2$ arcsec. For such cases the B_T and V_T photometry might consequently refer to one or more components while the Hp photometry for the same catalogue entry may refer to the combined light from the system (even though the separate components may have been spatially resolved by Hipparcos). Similarly, duplicity can be recognised for some partly unresolved double stars from a relation between the observed magnitude and orientation of the slit group during the observation.

1.3.4. Photometric Data from Ground-Based Observations

The Hipparcos Input Catalogue included V magnitudes and $B-V$ colour indices obtained from ground-based observations, along with estimated Hp magnitudes, based on the pre-mission calculations of the Hp passband. During the mission, the Hp passband was re-calibrated as a function of wavelength and time, and Hp magnitudes were re-calculated based on the reconstructed passband at the 'photometric reference epoch' JD 2 448 622.5 (1 January 1992). This passband defines the Hipparcos broad-band photometric system, to which all observations have been reduced (see Volume 3).

The Cousins' $(V-I)_{\mathrm{C}}$ colour index was adopted as the colour parameter characterising the astrometric and photometric calibration of Hipparcos—it was appropriate for describing changes in the passband, being a more linear function of spectral type than $B-V$. In the photometric calibration it was used to describe the detector response as a function of location and star colour. This was time-dependent due to the chromatic ageing of the detector, principally as a result of radiation damage of the optical elements of the detection chain. In the astrometric calibration the $(V-I)_{\mathrm{C}}$ index was used to account for (small) chromatic effects. A specific effort was therefore devoted to the acquisition and compilation of the $(V-I)_{\mathrm{C}}$ colour indices, using a variety of ground-based observations as well as reduced Tycho data obtained over the first half of the mission. Although most of the Hipparcos and Tycho Catalogue data were derived exclusively from the satellite observations, the colour indices represent such an important piece of astrophysical information that they have been updated and included in the catalogue.

The Hipparcos Catalogue includes both $B-V$ (Johnson) and $V-I$ (Cousins) colour indices. The $B-V$ colour index was taken either from ground-based observations or from Tycho photometry when the latter was more accurate. Since the Tycho B_T, V_T and Johnson B, V bands differ, a straightforward linear transformation from B_T-V_T to $B-V$ may show residuals of up to 0.1 mag depending on star reddening, gravity, and temperature. Accurate transformations therefore utilised spectral type information, if available, and distinct transformation equations for dwarf and giant stars. Similarly, the $(V-I)_C$ indices were updated on the basis of the Tycho photometry and a variety of ground based data acquired during the post-launch phase. The source of the $B-V$ index is given in Field H39, the source of the $(V-I)_C$ index in Field H42. The transformations from Tycho data to $B-V$ and $(V-I)_C$ indices are described in Section 1.3 Appendix 4.

The Tycho Catalogue also includes $B-V$ colour indices, but derived only from the B_T-V_T values using the simplified transformation given in Section 1.3 Appendix 4, spectral type information not being available for a large fraction of the Tycho Catalogue entries. Consequently, the Tycho Catalogue $B-V$ colour indices are less accurate than those given in the Hipparcos Catalogue, and the two will frequently differ, for the same object, simply because they have been derived in different ways.

The requirement to preserve a record of the $(V-I)_C$ colour index used for the astrometric and photometric reductions, while at the same time presenting the best-available (updated) colour indices, meant that two catalogue fields are dedicated to $(V-I)_C$: Field H40 provides the best-available colour index at the time of the catalogue completion, while Field H75 (not included in the printed catalogue) provides the (intermediate) value used for the astrometric and photometric reductions. Re-reduction of the astrometric and photometric data would have been possible in principle, but unrealistic in practice: partly from the perspective of the catalogue completion schedule, but also because the 'final' $(V-I)_C$ (and the published $B-V$) values, still largely derived from a wide variety of ground-based observations, cannot be considered as definitive or fully homogeneous. However, in the case of the astrometric reductions the effect of an erroneous $(V-I)_C$ value was very small. Stars for which an erroneous $(V-I)_C$ is likely to have been used for the data reductions are indicated by R in Field H52.

The Hipparcos Epoch Photometry can be corrected for the effects of an erroneous $(V-I)_C$ colour index, used for the photometric reductions, once a new or improved colour index becomes available. The $(V-I)_C$ value used in the data reductions (Field H75) is transformed into a pseudo-colour, $C_{\rm old}$, according to the prescription given in Table 1.3.2. $C_{\rm new}$ is derived from the same table on the basis of the improved $(V-I)_C$ index. The correction $\delta Hp = Hp_{\rm old} - Hp_{\rm new}$ is then derived as:

$$\delta Hp = (0.0537\,(t-t_0) - 0.0084) \times (C_{\rm old} - C_{\rm new}) \qquad [1.3.8]$$

where t and t_0 are measured in units of 1000 Julian days, and t_0 = 2448.6225 =1 January 1992. The standard deviation of δHp when applying a colour correction of 1 mag is approximately 0.003 mag. This approximate correction applies only to dc magnitudes, and ignores small field of view differences. More accurate corrections using information from the Hipparcos Epoch Photometry Annex Extension are provided in Volume 3, Chapter 14, where corrections for the ac magnitudes are also given.

Table 1.3.2. Definition of the pseudo-colour index, $C = a + b(V-I) + c(V-I)^2 + d(V-I)^3$

Interval	a	b	c	d
$V-I \le 0.85$	−0.48729	0.98554	−0.31968	0.592
$0.85 < V-I \le 2.00$	−1.03936	2.14720	−0.416	0.0
$V-I > 2.00$	+0.5152	0.592	−0.0256	0.0

1.3.5. Published Data Related to the Hipparcos Photometry

The Hipparcos photometry has been presented in three ways: the fully reduced observations (the Hipparcos Epoch Photometry Annex plus Annex Extension), the results from a provisional variability search (the Variability Annexes and light curves) and summary data in the main Hipparcos Catalogue. The information contained in each of these products is summarised in the following sections. Full descriptions of formats and contents can be found in the relevant parts of Section 2.

The Hipparcos Epoch Photometry Annex: This annex provides the calibrated *Hp* epoch photometric data (based on the mean signal level, i.e. the dc magnitudes), along with an error estimate, quality flags and the barycentric time of each observation. The barycentric time is expressed in JD(TT) (see Section 1.2.3). The dc magnitudes have been provisionally corrected for 5803 stars in double systems, indicated by the component flag in the header record (see also Section 1.3.1 and Volume 3). Header records provide information on the number of observations, the $(V-I)_{\rm C}$ colour index used in the reductions, the median magnitude and its estimated error, the 5th and 95th percentiles (see Section 1.3 Appendix 1), and the variability indicator as defined in Section 1.3 Appendix 2. This information is repeated in the main Hipparcos Catalogue.

The Hipparcos Epoch Photometry Annex Extension: The extension provides data supplementary to the epoch photometry: the background levels used in the two reduction processes, the photometry based on the amplitude of the modulation (i.e. the ac magnitudes), the position on the sky in the complementary field of view, and an index for identified coinciding objects from the complementary field of view. These data allow for a more detailed and specialised analysis of the Hipparcos photometry. The header records partly repeat information from the headers in the Epoch Photometry Annex. Additional information related to the ac component is also provided. Information on the median ac magnitude and its estimated error has been used in the definition of the variability flag. The determination of the ageing corrections for the ac magnitudes were not as comprehensive as for the dc magnitudes, and small residual systematic effects may still be present.

Variability annex: tabular data and light curves: A provisional analysis of the photometric data referred to above was carried out in parallel by two distinct groups (at the Geneva Observatory and the Royal Greenwich Observatory). The tables of periodic and unsolved variables are the result of this analysis. Given the very limited time available, these classifications should not be considered as exhaustive or conclusive. The Hipparcos photometric data were examined with various period searching algorithms and results were compared with literature references when available. Period searches were severely handicapped by often very poor coverage of epochs by the observations, in particular for stars close to the ecliptic plane. The character of the scanning law made the recognition of periods in the range 5 to 100 days unreliable, in particular for semi-regular variables. Possible periods are given in the notes, but in most cases these periods are very likely to be spurious. Similarly, it was not always possible to distinguish between eclipsing binaries and pulsation- or rotation-related variations, leading to an ambiguity in the period given. Minimal time for proper classifications was available given the adopted catalogue publication schedule, and in many cases no classification could be provided.

The tabular data were split into two parts, corresponding to objects for which a variability period could be, or could not be, determined. For the 'periodic variables' the tabular material provides periods (given to the full estimated precision), amplitudes, reference epochs, variability types, star names, and references to the literature. The methods used for the period optimisation and the determination of the amplitude and its estimated error are described in Section 1.3 Appendix 3. Stars were also included in this table if the literature gave a reliable period and reference phase, but where these could not be independently derived using the Hipparcos data alone. This applies in particular to some long-period and Algol-type variables. In these cases no Hipparcos period is given, and sometimes also no Hipparcos reference epoch.

For the 'unsolved variables', amplitudes, variable star names, and references to the literature are also given. This table includes stars which were considered as semi-regular in the literature, but for which the period presented in the literature could not be confirmed by the Hipparcos data. In general, a star appearing in the table of unsolved variables is not necessarily non-periodic: it may only be concluded that a period was not established from this preliminary analysis, or confirmed from the literature.

All variables appearing in the table for the 'periodic variables', except those with very long periods, have their folded light curve given in Volume 12, Section A. For some of the more interesting stars (in this case the more slowly evolving) among the 'unsolved variables' the epoch photometry is shown graphically in Volume 12, Section C.

Prior to the start of the Hipparcos observations it was realised that for large-amplitude semi-periodic and irregular variables the Hipparcos photometry needed support from ground-based data. This was also essential in planning of the astrometric measurements: a proper optimisation of the observing time required *a priori* knowledge of the magnitude of every object. A selection of 296 large amplitude variables was monitored successfully by the AAVSO, and the Hipparcos data for these stars are shown superimposed on the fitted curves through the AAVSO data in Volume 12, Section B. Some of these stars appear in the table of 'periodic variables', in which case there will also be a folded light curve presented in Volume 12, Section A.

Summary photometric data in the Hipparcos Catalogue: The main Hipparcos Catalogue contains a summary of information extracted from, and provided in, the header records of the Hipparcos Epoch Photometry Annex and Annex Extension. Other information comes from the Variability Annexes, except for Field H6. A coarse variability flag is given in Field H6, derived from the distribution of unit weight residuals as described in Section 1.3 Appendix 2. It provides an estimate for intrinsic variability present in the epoch photometry under the assumption that the underlying variations are approximately sinusoidal. No provision for possible eclipsing binaries were made.

Fields H44–50 and H52 summarise the epoch photometry through medians, scatter estimates, and a simplified variability indicator, all as given in the header records in the Hipparcos Epoch Photometry Annex. Field H51 gives a period (to an accuracy of no more than 0.001 days) when this period has been derived solely from Hipparcos data. Fields H53–54 provide reference flags to the tabular data and light curves respectively.

1.3.6. Published Data Related to the Tycho Photometry

A similar approach was followed for the Tycho photometric results as for the Hipparcos photometric results. Thus, the Tycho Epoch Photometry Annex contains 'epoch photometry', and the main Tycho Catalogue contains summary data. The main differences are: (1) only a relatively small number of the Tycho Catalogue entries are retained with epoch photometry, because of the lower precision of the individual B_T and V_T magnitudes; (2) the summary statistics differ in some details: a 'de-censored mean' rather than a direct median is used, and different percentiles of the distribution are used to characterise the scatter; (3) a systematic variability analysis was not carried out for the Tycho Catalogue entries, so there is no corresponding 'variability annex'.

Summary data provided in the Tycho Catalogue: The Tycho Catalogue provides the median or mean magnitude and related statistics for each catalogue entry.

Estimates of the median or mean B_T and V_T magnitudes could not be simply constructed from the observed photometric transits. A meaningful median magnitude could only be derived from the Tycho observations for stars brighter than V_T ~ 8 mag and B_T ~ 8.5 mag. For fainter stars an increasing number of observations fell below the detection threshold, with the observations becoming critically signal-to-noise limited and the detection probability becoming a strong function of stellar magnitude and instantaneous background intensity. Ignoring the non-detections would have resulted in a biased sample of observations. In practice, fainter Tycho mean magnitudes have been obtained using a 'survival analysis' technique taking into account the non-detections, and are referred to as 'de-censored mean magnitudes'.

Compared with the Hipparcos Catalogue, where the 5th and 95th percentiles are used to represent minimum and maximum magnitudes, the 95th percentiles are not well-defined for many of the fainter Tycho stars (because of the censoring of observations); the 15th and 85th percentiles are therefore provided instead.

Estimates of the standard errors of the B_T and V_T magnitudes were also affected by the censoring of the fainter observations. Moreover, the standard errors in the Tycho Catalogue are much larger than in the main Hipparcos Catalogue, and the points equivalent to the 15th and 85th percentiles are not well centred on the de-censored mean values, because of the non-linear transformation between intensities and magnitudes. Consequently, Fields T33 and T35 of the Tycho Catalogue provide estimates of the standard errors specifically towards *brighter* magnitudes:

$$\begin{aligned} \bar{\sigma}_{B_T} &= \langle B_T \rangle - B_T(\langle I_{B_T} \rangle + \sigma_{I_{B_T}}) \\ \bar{\sigma}_{V_T} &= \langle V_T \rangle - V_T(\langle I_{V_T} \rangle + \sigma_{I_{V_T}}) \end{aligned} \qquad [1.3.9]$$

where $\langle I_{B_T} \rangle$ and $\langle I_{V_T} \rangle$ are the de-censored mean intensities with standard errors $\sigma_{I_{B_T}}$ and $\sigma_{I_{V_T}}$, as determined in the 'de-censoring analysis' (see the introduction to Section 2.2, and Section 2.2 Fields T32–39). Uncertainties towards fainter magnitudes are larger than those towards brighter magnitudes. The latter has been chosen for the definition of the standard error because it may always be computed (unlike that towards fainter magnitudes, which is infinite when the standard error is as large as 0.753 mag, i.e. $\sigma_I = I$). Further details are given in Volume 4, Chapter 9.

Similarly, the change in magnitude corresponding to a shift of intensity by $n\,\sigma_I$ is given by:

$$\begin{aligned} \Delta B_T(n\sigma_{I_{B_T}}) &= |2.5 \log(1 + n - n\, 10^{0.4\bar{\sigma}_{B_T}})| \\ \Delta V_T(n\sigma_{I_{V_T}}) &= |2.5 \log(1 + n - n\, 10^{0.4\bar{\sigma}_{V_T}})| \end{aligned} \qquad [1.3.10]$$

where n is negative towards brighter magnitudes and positive towards fainter magnitudes. Thus 1σ uncertainties towards fainter magnitudes are given by:

$$\begin{aligned} \sigma^{+}_{B_T} &= \Delta B_T(+1\,\sigma_{I_{B_T}}) &= -2.5\log(2 - 10^{0.4\sigma^{-}_{B_T}}) \\ \sigma^{+}_{V_T} &= \Delta V_T(+1\,\sigma_{I_{V_T}}) &= -2.5\log(2 - 10^{0.4\sigma^{-}_{V_T}}) \end{aligned} \qquad [1.3.11]$$

As for B_T and V_T, the standard error interval of $B_T - V_T$ is not centred on the tabulated $B_T - V_T$ value, and one of the limits (or even both limits) could be undefined for a few stars. As described in Volume 4, Field T38 is derived from the larger of the two standard errors of $B_T - V_T$ (on the red and on the blue side, respectively), corresponding to $\pm 1\sigma_{I_{B_T}}$ and $\mp 1\sigma_{I_{V_T}}$. The individual uncertainties corresponding to $n\,\sigma_I$ are given approximately by:

$$\Delta(B_T - V_T)_{n\sigma_I} = 2.5\sqrt{[\log(1 + n - n\,10^{0.4\sigma^{-}_{B_T}})]^2 + [\log(1 - n + n\,10^{0.4\sigma^{-}_{V_T}})]^2} \qquad [1.3.12]$$

where n is negative on the blue side and positive on the red side; $\sigma^{-}_{B_T}$ and $\sigma^{-}_{V_T}$ are the uncertainties of B_T and V_T towards brighter magnitudes, as given in Fields T33 and T35 respectively.

The standard error of $(B - V)_J$ in Field T38 has been derived from Equations 1.3.12 and 1.3.22. The standard error of $(B - V)_T$ for a given Tycho star may be derived from the value in Field T38 by means of Equation 1.3.22, more simply than from Equation 1.3.12. Thus:

$$\sigma_{(B-V)_T} = \sigma_{(B-V)_J}/G \simeq \sigma_{(B-V)_J}/0.85 \qquad [1.3.13]$$

where G is given in Section 1.3 Appendix 4, Table 1.3.4.

Tycho Epoch Photometry Annex: Individual photometric observations in the B_T and V_T channels are provided in the Tycho Epoch Photometry Annex for a selection of the Tycho Catalogue entries. For each selected entry, a header record and a series of individual transit records are given. The header record contains summary photometric data, and also indicates the number of transit records following.

Two Tycho Epoch Photometry Annexes are published, differing in the number of catalogue entries for which transit records are included. Annex A, the smaller one, is part of the CD-ROM set in Volume 17 of the printed Hipparcos Catalogue. It contains transit data for 34 446 entries. The following groups of stars were selected (see Section 2.6 for details): (a) known or suspected variable stars and double stars; (b) a subset of the Tycho photometric standard stars. This selection was defined such as to include the most interesting subset of Tycho epoch photometry, while at the same time fitting onto a single CD-ROM.

Annex B, containing transit records for 481 553 catalogue entries, is archived at the CDS (Strasbourg). The selection includes all entries of Annex A, all stars brighter than $V_T = 10.25$ mag, and several small groups of stars of special interest. For details see Section 2.6.

The statistical significance of individual Tycho transits may be illustrated as follows. At $V_T = 9$ mag the mean photometric signal-to-noise ratio of a single slit group transit is of the order of 7. The censoring of transits is still fairly mild at this magnitude, but begins to become important at only slightly fainter magnitudes: the bias of a formal median magnitude is about 0.04 mag at $V_T = 9$ mag, increasing to about 0.20 and 0.80 mag at $V_T = 10$ and 11 mag.

Section 1.3 Appendix 1: Statistical Indicators

Different statistical indicators have been used to characterise the photometric stability or variability of stars in the Hipparcos and Tycho Catalogues, and the following provides a background to the choices made:

Quantiles: Let $x(p)$ denote the value of a random variable from a distribution, whose probability is p. Now consider N discrete (photometric) observations y_i, $i = 1...N$, ordered so that $y_i > y_{i-1}$. The observations y_i are mapped onto the distribution of $x(p)$ by setting $p = i/(N + 1)$, so that $x(p) = y_i$ for $i = 1...N$.

The complete distribution of $x(p)$ in [0,1] is then defined by the conventions $x(1/(N + 1)) = y_1$ and $x(N/(N + 1)) = y_N$. To this were added two artificial observations: $x(0) = x(1/(N + 1))$ and $x(1) = x(N/(N + 1))$, which avoids problems with estimates for low numbers of observations. The values of $x(p)$ at intermediate values of p are obtained by linear interpolation between adjacent points. $x(p)$ denotes the p-th quantile of the distribution. As explained below, different quantiles have been used as variability indicators in the case of the Hipparcos and Tycho Catalogues.

Error on the median: For the Hipparcos Catalogue entries, the median magnitude, m, is determined as $x(0.5)$. The standard error of $x(0.5)$ is given by:

$$\sigma_m = \frac{1}{2 f(z_{0.5}) \sqrt{N}} \qquad [1.3.14]$$

where $f(x)$ is the probability density function. For observations with identical variance σ^2 this reduces to:

$$\sigma_m = \sqrt{\frac{\pi}{2}} \frac{\sigma}{\sqrt{N}} \qquad [1.3.15]$$

representing a normal distribution of standard deviation σ. In the case of a variable star, the median may be very well defined despite large magnitude excursions in the observations. This is reflected in the expression for σ_m since the function $f(z_{0.5})$ represents the derivative of the cumulative probability function at the median. The expression for σ_m therefore conveys a local property of the observation distribution in the vicinity of the median, and remains largely insensitive to the wings, as does the median itself.

An evaluation of $f(z_{0.5})$, based on the difference of the empirical distribution function at the quantiles 0.35 and 0.65, provides a good compromise between the accuracy (being not far from the true slope) and the precision (since it includes, in general, a large number of data points). The resulting standard error on the median is then computed from:

$$\sigma_m = \frac{1}{\sqrt{N}} \frac{x(0.65) - x(0.35)}{0.615} \qquad [1.3.16]$$

where the coefficient 0.615 (or, more rigorously, 0.61488) is chosen such that the expectation of σ_m gives the factor $\sqrt{\frac{\pi}{2}}$ for a Gaussian distribution.

Scatter: the distribution of observations is ideally characterised by a small number of well-chosen parameters, less numerous than the observations themselves, but more than merely the location and its standard error. The scatter should provide information on the real scatter due to the noise, without being too much influenced by the variability, i.e. by the extended wings of the distribution.

The scatter of the observations has also been computed from specific percentiles of the distribution, while avoiding redundancy with the other characterisations of the distribution. A good compromise was to take the nearly half 2σ-width:

$$s = \frac{x(0.85) - x(0.15)}{2} \qquad [1.3.17]$$

whose expectation is 1.035σ for a Gaussian distribution. For constant stars, s gives an indication of the standard error of the individual observations, while a comparison with the maximum and minimum (defined in terms of the 5th and 95th percentiles of the distribution) can be taken as indicative of possible variability, since (min−max)/3.289 should be close to the sigma of an individual observation for a constant star.

In all calculations of medians, errors on medians and scatter values, it was assumed that all observations used had identical variances. This is not really true, and detailed interpretations of errors on medians, scatter values and other percentiles based data should be avoided. However, the median values are not expected to be seriously affected by different weights, and the expression used for calculating the errors on the median values still holds.

Section 1.3 Appendix 2: Variability Indicators

Proper investigation of variability of Hipparcos stars required careful assessment of the estimated errors on the Hipparcos epoch photometry. These error estimates were derived from a small number (between 5 and 10) of individual observations, each taking between 0.1 and 2 seconds. By calculating the variance of the mean from so few data points, a well-known bias is introduced, described by a Student's t distribution. These biases were empirically corrected by comparing the observed distributions of residuals for all standard stars with the expected distributions, as a function of magnitude and estimated error. Smooth corrections were determined and applied to the error estimates to bring them into agreement with the observed distributions. The resulting unit weight variance of the photometric data of a standard star is very close to 1.

Using the distribution of unit weight residuals, a χ^2 test was performed, comparing the observed distribution with a standard distribution based on about 20 000 apparently non-variable stars. This comparison distribution was close to Gaussian with unit variance, and independent of magnitude and colour. In the χ^2 test the residuals were binned according to the number of observations available and compared with the comparison distribution binned in the same way. Figure 1.3.2 shows the distribution of χ^2 values for all stars with at least 40 observations. In the following the 'χ^2 probability' refers to the formal probability of the star being constant, as based on the χ^2 test performed on the distribution of its unit weight residuals. Peculiarities recognised in the photometric data are summarised in Field H52 as follows:

Case 'C': All probably constant stars with the χ^2 probability larger than 0.5. In this context, constant means that the maximum undetectable amplitude is smaller than a magnitude-dependent threshold.

Case 'D': The distribution of unit weight residuals could also be affected by duplicity and colour errors (if the $(V-I)_{\rm C}$ index used in the reductions was erroneous). Duplicity could be recognised from two statistics: a comparison between the median ac and dc magnitudes, and a comparison between the estimated errors on the median ac and dc magnitudes (see Figure 1.3.3). Both indicators used the fact that for a double star the modulation amplitude is disturbed, and often indicates the presence of a fainter image than would be implied from the mean intensity. As explained in Section 1.3.1, the ac magnitude based statistic cannot be used for stars with the component flag set. These stars are also recognised as double in the double star processing, and are indicated as 'D' in Field H52.

Case 'M': Only stars with a χ^2 probability of less than 10^{-4} were considered in this category. The intrinsic amplitude of variability can only be estimated under certain assumptions—the assumption that the underlying signal is sinusoidal is reasonable for most small-amplitude pulsating and rotational modulation variables. Furthermore, it is assumed that the observed unit weight variance (U) is the sum of the variances caused by the measurement errors (= 1.0) and the weighted intrinsic variations, $U = I + 1.0$. If the mean squared weight of an observation is given by W, then the dispersion of the intrinsic variations is given by $A = \sqrt{I/W}$. For a sinusoidal signal $a\sin(\phi)$ a random sampling would produce a dispersion $A = a/\sqrt{2}$. The peak-to-peak amplitude of the underlying signal is then given by $A \times 2\sqrt{2} = 2a$. When below 0.03 mag, the variable is considered to be a 'micro-variable'. The underlying amplitude was considered insignificant when the value for (U) was less than 1.1. The coarse variability estimator (Field H6) was also derived from this amplitude estimate, dividing the intrinsic variability into three groups according to variability amplitude: '1' : less than 0.06 mag; '2' : between 0.06 and 0.6 mag; and '3' : more than 0.6 mag.

Case 'P' and case 'U': Stars which appeared to be variable were subjected to various period-searching algorithms, as well as compared with data available in the literature.

Case 'R': The epoch photometry for a star calibrated using an erroneous $(V-I)_C$ colour index shows up through a gradient with time in the data, and a systematic offset between the ac and dc magnitudes. Certain cases were flagged as described in Field H52. However, neither the epoch photometry, the summary photometry (Fields H44–46 and H49–50), or the epoch photometry header records were modified—any erroneous secular trends remain in the epoch photometry.

There is a certain amount of overlap between the various categories defined above. In Field H52 of the main catalogue this was dealt with through a strict setting of precedences (the resulting numbers of entries within each category are also given under Field H52). Every star passed through the following set of checks, in the given order, until it fulfilled one:

'R' : stars with confirmed $(V-I)_C$ error;
'P' : stars in variability annex Section 1 (periodic);
'U' : stars in variability annex Section 2 (unsolved);
'D' : stars with increased noise level on ac photometry;
'␣' : insufficient data for χ^2 statistics;
'C' : stars with probability > 0.5 of being constant;
'␣' : probability of being constant between 0.5 and 10^{-4};
'D' : remaining double stars;
'␣' : insignificant amplitude of variations;
'M' : micro-variables with amplitude below 0.03 mag;
'U' : remaining unsolved variables, not included in variability annex Section 2.

Since the Hipparcos photometry is photon noise limited, the detection threshold for variability (or for assessing constancy) is strongly magnitude dependent. Caution must therefore be exercised in considering whether stars flagged 'C' in Field H52 may be used as photometric standard stars. Stars flagged 'C' fainter than $Hp = 10$ mag, for example, will include most BY Dra, α Can Ven, β Cephei, and some δ Scuti stars. The amount of undetected variability ranges from a few millimagnitudes for the brighter stars, to several tenths of a magnitude at the fainter end.

The minimum peak-to-peak amplitude for the detection of confirmed variability is given in Table 1.3.3, which corresponds to the upper curve given in Figure 2.1.1 (under Field H52). The threshold for stars to be undetectable as variable is a factor of typically 0.88 of the quoted values, corresponding to the lower curve in Figure 2.1.1. The intermediate region corresponds to entries identified as suspected variables. Depending on the application, photometric standard stars may be selected according to any given maximum acceptable scatter. For catalogue entries with a number of photometric observations, N, differing from the mean value of about 110 (the actual number being given in Field H47) the corresponding threshold, T_N, scales approximately as:

$$T_N = T_{110}\sqrt{110/N} \qquad [1.3.18]$$

where T_{110} is the threshold corresponding to the mean number of photometric observations.

Table 1.3.3. The minimum peak-to-peak amplitude for stars to be confirmed as variables. Stars having detected variability at these levels have a probability of being constant of less than 0.001.

Hp	T_{110}	Hp	T_{110}	Hp	T_{110}
4.5	0.010	7.5	0.022	10.5	0.063
5.0	0.011	8.0	0.026	11.0	0.076
5.5	0.012	8.5	0.031	11.5	0.098
6.0	0.013	9.0	0.037	12.0	0.124
6.5	0.015	9.5	0.044	12.5	0.18
7.0	0.018	10.0	0.052	13.0	0.36

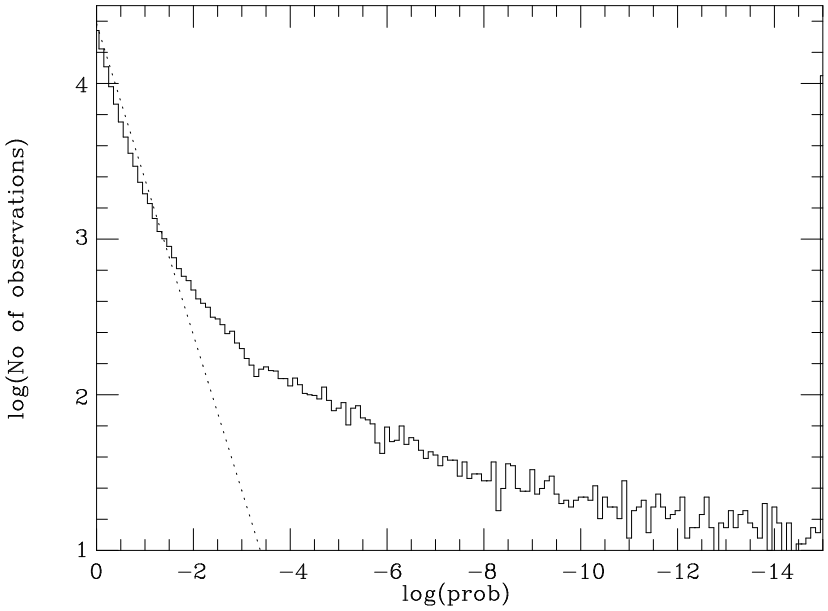

Figure 1.3.2. *The observed distribution of χ^2 values (full line) compared with the distribution for all stars being constant (dotted line).*

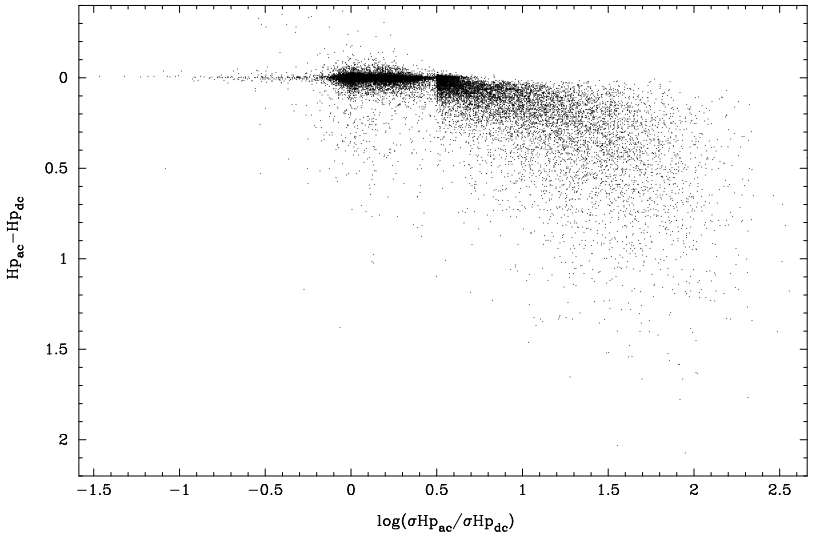

Figure 1.3.3. *The distribution of two statistical indicators of the Hipparcos Hp photometry. The noise ratio between the ac and the dc components increases for double stars, and the magnitude difference between the ac and dc components increases for double stars and extended objects. Variable stars can sometimes be found having smaller dispersion in the dc than in the ac component. For the central part of the diagram only a small selection of stars is displayed, in other parts all stars are shown.*

Section 1.3 Appendix 3: Period Optimisation and Amplitude Estimation

The periods detected with either the analysis of variance or the discrete Fourier analysis were hardly ever the optimal periods. The reason for this is that both methods assume certain characteristics of the data which in most cases are not fulfilled. This situation is made worse by the poor window functions characteristic of the Hipparcos data. Therefore, a simple procedure for fine-tuning the periods was developed that made use of the features of a given light curve. The following description applies strictly to the method used at the Royal Greenwich Observatory, whereas the method used at Geneva Observatory used different principles (see Volume 3 for details).

The first step was the fit of a spline function through the data, in such a way that the spline function was continuous in zero-, first- and second-order derivatives when going from phase 1 back to phase 0: the resulting fitted curve can be used as a periodic signal. The number of nodes and the positions of the nodes depend on the type of light curve and the total signal amplitude with respect to the noise on the data. In the case of some Algol-type variables a linear rather than a cubic spline was used.

If $f(\phi)$ is the function describing the light curve, and p is the period used to fold the signal, then the period correction can be obtained from a least-squares solution of the following observation equations:

$$O_i - f(\phi_i) = -\frac{t_i - t_0}{p}\frac{\Delta p}{p}\left(\frac{\partial f(\phi)}{\partial \phi}\right)_{\phi=\phi_i} \qquad [1.3.19]$$

where O_i represents observation i for which, when folded with period p the phase is given by $\phi_i = ((t_i - t_0)/p \bmod 1)$. The time of measurement (in barycentric Julian days) is give by t_i, while t_0 is an arbitrary zero-point roughly halfway through the total stretch of data. The new period is then $p' = p + \Delta p$.

The solution of this equation was iterated a few times with the solution for the curve fit $f(\phi)$, until period corrections became negligible. Solving the period through such an iteration had the advantage of optimising the period, while effectively putting most weight on those measurements that contain most information on the period: the measurements on the steepest parts of a light curve. The final solution provided an accuracy estimate for the period which, in most cases, appeared to be slightly on the optimistic side, and tends to depend to some extent on the actual curve fit $f(\phi)$. For automated processing, however, it was a practical solution, as it provided a measurement of the phases and magnitudes at minimum and maximum luminosity.

The amplitudes were derived from the maximum and minimum values of the fitted light curves. If the covariance matrix of the least-squares solution for $f(\phi)$ is given by A^{-1}, then the precision of the estimated value at a given phase ϕ can be derived from $\sigma f = s\sqrt{(f A^{-1} f^T)}$, where s is the standard deviation of the least-squares solution. The error on the amplitude was then calculated from the errors of the minimum and maximum magnitudes.

Section 1.3 Appendix 4: Photometric Transformations

The Hipparcos Hp photometry and the Tycho B_T and V_T photometry are the most substantial uniformly accurate collection of photometric data ever realised. At the time of the catalogue publication, the number of stars accurately measured by Hipparcos has already exceeded the number of stars measured in the major photometric system, Johnson UBV, during the past 45 years (some 108 000 stars).

The Hp magnitudes define a photometric reference system over the whole sky with an unprecedented accuracy, free from systematic errors as a function of right ascension or declination, and free from magnitude scale errors at the millimagnitude level. The Tycho two-colour system should also be considered as a new independent system, also free from systematic errors as a function of right ascension or declination, with only small departures from linearity at the bright and faint ends (at the faint end the possible systematic errors may be comparable to the quoted standard error). To avoid degrading these accuracies through approximate transformations it is recommended to use the magnitudes Hp, B_T and V_T directly, and to calibrate them in terms of astrophysical quantities.

Transformations used for the Tycho Catalogue

Using values of Johnson V_J and $(B-V)_J$ for 8000 standard stars with good Tycho (B_T, V_T) photometry, the following approximate linear transformations were derived between the two systems over the range $-0.2 < (B-V)_T < 1.8$:

$$\begin{aligned} V_J &= V_T - 0.090\,(B-V)_T \\ (B-V)_J &= 0.850\,(B-V)_T \end{aligned} \qquad [1.3.20]$$

giving errors generally below 0.015 mag in V_J and below 0.05 mag in $(B-V)_J$. The transformations apply to unreddened stars and ignore variations due to luminosity class. They should not be applied to M-type stars, even for $(B-V)_T < 1.8$ mag.

A more accurate transformation is obtained by linear interpolation of the values given in Table 1.3.4, where the factor G provides the slope of the local $(B-V)_J$ versus $(B-V)_T$ relation, and the values tabulated at the ends of the given interval are used for extrapolation. These relations have been used for the $(B-V)_J$ colour index given in the Tycho Catalogue. The formal errors on V_J and $(B-V)_J$ are well approximated by:

$$\sigma_{V_J} = \sqrt{1.09\,\sigma^2_{V_T} + 0.09\,\sigma^2_{B_T}} \qquad [1.3.21]$$

and:

$$\sigma_{(B-V)_J} = G \times \sigma_{(B-V)_T} \simeq G \times \sqrt{\sigma^2_{V_T} + \sigma^2_{B_T}} \qquad [1.3.22]$$

These equations do not take account of reddening and luminosity class (see Figure 1.3.6). The square root approximation in Equation 1.3.22 is only satisfactory if the errors of B_T and V_T are less than about 0.1 mag. For the computation of $\sigma_{(B-V)_J}$ in Field T38 the more accurate expression in Equation 1.3.12 has been used.

Table 1.3.4. Transformation from the Tycho photometric system to Johnson. The points given can be used in a linear interpolation, with deviations less than 0.005 mag from a more accurate spline fit.

$(B-V)_T$	≤ -0.2	0.1	0.5	1.4	≥ 1.8	
$V_J - V_T + 0.090(B-V)_T$	0.014	0.000	−0.005	−0.005	−0.015	
$(B-V)_J - 0.85(B-V)_T$	−0.006	0.000	0.046	−0.008	−0.032	
G-factor	0.85	0.87	0.97	0.79	0.79	0.85

Transformations used for the Hipparcos Catalogue

By construction, the Hp, B_T, V_T system is linked and normalised to the Johnson system by the conditions:

$$\begin{aligned} Hp &\equiv 0 \qquad \text{for } V_J = 0 \text{ and } B - V = 0 \\ V_T &\equiv 0 \qquad \text{for } V_J = 0 \text{ and } B - V = 0 \\ B_T &\equiv 0 \qquad \text{for } B_J = 0 \text{ and } B - V = 0 \end{aligned} \qquad [1.3.23]$$

The Relationship between Hp and V_J

The photometric data have been calibrated in the true instrumental Hp system as defined at a particular reference epoch. The actual response curve of Hp was a function of time, and the reference system that was implemented represents the Hp response for a date that was anticipated to be close to the middle of the mission, 1 January 1992. It applies strictly to the dc magnitudes (see Section 2.5 for details). There are very small differences in the time-dependent response function for the ac magnitudes, which have not been fully calibrated.

The definition of $(Hp - V_J)$ computed *a priori* on the basis of the instrumental calibration carried out on ground (on the basis of the nominal Hp response and stellar spectrophotometry) had to be revised in orbit for very red stars. The redetermination of the Hp response, and of the relation $(Hp - V_J)$, was problematic for stars redder than $(V - I)_C \sim 3.0$ mag because all such objects are highly variable, and therefore required simultaneous observations from the satellite and from the ground in order to provide a meaningful calibration.

The relationship was established by observing a set of long-period variables, of C and M type, with a CCD chain equipped with the Cousins' I band and Johnson/Geneva V band, in order to obtain $(V - I)_C$ and, immediately before or after, to measure the same Mirae with a classical photometer, to provide the original V_J magnitude. In parallel, AAVSO observers were requested to monitor these stars. This made it possible to define the relation $(V_{CCD} - V_J)$ versus $(V - I)_C$ and, at the epochs of photoelectric observations, the relations $(V_{AAVSO} - V_{CCD})$ and $(V_{AAVSO} - V_J)$. Hp magnitudes were deduced from the non-linear relations $(V_{AAVSO} - Hp)$ versus V_{AAVSO} as observed during the mission.

The resulting $(Hp - V_J)$ versus $(V - I)_C$ is very well defined from classical photometry in the range $-0.4 < V - I < 3.0$ mag, with uncertainties of less than 0.01 mag. The red extension down to $V - I = 5.4$ mag was defined using Mirae, with an uncertainty of 0.03–0.05 mag. Between $V - I = 3.8 - 5.4$ mag, this relation is linear. The values down to $V - I = 9.0$ mag follow from a linear extrapolation: they are given in order to cover the whole range of $(V - I)_C$ colours in the Hipparcos Catalogue.

The relation given in Table 1.3.5 holds, in principle, for O, B, A, F, G < G5 stars with low reddening, and for G5 to M8 giants. The relation for G, K and M dwarfs is given in Table 1.3.6. The difference between both relations is rather small, i.e. less than 0.030 mag. Figure 1.3.4 shows the transformations in graphical form.

Restrictions on the validity of these transformation equations for peculiar stars are the same as those described under the transformations for $(B - V)$ versus $(B_T - V_T)$.

Table 1.3.5. $(Hp - V_J)$ versus $(V - I)_C$ for spectral types O to G5 luminosity class II to V, and red giants of types G5III to M8III.

$V-I$	$Hp-V_J$	$V-I$	$Hp-V_J$	$V-I$	$Hp-V_J$	$V-I$	$Hp-V_J$
−0.50	−0.182	0.40	0.082	1.30	0.153	2.90	−0.065
−0.45	−0.164	0.45	0.089	1.35	0.147	3.00	−0.090
−0.40	−0.145	0.50	0.097	1.40	0.140	3.20	−0.155
−0.35	−0.126	0.55	0.106	1.45	0.135	3.40	−0.235
−0.30	−0.107	0.60	0.115	1.50	0.128	3.60	−0.325
−0.25	−0.088	0.65	0.125	1.60	0.116	3.80	−0.425
−0.20	−0.070	0.70	0.133	1.70	0.106	4.00	−0.535
−0.15	−0.053	0.75	0.141	1.80	0.096	4.20	−0.65
−0.10	−0.035	0.80	0.147	1.90	0.090	4.40	−0.76
−0.05	−0.018	0.85	0.154	2.00	0.082	4.60	−0.87
0.00	0.002	0.90	0.159	2.10	0.072	4.80	−0.98
0.05	0.018	0.95	0.164	2.20	0.060	5.00	−1.10
0.10	0.036	1.00	0.167	2.30	0.048	5.50	−1.38
0.15	0.050	1.05	0.168	2.40	0.032	6.00	−1.66
0.20	0.061	1.10	0.168	2.50	0.018	6.50	−1.94
0.25	0.068	1.15	0.165	2.60	0.001	7.00	−2.22
0.30	0.072	1.20	0.162	2.70	−0.018	8.00	−2.78
0.35	0.076	1.25	0.157	2.80	−0.040	9.00	−3.34

Table 1.3.6. $(Hp - V_J)$ versus $(V - I)_C$ for G, K, M dwarfs with $(V - I)_C > 0.70$ mag.

$V-I$	$Hp-V_J$	$V-I$	$Hp-V_J$	$V-I$	$Hp-V_J$	$V-I$	$Hp-V_J$
0.70	0.133	1.10	0.138	1.50	0.108	2.20	0.051
0.75	0.137	1.15	0.133	1.55	0.105	2.30	0.041
0.80	0.140	1.20	0.129	1.60	0.102	2.40	0.034
0.85	0.142	1.25	0.125	1.70	0.093	2.50	0.022
0.90	0.144	1.30	0.122	1.80	0.085	2.60	0.001
0.95	0.146	1.35	0.119	1.90	0.076	2.70	−0.023
1.00	0.145	1.40	0.115	2.00	0.066		
1.05	0.142	1.45	0.112	2.10	0.058		

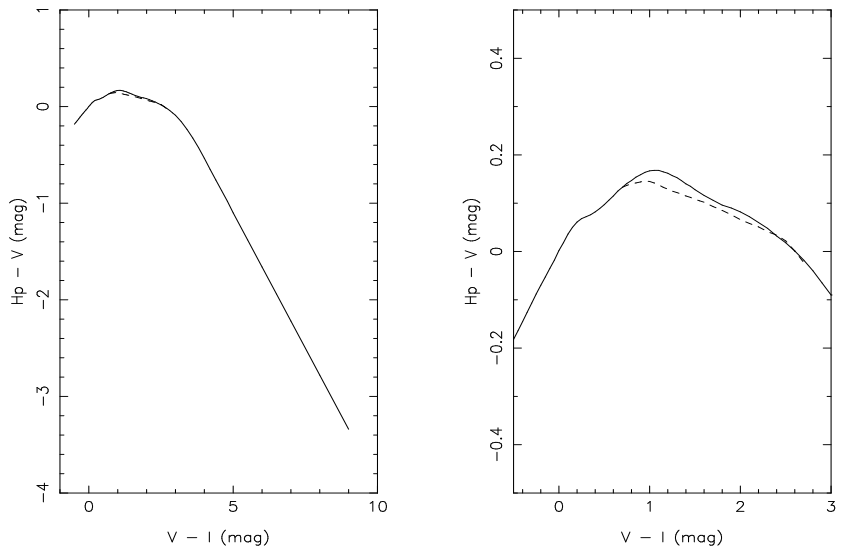

Figure 1.3.4. *The relation* $(Hp - V_J)$ *versus* $(V-I)_C$ *for different ranges of* $(V-I)_C$. *Solid lines: for spectral types O to G5 luminosity class II to V, and red giants of types G5III to M8III (from Table 1.3.5). Dashed lines: for G, K, M dwarfs with* $(V-I)_C$ *>0.70 mag (from Table 1.3.6).*

$(B-V)$ derived from $(B_T - V_T)$

Since the Tycho passbands, B_T and V_T (and in particular B_T), are different from the corresponding Johnson B, spectral features such as Balmer lines or molecular lines for late-type stars introduce differential effects, as do interstellar or circumstellar reddening. As a consequence, different relations are applicable to various spectral ranges, and must be separately applied in order to minimise the residuals arising from the transformation. The most sensitive spectral types from this point of view are the A-type stars, late-M, and Carbon stars. The following relations were used in the determination of the $B-V$ index based on $B_T - V_T$ (see Field H39) as a function of spectral type. Figure 1.3.5 illustrates the luminosity dependence and Figure 1.3.6 illustrates the effects of reddening for cases (a–c).

(a) for dwarfs (luminosity class V):

$B_T - V_T < 0.345$:

$$(B-V) = (B_T - V_T) + 0.021 - 0.130z - 0.08z^2 + 0.430z^3$$
$$z = B_T - V_T + 0.15 \qquad [1.3.24]$$

$0.345 < B_T - V_T < 0.50$:

$$(B-V) = (B_T - V_T) - 0.041 - 0.262z - 0.30z^2 + 1.030z^3$$
$$z = B_T - V_T - 0.60 \qquad [1.3.25]$$

$0.50 < B_T - V_T$:

$$(B-V) = (B_T - V_T) - 0.115 - 0.229z + 0.043z^3$$
$$z = B_T - V_T - 0.90 \qquad [1.3.26]$$

(b) for giants (luminosity class III with low reddening) with $B_T - V_T < 1.7$ mag:

$B_T - V_T < 0.65$:

$$(B-V) = (B_T - V_T) - 0.010 - 0.060z - 0.14z^3$$
$$z = B_T - V_T - 0.22 \qquad [1.3.27]$$

$0.65 < B_T - V_T < 1.10$:

$$(B-V) = (B_T - V_T) - 0.113 - 0.258z + 0.40z^3$$
$$z = B_T - V_T - 0.95 \qquad [1.3.28]$$

$1.10 < B_T - V_T$:

$$(B-V) = (B_T - V_T) - 0.173 - 0.220z + 0.01z^3$$
$$z = B_T - V_T - 1.20 \qquad [1.3.29]$$

(c) for late K giants, and luminous G and K stars (luminosity class I to II) with $B_T - V_T > 1.7$ mag:

$1.0 < B_T - V_T < 2.2$:

$$(B-V) = (B_T - V_T) - 0.173 - 0.220z + 0.01z^2$$
$$z = B_T - V_T - 1.20 \qquad [1.3.30]$$

(d) for Carbon stars, often surrounded by dust and showing extreme red colours:

$$(B-V) = +0.19 + 0.73\,(B_T - V_T) \qquad [1.3.31]$$

(e) for M giants, affected by the presence of TiO bands:

$$(B-V) = +0.046 + 0.824\,(B_T - V_T) \qquad [1.3.32]$$

When no luminosity classification was available, the relation defined for luminosity class III giants was used.

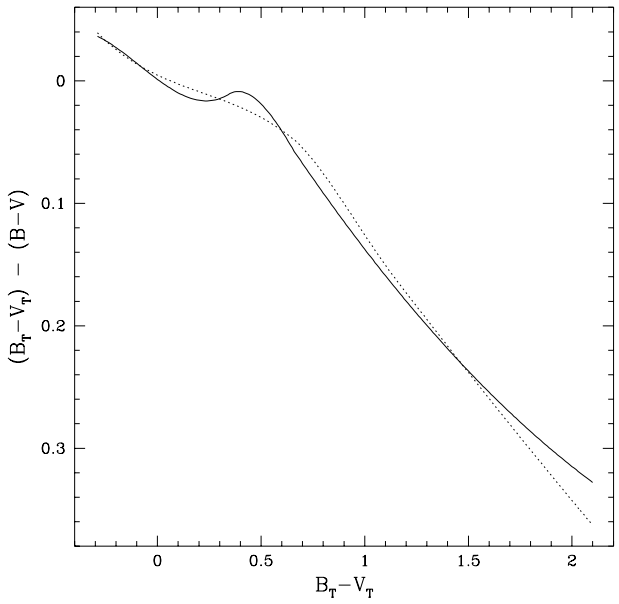

Figure 1.3.5. *The luminosity dependence of* $(B-V)$ *on* (B_T-V_T)*. The solid line corresponds to luminosity class V stars, while the dotted line corresponds to class III giants. The gravity effect, observable primarily through different absorption from the Balmer lines in* B_T *and* V_T*, reaches a maximum at around* B_T-V_T *~0.4 mag.*

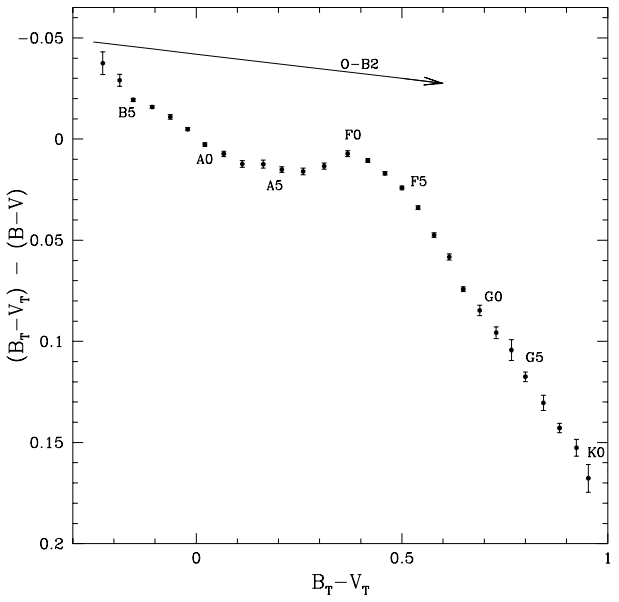

Figure 1.3.6. *The effect of reddening on the relationship between* $(B-V)$ *and* (B_T-V_T)*. The circles indicate the observed relationship for luminosity class V stars with accurate photoelectric photometry. The solid line shows the mean reddening direction for O–B2 stars (independent of luminosity class). Reddening for later-type stars moves the corresponding points parallel to this line.*

V_J derived from V_T

(a) for early-type stars and red stars up to and including K-type, the following relation is applicable to both dwarfs and giants:

$$V_J = V_T + 0.0036 - 0.1284(B_T - V_T) + 0.0442(B_T - V_T)^2 - 0.015(B_T - V_T)^3 \quad [1.3.33]$$

(b) for Carbon stars (R, N, C):

$$V_J = V_T + 0.007 - 0.024(B_T - V_T) - 0.023(B_T - V_T)^2 \quad [1.3.34]$$

(c) for M giants, the differential absorption by TiO, depending on the stellar temperature, metallicity, and gravity, means that the index $V_T - V_J$ becomes unrelated to $B_T - V_T$, since $(B_T - V_T)$ reaches a saturation value around 1.95, and then decreases again to about 1.45 for M5 stars. An indirect approach, allowing the degeneracy for M stars to be circumvented, consists of first evaluating the $V - I$ index from the $(Hp - V_T)$ versus $(B_T - V_T)$ relation, then applying a $(V_T - V_J)$ correction as a function of $(V - I)$ (see Figure 1.3.7). This results in the following relations:

$$\begin{aligned} V - I &= 3.55 - 2.44(dH + 0.60) - 0.60(dH + 0.60)^2 \qquad dH < 0.25 \\ V - I &= 2.02 - 6.00(dH + 0.12) - 11.0(dH + 0.12)^2 \qquad dH > 0.25 \end{aligned} \quad [1.3.35]$$

where $dH = (Hp - V_T) - 0.41(B_T - V_T - 1.9)^2$. V_J is then given by:

$$V_J = V_T - 0.20 - 0.03(V - I - 2.15) - 0.011(V - I - 2.15)^2 \quad [1.3.36]$$

(d) for M dwarfs, no relation between V_J and V_T has been defined, since all are too faint in B_T to provide a $B_T - V_T$ index precise enough to determine V_J from V_T and $B_T - V_T$.

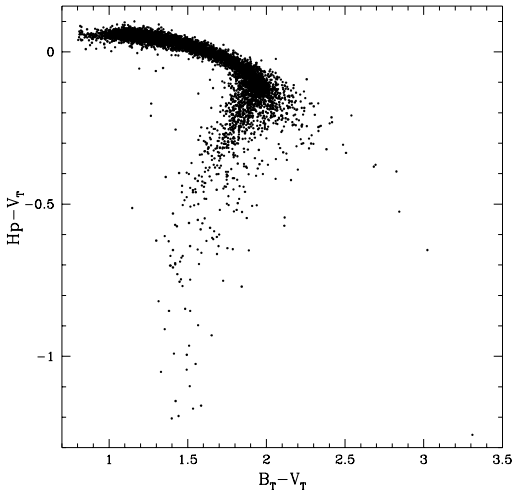

Figure 1.3.7. *The observed $(Hp - V_T)$ versus $(B_T - V_T)$ diagram for red giants. The G and K giants, and some Carbon stars, occupy the well-populated upper part of the diagram extending roughly horizontally up to $B_T - V_T$ ~2 mag (with reddened objects continuing in a descending arc towards the bottom right of the figure). The O-rich M stars form the descending sequence, with a vertical displacement from the region populated by the G–K giants being a direct measurement of the differential absorption on Hp and V_T, and directly related to the $V - I$ index (the decrease of $(B_T - V_T)$ with decreasing $Hp - V_T$ is due to an excess of TiO absorption on V_T relative to B_T).*

Section 1.3 Appendix 5: Determination of the $V - I$ Colour Index

The flag in Field H42 indicates the method adopted to estimate $(V - I)_C$. Twenty different methods were defined and applied in order to produce $(V-I)_C$ for all Hipparcos stars, and in the description below they are ranked according to their hierarchy of application. The reliability of the methods used may be inferred through the standard error on $(V - I)_C$ given in Field H41.

The $(V - I)_C$ colour index was determined to be the most appropriate to correct for chromatic residuals in the reduction of the astrometric data and, more importantly, for the photometric reductions, where the magnitudes were affected by colour-dependent transmission losses. In the context of Hipparcos, the $(V - I)_C$ index provided a way of monitoring and correcting for the chromatic evolution of the optics, applicable to stars of all colours, including the reddest long-period variables.

For a small fraction of the stars, the genuine Cousins' $(V - I)_C$ was available. Only when $(V - I)_C$ was derived from similar photometric systems are the photometric properties of this index, such as a temperature estimator with little dependence on reddening or metallicity, preserved.

When derived from other colour indices, the abundance and reddening dependencies affecting these indices are propagated into the resulting pseudo $(V - I)_C$ index. In stars with VRI photometry, an approximate $(V - I)_C$ was transformed from ground-based multi-colour photometric data, or from star mapper data with or without spectral-type information, or from a combination of an approximate $(B - V)$ and of the spectral type. Multi-colour photometric data necessary to produce $(V - I)_C$ were extracted from the General Catalogue of Photometric Data (GCPD), compiled at the Lausanne Institute of Astronomy (B. Hauck *et al.*, 1990, *Astronomy & Astrophysics Supplement*, 85, 989–998), and updated at mid-mission and at the end of the data reduction process.

For late-type stars, distinct relations were used for main-sequence and for giants, assuming a solar metallicity. The separation between dwarfs and giants was made according to an 'absolute magnitude estimator' (see method I). Ambiguous cases were treated individually using all external information, including some of the Hipparcos absolute magnitudes.

V, R, I Photometry (A–G)

Field H42 = A: $(V - I)_C$ measured directly in the Cousins' system. Only 2989 Hipparcos programme stars had genuine Cousins' $(V - I)_C$ colour index. They are mainly nearby parallax stars and metal poor stars. When several sources of data were available the weighted mean, and the precision on the mean $(V - I)_C$, were computed.

Field H42 = B: If only $(V - R)_C$ was available, the following transformations were applied:

$(V - R)_C$	$(V - I)_C$
< 0.0	$2.50\,(V - R)_C$
$[0.0, 0.6]$	$2.04\,(V - R)_C - 0.205\,(V - R)_C^2$
$[0.6, 1.0]$	$1.60\,(V - R)_C + 0.61\,(V - R)_C^2 - 0.034$
> 1.0	$2.70\,(V - R)_C - 0.52$

Field H42 = C: When stars were measured in the Johnson V, R, I system, and only $(V-I)_J$ was available, the following relations were used—when V_J and I_J were published separately, a zero point shift was needed to convert the raw magnitude difference into the classical $(V-I)_J$:

$(V-I)_J$	$(V-I)_C$
< 0.0	$0.713\,(V-I)_J$
$[0.0, 2.0]$	$0.778\,(V-I)_J$
$]2.0, 3.0]$	$0.835\,(V-I)_J - 0.13$

Field H42 = D: When stars were measured in the Johnson V, R, I system, and only $(V-R)_J$ was available, it was transformed into $(V-R)_C$ by the following relations (and then into $(V-I)_C$ by the relations given for method B):

$(V-R)_J$	$(V-R)_C$
< 1.0	$0.73\,(V-R)_J - 0.03$
> 1.0	$0.62\,(V-R)_J - 0.03$

Field H42 = E: When stars were measured in the Kron-Eggen V, R, I system, and $(V-I)_K$ was known, the transformation used was:

$(V-I)_K$	$(V-I)_C$
< 0.5	$0.936\,(V-I)_K + 0.27$
> 0.5	$1.000\,(V-I)_K + 0.24$

Field H42 = F: When stars were measured in the Kron-Eggen V, R, I system, and only $(R-I)_K$ was known, it was transformed into $(R-I)_C$ as follows:

$(R-I)_K$	$(R-I)_C$
$[0.29, 0.65]$	$1.049\,(R-I)_K + 0.092$
$]0.65, 1.15]$	$1.205\,(R-I)_K - 0.008$

$(R-I)_C$ was then transformed into $(V-I)_C$ as follows:

$(R-I)_C$	$(V-I)_C$
< 0.10	$1.69\,(R-I)_C$
$[0.10, 0.50]$	$2.26\,(R-I)_C - 0.05$
$]0.50, 0.75]$	$1.84\,(R-I)_C + 0.17$
> 0.75	$1.49\,(R-I)_C + 0.43$

Field H42 = G: When several V, R, I sources were available, a weighted mean was computed and the resulting $(V-I)_C$ index compiled using the appropriate combination of methods described above.

Multi–colour Photometry (H–K)

Field H42 = H: The $(B-V)_J$ colour from Johnson UBV system was transformed into $(V-I)_C$ according to the following transformations tabulated separately for early-type stars and red giants, and for late-type dwarfs. For stars with $(B-V)_J < 0.9$ mag, $(V-I)_C$ was interpolated in Table 1.3.7. Other categories derived from Table 1.3.7 are discussed under Field H42 = I, J, and K.

When stars had been observed in the Geneva, Strömgren and Walraven systems, colour indices of each system were first transformed into $(B-V)_J$, then transformed into $(V-I)_C$, as in the case of Johnson UBV data. Method H was used irrespective of the multi–colour system(s) used to produce $(V-I)_C$.

Table 1.3.7. $(V-I)_C$ versus $(B-V)_J$ for early-type stars and red giants

$(V-I)_C$	$(B-V)_J$	$(V-I)_C$	$(B-V)_J$	$(V-I)_C$	$(B-V)_J$	$(V-I)_C$	$(B-V)_J$
−0.379	−0.345	0.190	0.174	0.804	0.765	1.334	1.365
−0.299	−0.276	0.252	0.228	0.847	0.825	1.392	1.413
−0.231	−0.216	0.331	0.291	0.897	0.893	1.473	1.464
−0.168	−0.164	0.412	0.351	0.946	0.960	1.567	1.527
−0.105	−0.119	0.482	0.415	0.995	1.021	1.617	1.550
−0.050	−0.072	0.553	0.482	1.050	1.088	1.644	1.568
0.002	−0.020	0.617	0.543	1.107	1.143	1.724	1.583
0.040	0.021	0.667	0.597	1.155	1.196	1.831	1.604
0.072	0.062	0.722	0.659	1.211	1.253	1.882	1.615
0.124	0.110	0.770	0.717	1.271	1.311	2.021	1.635

Field H42 = I: Redder stars were separated into red giants, red dwarfs and long-period variables according to the value of the absolute magnitude estimator, M, defined as follows:

$$M = V_J + 5.0 \log_{10} (\text{proper motion}) + 1.505$$

where the proper motion is expressed in arcsec/yr. M larger than 5.2 indicates a late-type dwarf or a high-velocity giant. Marginal cases were treated star by star. For red giants with $(B-V)_J < 1.25$ mag, $(V-I)_C$ was derived from Table 1.3.7. Otherwise, for these late-type K and M dwarfs, $(V-I)_C$ was derived (Table 1.3.8) as follows:

Table 1.3.8. $(V-I)_C$ versus $(B-V)_J$ for late-type K and M dwarfs

$(V-I)_C$	$(B-V)_J$	$(V-I)_C$	$(B-V)_J$	$(V-I)_C$	$(B-V)_J$	$(V-I)_C$	$(B-V)_J$
0.631	0.550	1.042	0.999	1.567	1.348	2.725	1.650
0.670	0.601	1.103	1.050	1.645	1.390	2.874	1.700
0.707	0.648	1.175	1.100	1.785	1.445	3.008	1.750
0.747	0.699	1.244	1.149	1.905	1.472	3.144	1.800
0.788	0.749	1.333	1.199	2.054	1.498	3.478	1.900
0.840	0.800	1.386	1.228	2.255	1.524	3.630	1.955
0.893	0.850	1.410	1.250	2.440	1.550	4.100	2.114
0.941	0.898	1.494	1.300	2.544	1.575	4.328	2.198
0.997	0.949	1.535	1.326	2.601	1.600	4.630	2.300

Field H42 = J: Stars redder than $(B-V)_J = 1.25$ mag were treated according to their spectral type. For R, N, C type stars, the following linear relation was adopted:

$$(V-I)_C = 1.042\,(B-V)_J - 0.047$$

Reddened F, G, K < K5 stars, with $B-V > 1.55$ mag, follow the same relation. Otherwise their $(V-I)_C$ were interpolated in Table 1.3.7.

Field H42 = K: For giant stars later than K4, $(B-V)_J$ and $(V-I)_C$ become affected by TiO bands absorption. At a given $(B-V)_J$, the departure from the linear relation defining $(V-I)_C$ used for method J is a steep function of the spectral type, especially for the late-M sub-types. S and M types were not distinguished here. In this case, $\sigma_{(V-I)_C}$ is equal to $1.042\sigma_{(B-V)_J}$ added quadratically to σ_{type}, the observed scatter in $(V-I)_C$ for a given K or M sub-type.

Table 1.3.9. $(V-I)_C$ versus $(B-V)_J$ for giants later than K4

Type	$(V-I)_C$	σ_{type}	Type	$(V-I)_C$	σ_{type}
K5	$1.042\,(B-V)_J - 0.015$	0.09	M4	$1.042\,(B-V)_J + 0.978$	0.50
K5-9	$1.042\,(B-V)_J - 0.045$	0.14	M4.5	$1.042\,(B-V)_J + 1.329$	0.75
M0	$1.042\,(B-V)_J + 0.109$	0.15	M5	$1.042\,(B-V)_J + 1.679$	0.83
M0.5	$1.042\,(B-V)_J + 0.184$	0.16	M5.5	$1.042\,(B-V)_J + 2.040$	0.82
M1	$1.042\,(B-V)_J + 0.259$	0.17	M6	$1.042\,(B-V)_J + 2.399$	0.80
M1.5	$1.042\,(B-V)_J + 0.333$	0.18	M6.5	$1.042\,(B-V)_J + 2.754$	0.80
M2	$1.042\,(B-V)_J + 0.408$	0.21	M7	$1.042\,(B-V)_J + 3.109$	0.80
M2.5	$1.042\,(B-V)_J + 0.518$	0.22	M8.5	$1.042\,(B-V)_J + 3.459$	0.80
M3	$1.042\,(B-V)_J + 0.628$	0.30	M8	$1.042\,(B-V)_J + 3.820$	0.80
M3.5	$1.042\,(B-V)_J + 0.803$	0.37	M8+	$1.042\,(B-V)_J + 4.170$	0.80

$V-I$ from Hipparcos and Star Mapper Photometry (L–P)

At the beginning of the mission some 50 800 programme stars had no accurate ground-based photoelectric photometry, but were subsequently observed by the satellite's star mapper. The reduction of brighter star transits led to provisional B_T and V_T magnitudes. An updating of approximate $(B-V)_J$ given in the Hipparcos Input Catalogue was made at mid-mission using these provisional values, thus allowing an improvement in the final photometric and astrometric reductions to be made. Stars of types O to K4 had to be processed differently from the later type stars, the division being made according to the object's location in the provisional $(Hp-V_T)/(B_T-V_T)$ diagram.

At the very end of the data reduction phase the final Tycho photometric data then became available for about 113 000 stars. Most of the non-photoelectric $(V-I)_C$ could then be superseded by more accurate $(V-I)_C$ determined from (B_T-V_T) and partly from the relationship $(Hp-V_T)$ versus (B_T-V_T).

Except for M giants, (B_T-V_T) were first transformed into $(B-V)$ and then into $(V-I)_C$. Although carried out according to methods H, I, and J, these entries are all labelled as method L since they used colour indices from Tycho. M giants had their $(V-I)_C$ determined from an updated version of method O given under the description of the (B_T-V_T) to $(B-V)$ transformations in Section 1.3, Appendix 4. They are still flagged as method O.

As a result, methods M–P described below have an almost historical character, since they refer to stars, not reprocessed with the final Tycho photometric data; furthermore, since they make use of intermediate Hp and B_T-V_T which are no longer valid, the affected indices carry the subscript '*'.

Field H42 = L: The condition $(Hp-V_T)_*-0.786\,(B_T-V_T)_*+1.272<0$ selects stars without TiO absorption. Blue stars show a linear relation between $(B_T-V_T)_*$ and $(V-I)_C$. For $(B_T-V_T)_*<-0.05$ mag:

$$(V-I)_C = 1.192\,(B_T-V_T)_* + 0.058$$

For $-0.05<(B_T-V_T)_*<1.80$ mag, $(V-I)_C$ was obtained by interpolation in Table 1.3.10.

Table 1.3.10. $(V-I)_C$ versus $(B_T-V_T)_*$ for O to G stars, and K < K5 giants

$(V-I)_C$	$(B_T-V_T)_*$	$(V-I)_C$	$(B_T-V_T)_*$	$(V-I)_C$	$(B_T-V_T)_*$	$(V-I)_C$	$(B_T-V_T)_*$
−0.302	−0.326	0.136	0.152	0.597	0.557	0.977	1.151
−0.250	−0.258	0.177	0.193	0.630	0.591	1.006	1.200
−0.184	−0.202	0.217	0.225	0.658	0.642	1.040	1.250
−0.132	−0.165	0.248	0.252	0.690	0.684	1.075	1.300
−0.101	−0.135	0.284	0.282	0.719	0.726	1.112	1.350
−0.059	−0.096	0.337	0.317	0.754	0.773	1.155	1.400
−0.007	−0.047	0.398	0.357	0.790	0.829	1.210	1.467
0.024	0.014	0.441	0.392	0.832	0.892	1.262	1.536
0.053	0.052	0.476	0.429	0.866	0.957	1.330	1.611
0.069	0.085	0.529	0.480	0.908	1.026	1.403	1.679
0.103	0.118	0.569	0.520	0.939	1.084	1.492	1.756
						1.600	1.809

Field H42 = M: For stars with $(Hp-V_T)_*-0.786\,(B_T-V_T)_*+1.272>0$, the following relation was used for reddened G and K < K5 stars (assumed to be giants):

$$(V-I)_C = 1.156\,(B_T-V_T)_* - 0.532$$

Field H42 = N: For stars with $(Hp-V_T)_*-0.786\,(B_T-V_T)_*+1.272>0$, the following relations were used for K5 to M0.5 giants:

Type	$(V-I)_C$
K5	$1.156\,(B_T-V_T)_* - 0.500$
K5.5	$1.156\,(B_T-V_T)_* - 0.440$
M0	$1.156\,(B_T-V_T)_* - 0.376$
M0.5	$1.156\,(B_T-V_T)_* - 0.301$

Field H42 = O: For later M giants and for Carbon stars, iso-$(V-I)_C$ lines were defined in the $(Hp-V_T)_*/(B_T-V_T)_*$ diagram. For stars bluer than $(B_T-V_T)_*=2.8$ mag, $(V-I)_C$ was obtained for unreddened and reddened stars as follows:

(a) for $(Hp-V_T)_*-0.41\,[(B_T-V_T)_*-1.9]^2<0.05$:

$$(V-I)_C = -5.4\,\{(Hp-V_T)_*-0.41\,[(B_T-V_T)_*-1.9]^2\}+2.61$$

(b) for $(Hp-V_T)_*-0.41\,[(B_T-V_T)_*-1.9]^2>0.05$:

$$(V-I)_C = -7.0\,\{(Hp-V_T)_*-0.41\,[(B_T-V_T)_*-1.9]^2\}+2.68$$

Field H42 = P: Stars with $(B_T-V_T)_*>2.8$ mag are either Carbon stars or reddened G, K, or M supergiants. Their $(V-I)_C$ was estimated by the relation:

$$(V-I)_C = 0.890\,(B_T-V_T)\,* - 0.005$$

Long-Period Variables (Q)

Field H42 = Q: Long-period variables required a special treatment. Very few have been monitored over the whole light-curve cycle. In the photometric data base, the colour and the magnitude at maximum luminosity is normally given, rather than a mean colour index and magnitude, which are rarely defined. In order not to underestimate their mean colour index, the spectral type at maximum and minimum luminosity were searched for in the literature. This information was missing in the Hipparcos Input Catalogue, since complex spectral types were truncated.

A mean type was computed for each long-period variable; $(V-I)_C$ and $\sigma_{(V-I)_C}$ were deduced by linear interpolation in Table 1.3.11. Since the $E(V-I)_C$ colour excess is smaller than $E(B-V)$, at given A_V interstellar extinction, no attempt was made to correct $(V-I)_C$ for reddening. For emission line variables (suffix e), S stars, or for long-period variables with only one spectrum available, $\sigma_{(V-I)_C}$ = 1.20 mag was adopted.

Table 1.3.11. $(V-I)_C$ versus M sub-type for long-period variables

Type	$(V-I)_C$	$\sigma_{(V-I)}$	Type	$(V-I)_C$	$\sigma_{(V-I)}$	Type	$(V-I)_C$	$\sigma_{(V-I)}$
K5.5	1.61	0.14	M3	2.25	0.30	M6.5	4.32	0.80
M0	1.68	0.15	M3.5	2.40	0.37	M7	4.66	0.80
M0.5	1.76	0.16	M4	2.59	0.50	M7.5	5.03	0.80
M1	1.84	0.17	M4.5	2.91	0.75	M8	5.38	0.80
M1.5	1.94	0.18	M5	3.25	0.83	M8.5	5.75	0.80
M2	2.02	0.21	M5.5	3.61	0.82	M9	6.12	0.80
M2.5	2.13	0.22	M6	3.96	0.80	M10	6.80	1.20
Md	2.91	1.20	Me	3.00	1.20			

Stars without Colour, etc. (R–T)

Field H42 = R: When stars had no satellite colours nor photoelectric data, but an approximate V magnitude and a spectral type, and possibly a luminosity class, the intrinsic $(B-V)_J$ was derived from the spectral type. The reddened $(B-V)_J$ was estimated through a model galactic interstellar extinction, as a function of galactic coordinates and distance from the Sun (F. Arenou *et al.*, 1992, *Astronomy & Astrophysics*, 258, 104–111).

The $(V-I)_C$ was then deduced as in the case of genuine Johnson UBV data (method H), unless the stars are very red, reddened or of type M, R, S, N or C. For such stars the procedure was as for the photoelectric data (methods I to K).

Field H42 = S: When stars were reduced to the standard Hp system with an erroneous $(V-I)_C$ colour, the chromatic magnitude change, due to the irradiation of the optics in the space, was not adequately corrected. The resulting linear drift of magnitude could be used to recompute the true $(V-I)_C$. When the discrepancy was large and the stars non variable, the following relation was applied, where dHp/dt is the derivative of Hp, in magnitudes per day:

$$(V-I)_{new} = (V-I)_{old} - 1.429 \times 10^4 \, dHp/dt$$

Field H42 = T: This flag is used to signify stars with unknown colours reduced with $(V-I)_C = 0.666$ mag (Field H75), and also indicates entries where the final $V-I$ index was left blank. The latter was adopted when the final σ_{V-I} exceeded 0.25 mag for entries with $V-I < 1.5$ mag; the $(V-I)$ indices for redder stars, in particular long-period variables, are intrinsically inaccurate and were therefore retained in the catalogue independent of their associated errors (see Field H40).

Statistics

The number of entries in each of these categories is as follows:

H42	No.	H42	No.
A	2829	K	823
B	175	L	74269
C	1048	M	34
D	32	N	20
E	730	O	2631
F	455	P	13
G	209	Q	76
H	28369	R	1477
I	3170	S	177
J	406	T	1275

Section 1.4

Double and Multiple Systems

1.4. Double and Multiple Systems

This section provides the information necessary to interpret and use the results appearing under the header 'Multiplicity Data' of the main Hipparcos Catalogue (Fields H55–67, see Section 2.1), and the contents of the Double and Multiple Systems Annex (see Section 2.3). More extensive details of the processing of double and multiple star data are given in Volume 3.

1.4.1. Complications Arising from the Observations

The presence of double systems severely complicated the entire Hipparcos Catalogue production. If all the stars observed by the satellite had been single, and centred in the detector's instantaneous field of view, the five astrometric parameters per star would have been well constrained by the global observations. A well-defined reference system, and well-behaved photometric results, would have been obtained by a relatively straightforward process. Double or multiple systems, however, resulted in one-dimensional positions on the reference great circles which changed according to the satellite's scanning direction and the measurement epoch. These instantaneous positions had no well-defined common physical meaning for double star systems, except for close pairs (with separations less than about 0.30 arcsec) where the photocentre of the system was a good approximation to the Hipparcos observations. Careful screening of the observations and dedicated processing were necessary to avoid this having an effect on the resulting reference system at the level of the reference great circles, or at the level of the sphere solution.

In cases of detected duplicity the observation model had to be extended from the standard single-star model, essentially on a case-by-case basis, to account for resolved systems, systems with moving components, astrometric binaries, and multiple systems. Similar complications appeared when the magnitudes of individual components were derived from the combined detector signal. An additional difficulty was caused by the finite size of the detector's instantaneous field of view, of around 30 arcsec diameter. This meant that many double systems with separations comparable to this size had their astrometry and photometry affected by the resulting attenuation in the detector's response (Figure 1.4.1).

Systems with separations $< 0.1-0.15$ arcsec or magnitude differences $> 3.5-4$ mag were at the limit of what could be recognised as non-single and measured. The sensitivity of the detection and the quality of the solutions were also dependent on the ecliptic latitude of the star, as a consequence of the variation of sky coverage and scanning geometry resulting from the ecliptic-based scanning law. Although considerable attention was given to the optimised design of the modulating grid of the Hipparcos satellite to the detection of double stars, there are 'grey areas' in the parameter space where the astrometry and photometry of double and multiple systems must be considered as poorly defined. An additional problem was in trying to reconcile the Hipparcos results with relevant information (for example, system and component designation) already available from ground-based observations.

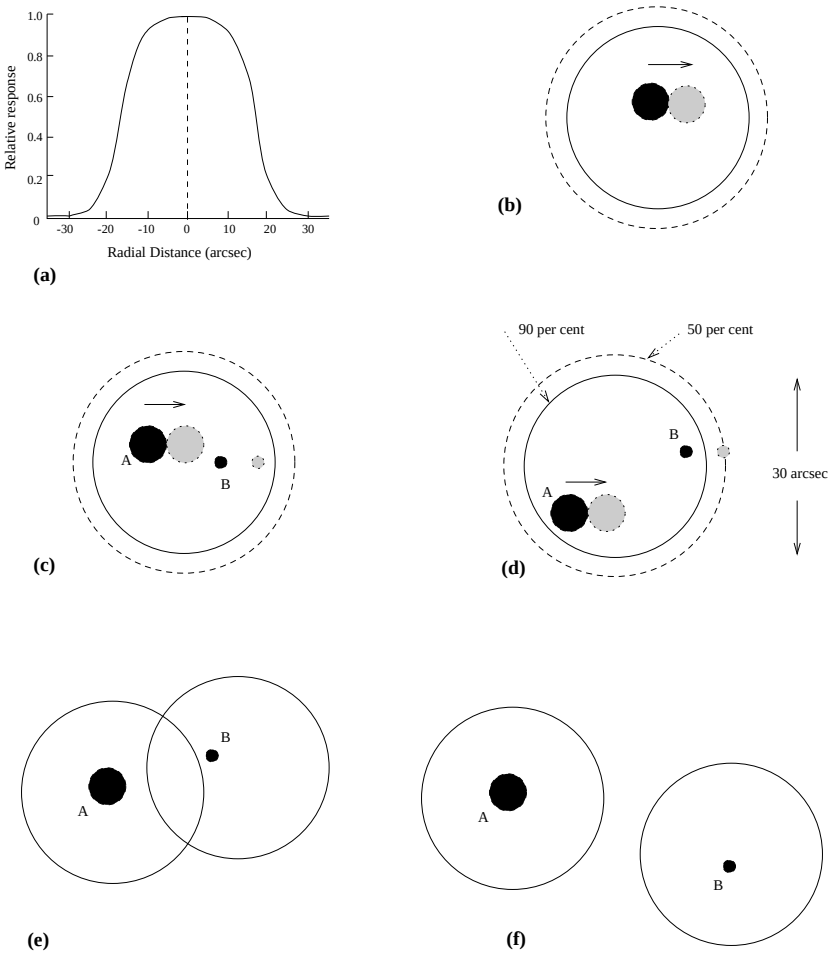

Figure 1.4.1. *(a) the (schematic) form of the detector's response profile in intensity, or the instantaneous field of view (IFOV). The geometric configuration of the double or multiple star affects the way in which reliable astrometric and photometric data could be acquired by the satellite. In (b) a single star has an a priori position such that it is well-centred within the detector's IFOV. Satellite attitude uncertainties (of less than a few arcsec) and discrete stepping of the IFOV during the star's transit across the instrument's focal plane (indicated by the solid and shaded images) leave the image well within the central part of the detector's response. In (c) a double star system, of a few arcsec separation, is still well-centred for the majority of observations, leading to reproducible and therefore reliable astrometric and photometric data. As the double star separation becomes comparable to or larger than the IFOV (d), attitude uncertainties lead to variations in the response as one or other of the components falls on the steep part of the detector's sensitivity profile—in such cases the resulting astrometry and/or photometry may be perturbed. In (e) the separation of the two components is too large for them to be observed within a single pointing of the IFOV, but small enough that consecutive pointings of the IFOV nevertheless 'interfere'. Such consecutive observations were reduced together, taking into account their mutual interference—the system is referred to as a two-pointing double. In (f) the component separation is large enough that they can be observed with two consecutive non-interfering IFOV pointings. Such components may or may not be part of a physically associated system: for Hipparcos such cases were treated no differently (for the observations, the reductions, and the presentation of astrometric and photometric results) to any other distinct catalogue entries.*

One major difficulty in the double star processing was a consequence of the large number of categories of double and multiple systems that had to be treated by distinctly different methods. While the majority of non-single systems are physical binaries, with either fixed relative positions over the mission duration or with an orbital motion that could be approximated by a linear function of time, some three thousand more complex systems were already included in the Hipparcos Input Catalogue, and many more were discovered by the satellite observations. Some such systems comprised more than two components, or had a significant orbital curvature over the time-scale of the satellite observations, or one or more of the components was found to be variable. Finally, the published results of the satellite observations may or may not be consistent with previously available ground-based observations.

Double and multiple systems therefore provided not only a challenge to the observations and data reductions, but also to the publication and presentation of the derived parameters. Any attempt to present information on previously known or newly discovered double or multiple systems in a simple and uniform manner was complicated by the large variety of configurations that exist: double or multiple stars may be contained within a single Hipparcos Catalogue 'entry', which means that the detector was always (nominally) pointed at the same point in the system, or they may appear as separate entries (because of the large component separation), or with one or more previously known components unobserved by the satellite (because of its faint magnitude, or due to its lack of high-priority scientific interest).

Catalogue users should thus be aware that the reliability of the published results for double and multiple systems depends on a variety of factors, some of which are not readily quantified in the form of standard errors and goodness-of-fit statistics. A particular difficulty, very specific to the Hipparcos mission, is the possible occurrence of 'grid-step' errors, where the derived position of a component may be displaced by a multiple of the main grid period, or about 1.2 arcsec. While this problem was readily soluble for single stars, some double or multiple systems with limited coverage in scanning directions may be quite susceptible to this kind of error, which then also affects the determination of the proper motion and parallax. Fortunately, the parallax is usually much less affected by this problem than the other parameters, and since the majority of objects received good observational coverage, their solutions are not likely to be affected by grid-step errors.

Although a quality rating of the component solutions according to their expected reliability has been attempted, based on factors such as the detection rate, rejection rate, and the level of agreement between the FAST and NDAC Consortia parameters, some caution must always be exercised in the interpretation of the double and multiple star results.

Figure 1.4.1 illustrates schematically the form of the detector's response profile (referred to as the instantaneous field of view), and the interplay between the geometric configuration of the double or multiple star and the reliability of the astrometric and photometric data acquired by the satellite. The numerical values of the instantaneous field of view profile used by both data reduction consortia are given in Table 1.4.1, and the corresponding profile in Figure 1.4.2. This function was used to correct the photometric data for systematic effects caused by components falling in the wings of the instantaneous field of view profile.

Table 1.4.1. The detector's response profile (ΔHp, in magnitudes) as a function of the distance to the centre of the instantaneous field of view (ϱ, in arcsec). The table gives the intensity attenuation for non-centred stars as adopted in the data reductions.

ϱ	ΔHp	ϱ	ΔHp	ϱ	ΔHp	ϱ	ΔHp	ϱ	ΔHp
0.0	0.0000	7.0	0.0223	14.0	0.3148	21.0	1.5960	28.0	4.9226
0.5	0.0000	7.5	0.0279	14.5	0.3638	21.5	1.7629	28.5	5.1868
1.0	0.0001	8.0	0.0347	15.0	0.4180	22.0	1.9445	29.0	5.4431
1.5	0.0002	8.5	0.0430	15.5	0.4776	22.5	2.1402	29.5	5.6884
2.0	0.0005	9.0	0.0530	16.0	0.5429	23.0	2.3493	30.0	5.9194
2.5	0.0010	9.5	0.0650	16.5	0.6140	23.5	2.5713	30.5	6.1330
3.0	0.0017	10.0	0.0793	17.0	0.6912	24.0	2.8056	31.0	6.3262
3.5	0.0028	10.5	0.0961	17.5	0.7746	24.5	3.0512	31.5	6.4962
4.0	0.0041	11.0	0.1159	18.0	0.8645	25.0	3.3063	32.0	6.6400
4.5	0.0059	11.5	0.1391	18.5	0.9613	25.5	3.5690	32.5	6.7559
5.0	0.0081	12.0	0.1658	19.0	1.0662	26.0	3.8371	33.0	6.8465
5.5	0.0107	12.5	0.1965	19.5	1.1807	26.5	4.1085	33.5	6.9153
6.0	0.0139	13.0	0.2314	20.0	1.3062	27.0	4.3813	34.0	6.9660
6.5	0.0177	13.5	0.2708	20.5	1.4442	27.5	4.6534	34.5	7.0022

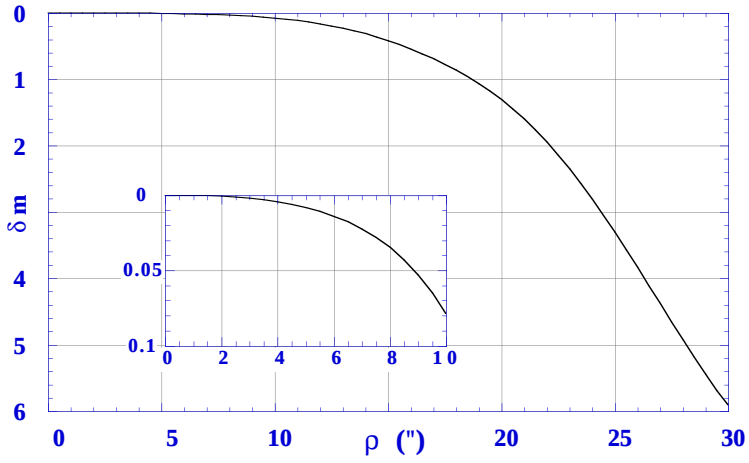

Figure 1.4.2. *The form of the detector's intensity response profile, or instantaneous field of view.*

1.4.2. Categorisation of Hipparcos Double Stars

When a Hipparcos Catalogue entry refers to a single object, the astrometric and photometric data are largely unambiguous. In the case of non-single objects, the situation is more complex in a number of ways, although not all combinations of separations and magnitude differences were observably non-single for Hipparcos. For the ones that were observably non single, and also for some non-resolved systems, the interpretation of the catalogue data requires some care. The following classification of the objects in terms of their separation (ϱ), magnitude difference (ΔHp), and orbital period (P) illustrates the categories of double and multiple systems that had to be accounted for:

(1) Effectively single systems:

(a) Close binaries with a maximum separation ϱ below 1–2 mas, corresponding to the final astrometric precision, showed no detectable photocentre offsets, and the observations effectively yielded the position, proper motion and parallax of the system's barycentre, plus the combined magnitude of the system. Such systems, being undetectable as binaries, appear simply as unresolved single entries in the main catalogue.

(b) Wide pairs with a minimum ϱ above some 30 arcsec, where only one component (at a time) was included in the instantaneous field of view. The separation is such that the components could be considered as 'non-interfering' (cf. the two-pointing doubles, 4b) and gave data for each target component as if it were a single object. Associated data do not appear in the Double and Multiple Systems Annex.

(2) Unresolved systems (separation $\varrho \sim$ 2–100 mas):

(a) Short-period binaries ($P <$ few months) presented the next lowest degree of complexity. The whole photocentric orbit was sampled, and the parallax and proper motions can be taken as referring to the barycentre of the system. (With a non-zero orbital eccentricity the position is however biased towards the apastron of the photocentric orbit). With increasing size of the photocentre orbit, there was an increasing departure between the observations and the single-star model, and many such cases fall within the 'stochastic' solution (see below).

(b) Intermediate-period binaries ($P \simeq$ 0.1 to 20 years), with $\varrho \geq 10$ mas, may have a significantly non-linear motion of the photocentre. In the upper range of this interval a non-linear proper motion could sometimes be fitted, but the separation of the (curved) orbital from the (rectilinear) barycentric motion was generally impossible, except in the relatively few cases where a full Keplerian orbit could be determined for the photocentre. The parallax was usually correctly estimated, unless the orbital period happened to be close to one year.

(c) Long-period binaries ($P >$ 10 years), at a distance where the projected separation was below 0.1 arcsec, presented a more complex situation. The parallax could still be correctly determined, but the proper motion reflects a combination of the barycentric motion and an approximately linear orbital component, being therefore indistinguishable from a normal single-star solution. If the object was not known from an external source to be non-single, the Hipparcos proper motion is thus slightly biased, and this effect has to be taken into account when comparing classical 'long-term' proper motions with the 'short-term' Hipparcos values (S. Söderhjelm, 1985, *Astrophys. Space Sci.*, 110, 77).

(3) Systems with large magnitude difference ($\Delta Hp \geq 4$ mag):

When the secondary component was sufficiently faint that effectively only the primary component was observed, the situation is analogous to categories 2(a–c) above, depending on the period of the system.

(4) Resolved systems ($0.1 < \varrho < 30$ arcsec *and* $\Delta Hp < 4$ mag):

(a) When the separation was below some 10 arcsec, both components fell well within the sensitive area of the instantaneous field of view, and they were observed simultaneously. There was usually little problem in analysing the combined signal as the sum of two point-like components. To determine correct photometry, it was only necessary to know if the instantaneous field of view of the image dissector tube was pointed at the primary, at the geometric centre, or at the photocentre of the system. More than 90 per cent of the resolved double-star solutions belong to this category.

(b) When $10 < \varrho < 30$ arcsec, the two components were sometimes included as separate entries in the Hipparcos Input Catalogue. Such 'two-pointing doubles' were observed through sequential pointings of the image dissector tube instantaneous field of view at the two distinct component positions, but using normally the data from both pointings in a combined solution for the astrometric parameters. With one of the components always in the steep wing of the instantaneous field of view profile some degradation of the precision was inevitable in these solutions, especially for the photometry, but for most systems the results are nevertheless reliable.

(5) Multiple systems:

All the above cases can be generalised to more than two components. Apart from the relatively easy cases with three or more bright components within 10 arcsec, there were many borderline cases where more than one model could fit the data. Many known triple stars were assigned a reasonably good double-star solution by neglecting the faintest component or by treating two close components as one for simplicity, although a full triple-star model might have fitted the data even better. The interpretation of the astrometric results in such cases must be done on a case-by-case basis, but in most cases the system parallax is quite reliable and unambiguous.

(6) Variable double stars:

A small-amplitude variability of one or the other component is not uncommon, and has normally rather little influence on the derived astrometric parameters. At least within the NDAC Consortium, however, the double star detection and solution methods turned out to be unexpectedly sensitive to photometric variability, in the sense that a single variable star could sometimes result in a double star solution with large ΔHp. Many hundreds of such solutions were rejected when they were not confirmed by the FAST Consortium solutions. For large-amplitude variable doubles, very few solutions could be obtained with standard methods, and a re-analysis of the data using more elaborate methods may be worthwhile for some systems.

1.4.3. Presentation of Double and Multiple Star Data

The results on double and multiple stars have been collected into the Double and Multiple Systems Annex (Volume 10), which comprises five separate parts:

- Part C giving solutions for systems resolved into distinct components (categories 4 or 5 in the preceding section);
- Part G for unresolved systems (probably astrometric binaries) where more than five parameters were needed to characterise the non-linear motion of the photocentre (category 2b, with periods above some 5 years);
- Part O for the orbital systems, when the Hipparcos observations could be used to determine some or all of the Keplerian elements of the absolute orbit of the photocentre (category 2b);
- Part V for a small number of objects where the duplicity has been inferred by a photocentric motion caused by the variability of one of the components ('Variability-Induced Movers', category 6);
- Part X, 'stochastic solutions' for objects where none of the other models, nor a single-star solution, could be found consistent with the observations (any category).

Detailed descriptions of these parts are found in Section 2.3. The main Hipparcos Catalogue (Volumes 5–9) provides a concise summary of the general properties of double and multiple systems for each relevant entry (Fields H55–67), with more extensive details of the solutions provided in the printed annex (Volume 10), and in the machine-readable files.

Of the five parts of the Double and Multiple Systems Annex, Part C contains the largest number of solutions and also the largest variety of configurations and problem cases. This part provides the magnitude, position, proper motion, and parallax for each of the resolved components in a system (in the case of the two-pointing doubles the two components were considered as independent single stars, although the solution took into account the mutual disturbance of their signals due to the size of the instantaneous field of view). For a double star, this involved the simultaneous determination of 12 parameters. However in many cases, a better solution may have been derived when constrained to give equal parallaxes for the two components, in an 11-parameter solution. In other cases, all internal motions were neglected, resulting in a 9-parameter solution.

Considering the many possible configurations of resolved double and multiple stars, involving one or more entries in the main catalogue, it is unavoidable that the multiplicity information given in the main catalogue will in many cases be incomplete. A summary of the multiplicity status is in all cases given in Fields H55–61. In particular Field H59 contains a pointer to the relevant part of the Double and Multiple Systems Annex, where the complete data are found. Whether more detailed information is given in the main catalogue depends on the actual configuration of the resolved system.

If the entry itself was resolved by the satellite observations into *precisely* two components, a summary of the system geometry and photometry is included in Fields H62–67. Where the entry was resolved into three or more components, no attempt has been made to summarise the geometric or photometric information in the main printed catalogue and, for details of the system, reference to the annexes must be made.

Irrespective of whether or not an entry may have been resolved by the satellite observations, the entry itself may also be associated with one or more distinct, more widely

separated components. Each such associated component may, or may not, have been observed separately by the satellite, and each may itself be double or multiple. No attempt was made to provide a summary of the geometric or photometric parameters of such a system in the main printed catalogue; but systems identified by their CCDM identifier (see Section 1.4.4), and whose components were observed by the satellite and jointly treated in the double-star reductions, are summarised in the Double and Multiple Systems Annex.

Depending on the precise geometry and photometry of the system, the astrometric and photometric data for an individual entry may be most meaningfully presented for a component of the system, or for the photocentre (or for one of the photocentres). This choice is found in Field H10 (for the astrometric data) and Field H48 (for the photometric data). Generally, for the astrometric data in the main catalogue, the photocentre is specified for component separations below about 0.30 arcsec (see Field H10), otherwise the primary is taken as the reference component. For the photometric data, photometry is presented according to the component separation as described in more detail under Field H48. Photometry is given for the combined system for objects with a single entry and with separations below 10 arcsec, for the primary component for separations larger than 10 arcsec, and for each component for all systems with two entries. For systems resolved into more than two components, the photometry in the main catalogue is not corrected for the detector's response profile, and the most complete information is contained in the Double and Multiple Systems Annex.

1.4.4. Hipparcos Catalogue Entries and Relationship to the CCDM

There are three levels of identification of a multiple system and its components in the Hipparcos Catalogue:

- the system identifier, based on the CCDM catalogue, which serves as the unique entry point to Part C of the Double and Multiple Systems Annex;
- the Hipparcos entry, according to which the main catalogue and all other annexes are organised;
- the component designation by upper-case letters (A, B, ...).

A system may be associated with one or several Hipparcos Catalogue entries, and each entry may correspond to one or several components according to the hierarchy of the system and to the separations between its components.

The definition of a Hipparcos Catalogue 'entry' depended on the separation of components, and has been influenced by the profile of the detector's instantaneous field of view. This is roughly 30 arcsec in diameter, with a flat central region, and more extended response wings (Figure 1.4.1). *A priori* known systems with components separated by less than 10 arcsec were considered as a single 'entry', or observing target, and the components were thus observed together. In terms of the pointing of the detector's sensitive area, either the photometric or geometric centre, or an individual component may have been targeted. For systems with components in the separation range 10–30 arcsec, observations were generally made by pointing the sensitive area of the detector to the various components individually, in order to adequately compensate

for the rapidly changing response profile in its outer regions—these are referred to as two-pointing systems (see Figure 1.4.1).

The basis for much of the preparatory work associated with the observations and treatment of double and multiple systems was the CCDM, the Catalogue of Components of Double and Multiple Stars (J. Dommanget & O. Nys, 1994, *Comm. Obs. R. de Belg.*, Serie A No. 115; and available from the CDS, ref. I-211), including a subset of 34 031 definitely identified systems. The CCDM identifier is based upon the approximate equatorial coordinates of the system at epoch and equinox J2000.0. For previously known systems this identifier is taken from the CCDM catalogue. New systems identified from ground-based observations were updated until 1 January 1994 using, in particular, a pre-release version of the WDS (The Washington Catalogue of Visual Double Stars; C.E. Worley & G.G. Douglass, US Naval Observatory, Washington).

Newly-discovered double and multiple systems have been allocated new CCDM numbers as part of the continual updating of the CCDM catalogue, following the rules described in its introduction. The CCDM identifier plays a special role in the identification and cross-referencing of double and multiple systems, and also establishes a link between the components of systems not present in the Hipparcos Catalogue. It is therefore included within the main catalogue (Field H55) for all the systems with component solutions, irrespective of whether they were previously known or discovered from the Hipparcos observations, and for all the entries of double and multiple systems of the Hipparcos Input Catalogue for which no solution could be determined from the Hipparcos data.

Field H56 summarises the 'discovery status' of double and multiple systems, in the form of the three flags:

H : double and multiple systems discovered by Hipparcos, and not identified in either the Hipparcos Input Catalogue, the CCDM, or the WDS;

I : double and multiple systems identified using the CCDM during construction of the Hipparcos Input Catalogue, and recorded in its double and multiple star annex;

M : systems identified between the preparation of the Input Catalogue and the completion of the Hipparcos observations. These are due either to the improvements of the CCDM (J. Dommanget & O. Nys, *Bulletin du CDS*, 46, 13 (1995) & 48, 19 (1996)), or to ground-based discoveries up to 1994.0, identified in more recently available catalogues and compilations, partially within the pre-release version of the WDS. The latter category also includes systems discovered by speckle interferometry, which were not included in the Hipparcos Input Catalogue.

Double or multiple systems, whether newly discovered by Hipparcos or not, should ideally have been allocated the component designations A, B, ... in order of decreasing brightness (increasing magnitude) or increasing angular separation from the primary. The differences in passbands, variability, rapid orbital motion with components of roughly equal magnitude, and errors, made such a scheme difficult to apply consistently. In any case, such a convention strictly applied to the Hipparcos double or multiple systems might be in conflict with systems previously measured by ground-based observers, not least because the component identification from ground-based observations depends on the angular separation as well as on the chronological order of discovery—hence one encounters complex designations reflecting the observing history of the system.

Table 1.4.2. Approximate number of entries considered in the double star processing by the reduction consortia FAST and NDAC. For each consortium the entries are divided into solved systems, systems detected as non-single but without a good solution, and entries considered as single stars ('undetected') but solved or detected by the other consortium. The total number of entries considered, 21 360, corresponds to the entries in Parts C, O and V of the Double and Multiple Systems Annex, plus those flagged as suspected non-single ('S' in Field H61).

	FAST solved	FAST detected	FAST undetected	Total
NDAC solved	12710	1030	2250	15990
NDAC detected	500	210	2190	2900
NDAC undetected	2310	160	–	2470
Total	15520	1400	4440	21360

The general principle adopted was to adhere as closely as possible to the previous identifications listed in the CCDM or in the literature. As a consequence, a newly-discovered wide component to a close pair AB may have been called C, even if it was brighter than B. A newly-discovered close component to component A of a normal wide pair AB might be called C, a, or P. Where this resulted in component B (for example) of a Hipparcos system being brighter than component A, B has been used as the reference component for the astrometric data (Field H10), to ensure that the values of ΔHp (Field H66) is always positive. Cases where the component designation adopted here differs from that given in previous catalogues are unavoidable. For newly discovered systems the components have always been designated as A, B, ... in order of increasing Hipparcos magnitude.

1.4.5. Statistics of Observed Double and Multiple Systems

On the basis of the double and multiple systems contained in the CCDM, the Hipparcos Input Catalogue contained 15 966 related entries. These entries, each assigned a specific HIC number, were part of the 14 162 systems (11 427 double, 2735 multiple) for which one or more targets were observed by the satellite. Of these 12 411 were systems with one target (or entry); 1703 were systems with two targets; 43 were systems with three targets; and 5 were systems with four targets (note that these *a priori* observational configurations do not correspond to the final catalogue classification of double or multiple systems).

Of these Hipparcos Input Catalogue CCDM-classified systems, some 11 000 were initially estimated to be observably non-single by the satellite, the precise number being highly dependent on the exact limits for plausible solutions, and on the quality of the ΔHp-data. Even with later updates of the CCDM and the inclusion of WDS data, the number of entries in known double systems was never more than about 11 500 in 'single-pointing' and 2000 in 'two-pointing' systems. To this would be added some 1000 entries in known multiple systems, resulting in a total of some 14 500 *a priori* known entries.

In constructing the final Hipparcos Catalogue, double or multiple star solutions were sought for all these known systems, and the detector signals were carefully screened for possible signatures of 'new' double stars to be added to this list. The uncertainties

inherent in the detection of binaries and the subsequent determination of the system parameters are illustrated by Table 1.4.2. Depending on the criteria for accepting an object as double or multiple, the number of systems in the Hipparcos Catalogue could have ranged between 10 000 (accepting only solutions where the consortia were in good agreement) and 19 000 (accepting all cases where at least some solution existed).

In the end a fairly conservative publication policy has been adopted. The solutions for many of the 14 162 previously known non-single systems observed by Hipparcos turned out to be not significantly better than single-star solutions, and the final number of resolved, known doubles (category 'I' or 'M' in Section 1.4.3) listed in the Hipparcos Catalogue is 10 210. Similarly, although some 15 000 'suspected non-singles' were initially selected and treated with double-star reduction methods by either FAST or NDAC, only 3001 new resolved doubles were finally fully 'accepted', with the remaining objects flagged in Field H61 as suspected doubles.

Part C of the Double and Multiple Systems Annex contains a total of 12 195 solutions. 12 005 of these are double star solutions, 182 are triple star solutions, and 8 are quadruple star solutions; the number of components is therefore 24 588.

The number of distinct entries in each part of the Hipparcos Double and Multiple Systems Annex is as follows: Part C: 13 211 entries; Part G: 2622 entries; Part O: 235 entries; Part V: 288 entries; Part X: 1561 entries.

Section 1.5

Transformation of Astrometric Data and Associated Error Propagation

1.5. Transformation of Astrometric Data and Associated Error Propagation

1.5.1. Introduction

This section describes the following, generally applicable, transformations of the astrometric data which may be of interest to users of the Hipparcos and Tycho Catalogues (and as incorporated in the *Celestia 2000* software):

- from equatorial to ecliptic coordinates;
- from equatorial to galactic coordinates;
- from the catalogue epoch $T_0 = \mathrm{J1991.25(TT)}$ to an arbitrary epoch T.

Although these or similar transformations are discussed in many textbooks, the corresponding transformation of covariances is usually not covered, and the epoch transformation not always treated at a level of approximation adequate for the present data.

Additionally, the calculation of rectangular space coordinates and space velocities in the equatorial and galactic systems is considered in Section 1.5.6. Section 1.5.7 describes some features of the relation between the reference system ICRS as materialised by the Hipparcos Catalogue, and the conventional coordinate system at J2000.0 previously realised by the FK5 Catalogue.

In this section the astrometric parameters are represented by vectors or column matrices $\mathbf{a}$, with subscripts indicating which coordinate system or epoch they refer to; the corresponding covariance matrices are denoted $\mathbf{C}$, cf. Equations 1.2.4 and 1.2.5. Specifically, $\mathbf{a}_0$ and $\mathbf{C}_0$ refer to the equatorial system at the common catalogue epoch $T_0 = \mathrm{J1991.25(TT)}$, and thus correspond exactly to the data as given in the Hipparcos and Tycho Catalogues (Fields H/T8–9 and H/T11–28) as explained in Section 1.2.

In the ecliptic coordinates the astrometric parameters are denoted $(\lambda, \beta, \pi, \mu_{\lambda *}, \mu_\beta)$, or in abbreviated vector form $\mathbf{a}_\mathrm{K}$; similarly in the galactic system $(l, b, \pi, \mu_{l*}, \mu_b)$, or $\mathbf{a}_\mathrm{G}$ in vector form. Here, $\mu_{\lambda *} = \mu_\lambda \cos\beta$ and $\mu_{l*} = \mu_l \cos b$. The subscript $_0$ may be added if the data specifically refer to the catalogue epoch T_0.

1.5.2. General Error Propagation

In Section 1.2.8 a standard model of stellar motion was introduced, and other, more complex models are discussed in Section 2.3. The numerical fitting of such a model to observational data generally results in an estimate both of the parameter vector **a** and of its covariance matrix **C**. With n free parameters, these are expressed respectively as matrices of dimension $n \times 1$ and $n \times n$.

From a statistical viewpoint, **a** and **C** jointly provide a complete specification of the fitted model and its uncertainties only in the context of linear estimation and normal (Gaussian) error distributions. The estimation problems encountered in the Hipparcos and Tycho data analyses are seldom strictly linear, and sometimes strongly non-linear, and the error distributions are in practice never Gaussian. Perhaps the most dramatic consequence of non-linearity is the possible existence of grid-step errors, which in unfortunate cases may result in positional errors of the order of an arcsec while the formal standard errors remain in the milliarcsec range. Additional statistics provided in the catalogue, such as the rejection rate and goodness-of-fit (Fields H29–30), provide some indication of the sometimes abnormal behaviour of data, but in practice no complete characterisation of the fit is possible. Nevertheless, in the vast majority of cases **a** and **C** provide an extremely useful approximation to complex reality.

If the parameters **a** are transformed into an alternative representation $\hat{\mathbf{a}} = \mathbf{f}(\mathbf{a})$ of the same dimension, then small errors in the parameters are transformed according to:

$$\Delta\hat{a}_i = \sum_j \frac{\partial f_i}{\partial a_j}\Delta a_j \qquad [1.5.1]$$

In matrix form this can be written:

$$\Delta\hat{\mathbf{a}} = \mathbf{J_f}(\mathbf{a})\Delta\mathbf{a} \qquad [1.5.2]$$

where $\mathbf{J_f}(\mathbf{a})$ is the Jacobian matrix of the transformation:

$$[\mathbf{J_f}]_{ij} = \frac{\partial f_i}{\partial a_j} \qquad [1.5.3]$$

evaluated at the point **a**. Now let $\Delta\mathbf{a}$ be the difference between the estimated and true parameter vectors. If the estimate is unbiased, then $\mathrm{E}(\Delta\mathbf{a}) = \mathbf{0}$, where E is the expectation operator, and the covariance of **a** is given by $\mathbf{C} = \mathrm{E}(\Delta\mathbf{a}\Delta\mathbf{a}')$, with the prime denoting matrix transposition. From Equation 1.5.2 it follows that $\hat{\mathbf{a}}$ is also unbiased, to the first order in the errors, and that its covariance is given by:

$$\hat{\mathbf{C}} = \mathbf{J_f}\,\mathbf{C}\,\mathbf{J_f}' \qquad [1.5.4]$$

Equation 1.5.4 is the basis for the error propagation discussed below.

If the inverse function $\mathbf{f}^{-1}$ exists, then it is possible to transform the data set [$\hat{\mathbf{a}}$ $\hat{\mathbf{C}}$] back to the original form [**a** **C**], and the two representations can be regarded as equivalent from the point of view of information content. A necessary condition for this is that $|\mathbf{J_f}| \neq 0$, in which case $\mathbf{J_{f^{-1}}} = \mathbf{J_f}^{-1}$. The transformations discussed here satisfy this condition.

1.5.3. Coordinate Transformations

In Section 1.2 the vectors representing celestial directions were effectively identified with the column matrices containing their components in the equatorial system; see for instance Equations 1.2.11, 1.2.15 and 1.2.19. When dealing with transformations between different coordinate systems it is useful to maintain the distinction between a vector as a physical entity and its numerical representation in some coordinate system. This requires that the basis vectors of the coordinate systems are explicitly introduced. The basis vectors in the equatorial system are here denoted [**x y z**], with **x** being the unit vector towards $(\alpha, \delta) = (0, 0)$, **y** the unit vector towards $(\alpha, \delta) = (+90°, 0)$, and **z** the unit vector towards $\delta = +90°$. The basis vectors in the ecliptic and galactic systems are respectively denoted [$\mathbf{x}_\mathrm{K}$ $\mathbf{y}_\mathrm{K}$ $\mathbf{z}_\mathrm{K}$] and [$\mathbf{x}_\mathrm{G}$ $\mathbf{y}_\mathrm{G}$ $\mathbf{z}_\mathrm{G}$]. Thus, the arbitrary direction **u** may be written in terms of the equatorial, ecliptic and galactic coordinates as:

$$\mathbf{u} = [\,\mathbf{x}\ \mathbf{y}\ \mathbf{z}\,] \begin{pmatrix} \cos\delta\cos\alpha \\ \cos\delta\sin\alpha \\ \sin\delta \end{pmatrix} = [\,\mathbf{x}_\mathrm{K}\ \mathbf{y}_\mathrm{K}\ \mathbf{z}_\mathrm{K}\,] \begin{pmatrix} \cos\beta\cos\lambda \\ \cos\beta\sin\lambda \\ \sin\beta \end{pmatrix} = [\,\mathbf{x}_\mathrm{G}\ \mathbf{y}_\mathrm{G}\ \mathbf{z}_\mathrm{G}\,] \begin{pmatrix} \cos b\cos l \\ \cos b\sin l \\ \sin b \end{pmatrix} \qquad [1.5.5]$$

The transformation between the equatorial and ecliptic systems is given by:

$$[\,\mathbf{x}_\mathrm{K}\ \mathbf{y}_\mathrm{K}\ \mathbf{z}_\mathrm{K}\,] = [\,\mathbf{x}\ \mathbf{y}\ \mathbf{z}\,]\,\mathbf{A}_\mathrm{K} \qquad [1.5.6]$$

where:

$$\mathbf{A}_\mathrm{K} = \begin{pmatrix} 1 & 0 & 0 \\ 0 & \cos\epsilon & -\sin\epsilon \\ 0 & \sin\epsilon & \cos\epsilon \end{pmatrix} = \begin{pmatrix} 1 & 0 & 0 \\ 0 & +0.917\,482\,062\,1 & -0.397\,777\,155\,9 \\ 0 & +0.397\,777\,155\,9 & +0.917\,482\,062\,1 \end{pmatrix} \qquad [1.5.7]$$

$\epsilon = 23° 26' 21.448'' = 23.^\circ439\,291\,111\,1\ldots$ is the conventional value of the obliquity of the ecliptic (Table 1.2.2).

The transformation between the equatorial and galactic systems is given by:

$$[\,\mathbf{x}_\mathrm{G}\ \mathbf{y}_\mathrm{G}\ \mathbf{z}_\mathrm{G}\,] = [\,\mathbf{x}\ \mathbf{y}\ \mathbf{z}\,]\,\mathbf{A}_\mathrm{G} \qquad [1.5.8]$$

where the matrix $\mathbf{A}_\mathrm{G}$ relates to the definition of the galactic pole and centre in the ICRS system. Currently no definition of this relation has been sanctioned by the IAU. In order to provide an unambiguous transformation for users of the Hipparcos and Tycho Catalogues, the north galactic pole is here defined by the following celestial coordinates in the ICRS system:

$$\begin{aligned} \alpha_\mathrm{G} &= 192.^\circ859\,48 \\ \delta_\mathrm{G} &= +27.^\circ128\,25 \end{aligned} \qquad [1.5.9]$$

The origin of galactic longitude is defined by the galactic longitude of the ascending node of the galactic plane on the equator of ICRS, which is here taken to be:

$$l_\Omega = 32.^\circ931\,92 \qquad [1.5.10]$$

Equations 1.5.9 and 1.5.10 are consistent with the previous (1960) definition of galactic coordinates to a level set by the quality of optical reference frames prior to Hipparcos.

The angles α_G, δ_G and l_Ω are to be regarded as exact quantities. From them, the transformation matrix A_G may be computed to any desired accuracy. To 10 decimal places the result is:

$$\mathbf{A}_G = \begin{pmatrix} -0.054\,875\,560\,4 & +0.494\,109\,427\,9 & -0.867\,666\,149\,0 \\ -0.873\,437\,090\,2 & -0.444\,829\,630\,0 & -0.198\,076\,373\,4 \\ -0.483\,835\,015\,5 & +0.746\,982\,244\,5 & +0.455\,983\,776\,2 \end{pmatrix} \qquad [1.5.11]$$

The current system of galactic longitudes and latitudes, (l^{II}, b^{II}), have been defined by adopting the coordinates of directions to the north galactic pole and the galactic centre, based on physical features in the Galaxy, with respect to the B1950 coordinate reference frame (A. Blaauw, C.S. Gum, J.L. Pawsey & G. Westerhout, 1960, *Mon. Not. R. Astron. Soc.*, 121, 123). It is clearly desirable that (l^{II}, b^{II}) computed from coordinates referred to the ICRS should be equal to those computed from coordinates referred to B1950. In principle this could be achieved by transforming the directions of the galactic axes first to the J2000 systems using standard precepts, and then to the ICRS, as realised by the Hipparcos Catalogue.

The main problem arises because the transformation from B1950 to J2000 consists not only of a pure rotation of axes due to changes in precession and equinox motion, but also a change in the convention by which stellar aberration is computed in the two systems. Prior to the adoption of the J2000 system, stellar aberration was based only on the circular component of the Earth's orbital velocity. The component depending on the eccentricity of the orbit, which can amount to 0.34 arcsec, and is approximately constant for a given direction over long intervals of time, was considered to be implicitly included in the mean catalogue positions of stars. Therefore if the galactic axes continue to be defined by the same physical features as in the 1960 definitions, they will no longer be mutually orthogonal. This is clearly unacceptable. Accordingly Murray (1989, *Astronomy & Astrophysics*, 218, 325) proposed that the axes defined in 1960 should be considered as absolute directions, unaffected by aberration; the angles given in Equations 1.5.9 and 1.5.10 were derived from his Equation 33 by rounding to five decimals of the degree.

The J2000 reference system is realised in practice by the FK5 Catalogue. The mean relation between this and the Hipparcos Catalogue involves a (time-dependent) rotation, which amounts to some 20 mas at the epoch J1991.25 (see Section 1.5.7). A precise and unambiguous determination of the difference in orientation between the two catalogues is however prevented by the much larger regional differences (~ 100 mas), and by colour and magnitude equations in FK5, which affect its orientation at the 20–30 mas level. It is therefore inappropriate to demand continuity with the previous definition at a level substantially below 100 mas. With this in mind, the orientation difference between ICRS and FK5 may be ignored in the present context.

The definition of the angles α_G, δ_G and l_Ω in Equations 1.5.9 and 1.5.10, using five decimals of the degree, implies a change in the directions of the principal axes, compared to the definition proposed by Murray (1989), by at most 18 mas. The ambiguity of the FK5/ICRS transformation does not warrant a higher numerical precision of the defining angles.

The ecliptic longitude and latitude are thus computed from:

$$\begin{pmatrix} \cos\beta\cos\lambda \\ \cos\beta\sin\lambda \\ \sin\beta \end{pmatrix} = \mathbf{A}'_K \begin{pmatrix} \cos\delta\cos\alpha \\ \cos\delta\sin\alpha \\ \sin\delta \end{pmatrix} \qquad [1.5.12]$$

and the galactic longitude and latitude from:

$$\begin{pmatrix} \cos b\cos l \\ \cos b\sin l \\ \sin b \end{pmatrix} = \mathbf{A}'_G \begin{pmatrix} \cos\delta\cos\alpha \\ \cos\delta\sin\alpha \\ \sin\delta \end{pmatrix} \qquad [1.5.13]$$

The variation in $\mathbf{u}$ due to small changes in the spherical coordinates can be written, in analogy with Equation 1.2.14:

$$\Delta\mathbf{u} = [\,\mathbf{p}\ \mathbf{q}\,]\begin{pmatrix}\Delta\alpha* \\ \Delta\delta\end{pmatrix} = [\,\mathbf{p}_\mathrm{K}\ \mathbf{q}_\mathrm{K}\,]\begin{pmatrix}\Delta\lambda* \\ \Delta\beta\end{pmatrix} = [\,\mathbf{p}_\mathrm{G}\ \mathbf{q}_\mathrm{G}\,]\begin{pmatrix}\Delta l* \\ \Delta b\end{pmatrix} \qquad [1.5.14]$$

where $\Delta\lambda* = \Delta\lambda\cos\beta$, etc.; $\mathbf{p}_\mathrm{K}$ and $\mathbf{q}_\mathrm{K}$ are unit vectors perpendicular to $\mathbf{u}$ in the directions of increasing λ and β, respectively, with corresponding notations in the galactic system. These vectors are parts of the normal triads $[\,\mathbf{p}_\mathrm{K}\ \mathbf{q}_\mathrm{K}\ \mathbf{r}\,]$ and $[\,\mathbf{p}_\mathrm{G}\ \mathbf{q}_\mathrm{G}\ \mathbf{r}\,]$ relative to the ecliptic and galactic systems, defined at the reference direction $\mathbf{r} = \mathbf{u}$ in analogy with the normal triad relative to the equatorial system introduced in Section 1.2.8 (Equation 1.2.15). They may be computed from:

$$\begin{aligned}\mathbf{p} &= \langle \mathbf{z}\times\mathbf{r}\rangle & \mathbf{q} &= \mathbf{r}\times\mathbf{p}\\ \mathbf{p}_\mathrm{K} &= \langle \mathbf{z}_\mathrm{K}\times\mathbf{r}\rangle & \mathbf{q}_\mathrm{K} &= \mathbf{r}\times\mathbf{p}_\mathrm{K}\\ \mathbf{p}_\mathrm{G} &= \langle \mathbf{z}_\mathrm{G}\times\mathbf{r}\rangle & \mathbf{q}_\mathrm{G} &= \mathbf{r}\times\mathbf{p}_\mathrm{G}\end{aligned} \qquad [1.5.15]$$

[Note that, with respect to the equatorial system, the components of $\mathbf{z}$ are given by the column matrix $(0, 0, 1)'$, while the components of $\mathbf{z}_\mathrm{K}$ and $\mathbf{z}_\mathrm{G}$ are given by the third columns in the matrices $\mathbf{A}_\mathrm{K}$ and $\mathbf{A}_\mathrm{G}$, respectively. Thus, the vector operations in Equation 1.5.15 could all be carried out in the equatorial system by means of standard operations on the corresponding column matrices.]

Using the orthonormality of the tangent vectors it follows from Equation 1.5.14 that:

$$\begin{pmatrix}\Delta\lambda* \\ \Delta\beta\end{pmatrix} = \begin{pmatrix}\mathbf{p}'_\mathrm{K}\mathbf{p} & \mathbf{p}'_\mathrm{K}\mathbf{q} \\ \mathbf{q}'_\mathrm{K}\mathbf{p} & \mathbf{q}'_\mathrm{K}\mathbf{q}\end{pmatrix}\begin{pmatrix}\Delta\alpha* \\ \Delta\delta\end{pmatrix} \qquad [1.5.16]$$

and:

$$\begin{pmatrix}\Delta l* \\ \Delta b\end{pmatrix} = \begin{pmatrix}\mathbf{p}'_\mathrm{G}\mathbf{p} & \mathbf{p}'_\mathrm{G}\mathbf{q} \\ \mathbf{q}'_\mathrm{G}\mathbf{p} & \mathbf{q}'_\mathrm{G}\mathbf{q}\end{pmatrix}\begin{pmatrix}\Delta\alpha* \\ \Delta\delta\end{pmatrix} \qquad [1.5.17]$$

The 2×2 matrices in the last two equations contain the partial derivatives of the ecliptic and galactic coordinates with respect to the equatorial ones. Computationally, they are obtained as scalar products of the relevant tangential vectors expressed in any convenient coordinate system, such as the equatorial. Considering the proper motion components as the time derivatives of $\Delta\alpha*$, $\Delta\delta$, etc. (with the tangent vectors regarded as fixed), their transformations are similarly given by:

$$\begin{pmatrix}\mu_{\lambda*} \\ \mu_\beta\end{pmatrix} = \begin{pmatrix}\mathbf{p}'_\mathrm{K}\mathbf{p} & \mathbf{p}'_\mathrm{K}\mathbf{q} \\ \mathbf{q}'_\mathrm{K}\mathbf{p} & \mathbf{q}'_\mathrm{K}\mathbf{q}\end{pmatrix}\begin{pmatrix}\mu_{\alpha*} \\ \mu_\delta\end{pmatrix} \qquad [1.5.18]$$

and:

$$\begin{pmatrix}\mu_{l*} \\ \mu_b\end{pmatrix} = \begin{pmatrix}\mathbf{p}'_\mathrm{G}\mathbf{p} & \mathbf{p}'_\mathrm{G}\mathbf{q} \\ \mathbf{q}'_\mathrm{G}\mathbf{p} & \mathbf{q}'_\mathrm{G}\mathbf{q}\end{pmatrix}\begin{pmatrix}\mu_{\alpha*} \\ \mu_\delta\end{pmatrix} \qquad [1.5.19]$$

The complete transformation of the equatorial position and proper motion into the ecliptic system is given by Equations 1.5.12 and 1.5.18; the parallax is of course independent of the coordinate system. Taking the five astrometric parameters in the standard order of Equation 1.2.4, the Jacobian matrix for the transformation is:

$$\mathbf{J} = \begin{pmatrix} c & s & 0 & 0 & 0\\ -s & c & 0 & 0 & 0\\ 0 & 0 & 1 & 0 & 0\\ 0 & 0 & 0 & c & s\\ 0 & 0 & 0 & -s & c\end{pmatrix} \qquad [1.5.20]$$

with $c = \mathbf{p}'_\mathrm{K}\mathbf{p} = \mathbf{q}'_\mathrm{K}\mathbf{q}$ and $s = \mathbf{p}'_\mathrm{K}\mathbf{q} = -\mathbf{q}'_\mathrm{K}\mathbf{p}$. The transformation of the equatorial parameters into the galactic system is similarly given by Equations 1.5.13 and 1.5.19; the Jacobian matrix is again given by Equation 1.5.20, now with $c = \mathbf{p}'_\mathrm{G}\mathbf{p} = \mathbf{q}'_\mathrm{G}\mathbf{q}$ and $s = \mathbf{p}'_\mathrm{G}\mathbf{q} = -\mathbf{q}'_\mathrm{G}\mathbf{p}$.

1.5.4. Epoch Transformation: Simplified Treatment

The simplistic formulae for transforming a celestial position (α, δ) from the catalogue epoch T_0 to the arbitrary epoch T are:

$$\begin{aligned} \alpha &= \alpha_0 + (T - T_0)\,\mu_{\alpha *0} \sec \delta_0 \\ \delta &= \delta_0 + (T - T_0)\,\mu_{\delta 0} \end{aligned} \qquad [1.5.21]$$

(where the $\sec \delta_0$ factor compensates the $\cos \delta_0$ factor implicit in $\mu_{\alpha *}$). This is not a good physical model of how the stars move on the sky: in general it describes a curved, spiralling motion towards one of the poles, whereas (unperturbed) real stars are expected to move along great-circle arcs. Although the difference with respect to a rigorous model (Section 1.5.5) is usually very small, it may become significant in special cases, in particular for stars near the celestial poles or when propagating over very long time intervals. Equation 1.5.21 should therefore not be used in software intended for general application. Nevertheless, it provides in many cases a useful first-order approximation suitable for hand calculation and for estimating the positional uncertainties at arbitrary epochs.

In this simplified model the slow changes in the proper motion components and in the parallax are neglected and the Jacobian matrix for the epoch transformation is then:

$$\mathbf{J} = \begin{pmatrix} 1 & 0 & 0 & t & 0 \\ 0 & 1 & 0 & 0 & t \\ 0 & 0 & 1 & 0 & 0 \\ 0 & 0 & 0 & 1 & 0 \\ 0 & 0 & 0 & 0 & 1 \end{pmatrix} \qquad [1.5.22]$$

with $t = T - T_0$. The covariance matrix for the five astrometric parameters at epoch T are obtained from Equation 1.5.4; this gives in particular for the variances in position:

$$\begin{aligned} \sigma^2_{\alpha *} &= \left[\sigma^2_{\alpha *} + 2t\rho^{\mu_{\alpha *}}_{\alpha *}\,\sigma_{\alpha *}\sigma_{\mu_{\alpha *}} + t^2\sigma^2_{\mu_{\alpha *}}\right]_0 \\ \sigma^2_{\delta} &= \left[\sigma^2_{\delta} + 2t\rho^{\mu_{\delta}}_{\delta}\,\sigma_{\delta}\sigma_{\mu_{\delta}} + t^2\sigma^2_{\mu_{\delta}}\right]_0 \end{aligned} \qquad [1.5.23]$$

(with all quantities in the right members referring to epoch T_0). Minimising these variances with respect to t results in the previously given expressions for the mean observational epochs in right ascension and declination; see Equations 1.2.6–1.2.10.

1.5.5. Epoch Transformation: Rigorous Treatment

In this section the rigorous transformation of parameters and covariances is formulated, based on the standard model of stellar motion described in Section 1.2.8. This is the epoch transformation incorporated in the *Celestia 2000* software. Because of its relative complexity, Fortran and C implementations of the transformation are included on ASCII CD-ROM disc 1 (see Section 2.11).

The six-dimensional parameter vector a: Recall that the standard model assumes uniform space velocity for the object: its path on the celestial sphere (as seen from the solar system barycentre, i.e. without the displacement due to parallax) is a great-circle arc. The angular velocity (proper motion) along this arc is variable, reaching a maximum when the object is at the point closest to the Sun along its rectilinear path; the distance (parallax) and distance rate (radial velocity) are also variable. In the rigorous treatment the variation of all *six* parameters α, δ, π, $\mu_{\alpha *}$, μ_{δ}, V_{R} must therefore be

considered, and the parameter vector **a** is now six-dimensional, associated with the 6×6 covariance matrix **C**. For computational reasons the sixth parameter is taken to be the radial velocity divided by distance, or more precisely:

$$\zeta = V_R \pi / A \qquad [1.5.24]$$

where A is the astronomical unit. ζ is conveniently measured in mas/yr, which is obtained by expressing V_R in km/s and A in km yr/s (= A_v in Table 1.2.2; see also the note after Equation 1.2.17). Its value as computed from the catalogue (referring to epoch T_0) is denoted ζ_0. The use of ζ instead of V_R as the sixth parameter allows the case of measured $\pi \le 0$ to be handled gracefully (if unphysically) by the general algorithm.

Propagation of a: The propagation of the barycentric direction, and hence of α and δ, is given by Equation 1.2.16. Using notations from Section 1.2.8 and introducing the distance factor:

$$f = |\mathbf{b}(0)|\,|\mathbf{b}(t)|^{-1} = [1 + 2\zeta_0 t + (\mu_0^2 + \zeta_0^2)t^2]^{-1/2} \qquad [1.5.25]$$

(where $\mu_0^2 = |\boldsymbol{\mu}_0|^2 = \mu_{\alpha*0}^2 + \mu_{\delta 0}^2$), the propagation of the barycentric direction is:

$$\mathbf{u} = [\mathbf{r}_0(1 + \zeta_0 t) + \boldsymbol{\mu}_0 t] f \qquad [1.5.26]$$

and the propagation of the parallax becomes:

$$\pi = \pi_0 f \qquad [1.5.27]$$

Direct differentiation of Equation 1.5.26 now gives the propagated proper motion vector:

$$\boldsymbol{\mu} = \frac{\mathrm{d}\mathbf{u}}{\mathrm{d}t} = \left[\boldsymbol{\mu}_0(1 + \zeta_0 t) - \mathbf{r}_0 \mu_0^2 t\right] f^3 \qquad [1.5.28]$$

while the propagated sixth parameter is found to be:

$$\zeta = \frac{\mathrm{d}b}{\mathrm{d}t}\frac{\pi}{A} = \left[\zeta_0 + (\mu_0^2 + \zeta_0^2)t\right] f^2 \qquad [1.5.29]$$

The barycentric direction and proper motion vector, taken at the catalogue epoch, are:

$$\mathbf{u}_0 = \mathbf{r}_0 \qquad [1.5.30]$$

$$\boldsymbol{\mu}_0 = \mathbf{p}_0 \mu_{\alpha*0} + \mathbf{q}_0 \mu_{\delta 0} \qquad [1.5.31]$$

where [$\mathbf{p}_0$ $\mathbf{q}_0$ $\mathbf{r}_0$] is the normal triad introduced in Section 1.2.8; its equatorial components are given by Equations 1.2.11 and 1.2.15.

The celestial coordinates (α, δ) at epoch T are obtained from **u** in the usual manner, using Equation 1.5.5. However, to obtain the proper motion components $(\mu_{\alpha*}, \mu_\delta)$ from the vector $\boldsymbol{\mu}$ it is necessary to resolve the latter along the tangential vectors **p** and **q** *at the propagated position*, i.e. with the tangent point located at **u** and with **p** pointing towards the local north. The proper motion components are thus:

$$\mu_{\alpha*} = \mathbf{p}'\boldsymbol{\mu} \qquad \mu_\delta = \mathbf{q}'\boldsymbol{\mu} \qquad [1.5.32]$$

with **p** and **q** defined in terms of **u** or (α, δ) (at epoch T) according to Equation 1.2.15 or 1.5.15.

The above formulae describe the transformation of $(\alpha_0,\ \delta_0,\ \pi_0,\ \mu_{\alpha*0},\ \mu_{\delta 0},\ V_{R0})$ at epoch T_0 into $(\alpha,\ \delta,\ \pi,\ \mu_{\alpha*},\ \mu_\delta,\ V_R)$ at epoch T. This transformation is rigorously reversible, so that a second transformation from T to T_0 recovers the original six parameters.

Propagation of C: The transformation of covariances requires the calculation of all 36 partial derivatives constituting the Jacobian matrix in $\mathbf{C} = \mathbf{J}\mathbf{C}_0\mathbf{J}'$. This is relatively straightforward, if somewhat tedious, and the complete expressions are given below. However, one further consideration is necessary. The proper motion components depend on the tangential vectors **p** and **q** (Equation 1.5.32), and these in turn depend on the reference direction **r** set equal to the propagated position **u** (Equation 1.5.15). The question arises whether the normal triad [**p q r**] should be regarded as a fixed, error-free reference frame for the proper motion vector, or whether the uncertainties in **u** should be propagated through the definition of this triad, and subsequently to the proper motion components.

It appears that either option could be adopted, as long as it is consistently applied, and that the choice between them is a matter of convention. The reduction procedures used to construct the Hipparcos and Tycho Catalogues implicitly adopt the first option, which also seems closer to an intuitive understanding of the uncertainty of the proper motion (as representing an uncertainty in the physical vector $\boldsymbol{\mu}$). Consequently the same convention has been adopted for the calculation of the Jacobian matrix below. The practical consequence is that the two normal triads [$\mathbf{p}_0$ $\mathbf{q}_0$ $\mathbf{r}_0$] and [**p q r**] must be regarded as fixed in all the calculations, which also motivates the somewhat formal distinction between the vectors $\mathbf{r}_0$ and $\mathbf{u}_0$, and between **r** and **u**.

The elements of the Jacobian matrix are given hereafter:

$$[\mathbf{J}]_{11} = \frac{\partial \alpha*}{\partial \alpha*_0} = \mathbf{p}'\mathbf{p}_0(1+\zeta_0 t)f - \mathbf{p}'\mathbf{r}_0\mu_{\alpha*0}tf \qquad [1.5.33]$$

$$[\mathbf{J}]_{12} = \frac{\partial \alpha*}{\partial \delta_0} = \mathbf{p}'\mathbf{q}_0(1+\zeta_0 t)f - \mathbf{p}'\mathbf{r}_0\mu_{\delta 0}tf \qquad [1.5.34]$$

$$[\mathbf{J}]_{13} = \frac{\partial \alpha*}{\partial \pi_0} = 0 \qquad [1.5.35]$$

$$[\mathbf{J}]_{14} = \frac{\partial \alpha*}{\partial \mu_{\alpha*0}} = \mathbf{p}'\mathbf{p}_0 tf \qquad [1.5.36]$$

$$[\mathbf{J}]_{15} = \frac{\partial \alpha*}{\partial \mu_{\delta 0}} = \mathbf{p}'\mathbf{q}_0 tf \qquad [1.5.37]$$

$$[\mathbf{J}]_{16} = \frac{\partial \alpha*}{\partial \zeta_0} = -\mu_{\alpha*}t^2 \qquad [1.5.38]$$

$$[\mathbf{J}]_{21} = \frac{\partial \delta}{\partial \alpha*_0} = \mathbf{q}'\mathbf{p}_0(1+\zeta_0 t)f - \mathbf{q}'\mathbf{r}_0\mu_{\alpha*0}tf \qquad [1.5.39]$$

$$[\mathbf{J}]_{22} = \frac{\partial \delta}{\partial \delta_0} = \mathbf{q}'\mathbf{q}_0(1+\zeta_0 t)f - \mathbf{q}'\mathbf{r}_0\mu_{\delta 0}tf \qquad [1.5.40]$$

$$[\mathbf{J}]_{23} = \frac{\partial \delta}{\partial \pi_0} = 0 \qquad [1.5.41]$$

$$[\mathbf{J}]_{24} = \frac{\partial \delta}{\partial \mu_{\alpha*0}} = \mathbf{q}'\mathbf{p}_0 tf \qquad [1.5.42]$$

$$[\mathbf{J}]_{25} = \frac{\partial \delta}{\partial \mu_{\delta 0}} = \mathbf{q}'\mathbf{q}_0 tf \qquad [1.5.43]$$

$$[\mathbf{J}]_{26} = \frac{\partial \delta}{\partial \zeta_0} = -\mu_{\delta}t^2 \qquad [1.5.44]$$

$$[\mathbf{J}]_{31} = \frac{\partial \pi}{\partial \alpha*_0} = 0 \qquad [1.5.45]$$

$$[\mathbf{J}]_{32} = \frac{\partial \pi}{\partial \delta_0} = 0 \qquad [1.5.46]$$

$$[\mathbf{J}]_{33} = \frac{\partial \pi}{\partial \pi_0} = f \qquad [1.5.47]$$

$$[\mathbf{J}]_{34} = \frac{\partial \pi}{\partial \mu_{\alpha*0}} = -\pi \mu_{\alpha*0} t^2 f^2 \qquad [1.5.48]$$

$$[\mathbf{J}]_{35} = \frac{\partial \pi}{\partial \mu_{\delta 0}} = -\pi \mu_{\delta 0} t^2 f^2 \qquad [1.5.49]$$

$$[\mathbf{J}]_{36} = \frac{\partial \pi}{\partial \zeta_0} = -\pi (1 + \zeta_0 t) t f^2 \qquad [1.5.50]$$

$$[\mathbf{J}]_{41} = \frac{\partial \mu_{\alpha*}}{\partial \alpha*_0} = -\mathbf{p}'\mathbf{p}_0 \mu_0^2 t f^3 - \mathbf{p}'\mathbf{r}_0 \mu_{\alpha*0} (1 + \zeta_0 t) f^3 \qquad [1.5.51]$$

$$[\mathbf{J}]_{42} = \frac{\partial \mu_{\alpha*}}{\partial \delta_0} = -\mathbf{p}'\mathbf{q}_0 \mu_0^2 t f^3 - \mathbf{p}'\mathbf{r}_0 \mu_{\delta 0} (1 + \zeta_0 t) f^3 \qquad [1.5.52]$$

$$[\mathbf{J}]_{43} = \frac{\partial \mu_{\alpha*}}{\partial \pi_0} = 0 \qquad [1.5.53]$$

$$[\mathbf{J}]_{44} = \frac{\partial \mu_{\alpha*}}{\partial \mu_{\alpha*0}} = \mathbf{p}'\mathbf{p}_0 (1 + \zeta_0 t) f^3 - 2\mathbf{p}'\mathbf{r}_0 \mu_{\alpha*0} t f^3 - 3\mu_{\alpha*}\mu_{\alpha*0} t^2 f^2 \qquad [1.5.54]$$

$$[\mathbf{J}]_{45} = \frac{\partial \mu_{\alpha*}}{\partial \mu_{\delta 0}} = \mathbf{p}'\mathbf{q}_0 (1 + \zeta_0 t) f^3 - 2\mathbf{p}'\mathbf{r}_0 \mu_{\delta 0} t f^3 - 3\mu_{\alpha*}\mu_{\delta 0} t^2 f^2 \qquad [1.5.55]$$

$$[\mathbf{J}]_{46} = \frac{\partial \mu_{\alpha*}}{\partial \zeta_0} = \mathbf{p}'[\boldsymbol{\mu}_0 f - 3\boldsymbol{\mu}(1 + \zeta_0 t)] t f^2 \qquad [1.5.56]$$

$$[\mathbf{J}]_{51} = \frac{\partial \mu_{\delta}}{\partial \alpha*_0} = -\mathbf{q}'\mathbf{p}_0 \mu_0^2 t f^3 - \mathbf{q}'\mathbf{r}_0 \mu_{\alpha*0} (1 + \zeta_0 t) f^3 \qquad [1.5.57]$$

$$[\mathbf{J}]_{52} = \frac{\partial \mu_{\delta}}{\partial \delta_0} = -\mathbf{q}'\mathbf{q}_0 \mu_0^2 t f^3 - \mathbf{q}'\mathbf{r}_0 \mu_{\delta 0} (1 + \zeta_0 t) f^3 \qquad [1.5.58]$$

$$[\mathbf{J}]_{53} = \frac{\partial \mu_{\delta}}{\partial \pi_0} = 0 \qquad [1.5.59]$$

$$[\mathbf{J}]_{54} = \frac{\partial \mu_{\delta}}{\partial \mu_{\alpha*0}} = \mathbf{q}'\mathbf{p}_0 (1 + \zeta_0 t) f^3 - 2\mathbf{q}'\mathbf{r}_0 \mu_{\alpha*0} t f^3 - 3\mu_{\delta}\mu_{\alpha*0} t^2 f^2 \qquad [1.5.60]$$

$$[\mathbf{J}]_{55} = \frac{\partial \mu_{\delta}}{\partial \mu_{\delta 0}} = \mathbf{q}'\mathbf{q}_0 (1 + \zeta_0 t) f^3 - 2\mathbf{q}'\mathbf{r}_0 \mu_{\delta 0} t f^3 - 3\mu_{\delta}\mu_{\delta 0} t^2 f^2 \qquad [1.5.61]$$

$$[\mathbf{J}]_{56} = \frac{\partial \mu_{\delta}}{\partial \zeta_0} = \mathbf{q}'[\boldsymbol{\mu}_0 f - 3\boldsymbol{\mu}(1 + \zeta_0 t)] t f^2 \qquad [1.5.62]$$

$$[\mathbf{J}]_{61} = \frac{\partial \zeta}{\partial \alpha*_0} = 0 \qquad [1.5.63]$$

$$[\mathbf{J}]_{62} = \frac{\partial \zeta}{\partial \delta_0} = 0 \qquad [1.5.64]$$

$$[\mathbf{J}]_{63} = \frac{\partial \zeta}{\partial \pi_0} = 0 \qquad [1.5.65]$$

$$[\mathbf{J}]_{64} = \frac{\partial \zeta}{\partial \mu_{\alpha*0}} = 2\mu_{\alpha*0} (1 + \zeta_0 t) t f^4 \qquad [1.5.66]$$

$$[\mathbf{J}]_{65} = \frac{\partial \zeta}{\partial \mu_{\delta 0}} = 2\mu_{\delta 0} (1 + \zeta_0 t) t f^4 \qquad [1.5.67]$$

$$[\mathbf{J}]_{66} = \frac{\partial \zeta}{\partial \zeta_0} = [(1 + \zeta_0 t)^2 - \mu_0^2 t^2] f^4 \qquad [1.5.68]$$

Initialization of $\mathbf{C}_0$: The Hipparcos and Tycho Catalogues provide the first five rows and columns of elements in $\mathbf{C}_0$ according to Equation 1.2.5. For the rigorous propagation this must be augmented with a sixth row and column related to the parameter $\zeta_0 = V_{\mathrm{R}0}\pi_0/A$. If the (spectroscopic) radial velocity $V_{\mathrm{R}0}$ has the standard error $\sigma_{V_{\mathrm{R}0}}$, and is assumed to be statistically independent of the astrometric parameters in the catalogue, then the required additional elements in $\mathbf{C}_0$ are:

$$\left.\begin{aligned} [\mathbf{C}_0]_{i6} = [\mathbf{C}_0]_{6i} &= (V_{\mathrm{R}0}/A)\,[\mathbf{C}_0]_{i3}, \quad i = 1 \ldots 5 \\ [\mathbf{C}_0]_{66} &= (V_{\mathrm{R}0}/A)^2\,[\mathbf{C}_0]_{33} + (\pi_0/A)^2\,\sigma^2_{V_{\mathrm{R}0}} \end{aligned}\right\} \qquad [1.5.69]$$

If the radial velocity is not known, ζ_0 should be set to zero and the corresponding elements in $\mathbf{C}_0$ could also be zeroed. However, it could also be argued that $\sigma_{V_{\mathrm{R}0}}$ should be set to the expected velocity dispersion of the stellar type in question, in which case $[\mathbf{C}_0]_{66}$ would in general still be positive according to Equation 1.5.69. This means that the unknown perspective acceleration is accounted for in the uncertainty of the propagated astrometric parameters. In the *Celestia 2000* software, $V_{\mathrm{R}0} = 0$ is assumed for all stars except the 21 listed in Table 1.2.3, and $\sigma_{V_{\mathrm{R}0}} = 0$ is assumed for all stars.

It should be noted that strict reversal of the transformation (from T to T_0), according to the standard model of stellar motion, is only possible if the full six-dimensional parameter vector and covariance is considered.

1.5.6. Calculation of Space Coordinates and Velocity

The calculation of the rectangular space coordinates and velocity of a star from the astrometric parameters, supplemented by the radial velocity, was considered already in Section 1.2.8, as part of the standard model of stellar motion. For convenience, the relevant formulae are summarized hereafter. All quantities may be taken to refer to the catalogue epoch J1991.25, although results for other epochs can be obtained by applying first the transformations in the preceding sections (for brevity, the subscript $_0$ is subsequently dropped).

Let $\mathbf{b}$ be the barycentric position of the star, measured in parsec, and $\mathbf{v}$ its barycentric space velocity, measured in km/s. According to Section 1.2.8, these vectors can be written:

$$\mathbf{b} = A_p\mathbf{u}/\pi \qquad [1.5.70]$$

where $\mathbf{u}$ is the direction defined by Equation 1.2.16, and:

$$\mathbf{v} = (\mathbf{p}\mu_{\alpha*}A_v/\pi + \mathbf{q}\mu_\delta A_v/\pi + \mathbf{r}V_{\mathrm{R}})k \qquad [1.5.71]$$

Here, $[\,\mathbf{p}\;\mathbf{q}\;\mathbf{r}\,]$ is the normal triad introduced in Section 1.2.8, with $\mathbf{r} = \mathbf{u}$. A_p = 1000 mas pc and A_v = 4.74047... km yr s^{-1} designate the astronomical unit expressed in the appropriate units (Table 1.2.2), and π, $\mu_{\alpha*}$ and μ_δ are the parallax and proper motion components in mas and mas/yr. $k = (1 - V_{\mathrm{R}}/c)^{-1}$ is the Doppler factor explained in connection with Equation 1.2.21.

In the equatorial system the components of the normal triad $[\,\mathbf{p}\;\mathbf{q}\;\mathbf{r}\,]$ are given by the matrix:

$$\mathbf{R} = \begin{pmatrix} p_x & q_x & r_x \\ p_y & q_y & r_y \\ p_z & q_z & r_z \end{pmatrix} = \begin{pmatrix} -\sin\alpha & -\sin\delta\cos\alpha & \cos\delta\cos\alpha \\ \cos\alpha & -\sin\delta\sin\alpha & \cos\delta\sin\alpha \\ 0 & \cos\delta & \sin\delta \end{pmatrix} \qquad [1.5.72]$$

(cf. Equations 1.2.11 and 1.2.15). The equatorial components of **b** and **v** may thus be written in matrix form as:

$$\begin{pmatrix} b_x \\ b_y \\ b_z \end{pmatrix} = \mathbf{R} \begin{pmatrix} 0 \\ 0 \\ A_p/\pi \end{pmatrix} \qquad [1.5.73]$$

and:

$$\begin{pmatrix} v_x \\ v_y \\ v_z \end{pmatrix} = \mathbf{R} \begin{pmatrix} k\mu_{\alpha*}A_v/\pi \\ k\mu_\delta A_v/\pi \\ kV_\mathrm{R} \end{pmatrix} \qquad [1.5.74]$$

The galactic components of **b** and **v** are obtained through pre-multiplication by $\mathbf{A}_\mathrm{G}'$, as in Equation 1.5.13.

For kinematical applications the covariance of the space velocity components may be required. More generally, the 6×6 covariance matrix of the position-velocity vector $\mathbf{s} \equiv (b_x, b_y, b_z, v_x, v_y, v_z)'$ may be calculated (again in equatorial coordinates) as:

$$\mathrm{Cov}(\mathbf{s}) = \mathbf{J} \begin{pmatrix} \mathbf{C} & \mathbf{0}_{51} \\ \mathbf{0}_{15} & \sigma_{V_\mathrm{R}}^2 \end{pmatrix} \mathbf{J}' \qquad [1.5.75]$$

where **C** is the 5×5 covariance matrix of the astrometric parameters, $\mathbf{0}_{mn}$ is the $m \times n$ matrix of zeroes, σ_{V_R} the standard error of the radial velocity, and:

$$\mathbf{J} = \begin{pmatrix} A_p p_x/\pi & A_p q_x/\pi & -A_p r_x/\pi^2 & 0 & 0 & 0 \\ A_p p_y/\pi & A_p q_y/\pi & -A_p r_y/\pi^2 & 0 & 0 & 0 \\ A_p p_z/\pi & A_p q_z/\pi & -A_p r_z/\pi^2 & 0 & 0 & 0 \\ 0 & 0 & -(p_x\mu_{\alpha*} + q_x\mu_\delta)A_v/\pi^2 & p_x A_v/\pi & q_x A_v/\pi & r_x \\ 0 & 0 & -(p_y\mu_{\alpha*} + q_y\mu_\delta)A_v/\pi^2 & p_y A_v/\pi & q_y A_v/\pi & r_y \\ 0 & 0 & -(p_z\mu_{\alpha*} + q_z\mu_\delta)A_v/\pi^2 & p_z A_v/\pi & q_z A_v/\pi & r_z \end{pmatrix} \qquad [1.5.76]$$

is the Jacobian matrix of the transformation from $(\alpha*, \delta, \pi, \mu_{\alpha*}, \mu_\delta, V_\mathrm{R})'$ to **s**. (The Doppler factor k has been neglected for the calculation of the partial derivatives.) The covariance of the space velocity is the lower-right 3×3 submatrix of Equation 1.5.75.

In the galactic system the components of the position-velocity vector are given by the 6×1 matrix **Gs**, where:

$$\mathbf{G} = \begin{pmatrix} \mathbf{A}_\mathrm{G}' & \mathbf{0}_{33} \\ \mathbf{0}_{33} & \mathbf{A}_\mathrm{G}' \end{pmatrix} \qquad [1.5.77]$$

according to Equation 1.5.13; the associated covariance is therefore:

$$\mathrm{Cov}(\mathbf{Gs}) = \mathbf{GJ} \begin{pmatrix} \mathbf{C} & \mathbf{0}_{51} \\ \mathbf{0}_{15} & \sigma_{V_\mathrm{R}}^2 \end{pmatrix} \mathbf{J}'\mathbf{G}' \qquad [1.5.78]$$

1.5.7. Relation to the J2000(FK5) Reference Frame

As explained in Section 1.2.2, the Hipparcos and Tycho Catalogues materialise the International Celestial Reference System by defining a reference frame, which may be designated ICRS(Hipparcos). This supersedes the optical reference frame defined by the FK5 catalogue, which was formally based on the mean equator and dynamical equinox of J2000 and therefore properly designated J2000(FK5).

Since all the stars in the basic FK5 catalogue are also contained in the Hipparcos Catalogue, the relationship between the two reference frames is open to investigation by direct comparison of the positions and proper motions in the two catalogues. The results of one such comparison are given in Volume 3.

A complete characterisation of the relation between J2000(FK5) and ICRS(Hipparcos) is difficult to achieve, given the relatively small number of stars defining the FK5 reference frame, and the intricate and possibly colour- and magnitude-dependent pattern of systematic (in particular zonal) differences, combined with the perturbing effects on the proper motions of undetected astrometric binaries. Nevertheless, certain relations on a global scale may be established with relative ease, in particular the most fundamental one corresponding to a difference in the mean orientation and spin between the two catalogues.

At the epoch T_0 = J1991.25 let $(\alpha_\mathrm{F}, \delta_\mathrm{F})$ be the barycentric coordinates of an object in the J2000(FK5) frame, and $(\alpha_\mathrm{H}, \delta_\mathrm{H})$ its coordinates in the ICRS(Hipparcos) frame. If the two frames are related by a pure rigid-body rotation, the coordinate differences can be written, in the small-angle approximation:

$$\begin{aligned}(\alpha_\mathrm{F} - \alpha_\mathrm{H})\cos\delta &= -\varepsilon_{0x}\,\sin\delta\cos\alpha - \varepsilon_{0y}\,\sin\delta\sin\alpha + \varepsilon_{0z}\,\cos\delta \\ \delta_\mathrm{F} - \delta_\mathrm{H} &= +\varepsilon_{0x}\,\sin\alpha - \varepsilon_{0y}\,\cos\alpha\end{aligned} \qquad [1.5.79]$$

(either set of coordinates may be used in the trigonometric factors). The vector $\varepsilon_0 = (\varepsilon_{0x}\ \varepsilon_{0y}\ \varepsilon_{0z})'$ represents the orientation difference between the frames, taken in the sense F−H, at epoch T_0 (L. Lindegren & J. Kovalevsky, 1995, *Astronomy & Astrophysics*, 304, 189). The differences in proper motion, to the extent they are described by a pure spin, can similarly be written:

$$\begin{aligned}(\mu_{\alpha*})_\mathrm{F} - (\mu_{\alpha*})_\mathrm{H} &= -\omega_x\,\sin\delta\cos\alpha - \omega_y\,\sin\delta\sin\alpha + \omega_z\cos\delta \\ (\mu_\delta)_\mathrm{F} - (\mu_\delta)_\mathrm{H} &= +\omega_x\,\sin\alpha - \omega_y\,\cos\alpha\end{aligned} \qquad [1.5.80]$$

where the vector $\omega = (\omega_x\ \omega_y\ \omega_z)'$ represents the spin difference between the frames, again taken in the sense F−H.

However, fitting the rotational parameters ε_0 and ω directly to the catalogue differences, by means of the above equations, results in a solution which is significantly affected by the non-zero projection of the largest zonal differences onto the rotational terms. For this reason a more general representation was preferred, in which the vector fields $[(\alpha_\mathrm{F} - \alpha_\mathrm{H})\cos\delta,\ \delta_\mathrm{F} - \delta_\mathrm{H}]$ and $[(\mu_{\alpha*})_\mathrm{F} - (\mu_{\alpha*})_\mathrm{H},\ (\mu_\delta)_\mathrm{F} - (\mu_\delta)_\mathrm{H}]$ are decomposed on a set of orthogonal vectorial harmonics. The first degree of these harmonics represents the pure rotation while the harmonics of higher degree account for the zonal differences. The root mean square of the residuals after removal of all significant terms allows the accuracy of each Fourier component of the decomposition to be estimated.

Applying this method to the estimation of the orientation and spin differences between the FK5 and the Hipparcos Catalogue gives:

$$\begin{aligned} \epsilon_{0x} &= -18.8 \pm 2.3 \text{ mas} \\ \epsilon_{0y} &= -12.3 \pm 2.3 \text{ mas} \\ \epsilon_{0z} &= +16.8 \pm 2.3 \text{ mas} \\ \omega_x &= -0.10 \pm 0.10 \text{ mas yr}^{-1} \\ \omega_y &= +0.43 \pm 0.10 \text{ mas yr}^{-1} \\ \omega_z &= +0.88 \pm 0.10 \text{ mas yr}^{-1} \end{aligned} \qquad [1.5.81]$$

where the orientation parameters refer to the epoch J1991.25. This preliminary result was based on the catalogue differences for all 1535 FK5 stars without filtering; no star was removed in the comparison. The remaining differences once the rotation has been applied may be as large as 150 mas, because of the large zonal differences which show up in the harmonics of higher degree.

A similar decomposition based on only 1232 FK5 stars, after the double stars and the suspected astrometric binaries had been excluded, led to very similar values for the orientation and spin. Likewise various binnings in cells of 100, 200 or 400 square degrees was attempted and found to give comparable results. Selecting stars according to their brightness produced different solutions for the rotation and spin parameters slightly outside the above standard errors, demonstrating the difficulty of establishing a well-defined relation between J2000(FK5) and ICRS(Hipparcos).

Section 2.1

Contents of the Hipparcos Catalogue

2.1. Contents of the Hipparcos Catalogue

Description of Left-Hand Pages (Fields H0–H30)

Field H0: The machine-readable (main) Hipparcos and Tycho Catalogues include a character indicating whether the associated record is derived from Hipparcos (H) or Tycho (T) data. Field H1/T1 then provides the Hipparcos Catalogue number (HIP) or the Tycho Catalogue identifier (TYC) accordingly, with the interpretation of subsequent fields being, in part, catalogue dependent (see Tables 2.1.1 and 2.2.1).

Field H1: Hipparcos Catalogue (HIP) identifier

The HIP identifier uniquely defines the stars observed by the Hipparcos satellite. Entries retain the same identifier within the final Hipparcos Catalogue as in the Hipparcos Input Catalogue—thus the Hipparcos Input Catalogue may conveniently be used to ascertain corresponding pre-Hipparcos data, cross-identifications, etc. Entries in the catalogue are referred to by their Hipparcos Catalogue (or HIP) number, emphasising that the data items associated with this number are different from those associated with the Hipparcos Input Catalogue (or HIC) number.

The printed catalogue is ordered by increasing HIP number (exceptions are noted below). This numbering follows very closely ordering by right ascension (within the reference system ICRS, and at the catalogue epoch J1991.25) independent of declination.

For entries originally considered as single, but discovered to be double or multiple on the basis of the satellite observations, the single HIP number is retained. Details are given in Fields H55–67, and in the Double and Multiple Systems Annex, along with all other double and multiple system data.

'*' indicates that the entry is 'out of sequence' (in the printed catalogue) in right ascension: there are a number of cases where ordering by HIP number results in a displacement in the ordering by right ascension by one or more catalogue places, n. In the printed catalogue, all $n + 1$ affected entries are indicated by an asterisk preceding the HIP number. This affects the following numbers of entries (those with $5 < n < 16$ are omitted here):

Displacement, n:	1	2	3	4	5	...	16	17	18
Number of entries:	3406	334	61	29	19	...	1	5	1

The only exception to the ordering by HIP number is for the 34 entries with HIP > 120 000. These are objects which were allocated revised HIP numbers during the early part of the mission following the identification of significant *a priori* errors in position and/or magnitude (a subset of these were already assigned in the published Hipparcos Input Catalogue). They are inserted in the printed catalogue at the position corresponding to their right ascension (and not indicated by an asterisk).

The machine-readable catalogue is ordered by right ascension, according to Field H8, with an ordering derived from Field H3 for the 263 cases where this field is blank. It may also be interrogated by HIP number through the index file supplied.

Statistics of entries: there are a total of 118 218 HIP entries. Of these, 117 955 have associated astrometry (of the other 263 entries, 10 entries had no astrometric solution and a further 253 inadequate solutions were suppressed); and 118 204 have associated photometry. The HIP entries follow precisely the HIC numbering, with the exception of one entry (HIC 99413) which was deleted from the Hipparcos observation programme after the publication of the Hipparcos Input Catalogue, and the entries 120 401 – 120 404 and 120 411 – 120 416 which were added to the programme at a late stage. Thus, in the range HIP 1 – 118 322, 138 numbers do not appear (137 were missing in HIC), while there are 34 HIP entries with a HIP number above 120 000. The affected entries are tabulated hereafter:

HIP >120000 ordered by HIP number

HIP	Right ascension J1991.25 (ICRS)	Declination J1991.25 (ICRS)
120001	05 10 42.43	−20 45 03.0
120002	05 59 25.13	+17 48 59.1
120003	06 31 09.63	+11 15 21.1
120004	08 25 48.50	−00 24 35.3
120005	09 14 26.19	+52 41 16.7
120006	14 53 20.87	−45 51 32.7
120027	03 19 13.13	−73 38 54.2
120046	07 03 52.64	−46 25 02.5
120047	07 15 18.66	−31 54 34.9
120071	10 07 38.10	−85 07 11.4
120082	11 39 49.86	+45 09 23.8
120121	16 04 48.15	−35 52 10.1
120132	18 00 09.95	−48 20 01.9
120148	20 03 00.82	+20 05 49.8
120155	20 21 31.73	+36 55 12.8
120159	21 22 59.03	−80 04 52.8
120212	12 27 48.08	+00 29 35.3
120229	21 58 41.72	+23 04 16.3
120248	06 49 50.74	+66 21 30.2
120250	21 10 01.55	−01 51 52.1
120276	10 02 04.27	+79 42 22.6
120290	16 57 40.96	+35 16 11.0
120306	23 06 44.99	−66 04 31.0
120313	13 45 35.69	+17 44 32.8
120401	07 57 31.75	−60 37 51.3
120402	07 57 47.68	−60 36 35.0
120403	07 57 49.18	−60 41 01.2
120404	07 58 02.92	−60 36 53.3
120411	04 47 58.18	−32 09 54.2
120412	05 23 33.71	−60 55 29.0
120413	11 46 36.46	−27 27 32.1
120414	11 51 37.00	−25 54 40.3
120415	20 20 04.64	−67 22 23.4
120416	20 12 58.08	−56 50 47.9

HIP >120000 ordered by right ascension

HIP	Right ascension J1991.25 (ICRS)	Declination J1991.25 (ICRS)
120027	03 19 13.13	−73 38 54.2
120411	04 47 58.18	−32 09 54.2
120001	05 10 42.43	−20 45 03.0
120412	05 23 33.71	−60 55 29.0
120002	05 59 25.13	+17 48 59.1
120003	06 31 09.63	+11 15 21.1
120248	06 49 50.74	+66 21 30.2
120046	07 03 52.64	−46 25 02.5
120047	07 15 18.66	−31 54 34.9
120401	07 57 31.75	−60 37 51.3
120402	07 57 47.68	−60 36 35.0
120403	07 57 49.18	−60 41 01.2
120404	07 58 02.92	−60 36 53.3
120004	08 25 48.50	−00 24 35.3
120005	09 14 26.19	+52 41 16.7
120276	10 02 04.27	+79 42 22.6
120071	10 07 38.10	−85 07 11.4
120082	11 39 49.86	+45 09 23.8
120413	11 46 36.46	−27 27 32.1
120414	11 51 37.00	−25 54 40.3
120212	12 27 48.08	+00 29 35.3
120313	13 45 35.69	+17 44 32.8
120006	14 53 20.87	−45 51 32.7
120121	16 04 48.15	−35 52 10.1
120290	16 57 40.96	+35 16 11.0
120132	18 00 09.95	−48 20 01.9
120148	20 03 00.82	+20 05 49.8
120416	20 12 58.08	−56 50 47.9
120415	20 20 04.64	−67 22 23.4
120155	20 21 31.73	+36 55 12.8
120250	21 10 01.55	−01 51 52.1
120159	21 22 59.03	−80 04 52.8
120229	21 58 41.72	+23 04 16.3
120306	23 06 44.99	−66 04 31.0

HIP numbers not represented in the Hipparcos Catalogue

672	15502	31865	39151	52081	60606	69217	86018	96578	106808
1569	18193	31869	39615	52754	60656	74720	86337	96685	108292
3814	18200	32720	40207	54637	60898	76367	86909	97453	110971
5200	19006	33870	41023	55419	61056	78626	87011	98686	111772
5791	20461	33967	43168	56283	63146	78778	88138	99413	112054
8402	24045	34232	45172	56288	63158	81359	88168	99630	112313
9584	24908	34593	47481	56804	64239	82616	89395	100410	112445
9626	25384	35175	47855	57147	65576	82846	90057	101609	114095
11119	26911	35292	48831	57354	66518	82924	90682	101775	114122
11916	27274	36230	49190	58156	67089	83437	90688	101872	115426
11961	28058	36353	49361	58209	67295	83470	91787	102008	116059
12388	28810	37807	49550	59097	67920	84039	91835	102079	116992
15088	31077	38450	50224	59304	67924	85550	92357	104519	
15417	31441	38452	51431	59860	68098	85754	96513	105516	

Field H2: Proximity flag

This field provides a coarse indication of the presence of nearby objects within a specific radial distance (10 arcsec) of the given entry. If non-blank, it indicates that there is one or more distinct Hipparcos Catalogue entries (or distinct components of the system from Part C of the Double and Multiple Systems Annex if double or multiple), or one or more distinct Tycho Catalogue entries, in either case irrespective of magnitude, within 10 arcsec of the position given in Fields H8–9. The flag is assigned according to the following hierarchy (i.e. if 'H' and 'T' both apply, 'H' is adopted):

H : there is one or more distinct Hipparcos Catalogue entries, or one or more distinct components of the relevant Hipparcos Catalogue entry, within 10 arcsec of the position given in Fields H8–9 (i.e. entries flagged 'G', 'O', 'V', 'X' in Field H59 or 'S' in Field H61 are not considered);

T : there is one or more distinct Tycho Catalogue entries within 10 arcsec of the position given in Fields H8–9.

The flag 'T' implies either an inconsistency between the Hipparcos and Tycho Catalogues (e.g. discordant positions resulting in different separations), or a deficiency in one or both of the catalogues (e.g. indicating that a component detected by Tycho was not detected, or could not be solved, in the Hipparcos double-star processing; or that the Tycho detection was spurious).

The number of entries in each of these categories is as follows: H = 10 800; T = 125 (107 of these are non-blank in Field H61, with 33 flagged 'S').

Fields H3–7: Descriptor

Fields H3–4: Positional identifier: truncated coordinates (epoch J1991.25, ICRS)

The approximate right ascension and declination are given in conventional sexagesimal units with truncated precision, for epoch J1991.25, and within the reference system ICRS. Fields H3–4 are rounded values of the positions given in Fields H8–9, and are included as a convenient way of object identification.

For the 263 cases where Fields H8–9 are missing (see Field H1), Fields H3–4 provide the position taken from the Hipparcos Input Catalogue, and propagated to the catalogue epoch J1991.25. Fields H3–4 were computed directly from the solution: computation from Fields H8–9 will lead to a few cases with an apparently discrepant final digit in the descriptor.

Field H5: V magnitude

The magnitude, V, in the Johnson UBV photometric system.

The V magnitude was not measured directly from the Hipparcos observations, but derived using a series of transformations according to stellar type and the photometric information available (see Field H7). As a result, the field provides an approximate but rather homogeneous indication of the Johnson V magnitude useful, for example, for identification purposes, and for the computation of absolute magnitudes in terms of M_V. Users should, however, be aware of the limitations arising from its construction.

The source of V is given in Field H7. If a genuine Johnson V magnitude (obtained either in UBV, Geneva, or Walraven photometry) was available and accurate, this was generally retained. When stars showed a significant

difference with respect to earlier ground-based data, V estimates from Hp and $V-I$, or from B_T and V_T, were preferred, since they correspond to the median magnitude during the mission. The V magnitude for variable stars are in principle derived from the satellite data only.

The most accurate estimate of V, produced either from the ground, from Tycho data, or from Hp and Tycho data, was selected. The transformations used are given in Section 1.3, Appendix 4. See also Field H43 for cases where the derived V magnitudes correspond to non-single stars.

Error estimates were computed in order to select the appropriate source of V. The internal accuracy is generally very high, with standard errors of the order of a few millimagnitudes. Nevertheless, the systematic errors induced by inadequacies of the transformation equations are larger. They are of the order of 0.01 mag for G and K stars, where $Hp-V_J$ is rather insensitive to colour index (see Figure 1.3.4). The offset may reach 0.03–0.08 mag, for example in the case of reddened stars, supergiants, WR stars, or double stars. Smaller systematic effects are also observed for metallic Am, Fm stars, and for metal-poor stars.

The selection of the appropriate transformation was made according to luminosity class. If no indication of luminosity class was available, the star was assumed to be a giant unless the 'absolute magnitude estimator' (see Field H42 = 'I' in Section 1.3, Appendix 5) indicated a late-type dwarf. The parallax was not used. The relations assume solar metallicity, and apply to low reddening stars.

Field H6: Coarse variability flag

A flag in this field indicates that the entry (or one of the components of the entry in the case of a resolved system) is variable, in Hp, at the level of:

1 : < 0.06 mag
2 : 0.06 – 0.6 mag
3 : > 0.6 mag

Fields H49–54 give further details of the photometric variability of the entry.

If, during the variability analysis, the entry was classified as a periodic or unsolved variable (Fields H52–53) the variability amplitude was taken directly from the tables in the Variability Annex (Section 2.4). Otherwise, entries were assigned this coarse variability flag according to the analysis described in Section 1.3, Appendix 2 (case 'M').

The number of entries in each of these categories is as follows: 1 = 4112; 2 = 6351; 3 = 1099.

Field H7: Source of V magnitude in Field H5

The source flag indicates that the V (Johnson) magnitude has been derived based upon:

G : ground-based multi-colour photometry, either directly in or reduced to the Johnson UBV system;
H : Hp (Field H44), combined with information on the colour index (either $V-I$ or B_T-V_T, Field H40 and Fields H32/34 respectively), in combination with the luminosity class (see Section 1.3, Appendix 4);
T : Tycho photometry, i.e. V_T and B_T-V_T from Fields H32–36 (see Section 1.3, Appendix 4);
␣ : no data available.

The number of entries in each category is as follows: G = 23 139; H = 94 669; T = 409; ␣ = 1.

Fields H8–30: Main Mission Astrometric Data

Positions are given at the catalogue epoch J1991.25. The astrometric positions and their errors can be propagated to the standard epoch J2000.0, or to any other epoch, within the ICRS system, by the methods described in Section 1.2.8. It is recommended that such propagation is based only on the five astrometric parameters given in Fields H8–13, supplemented with the radial velocity in cases where the perspective acceleration needs to be taken into account (including the 21 stars listed in Table 1.2.3). In particular the quadratic and cubic terms included in the 'acceleration solutions' ('G' in Field H59), and separately given in Part G of the Double and Multiple Systems Annex, are *not* intended for extrapolation beyond the observation interval (roughly 1989.9 to 1993.2); in this case the position and proper motion data in Fields H8–9 and H12–13, representing the mean linear motion over the mission interval, provide a more robust basis for extrapolation (see Section 2.3.3 for details). Field H8–30 are blank for the 263 entries noted under Field H1.

Fields H8–9: Equatorial coordinates (epoch J1991.25, ICRS)

The right ascension, α, and declination, δ, are expressed in degrees for the catalogue epoch J1991.25, and with respect to the reference system ICRS.

ICRS is consistent with the conventional coordinate system at J2000.0, previously realised by the FK5 Catalogue. The position is referred to the adopted common epoch for the whole catalogue, J1991.25. In practice, the satellite observations span slightly different epochs for each object; the effect is fully accounted for by providing positions, proper motions, and corresponding standard errors at the common catalogue epoch, along with the correlation coefficients.

For most entries, effective observational epochs can be computed from the data in Fields H14–28 according to precepts given in Section 1.2.7. The individual effective epochs form an approximately normal distribution with a median value of 1991.251 and with 85 per cent of the values falling between 1991.0 and 1991.5.

Field H10: Reference flag for astrometric parameters of double and multiple systems

The flag indicates that the astrometric parameters in Fields H3–4 and H8–30 refer to:

A, B,... : the specified component of a double or multiple system;

* : the photocentre of a double or multiple system included in Part C of the Double and Multiple Systems Annex;

\+ : the centre of mass. For such an entry, an orbit is given in Part O of the Double and Multiple Systems Annex, and an 'O' is given in Field H59.

Field H10 is given to account for the situations (because of the system geometry, and the magnitude difference between the components) where it is more appropriate to present the astrometric parameters of one or other of the components, or of a photocentre of two or more of the entries, or of the centre of mass. Field H10 is non-blank for all entries contained in Parts C, O, and V of the Double and Multiple Systems Annex (i.e. with 'C', 'O', or 'V' in Field H59). Entries in Parts G and X of the Double and Multiple Systems Annex ('G' or 'X' in Field H59) are blank in Field H10.

For resolved entries (with 'C' in Field H59) with separation $\varrho < 0.3$ arcsec the astrometric data in Fields H3–4 and H8–30 refer to the photocentre, which for these systems is generally better determined by the observations than the individual components (whose parameters are nevertheless given in Part C of the Double and Multiple Systems Annex).

For $\varrho \geq 0.3$ arcsec the astrometric parameters of the primary and secondary can be well estimated, and the primary is then used as the astrometric reference. If an individual component is used as reference, this will

always be the brightest component (in *Hp*), irrespective of whether this component has been identified in the literature as component A or B, etc. In certain multiple systems, it is in principle necessary to specify which components are included in the photocentre. For example, in a triple system ABC, the astrometric data may refer to the photocentre of the AB pair. This information is specified in a note (see Field H70). In practice, in all such cases in the Hipparcos Catalogue, it is AB which constitutes the adopted photocentre, never BC, AC, etc.

The number of entries in Field H10, and their relationship with the content of Field H59, is as follows:

Flag	Field H10	Field H59				
		C	G	O	V	X
A	9526	9526	0	0	0	0
B	1208	1208	0	0	0	0
C	87	87	0	0	0	0
D	10	10	0	0	0	0
E	2	2	0	0	0	0
G	1	1	0	0	0	0
S	2	2	0	0	0	0
*	2663	2375	0	0	288	0
+	235	0	0	235	0	0
Total non-blank	13734	13211	0	235	288	0

Field H11: Trigonometric parallax

The trigonometric parallax, π, is expressed in units of milliarcsec. The estimated parallax is given for every star, even if it appears to be insignificant or negative (which may arise when the true parallax is smaller than its error).

Fields H12–13: Proper motion components (epoch J1991.25, ICRS)

The proper motion components, $\mu_{\alpha*} = \mu_\alpha \cos\delta$ and μ_δ, are expressed in milliarcsec per Julian year (mas/yr), and are given with respect to the reference system ICRS.

Fields H14–15: Standard errors of the equatorial coordinates (epoch J1991.25)

The standard errors of the right ascension, $\sigma_{\alpha*} = \sigma_\alpha \cos\delta$, and declination, σ_δ, are given at the catalogue epoch, J1991.25, and are expressed in milliarcsec.

Field H16: Standard error of the trigonometric parallax

The standard error of the trigonometric parallax, σ_π, is given in milliarcsec.

Fields H17–18: Standard errors of the proper motion components

The standard errors of the proper motion components, $\sigma_{\mu_{\alpha*}} = \sigma_{\mu_\alpha \cos\delta}$ and σ_{μ_δ}, are expressed in milliarcsec per Julian year (mas/yr).

Fields H19–28: Correlation coefficients

The correlation coefficients (see Section 1.2.7) are given in per cent for the printed catalogue, but as (real) numerical values in the machine-readable version. They are given in the following order:

H19 = $\rho^{\delta}_{\alpha*}$
H20 = $\rho^{\pi}_{\alpha*}$
H21 = ρ^{π}_{δ}
H22 = $\rho^{\mu_{\alpha*}}_{\alpha*}$
H23 = $\rho^{\mu_{\alpha*}}_{\delta}$
H24 = $\rho^{\mu_{\alpha*}}_{\pi}$
H25 = $\rho^{\mu_{\delta}}_{\alpha*}$
H26 = $\rho^{\mu_{\delta}}_{\delta}$
H27 = $\rho^{\mu_{\delta}}_{\pi}$
H28 = $\rho^{\mu_{\delta}}_{\mu_{\alpha*}}$

corresponding to the sequence illustrated in the following table:

	$\alpha*$	δ	π	$\mu_{\alpha*}$	μ_{δ}
$\alpha*$	–	H19	H20	H22	H25
δ	H19	–	H21	H23	H26
π	H20	H21	–	H24	H27
$\mu_{\alpha*}$	H22	H23	H24	–	H28
μ_{δ}	H25	H26	H27	H28	–

The use of the asterisk notation, $\mu_{\alpha*} = \mu_{\alpha}\cos\delta$, etc., is not really required in the correlations, since the correlation coefficient is the same between (say) α and δ, as between $\alpha\cos\delta$ and δ. Nevertheless, it has been retained for uniformity.

Field H29: The percentage of rejected data, F1

This field gives the percentage of data that had to be rejected in order to obtain an acceptable astrometric solution.

This field provides a quality indicator for the astrometric data. It has been derived from an average of the two data reduction consortia values, and is insensitive to the precise definition of an observation (number of reference great circle observations, or field transits). It is given by: $100\ n_{\rm rej}/(n_{\rm acc}+n_{\rm rej})$, where $n_{\rm acc}$ and $n_{\rm rej}$ are the number of accepted and rejected observations. The field is non-blank for entries with an astrometric solution (but blank for the 263 entries without an astrometric solution).

A small percentage of rejections may be considered normal (due, for instance, to disturbing stars from the complementary field of view), whereas a large percentage is an indication of model mismatch. In all cases, including entries classified in one of the parts of the Double and Multiple Systems Annex, it corresponds to the percentage of data rejected in order to obtain the solution contained in Fields H8–28.

The precise number of observations associated with the astrometric results may be found from the file of intermediate astrometric data, which provides results at the level of each reference great-circle (see Section 2.8). An approximation to the number of astrometric observations (on great circles) may be obtained from Field H47 (the number of photometric observations, i.e. field transits) by dividing by a factor of 3.55.

Field H30: Goodness-of-fit statistic, F2

This number indicates the goodness-of-fit of the astrometric solution to the accepted data (i.e. excluding the percentage F1). For good fits, F2 should approximately follow a normal distribution with zero mean value and unit standard deviation. F2 values exceeding, say, +3 thus indicate a bad fit to the data.

The statistic F2 was computed from the goodness-of-fit statistic χ^2 of the least-squares fit (the sum of the squared normalised residuals, using the *a priori* standard error of each datum as the normalising factor), and ν, the number of degrees of freedom, according to the formula:

$$\mathrm{F2} = \left(\frac{9\nu}{2}\right)^{1/2} \left(\frac{\chi^2}{\nu}\right)^{1/3} + \frac{2}{9\nu} - 1$$

If χ^2 follows the chi-square distribution with ν degrees of freedom, then F2 is approximately normal with zero mean and unit standard deviation. The formula above corresponds to the well-known 'cube-root transformation' of the chi-square variable (e.g. M. Kendall & A. Stuart 1977, *The Advanced Theory of Statistics*, London). It is usually quoted to be valid for $\nu > 30$, but is in fact useful for much smaller ν. The transformation of (χ^2, ν) to F2 eliminates the inconvenience of having the distribution (and hence the significance levels) depend on the additional variable ν, which is generally not the same for different stars. The 'unit weight error' of the solution is given by $(\chi^2/\nu)^{1/2}$.

The resulting F2 distribution for single stars is close to normal, but with a mean of $\simeq 0.21$ and a standard deviation of 1.08; the former arising from the fact that the unit-weight error is about 1.015. For non-single stars there is an excess of large F2 values indicating the presence of modelling errors for many of these objects. Given the complexity of these solutions, even values above 3 can however sometimes represent rather 'good' solutions.

Field H30 is blank for solutions where the goodness-of-fit statistic provides no meaningful information about the fit, i.e. when the unit weight error (rms normalised residual) is equal to 1 by construction. This is the case for all 1561 stochastic solutions ('X' in Field H59), where the 'cosmic error' associated with the solution was defined precisely by the condition that the unit weight error equals 1 (see Section 2.3.6). It is also the case for the two exceptional cases of Sirius (HIP 32349) and 61 Cyg A (HIP 104214), where a realistic result could only be obtained by scaling up the formal observational errors (and consequently the astrometric standard errors in Fields H14–18) in such a way that the unit weight error became 1 (as explained in the individual notes to these objects). There are therefore 1563 entries with astrometric solutions in which Field H30 is blank.

Description of Right-Hand Pages (Fields H31–H70)

Field H31: Hipparcos Catalogue (HIP) identifier

As Field H1.

Fields H32–43: Tycho Photometry, and Colour Indices

B_T and V_T were derived from the star mapper observations, and are not available for 6301 Hipparcos Catalogue components (from the main Hipparcos Catalogue or from Part C of the Double and Multiple Systems Annex), corresponding principally to about 2300 faint entries in the main Hipparcos Catalogue (Section 1.1.1 gives further details of the relationship between the Hipparcos and Tycho Catalogues). The values of B_T and V_T listed in Field H32–35 are generally the same as the values listed in the Tycho Catalogue, Fields T32–35, for the corresponding entry, the exception being for double and multiple stars as indicated by Field H36. In these cases, furthermore, the values may be given for a different component, or combination of components, than indicated by the flags in Fields H10, H43, and H48 (see Field H36 for further details).

B_T and V_T were constructed according to the methods summarised in Section 2.2, and described in detail in Volume 4. In particular, the mean magnitudes given were based on a 'de-censoring' analysis, providing optimum estimates of the B_T and V_T magnitudes, taking into account the noise-limited nature of the fainter Tycho Catalogue observations. For further details of Fields H32–35, see the corresponding description of Fields T32–35 in Section 2.2. Field T36 in Section 2.2 summarises the methods used to obtain B_T and/or V_T, and indicates those cases where the magnitudes are not strictly 'de-censored' mean values.

The $B-V$ and $V-I$ colour indices (Fields H37–39 and H40–42 respectively) were constructed according to a variety of different methods, as indicated, and are included largely in order to complement interpretation of the Hipparcos astrometric data. Field H43 indicates those entries where particular attention must be given to the interpretation of these colour indices in the context of double or multiple star entries.

Field H32: Mean magnitude in the Tycho photometric system, B_T

Field H33: Standard error of the B_T magnitude, σ_{B_T}

Field H34: Mean magnitude in the Tycho photometric system, V_T

This magnitude is in the V_T passband, except if the B_T magnitude is missing in Field H32 (this occurs for 59 entries where V_T is given). In such cases Field H34, and the associated standard error in Field H35, refer to a passband which is a combination of B_T and V_T, as described under flag 'T' in Field T36 of the Tycho Catalogue.

Field H35: Standard error of the V_T magnitude, σ_{V_T}

Field H36: Reference flag for B_T and V_T (Fields H32–35)

This reference flag indicates, for non-single stars, the component measured in Tycho photometry (Fields T32–35), or indicates that several components have been directly measured together by Tycho, or have had their Tycho data combined in Fields H32–35.

Its purpose is to assist interpretation of the *Hp* photometric data with that in B_T and V_T, given the different resolutions of the two experiments. Thus a Tycho Catalogue entry may be resolved into two or more components in the Hipparcos Catalogue thus providing 'joint' (or combined) photometry for separate Hipparcos components. On the other hand, the Tycho Catalogue may include two or more entries corresponding to the same (main) Hipparcos Catalogue entry.

The flag takes the following values:

A, B, ... : Fields H32–35 refer to the designated Hipparcos Catalogue component;

* : Fields H32–35 refer to all components of the relevant Hipparcos entry. For systems not resolved into distinct components by Tycho, the star mapper observations provide, in principle, B_T and V_T for the combined system directly. When the system is also resolved in the Tycho observations the B_T and V_T data in Fields H32–35 have been combined from the separate Tycho Catalogue values, the photometric errors having been propagated assuming that the separate Tycho photometry errors are independent. In the case of a two-pointing triple system one entry will typically provide Tycho photometry for two of the three Hipparcos components, with Tycho photometry for the third component being associated with the second Hipparcos Catalogue entry;

– : the fields refer to a single-pointing triple system (the most common case for such a flag) or single-pointing quadruple system (in the cases of HIP 23624 and HIP 108519 only), for which only a close pair has been observed by Tycho, the other components being too faint to be detected by Tycho.

The combination and/or flagging of the Tycho Catalogue photometry for Fields H32–35 and H37–38 has been carried out to be consistent, where possible, with Field H48. In affected cases, the adjusted fields will differ from the corresponding Tycho fields for the same entry (Fields T32–35 and T37–38). Note that the detailed B_T/V_T photometry for separate Hipparcos Catalogue components is given in Part C of the Double and Multiple Systems Annex.

Close separation doubles are not always resolved in the Tycho Catalogue, and in such cases Field H36 may refer to a single Hipparcos component while Field H48 may refer to combined Hipparcos photometry (*). When the entry is not resolved by Tycho, the system's B_T and V_T magnitudes may be overestimated (i.e. the Tycho magnitudes are too faint) by an amount which depends on ϱ and Δm and which may reach several tenths of mag (especially in the range ϱ = 1 – 1.5 arcsec). The quoted standard errors on B_T and V_T do not reflect this systematic effect (although the flag in Field T49 may indicate such unresolved duplicity).

If one or more component of a multiple system is missing in the Tycho data, while the other is resolved, the main catalogue provides Tycho photometry for whichever component is brightest in V_T.

The number of entries in each of these categories is as follows: A = 4035; B = 857; C = 65; D = 7; E = 1; S = 2; * = 7795; – = 34.

Field H37: Colour index, $B - V$

The colour index in, or reduced to, the Johnson UBV system.

Although not derived directly from the Hipparcos data, the $B - V$ colour index has been included as being of direct astrophysical relevance to the interpretation of the Hipparcos astrometric data ($B_T - V_T$, the colour index in the Tycho photometric system, may be derived directly from Fields H32 and H34). See also the definition of the corresponding Tycho Catalogue quantity, Field T37.

The $B - V$ colour index has been taken either from existing ground-based observations, or derived by transforming $B_T - V_T$ according to equations given in Section 1.3, Appendix 4. The spectral type and luminosity class (Field H76) were frequently used to select the appropriate type of transformation. The source which has been adopted is given in Field H39. At the end of the construction of the $B - V$ indices, entries for which $V - I < 1.5$ mag and $\sigma_{V-I} > 0.25$ mag (see Fields H40–41) were considered as being of unacceptable quality, and Fields H37–38 were set to be blank for these entries.

Entries with relatively large values of σ_{B-V} (Field H38) may be found to occupy erroneous positions in the Hertzsprung-Russell diagram. Other entries, even with small formal errors on $B - V$, may remain with erroneous colour indices due to the use of incorrect material (such as the spectral classification) on which the transformations were based. A fraction of faint, nearby, K and M dwarfs had no photoelectric photometry in the Hipparcos Input Catalogue, and HIC colours were consequently highly uncertain. Magnitudes could be updated on the basis of the Hipparcos photometry, but if they were below the Tycho detection threshold their $B - V$ indices could not be improved. These objects (with large σ_{B-V} and $B - V > 1.5$ mag) are responsible for the apparent scatter above the lower main sequence; while their $B - V$ colour index appears systematically too red, no attempts to adjust the colour indices based on trigonometric parallax information have been made.

It should be noted that $B - V$ indices derived from such transformations will generally not reproduce a directly measured Johnson $B - V$ colour index, due to dependencies on metallicity, gravity, and reddening. The agreement should be very good for entries flagged with Field H39 = ‘G’ and Field H42 = ‘H’.

Ground-based observations will generally yield combined photometry for systems with separations $\varrho <$ 10 arcsec, and in those cases the $B - V$ colour index will therefore refer to components which may differ from that of the $B_T - V_T$ or Hp photometry for double systems with component separation in the range 8–12 arcsec (see Field H43).

Field H38: Standard error of the colour index, σ_{B-V}

The standard error of the $B - V$ colour index, either from the relevant ground-based observations, or from the Tycho $B_T - V_T$ data (see Field T38).

Field H39: Source of $B - V$

This field takes the following values:

G : indicates that $B - V$ was taken from ground-based observations;
T : indicates that $B - V$ has been determined from the transformed Tycho $B_T - V_T$ data (as described in Section 1.3, Appendix 4);
␣ : no data available.

The number of entries in each of these categories is as follows: G = 41 205; T = 75 732; ␣ = 1281.

Field H40: Colour index, $V - I$

The colour index in Cousins' system, derived as described in Section 1.3, Appendix 5. Field H40 represents the best available $V - I$ at the time of the Hipparcos Catalogue publication (i.e. frequently updated with respect to the value used for the astrometric and photometric reductions given in Field H75).

The $V - I$ colour index was used to correct for the chromatic residuals in the processing of both the astrometric and photometric data. For the astrometry the effects of an erroneous $V - I$ were small, while for the photometry the effects were more significant. One of the purposes of providing it is to permit a re-reduction of the epoch photometry as new $V - I$ colour indices become available (see Field H52). The $V - I$ index is also a useful quantity for the astrophysical interpretation of the Hipparcos astrometric data, in particular for the positioning of late K and M giants in the Hertzsprung-Russell diagram, where the $V - I$ index is more sensitive to temperature than $B - V$.

Therefore, efforts were made to present homogeneous and up-to-date information on $V - I$, including updates made on the basis of linear trends observed in the epoch photometry, or using transformed Tycho photometry. As a result, for any given entry, the value of $V - I$ used for the astrometric or photometric processing (Field H75) may not be the same as the final $V - I$ value given in Field H40. Where the value used for the data processing (given also in the Hipparcos Epoch Photometric Annex header record) differed from the true value of $V - I$, a spurious linear evolution of the Hp magnitude with time has resulted (see Field H52, flag 'R' for details).

At the end of the construction of the $V-I$ indices (as described in Field H42), entries for which $V-I < 1.5$ mag and $\sigma_{V-I} > 0.25$ mag were considered as being of unacceptable quality, and Fields H40–41 were set to be blank for these entries. The $V - I$ index for red stars ($V - I > 1.5$ mag), in particular long-period variables, are intrinsically inaccurate and were therefore retained in the catalogue independent of their associated errors.

$V - I$ indices derived from these transformations will not generally reproduce a directly measured Cousins' $V - I$ colour index, due to dependencies on metallicity, gravity, and reddening affecting the colour indices used to predict $V - I$. Ground-based observations will, furthermore, generally yield combined photometry for systems with separations $\varrho < 10$ arcsec, and in those cases the $V - I$ colour index will therefore refer to components which may differ from that of the $B_T - V_T$ or Hp photometry for close double systems (see Field H43).

Field H41: Standard error of the colour index, σ_{V-I}

See Field H40 and Section 1.3, Appendix 5 for further details.

Field H42: Source of the colour index $V - I$

The flag (A–T) in Field H42 indicates the method adopted to estimate $V - I$ given in Field H40. See Field H40 and Section 1.3, Appendix 5, for details.

For a small fraction of the stars, the genuine Cousins' $V-I$ was available. For the remaining programme stars, an approximate $V - I$ was derived from ground-based multicolour photometric data transformed into $V - I$, or from the Tycho data with or without spectral-type information, or from a combination of an approximate $B - V$ and the spectral type. Details of the construction of the adopted $V - I$ colour index for each star is given in Section 1.3, Appendix 5. The reliability of the methods used may be inferred from the standard error on $V - I$ given in Field H41.

Field H43: Reference flag for colour indices (Fields H37–42) and Field H5

A flag (*) indicates that the $B-V$ colour index and standard error (Fields H37–38), and also the $V-I$ colour index and standard error (Fields H40–41), refer to the combined light of double or multiple systems, otherwise resolved by the main mission astrometry and photometry.

The same flag also refers, with the same meaning, to the Johnson V magnitude given in Field H5.

Generally, this flagging results in consistency with the Hp photometry flag, Field H48. While for single-pointing double systems with $\varrho \gtrsim 10$ arcsec the $B-V$ and $V-I$ colour indices will therefore typically refer to the primary, the corresponding colour index information of the other component(s) of such systems are not provided in the catalogue.

The number of entries with '*' in this field is 10 783.

Fields H44–48: Main Mission Photometry

Field H44: Median magnitude in the Hipparcos photometric system, *Hp*

The median *Hp* magnitude, $x(0.5)$ in the notation of Section 1.3, Appendix 1, is defined on the basis of the accepted observations (or field transits) for a given star. The number of field transits, N, is different from star to star, and is given in Field H47.

The median is derived independently of any *a priori* or *a posteriori* knowledge of the object's variability. The median and related statistics (Fields H45–46 and 49–50) were determined from the epoch photometry derived on the basis of the $V - I$ colour index given in Field H75 (see also flag 'R' in Field H52).

Field H45: Standard error of the median *Hp* magnitude, σ_{Hp}

The standard error on the median was derived as:

$$\sigma_{Hp} = \frac{1}{\sqrt{N}} \frac{x(0.65) - x(0.35)}{0.615}$$

where N is the number of observations, and $x()$ the given quantile (see Section 1.3, Appendix 1).

Field H46: Scatter of the *Hp* observations, *s*

The scatter was derived as:

$$s = \frac{x(0.85) - x(0.15)}{2}$$

where $x()$ is the given quantile (see Section 1.3, Appendix 1).

In addition to the 14 entries for which no photometry is provided, Field H46 is blank for the secondary component of the 957 'two-pointing' double systems (but not blank for the secondary and/or tertiary components of a 'two-pointing' or 'three-pointing' *multiple* system). Entries in 'two-pointing' or 'three-pointing' systems are identified by the flags in Field H60.

Field H47: Number of *Hp* observations, *N*

This is the number of photometric observations used for the construction of the median, standard error, and scatter (Fields H44–46).

The number of photometric observations given in Field H47 is typically less than the total number of photometric transits recorded in the Hipparcos Epoch Photometry Annex, Field HH4. Only transits with certain values of the transit flag, Field HT4, have been used for the construction of the median.

Field H47 is blank for the same entries (and for the same reasons) as Field H46.

Field H48: Reference flag for the photometric parameters

For a double or multiple entry, this flag indicates that the photometry refers to:

A, B,... : the specified component of a double or multiple system;

* : combined photometry of a double system, corrected for attenuation by the detector's instantaneous field of view profile response (see Section 1.4);

– : combined photometry of a multiple system, *not* corrected for attenuation by the detector's instantaneous field of view profile response (see Section 1.4).

For single catalogue entries corresponding to double systems with separations up to about 10 arcsec, and indicated by '*' in Field H48, combined photometry is provided in the main catalogue. For these 'single-pointing' doubles this combined photometry has been corrected for the detector's response profile. The main catalogue photometry and the epoch photometry is fully consistent with the photometric data given in the Double and Multiple Systems Annex.

For single catalogue entries corresponding to double systems with separations larger than about 10 arcsec, and indicated by 'A', 'B', etc. in Field H48, photometry of the brightest component is provided in the main catalogue. For these 'single-pointing' doubles the photometry has also been corrected for the detector's response profile, although the corrections are larger and therefore relatively less accurate. The main catalogue photometry and the epoch photometry is fully consistent with the photometric data given in the Double and Multiple Systems Annex.

For double systems comprising two entries (i.e. the 'two-pointing doubles) Field H48 indicates the relevant component observed under each entry. The photometry for each entry was derived from the data collected during the observations of the brighter entry, using the magnitude difference determined from the double and multiple systems processing. They are corrected for the detector's response profile, although the corrections are usually rather uncertain. The main catalogue photometry and the epoch photometry is fully consistent for the brighter component, but not for the fainter. The photometric data in the Double and Multiple Systems Annex is consistent with the main catalogue photometry. The individual values in the Epoch Photometry Annex show large, usually spurious variations, especially for the fainter component.

For multiple star entries, indicated by '–' in Field H48 (i.e. the single-pointing, two-pointing, or three-pointing multiples) the main catalogue photometry and the epoch photometry have *not* been corrected for the detector's response profile—the photometric parameters refer to the light collected from all the components of the systems, each attenuated according to its position within the detector's field of view. Photometry of the components, corrected for the detector's response profile, are given in the Double and Multiple Systems Annex.

The number of entries in each of these categories is as follows:

Field H48	Entries	Field H48	Entries
A	1407	E	1
B	933	S	2
C	25	*	10590
D	4	–	249
	Total non-blank	13211	

Field H48 is non-blank for all 13 211 entries for which Field H59 = 'C'. The 249 entries flagged '–' are precisely the entries associated with the 'one-pointing', 'two-pointing' and 'three-pointing' *multiple* systems described further under Field H60. Entries for which Field H48 = '*' may have either '*' or one of the components given in Field H10.

Fields H49–54: Main Mission Variability

Fields H49–50: Observed magnitude at maximum and minimum luminosities

Fields H49–50 provide the 5th and 95th percentiles of the epoch photometry respectively, i.e. $x(0.05)$ and $x(0.95)$ in the notation of Section 1.3, Appendix 1. They thus provide an estimate of the magnitudes at maximum and minimum luminosities detected throughout the observational period.

In many cases, in particular for the entries flagged in Field H52 as 'C', the difference between the two values will not be statistically significant.

Fields H49–50, as well as the median and related statistics (Fields H44–46), were determined from the epoch photometry derived on the basis of the $V - I$ colour index given in Field H75 (see also flag 'R' in Field H52).

The percentiles are given even for entries with small numbers of Hp observations (Field H47), and in those cases appropriate caution must be exercised in interpreting the given values. In such cases, $Hp_{\rm max}$ and $Hp_{\rm min}$ may be equal or, due to rounding, the median magnitude may lie outside the tabulated values of $Hp_{\rm max}$ or $Hp_{\rm min}$. The number of transits accepted for photometry may be significantly less than the number of transits accepted for astrometry, so that there are also situations where entries with small N (Field H47) nevertheless correspond to an astrometric solution.

Fields H49–50 are blank for the same entries (and for the same reasons) as Field H46.

Field H51: Variability period from Hipparcos observations, P

The variability period, or a provisional estimate of such a period, was derived on the basis of the Hipparcos data (possibly in combination with ground-based observations). It is expressed in days, with a precision of 0.01 days.

Further details of the variability of the entry, including the variability period with the appropriate number of (significant) decimal places, are given in the Variability Annex (Section 2.4). Truncating the period to this fixed format precision means that the contents of Field H51 will generally differ from the (more precise) value given in the Variability Annex (Section 2.4, Field P11).

Periods presented in the Variability Annex may have been derived from the Hipparcos data (Field P11) or taken from the literature (Field P18). Field H51 is taken from Field P11 only; this means that some of the entries contained in the table of Periodic Variables (where the period has been taken only from the literature) may not have a period listed in the main catalogue.

Field H52: Type of variability

The sources of scatter in the photometric data are various, and the flag in Field H52 indicates the origin of the extra scatter, which may be astrophysical, or in some cases instrumental. A more detailed description of the following categories, and the manner in which they were derived, is given in Section 1.3, Appendix 2. Amongst astrophysical sources of variability, Field H52 only distinguishes between 'M' (micro-variables), 'P' (periodic variables), and 'U' (unsolved variables). Further variability details for the periodic or unsolved variables are included in the Variability Annex (see Field H53). The flag takes the following values (see Figure 2.1.1):

C : 'constant' stars or, more strictly, stars not detected as variable. These include stars used as photometric standards. The category also includes cases noted as variable in the Hipparcos Input Catalogue. Caution must be exercised in assuming that entries flagged 'C' are non-variable: they may be variable at levels below the Hipparcos detectability threshold (see Figure 2.1.1), or they may have shown variability in the past (e.g. Be stars, or long-period eclipsing binaries). For details of the use of such entries as photometric standard stars, see Section 1.3, Appendix 2;

D : a 'duplicity-induced variability' flag was assigned according to the difference between the 'dc' and 'ac' magnitudes (see Section 2.5) and according to the angular separation and magnitude difference of a double or multiple system. If 'D' is set, the entry is not necessarily a physical variable, and not necessarily seen as variable in Hp ('dc scale');

M : possibly micro-variable, with amplitude below 0.03 mag (stars classified with high confidence as micro-variable are flagged 'U');

P : periodic variable (see Field H53). This flag may supersede entries for which flag 'D' is also appropriate;

R : revised colour index. When the flag 'R' is set the $V - I$ colour index was corrected during the variability analysis. The effect of an erroneous $V - I$ index is a spurious linear trend in the Hp magnitude of the epoch photometry, with no physical origin. When identified during the data analysis, this could be taken into account in classifying the type of variability, i.e. whether spurious or not. Corrections on the $V - I$ index brought at a later stage are not flagged in this way;

U : unsolved variable (see Field H53). Entries are classified as 'unsolved' if they do not fall into the other variability categories—this class also includes irregular or semi-irregular variables, and possible variables with amplitudes $\gtrsim 0.03$ mag;

␣ : a blank indicates that the entry could not be classified as variable or constant with any degree of certainty (e.g. due to the presence of one or more outliers in the epoch photometry).

The flag 'D' is a photometric rather than strictly a 'duplicity' indicator, and indicates entries where there is a possibility that the Hp magnitudes may be disturbed; for other double or multiple star entries the photometry is unlikely to be affected. Thus 9722 of the 13 211 entries of Part C of the Double and Multiple Systems Annex are flagged 'D', 76 of the 2622 entries of Part G, 4 of the 235 entries of Part O, 2 of the 288 entries of Part V, and 155 of the 1561 entries of Part X.

Flag 'R' originates because (as explained in Section 1.3) the photometric reductions could only proceed on the basis of the best-available value of the $V - I$ colour index for each entry, as given in Field H75. Fields H44–46 and Fields H49–50 were derived from the resulting (possibly erroneous) epoch photometry, and the corresponding parameters (including the value of $V - I$ used) appear in the relevant header record of the epoch photometry annex. Subsequently, however, improved determinations of $V - I$ were available in some cases, and the $V - I$ colour index provided in Field H40 is the best available at the time of the catalogue publication.

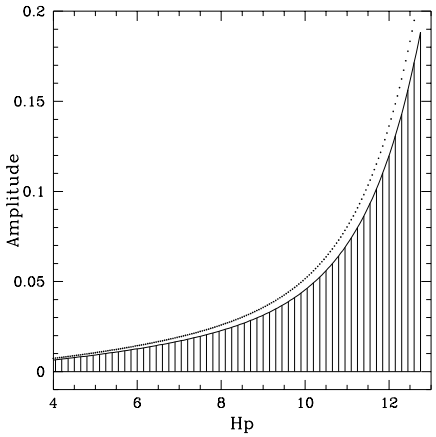

Figure 2.1.1. *The figure shows the peak-to-peak amplitude of variability which could be detected versus the Hp magnitude for an object observed an average number of times throughout the mission. To the upper left of the diagram, variability can be identified, and objects are classified as 'P' or 'U' accordingly. The shaded region is inaccessible to the Hipparcos variability analysis, and objects in that region are typically classified as 'C'. The narrow intermediate region is occupied by 'U' objects suspected as possible variables with amplitude* $\gtrsim$ *0.03 mag, or 'M' objects suspected as micro-variable with amplitude* $\lesssim$ *0.03 mag.*

Many of the significant revisions in $V - I$ were well correlated with the 1000 or so cases where the Hipparcos epoch photometry displays a secular change of magnitude with time. However, neither the epoch photometry, the summary photometry (Fields H44–46 and H49–50), or the epoch photometry header records were modified, so that they remain consistent with the value of $V - I$ given in Field H75.

A correction algorithm is included in Section 1.3.4, providing the details needed to make the appropriate corrections to the calibrated magnitudes and resulting statistics using any revised value of $V - I$, in particular that given in Field H40. This algorithm is also applicable to any new value of $V - I$ which becomes available in the future.

The number of entries in each category is as follows: C = 46 552; D = 12 361; M = 1045; P = 2708; R = 1172; U = 7784; ␣ = 46 596 (including the 14 entries for which no photometry is provided).

Field H53: Variability annex flag: tabular data

A flag indicates that variability periods, amplitudes, reference epochs, etc., compiled from the Hipparcos *Hp* data, along with associated ground-based data, are given in the corresponding tables of the Variability Annex (see Section 2.4 for further details):

1 : additional data are provided in a table of periodic variables (Volume 11, Part 1);
2 : additional data are provided in a table of 'unsolved' variables (Volume 11, Part 2).

Flags '1' and '2' generally correspond to flags 'P' and 'U' in Field H52 respectively, with the exception of some 'R' or 'D' flagged objects which occasionally superseded the 'P' and 'U' flags. Thus the 2712 entries in the periodic variables table, flagged '1', comprise all 2708 entries flagged 'P' in Field H52, and 4 entries flagged 'R'. The 5542 entries in the unsolved variables table, flagged '2', comprise 5486 of the entries flagged 'U' in Field H52, 55 flagged 'R', and 1 flagged 'D'.

Field H54: Variability annex flag: light curves

A flag in Field H54 indicates that a light curve, or folded light curve, compiled from the Hipparcos *Hp* data, is provided in the Variability Annex (see Section 2.4 for further details):

A : a (folded) light curve is given in Volume 12, Part A. This part corresponds to the 'periodic variables', generally with flag 'P' in Field H52, and with flag '1' in Field H53. The light curve has been folded at the period given in Field P11 of the Variability Annex (the period is truncated to 2 decimal places in Field H51). If Field P11 is blank, this indicates that no reliable period was obtained from the Hipparcos data, and in these cases the period as given in the literature (Field P18) was used to fold the data;

B : a light curve (not folded) is given in Volume 12, Part B. The light curve has been fitted to the data derived and transformed from the data base of the AAVSO (American Association of Variable Star Observers). This part corresponds to large-amplitude variable stars which have been observed systematically by ground-based observers for, and during, the Hipparcos mission. In these cases, a combination of the Hipparcos and AAVSO data have allowed a more complete light curve to be derived, including refined estimates of the maximum or minimum magnitudes during the mission. Entries for which the flag 'B' is set are also contained in the compilation of folded light curves if the variability is periodic; the corresponding folded light curve is then included at the relevant place according to its HIP running number;

C : a light curve (not folded) is given in Volume 12, Part C. This part generally corresponds to unsolved systems, with conspicuous features in their light curves, independent of amplitude. It includes irregular or semi-irregular variables.

The Hipparcos Catalogue Epoch Photometry Annex contains all of the data on which the light curves were based. From this, light curves not presented in the printed annexes, or constructed using different periods or data selection criteria, may be constructed.

The relationship between the non-blank entries in Fields H53 and H54 is summarised as follows:

	H53 = 1	H53 = 2	Total
H54 = A	2480+213*	–	2693*
H54 = B	213	61	274
H54 = C	8‡	819	827
H54 = ␣	11‡	4662	
Total	2712	5542	

* The 213 entries with Field H53 = '1' and Field H54 = 'B' are also included in Part A of the light curve compilation.

‡ The 8 periodic variables assigned to Part C of the light curve compilation, and the 11 periodic variables without published light curves, are variables with very long periods, well-established in the literature, where the Hipparcos data were considered to be better displayed unfolded or not at all.

For the majority of unsolved variables, flagged either 'U' in Field H52, and/or '2' in Field H53, unfolded light curves were considered to be of limited interest, showing mainly scatter, and are not included within Part C of the light curve compilation.

Fields H55–67: Multiplicity Data

Field H55: CCDM identifier (J2000.0)

The CCDM Catalogue, the Catalogue of Components of Double and Multiple Stars (described in Section 1.4.4) provides the principal cross-reference to information on double and multiple systems.

CCDM identifiers were taken from the CCDM Catalogue, and CCDM identifiers following the previous conventions were constructed for previously unknown double or multiple systems. These newly-constructed CCDM identifiers have, simultaneously, been included within the CCDM. The CCDM identifier is given if an entry is included in Part C of the Double and Multiple Systems Annex (see Field H59), or if a CCDM identifier was given in the Hipparcos Input Catalogue. Otherwise this field is blank.

There are a total of 19 393 entries with associated CCDM identifiers. A CCDM identifier has not been specifically assigned (as a result of the Hipparcos work) to entries in Part G (acceleration), Part O (orbital), Part V (variability-induced), or Part X (stochastic). CCDM identifiers associated with entries in Parts G, O, V and X arise from the assignment of CCDM identifiers to these entries in the Hipparcos Input Catalogue, and therefore have an 'I' in Field H56.

There are six cases where the CCDM identifier supersedes the corresponding CCDM identifier listed in the Hipparcos Input Catalogue:

HIP	CCDM (HIP)	CCDM (HIC)
18377	03558 + 4323	03557 + 4322
37037	07366 – 1428	07367 – 1427
47174	09367 + 5754	09368 + 5755
67635	13515 – 4626	13515 – 4627
80346	16258 + 4821	16242 + 4821
90273	18252 + 3017	18252 + 3015

Field H56: Historical status of the CCDM identifier

The flag takes the following values:

H : Hipparcos—indicates that the system was determined as double or multiple by the Hipparcos observations, and was previously unknown as double or multiple.

I : Input Catalogue—indicates that the system had been previously identified, as given in Annex 1 of the Hipparcos Input Catalogue.

M : miscellaneous—indicates that the system had been previously identified, after publication of the Hipparcos Input Catalogue, using other more recently available catalogues and compilations, in particular through the pre-release version of the Washington Catalogue of Visual Double Stars (WDS; C.E. Worley & G.G. Douglass, US Naval Observatory, Washington).

Of the 19 393 entries with associated CCDM identifiers, the number in each of these categories is as follows: H = 3001; I = 15 966; M = 426.

Field H57: Number of separate catalogue entries with the same CCDM identifier

The CCDM identifier links different components of an identified double or multiple system. If an entry itself comprises the double system, the CCDM identifier is associated only with that entry. If two or more entries are considered part of a double or multiple system, the entries are assigned the same CCDM identifier.

There are 19 393 entries with associated CCDM identifiers. Of these, 15 816 refer to a single entry, 1714 link two entries (i.e. affecting 3428 entries), 43 link three entries (affecting 129 entries), and 5 link four entries (affecting 20 entries). Part C of the Double and Multiple Systems Annex contains component information only for those cases where a catalogue entry comprises more than one component (i.e. Field H58 ≥ 2), and for those multiple entry systems taken together in the data reductions and referred to as the 'two-pointing' or 'three-pointing' doubles or multiples (there are no 'four-pointing' multiples). Entries which constitute part of a 'two-pointing' or 'three-pointing' system may be recognised by the flags 'P' (primary), 'F', 'I', or 'L' appearing in Field H60.

A double or multiple system which is comprised of two or more distinct, unresolved, and independently treated, catalogue entries, is not included in Part C of the Double and Multiple Systems Annex—the relative astrometric and photometric parameters may be derived from data for the separate catalogue entries (which are linked by their common CCDM identifier).

More complex systems may superficially appear to contradict this scheme. Thus the 4-entry (actually 6-component) system CCDM 05353–0524 comprises the 'three-pointing' system HIP 26220, HIP 26221 and HIP 26224, which all have Field H57 = 4 (four entries with the same CCDM identifier), Field H59 = 'C' (details provided in Part C of the Double and Multiple Systems Annex), and 'F' or 'P' in Field H60, indicating that they are part of a multiple-pointing system (in this case, a 'three-pointing' system). The fourth entry, HIP 26235, has Field H60 = ␣ (i.e. not observed as part of a multiple-pointing system). The 'C' in Field H59 arises because this entry is itself double (Field H58 = 2), not because of its association with CCDM 05353–0524. Similarly, two of the entries comprising the three-entry system CCDM 21555+5232 were observed as a 'two-pointing' system and have corresponding data in Part C, while the third entry was reduced independently, and is not referenced in Part C.

For entries in Part C of the Double and Multiple Systems Annex, the following table summarises the number of systems (n_s) in each of the multiple-pointing configurations (n_p = 1, 2, 3, corresponding to the 'single-pointing', 'two-pointing', and 'three-pointing' doubles or multiples respectively) as a function of the number of components in the system (n_c):

Components in system n_c	Multiple-pointing configuration, n_p			Total systems Σn_s	Total entries $\Sigma n_p n_s$	Total components $n_c \Sigma n_s$
	1	2	3			
2	11048	957	0	12005	12962	24010
3	129	50	3	182	238	546
4	6	1	1	8	11	32
Systems, Σn_s	11183	1008	4	12195	–	–
Entries, $n_p \Sigma n_s$	11183	2016	12	–	13211	–
Components, $\Sigma n_c n_s$	22507	2068	13	–	–	24588

The quadruple with two entries consists of AB for one entry and CD for the other, while the quadruple with three entries includes one entry resolved into two components. From these statistics, it follows that there are 11 101 (11 048 + 50 + 2 × 1 + 1) entries with relative double star information in the main Hipparcos Catalogue, Fields H63–67.

It also follows that the number of CCDM flagged entries which are not resolved into two or more components by Hipparcos is 4633 (15 816 – 11 183). There are 706 double systems (1714 – 1008) corresponding to 1412 entries in which two catalogue entries are linked by the same CCDM identifier but which were not 'reduced' as 'two-pointing' systems; and 39 triple systems (43 – 4) corresponding to 117 entries in which three catalogue entries are linked by the same CCDM identifier but which were not 'reduced' as 'three-pointing' systems. The further 5 CCDM identifiers each linking four entries (affecting 20 entries) were also not reduced as multiple-pointing systems.

Field H58: Number of components into which the entry was resolved

This field gives the number of components into which the entry was resolved as a result of the satellite observations and data reductions.

A value of '1' is given in Field H58 for all entries not in Part C of the Double and Multiple Systems Annex (thus, entries with 'G', 'O', 'V' or 'X' in Field H59 are not considered as resolved by Hipparcos and are assigned a value of '1'). For entries in Part C, Field H58 may take a value of 1, 2, 3, or 4 (for example, the value 1 occurs in the 1975 cases where an unresolved entry is nevertheless 'linked' to another entry, through a common CCDM identifier) in those cases where the reduction of the combined data was made as part of a 'single-pointing', 'two-pointing' or 'three-pointing' double or multiple.

Thus a single star has Field H58 = 1; a resolved double system contained within a single entry has Field H58 = 2; a double system represented by two entries has Field H58 = 1 for each entry; a resolved triple system contained within a single entry has Field H58 = 3; a triple system comprising two entries has Field H58 = 1 for the unresolved entry and Field H58 = 2 for the close pair, etc.

Only when Field H58 = 2 is relative information given in Fields H62–67 (this information is given irrespective of the quality of the solution). In particular, for 'two-pointing' doubles (where both entries have Field H58 = 1) values of ϱ, θ and ΔHp are not given.

The number of entries in each of these categories as follows: 1 = 106 719; 2 = 11 101; 3 = 129; 4 = 6; ␣ = 263. The 263 blank entries correspond to those without final astrometric solutions, with the total number of entries 1+2+3+4 = 117 955.

Field H59: Double and multiple systems annex flag

A flag indicates that further details of this system are given in one of the five (mutually exclusive) parts of the Double and Multiple Systems Annex (see Section 2.3). These five parts are labelled C, G, O, V, and X. The flags, and the corresponding parts of the annex, refer to the following types of solution:

C : component solutions; solutions are given for double and multiple stars in which the relative motions of the components can be described, to the precision of the observations, as a linear function of time. This condition is generally met for systems having orbital periods longer than several times the length of the Hipparcos observing interval (3.3 years), which applies to the majority of systems resolved into components by the Hipparcos instrument, or to systems not physically linked;

G : acceleration (or higher-order) terms; for some apparently single (unresolved) stars it was found that the observed motion on the sky could not be properly modelled by the standard five astrometric parameters, while an acceptable solution was obtained by adding higher-order terms to the model. These objects are probably astrometric binaries with periods above some 10 years, so that the photocentric motion over the

mission interval (roughly 1989.9–1993.2) is adequately represented by a quadratic or cubic polynomial in time. In these cases, the proper motion given in Fields H12–13 is a mean value over the mission duration;

O : orbital solutions; for a few hundred systems observed with Hipparcos it has been possible to determine at least one of the orbital elements from the space observations, in addition to the five astrometric parameters referring to the centre of mass. The remaining orbital elements, varying in number from zero to seven, had to be adopted from ground-based data such as the published orbits of spectroscopic binaries. The main results on the orbital elements are given in the annex, while the astrometric parameters for the centre of mass are given in the main catalogue. Such a solution always corresponds with '+' in Field H10 (parameters referred to the centre of mass);

V : 'variability-induced movers'; in which the apparent motion of the photocentre is considered to arise from variability of one of the components of a double system;

X : stochastic solution; for some unresolved stars it was not possible to find an acceptable single or double star solution in reasonable agreement with the statistical uncertainties (standard errors) assigned to the individual measurements. These objects are probably astrometric binaries with relatively short periods (< 3 years), for which a simple polynomial model was clearly inadequate, while the satellite data alone did not allow a full orbital solution. In the individual measurements, the displacement of the photocentre from an assumed linear motion of the centre of mass thus appears like a random scatter in excess of the measurement noise. For the stochastic solutions, the solution's goodness-of-fit, Field H30, is left blank.

This flag is tied to the entry and not to the system: e.g. HIP 185 is an unresolved entry, but with the same CCDM identifier as the close double HIP 190. Data for the two close components contained within the entry for HIP 190 are given in the annex, but no data are given there for HIP 185.

The number of entries in each of these categories is as follows: C = 13 211; G = 2622 (2163 7-parameter and 459 9-parameter solutions); O = 235; V = 288; X = 1561. The 13 211 'C' entries correspond to the 12 195 single- or multiple-pointing systems distributed according to the observational configuration summarised under Field H57.

For some entries with Field H59 non-blank, standard errors may be large compared with the single stars solutions (e.g. HIP 66182 has σ_π = 114 mas), rejection rates (Field H29) reach 47 per cent, and the goodness-of-fit (Field H30) is as large as F2 = 27.22. In exceptional cases such behaviour has been accepted, in view of the complexity of the solutions, in preference to providing no data at all.

Field H60: Source of the absolute astrometry in Fields H8–30

This field qualifies the source of astrometry in Fields H8–30 for some of the entries with a 'C' in Field H59 (and which therefore appear also in Part C of the Double and Multiple Systems Annex). Flags 'F', 'I', 'L', and 'P' indicate a component of a 'two-pointing' or 'three-pointing' system in which the astrometric solution may have been constrained in a certain way (these flags provide the only method of determining whether a given entry was observed as part of a 'two-pointing' or 'three-pointing' system).

Flag 'S' indicates that the astrometric parameters of the photocentre were constrained to the values obtained by treating the system as a single star, i.e. by merging of the intermediate astrometry from the two data reduction consortia. This procedure was

used, when possible, for close binaries (separation $\varrho < 0.2$ arcsec), where the single-star processing generally gave a more accurate determination of the photocentre than the double-star processing. The quality of the astrometric data in Fields H8–30 is then comparable to that of 'single' stars (blank in Field H59), and in particular the standard errors in Fields H14–18 are on exactly the same scale as for the single stars—and therefore generally more reliable than for other double and multiple systems. Full consistency between Fields H8–30 and the component data in Part C of the Double and Multiple Systems Annex, also for the 'S' systems, has been achieved by means of very small adjustments of the component data resulting from the double-star processing.

The flag in this field has the following meaning:

- F : this is the secondary or tertiary target of a two-pointing or three-pointing system solved, in the double-star processing, as a 'fixed' system (solution type 'F'). Consequently its parallax and proper motion were constrained to be the same as for the primary target—the latter identified by a 'P' in this field and the same CCDM identifier as the current entry;
- I : this is the secondary or tertiary target of a two-pointing or three-pointing system solved, in the double-star processing, as an 'independent' system (solution type 'I'). Consequently the parallax and proper motion were not constrained with respect to their values for the primary target—the latter identified by a 'P' in this field and the same CCDM identifier as the current entry;
- L : this is the secondary or tertiary target of a two-pointing or three-pointing system solved, in the double-star processing, as a 'linear' system (solution type 'L'). Consequently its parallax, but not the proper motion, was constrained to be the same as for the primary target—the latter identified by a 'P' in this field and the same CCDM identifier as the current entry;
- P : this is the primary target of a two-pointing or three-pointing system;
- S : Fields H8–30 were taken from the 'single-star merging' process. This flag implies a binary with separation $\varrho < 0.2$ arcsec (Field H64), with astrometry and photometry referred to the photocentre (Field H10 = '*' and Field H48 = '*');
- ␣ : the astrometric data in Fields H8–30 have been obtained from the double-star processing (if Field H59 = 'C') or from the single-star merging (otherwise).

The primary of a two-pointing or three-pointing system is flagged 'P', while secondary or tertiary components are flagged 'F', 'I' or 'L' as described above. An entry can therefore be recognised as a component of such a system by the flags in this field. (In the Double and Multiple Systems Annex, Field DC3 gives the corresponding flag for all solutions, not only the multiple-pointing ones).

Of the 3236 non-blank entries, the number in each of these categories is as follows: F = 129; I = 843; L = 44; P = 1012; S = 1208.

These entries may be understood as follows. There are 1012 'two-pointing' or 'three-pointing' systems. These comprise 1012 entries related to primary targets (flagged P), and 1016 entries related to secondary targets (flagged F, I, or L), giving a total of 2028 affected entries, all of which have Field H57 > 1 and Field H59 = C. Of these, there are 1008 'two-pointing' systems with 2016 related entries, themselves comprising 957 two-pointing double systems (1914 entries), 50 two-pointing triple systems (100 entries), and 1 two-pointing quadruple system (2 entries). The remaining 'three-pointing' systems have 12 related entries, comprising 3 three-pointing triple systems (9 entries), and 1 three-pointing quadruple system (3 entries).

Field H61: Solution quality flag

This provides an indication of the reliability of the double or multiple star solution; the flag is set for all entries in Part C of the Double and Multiple Systems Annex. An additional flag, 'S', gives further indications of suspected non-single systems. The quality rating of a solution was made according to a combination of criteria based on the availability and agreement of solutions from the two data reduction consortia, and on the ease by which the system was resolved by Hipparcos. The flags can be understood as follows (further details for cases A–D are given in Section 2.3, Field DC5):

A : 'good', or reliable solution;
B : 'fair', or moderately reliable solution;
C : 'poor', or less reliable solution;
D : 'uncertain' solutions;
S : suspected non-single, i.e. possible double or multiple, although no significant or convincing non-single star solution was found. Flag 'S' may or may not be associated with 'X' in Field H59 (these flags were derived independently), but is not associated with any other flags in Field H59.

The number of entries in each of these categories is as follows: A = 9521; B = 1668; C = 909; D = 1113; S = 7624. The total number of entries A+B+C+D = 13 211 is equal to the number of entries in Part C of the Double and Multiple Systems Annex.

643 entries have 'S' in Field H61 and 'X' in Field H59. A large part of the 7624 'S'-flagged entries are probably effectively single as observed by Hipparcos, with the flag induced by photometric variability or inadequate astrometric sampling. There is however an increased probability for real non-singles in this group as compared with the 'non-S' entries, as can be seen by the ratio of the 643 'X' (Field H59) among the 'S' entries, compared with 918 among roughly 100 000 'non-S' entries.

The totality of entries classified as either known or suspected to be double or multiple is given by entries which are non-blank in Field H59, combined with entries with 'S' in Field H61 (some of which may also have 'X' in Field H59), combined with separate entries linked by a common CCDM identifier but not observed as part of a multiple-pointing system (the statistics of solved or detected systems do not include the latter).

Corresponding data are given in Fields H62–67 when Field H58 = 2 only, irrespective of the solution quality flag in Field H61; however, for Field H61 = D there will be alternative values of ΔHp, θ, and ϱ given in a note, as described under Field DC5 of the Double and Multiple Systems Annex.

Field H62: Component designation for parameters in Fields H63–67

The first letter of Field H62 gives the 'reference' component, with the second letter giving the subsidiary component. In the case of the Hipparcos observations, the reference component is always defined to be the brighter component (in median Hp), such that the magnitude difference between the components (Field H66) is always positive.

Thus, in particular, the position angle in Field H63 is for the fainter component (in median Hp) relative to the brighter component. Maintaining conformity with existing designations of certain previously known double systems therefore requires that the components considered are explicitly stated. Of the 11 101 entries with Field H62 non-blank, 10 200 are designated 'AB'. Other combinations occur: AC, AD, AE, AF, AG, AK, AP, BA, BC, BD, CA, CB, CD, CR, DC, DE, EN, GH, and PA. AS is used for cases where component identification is doubtful (for close binaries with a small magnitude difference) and consequently where the system is to be interpreted as either AB or BA.

Fields H63–64: Position angle and angular separation (epoch J1991.25), rounded

These fields give rounded values for the position angle between the components, θ, expressed in degrees, and the angular separation, ϱ, expressed in arcsec, respectively. The position angle is that of the component given by the second letter of Field H62 with respect to the component given by the first letter of Field H62.

Fields H63–64 provide information on the system geometry in the more standard 'double star' form for entries observed as precisely double, i.e. where Field H58 = 2. The position angle is measured counterclockwise, as seen on the sky, from the $+\delta$ direction. The position angle and the component separation are referred to the catalogue epoch, on the basis of the geometrical model defined in the Double and Multiple Systems Annex. Details, with full numerical precision, are given only in the Double and Multiple Systems Annex.

Providing corresponding information for systems with two or more separate entries was considered impractical in such a concise summary format, given that one or more of the related entries could themselves be double or multiple. Determination of which catalogue entries constitute such separated systems should utilise the CCDM identifier of the system (Field H55) from which relative astrometric and photometric data may be inferred from the parameters of the individual entries. Separate entries treated as 'multiple-pointing' systems are, however, also contained explicitly within Part C of the Double and Multiple Systems Annex.

The tabulated value of ϱ was derived rigorously from the absolute positions. For $\varrho \sim 20$ arcsec the resulting differences compared with a linear approximation, based on $\Delta\alpha \cos\delta$ and $\Delta\delta$, may reach several milliarcsec.

Field H65: Standard error of the angular separation, σ_ϱ

The standard error of the angular separation is given in arcsec.

The standard error of the position angle is not given in the catalogue, but may be computed from the complete data given in Part C of the Double and Multiple Systems Annex. It may be roughly estimated as $\sigma_\theta \sim \sigma_\varrho / \varrho$ (in radians).

Field H66: Magnitude difference of components, ΔHp

This field gives the magnitude difference between the components, expressed in mag.

The magnitude difference, ΔHp, assumed to be constant with time, was derived on the basis of the geometrical model defined in the Double and Multiple Systems Annex. ΔHp is always positive since the reference component given in Field H62 is the brighter component.

For 'multiple-pointing' systems, no relative information is given (as explained under Fields H63–64). For non-single variables, the standard variability information is given in Fields H49–54, and ΔHp is always an average value of some real (but unspecified) variability.

Field H67: Standard error of the magnitude difference, $\sigma_{\Delta Hp}$

The standard error of the magnitude difference, $\sigma_{\Delta Hp}$, is given in magnitudes.

Fields H68–70: Miscellaneous

Field H68: Flag indicating 'survey' star

The 'survey' was the basic list of bright stars added to and merged with the total list of proposed stars, to provide a stellar sample (almost) complete to well-defined limits. A flag 'S' given in Field H68 indicates that the entry is contained within this 'survey', whose limiting magnitude is a function of the star's spectral type and galactic latitude, b, and is defined by:

$V \leq 7.9 + 1.1|\sin b|$ for spectral types earlier or equal to G5

$V \leq 7.3 + 1.1|\sin b|$ for spectral types later than G5

If no spectral type was available, the break was taken at $B - V = 0.8$ mag. The survey was defined during the construction of the Hipparcos Input Catalogue, using HIC data for V, b, and spectral type, and was not adjusted as a result of revised Hipparcos photometry. 52 045 entries are flagged as 'S'.

Field H69: Flag indicating identification chart

Where identification of the star using ground-based telescopes might prove difficult or ambiguous (e.g. for faint stars, for crowded zones, or for components of double or multiple systems), identification charts were constructed and are included in Volume 13 of the printed catalogue. Charts correspond to the object observed by the satellite (i.e. at the position given in the Hipparcos Catalogue), even if it was not the intended target. The flag takes the following values:

D : charts produced directly from the STScI Digitized Sky Survey (776 entries);
G : charts constructed from the Guide Star Catalog (10 877 entries).

Field H70: Flag indicating a note given at the end of the volume(s)

Three categories of notes have been compiled during the construction of the Hipparcos Catalogue: notes associated with the general catalogue compilation; notes specifically associated with the photometry or variability of the entry; and notes associated with the double or multiple solution determined for the entry.

General notes are included at the end of the relevant volume of the main catalogue (Volumes 5–9). Photometric notes are collected together at the end of the Variability Annex (Volume 11), although these also include certain notes to stars considered as non-variable by Hipparcos. Notes specifically related to double and multiple systems are collected together at the end of the Double and Multiple Systems Annex.

The flag has the following meaning:

D : double and multiple systems note only (Volume 10);
G : general note only (Volumes 5–9);
P : photometric (including variability) notes only (Volume 11);
W : 'D' + 'P' only;
X : 'D' + 'G' only;
Y : 'G' + 'P' only;
Z : 'D' + 'G' + 'P'.

The general notes in Volumes 5–9 also include a pointer to 'D'- and 'P'-type notes where appropriate (i.e. if Field H70 is 'X', 'Y', or 'Z', then the general notes will include 'D', 'P', or both additional pointers, respectively).

The same note flag given in Field H70 is strictly reproduced in Field P16/U16 of the Variability Annex (Section 2.4), and in Field DC6, DG12, DO17, DV12, and DX4 of the Double and Multiple Systems Annex (Section 2.3), so that notes on a given entry—independently of their source—may be simply identified.

References, included within the photometric notes, can be located for variable stars directly using Fields P23 or U23 of the Variability Annex. They cannot be located directly from Field H70, but only via their sequential HIP number.

The 'general notes' cover the following situations:

- entries with no astrometric or photometric solution, including entries where no signal was detected at the position specified in the Hipparcos Input Catalogue;
- misidentified stars mentioned in the photometric notes;
- poorly observed stars with rejected solution;
- stochastic solutions (see Part X of the Double and Multiple Systems Annex) with associated 'cosmic error' larger than 100 mas, or stochastic solutions rejected for other reasons;
- general notes produced during the construction of the Double and Multiple Systems Annex;
- noted and updates related to the CCDM (Field H55);
- extended sources.

The formats of the machine-readable notes are given in Section 2.11.

Fields not in the Printed Catalogue (Fields H71–77)

The following fields are included only in the machine-readable version (ASCII CD-ROMs). Additional cross-identifications are available through the Hipparcos Input Catalogue (printed as ESA SP–1136, 1992; on the Hipparcos Input Catalogue CD-ROM; on *Celestia 2000*; and through the CDS).

The HD, and DM (BD, CoD, and CPD) identifiers have been derived as a result of cross-identifications using the CDS's SIMBAD facility. As of mid-1996, about half of the DM stars are not included in SIMBAD. For all other cross-identifications, the user is referred to the 'star names resolving facility' of SIMBAD, where the Hipparcos Catalogue identifier (HIP) is included.

Reliability tests were performed during the construction of the Hipparcos Input Catalogue, to check, for example, the coherence between the zones of the DM (BD, CoD, and CPD) and the declination at the mean epoch of the catalogue (1855 for BD, 1875 for CoD and CPD), and for typing errors (originating from the source catalogue, from an intermediate transcription, or confusion between the CoD and CPD identifiers). Resulting corrections were included in the Hipparcos Input Catalogue. Additional corrections are included in the corresponding fields; if the corresponding fields differ, the associated cross-identifications given in the Hipparcos Input Catalogue should be considered with caution.

Field H71: HD/HDE/HDEC identifier

Cross-identifications are given to stars in the HD Catalogue, with numbers in the range 1 – 225 300 (A.J. Cannon & E.C. Pickering, 1918–24, *Ann. Harvard Obs.*, 91–99), and its two extensions: HDE numbers in the range 225 301 – 272 150 (A.J. Cannon, 1925–36, *Ann. Harvard Obs.*, 100), and HDEC numbers in the range 272 151 – 359 083 (A.J. Cannon & M. Walton Mayall, 1949, *Ann. Harvard Obs.*, 112).

Field H72: DM identifier (BD)

This gives the DM identifier for objects contained within the Bonner Durchmusterung (BD), with the format B±ZZ␣NNNNa (coded with leading zeros in ZZ where appropriate). BD identifiers, unlike the CoD and CPD identifiers, may carry a lower-case suffix letter for additional stars, i.e. stars with suffix 'a', 'b', 'p', or 's' (these stars were added to the BD Catalogue after the original numbering was made; such suffixes do not imply that the entry is a component of a double or multiple system).

Field H73: DM identifier (CoD)

This gives the DM identifier for objects contained within the Cordoba Durchmusterung (CoD), with the format C±ZZ␣NNNNN (coded with leading zeros in ZZ where appropriate).

Field H74: DM identifier (CPD)

This gives the DM identifier for objects contained within the Cape Durchmusterung (CPD), with the format P±ZZ␣NNNNN (coded with leading zeros in ZZ where appropriate).

Field H75: $V - I$ used for the photometric processing

This is not necessarily the same as the 'final' value of $V - I$ given in Field H40. See Field H40 for details.

The value which has been used for the astrometric processing is the same as the value given in Field H75, to within 0.01 mag, for all entries except the following eight, which had their colours updated at a late stage of the processing:

HIP	H75	astrometric processing
87863	+0.31	+0.021
99483	+1.58	+2.220
102964	+1.05	+0.516
120401	+0.12	+0.090
120402	+0.00	−0.080
120403	+0.07	+0.040
120404	−0.04	−0.120
120415	−0.16	−0.250

Field H76: Spectral type

Acquired from ground-based compilations, the spectral types given in this field come primarily from the Hipparcos Input Catalogue, with some updates, especially for variable stars. Spectral types that were published in a truncated form in the Hipparcos Input Catalogue (composite spectra, or spectra with many peculiarities) are given here in their original form for a subset.

The spectral type has not been derived from the satellite observations, and is therefore not considered as a product of the mission. It is nevertheless provided partly for its astrophysical relevance, but also because it was used for the photometric transformations between B_T/V_T and $V/B-V$ for a subset of the entries (see Section 1.3, Appendix 4, and Field H37 for further details). A complete listing of the available spectral types is also given in Volume 11.

The data included in the Variability Annex (Volume 11, see also Section 2.4) includes the object's spectral type. This means that for variable stars, the spectral type is found in the ASCII files in two places (within the main catalogue Field H76, and within the Variability Annex, see Section 2.4, Field P3 and U3).

Spectral types in the Hipparcos Input Catalogue were taken from the SIMBAD data base or from the original proposal when the data were not available in SIMBAD. The latter included data from the Michigan Spectral Survey, Volumes 1–3; Volume 4 was also made available to the INCA Consortium in 1988. For variable stars, many spectral types were taken from the Fourth Edition of the General Catalogue of Variable Stars. Furthermore, many additions and corrections were made from the various programmes proposed for Hipparcos observation, or from individual searches in the literature. Confidence tests were performed from a correspondence between the spectral types and the colour index when both B and V magnitudes were considered reliable, and subsequently between the spectral type and B_T and V_T. Many resulting corrections were made either to the spectral types or to the photometric data.

Spectral types follow various classification systems (MK, HD, etc.). In the case of the MK classification system, the spectral type, luminosity class, and peculiarity code are given with the following designations:

- O, B, A, F, G, K, M plus sub-type (0, 1, etc.), and sometimes intermediate sub-type (for example F7.2, F7.5, F7.7) for the spectral types of 'normal stars';
- R, S, N, C for carbon stars;
- DB, DA, DF, DG for white dwarfs;
- WR, WN, WC for Wolf-Rayet stars.

For the luminosity class, the following designations are used: Ia0, Ia, Iab, Ib for supergiants, II for bright giants, III for giants, IV for sub-giants, V for dwarfs. The sub-dwarfs are either noted sd followed by the spectral type, or class VI. Peculiarities of the spectra are noted in lower case letters (e for emission lines, m for enhanced metallic lines, n for nebulous lines, nn for very nebulous, p for peculiarity in the chemical composition, s for sharp lines, sh for a shell, v for variations in the spectrum, w for weak lines, etc.). CN indicates stars cyanogen abundance anomaly.

Additional qualifiers have the following meaning:

: indicates some doubt about the determination of the spectral type or luminosity class;
/ between two spectral types or luminosity classes indicates that the two classifications were made during the Michigan Spectral Survey;
– between two spectral types or luminosity classes indicates that the parameter is intermediate between those given;
\+ indicates composite spectra (the second spectrum is not given in these cases);
... indicates truncated spectra (the source catalogue gives further details, including peculiarities).

The above description does not cover all MK designations which may be found in Field H76. A more complete description can be found in the introduction to the Michigan Spectral Survey.

Spectral types given in this field are homogeneous for the HD and HDE numbered stars from $-90°$ to $-12°$ in declination (i.e. in the zones covered by the Michigan Spectral Survey, Volumes 1–4). North of $-12°$ their quality is heterogeneous. This compilation of spectral types is provided for the convenience of the catalogue users. Although the highest quality spectral classification was selected to produce estimates of $B - V$ and $V - I$ where appropriate, no claims about the reliability of the spectral types are implied. For more careful use, SIMBAD or other original sources should be consulted.

Field H77: Source of spectral type

The flag indicates the source of the spectral type, as follows:

1 : Michigan Spectral Survey, Vol. 1 (N. Houk & A.P. Cowley, 1975, Univ. Michigan);
2 : Michigan Spectral Survey, Vol. 2 (N. Houk, 1978, Univ. Michigan);
3 : Michigan Spectral Survey, Vol. 3 (N. Houk, 1982, Univ. Michigan);
4 : Michigan Spectral Survey, Vol. 4 (N. Houk & A. Smith-Moore, 1988, Univ. Michigan);
G : updated after publication of the Hipparcos Input Catalogue;
K : Fourth Edition of the General Catalogue of Variable Stars (GCVS, P.N. Kholopov (ed.), 1985, 1987, Moscow);
S : SIMBAD;
X : miscellaneous;
␣ : entry without corresponding information.

As indicated under Field H76, spectral types and corresponding source flags were generally taken directly from the Hipparcos Input Catalogue (HIC) compilation. In cases where the spectral type given here differed from the HIC value (either because it was truncated in the HIC compilation, or because it was updated following investigations in view of discordant photometric data), the flag 'G' has been assigned. The number of entries in each category, compared with those in HIC are as follows:

	H77	HIC
1	12201	12348
2	9309	9375
3	11122	11232
4	10181	10304
G	1223	0
K	696	929
S	56983	57081
X	13469	13993
␣	3034	2947
Total	118218	118209

Table 2.1.1. Summary of the machine-readable Hipparcos Catalogue format
(a) fields also in the printed Hipparcos Catalogue, and in common with the Tycho Catalogue

Field	Bytes	Format	Description
H0/T0	1–2	A1,X	Catalogue (H = Hipparcos, T = Tycho)
H1	3–15	6X,I6,X	Identifier (HIP number)
T1	„	I4,I6,I2,X	TYC1–3 (TYC number)
H2/T2	16–17	A1,X	Proximity flag
H3/T3	18–29	A11,X	Identifier RA, h m s (J1991.25)
H4/T4	30-41	A11,X	Identifier Dec, ± ° ′ ″ (J1991.25)
H5/T5	42–47	F5.2,X	V (Johnson) magnitude
H6	48–49	A1,X	Coarse variability flag
T6	„	1X,X	Blank for Tycho
H7/T7	50–51	A1,X	Source of magnitude identifier
H8/T8	52–64	F12.8,X	α, degrees (J1991.25)
H9/T9	65–77	F12.8,X	δ, degrees (J1991.25)
H10/T10	78–79	A1,X	Reference flag for astrometry
H11/T11	80–87	F7.2†,X	Trigonometric parallax (mas)
H12/T12	88–96	F8.2†,X	$\mu_{\alpha*} = \mu_\alpha \cos\delta$ (mas/yr)
H13/T13	97–105	F8.2†,X	μ_δ (mas/yr)
H14/T14	106–112	F6.2†,X	Standard error in $\alpha*$ at J1991.25 (mas)
H15/T15	113–119	F6.2†,X	Standard error in δ at J1991.25 (mas)
H16/T16	120–126	F6.2†,X	Standard error in π (mas)
H17/T17	127–133	F6.2†,X	Standard error in $\mu_{\alpha*}$ (mas/yr)
H18/T18	134–140	F6.2†,X	Standard error in μ_δ (mas/yr)
H19/T19	141–146	F5.2,X	Correlation, $\rho^{\delta}_{\alpha*}$
H20/T20	147–152	F5.2,X	Correlation, $\rho^{\pi}_{\alpha*}$
H21/T21	153–158	F5.2,X	Correlation, ρ^{π}_{δ}
H22/T22	159–164	F5.2,X	Correlation, $\rho^{\mu_{\alpha*}}_{\alpha*}$
H23/T23	165–170	F5.2,X	Correlation, $\rho^{\mu_{\alpha*}}_{\delta}$
H24/T24	171–176	F5.2,X	Correlation, $\rho^{\mu_{\alpha*}}_{\pi}$
H25/T25	177–182	F5.2,X	Correlation, $\rho^{\mu_{\delta}}_{\alpha*}$
H26/T26	183–188	F5.2,X	Correlation, $\rho^{\mu_{\delta}}_{\delta}$
H27/T27	189–194	F5.2,X	Correlation, $\rho^{\mu_{\delta}}_{\pi}$
H28/T28	195–200	F5.2,X	Correlation, $\rho^{\mu_{\delta}}_{\mu_{\alpha*}}$
H29	201–204	I3,X	Data points rejected (per cent)
T29	„	I3,X	Data points accepted, $N_{\rm astrom}$
H30/T30	205–210	F5.2,X	F2 (goodness-of-fit)
H31/T31	211-217	I6,X	HIP number
H32/T32	218–224	F6.3,X	B_T (mag)
H33/T33	225–230	F5.3,X	σ_{B_T} (mag)
H34/T34	231–237	F6.3,X	V_T (mag)
H35/T35	238–243	F5.3,X	σ_{V_T} (mag)
H36/T36	244–245	A1,X	Reference flag for B_T and V_T
H37/T37	246–252	F6.3,X	$B-V$ (mag)
H38/T38	253–258	F5.3,X	σ_{B-V} (mag)
H39	259–260	A1,X	Source of $B-V$
T39	„	1X,X	Blank for Tycho

† For these fields, the second decimal digit for the Tycho format is always blank

The Hipparcos and Tycho Catalogues are similar up to Field H39/T39; thereafter, the fields and their meanings are catalogue specific. Thus Tables 2.1.1(a) and 2.2.1(a) are identical. Due care must be taken in ensuring that blank fields are not interpreted as numerically zero.

Table 2.1.1. Summary of the machine-readable Hipparcos Catalogue format (cont.)
(b) Hipparcos specific catalogue data, also contained in the printed Hipparcos Catalogue

Field	Bytes	Format	Description
H40	261–265	F4.2,X	$V - I$ (mag)
H41	266–270	F4.2,X	σ_{V-I} (mag)
H42	271–272	A1,X	Source of $V - I$
H43	273–274	A1,X	Reference flag for colour indices
H44	275–282	F7.4,X	Median Hp (mag)
H45	283–289	F6.4,X	σ_{Hp} (mag)
H46	290–295	F5.3,X	Scatter, s (mag)
H47	296–299	I3,X	Accepted transits, N
H48	300–301	A1,X	Reference flag for photometry
H49	302–307	F5.2,X	Mag at max, Hp (5th percentile)
H50	308–313	F5.2,X	Mag at min, Hp (95th percentile)
H51	314–321	F7.2,X	Period (days)
H52	322–323	A1,X	Flag (variability type)
H53	324–325	A1,X	Flag (variability tables)
H54	326–327	A1,X	Flag (light curves)
H55	328–338	A10,X	CCDM Identifier
H56	339–340	A1,X	Historical status flag
H57	341–343	I2,X	Number of catalogue entries
H58	344–346	I2,X	Number of components
H59	347–348	A1,X	Double/Multiple Systems Annex flag
H60	349–350	A1,X	Astrometric source flag
H61	351–352	A1,X	Solution quality
H62	353–355	A2,X	Component identifiers
H63	356–359	I3,X	Position angle (degrees)
H64	360–367	F7.3,X	Angular separation (arcsec)
H65	368–373	F5.3,X	σ_ϱ (arcsec)
H66	374–379	F5.2,X	ΔHp (mag)
H67	380–384	F4.2,X	$\sigma_{\Delta Hp}$ (mag)
H68	385–386	A1,X	Survey flag
H69	387–388	A1,X	Chart flag
H70	389–390	A1,X	Notes

Table 2.1.1. Summary of the machine-readable Hipparcos Catalogue format (cont.)
(c) Hipparcos specific catalogue data, not contained in the printed Hipparcos Catalogue

Field	Bytes	Format	Description
H71	391–397	I6,X	HD identifier
H72	398–408	A10,X	DM (BD) identifier
H73	409–419	A10,X	DM (CoD) identifier
H74	420–430	A10,X	DM (CPD) identifier
H75	431–435	F4.2,X	$V - I$ (mag) used for reductions
H76	436–448	A12,X	Spectral type
H77	449–450	A1,X	Source of spectral type

Section 2.2

Contents of the Tycho Catalogue

2.2. Contents of the Tycho Catalogue

Overview of the Tycho Catalogue: The Tycho Catalogue provides astrometry (positions, parallaxes and proper motions) and two-colour photometry (in B_T and V_T) for more than one million stars brighter than $V_T = 11.5$ mag. The median precision (standard error) is 25 mas in position and 0.10 mag in the $B_T - V_T$ colour index. These values apply at the median magnitude $V_T = 10.5$ mag for stars of median colour index $B_T - V_T \simeq 0.7$ mag. The Tycho Catalogue contains 1 058 332 entries: comprising 1 052 031 entries (stars) observed by Tycho, supplemented by the 6301 entries from the Hipparcos Catalogue and Part C of the Double and Multiple Systems Annex that were not observed by Tycho. The Tycho Catalogue contains roughly 40 000 stars brighter than $V_T = 9$ mag which are not contained in the Hipparcos Catalogue. For these stars the median precision is 7 mas in position, parallax and annual proper motion and 0.019 mag in $B_T - V_T$. Double stars with separations larger than 2 arcsec and with moderate magnitude difference are usually resolved.

The Tycho Catalogue, and its associated Tycho Epoch Photometry Annex, is strictly an observational catalogue. It contains data derived exclusively from the Hipparcos satellite's star mapper observations, with the exception of certain cross-identifications.

The reduced data comprise two parts. The main catalogue (the Tycho Catalogue, or TYC, described in this section) contains the astrometric and summary photometric data for each star. The Tycho Epoch Photometry Annex (described in Section 2.6) contains 'epoch photometry' (photometry at each epoch of observation) for a subset of stars observed with sufficiently high signal-to-noise ratio. In structure, the Tycho Catalogue and its Epoch Photometry Annex resemble the corresponding machine-readable parts of the Hipparcos Catalogue and associated Epoch Photometry Annex.

Solar system objects observed as part of the Tycho experiment are contained within the general annex of solar system observations (see Section 2.7).

Tycho Catalogue Completeness: Some Hipparcos Catalogue stars were not observable by the star mapper. The dynamic range of the star mapper detector resulted in non-linearity at the brightest magnitudes (Sirius was not observable). The faintest Hipparcos Catalogue stars fell below the detection threshold of the star mapper detectors. Stars in very dense clusters and other dense fields could not be observed by Tycho, thus leaving the resulting Tycho Catalogue incomplete in such regions (see, for example, entries flagged 'R' in Field T42). Section 1.1.1 gives further details of the relationship between the Tycho and Hipparcos Catalogues and entries.

All 6301 single star entries and double and multiple star components contained within the Hipparcos Catalogue but not observed by Tycho have nevertheless been included in the Tycho Catalogue for completeness, and assigned a corresponding TYC number. In these cases (flag 'H' in Field T42), the truncated astrometric and photometric descriptor taken from the Hipparcos Catalogue (Fields H3–5) has been included in the Tycho Catalogue at the appropriate location (Fields T3–5). The position of the entry taken from the Hipparcos Catalogue (Fields H8–9) is also included in Fields T8–9 to assist cross-identification between the catalogues.

Among the 120 000 stars in the PPM catalogue brighter than 9.0 mag, about 120 are not contained in the Tycho Catalogue (see Chapter 17, Volume 4 for details).

The following table gives the number of stars in TYC and the number of TYC stars not included in HIP, along with the corresponding median standard errors for stars within the given intervals of V_T magnitude (the column 'All' also including entries for which V_T is not available). Systematic errors in astrometry are less than 1 mas and 1 mas/yr, although the external standard errors (the true accuracies) may be up to 50 per cent larger than the quoted standard errors for faint stars. In photometry, systematic errors may reach the level of the quoted standard errors for faint stars. The photometry for about 20 000 stars is considered to be uncertain, for example when the standard errors are larger than 0.3 mag.

Interval of V_T	<6.0	6–7.0	7–8.0	8–9.0	9–10.0	10–11.0	>11.0	All	<9.0
Median V_T, mag	5.38	6.63	7.62	8.62	9.61	10.58	11.19	10.47	8.33
N (TYC)	4553	9550	27750	78029	211107	515029	205934	1052031	119882
N (not in HIP)	4	55	3485	36511	182773	506720	205275	934901	40055
Median standard errors in astrometry (mas):									
Position (J1991.25)	1.8	2.6	4.0	6.7	12.9	27.2	39.2	24.6	5.6
Parallax	2.5	3.6	5.3	8.6	16.4	34.3	49.6	31.2	7.2
Proper motion/yr	2.3	3.3	5.0	8.3	16.0	33.5	48.6	30.2	7.0
Median standard errors in photometry (mag):									
B_T	0.003	0.006	0.010	0.018	0.036	0.084	0.128	0.074	0.014
V_T	0.003	0.005	0.008	0.014	0.027	0.064	0.122	0.057	0.012
$B_T - V_T$	0.005	0.008	0.014	0.024	0.049	0.117	0.200	0.104	0.019
$B - V$	0.004	0.007	0.012	0.020	0.041	0.098	0.171	0.087	0.017

Tycho Photometry: Tycho photometry was obtained in two colour bands, B_T and V_T, closely corresponding to B and V in the Johnson UBV system. The Tycho colour index, written $B_T - V_T$ or $(B-V)_T$, is not explicitly given, but may be simply derived from the difference of the published magnitudes. Approximate values of the Johnson V magnitude (Field T5) and colour index $B - V$ (Field T37) are also provided, derived by the transformations in Section 1.3, Appendix 4. Because it is a strict observable, and unaffected by the uncertainties inherent in such a transformation, the Tycho colour index rather than the derived Johnson colour index is recommended for use whenever appropriate.

A simple linear transformation from the Tycho B_T, V_T magnitudes to B, V magnitudes in the Johnson photometric system is:

$$V \simeq V_T - 0.090\,(B_T - V_T) \qquad [2.2.1]$$

$$B - V \simeq 0.850\,(B_T - V_T) \qquad [2.2.2]$$

In the interval $-0.2 < B_T - V_T < 1.8$ mag the systematic errors of this simple transformation do not exceed 0.015 mag for V and 0.05 mag for $B - V$ for unreddened main-sequence stars.

Proximity Flag: In analogy with the Hipparcos Catalogue, Field T2 provides a 'proximity flag' giving a coarse indication of the presence of nearby objects (within 10 arcsec). These may be separate Tycho Catalogue entries, or separate Hipparcos Catalogue entries (or components). Further information on nearby objects can be derived from an examination of the relevant Hipparcos or Tycho Catalogue entries, or from Field T49 indicating unresolved duplicity.

Reference Stars: A distinct flag, Field T10, indicates whether the Tycho Catalogue entry is considered as a 'recommended' astrometric reference star. This flag is assigned to classification of the entry as an astrometric reference star since there are several considerations, aside from (possible) duplicity, which may disqualify the object from being classified as a Tycho Catalogue astrometric reference star. Further details are given under Field T10. Hipparcos Catalogue objects not observed by Tycho (i.e. where Field T42 contains 'H') are flagged as dubious Tycho astrometric reference stars even though the object could be a well-behaved, single object within the Hipparcos Catalogue. This distinction has been preserved in order to maintain the consistency of the Tycho Catalogue as an independent observational catalogue.

Most of the Tycho Catalogue magnitudes have sufficient accuracy for calibration of magnitudes derived from photographic survey plates in colour bands near to B or V. Selection according to the criteria adopted under Field T34 results in the availability of about 520 000 Tycho photometric reference stars suitable for such purposes.

Transits, Detections, Measurements: In the terminology of the Hipparcos Catalogue, a star 'transit' is defined as a crossing of the star across the main modulating grid (2688 slits covering a field of view of approximately $0\overset{\circ}{.}9 \times 0\overset{\circ}{.}9$). In the terminology of the Tycho Catalogue, a 'transit' refers to the crossing of the star across a star mapper slit system (either of a set of four vertical or inclined slits of 40 arcmin length, located at the edge of the main field of view, and used primarily for the satellite real-time attitude determination). Such a transit is defined irrespective of whether or not such a crossing yields 'useful' astrometric and/or photometric information. The transit yields useful astrometric and/or photometric information when the star is not too faint, when the background was below a certain limit, when an accurate attitude determination was available, and when the observations were not perturbed by nearby bright stars. Details of the measurements and reductions are given in Volumes 2 and 4.

All relevant transits related to a given star have been combined to provide the astrometric data and the summary photometric data contained in the main Tycho Catalogue, and individual transit records (providing 'epoch photometry') are contained in the Tycho Epoch Photometry Annex. The summary photometric data provide median magnitudes for bright stars and 'de-censored mean magnitudes' for fainter stars, and a set of parameters and flags giving an overview of the variability. The Tycho Epoch Photometry Annex includes details of each transit including background, observation epoch, and related quantities and flags.

In practice, the detection process giving a signal amplitude and a transit time was carried out on a signal where the photon counts in the B_T and V_T channels had been added, forming the so-called T channel. The term 'detected transit' is used to refer to a transit containing a significant signal belonging to the relevant star, and this signal itself is called a detection. When a signal was detected above a signal-to-noise ratio of 1.5 in the T channel an estimation (or measurement) of the signal amplitude was carried out in the B_T and V_T channels separately whenever possible. If no such measurement was available, a flag in the first two bits of Field TT13 (see Table 2.6.2) indicates that the magnitude could not be measured in one or other of the separate channels.

Valid and Invalid Transits for Photometry: Transits were used for Tycho (mean value) photometry irrespective of whether or not the object was actually detected in the predicted 'transit interval' of a few arcsec length for the corresponding slit group—the condition for using the transit being simply that the relevant data interval was considered to be 'valid'. Such a transit interval could contain several detections (either real detections due to the predicted star or to another star, or false detections due simply to photon noise) or it could contain no detection at all.

Certain transit intervals were considered as 'invalid', and subsequently excluded from use in Tycho photometry, for a variety of reasons:

(a) if the satellite attitude was poorly known, or if (attitude-control) jet firings were affecting the satellite attitude estimation at the moment of the observations;
(b) if the detector background was high, for example as a result of a passage of the satellite through the van Allen radiation belts—a higher background was acceptable for astrometry than for photometry;
(c) because the star crossed the star mapper slit system too close to the end of the slit, or to the 90° angle of the inclined slits—in such cases, attitude uncertainties may have made it infeasible to distinguish between 'uncaptured' transits, and transits where the signal was below the detectability threshold.

Non-Detections and De-Censored Magnitudes: A valid transit interval was classified as 'non-detected' or 'censored' if it contained no detection, in the T channel, close enough to the predicted transit time for the relevant star. The criterion for rejection was that all residuals of detections in the astrometric adjustment of the transit interval were larger than given limits.

Limits used in astrometry for the rejection of detections were $|\Delta u| > 1.0$ arcsec or $|\Delta u| > 3\sigma_u$, where Δu is the difference between the observed and computed transit times (converted to an angular distance using the instantaneous satellite scan speed across the slit group), and σ_u is the standard error of Δu. A single limit was used in the de-censoring analysis, $|\Delta u| > 0.6$ arcsec. Since transit detection was based on preliminary predicted transit times, which were sometimes in error by a large amount, the real transit occasionally occurred outside the predicted transit interval. Such detected transits were not assigned to the correct star and were thus lost, even when the improved transit times were introduced at a later stage. As a consequence, non-detections were occasionally associated even with bright stars. This problem was accommodated within the mathematical model for the de-censoring analysis by assuming that there was a probability of 6 per cent that a predicted Tycho star transit resulted in a non-detection even for a bright star. This is referred to as the assumption of 6 per cent 'spurious non-detections', and users of the Tycho epoch photometry should be aware of this deficiency. Photometric standard star observations were used for checking the validity of the de-censoring analysis and for correcting final small biases, as described in further detail in Volume 4, Chapter 9.

The use of non-detected transits has two reasons. First, because detectability depends on the signal-to-noise ratio of a given transit, mean or median magnitudes have not simply been constructed from the detected transits—rather, a 'de-censored mean magnitude' in B_T and V_T was constructed, using model-based inferred magnitudes in place of transits which were either not detected in the T-channel, or detected but not measured in the B_T or V_T channels. All valid transits were thus taken into account, whether detected or not (see Volume 4 for details). Second, non-detected transits may be relevant in variability studies, where it may be important to identify whether a photometric data point is absent because the object's magnitude fell below the threshold at that epoch, or simply because no data were acquired at that epoch. But a non-detection is not always

an indication that the star was too faint to be detected due to the 6 per cent spurious non-detections described above.

For bright stars with $B_T \leq 8.5$ mag and $V_T \leq 8.0$ mag a median magnitude was derived from the measured signal in the B_T and V_T channels respectively. This median magnitude is equivalent, within 0.005 mag, to a de-censored mean magnitude because bright stars resulted in very few non-detections. The median magnitude was adopted for bright stars since the median could also be constructed for variable stars, while the de-censoring analysis was based on the assumption that the star is constant.

Parasites: Some transits have been flagged as disturbed by a 'parasite', i.e. a fairly bright star which was close in transit time to that of the star considered, according to calculations based on the stars in the Tycho Input Catalogue Revision, described in further detail in Volume 4. Such transits were rejected in the astrometric adjustment, and (partly) in the de-censoring analysis since these analyses were sensitive to outlying observations. They are however included in the Tycho Epoch Photometry Annex (flagged in bit 2 of Field TT13, see Table 2.6.2) if none of the conditions (a–c) discussed under 'Valid and Invalid Transits for Photometry' also caused a rejection in the astrometric adjustment. The flag was not used in the construction of median magnitudes since the median is only weakly affected by outliers, and since such transits in fact often do not suffer from any significant photometric disturbance.

Number of Transits: The number of valid transits for a given TYC entry, including the non-detections, is denoted by $N_{\rm transits}$. The Tycho Epoch Photometry Annex contains $N_{\rm transits}$ transits for the selected stars, and the number is given in Field TH4 of the corresponding header record (see Section 2.6).

The final astrometric and photometric results for each star have typically been constructed from different numbers of star transits in each case—individual transits having been used, or rejected, for the final catalogue for a variety of reasons. The number of transits used in the *astrometric* adjustment, $N_{\rm astrom}$, is given in Field T29 of the main Tycho Catalogue. It excludes non-detections and detections affected by parasites.

The number of transits used in Tycho mean value photometry, $N_{\rm photom}$, is given in Field T43 of the main Tycho Catalogue. $N_{\rm astrom}$ and $N_{\rm photom}$ are about 25 per cent less than $N_{\rm transits}$. The number of valid transits was slightly lower for photometry than for astrometry because a higher background was acceptable in astrometry. The process of photometric de-censoring used both detections which were unaffected by parasites, and the non-detections. Therefore, for stars brighter than $V_T \simeq 10$ mag with few non-detections the ratio $N_{\rm photom}/N_{\rm astrom} \simeq 0.80$, while for fainter stars with many non-detections the ratio may be as large as 1.5. For median magnitudes only detections were used, including those affected by parasites, since these were too few to have any significant effect on the median.

Format of the Tycho Catalogue

Unlike the main Hipparcos Catalogue, the Tycho Catalogue and the Tycho Epoch Photometry Annex are not made available in printed form, but only as a machine-readable version.

The Tycho Catalogue format is largely identical to that of the Hipparcos Catalogue up to and including Field H39/T39. This approach is intended to facilitate use of both catalogues. Thereafter, additional Tycho Catalogue fields are included with astrometric and photometric information and cross-identifications to other catalogues. Flags indicate variable stars, detected duplicity or multiplicity, or notes.

Entries of the Tycho Catalogue are given in the sequence of the hierarchical TYC1–3 identifier (Field T1), i.e. corresponding to organisation according to the GSC (Guide Star Catalog) region number (and not in sequence of right ascension).

The same conventions and units are adopted for the Tycho Catalogue as for the main Hipparcos Catalogue. Thus, definitive values of right ascension and declination are expressed in degrees and decimals of a degree, while all other astrometric parameters, and errors, are expressed in milliarcsec, even though some digits may not be significant. The catalogue epoch is J1991.25, and positions and errors are given for that epoch. Astrometric correlations are also provided. All parameters are expressed within the reference system ICRS (see Section 1.2.2). Positions are also provided in conventional sexagesimal units, with truncated precision. Similar approaches have also been adopted for the categorisation of variability data.

Double and multiple star detection differs significantly between the Hipparcos main mission and Tycho, and fields dedicated to summary double and multiple star data in the main Hipparcos Catalogue are accordingly absent in the Tycho Catalogue.

Fields T0–2: Tycho Identifier/Proximity Flag

Field T0: The machine-readable (main) Hipparcos and Tycho Catalogues include a character indicating whether the associated record is derived from Hipparcos (H) or Tycho (T) data. Field H1/T1 then provides the Hipparcos Catalogue number (HIP) or the Tycho Catalogue identifier (TYC) accordingly, with the interpretation of subsequent fields being, in part, catalogue dependent (see Tables 2.1.1 and 2.2.1).

Field T1: TYC identifier

The designation of the object within the Tycho Catalogue uses the Guide Star Catalog (GSC) numbering system (a region number, designated here TYC1; and a number within the region, designated here TYC2) followed by a Tycho Catalogue specific component number (TYC3). As well as giving a cross-identification to an important star catalogue, this designation system has the advantage of giving a rough position indication. For objects contained in the GSC, TYC1 and TYC2 are identical to the identifiers defined by the GSC numbering system.

In the few cases where no corresponding GSC object exists close to the Tycho Catalogue object, values of TYC1 and TYC2 consistent with the GSC numbering system were created with the assistance of the Guide Star Catalog team. The component number (TYC3) gave necessary flexibility for addition of objects during the Tycho Catalogue production discovered close to the GSC object designated by the values of TYC1 and TYC2. The TYC3 numbers have been assigned starting with 1 and increasing with the V_T magnitude. Components with TYC3 > 1 are always located within a distance of 15 arcsec from the corresponding star with TYC3 = 1.

The recommended TYC designation contains a hyphen between the TYC numbers, e.g. for the first star in the Tycho Catalogue the designation is 'TYC 1–13–1', corresponding to 'GSC 1–13'. The TYC identifier of the first entry in the catalogue is ' 1   13 1'.

The maximum value for each of the TYC numbers is as follows: TYC1 = 9537; TYC2 = 12119; TYC3 = 4. The number of entries with each of the occurring TYC3 numbers is as follows: 1 = 1 051 966; 2 = 6334; 3 = 31; 4 = 1. The entry with 4 TYC3 components is TYC 1327–606–1 to –4 = HIP 30075 ABCD of which the components C and D were only measured by Hipparcos.

All stars contained within the Hipparcos Catalogue but not observed by Tycho have also been included in the Tycho Catalogue for completeness (see Field T42) and assigned a corresponding TYC number.

Field H31, which appears as the first column of the right-hand page of the printed Hipparcos Catalogue, contains the Hipparcos Catalogue (HIP/HIC) identifier. This is retained for the Tycho Catalogue, so that Fields T31 and T51 (which gives the Hipparcos component identifier, if any) provide the links between the Hipparcos and Tycho Catalogues.

Field T2: Proximity flag

This field provides a coarse indication of the presence of nearby objects. If non-blank, it indicates that there is one or more distinct Hipparcos Catalogue entries (or distinct components of the system if double or multiple), or one or more distinct Tycho Catalogue entries, in either case irrespective of magnitude, within 10 arcsec of the position given in Fields T8–9. The term 'distinct' means simply that a proximity flag is not assigned to a Tycho Catalogue entry cross-identified with the same (single) star contained within the Hipparcos Catalogue.

The flag is assigned according to the following hierarchy (i.e. if 'H' and 'T' both apply, 'H' is adopted):

H : there is one or more distinct Hipparcos Catalogue entries, or one or more distinct components of the relevant Hipparcos Catalogue entry, within 10 arcsec of the position given in Fields T8–9. This includes the cases where two Hipparcos components are merged into one Tycho entry (see also Field T51);

T : there is one or more additional Tycho Catalogue entries within 10 arcsec of the position given in Fields T8–9.

The number of entries in each of these categories is as follows: H = 12 812; T = 5851.

Fields T3–7: Descriptor

Fields T3–4 provide an approximation to the position given in Fields T8–9, and are included as a convenient way of object identification. Fields T5–7 provide an approximate but rather homogeneous indication of the V magnitude in the Johnson UBV system, along with a source flag.

Fields T3–4: Positional identifier: truncated coordinates (epoch J1991.25, ICRS)

The approximate right ascension and declination are given in conventional sexagesimal units with truncated precision, for epoch J1991.25, and within the reference system ICRS. Fields T3–4 are rounded values of the positions given in Fields T8–9, and are included as a convenient way of object identification. Since the identifier is strictly constructed from the Tycho position, identifiers for entries contained in both the Hipparcos and Tycho Catalogues will not necessarily be identical.

Field T5: V magnitude

The V magnitude is given mainly for identification purposes (see Field T7). Normally this V magnitude is in the Johnson UBV photometric system, although this is not the case for some entries as specified in Field T7.

The field is blank for 3217 entries, all faint ($Hp > 10.9$ mag) Hipparcos double star components.

Although Tycho observations give magnitudes in the photometric bands referred to as B_T and V_T, the magnitude identifier has been transformed from the available B_T and V_T data to a magnitude in the V band, for consistency with the information given in the Hipparcos Catalogue, using the transformations defined in Section 1.3, Appendix 4. Magnitudes are given to two decimal places, with typical systematic errors of about 0.01 mag, although much larger systematic errors are expected especially for red stars, i.e. with $B - V > 1.5$ mag.

The standard error is usually $\simeq 1.1\sigma_{V_T}$, but may be calculated more accurately using Equation 1.3.21. The magnitude is very uncertain if Field T57 is not blank, in particular if it contains 'M'.

Field T6: This field (coarse variability flag for HIP) is blank for Tycho

Field T7: Source of magnitude given in Field T5

The V magnitude, considered primarily as a magnitude 'identifier' (although with astrophysical relevance) has usually been derived from the available B_T and V_T data, as described under Field T5. Otherwise, if non-blank, the field has the following meaning:

- B : no V_T magnitude is available, therefore the B_T value was adopted;
- D : derived from approximate B_T and V_T magnitudes, corresponding to flag 'D' in Field T36;
- T : only an approximate V_T magnitude has been derived, as indicated by flag 'T' in Field T36; in these cases, the V magnitude given in Field T5 is simply the approximate V_T magnitude given in Field T34;
- V : no B_T magnitude is available, therefore the V_T value was adopted;

The number of entries in each of these categories is as follows: B = 79; D = 3314; T = 1333; V = 173.

Fields T8–30: Astrometric Data

The data in Fields T8–30 are the same in both format and meaning in the Tycho Catalogue as in the Hipparcos Catalogue, i.e. position, proper motion, parallax, astrometric standard errors and correlations, and solution flags. Positions are expressed in degrees. Annual proper motion components, trigonometric parallaxes, and all astrometric errors (including those of positions) are expressed in milliarcsec. Angular measures are along a great circle, including the factor of $\cos\delta$ for positional error in right ascension, for proper motion in right ascension, and for proper motion error in right ascension. If parameters such as the proper motion or parallax were not calculated (e.g. for a close companion having too few observations) the corresponding field will be blank.

The right ascension and declination are referred to the catalogue epoch, J1991.25, as described in Section 1.2.6. Corresponding standard errors, also at the catalogue epoch, are given in Fields T14–18. Positions and proper motions are referred to ICRS, as described in Section 1.2.2. The astrometric positions and their errors can be propagated to the standard epoch J2000.0, or to any other epoch, within the ICRS frame, by the methods described in Section 1.2.8. [Since for many Tycho Catalogue entries the proper motion will have a standard error larger than the expected proper motion itself ($\mu \simeq 20$ mas/yr for a star of spectral type F5 and $V = 11$ mag), a more accurate position for faint stars at a different epoch may often be predicted by assuming a zero proper motion.]

Fields T8–9: Equatorial coordinates (epoch J1991.25, ICRS)

The right ascension, α, and declination, δ, are expressed in degrees for the catalogue epoch J1991.25, and with respect to the reference system ICRS.

ICRS is consistent with the conventional coordinate system at J2000.0, previously realised by the FK5 Catalogue.

The source of astrometric data is detailed in Field T42. If only the position is given (i.e. if Field T42 is non-blank), Fields T11–13 and T16–28 will be blank, and sometimes also other fields. Formal positional standard errors are still given in Fields T14–15 if Field T42 = ‘P’ or ‘R’, although they will be less reliable than the standard errors corresponding to a full astrometric solution. If Field T42 = ‘H’, the position given in Fields T8–9 is the position taken directly from the Hipparcos Catalogue.

Field T10: Reference flag for the astrometric parameters

This flag indicates that the astrometric parameters in Fields T8–30 refer to:

␣ : a recommended astrometric reference star, having good Tycho astrometric quality, and not recognised as double;

X : a dubious astrometric reference star in the context of the Tycho Catalogue.

A star is flagged as a dubious astrometric reference star either because the quality flag in Field T40 is $Q \geq 6$, or because Fields T2 or T42 are non-blank, or because Field T49 = ‘D’ or ‘S’ indicating possible duplicity, or because Field T57 = ‘J’, ‘K’ or ‘L’ indicating dubious astrometry. The case where Field T42 contains ‘H’ (Hipparcos entry not observed by Tycho) is systematically classified as ‘dubious’ within the context of the Tycho Catalogue, even though it could be a well-behaved, single object within the Hipparcos Catalogue.

The number of entries in each of these categories is as follows: ␣ = 886 621; X = 171 711. The catalogue thus contains nearly 900 000 recommended astrometric reference stars.

Field T11: Trigonometric parallax

The trigonometric parallax, π, is expressed in units of milliarcsec. The estimated parallax is given for every star, even if it appears to be insignificant or negative (which may arise when the true parallax is smaller than its error).

Fields T12–13: Proper motion components (epoch J1991.25, ICRS)

The proper motion components, $\mu_{\alpha*} = \mu_\alpha \cos\delta$ and μ_δ, are expressed in milliarcsec per Julian year (mas/yr), and are given with respect to the reference system ICRS.

Fields T14–15: Standard errors of the equatorial coordinates (epoch J1991.25)

The standard errors of the right ascension, $\sigma_{\alpha*} = \sigma_\alpha \cos\delta$, and declination, σ_δ, are given at the catalogue epoch, J1991.25, and are expressed in milliarcsec.

Field T16: Standard error of the trigonometric parallax

The standard error of the trigonometric parallax, σ_π, is given in milliarcsec.

Fields T17–18: Standard errors of the proper motion components

The standard errors of the proper motion components, $\sigma_{\mu_{\alpha*}} = \sigma_{\mu_\alpha \cos\delta}$ and σ_{μ_δ}, are expressed in milliarcsec per Julian year (mas/yr).

Fields T19–28: Correlation coefficients

The correlation coefficients (see Section 1.2.7) are given as (real) numerical values in the following order:

T19 = $\rho^{\delta}_{\alpha*}$
T20 = $\rho^{\pi}_{\alpha*}$
T21 = ρ^{π}_{δ}
T22 = $\rho^{\mu_{\alpha*}}_{\alpha*}$
T23 = $\rho^{\mu_{\alpha*}}_{\delta}$
T24 = $\rho^{\mu_{\alpha*}}_{\pi}$
T25 = $\rho^{\mu_{\delta}}_{\alpha*}$
T26 = $\rho^{\mu_{\delta}}_{\delta}$
T27 = $\rho^{\mu_{\delta}}_{\pi}$
T28 = $\rho^{\mu_{\delta}}_{\mu_{\alpha*}}$

corresponding to the sequence illustrated in the following table:

	$\alpha*$	δ	π	$\mu_{\alpha*}$	μ_δ
$\alpha*$	–	T19	T20	T22	T25
δ	T19	–	T21	T23	T26
π	T20	T21	–	T24	T27
$\mu_{\alpha*}$	T22	T23	T24	–	T28
μ_δ	T25	T26	T27	T28	–

The use of the asterisk notation, $\mu_{\alpha *} = \mu_\alpha \cos\delta$, etc., is not really required in the correlations, since the correlation coefficient is the same between (say) α and δ, as between $\alpha\cos\delta$ and δ. Nevertheless, it has been retained for uniformity.

Field T29: The number of transits retained in the astrometric adjustment, $N_{\rm astrom}$

The number of transits retained in the astrometric adjustment corresponds to those remaining after the rejection of outliers, as defined in the introduction to the present section.

While Field H29 gives the fraction of rejected observations for the main Hipparcos Catalogue, the number of rejected transits is of no value in assessing a goodness-of-fit for objects in the Tycho Catalogue—it is usually of the order of 50 per cent, due to the definition of the identified transits.

Field T30: Goodness-of-fit parameter, F2

This number indicates the goodness-of-fit of the solution to the accepted data. For good fits F2 should approximately follow a normal distribution with zero mean value and unit standard deviation. F2 values exceeding +2.5 to +3 thus indicate a bad fit to the data. Its construction and interpretation are explained further under Field H30 (Section 2.1). The F2 value was, however, not used for generating the astrometric quality flag in Field T40, where classification measures derived from other aspects of the data reduction were found to be more informative.

The resulting F2 distribution is close to normal for single stars, i.e. for the recommended astrometric reference stars with no flag set in Field T10. The mean of the distribution is $\simeq 0.73$ and the standard deviation 1.20; the former arising from the fact that the unit weight error, $(\chi^2/\nu)^{1/2}$, is about 1.04. The unit weight error is included as a factor in the astrometric standard errors (see Volume 4, Equation 11.2) given in Fields T14–18 (but not in the corresponding errors for Hipparcos, Fields H14-18). The effect of this factor is discussed in Volume 4, Section 18.1. The unit weight error may be calculated for a star if F2 is given, as:

$$\text{unit weight error} = \left[\left(\frac{2}{9\nu}\right)^{1/2} \text{F2} + 1 - \frac{2}{9\nu}\right]^{\frac{3}{2}}$$

where $\nu = N_{\rm astrom} - 5$.

Field T31: Hipparcos Catalogue number, as Field H31

The Hipparcos Catalogue number is given for 123 431 entries (there are 117 955 different HIP numbers, in agreement with the number of entries in the Hipparcos Catalogue with an astrometric solution).

Field H1 gives further details of the HIP identifier.

The number of Tycho Catalogue entries with cross-identification to the Hipparcos Catalogue is larger than the number of entries in the main Hipparcos Catalogue since the corresponding HIP number is also given, where appropriate, for Tycho Catalogue entries corresponding to components contained in the Hipparcos Catalogue Double and Multiple Systems Annex (see also Field T51). The associated CCDM component identifier, if relevant, is given in Field T51 for 18 687 entries.

Fields T32–39: Photometric Data

These fields generally retain the same structure as the corresponding fields of the Hipparcos Catalogue. Fields T32–35 contain B_T and V_T magnitudes, and associated standard errors, precisely the same as the values given under Fields H32–35. The flag in Field T36 specifies how these 'mean' magnitudes have been obtained, i.e. as 'de-censored mean', as 'median' or 'approximate'.

For most stars (96 per cent) de-censored mean magnitudes are given because of the 'censoring' (non-detection) of faint transits in the case of Tycho observations, as described in the introduction (a simple median or mean value of the detected amplitudes would result in a biased estimate of the star's magnitude). Thus Fields T32 and T34 provide 'de-censored mean magnitudes' if the flag 'N' is given in Field T36. These magnitudes are derived from an analysis taking specific account of individual transits likely to have fallen below the detectability threshold for a subset of the observations. Estimates of the standard errors, and a description of the notation $\sigma^-_{B_T}$ and $\sigma^-_{V_T}$, are given in Section 1.3.6.

For bright stars median magnitudes B_T, V_T were computed with the errors obtained from the 15th and the 85th percentile of the distribution. (Note that for the *Hp* photometry included in the main Hipparcos Catalogue, *median* magnitudes were derived from all observations, and the error on the median was computed from the 35th and 65th percentiles of the distribution—as described in Section 1.3.6.)

Approximately 10 000 photometric standards were effectively used in the Tycho photometric calibration, making use of *a priori* B_T and V_T magnitudes derived from ground-based observations, appropriately transformed to magnitudes in the Tycho photometric system. These *a priori* values are considered of limited relevance for the Tycho Catalogue, and are not provided.

The magnitudes, colour indices and standard errors are given as obtained by computation from the individual photometric observations, thus accepting sometimes rather unreasonable results for faint stars. The following limitation of intervals has however been carried out in Fields T32–35, T37–38, and T45–46:

- for Fields T32–35: magnitudes fainter than 15.0 mag in B_T and V_T derived by de-censoring and their standard errors were replaced by blanks. If both B_T and V_T were then missing a V_T magnitude of 15.0 mag was adopted. The reason for this limitation is that the distribution of de-censored magnitudes fainter than 15.0 mag clearly indicated that these magnitudes were incorrect, probably arising from stellar variability or photon noise. Although highly uncertain, it was considered more appropriate to assign such a magnitude—in order to have been detected by Tycho the star must, at least during some interval, have been brighter than the detection limit of $V_T \simeq 12$ mag;
- for Field T37–38: the $B - V$ colour index has been omitted if the value was outside the interval $-2.0 < B - V < +5.0$ mag, leaving blanks in these fields;
- for Fields T45–46: magnitudes of the percentiles in Field T46 fainter than 15.0 mag were replaced by blank. This never happened in Field T45.

Fields T32–33: The B_T mean magnitude, $\langle B_T \rangle$, and standard error $\sigma^-_{B_T}$

The number of entries with standard errors of B_T in given ranges is as follows: < 0.1 = 681 190; 0.1 – 0.3 = 352 552; > 0.3 = 16 783. See also Fields T34–35.

Fields T34–35: The V_T mean magnitude, $\langle V_T \rangle$, and standard error $\sigma^-_{V_T}$

The number of entries with standard errors of V_T in given ranges is as follows: < 0.1 = 840 854; 0.1 – 0.3 = 206 435; > 0.3 = 4634.

The B_T and V_T magnitudes are considered to be very uncertain if Field T57 is not blank, especially if it contains 'M'. The choice of suitable photometric reference stars from the Tycho Catalogue for B_T and V_T will depend on the application, but should generally require that Field T36 = 'M' or 'N', and Fields T2 = T47 = T48 = T57 = ␣, and Field T49 is not 'D' or 'S'. Additional criteria on σ_{B_T} and σ_{V_T} may be defined by the user. If this latter requirement is $\sigma < 0.1$ mag, for example, a total of 520 631 Tycho photometric reference stars are available for calibration of photographic survey plates.

Field T36: Source of photometric data

The source flag has the following meaning:

D : approximate B_T, V_T magnitudes obtained during astrometric processing of resolved double stars, based on photometric signal amplitudes; no percentiles are given;

M : the B_T, V_T data are median values, rather than de-censored mean values (mainly relevant for bright stars with $B_T \leq 8.5$ mag and $V_T \leq 8.0$ mag);

N : the B_T, V_T data are de-censored mean values derived from the de-censoring analysis from the (normal) photometric processing for faint stars;

T : an approximate magnitude is given in Field T34 for V_T, and Field T32 for B_T is blank. The magnitude estimate was obtained from a combination of B_T and V_T observations during the Tycho Input Catalogue Revision (see Field T43) or the astrometric processing. These magnitudes are systematically too bright, by up to 1 mag for stars of $T = 11$ mag, and epoch photometry or percentiles can sometimes not be given. In these cases, the V magnitude given in Field T5 and flagged in Field T7 is simply this approximate V_T magnitude;

␣ : the Hipparcos stars (Field T42 = 'H').

The number of entries in each of these categories is as follows: D = 3314; M = 29 524; N = 1 017 860; T = 1333; ␣ = 6301.

Fields T37–38: The $B - V$ colour index, and standard error

These values give an indication of the Johnson $B - V$ colour index and standard error. The value of $B - V$ is derived strictly from Fields T32 and T34 if both these fields are non-blank (i.e. from $B_T - V_T = \langle B_T \rangle - \langle V_T \rangle$) according to the transformations given in Section 1.3, Appendix 4. If either B_T or V_T are not available, then the field is blank.

Unlike the case for the Hipparcos Catalogue, the colour index in Field T37 is never derived from ground-based data. In those cases where Field H37 contains a better estimate of $B - V$ than that derived from the Tycho data, Fields H37 and T37 will therefore be different. These two fields may also differ because effects of luminosity and reddening have been taken into account in constructing Field H37, but not in Field T37. Because of these limitations, the $B - V$ colour index given in the Tycho Catalogue is therefore only indicative; it is consequently recommended to make use, wherever possible, of the directly observed index $B_T - V_T$ (and correspondingly to use V_T rather than the V magnitude given in Field T5). Standard errors in $B - V$ and $B_T - V_T$ are related approximately by $\sigma_{(B-V)} \simeq 0.85\,\sigma_{(B-V)_T}$ (see Section 1.3.6).

The number of entries with standard errors of $B - V$ in given ranges is as follows: < 0.1 = 592 918; 0.1 – 0.3 = 423 105; > 0.3 = 33 556; ␣ = 8753. The number of entries with standard errors of $B_T - V_T$ in given ranges is as follows: < 0.1 = 504 132; 0.1 – 0.3 = 485 910; > 0.3 = 59 537; ␣ = 8753.

Field T39: blank for Tycho

Tycho-Specific Fields

Fields H40–70 of the Hipparcos Catalogue (which contain certain colour indices, variability data, multiplicity data, and certain flags), are not relevant to the Tycho Catalogue. Fields T40–57 are used for Tycho specific parameters, other flags, and cross-identifications.

Fields T40–42: Astrometry Related

Field T40: Astrometric quality flag, Q

The astrometric quality is defined for the Tycho data according to the following table, where N gives the number of stars in the Tycho Catalogue of each quality class, Q:

Q	$\sigma_{\rm max}$ (mas)	F_S	$\sigma_{\rm obsf}$ (mas)	N	$\sigma_{\rm med}$ (mas)	Astrometric quality
1	< 5	> 5	< 300	23147	2.6	very high
2	$5 - 10$	> 5	< 300	70945	5.5	very high
3	$10 - 25$	> 5	< 300	259695	13	high
4	$25 - 50$	> 5	< 300	430182	26	high
5	$50 - 150$	> 5	< 300	146520	39	medium
6	< 150	> 5	≥ 300	41695	44	perhaps non-single
7	< 150	$3 - 5$	< 300	37821	45	low
8	< 150	$3 - 5$	≥ 300	28949	54	perhaps non-stellar
9	$\equiv 200$	–	–	13077	–	low, ‘R’ in Field T42
␣	–	–	–	6301	–	unassigned, ‘H’ in Field T42
any	–	–	–	1058332	25	all entries

$\sigma_{\rm max}$ is the largest of the five astrometric standard errors for a given star; F_S is the signal-to-noise ratio given in Field T41; $\sigma_{\rm obsf}$ is the formal standard error of the single observation, being a measure of the half-width of the observed star image: $\sigma^2_{\rm obsf} = 0.25(\sigma_x^2 + \sigma_y^2)(N_{\rm astrom} - 5)$, where σ_x and σ_y are the standard errors of the two position components; and $\sigma_{\rm med}$ gives the median standard error of a position coordinate at the catalogue epoch J1991.25 (the errors at the mean epoch of observation of any given star are typically about 5 per cent smaller).

Objects with $Q \leq 8$ in the Tycho Catalogue all have $F_S > 3$, $\sigma_{\rm max} < 150$ mas, $\sigma_{\rm obsf} < 450$ mas, and $N_{\rm astrom} > 30$ (excluding objects for which $N_{\rm astrom} \leq 30$ only has the effect of excluding less than 100 stars of low quality, because the F_S limit is the strongest criterion). Objects with $Q = 9$ have lower astrometric quality, and are included for the sake of their photometric data—these objects are flagged by ‘R’ in Field T42. The goodness-of-fit parameter (Field T30) did not provide additional useful information in defining the astrometric quality. The last line in the table shows that 6301 entries have ‘H’ in Field T42, showing that they are contained in the Hipparcos Catalogue, but were not observed by Tycho.

Field T41: Signal-to-noise ratio of the star image, F_s

This is defined as $F_s = (n_1 - n_2)/\sqrt{n_1 + n_2}$, where n_1 is the number of detections within 0.7 arcsec along scan from the mean position, and n_2 is the number of detections between 0.7 and 1.4 arcsec (which provides a measure of the rate of background detections). In the special but rather common case of a sharp image on a negligible background, $n_1 \sim N_{\rm astrom}$, $n_2 \sim 0$ and $F_s \sim \sqrt{N_{\rm astrom}}$. The field is blank for stars flagged as 'R' in Field T42.

Field T42: Source of astrometric and other data

For the majority of Tycho entries this field is blank, indicating that the astrometric data is derived from the standard data processing. Otherwise, this field has the following meaning:

H : for the Hipparcos stars not observed by Tycho (i.e. a few bright stars, some stars in double and multiple systems, and in clusters and other dense fields, and faint Hipparcos stars below the observability limit of Tycho), this flag indicates that a GSC-type identifier has been created for Field T1, with the astrometric and photometric descriptor, taken from the Hipparcos Catalogue (Fields H3–5, and H8–9), inserted in Fields T3–5, and T8–9: no magnitude is, however, given in Field T5 for Hipparcos components from Part C of the Double and Multiple Systems Annex. The HIP number and the CCDM component identifier are inserted in Fields T31 and T51 respectively;

P : only the position was determined, either because the entry is a component of a double star resolved in Tycho astrometric analysis of suspected doubles, or because incomplete information was acquired for the entry. In these cases, Fields T11–13, and T16–28 are blank;

R : indicates that only an approximate position (with an accuracy of about ±200 mas) derived from the Tycho Input Catalogue Revision is given, because many transits were flagged as potentially disturbed by a parasite (see the introductory remarks to this section). Nevertheless, many of the transits were still considered to have yielded useful photometric information, and they are therefore included in the Tycho Epoch Photometry Annex. The astrometric quality of such an entry (Field T40) is given by $Q = 9$, and Fields T11–13, T16–30, and T41 are blank.

The number of entries in each of these categories is as follows: H = 6301; P = 3509; R = 13 077.

Fields T43–50: Photometry Related

Field T43: The number of transits used in Tycho mean photometry, $N_{\rm photom}$

This number is discussed in the introduction to this section. In the case of median magnitudes, i.e. flag 'M' in Field T36, this is the number of photometrically valid transits, including all detections, even those affected by parasites, but excluding the non-detections. In case of de-censored mean magnitudes, i.e. flag 'N' in Field T36, this is the number of photometrically valid transits, including the non-detections and the detections not affected by parasites. In case of 'D' or 'T' in Field T36 the number is equal to $N_{\rm astrom}$, except for magnitudes from the Tycho Input Catalogue Revision where the field has been set blank.

Field T44: V_T scatter, s

An estimate of the scatter for the Hipparcos Hp photometric data (Field H46) is given by $s = \frac{1}{2}[x(0.85) - x(0.15)]$ (see Section 1.3, Appendix 1). The same definition of the scatter is used for stars with median magnitudes ('M' in Field T36).

For the fainter Tycho observations with de-censored mean magnitudes ('N' in Field T36) where the 85th (fainter) percentile may be undetermined, the scatter in V_T has been defined by $s = V_T(0.50) - V_T(0.15)$, where $V_T(0.50)$ is the de-censored median and $V_T(0.15)$ is the 15th (brighter) percentile. This definition is similar to that used for the Hipparcos main mission photometry.

For Fields T44–46, non-detected transits are accounted for in the de-censoring analysis on the assumption that the star is not variable.

Field T45: V_T magnitude at maximum luminosity

This is given by the 15th percentile of the $N_{\rm photom}$ transits. This quantity is given for entries with 'M' or 'N' in Field T36.

Note that the 5th percentile (rather than the 15th percentile) is given in the Hipparcos Catalogue for the corresponding Hp magnitude at maximum luminosity.

Field T46: V_T magnitude at minimum luminosity

This is given by the 85th percentile of the $N_{\rm photom}$ transits. This quantity is given for entries with 'M' or 'N' in Field T36, except for the faintest stars. The field is blank for about 150 000 stars for which Field T45 is given.

Note that the 95th percentile (rather than the 85th percentile) is given in the Hipparcos Catalogue for the corresponding Hp magnitude at minimum luminosity.

Field T47: Previously known or suspected as variable

The flag indicates that the star is, according to SIMBAD, listed in either the GCVS or the NSV as follows:

G : GCVS, General Catalogue of Variable Stars, 4th edition (P.N. Kholopov *et al.*, Publ. Office 'Nauka', Moscow, 1985–88);

N : NSV, New Catalogue of Suspected Variable Stars (P.N. Kholopov, *et al.*, Publ. Office 'Nauka', Moscow, 1982).

This field has been constructed using the data available from CDS (SIMBAD) as of April 1996.

The astrometric quality of the GCVS and NSV Catalogues is generally rather poor, and the assignment of the flag must therefore be interpreted with appropriate caution. [For example, after completion of the Tycho Catalogue, it was noted that for the variable GQ Ori, TYC 734–1163-1 rather than TYC 734–627–1 had been assigned flag 'G'; the same error is present in the Hipparcos Input Catalogue for HIC 29386.]

The number of entries in each of these categories is as follows: G = 4068; N = 2624.

Field T48: Flag indicating variability of the Tycho measurements

The flag has the following meaning:

U : apparent variability in the Tycho data; this may be due to duplicity, and the flag is only set if an indication of duplicity was also found, i.e. Field T49 = 'R' or 'S';

V : strong evidence of variability in the Tycho data; no correlation with position angle was evident, suggesting that the variability is intrinsic and not an apparent effect due to duplicity;

W : variability suspected in the Tycho data; this may be due to intrinsic variability since no correlation with position angle was evident. But no thorough investigation has been carried out to eliminate other reasons intrinsic to the Tycho measurements.

The number of entries in each of these categories is as follows: U = 15 795; V = 13 994; W = 75 730.

Tycho photometry has not yet been thoroughly used to investigate intrinsic stellar variability. The brightest 384 000 stars have been investigated to find stars having standard errors of the median magnitude exceeding those expected for constant stars with the same number of transits and the same magnitude (see Volume 4). Flags 'V' and 'W' can therefore only be used as an indication of an unexpectedly large scatter of the measurements, and do not necessarily mean that the object is intrinsically variable. The scatter may also be due to duplicity (see below) and disturbances by faint (undetected) stars crossing the star mapper slits at the same time as the Tycho star.

Correspondingly, the proportion of stars flagged 'V' and 'W' is larger in dense regions of the sky. On the other hand for a star satisfying the conditions $V_T \leq 9.5$ mag and $N_{\mathrm{photom}} \geq 80$ a 'blank' may be taken as an indication that the star was constant during the period of the Tycho observations.

A comparison with results from Hipparcos photometry indicates that the classification 'V' is mostly correct for stars brighter than $V_T \simeq 9.0$ mag, while for most stars fainter than $V_T \simeq 9.8$ mag 'V' may be a misleading indicator of variability.

Since duplicity may mimic variability in the Tycho observations, it is not always straightforward to disentangle these effects (see also Field T49). Investigations on variability and duplicity are separate processes, but the resulting lists of candidate variables or doubles do have a lot of stars in common. Stars have therefore been flagged as follows: if a star was found to be clearly double (Field T49 = 'D') then any suspected variability has been assumed to be caused by this duplicity, and thus Field T48 has been set to '␣' (blank).

Field T48 = 'U' was introduced to reflect those cases where it was not possible to decide between variability and duplicity. If a star was found to be a suspected double star (Field T49 = 'S') then Field T48 is set to 'U'. If a star was found to have an indication of variability and also a weak indication of duplicity, lower than the limit corresponding to Field T49 = 'S', Field T49 was set to 'R' and Field T48 was set to 'U'.

Field T49: Flag indicating unresolved duplicity status from Tycho data analysis

The flag has the following meaning:

D : duplicity (unresolved) was clearly indicated in about 8400 stars by Tycho data analysis (the published Tycho mean photometry is for the combined light, except for the astrometrically resolved components with Field T36 = 'D');

R : weak indication of duplicity, combined with indication of variability. This was found for some 11 500 stars which are then also flagged with Field T48 = 'U';

S : suspected duplicity from Tycho data analysis, although this duplicity cannot be regarded as certain. About 11 600 stars are assigned this flag, and 4500 of these also have Field T48 = 'U';

Y : an investigation was carried out on the Tycho data, but no indication of duplicity was found for about 450 000 stars;

Z : no investigation for duplicity was carried out on the Tycho data for about 570 000 stars mainly with $V_T > 10.5$ mag;

␣ : the Hipparcos stars (Field T42 = 'H').

The number of entries in each of these categories is as follows: D = 8441; R = 11 523; S = 11 639; Y = 449 209; Z = 571 219; ␣ = 6301.

Whenever an object observed by Tycho was clearly resolved into two stars, these were separated into two distinct catalogue entries, and the two stars assigned TYC1–3 designations as described under Field T1. Generally this was feasible for separations down to about 2 arcsec. However, it is also possible to detect doubles at smaller separations, down to about 0.8 arcsec (for bright stars even down to 0.6 arcsec). Such (unresolved) duplicity causes a perturbation (broadening) of the light curve produced by a transit of the object through the Tycho slits. A search for such perturbations was carried out in the Tycho data by two different methods, as described in Volume 4, Chapter 14. Field T49 represents the result of this search.

One of the methods was to search for a significant correlation between the estimated magnitude of the transit and the position angle of the measuring slit. This method was applied to about 510 000 stars with $V_T \leq 10.5$ mag. The other method was applied to the raw photon counts, and attempted to resolve the perturbed single peak into two peaks for every observation of a star. This method was applied to about 22 000 stars. The application of the two methods resulted in the flagging of about 20 000 stars with 'D' or 'S'.

Field T50: Flag indicating availability of epoch photometry for this object

The flag has the following meaning:

␣ : a blank field indicates that epoch photometry is not provided;

A : epoch photometry is given for these stars in the machine-readable Tycho Epoch Photometry Annex A, as made available on the ASCII CD-ROMs;

B : epoch photometry is not given in the Annex A but is given in a machine-readable data set, Annex B, made available at CDS, Strasbourg, containing also the stars from the Annex A.

The number of entries in each of these categories is as follows: A = 34 446; B = 447 107.

Tycho Epoch Photometry Annex B includes objects flagged 'A' as well as those flagged 'B', and therefore contains 34 446 + 447 107 = 481 553 entries.

Fields T51–57: Cross-identifications and Notes

In addition to the cross-identification to HIP/HIC (Field T31), the PPM, HD, and DM (BD, CoD, and CPD) identifiers are included.

These have been derived as a result of cross-identifications using the SIMBAD facility of the CDS, supplemented in the southern sky by direct use of the PPM Catalogue. As of April 1996, about half of the DM stars were not included in SIMBAD. A given DM identifier may be associated with more than one TYC entry because of the low accuracy of the DM positions. The cross-identification with the Hipparcos Catalogue identifier (HIP), combined with the component identifier if any, is unique, with the identity having been accepted if the TYC entry has a position within 1.0 arcsec of the Hipparcos Catalogue component at the epoch J1991.25. In 57 cases, however, a distance up to 2.0 arcsec was accepted when the identity appeared to be unambiguous and the position given by either catalogue was believed to be particularly uncertain. However, the astrometric quality of the HD and DM catalogues in particular is generally rather poor, and the resulting cross-identifications are therefore not always fully reliable or consistent.

For all other cross-identifications, the user is referred to the 'star names resolving facility' of SIMBAD, where the Tycho Catalogue identifier is included. Implicitly, the cross-identification to the variable star catalogues GCVS and NSV are given by the flag indicating known or suspected variability (see Field T47). The GCVS name and NSV number are specifically included in the *Celestia 2000* interrogation package, along with SAO Catalogue and HR Catalogue numbers and names of bright stars.

For HIP entries, reliability tests were performed, during the construction of the Hipparcos Input Catalogue, to check the coherence between the zones of the DM (BD, CoD, and CPD) numbers and the declination at the epoch of the catalogue (1855 for BD, 1875 for CoD and CPD), and also to check that the numbers increased with increasing right ascension at the epoch of the catalogue. Resulting corrections (from typing errors in the numbers or in the coordinates, originating from the source catalogue themselves or from an intermediate transcription, or confusion between the CoD and CPD identifiers) have been included.

Field T51: CCDM component identifier

The HIP number alone may be insufficient to identify uniquely the object in the Hipparcos Catalogue (if any) corresponding to the relevant Tycho Catalogue entry. This happens when the HIP entry has been resolved into two or more components, as listed in Part C of the Hipparcos Double and Multiple Systems Annex. These components are however uniquely identified by the HIP number combined with the component identifier in Field DC7 of the Double and Multiple Systems Annex. For such objects, Field T51 thus contains the CCDM component identifier taken from Field DC7.

There are 18 687 such entries in the Tycho Catalogue. The component identifier is normally a single letter: thus 'A' means that the TYC entry corresponds to the 'A' component of the HIP entry specified in Field T31. However, in about 6000 cases where two components of the Annex appear to correspond to one Tycho Catalogue entry, the two values from Field DC7 are combined, e.g. to 'AB'. In only three cases, indicated by 'TT', there were three components: ABC. Note that the components are given in lexical order (cf. Field H62 where, for example, 'AB' and 'BA' both occur).

The component identifiers originate from the CCDM catalogue (see Section 1.4), and therefore in principle refer to the systems identified by their CCDM numbers—which are not given in TYC. Such a system may have more than one HIP number, if the components are well separated, but a given HIP number can only have one CCDM number (given in Field H55 of the Hipparcos Catalogue). Consequently the HIP number plus the CCDM component identifier uniquely specifies a component.

Field T52: PPM identifier

The PPM (Catalogue of Positions and Proper Motions, U. Bastian & S. Röser 1994) is the largest source to date for high-precision proper motions, containing a very significant fraction (about 42 per cent) of the Tycho Catalogue stars.

Cross-identification was relatively straightforward, because of the positional precision of both the Tycho Catalogue and the PPM. Identity was accepted for stars in PPM with positions at J1991.25 having the closest TYC star within 2.5 arcsec separation in both coordinates. In the cases of 1700 single PPM stars, however, there were two TYC stars in this window, but none of them were accepted since the purpose was to give only reliable PPM proper motions. About 4600 of these 447 097 PPM proper motions disagreed significantly with the Tycho proper motion (as flagged by 'L' in Field T57).

The *Celestia 2000* interrogation package includes the PPM proper motions, which are, for a significant fraction of the Tycho stars, more precise than the Tycho proper motions. However, because of possible systematic and regional errors, and to retain the purely observational nature of the Hipparcos and Tycho Catalogues, the PPM proper motions are not included within the main mission data products.

Field T53: HD/HDE/HDEC identifier

Cross-identifications are given to 252 457 stars in the HD Catalogue, with numbers in the range 1 – 225 300 (A.J. Cannon & E.C. Pickering 1918–24, *Ann. Harvard Obs.*, 91–99), and its two extensions: HDE numbers in the range 225 301 – 272 150 (A.J. Cannon 1925–36, *Ann. Harvard Obs.*, 100), and HDEC numbers in the range 272 151 – 359 083 (A.J. Cannon & M. Walton Mayall 1949, *Ann. Harvard Obs.*, 112).

The number of cross-identifications in each of these categories is as follows: HD = 211732; HDE = 16540; HDEC = 24185.

Field T54: DM identifier (BD)

This field gives the DM identifier for 244 470 objects contained within the Bonner Durchmusterung (BD), with the format B±ZZ␣NNNNa (coded with leading zeros in ZZ where appropriate). Note that BD identifiers, unlike the CoD and CPD identifiers (Fields T55–56), may carry a lower-case suffix letter for additional stars, i.e. stars with suffix 'a', 'b', 'n', 'p' or 's': these stars were added to the BD Catalogue after the original numbering was made; such suffixes do not imply that the entry is a component of a double or multiple system (the suffixes 'b' and 'n' occur very seldom).

Field T55: DM identifier (CoD)

This field gives the DM identifier for 134 898 objects contained within the Cordoba Durchmusterung (CoD), with the format C±ZZ␣NNNNN.

Field T56: DM identifier (CPD)

This field gives the DM identifier for 154 604 objects contained within the Cape Durchmusterung (CPD), with the format P±ZZ␣NNNNN.

Field T57: Notes on dubious entries

If non-blank, this field has the following meaning (in decreasing sequence of priority):

J : disagreement with position or magnitude given in the Guide Star Catalog (GSC Version 1.1): in about 8000 cases the positions differ by more than 5 arcsec or 3σ, or the magnitudes differ by more than 1.5 mag. The B_T magnitude was used for the comparison if the GSC magnitude was derived from a blue plate, and the V_T magnitude in case of a visual plate. Tycho proper motions were used in the comparison of positions. Such flagged entries may be double stars, stars with extreme colours, galaxies, or planetary nebulae. However many are quite normal stars having erroneous positions, proper motions or magnitudes in the Tycho Catalogue or in the Guide Star Catalog;

K : dubious Tycho parallax: either (1) the parallax is significantly negative, less than $-4\sigma_\pi$; or (2) the difference, $|\Delta\pi|$, between the parallaxes from Hipparcos and Tycho is larger than $4\sigma_{\Delta\pi}$; or (3) a non-Hipparcos star has a Tycho parallax $> 40 + 4\sigma_\pi$ mas, which will in only very few cases be a real nearby star since nearly all nearby stars with parallaxes > 40 mas are Hipparcos stars;

L : dubious Tycho proper motion: a Tycho proper motion component, $\mu_\alpha \cos\delta$ or μ_δ, deviates $> 4\sigma_{\Delta\mu_{\rm comp}}$ from the PPM proper motion;

M : Tycho magnitude very uncertain: a subset of about 20 000 stars have a standard error larger than 0.3 mag in either B_T or V_T, or either of these magnitudes are missing. This may indicate variability, or may be due to an extreme colour index or to special observational circumstances, or the star may be very faint (see further details of the magnitudes described in the introduction to Fields T32–39).

Each of the astrometric criteria 'K' and 'L' identifies about 0.5 per cent of the catalogue entries as having large residuals, $> 4\sigma$. This is considered to be an acceptably small number of large residuals in astrometric observational data, since the tails of the distributions of such data rarely follow an ideal Gaussian distribution (for which a corresponding fraction of outliers of only 0.006 per cent would be predicted).

Under item 'K', condition (3) includes entries with large parallaxes not contained in the Hipparcos Catalogue, and is derived simply on the assumption that all such nearby objects are already contained within the Hipparcos Catalogue—an extreme, and presumably incorrect, assumption. The number of non-Hipparcos stars with Tycho Catalogue parallaxes larger than $40 + 4\sigma_\pi$ mas is 1245. This tail on the parallax error distribution will result in a number of erroneously large parallaxes—appropriate care will be required in using the Tycho parallaxes, together with other supplementary data, in the search for stars with real large parallaxes.

The number of entries in each of these categories is as follows: J = 7925; K = 5555; L = 4446; M = 18 791; total = 36 717. The number of entries corresponding to each of the criteria individually is as follows: J = 7925; K = 5763; L = 4653; M = 20 688. Thus the categories of stars satisfying the three first mainly astrometric criteria have little overlap. About 1400 stars satisfying 'J' would also satisfy 'M'.

Table 2.2.1. Summary of the machine-readable Tycho Catalogue format
(a) fields in common with the Hipparcos Catalogue

Field	Bytes	Format	Description
H0/T0	1–2	A1,X	Catalogue (H = Hipparcos, T = Tycho)
H1	3–15	6X,I6,X	Identifier (HIP number)
T1	„	I4,I6,I2,X	TYC1–3 (TYC number)
H2/T2	16–17	A1,X	Proximity flag
H3/T3	18–29	A11,X	Identifier RA, h m s (J1991.25)
H4/T4	30-41	A11,X	Identifier Dec, ± ° ′ ″ (J1991.25)
H5/T5	42–47	F5.2,X	V (Johnson) magnitude
H6	48–49	A1,X	Coarse variability flag
T6	„	1X,X	Blank for Tycho
H7/T7	50–51	A1,X	Source of magnitude identifier
H8/T8	52–64	F12.8,X	α, degrees (J1991.25)
H9/T9	65–77	F12.8,X	δ, degrees (J1991.25)
H10/T10	78–79	A1,X	Reference flag for astrometry
H11/T11	80–87	F7.2†,X	Trigonometric parallax (mas)
H12/T12	88–96	F8.2†,X	$\mu_{\alpha*} = \mu_\alpha \cos\delta$ (mas/yr)
H13/T13	97–105	F8.2†,X	μ_δ (mas/yr)
H14/T14	106–112	F6.2†,X	Standard error in $\alpha*$ at J1991.25 (mas)
H15/T15	113–119	F6.2†,X	Standard error in δ at J1991.25 (mas)
H16/T16	120–126	F6.2†,X	Standard error in π (mas)
H17/T17	127–133	F6.2†,X	Standard error in $\mu_{\alpha*}$ (mas/yr)
H18/T18	134–140	F6.2†,X	Standard error in μ_δ (mas/yr)
H19/T19	141–146	F5.2,X	Correlation, $\rho^{\delta}_{\alpha*}$
H20/T20	147–152	F5.2,X	Correlation, $\rho^{\pi}_{\alpha*}$
H21/T21	153–158	F5.2,X	Correlation, ρ^{π}_{δ}
H22/T22	159–164	F5.2,X	Correlation, $\rho^{\mu_{\alpha*}}_{\alpha*}$
H23/T23	165–170	F5.2,X	Correlation, $\rho^{\mu_{\alpha*}}_{\delta}$
H24/T24	171–176	F5.2,X	Correlation, $\rho^{\mu_{\alpha*}}_{\pi}$
H25/T25	177–182	F5.2,X	Correlation, $\rho^{\mu_{\delta}}_{\alpha*}$
H26/T26	183–188	F5.2,X	Correlation, $\rho^{\mu_{\delta}}_{\delta}$
H27/T27	189–194	F5.2,X	Correlation, $\rho^{\mu_{\delta}}_{\pi}$
H28/T28	195–200	F5.2,X	Correlation, $\rho^{\mu_{\delta}}_{\mu_{\alpha*}}$
H29	201–204	I3,X	Data points rejected (per cent)
T29	„	I3,X	Data points accepted, $N_{\rm astrom}$
H30/T30	205–210	F5.2,X	F2 (goodness-of-fit)
H31/T31	211-217	I6,X	HIP number
H32/T32	218–224	F6.3,X	B_T (mag)
H33/T33	225–230	F5.3,X	σ_{B_T} (mag)
H34/T34	231–237	F6.3,X	V_T (mag)
H35/T35	238–243	F5.3,X	σ_{V_T} (mag)
H36/T36	244–245	A1,X	Reference flag for B_T and V_T
H37/T37	246–252	F6.3,X	$B-V$ (mag)
H38/T38	253–258	F5.3,X	σ_{B-V} (mag)
H39	259–260	A1,X	Source of $B-V$
T39	„	1X,X	Blank for Tycho

† For these fields, the second decimal digit for the Tycho format is always blank

The Hipparcos and Tycho Catalogues are similar up to Field H39/T39; thereafter, the fields and their meanings are catalogue specific. Thus Tables 2.1.1(a) and 2.2.1(a) are identical. Due care must be taken in ensuring that blank fields are not interpreted as numerically zero.

Table 2.2.1. Summary of the machine-readable Tycho Catalogue format (cont.)
(b) Tycho specific catalogue data

Field	Bytes	Format	Description
T40	261–262	I1,X	Astrometric quality flag, Q
T41	263–267	F4.1,X	S/N ratio, F_S
T42	268–269	A1,X	Source of astrometric data
T43	270–273	I3,X	$N_{\rm photom}$
T44	274–279	F5.3,X	V_T scatter, s (mag)
T45	280–285	F5.2,X	Mag at max, V_T (15th percentile)
T46	286–291	F5.2,X	Mag at min, V_T (85th percentile)
T47	292–293	A1,X	Variability (from GCVS/NSV)
T48	294–295	A1,X	Variability (from Tycho)
T49	296–297	A1,X	Duplicity (from Tycho)
T50	298–299	A1,X	Flag (epoch data)
T51	300–302	A2,X	CCDM component identifier
T52	303–309	I6,X	PPM identifier
T53	310–316	I6,X	HD identifier
T54	317–327	A10,X	DM (BD) identifier
T55	328–338	A10,X	DM (CoD) identifier
T56	339–349	A10,X	DM (CPD) identifier
T57	350	A1	Notes

Section 2.3

Hipparcos Catalogue: Double and Multiple Systems Annex

2.3. Hipparcos Catalogue: Double and Multiple Systems Annex (DMSA)

2.3.1. Overview of the DMSA

The main Hipparcos Catalogue (Volumes 5–9) contains the principal astrometric and photometric results on all stellar objects observed with the satellite. For the majority of apparently single objects this adequately summarises the Hipparcos observations in terms of the standard astrometric single-star model, represented by the five parameters α, δ, π, $\mu_{\alpha*}$, μ_δ (see Section 1.2.8).

For a number of double and multiple stars the single-star model was not sufficient to represent the observations to within their intrinsic uncertainties, and more complex models, involving additional parameters, had to be used. The complementary information derived from these solutions are given in Volume 10 of the Hipparcos Catalogue, containing the Double and Multiple Systems Annex (DMSA).

The models (or solutions) used for the manifestly or suspected non-single stars are of five different kinds. Accordingly, the DMSA is divided into the five parts:

DMSA/C: Component solutions
DMSA/G: Acceleration solutions
DMSA/O: Orbital solutions
DMSA/V: 'VIM' (variability-induced movers) solutions
DMSA/X: Stochastic solutions

The various models are briefly explained below, and in some detail in the following sections. In the printed catalogue, the fields (or columns) are identified by numbers shown in the column header on every page. To avoid confusion between the different parts of the DMSA these fields are normally referenced by letters DC, DG, DO, DV and DX followed by the number in the column header.

Component Solutions: The component solutions in DMSA/C comprise resolved systems in which the individual components were modelled similarly to the single stars, using, for each component, five astrometric parameters and a magnitude. Clearly this applies to 'optical' double stars, but also to long-period binary and multiple systems, where the configuration of components remains approximately fixed over the observing interval, or where the relative motions can be represented as linear functions of time (i.e. by assigning different absolute proper motions to the different components). The layout of this information in the printed DMSA/C mirrors the corresponding columns of the main catalogue, except that the data are given for each component.

Acceleration Solutions: DMSA/G lists apparently single (unresolved) stars, for which the motion appears to be significantly non-linear. They are probably 'astrometric binaries': either too close to be resolved ($\varrho \lesssim 0.1$ arcsec), or with a companion too faint to be seen by Hipparcos. If an orbital solution can be obtained, usually with the help

of ground-based data, then the result is given in DMSA/O. In DMSA/G only those (long-period) astrometric binaries are included for which the motion of the photocentre, as observed by Hipparcos, could be adequately described by quadratic or cubic polynomials in time. DMSA/G contains the non-linear terms of their motions. (The 'G', as well as the designations g and $\dot{g}$ chosen for the acceleration terms, derive from the word 'gravity'.)

Orbital Solutions: DMSA/O contains results for orbital binaries where the Hipparcos observations could be used to determine some or all of the elements of the *absolute* Keplerian orbit of the system's photocentre. These solutions often involve ground-based data for the determination of certain orbital elements (such as the period), and the sometimes complex interdependence of space and ground-based data cannot easily be specified in compact form. Therefore, only the main results of the orbital solutions are given in a simple tabular form, while detailed discussions of the individual systems will be published separately.

VIM Solutions: 'Variability-Induced Movers', or VIMs, are unresolved binaries in which one of the components is variable. The photocentre of such a system shows a specific motion on the sky, coupled to the system's total brightness variation. Specification of the variability-induced motion requires two additional parameters that can be determined together with the normal five astrometric parameters used for single stars. DMSA/V contains the additional parameters and reference data describing the VIMs.

Stochastic Solutions: DMSA/X finally lists the objects for which no solution of the previous types could be found in reasonable agreement with the standard errors of the Hipparcos observations. These objects could be double or multiple stars of unknown characteristics, or short-period astrometric binaries for which the displacement of the photocentre from the assumed linear motion of the centre of mass mimics a random scatter among the individual observations. In this case a stochastic model was adopted for the deviations from a linear motion, by postulating the presence of a non-zero physical scatter in excess of the measurement noise. DMSA/X lists the excess scatter or 'cosmic error' of these objects, the 'X' symbolising its unknown origin.

G, V and X type solutions are new classifications of astrometric phenomena, made possible by the specific observational capabilities of Hipparcos. In particular the high positional accuracy obtained in numerous individual observations spread over a relatively short time interval (few years) enables the detection of small deviations from the expected uniform motion of an apparently single star. Such deviations are most likely manifestations of the binary nature of the star, and as such belong in the DMSA of the Hipparcos Catalogue.

The relations between the astrometric parameters given in the main catalogue and the additional information in the G, O and V parts of the DMSA are further illustrated in Figures 2.3.1–3. In these, the motion according to the five astrometric parameters in the main catalogue is represented by the dashed line, while the solid curves describe the superposed non-linear motions of the photocentre as represented by the additional parameters in the DMSA.

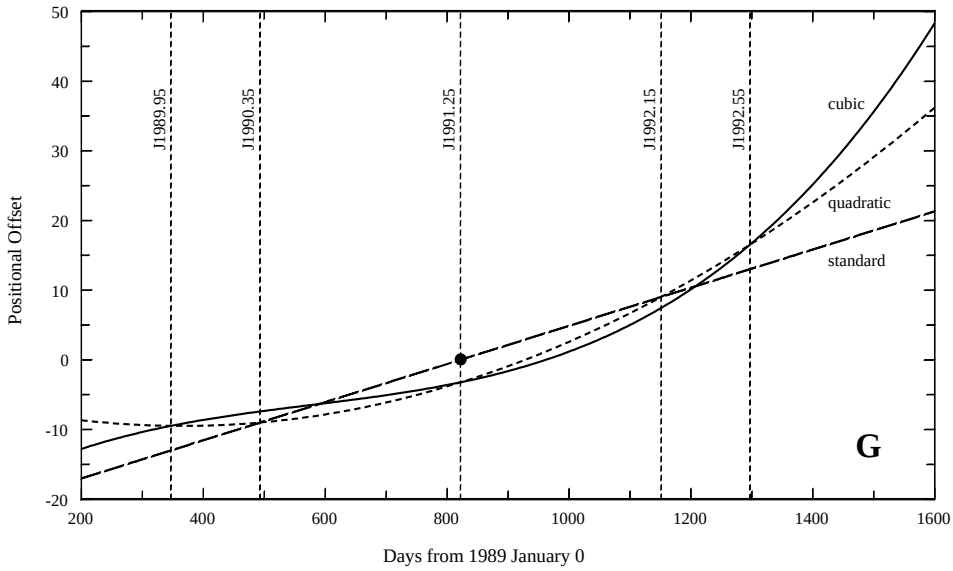

Figure 2.3.1. *Schematic representation of the barycentric position of the photocentre, as a function of time, in a 'G' type (acceleration) solution. The curves marked 'quadratic' and 'cubic' illustrate the positional offset in one coordinate (e.g. right ascension) for a solution including the g terms (quadratic), and g and $\dot{g}$ terms (cubic). The dashed line marked 'standard' represents the offset for the standard model (Section 1.2.8) using only the five astrometric parameters given in the main catalogue. The heavy dot, in particular, corresponds to the position at the catalogue epoch J1991.25 as given in Field H8 or H9 of the main catalogue, and the slope of the dashed line corresponds to the proper motion in Field H12 or H13. Note that these parameters approximately describe the mean motion over the mission interval, rather than the instantaneous motion at 1991.25. See Section 2.3.3 for the significance of the epochs J1989.95, J1990.35, J1992.15 and J1992.55.*

Combinations of the five models C, G, O, V and X could well be envisaged, but for reasons of logistics no overlap has been allowed between the five parts of the DMSA. A given HIP entry consequently occurs in at most one of them, as specified by the flag (C, G, O, V or X) in Field H59 of the main catalogue. An alternative interpretation of the object may nevertheless be indicated among the Notes. (The presence of a note is flagged in Field H70 of the main catalogue and in the corresponding field of the DMSA: DC6, DG12, DO17, DV12, or DX4.)

The decision as to which model to adopt for an object is made according to the following list of priorities:

1. Component solutions
2. Orbital solutions
3. VIM solutions
4. Acceleration solutions
5. Stochastic solutions
6. Single-star solutions
7. Invalid solutions (not retained in the published catalogue)

That is, a component solution, if significant and of acceptable quality, takes precedence over an orbital solution of the same HIP entry, etc. This particular order of priorities is

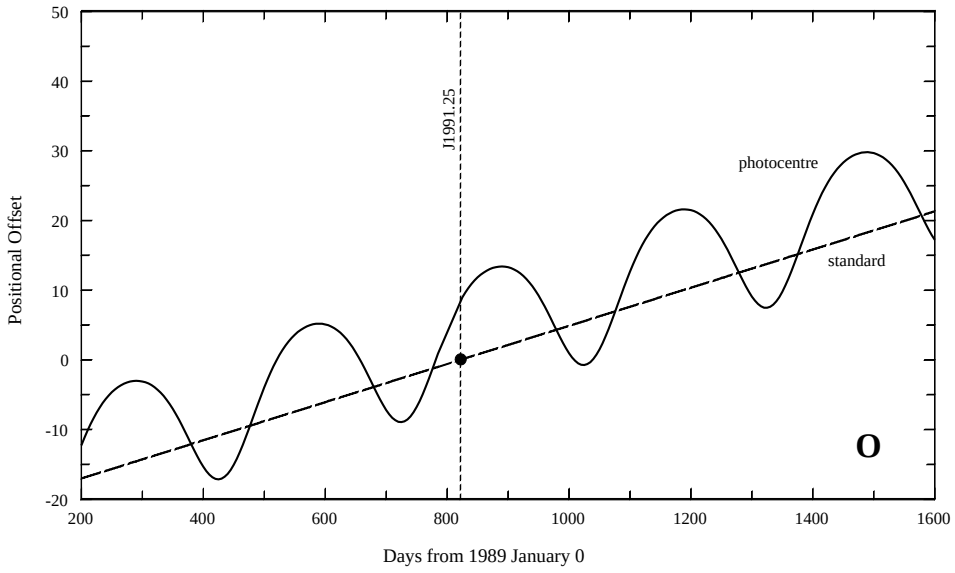

Figure 2.3.2. *This figure illustrates the motions of the photocentre (solid curve) and centre of mass (dashed line) in an 'O' type (orbital) solution. The main catalogue gives, in this case, the astrometric parameters for the centre of mass.*

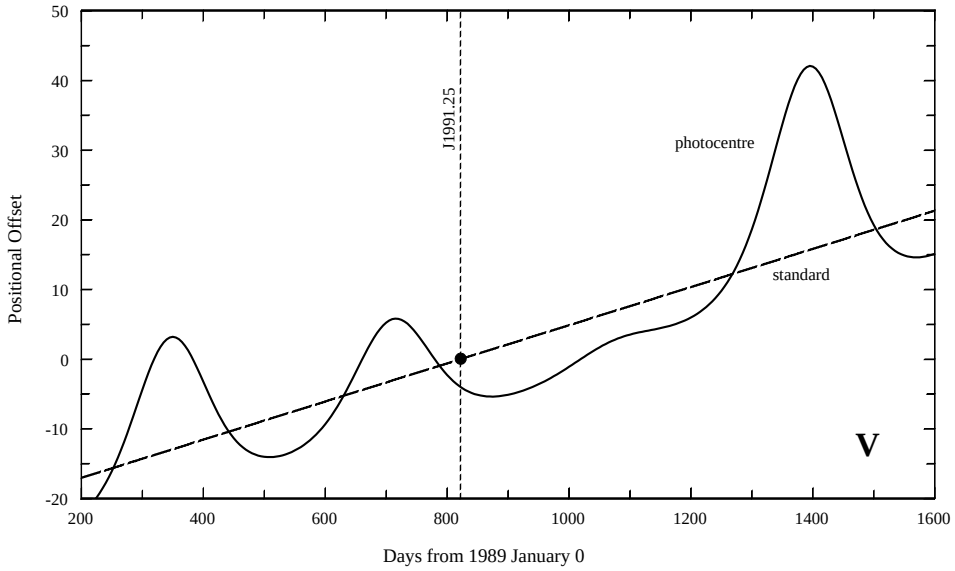

Figure 2.3.3. *For a 'Variability-Induced Mover' (VIM) the photocentre (solid curve) describes an oscillating motion between the binary components in phase with the variations of the total luminosity of the system. The dashed line, corresponding to the astrometric parameters in the main catalogue, gives the hypothetical motion of the photocentre, had the total magnitude been constant and equal to the reference magnitude in Field DV2.*

mainly based on practical considerations in the complex task of assembling the DMSA from several different processes; there is consequently no guarantee that the best solution was invariably selected for each object, although in general the classification was unproblematic. It should be noted however that the adopted criteria for accepting or rejecting a particular kind of solution are always to some extent arbitrary, and could greatly affect the number of objects in each category.

In practice, for the entries remaining after the resolved double and multiple stars (part C), orbital astrometric binaries (part O), and VIMs (part V) had been selected, the choice between the G solutions (7-parameter, g; or 9-parameter, $\dot{g}$) and X solutions was made as follows, depending on the rejection (outlier) rate F1 and the goodness-of-fit F2 (as described in further detail in subsequent sections):

– the 9-parameter solution was chosen if significant ($F_{\dot{g}} > 3.44$), if the goodness-of-fit F2 < 4, if F1 < 7 per cent, and if the 7-parameter solution would otherwise have been accepted (the resulting g terms may or may not be significant);

– the 7-parameter solution was chosen if significant ($F_g > 3.44$), if the goodness-of-fit F2 < 4, and if F1 < 7 per cent;

– the X solution was chosen if significant (cosmic error > 5σ) or if the 5-parameter solution would give F1 > 20 per cent; the X solution was however rejected if the associated cosmic error exceeded 100 mas;

– otherwise the 5-parameter solution was chosen.

For a few hundred stars no sensible solution could be found according to this scheme. In a stochastic solution they would have had an unphysically large cosmic error, while in a standard 5-parameter solution most of the observations would have been rejected. These are most likely strongly affected by unresolved grid-step errors, in which case neither solution would be useful. No astrometric data is provided for these objects.

Field H59 is the pointer from the main catalogue to the relevant part of the DMSA. The detailed information in parts G, O, V and X of the DMSA is given under the corresponding HIP number. In contrast, the data in DMSA/C are given according to the CCDM numbers (see Section 1.4.4) and component identifiers (a single letter). The reason for this is that the HIP number of systems in part C has no simple relation to the double and multiple systems or their components: a given HIP number may correspond to several components, while a given double or multiple system may contain components with different HIP numbers. The entry point to DMSA/C is thus provided by the CCDM identifier given in Field H55 of the main catalogue.

Although the DMSA (together with the main catalogue) provides the full details of the solutions for the non-single object models, the main astrometric and photometric parameters are always given in the main catalogue. These data must then be interpreted with some caution, as they are necessarily incomplete. For example, the position and proper motion given in the main catalogue may refer to a particular component of a resolved binary, to the photocentre or centre of mass of the system, or to the mean motion of the system over the Hipparcos mission. The flags in Fields H10 and H57–60 must be consulted to ensure proper interpretation of the main astrometric data; similarly Fields H36, H43 and H48 must be consulted for the main photometric data.

2.3.2. DMSA/C: Component Solutions

The Component Solutions part of the DMSA (DMSA/C) contains the Hipparcos results on double and multiple stars resolved into distinct components, whose motions can be described, to the precision of the observations, as linear functions of time. This latter condition is generally met for systems having orbital periods longer than several times the length of the observing interval (3.3 years), and applies to the majority of systems resolved by the Hipparcos instrument. General considerations related to the observation and classification of double and multiple systems are given in Section 1.4.

While all other parts of the Hipparcos Catalogue are organised according to the HIP numbers, the unique entry point to DMSA/C is the CCDM identifier of the double or multiple system. This choice was motivated by the fact that, in many cases, two or more different HIP entries had to be treated together in the double-star analysis (typically this applies to systems with a separation between 10 and 30 arcsec, and referred to as 'two-pointing' or 'three-pointing' systems). For a given CCDM number the different components are uniquely identified by letters (A, B, ...). A given component is always associated with a single HIP number, namely that under which it was observed by the Hipparcos satellite; the reverse relation is however not unique: several components (within a radius of up to 15–20 arcsec) may be associated with the same HIP number.

Each line in the printed DMSA/C corresponds to a single component, as seen by Hipparcos. The system and component identifiers are given in Fields DC1 and DC7, respectively, while the HIP number under which the component was observed is given in Field DC8.

While the system and component identifiers uniquely define each component under consideration, a further identifier is needed to specify which components were jointly considered in a solution for their astrometric and photometric parameters. Normally a double or multiple star solution may be confined to the components within a radius of approximately 30 arcsec from the main star of each HIP entry; more distant companions or field stars can usually be ignored. Since many systems in the CCDM catalogue are much larger than this, it may happen that two independent solutions (involving different sets of components) are made under the same CCDM number. The solution identifier 'S' in Field DC2 was introduced to distinguish between such solutions. It can be regarded as a division of the whole system (as defined by a single CCDM number) into subsystems suitable for the special double and multiple star reduction. A well-known example is the multiple system ϵ Lyr (CCDM 18443+3938), which in the Hipparcos reductions was treated as two independent double stars; in DMSA/C the results are listed under S = 1 for components A and B, and under S = 2 for C and D.

For the user's convenience certain *relative* astrometric information is added in relevant cases (Fields DC25–29): the position angle and separation of one component relative to another and the rate of change of these angles. These data are uniquely derived from the absolute astrometric information in the preceding fields and rounded according to their uncertainties. When an entry contains precisely two components, summary data (including position angle, separation and magnitude difference) are given in the main catalogue, Fields H62–67. Again, these are uniquely derived from the absolute data contained in DMSA/C.

The DMSA/C contains the results of 12 195 solutions, of which 12 005 are double star solutions, 182 triple star solutions, and 8 quadruple star solutions. The total number of

components, therefore, is $12\,005 \times 2 + 182 \times 3 + 8 \times 4 = 24\,588$; the number of different HIP entries concerned is 13 211.

The contents of the printed DMSA/C are described in detail below. Further details on the machine-readable version are given in Section 2.3.7, in particular Table 2.3.2.

Field DC1: System Identifier

Field DC1: CCDM number

The Catalogue of Components of Double and Multiple Stars (CCDM), described in Section 1.4.4, provides the principal cross-reference to information on double and multiple systems. In DMSA/C the CCDM number is used as the unique entry to the Hipparcos results on resolved components of double and multiple systems. For previously uncatalogued systems new CCDM identifiers were constructed according to the conventions of the CCDM Catalogue, and the newly-constructed identifiers have been included within the CCDM data base.

The CCDM identifier is based on the approximate equatorial coordinates of the system at epoch and equinox J2000.0, rounded to the nearest 0.1^{m} in α and 1 arcmin in δ (but taking into account other systems in order to guarantee the uniqueness of the identifier). System identifiers already included in the CCDM before the construction of the Hipparcos Catalogue have not been changed.

Fields DC2–6: Solution Details

Field DC2: Solution identifier, S

This field contains a digit (S = 1, 2, ...) identifying different solutions pertaining to the same CCDM number in Field DC1. More than one solution may occur if the system was split up into different parts (regions) subject to separate solutions. This field is related to the 'two-pointing' and 'three-pointing' systems (F, I, L, or P in Field H60) where components having more than one HIP identifier have the same CCDM number (Field DC1 and H55) and the same solution identifier.

The number of solutions for the system is given in the header record of the machine-readable DMSA/C as N_{S}. There are 12 157 systems with $N_{\mathrm{S}} = 1$, 19 with $N_{\mathrm{S}} = 2$ and none with $N_{\mathrm{S}} \geq 3$, resulting in $12\,157 + 2 \times 19 = 12\,195$ solutions in total.

Field DC3: Type of solution

This field provides a summary of the type of double or multiple star solution, and has the following meaning:

F : fixed double or multiple system: the components are assumed to have identical proper motions and parallaxes;
I : individual parallaxes and linear (relative) motion (possible optical double star);
L : linear double or multiple system: the components may have different proper motions, but curved motions are not considered, and the components are assumed to have the same parallax.

The following table summarises what the different solution types imply in terms of constraints and the total number of estimated parameters.

Summary of the properties of the various solution types in terms of constraints among the parallaxes and absolute proper motions of the different components of a system, and the total number of estimated parameters in the solution, including the magnitude of the component (N_P). N_C is the number of components.

Solution Type	Constraints	Number of Parameters
F	same π, $\mu_{\alpha*}$, μ_δ	$3 + 3N_C$
I	no constraint	$6N_C$
L	same π	$1 + 5N_C$

Field DC4: Source of solution

Most solutions are obtained by combining the results from the two data reduction consortia (FAST and NDAC), while some originate from one consortium only:

C : combined FAST+NDAC solution;
F : solution taken from the FAST Consortium only;
N : solution taken from the NDAC Consortium only.

Field DC5: Quality of solution

This provides an indication of the reliability of the double or multiple star solution on a scale from A to D. The quality flag was computed according to the availability, mutual agreement and estimated quality (first/second class) of the individual FAST and NDAC solutions. This was done regardless of whether the adopted solution agreed with ground-based data as given, for instance, in the Hipparcos Input Catalogue. Cases of severe disagreement are instead indicated in a note (see Field DC6). The quality flags can be understood as follows:

A : 'good', or reliable solution: this solution was obtained by combining two first-class solutions in good mutual agreement;
B : 'fair', or moderately reliable solution: based on only one first-class solution, or a combination of a first-class and a second-class solution in mutual agreement;
C : 'poor', or less reliable solution: based on only one second-class solution, or a combination of two second-class solutions in mutual agreement;
D : 'uncertain' solution: this flag is a warning that FAST and NDAC found distinctly different solutions and that a choice between them had to be made according to certain criteria. The source of the retained solution is given in Field DC4. The main parameters (ΔHp, θ, ϱ) of the rejected solution are given among the Notes at the end of the volume (see Field DC6).

Field DC6: Flag indicating a note

Notes are included at the end of the relevant volumes: Volumes 5–9 for general notes, Volume 10 for double and multiple systems, and Volume 11 for photometric notes (see Field H70 for explanation of the Notes system). The flag has the following meaning:
D : double and multiple systems note only;
G : general note only;
P : photometric (including variability notes) only;
W : 'D' + 'P' only;
X : 'G' + 'D' only;
Y : 'G' + 'P' only;
Z : 'G' + 'D' + 'P'.

Fields DC7–8: Component Identifiers

Field DC7: Component identifier

This field contains a single letter (A, B, C, ...) designating the component of the double or multiple system considered in subsequent fields. 'A' designates the primary, usually the brightest component; 'B' the secondary, usually the second brightest component; etc. An effort has been made to use the same component designations as in the CCDM catalogue for systems already known from ground-based observations, while new designations have been assigned to the newly discovered components.

What is referred to here as a component is the smallest entity considered in the published Hipparcos solution. It can in reality consist of more than one star, in which case the given position refers to the photocentre of the unresolved object in the passband of the *Hp* magnitude. In such cases the single-letter identifier given here may in other catalogues designate just one of the unresolved components. Thus, a known triple star ABC may be given as a double star with component identifiers A and C, although the A component may actually be the photocentre of A and B.

Close binaries with a small magnitude difference sometimes present an ambiguity in the component identification caused by possible orbital motion since the (often old) ground-based identification. In doubtful cases such binaries are given the component designations A and S. The system AS could thus be interpreted as either AB or BA.

The total number of (resolved) components in the solution is given in the machine-readable DMSA/C as N_C. There are 12005 solutions with $N_C = 2$, 182 with $N_C = 3$ and 8 with $N_C = 4$.

Field DC8: Hipparcos Catalogue identifier

This field gives the HIP number under which the component was observed.

Components confined to the roughly 30 arcsec diameter sensitive area of the primary detector were usually observed under the same HIP number. If two components with not too unequal magnitudes were known *a priori* in the Hipparcos Input Catalogue (HIC) to be within 10–30 arcsec of each other, they were considered as individual targets and given separate HIC numbers; this numbering is retained in the Hipparcos Catalogue.

A given HIP number cannot occur under more than one system identifier (Field DC1). The CCDM number, if any, for a given HIP number is found in Field H55 of the main catalogue.

Fields DC9–14: Component Photometric Data

Field DC9: Magnitude of component in the Hipparcos photometric system, Hp

Field DC10: Standard error of the Hp magnitude, σ_{Hp} (mag)

These fields give the magnitude of the component in the broad-band Hp photometric system, as derived from the astrometric and photometric processing, with its estimated standard error. For variable stars the magnitude should be understood as a median value, and the standard error includes a contribution from the variability.

Field DC11: Magnitude of component in the Tycho photometric system, B_T

Field DC12: Standard error of the B_T magnitude, σ_{B_T} (mag)

Field DC13: Magnitude of component in the Tycho photometric system, V_T

Field DC14: Standard error of the V_T magnitude, σ_{V_T} (mag)

Fields DC11–14 give, when available, the (corrected or 'de-censored') mean B_T and V_T magnitudes and standard errors of the component as derived in the Tycho data analysis (see Section 2.2 for details). Blank fields indicate that no component data were available from the Tycho data analysis. This usually means either that the component was too faint ($\gtrsim$ 11 mag), or that it could not be separated from another component ($\varrho \lesssim 2$ arcsec).

Fields DC15–19: Component Astrometric Data

Fields DC15–16: Equatorial coordinates at the epoch J1991.25, α and δ (deg)

Field DC17: Trigonometric parallax, π (mas)

Fields DC18–19: Proper motion, $\mu_{\alpha*}$ and μ_δ (mas/yr)

The position (α, δ) and the proper motion components in right ascension, $\mu_{\alpha*} = \mu_\alpha \cos\delta$, and declination, μ_δ, refer to the epoch J1991.25 and are given with respect to the reference system of ICRS. The proper motion is expressed in milliarcsec per Julian year (mas/yr).

Fields DC20–24: Standard Errors of Component Astrometry

Fields DC20–21: Standard errors of the position at the epoch J1991.25, $\sigma_{\alpha*}$ and σ_δ (mas)

The standard error in right ascension is given as a great-circle measure, $\sigma_{\alpha*} = \sigma_\alpha \cos\delta$.

Field DC22: Standard error of the trigonometric parallax, σ_π (mas)

Fields DC23–24: Standard errors of the proper motion at the epoch J1991.25, $\sigma_{\mu_{\alpha*}}$ and σ_{μ_δ} (mas/yr)

Fields DC25–29: Relative Astrometry

The relative astrometric data given in Fields DC25–29 are computed from the data in Fields DC15–19 for the relevant components. Fields DC26–29 may be of truncated precision compared to the absolute data, and no standard errors are given. They are provided merely as a convenient way to form an overview of the geometry of a system and of the relative motions of the components. All relative data refer to the catalogue epoch, J1991.25.

Fields DC25–29 are blank for the first component in a solution. Fields DC28–29 are blank also for the other component(s) of a fixed solution (type F in Field DC3), where $d\theta/dt = 0$ and $d\varrho/dt = 0$ are enforced by the solution process.

Field DC25: Reference component for the data in Fields DC26–29

This field designates the reference component for the relative data of the current component (Field DC7).

Fields DC26–27: Position angle and separation, θ (deg) and ϱ (arcsec)

The position angle, θ, of the current component (Field DC7) relative to the reference component (Field DC25) is measured counterclockwise, as seen on the sky, from the $+\delta$ direction.

Fields DC28–29: Rate of change of position angle and separation, $d\theta/dt$ (deg/yr) and $d\varrho/dt$ (arcsec/yr)

These data are given only for solutions of type L and I (see Field DC3).

Charts of Double and Multiple Systems

All systems in DMSA/C are graphically depicted at the bottom of the printed page on which the data appear. Each chart is labelled, immediately below its frame, with the CCDM number of the system (from Field DC1), the solution identifier (Field DC2) if there is more than one solution for the system, and the scale of the chart expressed as the side length in arcsec.

The orientation of the charts is such that right ascension increases towards the left and declination towards the top. Component identifiers are shown as appropriate.

2.3.3. DMSA/G: Acceleration Solutions

For some apparently single (unresolved) stars it was found that the observed motion on the sky could not be properly modelled by the standard five astrometric parameters, while an acceptable solution was obtained by adding acceleration terms to the model. These objects are probably astrometric binaries with periods above some 10 years, so that the photocentric motion over the Hipparcos observation interval (roughly 1990.0–1993.2) is adequately represented by a quadratic or cubic polynomial in time. DMSA/G gives the non-linear (acceleration, or higher-order) terms for these objects.

The acceleration models are polynomial extensions of the single-star model with five astrometric parameters (α, δ, π, $\mu_{\alpha*}$, μ_δ). The additional parameters are the accelerations in right ascension and declination, or approximately $g_{\alpha*} = \mathrm{d}\mu_{\alpha*}/\mathrm{d}t$, $g_\delta = \mathrm{d}\mu_\delta/\mathrm{d}t$; and in some cases also the second derivatives of the proper motions, or approximately $\dot{g}_{\alpha*} = \mathrm{d}^2\mu_{\alpha*}/\mathrm{d}t^2$, $\dot{g}_\delta = \mathrm{d}^2\mu_\delta/\mathrm{d}t^2$. A stricter definition is given below.

Using a polynomial model for the motion is, from a physical viewpoint, a very unsatisfactory substitute for a complete orbital model. Probably it is still the most practical and compact representation of the Hipparcos measurements of astrometric binaries following an otherwise unknown, long-period orbit. The polynomial fit must however *never* be used to extrapolate the motion significantly outside the observation interval. Since the extrapolation of stellar positions by means of observed proper motions is nevertheless a legitimate use of the catalogue, a special provision has been made to somewhat reduce the risk of this procedure. Basically, the main catalogue (Fields H8–9 and H12–13) gives the best *linear* approximation of the motion over the observation interval, while DMSA/G gives the non-linear deviation from that motion. The recommended procedure for extrapolating to distant epochs is to rely entirely on the parameters in the main catalogue, thus ignoring the acceleration terms. While this may still lead to considerable errors in the presence of actual accelerations, it is obviously safer than the use of polynomial models.

The acceleration terms are defined in terms of local rectangular coordinates (ξ, η) valid in a small area around the object; cf. Section 1.2.9 and Figure 1.2.3. (ξ and η are positional offsets in the directions of $+\alpha$ and $+\delta$, respectively, from a fixed reference position; i.e. $\xi \simeq \Delta\alpha\cos\delta$, $\eta \simeq \Delta\delta$.) The model for the accelerated motion is:

$$\begin{aligned} \xi(t) &= \xi_{\mathrm{s}}(t) + \tfrac{1}{2}(t^2 - a)g_{\alpha*} + \tfrac{1}{6}(t^2 - b)t\dot{g}_{\alpha*} \\ \eta(t) &= \eta_{\mathrm{s}}(t) + \tfrac{1}{2}(t^2 - a)g_\delta + \tfrac{1}{6}(t^2 - b)t\dot{g}_\delta \end{aligned} \qquad [2.3.1]$$

where the time t is reckoned from the catalogue epoch J1991.25. Here, $\xi_{\mathrm{s}}(t)$ and $\eta_{\mathrm{s}}(t)$ give the motion according to the standard single-star model described in Section 1.2.8; this is specified by the five astrometric parameters given in Fields H8–13 of the main catalogue. a and b are the fixed constants:

$$a = 0.81\ \mathrm{yr}^2\,, \quad b = 1.69\ \mathrm{yr}^2 \qquad [2.3.2]$$

introduced in order to make the g and $\dot{g}$ terms approximately orthogonal to the position and proper motion terms implicit in $\xi_{\mathrm{s}}(t)$ and $\eta_{\mathrm{s}}(t)$. As a consequence, the position and proper motion given in the main catalogue represent the mean position and mean proper motion over the observation interval, rather than the instantaneous position and proper motion at epoch J1991.25 according to the fitted acceleration model.

The g terms vanish precisely at the two epochs J1990.35 and J1992.15 ($t = \pm\sqrt{a}$) while the $\dot{g}$ terms vanish at J1989.95, J1991.25 and J1992.55 ($t = 0, \pm\sqrt{b}$). This permits the following interpretation of the position and proper motion parameters in the main catalogue in terms of the fitted quadratic or cubic motion: the position in Fields H8–9 is the mid-point of the fitted locations at J1990.35 and J1992.15, and the proper

motion in Fields H12–13 is the mean annual motion between the fitted locations at J1989.95 and J1992.55 (see Figure 2.3.1).

Note that any contribution from the secular acceleration (a geometrical effect due to the star's radial velocity; see Section 1.2.8) is included in the definition of $\xi_S(t)$ and $\eta_S(t)$, at least if it would exceed 0.1 mas during the mission. The g and $\dot{g}$ terms, when significant, therefore represent a true physical action on the object.

The g and $\dot{g}$ terms were initially estimated for all stars, but depending on their statistical significance, the finally adopted solution was constrained to n = 5, 7 or 9 parameters. This corresponds, respectively, to the standard astrometric model (with no entry in DMSA/G), the quadratic, and the cubic model. The first five parameters are given in Fields H8–13 of the main Hipparcos Catalogue, while the additional quadratic and cubic terms are given in Fields DG2–3 and DG7–8. The standard errors of all n parameters are also given in the printed catalogue (Fields H14–18, DG4–5 and DG9–10).

The significance of the g and $\dot{g}$ terms was determined by means of the statistics F_g and $F_{\dot{g}}$ given (in significant cases) in Fields DG6 and DG11. They are defined by:

$$F_g^2 = \begin{pmatrix} g_{\alpha*} & g_\delta \end{pmatrix} \begin{pmatrix} \sigma^2_{g_{\alpha*}} & \rho_g \sigma_{g_{\alpha*}} \sigma_{g_\delta} \\ \rho_g \sigma_{g_{\alpha*}} \sigma_{g_\delta} & \sigma^2_{g_\delta} \end{pmatrix}^{-1} \begin{pmatrix} g_{\alpha*} \\ g_\delta \end{pmatrix} \qquad [2.3.3]$$

and:

$$F_{\dot{g}}^2 = \begin{pmatrix} \dot{g}_{\alpha*} & \dot{g}_\delta \end{pmatrix} \begin{pmatrix} \sigma^2_{\dot{g}_{\alpha*}} & \rho_{\dot{g}} \sigma_{\dot{g}_{\alpha*}} \sigma_{\dot{g}_\delta} \\ \rho_{\dot{g}} \sigma_{\dot{g}_{\alpha*}} \sigma_{\dot{g}_\delta} & \sigma^2_{\dot{g}_\delta} \end{pmatrix}^{-1} \begin{pmatrix} \dot{g}_{\alpha*} \\ \dot{g}_\delta \end{pmatrix} \qquad [2.3.4]$$

where $\sigma_{g_{\alpha*}}$, σ_{g_δ}, $\sigma_{\dot{g}_{\alpha*}}$ and $\sigma_{\dot{g}_\delta}$ are the standard errors of the g and $\dot{g}$ terms (Fields DG4–5 and DG9–10), ρ_g is the correlation coefficient between $g_{\alpha*}$ and g_δ, and $\rho_{\dot{g}}$ the correlation coefficient between $\dot{g}_{\alpha*}$ and $\dot{g}_\delta$. (These two correlation coefficients are not given in the printed catalogue, but are contained in the machine-readable file as the 21st and 36th coefficients, ρ_{21} and ρ_{36}, respectively; see Table 2.3.3.)

In the absence of real accelerations, the g and $\dot{g}$ terms are expected to be random variables, following a centred multivariate normal distribution with the given standard deviations and correlations. In this case F_g^2 and $F_{\dot{g}}^2$ each follow the χ^2 distribution with two degrees of freedom. The probability that $F_g > x$ is then given by $\exp(-\frac{1}{2}x^2)$, and similarly for $F_{\dot{g}}$. The g terms were considered to be significant if $F_g > 3.44$, and the $\dot{g}$ terms were considered to be significant if $F_{\dot{g}} > 3.44$. This gives the same level of significance (0.27 per cent) as the two-sided 3σ criterion for a normal distribution.

The quadratic model (n = 7) was adopted if a seven-parameter fit resulted in significant g terms ($F_g > 3.44$) and an acceptable goodness-of-fit (F2 < 4 in Field H30) with a reasonable rejection rate (F1 < 7 per cent). If, however, the addition of the $\dot{g}$ terms produced a significant solution ($F_{\dot{g}} > 3.44$), then the cubic model (n = 9) was instead adopted.

The fields of the printed DMSA/G are described below. Further details on the machine-readable version are given in Section 2.3.7, in particular Table 2.3.3.

Field DG1: Identifier

Field DG1: Hipparcos Catalogue identifier

This field gives the HIP number under which the object was observed.

Fields DG2–6: Acceleration of Photocentre

Fields DG2–3: Components in right ascension and declination of the apparent acceleration of the photocentre at epoch J1991.25, $g_{\alpha *}$ and g_δ (mas/yr^2)

Fields DG4–5: Standard errors of the acceleration terms, $\sigma_{g_{\alpha *}}$ and σ_{g_δ} (mas/yr^2)

The acceleration (g) terms describe the quadratic deviation of the path of the photocentre on the sky from the motion predicted for a single star. They may be interpreted as the rates of change of the proper motion components, $g_{\alpha *} = \mathrm{d}\mu_{\alpha *}/\mathrm{d}t$ and $g_\delta = \mathrm{d}\mu_\delta/\mathrm{d}t$, after correction for the perspective acceleration (see the preceding discussion).

Field DG6: Statistic for the significance of the acceleration terms, F_g

The quadratic model is only adopted if the g terms are significant, i.e. $F_g > 3.44$; see Equation 2.3.3.

Fields DG7–11: Third-Order Motion of Photocentre

Fields DG7–8: Components in right ascension and declination of the rate of change of the apparent acceleration of the photocentre, $\dot{g}_{\alpha *}$ and $\dot{g}_\delta$ (mas/yr^3)

Fields DG9–10: Standard errors of the $\dot{g}$ terms, $\sigma_{\dot{g}_{\alpha *}}$ and $\sigma_{\dot{g}_\delta}$ (mas/yr^3)

Together with the g terms, the $\dot{g}$ terms describe the deviation of the path of the photocentre on the sky from the linear motion predicted for a single star. The $\dot{g}$ terms express a linear variation with time of the acceleration (g) terms, with DG2–3 being the instantaneous accelerations at epoch J1991.25.

Field DG11: Statistic for the significance of the $\dot{g}$ terms, $F_{\dot{g}}$

The third-order (cubic) model is only adopted if the $\dot{g}$ terms are significant, i.e. $F_{\dot{g}} > 3.44$; see Equation 2.3.4.

Fields DG7–11 are blank unless a solution was found with significant cubic terms ($F_{\dot{g}} > 3.44$).

Fields DG12: Notes

Field DG12: Flag indicating a note

Notes are included at the end of the relevant volumes: Volumes 5–9 for general notes, Volume 10 for double and multiple systems notes, and Volume 11 for photometric notes (see Field H70 for explanation of the Notes system). The flag has the following meaning:

D : double and multiple systems note only;
G : general note only;
P : photometric (including variability notes) only;
W : 'D' + 'P' only;
X : 'G' + 'D' only;
Y : 'G' + 'P' only;
Z : 'G' + 'D' + 'P'.

2.3.4. DMSA/O: Orbital Solutions

The astrometric solution for the systems described in DMSA/O is the superposition of two models (see Figure 2.3.2):

1. a model for the uniform space motion of the centre of mass: this is described by the same five parameters as used for a single star (α, δ, π, $\mu_{\alpha*}$, μ_δ);
2. a model for the orbital motion of the photocentre around the centre of mass: this assumes a Keplerian orbit and is consequently fully specified by seven orbital elements (P, T, a_0, e, ω, i, Ω).

The astrometric parameters for the centre of mass are given in the main catalogue (as indicated by '+' in Field H10), while the results for the orbital elements are given in DMSA/O. It was not always possible to determine all seven orbital elements uniquely from the Hipparcos data. In many cases some of the elements (and in a few cases all the orbital elements) were adopted from the literature; these are indicated by the presence of a reference number in Field DO16 and by blanks in Fields DO9–15 for the standard errors of the adopted elements. In other cases where no published orbit was used, and where Field DO16 is consequently blank, it was nevertheless necessary to constrain the solution by assuming a circular orbit ($e = \omega = 0$); in these cases Fields DO12–13 are blank. The status of each parameter—estimated or constrained—is thus consistently flagged by the presence or absence of numerical data in Fields DO9–15, and also by Field DOM1 in the machine-readable DMSA/O (Table 2.3.4a).

The elements given in DMSA/O are the classical ones normally used to describe binary orbits from visual and spectroscopic observations (see, e.g. L. Binnendijk, 1960, *Properties of Double Stars*, Philadelphia, and A.H. Batten, 1973, *Binary and Multiple Systems of Stars*, Oxford). Note however that the present elements always describe the *absolute* orbit of the photocentre with respect to the mass centre of the binary, whereas ground-based observations usually give the *relative* orbit of the secondary with respect to the primary star.

The definition of each element is contained in the descriptions of Fields DO2–8. For convenience the complete formulae to compute the positional offset of the photocentre with respect to the centre of mass are given below. The offset is expressed in the local rectangular coordinates (ξ, η), cf. Section 1.2.9 and Figure 1.2.3. (ξ and η are positional offsets in the directions of $+\alpha$ and $+\delta$, respectively, from a fixed reference position; i.e. $\xi \simeq \Delta\alpha \cos\delta$, $\eta \simeq \Delta\delta$.) With $\xi_s(t)$, $\eta_s(t)$ representing the motion of the centre of mass as described by the five astrometric parameters (Fields H8–13 of the main Hipparcos Catalogue) in terms of the standard model discussed in Section 1.2.8, the motion of the photocentre is given by:

$$\xi(t) = \xi_s(t) + B\,X(t) + G\,Y(t), \quad \eta(t) = \eta_s(t) + A\,X(t) + F\,Y(t) \qquad [2.3.5]$$

where A, B, F, G are the Thiele-Innes elements:

$$\begin{aligned} A &= a_0(+\cos\omega\cos\Omega - \sin\omega\sin\Omega\cos i) \\ B &= a_0(+\cos\omega\sin\Omega + \sin\omega\cos\Omega\cos i) \\ F &= a_0(-\sin\omega\cos\Omega - \cos\omega\sin\Omega\cos i) \\ G &= a_0(-\sin\omega\sin\Omega + \cos\omega\cos\Omega\cos i) \end{aligned} \qquad [2.3.6]$$

(expressed in mas), and (X, Y) the time-dependent dimensionless coordinates in the orbital plane:

$$X(t) = \cos E - e, \quad Y(t) = (1 - e^2)^{1/2} \sin E \qquad [2.3.7]$$

The eccentric anomaly, E, is obtained from Kepler's equation:

$$\frac{2\pi}{P}(t - T) = E - e \sin E \qquad [2.3.8]$$

The fields of the printed DMSA/O are described below. Further details on the machine-readable version are given in Section 2.3.7, in particular Table 2.3.4.

Field DO1: Identifier

Field DO1: Hipparcos Catalogue identifier

This field gives the HIP number under which the binary was observed.

Fields DO2–8: Orbital Elements of the Photocentre

Field DO2: Orbital period, P (days)

This is the time interval in days between successive periastron passages (cf. Field DO3).

Field DO3: Time of periastron passage, T (days)

This is the date when the photocentre is closest to the centre of mass in the orbital plane. This is equivalent to the closest approach of the stellar components, so that the event may be called 'periastron passage' without ambiguity. The date is expressed in days from JD2 440 000.0(TT).

Field DO4: Semi-major axis of photocentre orbit, a_0 (mas)

This is the semi-major axis of the absolute orbit of the photocentre, as measured in the orbital plane.

Field DO5: Eccentricity, e

This is the eccentricity of the true orbit. $0 \leq e < 1$.

Field DO6: Argument of periastron, ω (deg)

This is the angle in the orbital plane from the line of nodes to the major axis. It is measured from the nodal point (Ω in Field DO8) to the periastron in the direction of motion. $0 \leq \omega < 360°$.

Field DO7: Inclination, i (deg)

This is the inclination of the orbital plane to the tangent plane of the sky. It is taken to be in the first quadrant if the apparent motion is direct (counter-clockwise) and in the second quadrant for retrograde (clockwise) apparent motion. $0 \leq i \leq 180°$.

Field DO8: Position angle of the node, Ω (deg)

This is the position angle (measured counterclockwise, as seen on the sky, from the $+\delta$ direction) of the line of nodes, or the intersection of the orbital and tangent planes. If the radial motion of the components is known from spectroscopic studies, then Ω should give the position angle of the *ascending node*, at which the primary star crosses the tangent plane while receding from the observer. In the absence of spectroscopic information Ω refers to the node with the smallest positive position angle (which may then actually be the descending node). This ambiguity has no effect on the calculation of the positional offset on the sky. $0 \leq \Omega < 360°$.

Fields DO9–15: Standard Errors

Field DO9: Standard error of P (days)

Field DO10: Standard error of T (days)

Field DO11: Standard error of a_0 (mas)

Field DO12: Standard error of e

Field DO13: Standard error of ω (deg)

Field DO14: Standard error of i (deg)

Field DO15: Standard error of Ω (deg)

These fields contain the standard errors of each element of the photocentre determined or improved by the Hipparcos observations. A blank field signifies either that the corresponding element was adopted from the literature (in which case a reference number is given in Field DO16), or that the element was otherwise constrained in the solution (viz. by assuming a circular orbit, $e = \omega = 0$).

Fields DO16–17: References and Notes

Field DO16: Reference number

This number points to the references to adopted ground-based orbital elements given at the end of DMSA/O. This field is blank when no ground-based orbit exists, or when the orbital elements were determined without regard to any previous determination.

Field DO17: Flag indicating a note

Notes are included at the end of the relevant volumes: Volumes 5–9 for general notes, Volume 10 for double and multiple systems notes, and Volume 11 for photometric notes (see Field H70 for explanation of the Notes system). The flag has the following meaning:

D : double and multiple systems note only;
G : general note only;
P : photometric (including variability notes) only;
W : ‘D’ + ‘P’ only;
X : ‘G’ + ‘D’ only;
Y : ‘G’ + ‘P’ only;
Z : ‘G’ + ‘D’ + ‘P’.

2.3.5. DMSA/V: VIM Solutions

The photocentre of an unresolved binary, in which one component is a variable star, shows a specific motion on the sky, coupled to the variation in the total brightness of the system. Such an object is called a 'Variability-Induced Mover', abbreviated as VIM. The detailed theory of VIMs is described elsewhere (R. Wielen, 1996, *Astronomy & Astrophysics*, 314, 679). Only a concise description is given here.

The variable star is called V; the other star C is assumed to have the (unknown) constant magnitude $Hp_{\rm C}$. The total magnitude of the system at time t, observed by Hipparcos, is $Hp_{\rm tot}(t)$. The (unknown) angular separation between the two stars is ϱ. The equatorial components of ϱ are called $d_{\alpha *} = \varrho \sin\theta_{\rm C}$ and $d_\delta = \varrho\cos\theta_{\rm C}$, where $\theta_{\rm C}$ is the position angle of C with respect to V. It is assumed that the relative geometry of the double star, defined by ϱ and $\theta_{\rm C}$, does not change significantly over the observational period of Hipparcos (3.3 years). This is probably a good approximation for most of the VIMs found by Hipparcos.

If the system had always the same total brightness, then the photocentre would be fixed with respect to the two components, and hence with respect to the centre of mass of the system; consequently the photocentre would move like a single star and could be described by the usual five astrometric parameters. Such an (unresolved) object would not be recognised as a binary by Hipparcos, and indeed many of the 'single' stars in the Hipparcos Catalogue may be of this kind.

If one of the components is variable, the photocentre is not fixed with respect to the centre of mass but moves back and forth on the line joining the two components. In order to apply the five astrometric parameters to such a VIM, a 'reference magnitude' $Hp_{\rm ref}$ is chosen for the object, and the 'reference point' of the system is defined as the position of the photocentre when the total magnitude equals $Hp_{\rm ref}$. The choice of reference magnitude is arbitrary in principle, but should be close to the mean magnitude of the system for practical reasons. Clearly the reference point moves like a single star and can be described by the standard astrometric model (Section 1.2.8) in terms of the five parameters α, δ, π, $\mu_{\alpha *}$ and μ_δ. These are given in the main Hipparcos Catalogue as for a single star (Fields H8–13). The variability-induced motion, specified by the two parameters $D_{\alpha *}$ and D_δ together with the light curve, is superposed on the standard model, giving the observed motion of the photocentre (see Figure 2.3.3).

The DMSA/V gives the estimates of $D_{\alpha *}$ and D_δ, for a specified reference magnitude, together with their standard errors. The machine-readable DMSA/V additionally provides the complete set of correlation coefficients among the seven estimated parameters. Three more quantities, derived from the above parameters, are given in the DMSA/V. These are the position angle $\theta_{\rm C}$ of the constant star with respect to the variable star; a lower limit $\varrho_{\rm min}$ on their separation; and the approximate size $d_{\rm var}$ of the VIM effect. Finally the statistical significance of the solution, F_D, is also given.

The additional variability-induced motion can be expressed as small offsets in the local rectangular coordinates (ξ, η); cf. Section 1.2.9 and Figure 1.2.3. With $\xi_{\rm S}(t)$, $\eta_{\rm S}(t)$ representing the motion of the reference point, as defined by the five astrometric parameters in the main Hipparcos Catalogue, and $Hp_{\rm C}$ the Hp magnitude of component C, the motion of the actual photocentre is found to be:

$$\begin{aligned} \xi(t) &= \xi_{\rm S}(t) + \left(10^{-0.4(Hp_{\rm C}-Hp_{\rm tot}(t))} - 10^{-0.4(Hp_{\rm C}-Hp_{\rm ref})}\right) d_{\alpha *} \\ \eta(t) &= \eta_{\rm S}(t) + \left(10^{-0.4(Hp_{\rm C}-Hp_{\rm tot}(t))} - 10^{-0.4(Hp_{\rm C}-Hp_{\rm ref})}\right) d_\delta \end{aligned} \qquad [2.3.9]$$

This depends on the three unknowns $d_{\alpha*}$, d_δ and $Hp_{\rm C}$, which however cannot be separated by observing only the photocentre. Introducing:

$$\begin{aligned} D_{\alpha*} &= 10^{-0.4(Hp_{\rm C}-Hp_{\rm ref})} d_{\alpha*} \\ D_\delta &= 10^{-0.4(Hp_{\rm C}-Hp_{\rm ref})} d_\delta \end{aligned} \qquad [2.3.10]$$

the motion of the photocentre can be written:

$$\begin{aligned} \xi(t) &= \xi_{\rm s}(t) + \left(10^{0.4(Hp_{\rm tot}(t)-Hp_{\rm ref})} - 1\right) D_{\alpha*} \\ \eta(t) &= \eta_{\rm s}(t) + \left(10^{0.4(Hp_{\rm tot}(t)-Hp_{\rm ref})} - 1\right) D_\delta \end{aligned} \qquad [2.3.11]$$

Since $Hp_{\rm tot}(t)$ is known, and $Hp_{\rm ref}$ is an adopted value, $D_{\alpha*}$ and D_δ (measured in mas) can be obtained in a simultaneous least-squares solution together with the five standard astrometric parameters. The full solution is therefore a seven-parameter solution.

Because $Hp_{\rm C}$ is unknown, it is not possible to derive the separation ϱ of a VIM. However, a lower limit can be computed, since obviously $Hp_{\rm C} \geq Hp_{\rm tot,\,min}$, the total magnitude of the system at its minimum luminosity:

$$\varrho \geq \varrho_{\rm min} = 10^{0.4(Hp_{\rm tot,\,min}-Hp_{\rm ref})}(D_{\alpha*}^2 + D_\delta^2)^{1/2} \qquad [2.3.12]$$

To determine this value, the faintest magnitude actually observed by Hipparcos has been used. For some Mira stars and other objects a larger $\varrho_{\rm min}$ could be derived by using fainter ground-based values of $Hp_{\rm tot,\,min}$.

The size of the VIM effect is indicated by the total displacement of the photocentre between the (observed) minimum and maximum luminosity:

$$d_{\rm var} = \left(10^{0.4(Hp_{\rm tot,\,min}-Hp_{\rm ref})} - 10^{0.4(Hp_{\rm tot,\,max}-Hp_{\rm ref})}\right)(D_{\alpha*}^2 + D_\delta^2)^{1/2} \qquad [2.3.13]$$

The significance of the VIM solution is determined by means of the statistic F_D defined in analogy with F_g and $F_{\dot g}$ (Fields DG6 and DG11):

$$F_D^2 = (\,D_{\alpha*} \quad D_\delta\,) \begin{pmatrix} \sigma_{D_{\alpha*}}^2 & \rho_D \sigma_{D_{\alpha*}} \sigma_{D_\delta} \\ \rho_D \sigma_{D_{\alpha*}} \sigma_{D_\delta} & \sigma_{D_\delta}^2 \end{pmatrix}^{-1} \begin{pmatrix} D_{\alpha*} \\ D_\delta \end{pmatrix} \qquad [2.3.14]$$

where ρ_D is the correlation coefficient between $D_{\alpha*}$ and D_δ (this correlation is only given in the machine-readable DMSA/V; see Table 2.3.5). An object is accepted as a VIM, if $F_D > 2.15$. This corresponds to a 10 per cent probability of wrongly accepting an object as a VIM. The adopted limit for F_D (2.15) is smaller than for F_g and $F_{\dot g}$ (3.44), since the warning on the possible binary nature of the variable star is considered to be important even for less certain cases.

As previously explained, the positional parameters α and δ given in Fields H8–9 refer to the reference point, and are valid for the chosen reference brightness $Hp_{\rm ref}$ of the object. The corresponding parameters for the variable star itself are given by $\alpha_{\rm V} = \alpha - D_{\alpha*} \sec\delta$ and $\delta_{\rm V} = \delta - D_\delta$. The position of the constant star cannot be derived. Due to the assumption of ϱ and $\theta_{\rm C}$ being fixed, the given proper motion of the reference point (Fields H12–13) is identical to the proper motions of the centre of mass, of the constant star, and of the variable star.

The fields of the printed DMSA/V are described below. Further details on the machine-readable version are given in Section 2.3.7, in particular Table 2.3.5.

Fields DV1–2: Identifier and Reference Magnitude

Field DV1: Hipparcos Catalogue identifier

This field gives the HIP number under which the object was observed.

Field DV2: Adopted reference magnitude for the object, $Hp_{\rm ref}$

The reference magnitude is freely chosen and defines the reference point for the object. The positional parameters α and δ (Fields H8–9 of the main Hipparcos Catalogue) and the VIM elements $D_{\alpha*}$ and D_δ (Fields DV3–4) depend on the chosen $Hp_{\rm ref}$. Fields DV7–11, on the other hand, do not depend on $Hp_{\rm ref}$.

Fields DV3–6: Elements of the VIM

Fields DV3–4: Elements of the variability-induced motion in right ascension, $D_{\alpha*}$, and declination, D_δ, in mas, valid for the reference magnitude $Hp_{\rm ref}$ (Field DV2)

Fields DV5–6: Standard errors of the VIM elements in right ascension, $\sigma_{D_{\alpha*}}$, and declination, σ_{D_δ}, in mas

Field DV7: Statistic for the significance of the detection of the variability-induced motion, F_D

See Equation 2.3.14 for the definition of F_D. The VIM solution is only accepted if $F_D > 2.15$.

Fields DV8–11: Derived Quantities

Field DV8: Position angle $\theta_{\rm C}$ of the constant component of the binary with respect to the variable component, in degrees

The position angle is measured counterclockwise, as seen on the sky, from the $+\delta$ direction. It is derived from $D_{\alpha*}$ and D_δ given in Fields DV3–4.

Field DV9: Standard error $\sigma_{\theta_{\rm C}}$ of the position angle, in degrees

Field DV10: Lower limit for the separation of the binary, $\varrho_{\rm min}$, in mas

From the Hipparcos observations only this lower limit for the separation can be derived.

Field DV11: Displacement of photocentre between the minimum and maximum luminosity of the system, $d_{\rm var}$, in mas

This quantity is provided as an indication of the size of the VIM effect.

Field DV12: Notes

Field DV12: Flag indicating a note

Notes are included at the end of the relevant volumes: Volumes 5–9 for general notes, Volume 10 for double and multiple systems notes, and Volume 11 for photometric notes (see Field H70 for explanation of the Notes system). The flag has the following meaning:

D : double and multiple systems note only;
G : general note only;
P : photometric (including variability notes) only;
W : 'D' + 'P' only;
X : 'G' + 'D' only;
Y : 'G' + 'P' only;
Z : 'G' + 'D' + 'P'.

2.3.6. DMSA/X: Stochastic Solutions

For some unresolved stars it was not possible to find an acceptable single or double star solution in reasonable agreement with the statistical uncertainties (standard errors) assigned to the individual measurements. These objects could for instance be astrometric binaries with relatively short periods (< 3 years), for which a simple polynomial model was clearly inadequate, while the space data alone did not allow a full orbital solution. In the individual measurements, the displacement of the photocentre from an assumed linear motion of the centre of mass thus appears like a random scatter in excess of the measurement noise.

Lacking an acceptable deterministic model for such objects, a reasonable treatment would be to assume a stochastic model for the photocentric displacements superposed on a uniform motion of the centre of mass. Practically, the stochastic model is implemented by quadratically adding a certain amount ϵ to the standard errors of all the observations of the object, thereby reducing their statistical weights in the least-squares determination of the single-star parameters. The size of ϵ for a given object is adjusted to bring the modified weights in statistical agreement with the residuals of the fit, taking into account that occasional outliers could still exist. As a consequence, the standard errors in the main catalogue (Fields H14–18) fully reflect the increased uncertainty of the solution. Furthermore, the rms residual (or 'unit weight error') for the X solutions is, by construction, exactly equal to 1, resulting in a goodness-of-fit statistic F2 (see the description for Field H30) close to zero. This statistic is normally given in Field H30 of the main catalogue, which however is left blank for the X solutions. In this way the user should avoid the false impression that the five-parameter model provides an excellent fit to the observations.

The quantity ϵ may be referred to as the 'cosmic error' of the (suspected) astrometric binary. To the extent that the cosmic error actually represents a physical scatter in excess of the measurement noise, its value provides an order-of-magnitude estimate of the size of the orbit of the photocentre, and may consequently be of considerable astrophysical interest. The adopted quantities ϵ are given in DMSA/X, while the corresponding single-star parameters describing the mean motion of the object are given in the main catalogue.

It should be noted that the stochastic model is applied only to objects where other models fail and a forced application of the single-star model would lead to the rejection of a significant fraction of the data, or where the cosmic error is highly significant. For instance, if an acceptable fit can be obtained by rejecting only a few data points, then that method is generally preferred to the stochastic model. The quality of such a fit is generally specified by the percentage of rejected observations (F1) and the resulting goodness-of-fit statistic (F2), as given in the main catalogue (Fields H29 and H30, respectively).

In cases where there is in fact an unmodelled scatter above the measurement noise, the stochastic model has however two important advantages over the standard single-star solution with rejection of outliers: firstly, it avoids the rather arbitrary designation of some measurements as outliers, while others retain their full weight; in this way, the stochastic model often produces more realistic values of the astrometric parameters. Secondly, the weight reduction causes the standard errors of the estimated single-star parameters to become larger, reflecting the actual scatter of the observations, and hence being more realistic.

The stochastic model can also be regarded as a kind of robust estimation. However, in contrast to most standard robust techniques, which are designed to deal for instance with strongly non-Gaussian tails of the error distribution, the present model assumes a fairly uniform contribution of the excess scatter to all the observations (while exceptional outliers are still rejected). Moreover, it provides a direct estimate of the excess scatter, or cosmic error, and assigns a possible physical significance to it.

The fields of the printed DMSA/X are described below. Further details on the machine-readable version are given in Section 2.3.7, in particular Table 2.3.6.

Field DX1: Identifier

Field DX1: Hipparcos Catalogue identifier

This field gives the HIP number under which the object was observed.

Fields DX2–3: Cosmic Error

Field DX2: Cosmic error, ϵ (mas)

This field gives the excess rms observational noise. The astrometric data in Fields H8–30 have been derived from one-dimensional measurements (abscissae) after their *a priori* standard errors were modified according to the formula:

$$\sigma_{\mathrm{absc,\ adopted}} = \sqrt{\sigma^2_{\mathrm{absc,}\ a\ priori} + \epsilon^2} \qquad [2.3.15]$$

Field DX3: Estimated standard error of the cosmic error, σ_ϵ (mas)

Field DX4: Notes

Field DX4: Flag indicating a note

Notes are included at the end of the relevant volumes: Volumes 5–9 for general notes, Volume 10 for double and multiple systems notes, and Volume 11 for photometric notes (see Field H70 for explanation of the Notes system). The flag has the following meaning:

D : double and multiple systems note only;
G : general note only;
P : photometric (including variability notes) only;
W : 'D' + 'P' only;
X : 'G' + 'D' only;
Y : 'G' + 'P' only;
Z : 'G' + 'D' + 'P'.

2.3.7. The Machine-Readable DMSA

The machine-readable version of the DMSA contains strictly the same data as the printed version, plus information on the statistical correlations among the estimated parameters. Further fields have been added to facilitate the automatic interpretation of the files. Tables 2.3.1–6 summarise the contents of the machine-readable files.

The correlation coefficients among the five astrometric parameters α, δ, π, $\mu_{\alpha*}$ and μ_δ are given in the main catalogue (Fields H19–28) rounded to the nearest per cent. The DMSA contains the results of the fitting of more complex models to the observations, involving the statistical estimation of additional parameters or unknowns. The machine-readable DMSA provides the complete set of correlations for these model fits, including (for convenience) the correlations already specified in the main catalogue. The main reason for systematically providing correlations in DMSA is to allow a correct derivation of the standard errors of transformed quantities such as space velocities in galactic coordinates.

Coding of correlation coefficients in DMSA: The estimation of the astrometric parameters for single stars is usually well conditioned, resulting in small or moderate correlations, for which values percentage values (as given in the main catalogue) are generally sufficient.

The situation is often rather different in the estimation problems connected with double and multiple stars, astrometric binaries and orbital systems: some of the estimated parameters may exhibit a very high degree of (positive or negative) correlation. Correlation coefficients (ρ) of ± 0.999 or even ± 0.9999 are not uncommon, for instance between the component magnitudes of a close binary. In such cases a correlation coefficient rounded to the nearest per cent would lead to unacceptable errors in the calculation of the standard errors of transformed quantities. A special coding was therefore adopted for the correlation coefficients in the machine-readable DMSA, using a non-linear mapping of $-1 \le \rho \le +1$ onto the integers $-99 \le I \le 999$. This mapping is given by:

$$I = \text{round}\,(450.0 + 349.5 \times \arcsin \rho) \qquad [2.3.16]$$

where round() represents rounding to the nearest integer. The inverse mapping (decoding) is given by:

$$\rho = \sin((I - 450.0)/349.5) \qquad [2.3.17]$$

where the argument of the sine function is expressed in radians. The number 349.5 should be regarded as exact: it is adopted as a convenient approximation to $(999+99)/\pi$. The numerically largest correlations that are distinct from unity in this coding are $\rho = \pm 0.9999960$.

Sequence of correlation coefficients: In a solution with N parameters, $N(N-1)/2$ correlation coefficients must be specified, corresponding to the triangular part of the (symmetric) correlation matrix above or below the main diagonal. These coefficients are always given in a fixed sequence, corresponding to the columns of the upper-triangular matrix or, equivalently, the rows of the lower-triangular matrix; the order of reading is top to bottom and left to right.

The number of parameters varies between the different solution types depending on the specific models used. For DMSA/C and DMSA/O the situation is further complicated by constraints among the parameters: in the component solutions this means, for instance, that the two components in an F or L type binary solution are assumed to

have the same parallax. Similarly, in the orbital solutions, certain elements may be constrained to their values from ground-based orbit determinations, and consequently not estimated from the Hipparcos data. In order to avoid unnecessarily complex and variable data structures, the correlations among all of the model parameters are given in the machine-readable files. This allows the use of a fixed sequence for the parameters, and hence also for the correlation coefficients. The required distinction between the separately estimated (or 'active') parameters, and the constrained (or 'passive') ones is provided by an array of status flags, one for each parameter. The status flag is 1 if the parameter is active, otherwise 0. A non-redundant set of parameters and the corresponding correlation matrix can thus be constructed from the full set given in the files by deleting parameters with status flag 0 as well as the corresponding rows and columns of the correlation matrix.

The correlation coefficients are placed at the end of the data record, following the fields of the printed DMSA. However, for DMSA/C a slightly different arrangement was necessary because of the variable number of components. For each component there are six parameters (Hp, α, δ, π, $\mu_{\alpha*}$, μ_δ), so the number of parameters in the solution ranges from 12 to 24 and the number of correlation coefficients from 66 to 276. Choosing a record length to accommodate the actual maximum number of coefficients would be highly impractical. Instead, at most 66 coefficients are given in a record, which suffices for the vast majority of objects, but there may be up to five such records for a given solution. In DMSA/C there are consequently two record types: component records and correlation records. They are distinguished by the word 'COMP' and 'CORR', respectively, in Field DCM5. The first 32 bytes are identical in each record of a solution. The component records correspond to the lines of the printed DMSA/C.

Table 2.3.1. Overview of the machine-readable DMSA

This table summarises the files constituting the machine-readable DMSA
The file names are given in Section 2.11.2

Part of DMSA	Record length (bytes)	Number of records	Format description
C	238	37179	Table 2.3.2
G	195	2622	Table 2.3.3
O (data)	337	235	Table 2.3.4a
O (references)	80	118	Table 2.3.4b
V	144	288	Table 2.3.5
X	22	1561	Table 2.3.6

Table 2.3.2a. The Machine-Readable DMSA/C: Component Record

Fields designated DCM... appear only in the machine-readable catalogue

Field	Bytes	Format	Description
DC1	1–11	A10,X	System identifier (CCDM number)
DC2	12–13	I1,X	Solution identifier, S (1 to N_S)
DC3	14–15	A1,X	Type of solution (F, I, L)
DC4	16–17	A1,X	Source of solution (C, F, N)
DC5	18–19	A1,X	Quality of solution (A, B, C, D)
DC6	20–21	A1,X	Flag indicating a note at the end of relevant volume
DCM1	22–23	I1,X	Number of solutions pertaining to the system, N_S
DCM2	24–26	I2,X	Number of components in this solution, N_C
DCM3	27–29	I2,X	Number of free parameters in this solution, N_P
DCM4	30–32	I2,X	Number of correlation records in this solution, N_R
DCM5	33–37	A4,X	This field contains the word 'COMP'
DCM6	38–40	I2,X	Sequential component number in this solution (1 to N_C)
DC7	41–42	A1,X	Component identifier (A, B, C, ...)
DC8	43–49	I6,X	Hipparcos Catalogue (HIP) identifier
DC9	50–56	F6.3,X	Magnitude of component, Hp (mag)
DC10	57–62	F5.3,X	Standard error of Hp magnitude, σ_{Hp} (mag)
DC11	63–69	F6.3,X †	Magnitude of component, B_T (mag)
DC12	70–75	F5.3,X †	Standard error of B_T magnitude, σ_{B_T} (mag)
DC13	76–82	F6.3,X †	Magnitude of component, V_T (mag)
DC14	83–88	F5.3,X †	Standard error of V_T magnitude, σ_{V_T} (mag)
DC15	89–101	F12.8,X	Right ascension, α (deg)
DC16	102–114	F12.8,X	Declination, δ (deg)
DC17	115–122	F7.2,X	Trigonometric parallax, π (mas)
DC18	123–131	F8.2,X	Proper motion in right ascension, $\mu_{\alpha *}$ (mas/yr)
DC19	132–140	F8.2,X	Proper motion in declination, μ_δ (mas/yr)
DC20	141–147	F6.2,X	Standard error of α, $\sigma_{\alpha *}$ (mas)
DC21	148–154	F6.2,X	Standard error of δ, σ_δ (mas)
DC22	155–161	F6.2,X	Standard error of π, σ_π (mas)
DC23	162–168	F6.2,X	Standard error of $\mu_{\alpha *}$, $\sigma_{\mu_{\alpha *}}$ (mas/yr)
DC24	169–175	F6.2,X	Standard error of μ_δ, σ_{μ_δ} (mas/yr)
DC25	176–177	A1,X	Reference component for the data in Fields DC26–29
DC26	178–185	F7.3,X †	Position angle relative to reference component, θ (deg)
DC27	186–194	F8.3,X †	Separation from reference component, ϱ (arcsec)
DC28	195–203	F8.3,X †	Rate of change of θ, $\mathrm{d}\theta/\mathrm{d}t$ (deg/yr)
DC29	204–210	F6.3,X †	Rate of change of ϱ, $\mathrm{d}\varrho/\mathrm{d}t$ (arcsec/yr)
DCM7	211–213	I2,X ‡	Sequential record number for the reference component in Field DC25
DCM8	214–238	6I1,19X	Status flags for Hp, α, δ, π, $\mu_{\alpha *}$ and μ_δ: 1 = estimated 0 = constrained to the value for the first component

† blank if undefined ‡ set to zero if Field DC25 is blank

Table 2.3.2b. The Machine-Readable DMSA/C: Correlation Record

Fields designated DCM... appear only in the machine-readable catalogue
Bytes 1–32 are copied from the corresponding component records

Field	Bytes	Format	Description
DC1	1–11	A10,X	System identifier (CCDM number)
DC2	12–13	I1,X	Solution identifier, S (1 to N_S)
DC3	14–15	A1,X	Type of solution (F, I, L)
DC4	16–17	A1,X	Source of solution (C, F, N)
DC5	18–19	A1,X	Quality of solution (A, B, C, D)
DC6	20–21	A1,X	Flag indicating a note
DCM1	22–23	I1,X	Number of solutions pertaining to the system, N_S
DCM2	24–26	I2,X	Number of components in this solution, N_C
DCM3	27–29	I2,X	Number of free parameters in this solution, N_P
DCM4	30–32	I2,X	Number of correlation records in this solution, N_R
DCM5	33–37	A4,X	This field contains the word 'CORR'
DCM6	38–40	I2,X	Sequential number of this correlation record (1 to N_R)
DCM9	41–238	66I3 ‡	Up to 66 correlation coefficients in a non-linear coding

† blank if undefined ‡ trailing undefined values are blank

The correlation records contain the correlation coefficients among the maximum set of $6N_C$ parameters (i.e. Hp_i, α_i, δ_i, π_i, $\mu_{\alpha*i}$, $\mu_{\delta i}$ for each component, $i = 1, \ldots, N_C$). The number of correlation coefficients is $6N_C(6N_C - 1)/2 = 66$, 153, and 276 for $N_C = 2$, 3, and 4. A correlation record contains up to 66 coefficients; thus respectively 1, 3 and 5 records are needed for a double, triple or quadruple star. The order of the correlation coefficients is indicated by the table below. They are coded as integers between −99 and 999 using the arcsine transformation (Equation 2.3.16).

Depending on the solution type (Field DC3) some of the parameters may be common for the components, in which case the correlation coefficients are replicated for the respective parameters. For instance, a double star solution of type L implies that $\pi_2 = \pi_1$; then $\rho_{37} = \rho_4$, $\rho_{38} = \rho_5$, $\rho_{39} = \rho_6$, $\rho_{40} = 1$, etc. The subset of 'active' (free, or non-redundant) parameters ($N_P \le 6N_C$) is defined by the status flags in Field DCM8 of the component records.

	Hp_1	α_1	δ_1	π_1	$\mu_{\alpha*1}$	$\mu_{\delta1}$	Hp_2	α_2	δ_2	π_2	$\mu_{\alpha*2}$	$\mu_{\delta2}$	Hp_3	...
Hp_1	1	ρ_1	ρ_2	ρ_4	ρ_7	ρ_{11}	ρ_{16}	ρ_{22}	ρ_{29}	ρ_{37}	ρ_{46}	ρ_{56}	ρ_{67}	⋯
α_1	ρ_1	1	ρ_3	ρ_5	ρ_8	ρ_{12}	ρ_{17}	ρ_{23}	ρ_{30}	ρ_{38}	ρ_{47}	ρ_{57}	ρ_{68}	⋯
δ_1	ρ_2	ρ_3	1	ρ_6	ρ_9	ρ_{13}	ρ_{18}	ρ_{24}	ρ_{31}	ρ_{39}	ρ_{48}	ρ_{58}	ρ_{69}	⋯
π_1	ρ_4	ρ_5	ρ_6	1	ρ_{10}	ρ_{14}	ρ_{19}	ρ_{25}	ρ_{32}	ρ_{40}	ρ_{49}	ρ_{59}	ρ_{70}	⋯
$\mu_{\alpha*1}$	ρ_7	ρ_8	ρ_9	ρ_{10}	1	ρ_{15}	ρ_{20}	ρ_{26}	ρ_{33}	ρ_{41}	ρ_{50}	ρ_{60}	ρ_{71}	⋯
$\mu_{\delta1}$	ρ_{11}	ρ_{12}	ρ_{13}	ρ_{14}	ρ_{15}	1	ρ_{21}	ρ_{27}	ρ_{34}	ρ_{42}	ρ_{51}	ρ_{61}	ρ_{72}	⋯
Hp_2	ρ_{16}	ρ_{17}	ρ_{18}	ρ_{19}	ρ_{20}	ρ_{21}	1	ρ_{28}	ρ_{35}	ρ_{43}	ρ_{52}	ρ_{62}	ρ_{73}	⋯
α_2	ρ_{22}	ρ_{23}	ρ_{24}	ρ_{25}	ρ_{26}	ρ_{27}	ρ_{28}	1	ρ_{36}	ρ_{44}	ρ_{53}	ρ_{63}	ρ_{74}	⋯
δ_2	ρ_{29}	ρ_{30}	ρ_{31}	ρ_{32}	ρ_{33}	ρ_{34}	ρ_{35}	ρ_{36}	1	ρ_{45}	ρ_{54}	ρ_{64}	ρ_{75}	⋯
π_2	ρ_{37}	ρ_{38}	ρ_{39}	ρ_{40}	ρ_{41}	ρ_{42}	ρ_{43}	ρ_{44}	ρ_{45}	1	ρ_{55}	ρ_{65}	ρ_{76}	⋯
$\mu_{\alpha*2}$	ρ_{46}	ρ_{47}	ρ_{48}	ρ_{49}	ρ_{50}	ρ_{51}	ρ_{52}	ρ_{53}	ρ_{54}	ρ_{55}	1	ρ_{66}	ρ_{77}	⋯
$\mu_{\delta2}$	ρ_{56}	ρ_{57}	ρ_{58}	ρ_{59}	ρ_{60}	ρ_{61}	ρ_{62}	ρ_{63}	ρ_{64}	ρ_{65}	ρ_{66}	1	ρ_{78}	⋯
Hp_3	ρ_{67}	ρ_{68}	ρ_{69}	ρ_{70}	ρ_{71}	ρ_{72}	ρ_{73}	ρ_{74}	ρ_{75}	ρ_{76}	ρ_{77}	ρ_{78}	1	⋯
⋮	⋮	⋮	⋮	⋮	⋮	⋮	⋮	⋮	⋮	⋮	⋮	⋮	⋮	

Table 2.3.3. The Machine-Readable DMSA/G

Fields designated DGM... appear only in the machine-readable catalogue

Field	Bytes	Format	Description
DG1	1–7	I6,X	Hipparcos Catalogue (HIP) identifier
DG2	8–15	F7.2,X	$g_{\alpha*} = \mathrm{d}\mu_{\alpha*}/\mathrm{d}t$ at J1991.25 (mas/yr^2)
DG3	16–23	F7.2,X	$g_\delta = \mathrm{d}\mu_\delta/\mathrm{d}t$ at J1991.25 (mas/yr^2)
DG4	24–31	F7.2,X	Standard error of $g_{\alpha*}$, $\sigma_{g_{\alpha*}}$ (mas/yr^2)
DG5	32–39	F7.2,X	Standard error of g_δ, σ_{g_δ} (mas/yr^2)
DG6	40–45	F5.2,X	Significance of the g terms, F_g
DG7	46–53	F7.2,X †	$\dot{g}_{\alpha*} = \mathrm{d}^2\mu_{\alpha*}/\mathrm{d}t^2$ at J1991.25 (mas/yr^3)
DG8	54–61	F7.2,X †	$\dot{g}_\delta = \mathrm{d}^2\mu_\delta/\mathrm{d}t^2$ at J1991.25 (mas/yr^3)
DG9	62–69	F7.2,X †	Standard error of $\dot{g}_{\alpha*}$, $\sigma_{\dot{g}_{\alpha*}}$ (mas/yr^3)
DG10	70–77	F7.2,X †	Standard error of $\dot{g}_\delta$, $\sigma_{\dot{g}_\delta}$ (mas/yr^3)
DG11	78–83	F5.2,X †	Significance of the $\dot{g}$ terms, $F_{\dot{g}}$
DG12	84–85	A1,X	Flag indicating a note at the end of relevant volume
DGM1	86–87	I1,X	Number of astrometric parameters, n = 7 or 9
DGM2	88–195	36I3 †	(Up to) 36 correlation coefficients in a non-linear coding

† blank for undefined values

The complete set of $n(n-1)/2$ correlation coefficients (where $n = 7$ for a quadratic and $n = 9$ for a cubic model of the photocentric motion) is given in the order indicated by the following table:

	α	δ	π	$\mu_{\alpha*}$	μ_δ	$g_{\alpha*}$	g_δ	$\dot{g}_{\alpha*}$	$\dot{g}_\delta$
α	1	ρ_1	ρ_2	ρ_4	ρ_7	ρ_{11}	ρ_{16}	ρ_{22}	ρ_{29}
δ	ρ_1	1	ρ_3	ρ_5	ρ_8	ρ_{12}	ρ_{17}	ρ_{23}	ρ_{30}
π	ρ_2	ρ_3	1	ρ_6	ρ_9	ρ_{13}	ρ_{18}	ρ_{24}	ρ_{31}
$\mu_{\alpha*}$	ρ_4	ρ_5	ρ_6	1	ρ_{10}	ρ_{14}	ρ_{19}	ρ_{25}	ρ_{32}
μ_δ	ρ_7	ρ_8	ρ_9	ρ_{10}	1	ρ_{15}	ρ_{20}	ρ_{26}	ρ_{33}
$g_{\alpha*}$	ρ_{11}	ρ_{12}	ρ_{13}	ρ_{14}	ρ_{15}	1	ρ_{21}	ρ_{27}	ρ_{34}
g_δ	ρ_{16}	ρ_{17}	ρ_{18}	ρ_{19}	ρ_{20}	ρ_{21}	1	ρ_{28}	ρ_{35}
$\dot{g}_{\alpha*}$	ρ_{22}	ρ_{23}	ρ_{24}	ρ_{25}	ρ_{26}	ρ_{27}	ρ_{28}	1	ρ_{36}
$\dot{g}_\delta$	ρ_{29}	ρ_{30}	ρ_{31}	ρ_{32}	ρ_{33}	ρ_{34}	ρ_{35}	ρ_{36}	1

ρ_{22} to ρ_{36} are blank if $n = 7$. All correlation coefficients are coded as integers between −99 and 999 using the arcsine transformation (Equation 2.3.16). Note that ρ_1 to ρ_{10} are also given, to the nearest percentages, in the main catalogue (Fields H19–28).

Table 2.3.4a. The Machine-Readable DMSA/O (Data)

Fields designated DOM... appear only in the machine-readable catalogue

Field	Bytes	Format	Description
DO1	1–7	I6,X	Hipparcos Catalogue (HIP) identifier
DO2	8–18	F10.4,X	Orbital period, P (days)
DO3	19–30	F11.4,X	Time of periastron passage, T (days from JD2 440 000.0)
DO4	31–39	F8.2,X	Semi-major axis of photocentre orbit, a_0 (mas)
DO5	40–46	F6.4,X	Eccentricity, e
DO6	47–53	F6.2,X	Argument of periastron, ω (deg)
DO7	54–60	F6.2,X	Inclination, i (deg)
DO8	61–67	F6.2,X	Position angle of the node, Ω (deg)
DO9	68–76	F8.4,X †	Standard error of P (days)
DO10	77–86	F9.4,X †	Standard error of T (days)
DO11	87–92	F5.2,X †	Standard error of a_0 (mas)
DO12	93–99	F6.4,X †	Standard error of e
DO13	100–106	F6.2,X †	Standard error of ω (deg)
DO14	107–113	F6.2,X †	Standard error of i (deg)
DO15	114–120	F6.2,X †	Standard error of Ω (deg)
DO16	121–124	I3,X	Reference to the literature for the orbital parameters
DO17	125–126	A1,X	Flag indicating a note at the end of relevant volume
DOM1	127–139	12I1,X	Status flags for the 12 astrometric and orbital parameters taken in the order indicated below (1 = estimated, 0 = not estimated)
DOM2	140–337	66I3	66 correlation coefficients in a non-linear coding

† blank if the element is not estimated but assumed or adopted from the literature (status 0 in Field DOM1)

The order of the correlation coefficients in Field DOM2 is indicated by the table below. Correlation coefficients which are undefined (corresponding to blanks in the standard error Fields DO9–15, and a status flag = 0 in Field DOM1) are set to zero. The table also indicates the order of the 12 astrometric and orbital parameters relevant for the status flags. All correlation coefficients are coded as integers between −99 and 999 using the arcsine transformation (Equation 2.3.16); undefined values are thus coded as 450. Note that ρ_1 to ρ_{10} are also given, to the nearest percentages, in the main catalogue (Fields H19–28).

	α	δ	π	$\mu_{\alpha*}$	μ_δ	P	T	a_0	e	ω	i	Ω
α	1	ρ_1	ρ_2	ρ_4	ρ_7	ρ_{11}	ρ_{16}	ρ_{22}	ρ_{29}	ρ_{37}	ρ_{46}	ρ_{56}
δ	ρ_1	1	ρ_3	ρ_5	ρ_8	ρ_{12}	ρ_{17}	ρ_{23}	ρ_{30}	ρ_{38}	ρ_{47}	ρ_{57}
π	ρ_2	ρ_3	1	ρ_6	ρ_9	ρ_{13}	ρ_{18}	ρ_{24}	ρ_{31}	ρ_{39}	ρ_{48}	ρ_{58}
$\mu_{\alpha*}$	ρ_4	ρ_5	ρ_6	1	ρ_{10}	ρ_{14}	ρ_{19}	ρ_{25}	ρ_{32}	ρ_{40}	ρ_{49}	ρ_{59}
μ_δ	ρ_7	ρ_8	ρ_9	ρ_{10}	1	ρ_{15}	ρ_{20}	ρ_{26}	ρ_{33}	ρ_{41}	ρ_{50}	ρ_{60}
P	ρ_{11}	ρ_{12}	ρ_{13}	ρ_{14}	ρ_{15}	1	ρ_{21}	ρ_{27}	ρ_{34}	ρ_{42}	ρ_{51}	ρ_{61}
T	ρ_{16}	ρ_{17}	ρ_{18}	ρ_{19}	ρ_{20}	ρ_{21}	1	ρ_{28}	ρ_{35}	ρ_{43}	ρ_{52}	ρ_{62}
a_0	ρ_{22}	ρ_{23}	ρ_{24}	ρ_{25}	ρ_{26}	ρ_{27}	ρ_{28}	1	ρ_{36}	ρ_{44}	ρ_{53}	ρ_{63}
e	ρ_{29}	ρ_{30}	ρ_{31}	ρ_{32}	ρ_{33}	ρ_{34}	ρ_{35}	ρ_{36}	1	ρ_{45}	ρ_{54}	ρ_{64}
ω	ρ_{37}	ρ_{38}	ρ_{39}	ρ_{40}	ρ_{41}	ρ_{42}	ρ_{43}	ρ_{44}	ρ_{45}	1	ρ_{55}	ρ_{65}
i	ρ_{46}	ρ_{47}	ρ_{48}	ρ_{49}	ρ_{50}	ρ_{51}	ρ_{52}	ρ_{53}	ρ_{54}	ρ_{55}	1	ρ_{66}
Ω	ρ_{56}	ρ_{57}	ρ_{58}	ρ_{59}	ρ_{60}	ρ_{61}	ρ_{62}	ρ_{63}	ρ_{64}	ρ_{65}	ρ_{66}	1

Table 2.3.4b. References to DMSA/O

This file is an alphabetical list of references to the literature for orbital elements adopted in the orbital solutions or used as starting values for the solution. The references are numbered sequentially, with Field DO16 in Table 2.3.4a pointing to the relevant reference. Each reference consists of up to nine lines of text, with a maximum of 72 characters in each line.

Fields designated DOM... appear only in the machine-readable catalogue

Field	Bytes	Format	Description
DO16	1–4	I3,X	Reference number from Field DO16
DOM3	5–6	I1,X	Number of records (N) under this reference number
DOM4	7–8	I1,X	Sequential number (1 to N) of this record
DOM5	9–80	A72	Text

Table 2.3.5. The Machine-Readable DMSA/V

Fields designated DVM... appear only in the machine-readable catalogue

Field	Bytes	Format	Description
DV1	1–7	I6,X	Hipparcos Catalogue (HIP) identifier
DV2	8–13	F5.2,X	Adopted reference magnitude, $Hp_{\rm ref}$ (mag)
DV3	14–21	F7.2,X	VIM element in right ascension, $D_{\alpha *}$ (mas)
DV4	22–29	F7.2,X	VIM element in declination, D_δ (mas)
DV5	30–37	F7.2,X	Standard error of $D_{\alpha *}$, $\sigma_{D_{\alpha *}}$ (mas)
DV6	38–45	F7.2,X	Standard error of D_δ, σ_{D_δ} (mas)
DV7	46–51	F5.2,X	Significance of the VIM elements, F_D
DV8	52–58	F6.2,X	Position angle of the constant component, $\theta_{\rm C}$ (deg)
DV9	59–65	F6.2,X	Standard error of the position angle, $\sigma_{\theta_{\rm C}}$ (deg)
DV10	66–72	F6.1,X	Lower limit for the separation of the binary, $\varrho_{\rm min}$ (mas)
DV11	73–79	F6.1,X	Displacement of photocentre between maximum and minimum luminosity, $d_{\rm var}$ (mas)
DV12	80–81	A1,X	Flag indicating a note at the end of relevant volume
DVM1	82–144	21I3	21 correlation coefficients in a non-linear coding

The correlation coefficients in Field DVM1 are given in the sequence indicated by the following table:

	α	δ	π	$\mu_{\alpha *}$	μ_δ	$D_{\alpha *}$	D_δ
α	1	ρ_1	ρ_2	ρ_4	ρ_7	ρ_{11}	ρ_{16}
δ	ρ_1	1	ρ_3	ρ_5	ρ_8	ρ_{12}	ρ_{17}
π	ρ_2	ρ_3	1	ρ_6	ρ_9	ρ_{13}	ρ_{18}
$\mu_{\alpha *}$	ρ_4	ρ_5	ρ_6	1	ρ_{10}	ρ_{14}	ρ_{19}
μ_δ	ρ_7	ρ_8	ρ_9	ρ_{10}	1	ρ_{15}	ρ_{20}
$D_{\alpha *}$	ρ_{11}	ρ_{12}	ρ_{13}	ρ_{14}	ρ_{15}	1	ρ_{21}
D_δ	ρ_{16}	ρ_{17}	ρ_{18}	ρ_{19}	ρ_{20}	ρ_{21}	1

All correlation coefficients are coded as integers between −99 and 999 using the arcsine transformation (Equation 2.3.16). Note that ρ_1 to ρ_{10} are also given, to the nearest percentages, in the main catalogue (Fields H19–28).

Table 2.3.6. The Machine-Readable DMSA/X

Field	Bytes	Format	Description
DX1	1–7	I6,X	Hipparcos Catalogue (HIP) identifier
DX2	8–14	F6.2,X	Cosmic error, ϵ (mas)
DX3	15–21	F6.2,X	Standard error of ϵ, σ_ϵ (mas)
DX4	22	A1	Flag indicating a note at the end of relevant volume

Section 2.4

Hipparcos Catalogue: Variability Annex

2.4. Hipparcos Catalogue: Variability Annex

The variability annex has been compiled from an analysis of the (calibrated) Hipparcos epoch photometry data, described in Section 2.5. The variability annex is divided into two tabular sections (contained in Volume 11 of the printed catalogue), with three additional parts containing light curves or folded light curves (contained in Volume 12 of the printed catalogue). The criteria for including an object in the Variability Annex are described in Section 1.3.5.

The results presented in the context of the Hipparcos Catalogue publication are inevitably a compromise between the objectives of the data analysis groups to provide useful variability classification at the time of the catalogue publication, and the conflicting requirement to make the final catalogue available as rapidly as possible. Terms such as 'newly-discovered as variable by Hipparcos', assigned variability types, or inferred absence of variability, should be understood in this context.

Description of the Tabular Data

Volume 11, Section 1 is the subset of variable stars ('periodic variables') for which a period and variability amplitude has been derived on the basis of the Hipparcos data. There are also cases where the Hipparcos data were insufficient to determine a period but, when folded with the period given in the literature, confirm that period—in some cases this has provided a new determination of the reference epoch. In nearly 200 cases, mainly involving Algol-type eclipsing binaries, for which the Hipparcos observations covered the full period of the light curves inadequately, periods and reference epochs from the literature were used to fold the data. In these cases, an object may appear in the section of periodic variables even though no period is given in the main catalogue, Field H51.

Volume 11, Section 2 contains relevant information for what are referred to as 'unsolved variables', i.e. for objects which could be classified as variable on the basis of the Hipparcos data, but for which periods could not be determined from the Hipparcos data, or where Hipparcos could not confirm a periodicity given in the literature. The majority of these are small-amplitude variables ('micro-variables' without established periods are flagged 'M' in Field H52 of the main Hipparcos Catalogue, and are not included in the sections on periodic or unsolved variables). Consequently, in those cases where the Hipparcos observations have been unable to confirm a period given in the literature, an object may appear in the section of unsolved variables, even though a period may have been given in the literature (Field U18).

Both tabular sections are organised according to the Hipparcos Catalogue (HIP) identifier. A flag in the main catalogue, Field H53, takes the value '1' or '2' depending on the section where the given object is to be found.

Both sections have a similar structure, with spectral type and variability type given (generally from the literature where known), along with information on the period,

maximum and minimum magnitudes, variable star name, and other related information from the literature. For the periodic variables, information on the period and estimated values of the maximum and minimum *Hp* magnitudes from the light-curve fitting are given, while directly observed quantities are given in the case of the unsolved variables. In both cases, notes or cross-references to published light curves are given.

Within the section devoted to unsolved variables, the reference epoch and period from the literature are mainly of relevance for the semi-regular variables, where Hipparcos has been unable to confirm or update the period given in the literature—in most of these cases the information in these fields is only of historical interest, with periods given in the literature frequently being unconfirmed in the Hipparcos data.

Information entered in Fields P18–P22 and U18–U22 is largely taken from the General Catalogue of Variable Stars, 4th edition GCVS; P.N. Kholopov *et al.*, Publ. Office 'Nauka', Moscow, 1985–88) and its updates, either through the CDS (Strasbourg), or from the data base of the American Association of Variable Star Observers (AAVSO), as communicated by J. Mattei. There has not been a systematic attempt to incorporate similar published information from other sources. In a few cases, information from the recent literature has been added in these fields to support the interpretation of the Hipparcos results.

Description of the Light Curves

Field P15 in the periodic variables, and Field U15 in the unsolved variables, contains a pointer to one of the three sections of light curves contained in Volume 12. These sections provide light curves extending over the total mission duration in the case of the non-periodic variables, or folded light curves in those cases where periods are available or have been derived. A section is also devoted to objects for which light curves supplied by the AAVSO have been transformed to the same photometric system, and superimposed on the Hipparcos results (these may be periodic or non-periodic).

Fields P1–19: Periodic Variables

Field P1: The Hipparcos Catalogue (HIP) identifier

The variability annex contains no provision for a component identifier. Even though in some cases there are double/multiple star solutions with individual photometry for two variable components, it has almost always been preferable to fix the magnitude of one component, and solve for only one variable. This means that the only difference between the 'combined photometry' and the 'component photometry' is a fixed amount of subtracted light. In the large majority of cases, the primary has been assumed to be the variable component, but for a few tens of cases, there is good evidence that the variability originates mainly in the secondary. This information has been indicated in a note to the entry in the Double and Multiple Systems Annex (Part C).

Field P2: Flag for newly-classified variable entries

A flag (*) indicates that the object has been newly-classified as variable on the basis of the Hipparcos observations and the preliminary variability analysis.

Field P3: Spectral type

The spectral type has generally been taken from the SIMBAD data base of the CDS, Strasbourg, and updated by the Hipparcos Input Catalogue Consortium in some cases. Spectral types given in the Hipparcos Input Catalogue were frequently truncated (e.g. B8+... for B8+K2Ibe; for most eclipsing variables, the type of the hotter component was generally given, even if fainter). Since Field P3 gives the full description of the spectral type, and because of the updating, there are certain inconsistencies between the HIP spectral types (given here) and those given in the Hipparcos Input Catalogue.

Field P4: 1-letter variability type

This field repeats the single-character variability identifier given in the Hipparcos Catalogue, Field H52. It is 'P' for all entries contained in the section on periodic variables, except for one entry, for which the $(V-I)$ colour was revised (see Field H52) and which is consequently indicated by 'R'.

Field P5: 6-letter variability type

The 6-letter variability type was taken, when available, from the GCVS and NSV Catalogues. Table 2.4.1 summarises the main types of variability given in these source catalogues (e.g. eruptive, pulsating, rotating, cataclysmic, and eclipsing stars). A semicolon, ':', following the variability type indicates that the type is uncertain. The type 'SR' has been used to indicate not only semi-regular pulsating stars, but also other apparently semi-regular light curves, and could also include some rotational modulation variables. Where appropriate, updated or newly-defined variability types have been entered, according to the preliminary analysis of the Hipparcos photometric data.

Table 2.4.1. Types of variability

Code	Description	Class of Variable
ACV	α^2 Canum Venaticorum type (including ACVO)	rotating
ACYG	α Cygni type	pulsating
BCEP	β Cephei type (including BCEPS)	pulsating
BY	BY Draconis type	rotating
CEP	Cepheids (including CEP(B))	pulsating
CST	constant stars (considered as variable by some observer(s))	–
CW	W Virginis type	pulsating
CWA	W Virginis type (periods > 8 days)	pulsating
CWB	W Virginis type (periods < 8 days)	pulsating
DCEP	δ Cephei type (including DCEPS)	pulsating
DSCT	δ Scuti type (including DSCTC)	pulsating
E	(E+, E/ ..)	eclipsing binary
EA	Algol type (EA+, EA/ ..)	eclipsing binary
EB	β Lyrae type (EB/ ..)	eclipsing binary
ELL	rotating ellipsoidal (ELL+.. or /..)	rotating
EW	W Ursae Majoris type (EW/ ..)	eclipsing binary
FKCOM	FK Comae Berenices type	rotating
GCAS	γ Cassiopeiae type	eruptive
I	irregular (I, IA, IB, In, InT, Is)	eruptive
IN	irregular (INA, INAT, INB, INSA, INSB, INST, INT)	eruptive
IS	irregular (ISA, ISB)	eruptive
L	slow irregular (L, LB, LC)	pulsating
M	Mira Ceti type	pulsating
N	slow novae (NB, NC)	cataclysmic
NA	fast novae	cataclysmic
NL	nova-like	cataclysmic
NR	recurrent novae	cataclysmic
PVTEL	PV Telescopii type	pulsating
RCB	R Coronae Borealis type	eruptive
RR	RR Lyrae type (RR, RRAB, RRB, RRC)	pulsating
RS	RS Canum Venaticorum type	eruptive
RV	RV Tauri type (RV, RVA, RVB)	pulsating
SARV	small-amplitude red variables	pulsating/rotating
SDOR	S Doradus type	eruptive
SPB	slowly pulsating B stars	pulsating
SR	semi-regular (SR, SRA, SRB, SRC, SRD)	pulsating
SXARI	SX Arietis type	rotating
SXPHE	SX Phœnicis type	pulsating
UV	UV Ceti type	eruptive
WR	Wolf-Rayet	eruptive
XNG	X-ray nova-like system	X-ray binary
XP	X-ray pulsar	X-ray binary
ZAND	Z Andromedae type	cataclysmic

Field P6: Flag indicating newly-assigned variability type

A flag (*) indicates that a previously known variable has been assigned a different variability type in Field P5 than that previously given in the literature, on the basis of the Hipparcos analysis (a flag in Field P6 therefore never coincides with a newly-discovered variable flag in Field P2). Further details are given in the notes.

Field P7–9: Magnitudes at maximum and minimum luminosities

Fields P7 and P9 provide the magnitudes at maximum and minimum luminosities. These were derived from (folded) light-curve fitting on the basis of the *Hp* photometry for approximately 90 per cent of the stars in the section of periodic variables. These cases are assigned an associated error value in Field P10. The remaining 10 per cent (where no value is given in Field P10) had these magnitudes estimated from the light curves; in these cases the estimated errors on the period (Field P12) and reference phase (Field P14) were based on general relations between periods and accuracies.

A flag (>) in Field P8 indicates that the true magnitude at minimum luminosity is likely to be larger than the value of $Hp_{\rm min}$ given in Field P9.

For large-amplitude and faint variables, the fitted light-curve generally gives a more reliable estimate of $Hp_{\rm min}$, especially when the minimum is fainter than the detection threshold (cf. the AAVSO/Hipparcos light curves). For some stars with partial observations, fitting is not possible near the minimum, although it may be clear that the true minimum is fainter than the minimum luminosity observed.

Maximum and minimum magnitudes are given to 1, 2, or 3 decimal places, depending on the accuracy estimated for these values during the light-curve fitting process. The use of three decimals is generally only appropriate for the very brightest stars. The intrinsic uncertainty of the light-curve fitting, and the variability of the levels of the minima and maxima themselves, imply that resulting variations will typically be larger than 0.005 mag. In particular, for large amplitude or faint stars, only two or even one decimal are significant if σ_A/A (see Field P10) is large.

Some subjectivity is therefore involved in assigning the number of significant decimals. Appropriate caution should be exercised in their interpretation and, in general, users should establish their own reliability criteria on the basis of the epoch photometry data. Attention is drawn to the fact that interpretation of the significance of the machine-readable data, given as an ASCII string, must be carried out by explicitly testing for the number of significant digits retained.

The values given in Field P7 and P9 are generally different from the corresponding magnitudes at maximum and minimum luminosities given in the main Hipparcos Catalogue, Fields H49–50; the former having been derived from the light-curve fitting (and thus subject to modelling uncertainties), the latter having been strictly and consistently (for all objects with Field P4 having a value of U, P or R) derived from the 5th and 95th percentiles of the magnitude distribution respectively. The corresponding Fields H49–50 in the main Hipparcos Catalogue are given uniformally to 2 decimal digits.

Field P10: Relative error on the peak-to-peak amplitude, $\log_{10}(\sigma_A/A)$

An indication of the uncertainty on the magnitudes given in Fields P7–9 is given by σ_A/A, where A is the difference between the (fitted) magnitudes at maximum and minimum luminosity ($Hp_{\max} - Hp_{\min}$) given in Fields P7–9, and σ_A is the root-sum-square of the errors on the maximum and minimum magnitudes. The field is blank in some cases (see Fields P7–9).

The majority of known and newly-discovered small-amplitude variables have A in the range 0.005 mag for the brightest to 0.05 mag. For low signal-to-noise ratio, i.e. $\sigma_A/A > 0.05$, the fraction of solutions with spurious values of amplitude and period increases rapidly, to 50 per cent or more. In contrast, for large-amplitude variables σ_A/A, if not small, may reflect the irregularity of the light-curve. Thus σ_A is less related to A than σ_P is to P, since it depends on the amplitude/noise ratio, on the regularity of the variation, on the number of modes (which may be several in the case of early-type low-amplitude variables), and on the ratio between mode amplitudes. It also depends on the degrees of freedom used to fit the light-curve. When the amplitudes are small, non-linear effects disappear and a fit with a single harmonic leads to the most stable and physical solution. The maximum number of degrees of freedom used for the folded-curve fitting depended on the character of the light curve, and the number of data points available, as well as on the intrinsic errors on the measurements relative to the amplitude of the light curve. Consequently, the determination of σ_A/A is also dependent on the adopted fitting method. In summary, $\log_{10}(\sigma_A/A)$ provides a crude classification of the variability amplitudes.

The photometric reductions were made assuming a measured or derived value of $V - I$. Because of the chromatic ageing of the instrument's optics, there may be differences between the true and the derived light-curves due to this adopted value. An incorrect value of $V - I$ may lead, for example, to a spurious linear trend of the calibrated Hipparcos photometry with time. Similarly, for variable objects where $V - I$ varies with phase, the simplistic assumption of a mean $V - I$ index at mean magnitude will contribute to an error on the magnitude and on σ_A (see Field H52 and Section 1.3.4 for further details).

Field P11: Mean period during the mission, derived from the Hipparcos data (days)

The Hipparcos Catalogue provides the variability period (Field H51) uniformally truncated to 2 decimal places for reasons of catalogue presentation and user convenience. The wide variation of variability periods and corresponding precisions means that it would strictly be more appropriate to present a variable number of decimal digits (inconvenient for the machine-readable catalogue), or express the variability period as $1/P$ or $\log(P)$ (inconvenient for visual inspection of the printed catalogue).

In the Variability Annex, a more complete description of the variability type and period is given, and a variable number of decimal digits has been adopted in order to reflect the significance of the derived period (the error being approximately proportional to the square of the period). Depending on the quality of the solution, and the stability of the period, this means that for a period below 0.1 day, some 5–6 positions following the decimal point are significant, while for a 300-day period the significance is at best a few days.

While convenient for visual inspection of the printed catalogue, a variable number of decimal digits is less tractable for the machine-readable version, where the number of trailing blanks must be specifically determined. See further comments under the description of Field P12.

Field P12: Precision on the period, $\log_{10}\sigma_P$

Field P12 provides $\log_{10}\sigma_P$ to one decimal place. As noted under the description of the period (Field P11) the use of a variable number of significant decimal digits for the period is convenient for the printed catalogue, but inconvenient for the machine-readable version, where assessment of significance would need to be based on the number of trailing blanks. $\log_{10}\sigma_P$ is almost the same as the (negative) number of significant decimals, but it is more well-defined and provides uniform relative precision on σ_P.

The number of significant decimal digits in the period (Field P11) and in the reference epoch (Field P13) are closely related through the error estimate on the period, which itself is rather unreliable. The error given on the period depends on the resulting curve-fit, and can be underestimated rather easily: the relevant factor is the derivative of the fitted curve and measurements contribute weight according to this derivative. A slightly poorer fit tends to produce locally higher derivatives due to unrealistic and uncontrolled fluctuations of the fitted curve. While acting as weights, these derivatives distort the real amount of period information contained in the data. However, what is also to be avoided is a loss of precision on the phase of the light-curve at any time during the mission, since the phase error is directly proportional to $N_{\rm cycles}\times\sigma_P$.

Field P13: Reference epoch from solution, BJD(TT)−2 440 000.0

In general, this gives the epoch of the first zero phase after JD 2 448 500. The phase of the maximum is used, except for eclipsing binaries and RV Tau variables where the zero phase is determined by the phase of the primary minimum (which can be ambiguous in the case of EW and some EA types).

The reference epoch is usually given to (a maximum of) 3 decimals (i.e, to a maximum precision of 86 s); providing four decimal places is not justified except in one or two exceptional cases. In the printed and machine-readable catalogues, the number of trailing decimals is related to the precision on the reference epoch (Field P14), typically given to a precision of 0.01 times the period (with extremes from 0.1 for semi-regular variables to 0.002 for some Algol-like eclipsing binaries) with a minimum resolution of 1 day.

Field P14: Flag indicating precision on the reference epoch

If the proposed light-curve is reasonably well-behaved, the precision on the reference epoch, σ_ϕ, lies typically in the range 0–1 days. Since the precision of the reference epoch is itself rather inaccurate, this field contains an integer (in the range 0–5) indicating the significance of the reference epoch given in Field P13. The field gives $1-\log_{10}\sigma_\phi$, i.e. 0 for an accuracy of order 10 days, 1 for an accuracy of order 1 day, 2 for 0.1 day, 3 for 0.01 day, 4 for 0.001 day, and 5 for 0.0001 day. The field is blank if Field P13 is blank.

If Field P10 is blank the precision on the reference epoch was estimated on the basis of the period and type of light curve, rather than from the fitted light curve.

One purpose of providing the error on the reference epoch is to allow observers to evaluate the errors on the extrapolated Hipparcos light-curves before and after the mission. The traditional way of determining the reference epoch of a pulsating variable is from the phase of the maximum—often poorly defined. The phase of the folded light-curve is not necessarily determined precisely, and depends on several parameters, namely the level of regularity, the amplitude, and the shape of the light-curve (e.g. the number of harmonics used to describe it).

Field P15: Variability annex flag

A flag indicates that a light curve, or folded light curve, compiled from the Hipparcos *Hp* data, is provided in the corresponding variability annex (Volume 12). The flag is identical to that given in Field H54, and has the following meaning:

A : light curve, folded at the period given in Field P11;
B : light curve, fitted to the data derived and transformed from the data base of the AAVSO (American Association of Variable Star Observers);
C : light curve (not folded).

Most entries classified as a periodic variable have a folded light curve in Part A. Entries indicated with 'B', which takes precedence in this field, also have a curve in Part A if they are periodic (see also Field H54). A few very long-period variables are contained within the section of non-folded light curves (Part C).

Flag 'B' corresponds to large-amplitude variable stars which have been observed systematically by ground-based observers during the Hipparcos mission. In these cases, a combination of the Hipparcos and AAVSO data have allowed a more complete light curve to be derived, including refined estimates of the maximum or minimum magnitudes during the mission. Note that an entry for which the flag 'B' is set may also be contained in the section on folded light curves if it is periodic. The folded light curve, if available, is included at the relevant place according to its HIP running number.

Field P16: Flag indicating note

A flag indicates that a note is associated with the entry drawing attention, for example, to a discrepant period, amplitude, or variability type. The flag is also used to indicate that another solution is also possible, e.g. eclipsing or pulsating with period differing by a factor two, or any special feature of the light-curve. Notes on the variability are compiled with the literature references at the end of the variability annexes (Volume 11). The note flag has the same content and meaning as the flag used for the main Hipparcos Catalogue, Field H70 (where further details are given), thus:

D : double and multiple systems note only (Volume 10);
G : general note only (Volumes 5–9);
P : photometric (including variability) notes only (Volume 11);
W : 'D' + 'P' only;
X : 'G' + 'D' only;
Y : 'G' + 'P' only;
Z : 'G' + 'D' + 'P'.

Field P17: Variable star name

The variable star name has been taken from the literature if the star was already known to be variable. Names have been assigned under the auspices of the IAU by N.N. Samus and colleagues (Moscow) to Hipparcos stars with unambiguous status as newly-discovered variables.

The general Hipparcos and Tycho Catalogue publication policy has been to preserve full identity between the printed and machine-readable versions—and thus to use exclusively ASCII coding. Nevertheless, the use of Greek letters for the variable star names in the printed catalogue (Field P17 and U17) has been adopted as being more appropriate, with the phonetic equivalent being used in the machine-readable version.

The following table lists the adopted equivalence:

α	alf	ι	iot	ρ	rho
β	bet	κ	kap	σ	sig
γ	gam	λ	lam	τ	tau
δ	del	μ	mu.	υ	ups
ϵ	eps	ν	nu.	ϕ	phi
ζ	zet	ξ	ksi	χ	chi
η	eta	o	omi	ψ	psi
θ	the	π	pi.	ω	ome

Note that, as in SIMBAD, a dot is added to mu, nu, and pi, in order to make three letters; this is intended to ease distinction between, e.g. the variable star MU Cep and the Greek-letter name μ Cep. [SIMBAD also supports the conventions χ = 'khi', θ = 'tet'.]

In addition, an underscore is used in the machine-readable version to tie the two parts of the variable star name, in order to facilitate reading in of Fields P17 and U17 using standard text editors. Thus, β Lyr in the printed catalogue is represented as 'bet_Lyr' in the machine-readable catalogue.

Field P18: Period (days), taken from the literature

Field P19: Reference epoch from literature, Julian Date

Due to the range of reference epochs found in the literature, this field gives the complete Julian Date of the reference epoch. Note that the time scale used in the literature for the Julian Date specification (e.g. UTC, TT, with or without barycentric correction) is frequently omitted in the literature and is not specified here.

Field P20: Magnitude at maximum luminosity, taken from the literature

Field P21: Magnitude at minimum luminosity, taken from the literature

Field P22: Photometric band for the minimum and maximum magnitudes taken from the literature, given in Fields P20–21

The letters U, B, V, K, I, R refer to the Johnson broad-band system passbands, or closely related passbands. P refers to photographic magnitude, Y and b for the Strømgren y and b bands.

Field P23: Flag (R) indicating that references are given to the literature

References are included, with the notes, at the end of the variability annexes (Volume 11). See the main catalogue, Field H70, for further details of the relationship between this field and the note flag (Field P16).

Fields U1–19: Unsolved Variables

Field U1 ≡ Field P1: The Hipparcos Catalogue (HIP) identifier

Field U2 ≡ Field P2: Flag for newly-classified variable entries. Details as for Field P2.

Field U3 ≡ Field P3: Spectral type (details as for Field P3)

Field U4 ≡ Field P4: 1-letter variability type (details as for Field P4, with 21 entries indicated by 'R')

Field U5 ≡ Field P5: 6-letter variability type (details as for Field P5)

Field U6 ≡ Field P6: Flag indicating newly-assigned variability type (details as for Field P6)

Fields U7–9 ≡ Field P7–9: Magnitudes at maximum and minimum luminosities

Fields U7 and U9 provide the magnitudes at maximum and minimum luminosities observed during the mission, derived from the 5th and 95th percentiles. In certain cases, the AAVSO data may provide more relevant values for the magnitudes at maximum and minimum luminosities; where available, these are included in the notes.

These magnitudes are given to 1, 2, or 3 decimal places, depending on the accuracy estimated for these values (see Fields P7–P9 for further details).

Note that Fields U7 and U9, and the corresponding magnitudes at maximum and minimum luminosity given in the main Hipparcos Catalogue, Fields H49–50, are the same for the unsolved variables (unlike the case for the periodic variables, Fields P7 and P9), both having been derived strictly and consistently, for all objects with inferred variability larger than 0.03 mag, from the 5th and 95th percentiles of the magnitude distribution.

For small-amplitude variables, and multi-periodic or spotted stars, the percentile values could in principal have been corrected for the photon and reduction noise, although such a procedure would be subject to some uncertainties in the case of, e.g. irregular variables or Be stars. Such corrections have therefore not been made.

Field U10 ≢ Field P10: Median value of *Hp* (as given in the main Hipparcos Catalogue, Field H44)

Field U11 ≢ Field P11: Intrinsic variability amplitude, *A*

The intrinsic variability amplitude has been derived from the observed scatter, *s*, as given in Field H46, by correcting for reduction and photon noise—thus Field U11 is not precisely the same as Field H46. (The difference between raw and corrected scatter is negligible for large-amplitude variables but very significant for micro-variables.)

Field U12 ≢ Field P12: Standard error of A, σ_A

Field U13: Blank for unsolved variables

Field U14: Blank for unsolved variables

Field U15 ≡ Field P15: Variability annex flag

A flag indicates that a light curve, compiled from the Hipparcos *Hp* data, is provided in the corresponding variability annex (Volume 12). The flag is identical to that given in Field H54, and has the following meaning:

B : light curve, fitted to the data derived and transformed from the data base of the AAVSO (American Association of Variable Star Observers);

C : light curve (not folded).

[Flag 'A', which may appear in Field H54 of the main catalogue (indicating that a folded light curve is provided in Volume 12) is not relevant for unsolved variables.]

Field U16 ≡ Field P16: Flag indicating that a note is associated with the entry (see Field P16 for further details)

Field U17 ≡ Field P17: Variable star name (details as for Field P17)

Field U18 ≡ Field P18: Period (days), taken from the literature

Field U19 ≡ Field P19: Reference epoch from literature, Julian Date

The combination of unsolved variables with a meaningful reference epoch is rarely relevant, but applies to a few semi-regular variables where a period is not apparent from the Hipparcos data, and where Field U19 takes the reference epoch obtained from the literature.

Field U20 ≡ Field P20: Magnitude at maximum luminosity, taken from the literature

Field U21 ≡ Field P21: Magnitude at minimum luminosity, taken from the literature

Field U22 ≡ Field P22: Photometric band for the magnitudes given in Fields U20–21

Field U23 ≡ Field P23: Flag (R) indicating that references are given to the literature (see Field P23 for further details)

Table 2.4.2. Machine-readable Variability Annex

Field	Bytes	Format	Description
P1/U1	1– 7	I6,X	Identifier (HIP)
P2/U2	8– 9	A1,X	Flag if new variable
P3/U3	10– 22	A12,X	Spectral type
P4/U4	23– 24	A1,X	Variability type (1-letter)
P5/U5	25– 31	A6,X	Variability type (6-letter)
P6/U6	32– 33	A1,X	Flag if newly classified by Hipparcos
P7	34– 40	F6.3,X	Magnitude at max from curve fitting
U7	„	„	Magnitude at max from percentiles
P8/U8	41– 42	A1,X	Limit flag (>)
P9	43– 49	F6.3,X	Magnitude at min from curve fitting
U9	„	„	Magnitude at min from percentiles
P10	50– 56	2X,F4.1,X	$\log_{10}(\sigma_A/A)$
U10	„	F6.3,X	Median Hp (mag)
P11	57– 69	F12.7,X	Mean period (days)
U11	„	7X,F5.3,X	Intrinsic variability amplitude, A (mag)
P12	70– 76	2X,F4.1,X	$\log_{10}\sigma_P$
U12	„	F6.3,X	σ_A
P13	77– 86	F9.4,X	Epoch from solution (days)
U13	„	10X	Blank for unsolved variables
P14	87– 88	I1,X	Precision flag
U14	„	2X	Blank for unsolved variables
P15/U15	89– 90	A1,X	Annex flag
P16/U16	91– 92	A1,X	Note flag
P17/U17	93–105	A12,X	Variable star name[1]
P18/U18	106–116	F10.5,X	Period from literature (days)
P19/U19	117–127	F10.2,X	Epoch from literature (Julian Date)
P20/U20	128–133	F5.2,X	Magnitude at max from literature
P21/U21	134–139	F5.2,X	Magnitude at min from literature
P22/U22	140–141	A1,X	Photometric band
P23/U23	142	A1	Reference flag

[1] a different representation is used for the printed catalogue (see description of Field P17 for details)

Section 2.5

Hipparcos Catalogue: Epoch Photometry Annex (and Extension)

2.5. Hipparcos Catalogue: Epoch Photometry Annex (and Extension)

The results of the detailed Hipparcos epoch photometry have been compiled into the Hipparcos Catalogue Epoch Photometry Annex, ordered by HIP number.

The epoch photometry has been used to derive the median magnitudes and related statistics given in the Hipparcos Catalogue (Fields H44–48), and also the variability characteristics summarised in the Hipparcos Catalogue (Fields H49–54) and provided in detail within the Variability Annex (Section 2.4, and Volumes 11–12).

The Hipparcos Epoch Photometry Annex consists of three header records for each object in the Hipparcos Catalogue, containing summary photometric data for the object (Table 2.5.1), followed by N transit records, one record for every star transit in the Annex (Table 2.5.2). The transit records contain the transit time (i.e. the observation epoch), followed by the calibrated Hp magnitudes and related quantities, and flags providing further observational details. Transits are presented strictly in chronological order. For resolved systems, data are provided for the combined system, or for the individual components, as specified by the component flag, Field H H2.

The mean number of transits per star is roughly 110, varying approximately in the range 30–380, depending principally on the object's ecliptic latitude. This gives a total of some 13 million transits in the Hipparcos Catalogue Epoch Photometry Annex.

Hp magnitudes contained in the Hipparcos Catalogue and in the Epoch Photometry Annex (and where appearing without further qualification) refer to $Hp_{\rm dc}$, a magnitude estimate derived from the 'dc', or unmodulated, part of the signal intensity. Magnitude estimates derived from the 'ac', or modulated, part of the signal intensity are denoted $Hp_{\rm ac}$. $Hp_{\rm ac}$, and supplementary information related to the photometric reduction, are provided for more specialist use in the Epoch Photometry Annex Extension.

Further details of the derivation of $Hp_{\rm dc}$, and the difference between $Hp_{\rm dc}$ and $Hp_{\rm ac}$, can be found in Volume 3. Median values, as tabulated in the Hipparcos Catalogue (Field H44), are referred to in this section as $\overline{Hp}$ to distinguish them from the calibrated magnitudes derived for each transit. Usually, the difference between the individual transit value, and the median value derived from all transits for a given star, is clear from the context.

Description of the Hipparcos Epoch Photometry Annex

Header Records (Table 2.5.1)

The header structure follows closely the contents of the summary photometric data presented in the main catalogue, with the corresponding data content being identical. The header is divided into three records, each of 28 bytes, for consistency with the individual transit records (see Table 2.5.2). Note that *all* transits of each star are included in the file, with those considered photometrically suspect being flagged within the relevant transit record. Values given in the header records indicate the total number of transits in the file, $N_{\rm tot}$, and the number of photometrically accepted records, $N_{\rm acc}$.

Field HH1: HIP number

Field HH2: Component flag for a double or multiple entry

This indicates whether the subsequent photometric records refer to a photocentre (*), to one of the components (A, B,..), or to combined photometry from a multiple system (–). The flag has the same value as that given in the Hipparcos Catalogue, Field H48.

Field HH3: $V - I$ colour index used for the photometric reductions

As explained under Fields H40 and H52 of the main Hipparcos Catalogue, this value of $V - I$ (typically taken from ground-based observations) may subsequently have been found to be incorrect: a systematic linear trend of the calibrated Hp magnitude with time may have arisen specifically because of such an error. $V - I$ values given in Field H40 have been updated where relevant. Field HH3 gives the value of $V - I$ used for the photometric reductions (this value is also given in the Hipparcos Catalogue, Field H75); it is not necessarily the same as given in Field H40.

Field HH4: Total number of transits in the file, $N_{\rm tot}$

$N_{\rm tot}$ gives the number of individual transits for the star following the header.

The first and last observation epochs for a given star can be accessed through the first and last transit records. Transits that are considered photometrically suspect are flagged accordingly (see Field HT4).

Field HH5: Number of transits considered to be photometrically accepted, $N_{\rm acc}$

Generally, transits were not considered as photometrically accepted if any of bits 3–5 or 7–8 in Field HT4 were set. However, for all entries of 'two-pointing' double systems with separation less than about 35 arcsec (irrespective of whether or not they were resolved), and for all resolved single entries with separations larger than 10 arcsec, transits with bit 4 set were also photometrically accepted.

Only photometrically accepted transits were used for the determination of the median magnitude and related statistics given in Fields H44–48 of the main catalogue, and in Fields HH6–9 of this annex. The number of Hp observations listed in Field H47 is equal to the number of photometrically accepted transits, $N_{\rm acc}$, which is typically less than the total transits given in the Epoch Photometry Annex. As explained under Field HT4, transits with bit 6 set should also, ideally, have been excluded from those accepted photometrically, although this was not done in practice. Rigorous exclusion of transits with bit 6 set would, however, not have a large effect on the resulting statistics.

Field HH6: Median magnitude in the Hipparcos photometric system, $\overline{Hp}$

This value is generally the same as that given in the Hipparcos Catalogue, Field H44. There are differences in the case of two-pointing double systems (as explained in Section 1.3): for the faint companion of a 'two-pointing' double system Field HH6 is derived from the individual transits, while Field H44 of the main Hipparcos Catalogue was obtained from observations with the detector pointing at the brighter component, using the magnitude difference determined in the double star solution. Therefore, while the difference between the two median Hp magnitudes given in Field H44 for the two components is identical to the magnitude difference ΔHp given in Field H66 of the main Hipparcos Catalogue, this is not true for the magnitude difference based on Field HH6.

Field HH7: Standard error of the median magnitude, $\sigma_{\overline{Hp}}$

Typically this value is the same as that given in the Hipparcos Catalogue, Field H45. There are differences in the case of two-pointing double systems, as explained in Section 1.3.2.

Fields HH8–9: 5th and 95th percentiles of the epoch photometry data points

Typically these values are the same as those given in the Hipparcos Catalogue, Fields H49–50. There are differences in the case of two-pointing double systems, as explained in Section 1.3.2.

Field HH10: Variability period, P (days)

The period is as given in the Variability Annex, Section 2.4, Field P11. As explained in Section 2.4, the period given in the Variability Annex is given with greater precision than that in the Hipparcos Catalogue (Field H51).

Field HH11: Reference epoch, BJD(TT)−2 440 000.0

The reference epoch gives the epoch of the first zero phase after JD(TT) 2 448 500.0. See the Variability Annex, Section 2.4, Field P13, for further details.

Field HH12: 1-letter variability type

The 1-letter variability type is that given in the Hipparcos Catalogue (Field H52) and in the Variability Annex, Section 2.4, Field P4.

Field HH13: Annex flag

This flag, identical to that given in Field H53 of the main Hipparcos Catalogue, indicates that further data are tabulated in the Variability Annex (see Section 2.4, and Volume 11).

Field HH14: Annex flag

This flag, identical to that given in Field H54 of the main Hipparcos Catalogue, indicates that (folded) light curves are included in the Variability Annex (see Section 2.4, and Volume 12).

Description of the Hipparcos Epoch Photometry Annex
Individual Transit Record (Table 2.5.2)

Field HT1: Observation epoch

This is specified in (barycentric) Julian Date, with respect to JD(TT) 2 440 000.0.

Observation epochs are given in Terrestrial Time (TT), and have been corrected for light propagation time to the solar system barycentre. They are therefore referred to as BJD(TT). Observation epochs are given with a resolution of 10^{-5} days = 0.864 s.

Field HT2: Calibrated *Hp* magnitude for this transit

Field HT3: Estimated standard error of the magnitude given in Field HT2, σ_{Hp}

Field HT4: Quality flag

If the flag is not set, then the data are considered to be photometrically reliable. If the flag is non-zero, caution must be used in interpreting the data. The various bit settings of the quality flag are given in Table 2.5.2.

If only bit 0 or bit 1 is set, the data may be reliable, but no cross-check between the consortia was possible, since the data were obtained from one consortium only (the corresponding data having been rejected by the other consortium for a variety of reasons which were not precisely the same for both consortia).

Bit 2 was not used.

If any of bits 3–8 are set, the data are likely to be unreliable:

• bit 3 was set for transits observed during intervals of high background level (e.g. during certain parts of the satellite's orbit). For stars brighter than 10 mag the data may be reliable even when bit 3 is set;

• bit 4 was set when an object, either in the same or in the complementary field of view, was likely to have perturbed the resulting photometry. For some 'two-pointing doubles' (see Section 1.4) bit 4 is set for all transits, since there is a strong possibility of the photometry of each of the components being affected by the companion;

• bit 5 flags correspond to transits which the FAST Consortium flagged as suspect as a result of poor attitude reconstruction;

• bit 6 flags were assigned, as a result of a detailed investigation of outliers in the photometric data, where a cause could be identified for the perturbation. Such flagged transits typically originate from events which are generally clustered in time: thus *Hp* estimates were found to be systematically too bright near to some shutter closures (close to Earth occultations), and systematically too faint during periods of poor instrument pointing. While future investigations should suppress these flagged transits, they have been included in (and will weakly influence) the published statistical results of the Hipparcos photometry (Fields H44–47);

• bit 7 flags were assigned to identify observations acquired during (relatively short) intervals of satellite Sun pointing. It is believed that the data quality are affected by the non-nominal thermal environment of the satellite.

Transits with any of bits 1–8 set are not plotted on the folded or unfolded light curves. Transits with bit 0 set are plotted, using a different symbol.

Table 2.5.1. Hipparcos Epoch Photometry Annex: star header

Record	Field	Bytes	Format	Description
1	HH1	1– 7	I6,X	HIP number
	HH2	8– 9	A1,X	Component flag
	HH3	10–16	F6.3,X	$V - I$ (mag)
	HH4	17–20	I3,X	Total transits, $N_{\rm tot}$
	HH5	21–28	I3,5X	Accepted transits, $N_{\rm acc}$
2	HH6	1– 8	F7.4,X	Median magnitude, $\overline{Hp}$ (mag)
	HH7	9–15	F6.4,X	$\sigma_{\overline{Hp}}$ (mag)
	HH8	16–21	F5.2,X	5th percentile (max) (mag)
	HH9	22–28	F5.2,2X	95th percentile (min) (mag)
3	HH10	1–12	F11.7,X	Variability period, P (day)
	HH11	13–22	F9.4,X	Reference epoch (day)
	HH12	23–24	A1,X	Variability type
	HH13	25–26	A1,X	Annex flag (tables)
	HH14	27–28	A1,X	Annex flag (light curves)

Table 2.5.2. Hipparcos Epoch Photometry Annex: individual transit record

Field	Bytes	Format	Description
HT1	1–11	F10.5,X	BJD(TT), (barycentric) Julian Date (TT)–2 440 000.0 (days)
HT2	12–19	F7.4,X	Hp for the transit (mag)
HT3	20–25	F5.3,X	σ_{Hp} (mag)
HT4	26–28	I3	Quality flag (bit): 0 NDAC data only 1 FAST data only 2 (not used) 3 Very high background estimate (threshold 70 Hz) 4 Possible interfering object in either field of view 5 FAST quality flag set 6 Perturbed for other identified reasons 7 Observation during Sun-pointing mode 8 Significant difference between FAST and NDAC data

Note: see Section 2.11.1 for interpretation of the bit settings in Field HT4.

The Hipparcos Epoch Photometry Annex Extension

As described previously, the median $\overline{Hp}$ magnitudes contained in the Hipparcos Catalogue, and the individual Hp magnitudes in the Hipparcos Epoch Photometry Annex, refer to $Hp_{\rm dc}$, a magnitude estimate derived from the unmodulated part of the signal intensity. Magnitude estimates from the modulated part of the signal intensity, denoted $Hp_{\rm ac}$, were derived as part of the photometric reductions (further details of the derivation of $Hp_{\rm dc}$, and the difference between $Hp_{\rm dc}$ and $Hp_{\rm ac}$, can be found in Volume 3).

For most users of the epoch photometry, the Hipparcos Epoch Photometry Annex will contain much if not all of the information needed. However, $Hp_{\rm ac}$, and supplementary information related to the photometric reduction, are provided for more specialist use within the Hipparcos Epoch Photometry Annex Extension.

The information contained in the Hipparcos Epoch Photometry Annex Extension is provided to allow users to verify the quality of individual photometric measurements at a particular epoch (further verification by the Hipparcos data analysis teams could have been carried out, but at the expense of delaying the publication of the results).

Such verification may fall into the following categories:

(a) verification of the overall photometric calibration with respect to photometric standard stars. As described in Volume 3, the photometric calibration was a complex process, dependent on the field of view and position in the field of view, time, magnitude, colour index, and background intensity. Recalibration would require a reordering of all transits in order of acquisition, and provision of additional geometrical information related to the viewing configuration. Since the final photometric calibration was consistent at the level of the photon noise statistics, such information has not been preserved, and such a re-calibration is essentially precluded;

(b) differences between $Hp_{\rm dc}$ and $Hp_{\rm ac}$, derived on the basis of the unmodulated and modulated components of the signal respectively, provide a sensitive indication of the presence of resolved structure within the target, i.e. whether the entry is possibly double, multiple, or extended. Since the signal amplitudes of the modulated and unmodulated components will depend on the scanning geometry, the resulting time-dependent variations may mimic variability. Specialist users may wish to verify the presence or absence of such multiplicity, and its possible effects on the inferred variability. For these reasons, $Hp_{\rm ac}$ is provided within the Hipparcos Epoch Photometry Annex Extension;

(c) although a careful calibration of the magnitudes took account of background variations (both sky, and van Allen radiation background induced), modelling of the background was performed differently by the two reduction groups. The two separate background estimates are included in the Hipparcos Epoch Photometry Annex Extension;

(d) less easy to take rigorously into account was the possible perturbing influence of one or more stars (within the instantaneous field of view of the detector's response profile) coming from the other field of view—the Hipparcos observations being acquired from two such superposed fields of view, separated by about 58° on the sky. Possibly interfering objects known from the Tycho Input Catalogue have been considered, and clearly perturbed observations have been flagged in the list of transits compiled in the Hipparcos Epoch Photometry Annex (see Field HT4). The Hipparcos Epoch Photometry Annex Extension provides sufficient information for the specialist user to verify whether an object from the other field of view (identified during the Hipparcos data reductions or not) might have perturbed a transit at any given epoch, by providing the coordinates of the other field of view at that epoch.

In summary, the general user will find most of the information needed within the Hipparcos Epoch Photometry Annex. Transits flagged already as suspect should typically be rejected from further use. Users interested in assessing whether duplicity/multiplicity might have affected the light curves may wish to investigate the values of $Hp_{\rm ac}$ in further detail. Those wanting to verify the nature of identified perturbing objects in the complementary field of view, or wanting to assess the effects of (faint) stars in the complementary field of view, will make use of the coordinates of the complementary field of view given in the Hipparcos Epoch Photometry Annex Extension.

In general, for double and multiple objects the median ac magnitude is higher than the median dc magnitude, since extended structure decreases the signal modulation so that the object appears fainter in the modulated signal. Also the ratio between the standard errors on the ac and dc magnitudes will be higher than for single objects. For extended objects (e.g. planetary nebulae) the ac magnitudes will be higher than the dc magnitudes, but the ratio between the standard errors will be much the same as for a single object (see Volume 3). For variable stars, the standard error of the ac magnitudes can become smaller than that of the dc magnitudes.

There are two reasons for retaining possibly perturbed transits in the Hipparcos Epoch Photometry Annex and its Extension. First, the criteria used for flagging has been rather severe, and there will be cases where the disturbance, for many applications, is not too serious. Second, it is in principle possible to correct for perturbations from the complementary field of view when the separation from the centre of the instantaneous field of view is small (a few arcsec). Such corrections have not been made for the published data, since the available magnitudes and colours of the disturbing objects were often very uncertain.

Description of the Epoch Photometry Annex Extension

Header Records (Table 2.5.3)

The Extension file is organised exactly in parallel with the Annex file, but with records of 44 byte length. The Extension consists of three header records for each object in the Hipparcos Catalogue (as for the Annex file, facilitating the synchronous reading of the both files, see Table 2.5.3), followed by N transit records (Table 2.5.4). The transit records in the Extension are for the same epochs as the individual transit records in the Annex. The first header record of the Extension is a copy of the first header record of the Annex. The second record contains the median $\overline{Hp}_{\rm ac}$ and $\sigma_{\overline{Hp}_{\rm ac}}$, i.e. analogous to the Annex header, but containing the Hp magnitudes derived from the modulated signal (i.e. $Hp_{\rm ac}$ instead of $Hp_{\rm dc}$). It also contains parameters derived from $\overline{Hp}_{\rm dc}$ and $\overline{Hp}_{\rm ac}$ providing indirect information on the likelihood of data being disturbed by duplicity or background objects.

Field HHE1: HIP number (as Field HH1)

Field HHE2: The component flag for a double or multiple entry

This is the same as given in the Hipparcos Catalogue (Field H48) and in Field HH2. However the photometric data in the Annex Extension always refer to the combined system, with no correction for duplicity or for the attenuation profile of the detector.

Field HHE3: $V - I$ colour index (as Field HH3)

Field HHE4: Total number of transits in the file $N_{\rm tot}$ (as Field HH4)

Field HHE5: Number of photometrically accepted transits, $N_{\rm acc}$ (as Field HH5)

Field HHE6: Median magnitude for the modulated signal component, $\overline{Hp}_{\rm ac}$

Field HHE7: Standard error of the median $\overline{Hp}_{\rm ac}$ magnitude, $\sigma_{\overline{Hp}_{\rm ac}}$

Fields HHE8: $\overline{Hp}_{\rm dc} - \overline{Hp}_{\rm ac}$ (the difference between Fields HH6 and HHE6)

Fields HHE9: Ratio of the standard errors on the medians, $\log_{10}(\sigma_{\overline{Hp}_{\rm ac}} / \sigma_{\overline{Hp}_{\rm dc}})$

This is a good approximation to the ratio between the standard deviations in $Hp_{\rm ac}$ and $Hp_{\rm dc}$, since $N_{\rm acc}$ is the same for both parameters.

Field HHE10: Coincidence pointer offset

This is used in combination with a coincidence index in the transit record (Field HTE8) to determine possibly perturbing objects in the complementary field of view.

Field HHE11: Double star correction

The correction applied to the epoch photometry and summary data to account for the effect of a companion, calculated as part of the double star processing (see Section 1.3.2).

Description of the Epoch Photometry Annex Extension
Individual Transit Record (Table 2.5.4)

Field HTE1: $Hp_{\rm ac}$ magnitude for this transit

$Hp_{\rm ac}$ is given to three decimals, compared with four decimals for $Hp_{\rm dc}$, reflecting the larger error on the magnitude derived from the modulated signal component. The epoch of the transit is precisely that given for the corresponding transit in the Hipparcos Epoch Photometry Annex.

Field HTE2: Estimated standard error of the magnitude given in Field HTE1, $\sigma_{Hp_{\rm ac}}$

Field HTE3: Background determined by the FAST Consortium, b_F, in Hz

The field is blank if no data from this consortium were available for this transit.

Field HTE4: Background determined by the NDAC Consortium, b_N, in Hz

The field is blank if no data from this consortium were available for this transit.

Field HTE5: Field of view index

This takes the value:
0 : for observations made in the following field of view;
1 : for observations made in the preceding field of view.

Field HTE6–7: Right ascension and declination of the complementary field of view

The measurement principle of Hipparcos involved the superposition of two fields of view, separated by approximately 58° on the sky. The photometric (and astrometric) measurements were affected if objects of sufficient brightness from the complementary field of view were superposed on the target field of view. To permit further consideration of the possibility that photometry at a given observation epoch was perturbed due to the geometrical configuration at that epoch, the equatorial coordinates of the complementary field of view are provided. Resulting contaminating objects already identified from the Tycho Input Catalogue are included in a corresponding 'coincidence file', see Field HTE8. The complimentary field of view coordinates were only retained by the NDAC Consortium, and thus if no NDAC data are available these two fields are blank.

Field HTE8: Coincidence index

The 'coincidence file' contains about 100 000 entries, and provides information on identified objects in the other field of view (details of the file are given in Table 2.5.5). Transits are indicated as 'perturbed by an identified object in the other field of view' (as found in the Tycho Input Catalogue) by a non-zero value of the 'coincidence index' given in the transit record. More than one object may have been identified in the 'other field of view'. When added to the 'coincidence pointer offset' given in the header, the 'coincidence index' provides a pointer to the first of these identified objects. Subsequent objects may follow, as indicated by a 'pointer terminator'. This will be set to 1 if the last entry related to the relevant transit has been found. It will be set to 0 if the next entry is also related to the same transit. In the majority of cases, however, only one entry will be found for a transit, thus the 'pointer terminator' will usually be 1.

Table 2.5.3. Hipparcos Epoch Photometry Annex Extension: star header

Record	Field	Bytes	Format	Description
1	HHE1	1– 7	I6,X	HIP number
	HHE2	8– 9	A1,X	Component flag
	HHE3	10–16	F6.3,X	$V - I$ (mag)
	HHE4	17–20	I3,X	Total transits, $N_{\rm tot}$
	HHE5	21–23	I3	Accepted transits, $N_{\rm acc}$
		24–44	21X	
2	HHE6	1– 8	F7.4,X	Median magnitude, $\overline{Hp}_{\rm ac}$ (mag)
	HHE7	9–15	F6.4,X	$\sigma_{\overline{Hp}_{\rm ac}}$ (mag)
	HHE8	16–22	F6.3,X	$\overline{Hp}_{\rm dc} - \overline{Hp}_{\rm ac}$ (mag)
	HHE9	23–28	F6.3	$\log_{10}(\sigma_{\overline{Hp}_{\rm ac}} / \sigma_{\overline{Hp}_{\rm dc}})$
		29–44	16X	
3	HHE10	1– 7	I6,X	Coincidence pointer offset
	HHE11	8–14	F7.4	Double star correction (mag)
		15–44	30X	

Table 2.5.4. Hipparcos Epoch Photometry Annex Extension: individual transit record

Field	Bytes	Format	Description
HTE1	1– 7	F6.3,X	$Hp_{\rm ac}$ for the transit (mag)
HTE2	8–13	F5.3,X	$\sigma_{Hp_{\rm ac}}$ (mag)
HTE3	14–17	I3,X	Background, b_F (Hz)
HTE4	18–21	I3,X	Background, b_N (Hz)
HTE5	22–23	I1,X	Field of view index
HTE6	24–32	F8.4,X	RA of other field of view (degrees)
HTE7	33–41	F8.4,X	Dec of other field of view (degrees)
HTE8	42–44	I2,X	Coincidence index

Table 2.5.5. Hipparcos Epoch Photometry Annex Extension: coincidence file

Field	Bytes	Format	Description
HCE1	1– 5	F4.1,X	Distance from IFOV centre (arcsec)
HCE2	6–10	F4.1,X	Magnitude (mag)
HCE3	11–15	F4.1,X	Colour index, if known (mag)
HCE4	16	I1	Coincidence terminator flag

Section 2.6

Tycho Catalogue: Epoch Photometry Annex

2.6. Tycho Catalogue: Epoch Photometry Annex

A general introduction to the published data related to the Tycho experiment is given in Section 1.3.6. Details of the fields of the Tycho Catalogue, including an explanation of the quantities relevant for an understanding of the contents of the Annex, are given in the introduction to Section 2.2.

Results of the individual, calibrated, Tycho photometric measurements at each epoch of observation are made available as the Tycho Epoch Photometry Annex. In principle, an annex comprising individual transit data for every object in the Tycho Catalogue could have been provided. In practice, for most of the faint Tycho stars, the epoch photometry is not considered to be of sufficient importance to merit general publication.

Two subsets of the data have consequently been selected. Transit data related to Tycho Catalogue objects considered to be of greatest astrophysical value constitute the Tycho Epoch Photometry Annex A. It forms part of the ASCII CD-ROMs accompanying the printed Hipparcos Catalogue, where transit data for 34 446 objects are given. Epoch photometry for a significantly larger fraction of the Tycho Catalogue objects (481 553) is made available as the Tycho Epoch Photometry Annex B through the CDS, Strasbourg. Finally, the epoch photometry data for all Tycho Catalogue objects is kept in an archive of the Tycho Consortium.

Field T50 of the main Tycho Catalogue (see Section 2.2) indicates which objects are included in Annexes A and B, respectively. The selection criteria are detailed below.

Each Tycho Epoch Photometry Annex is ordered by the TYC identifier (see also Section 2.11). It consists of header records and transit records. The header records (Table 2.6.1) contain summary photometric data. When provided, the transit records contain the transit time (i.e. the observation epoch), estimated magnitudes and related quantities, and flags providing further details related to each observation, as well as information on the quality of the resulting data.

The number of valid transits, N_{transits} (i.e. including both detected and non-detected transits) are given in Field TH4 of the header record. The criteria used to determine whether the transit provides valid photometric data are described in the introduction to Section 2.2. As explained there, a valid photometric transit does not necessarily provide a statistically meaningful estimate of the object's magnitude.

Selection Criteria for the Presentation of Transit Records

The Tycho Epoch Photometry Annex A, provided on the ASCII CD-ROMs, gives epoch photometry for objects which fall into one or more of the following categories:

- a selection of 6100 photometric standard stars;
- known or suspected variable stars from the General Catalogue of Variable Stars (GCVS, 1985) and the New Catalogue of Suspected Variables (NSV). These stars have flags 'G' and 'N' in Field T47 of the Tycho Catalogue;
- stars showing strong indication of variability in the Tycho measurements (flag 'V' in Field T48);
- stars showing clear indication of (unresolved) duplicity in the Tycho measurements (flag 'D' in Field T49).

The selection of objects for Annex A was defined such as to provide the most interesting subset of the Tycho epoch photometry, while at the same time selected to fit onto a single CD-ROM. The number of objects with transit records in Annex A is 34 446.

The Tycho Epoch Photometry Annex B made available through the CDS includes all the above objects, supplemented by objects which fall into one or more of the following categories:

- all stars brighter than $V_T = 10.25$ mag;
- stars with weak indication of variability in the Tycho measurements, or photometric disturbance that may be due to other reasons (flag 'U' or 'W' in Field T48);
- stars with weak indication of duplicity in the Tycho measurements (flag 'R' or 'S' in Field T49);
- stars with astrometric quality flag '9' in Field T40;
- stars with the note flag set in Field T57.

Some of the criteria for Annex B especially select objects with low signal-to-noise ratio or with dubious astrometric or photometric results. They are included in Annex B so that a better summary photometry may be obtained by a more thorough study than was possible until now. Improved astrometry may in principle also be derived since the individual transit records (Table 2.6.2) contain the required information. The number of objects with transit records in Annex B is 481 553 (these are the 34 446 objects of Annex A, flagged 'A' in Field T50 of the Tycho Catalogue, and 447 107 additional objects, flagged 'B' in Field T50 of the Tycho Catalogue).

Description of the Header Record (Table 2.6.1)

Fields TH1–3: Tycho identifier

The Tycho identifier is described under Field T1 (Section 2.2). For double stars resolved in the special astrometry analysis, but not separated in photometry, the full set of transits are given under both entries.

Field TH4: Number of transit records following this header record, $N_{\rm transits}$

If provided, these are the records belonging to 'valid' transits in the terminology of the Tycho photometry treatment. The introduction to Section 2.2 provides details of the criteria used to define the 'valid' transits.

Field TH5: Number of detected transits measured in the B_T band, $N_{B,\ \rm measured}$

The number of detected transits measured in B_T, referred to as $N_{B,\ \rm measured}$, corresponds to the total number of transits where bit 0 of Field TT13 is not set. An appropriate subset of transits classified as 'measured' and 'not-measured' were used to construct the summary photometric data given in the following fields (see the introduction to Section 2.2 for further details).

Each measured transit corresponds to a detection of the relevant star above a signal-to-noise ratio of 1.5 in the T channel. However, some detections may be 'not-measured' in either B_T or V_T. The total number $N_{\rm transits}$ for a given star is related to the number of transits 'measured' and 'not-measured' in each photometric band as follows:

$$\begin{aligned} N_{\rm transits} &= N_{B,\ \rm measured} + N_{B,\ \rm not-measured} \\ &= N_{V,\ \rm measured} + N_{V,\ \rm not-measured} \end{aligned} \qquad [2.6.1]$$

where the values $N_{B,\ \rm measured}$ and $N_{V,\ \rm measured}$ are given in Fields TH5 and TH10.

Fields TH6–9: Summary photometric data for the B_T observations

These fields provide, for the B_T observations, the mean magnitude (either median or de-censored mean), the standard error of the mean magnitude, and the 15th and 85th percentile points (together providing an indication of the scatter of the measurements). More details can be found in the descriptions of Fields T32–T39 and Fields T45–46 in Section 2.2. The definition and derivation of the relevant quantities in the context of the Tycho observations are given in Section 1.3.6.

Field TH10: Number of detected transits measured in the V_T band, $N_{V,\ \rm measured}$

The number of detected transits measured in V_T, referred to as $N_{V,\ \rm measured}$, corresponds to the total number of transits where bit 1 of Field TT13 is not set. See Field TH5 for details.

Fields TH11–14: Summary photometric data for the V_T observations

See Fields TH6–9 for details.

Fields TH15–16: Header flags (see Table 2.6.1 and Volume 4 for details)

Table 2.6.1. Tycho Epoch Photometry Annex: star header

Field	Bytes	Format	Description
TH 1	1– 5	I4,X	TYC1 (GSC region)
TH 2	6–11	I5,X	TYC2 (star number)
TH 3	12–13	I1,X	TYC3 (component)
TH 4	14–17	I3,X	Number of transits in epoch photometry, N_{transits}
TH 5	18–21	I3,X	Number of detected and measured transits, $N_{B,\text{ measured}}$
TH 6	22–28	F6.3,X	Mean magnitude B_T (mag)
TH 7	29–34	F5.3,X	σ_{B_T} (mag)
TH 8	35–41	F6.3,X	15th percentile for B_T (mag)
TH 9	42–48	F6.3,X	85th percentile for B_T (mag)
TH10	49–52	I3,X	Number of detected and measured transits, $N_{V,\text{ measured}}$
TH11	53–59	F6.3,X	Mean magnitude V_T (mag)
TH12	60–65	F5.3,X	σ_{V_T} (mag)
TH13	66–72	F6.3,X	15th percentile for V_T (mag)
TH14	73–79	F6.3,X	85th percentile for V_T (mag)
TH15	80–82	I2,X	Header flags (bit): 0: approximate magnitude (see Field T36) 1: variable/suspected variable from GCVS/NSV (set if Field T47 non-blank) 2: variable/suspected variable from Tycho analysis (set if Field T48 = 'U', 'V' or 'W') 3: close pair, known from Hipparcos or Tycho (set if Field T2 non-blank) 4: double/suspected double, unresolved by Tycho (set if Field T49 = 'D', 'R' or 'S') 5: variable/suspected variable from Hipparcos analysis (set if Field H6 non-blank)
TH16	83–84	I2	Header flags (bit): 0: standard star for photometric calibration (in normal processing) 1: standard star for photometric calibration (in reprocessing) 2: photometric reduction used instrument parameters from reprocessing

See Section 2.11.1 for interpretation of bit settings in Fields TH15–16 (bit 0 is the least-significant bit).

Description of the Individual Transit Record (Table 2.6.2)

Field TT1: Observation epoch

This is specified in (barycentric) Julian Date, with respect to JD(TT) 2 440 000.0.

Observation epochs are given in Terrestrial Time (TT), and have been corrected for light propagation time to the solar system barycentre. They are therefore referred to as BJD(TT). Observation epochs are given with a resolution of 10^{-5} days = 0.864 s.

Fields TT2–4: Photometric quantities for the transit in B_T

These fields give the calibrated magnitude for the transit (B_T), the standard error (σ_{B_T}), and the background (b_B) in counts per sample (i.e. counts per $\frac{1}{600}$ s). If a magnitude is not measured, then the value $B_{\rm det}$, corresponding to the measurement limit, i.e. an upper limit on the brightness, is entered as B_T. The value is calculated assuming an appropriate value of the signal-to-noise ratio, the background, and the slit group (see Volume 4). It is noted that $B_{\rm det}$ is not a completely reliable upper limit on the brightness, because about 6 per cent of all transits are spurious non-detections. A value of 327.67 counts per sample in Field TT2 or Field TT4 means that the measured background was equal to or higher than that value. For further explanation see Section 2.2.

Fields TT5–7: Photometric quantitities for the transit in V_T

Details as for Fields TT2–4.

Fields TT8–9: Instrumental geometry for the transit

Field TT8 provides the z-coordinate at which the star transitted the star mapper slits at the given epoch. Field TT9 provides the corresponding position angle of the slit normal, p_n, reckoned positive in the direction of motion of the star in the field of view.

The position angle allows a photometric analysis to be made as a function of this parameter—a dependence is expected for close double stars, which might therefore be discovered in this way. The user must still distinguish between vertical and inclined slits with respect to resolution. The position of the slits on the sky can also be calculated at the transit time using the position angle p_n along with the z-coordinate (see Volume 4 for further details). The position angle is measured counterclockwise, as seen on the sky, from the $+\delta$ direction.

Field TT10: Astrometric residual of the transit, Δu

This is the difference between the transit time of the star and the transit time expected from the adjusted position of the star, the satellite attitude, and the geometric calibration of the instrument. This time difference is multiplied by the instantaneous scan speed of the slit group, giving an angular distance Δu expressed in mas.

The user may restrict further the range of Δu for which the photometric transits are to be accepted for an analysis of epoch photometry. If two detected transits from the same group crossing were accepted by the astrometric adjustment, the one with the smallest absolute Δu is selected as being associated with the photometric parameters of the candidate object.

Field TT11: Expected standard error of the astrometric residual σ_u

The expected standard error of the astrometric residual given in Field TT10 has been computed from the known uncertainties of the satellite attitude, the geometric instrument calibration, and the photon noise of the raw Tycho signal.

Field TT12: Goodness-of-fit

The numerical value of the goodness-of-fit indicates possible (unrecognised) duplicity, and unrecorded parasite disturbances. The goodness-of-fit has been constructed as described in Volume 4.

Field TT13: Transit flags

The bits are defined in Table 2.6.2. If a transit is not detected in the T-channel bits 0 and 1 are set = 1, Fields TT8–9 are given, but Fields TT10–12 are blank. These blank fields characterise unambiguously a non-detection.

Table 2.6.2. Tycho Epoch Photometry Annex: individual transit record

Field	Bytes	Format	Description
TT 1	1–11	F10.5,X	BJD(TT), (barycentric) Julian Date −2 440 000.0 (days)
TT 2	12–18	F6.3,X	B_T for the transit (mag)
TT 3	19–24	F5.3,X	σ_{B_T} (mag)
TT 4	25–31	F6.2,X	Background, b_B (cts/smp)
TT 5	32–38	F6.3,X	V_T for the transit (mag)
TT 6	39–44	F5.3,X	σ_{V_T} (mag)
TT 7	45–51	F6.2,X	Background, b_V (cts/smp)
TT 8	52–59	F7.1,X	z-coordinate, z (arcsec)
TT 9	60–65	F5.1,X	Position angle, p_n (degrees)
TT10	66–71	I5,X	Residual, Δu (mas)
TT11	72–76	I4,X	Standard error, σ_u (mas)
TT12	77–82	F5.1,X	Goodness-of-fit
TT13	83–84	I2	Transit flags (bit): 0: magnitude not measured in B_T 1: magnitude not measured in V_T 2: transit rejected in astrometry and in de-censoring (due to suspected parasite) 3: transit on the vertical/inclined slit (0 = vertical, 1 = inclined) 4: transit in following/preceding field (0 = following, 1 = preceding)

See Section 2.11.1 for interpretation of bit settings in Field TT13 (bit 0 is the least-significant bit).

Section 2.7

Solar System Objects

2.7. Solar System Objects

2.7.1. Hipparcos (Main Mission) Observations

The Hipparcos observing programme included careful selection of all solar system objects observable by the satellite (major planets, natural satellites and minor planets). One of the primary motivations for including these objects was to provide the necessary material for the construction of a dynamical reference frame based upon the absence of local rotation in their equations of motion. These objects are brighter than 13 mag and smaller than 1 arcsec; in addition, the planetary satellites observed had to be sufficiently far from the planet to be observable beyond the corresponding envelope of scattered light. In total, 48 asteroids were observed (among the IAU list from (1) Ceres to (704) Interamnia), and three planetary satellites (J II–Europa, S VI–Titan and S VIII–Iapetus).

Positions and proper motions in the Hipparcos and Tycho Catalogues are given within the International Celestial Reference System (ICRS), and therefore represent an extension, at optical wavelengths, of the (extragalactic) radio reference system (see Section 1.2.2). The minor planet observations have been explicitly excluded from the construction of the Hipparcos reference system. Rather, the construction of a self-consistent dynamical reference frame will be a complex, long-term project, complicated by the phase and geometrical effects mentioned below, and somewhat constrained by the relatively short observation interval. The eventual comparison of the two resulting reference frames has been considered as a problem quite distinct from the construction of the Hipparcos Catalogue, and will only be undertaken after catalogue publication.

Some specific remarks are relevant for the astrometric measurements of solar system objects. Due to the particular scanning law of the satellite, observations only occur during the 18 seconds of an object's transit in one of the telescope's fields of view; they are spread around the quadratures (when the phase angle is maximum), and are not uniformly distributed in time. Since the scanning circles always subtend angles with the ecliptic of more than 47°, Hipparcos yields in general more accurate information on the object's ecliptic latitude than on its ecliptic longitude.

Each observation corresponds to a transit of the object across the instrument main grid. Because the observations are essentially one-dimensional (namely, in the direction perpendicular to the grid slits at the epoch of observation), and because solar system objects have a large daily motion, the observed direction cannot be given in the form of conventional, two-dimensional coordinates such as right ascension and declination. Instead, the observed quantity is the abscissa v of the projected position on a reference great circle with (positive) pole P; no information is given on the object's ordinate r on this great circle, except that $|r| \lesssim 1°$ (see Figure 2.7.1). The observed position is somewhere on an arc of a great circle perpendicular to this reference great circle, where the abscissa on the reference great circle is precisely the value given by the observation.

Table 2.7.1. Object numbering for Hipparcos and Tycho.

	Name	Number
Minor planets:	(1) Ceres	1
	...	IAU Number
	(704) Interamnia	704
Satellites:	J II–Europa	901
	J III–Ganymede	902
	J IV–Callisto	903
	S VI–Titan	904
	S VIII–Iapetus	905
Major planets:	Uranus	906
	Neptune	907

The published quantities defining this arc are reckoned in the tangent plane of a particular point. This particular point, referred to as the reference point, is chosen to be as close as possible to the actual position as given by the ephemerides. The reference point thus corresponds to the observed coordinate in the scanning direction, and to the calculated coordinate in the perpendicular direction (Figure 2.7.1). In this context, references to 'place' or 'position' correspond to the arc of a circle perpendicular to the reference great circle passing through the reference point, a one-dimensional quantity referred to hereafter as the 'position locus'.

All positions are referred to the reference frame defined by the Hipparcos Catalogue. The data for one observation consist of:

(1) the astrometric coordinates (α_0, δ_0) of the reference point, i.e. the geocentric direction corrected for stellar aberration; and the direction **w** in its tangent plane, of the slit motion (i.e. the trace of the reference great circle);

(2) the mean epoch of the transit, reduced to the geocentre, and expressed on the TT time scale (see Section 1.2.3);

(3) the apparent magnitude *Hp* in the Hipparcos photometric system.

Object Numbering for Solar System Objects

Identification numbers used for the observation of solar system objects are specific to this section, and should not be confused with the HIP identification number of entries in the main Hipparcos Catalogue. The same solar system object number applies to objects observed either by Hipparcos or by Tycho.

The numbering of minor planets corresponds to the IAU number. For the satellites and major planets the adopted numbering code has been chosen specifically for the Hipparcos/Tycho observations, and is given in Table 2.7.1.

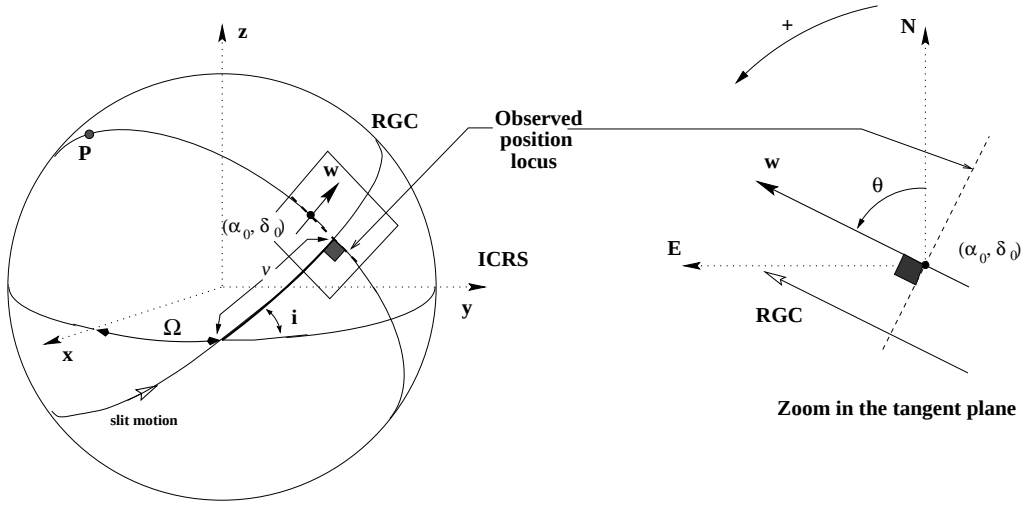

Figure 2.7.1. *One dimensional position locus for solar system objects observed by Hipparcos, on the celestial sphere (left), and on the tangent plane (right).*

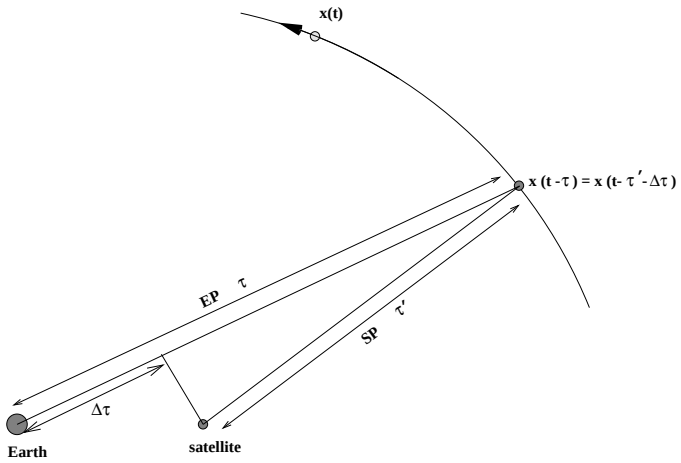

Figure 2.7.2. *Planetary aberration and the correction of light travel time.*

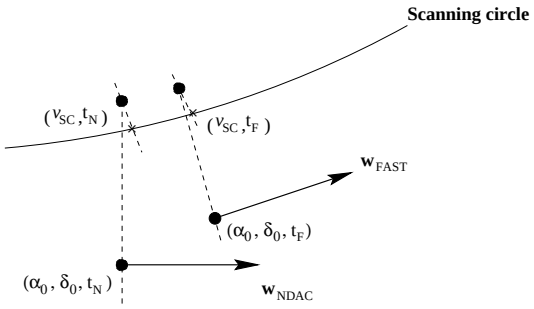

Figure 2.7.3. *FAST and NDAC observed reference points and position loci for two different* **w** *directions (or reference great circles) and for the different epochs* t_F *and* t_N.

2.7.2. Hipparcos Astrometry

The catalogue of minor planets and natural satellites consists of the separate FAST and NDAC consortia results. The main difference between the two reductions is in the expansion of the modulated light signal: using only the first harmonic for NDAC, but the first and second harmonics in the case of FAST. This has a negligible effect for the smallest bodies (with apparent diameters smaller than approximately 0.1 arcsec); then the positions correspond, to a first approximation, to the position of the photocentre. For the largest bodies, care must be taken in the actual definition of the observed direction. If the modulated signal is written in the form:

$$S(t) = I\ [1 + M\ \cos(\omega t + \varphi) + N\ \cos(2\ \omega t + 2\ \psi)] \qquad [2.7.1]$$

then the NDAC abscissa definition corresponds to the phase of the first harmonic $v_N = f(\varphi)$; while the FAST abscissa definition corresponds to a weighted mean of both harmonic phases $v_F = f(3/4\ \varphi + 1/4\ \psi)$ (where f is the application expressing the whole reduction process). For a point source the calibrated phases φ and ψ are equal so that $E(v_F - v_N) = 0$. For an extended source, $E(v_F - v_N) \sim f(1/4\ (\psi - \varphi))$ depending on the physical properties of the minor planet or satellite (such as apparent diameter, albedo contrast, and light scattering by the surface).

In particular the FAST abscissa for larger objects does not correspond to the conventional definition of the photocentre of the body. For this reason, no merging of the solutions has been performed, for any of the minor planets, on the FAST and NDAC catalogues. For a similar reason, only astrometric data within NDAC can be given for the two satellites J II–Europa and S VI–Titan. In fact, the FAST astrometric reduction procedure is unsuitable for objects with an apparent diameter larger than roughly 0.7 arcsec, i.e. when the second harmonic amplitude is too small. Table 2.7.2 summarises the data obtained by the Hipparcos (main mission) observations. In general, both FAST and NDAC observed abscissae are provided for each transit (a few transits do not appear in both consortia results). The corresponding position loci are perpendicular to two different **w** directions, the latter being close to the actual scanning motion (see Figure 2.7.3). The corresponding epochs are also different.

The various steps of the reduction procedure took into account effects down to the order of one milliarcsec. The observations are referred to the geocentre; they are corrected for stellar aberration (due to the satellite's barycentric velocity **v**, and expanded to second order in $|\mathbf{v}|/c$), and general relativistic light deflection (due to the Sun's spherical gravitational field). Conversely, effects not modeled with the observing precision are discarded, in particular no attempt has been made to account for phase, shape, or albedo corrections. In general the observed minor planets are small (with an apparent diameter of less than 0.1 arcsec); in such cases the systematic photocentre offset between the observed centre of light and the centre of gravity may be smaller than the measurement noise, but still of the order of a few milliarcsec.

As stated previously, a single mean coordinate is given for the mid-time of each 18 s transit across the main field of view. For this reduction the movement of the object along the **w** direction was assumed to be linear in time and with a known velocity. One resulting normal point corresponds to the median (FAST) or a weighted mean (NDAC) of typically eight single measurements, so that the corresponding error distribution will not follow a normal distribution but rather a Student's t-like distribution. Some transits were discarded during one or other of the consortia's great circle data reductions, and also during the transit reductions. The latter correspond essentially to measurements

corrupted by parasitic light (for example due to the parent planet in the case of planetary satellites, or veiling-glare by a star) and/or a badly centered instantaneous field of view.

The treatment of grid-step ambiguities for minor planets or natural satellites also differs from that applied in the case of stars. The basic measurement of the modulation phases φ and ψ in Equation 2.7.1, when translated to a one-dimensional geometrical coordinate, only gives the fraction of the grid period (1.2074 arcsec) counted from the centre of the nearest slit; to this must be added the coordinate of this nearest slit, which is assumed to be the nearest to the calculated ephemeris position of the object. The validity of the resulting position locus can only be verified in comparison with the improved ephemerides obtained after incorporating the Hipparcos observations. In this process, it may occasionally be necessary to correct the abscissae by ±1.2074 in the scanning direction. As a rule, abscissae differing from the calculated abscissa by more than 0.801 arcsec in modulus were corrected by one grid period. This correction was only necessary for a very small number of observations. The data for minor planet (27) Euterpe are more troublesome. After rejection of suspicious transits, sometimes no satisfactory solution was found for the treatment of grid-step correction, so only the data uncorrected for possible grid-step errors are given. This means that some of the transits may be suspicious, or erroneous by one grid period (the transits concerned are in the time window $8200.5 < t - 2\,440\,000.0 < 8380.5$).

The published quantities defining the arc of a great circle of the observed positions are:

(a) the reference point (α_0, δ_0) of this arc such that its abscissa on the reference great circle is the observed one, and its (unobserved) ordinate on this great circle is taken from the ephemerides ($v = v^{\mathrm{obs}}$; $r = r^{\mathrm{calc}}$). The reference point is generally within ~ 1 arcsec of the true position;

(b) the position angle θ between the direction **w** of the slit motion and north (see Figure 2.7.1). The **w** axis is also oriented in the sense of increasing abscissae v, with the position angle θ reckoned positive from north through east;

(c) the standard error in the **w** direction, $\sigma_{v*} = \sigma_v \cos r^{\mathrm{calc}}$. There is no astrometric measurement, and thus no similar quantity, along the perpendicular direction ($\theta \pm \pi/2$).

The position locus and epoch of observation are both corrected to the geocentre. The astrometric direction corresponds to the position of the object at time $t - \tau$, where t is the published epoch of observation and τ the light time delay to the geocentre.

The epoch at the Hipparcos satellite can be calculated by $t' = t - \Delta\tau$ where the difference $\Delta\tau \equiv \tau' - \tau$ is provided as additional data (see Figure 2.7.2). Since the latter is a small quantity when compared to the time resolution of the basic measurement, no use of a special relativistic formalism has been made; this time offset is then calculated as:

$$\Delta\tau \equiv \tau' - \tau = \frac{EP - SP}{c} \qquad [2.7.2]$$

where EP and SP are respectively the geocentric and satellitocentric distances of the planet apparent position, and c the velocity of light.

When comparing the published coordinates with independent two dimensional equatorial coordinates (α^c, δ^c)—which may be either calculated or observed—the strictly one-dimensional nature of the Hipparcos observations must be taken into account,

since the published direction (α_0, δ_0) effectively constrains the position in only this single dimension (see Figure 2.7.1). Thus, for comparison with the observed positions, the residuals (i.e. the differential equatorial coordinates):

$$\begin{pmatrix} \Delta\alpha* \\ \Delta\delta \end{pmatrix} = \begin{pmatrix} (\alpha_0 - \alpha^c)\cos\delta_0 \\ \delta_0 - \delta^c \end{pmatrix} \qquad [2.7.3]$$

should be projected onto the great circle:

$$\begin{pmatrix} \Delta v* \\ \Delta r \end{pmatrix} \sim \begin{pmatrix} \sin\theta & \cos\theta \\ -\cos\theta & \sin\theta \end{pmatrix} \begin{pmatrix} \Delta\alpha* \\ \Delta\delta \end{pmatrix} \qquad [2.7.4]$$

from which only the single equation of condition:

$$\Delta v* = v^{\rm obs} - v^{\rm calc} \sim (\sin\theta \quad \cos\theta)\ \mathbf{M}\,\Delta\mathbf{x^c} \qquad [2.7.5]$$

is retained, instead of the usual system of two equations:

$$\begin{pmatrix} \Delta\alpha* \\ \Delta\delta \end{pmatrix} \sim \mathbf{M}\,\Delta\mathbf{x^c} \qquad [2.7.6]$$

where **M** is the matrix yielding the differential equatorial coordinates from the variation in orbital elements $\Delta\mathbf{x^c}$; and where small terms due to the projection from the celestial sphere to the tangent plane are neglected.

2.7.3. Hipparcos Photometry

The published photometric data is the result of a single data reduction consortium (the FAST Consortium) and is restricted to minor planets only. The reduction of the data was similar to that adopted for double stars. Two different estimations of the apparent magnitude ($Hp_{\rm dc}$ and $Hp_{\rm ac}$) are given for each transit in the Hipparcos photometric system *Hp* (see Section 1.3 and Section 2.5). The correction to the geocentre of the epoch of observation is irrelevant for the photometry and, in contrast with the astrometric data, is not applied.

The magnitude estimator $Hp_{\rm dc}$, derived from the integrated light, corresponds to the 'true' magnitude; while the estimator $Hp_{\rm ac}$, derived from the two harmonics of the modulated part of the light, is biased and of lower accuracy. Although the difference between these two estimations depends on the scanning direction, shape, albedo contrast, and light scattering on the surface of the object, it depends mostly on the object's apparent diameter. Moreover $\Delta Hp = Hp_{\rm ac} - Hp_{\rm dc} > 0$ and in a first approximation $\Delta Hp(\varrho,\alpha) = a\varrho^2 + o(\varrho^4) + o(\alpha)$, where a is a scalar, ϱ the apparent diameter and α the solar phase angle. For the smallest asteroids, the difference between these two determinations is however smaller than the measurement noise.

Due to the rather random observation epochs of the objects, the data rarely yield magnitudes over a rotation period, nor representative light curves. They can nevertheless be used for deriving absolute magnitudes (accurate to about 0.03 mag) over a large range of phase angles and rotational phase. Some aspect data are also provided for convenience: these are the Sun-asteroid and satellite-asteroid distances, and the solar phase angle.

Due to the perturbation by the planet, which contributed significantly to the background scattered light, no photometry is provided for the planetary satellites.

Table 2.7.2. Solar system objects observed by the Hipparcos main mission. Apparent magnitudes are from the FAST Consortium only. Astrometry results have been derived from the separate FAST and NDAC reductions.

	Name	Photometry	Astrometry
Minor planets:	(1) Ceres	FAST	FAST + NDAC
	...	FAST	FAST + NDAC
	(704) Interamnia	FAST	FAST + NDAC
Satellites:	J II–Europa	–	NDAC
	S VI–Titan	–	NDAC
	S VIII–Iapetus	–	FAST + NDAC

Table 2.7.3. Solar system objects observed by Tycho. The star mapper observations yield astrometry for the objects listed, and photometry for the smallest objects only.

	Name	Photometry	Astrometry
Minor planets:	(1) Ceres	√	√
	(2) Pallas	√	√
	(4) Vesta	√	√
	(6) Hebe	√	√
	(7) Iris	√	√
Satellites:	J III–Ganymede	–	√
	J IV–Callisto	–	√
	S VI–Titan	√	√
Major planets:	Uranus	–	√
	Neptune	–	√

Table 2.7.4. Number of observations for Hipparcos and Tycho.

Hipparcos			
N	Astrometry		Photometry
	NDAC	FAST	FAST
1	72	65	65
2	66	63	63
3	67	61	60
4	55	58	58
5	89	81	81
6	100	95	91
7	73	71	69
8	58	56	56
9	43	40	40
10	62	51	51
11	83	68	68
12	24	24	24
13	37	34	34
14	51	45	45
15	96	84	83
16	56	49	49
18	110	100	100
19	30	30	30
20	62	62	61
22	67	63	63
23	69	66	66
27	38	35	35
28	35	34	33
29	85	75	74
30	47	48	48
31	17	14	14
37	40	33	32
39	123	114	112
40	107	103	103
42	53	51	51
44	53	53	53
51	15	15	14
63	15	12	12
88	36	36	36
115	31	33	33
129	46	41	40
192	33	32	32
196	18	14	14
216	22	21	21
230	33	35	35
324	74	73	73
349	108	94	92
354	103	98	98
451	31	29	29
471	114	112	112
511	62	64	64
532	41	40	40
704	87	82	82
901	64	0	0
904	38	0	0
905	5	8	0

Tycho		
N	Astrometry	Photometry
1	43	43
2	31	31
4	40	40
6	12	12
7	24	24
902	16	0
903	13	0
904	19	19
906	51	0
907	42	0

2.7.4. Tycho Observations

The data gathered by the star mapper yield valuable results for some of the minor planets, satellites and planets, as given in Table 2.7.3. The main differences between the Tycho and Hipparcos results are that Tycho provides: (a) photometry in the B_T and V_T bands; (b) more conventional two-dimensional astrometry; (c) astrometry for larger angular diameter objects. The theory of Tycho astrometric reduction of solar system objects is given in Volume 4.

Photometry can only be provided for objects smaller than the width of the modulating slit, i.e. 0.91 arcsec; while astrometry can be obtained for larger objects up to approximately 5 arcsec. For the smallest objects both photometric and astrometric data can be obtained (see Table 2.7.3); for major planets, the Tycho observations only provide astrometric information.

No attempt has been made to account for phase, shape, or albedo corrections. The published Tycho astrometric position corresponds to the photocentre for objects smaller than the slit width, where the photocentre is the 'centre of gravity of light'.

The astrometric position of the single slit group crossing corresponds to the projection of the slit group on the sky at the time of transit determined by the Tycho detection algorithm (see Volume 4).

For the largest natural satellites and for the major planets, it is assumed that (1) the time offset between the two slit group crossings is small enough and (2) the distribution of light is sufficiently symmetric, so that the published position corresponds, to a first approximation, to the photocentre. Additional data are provided to enable the user to reconstruct the slit geometry during the observation if a more comprehensive treatment is undertaken.

Each observation corresponds to a transit, on both vertical and inclined slits, across the star mapper for one of the fields of view. One (mean) position is constructed assuming that the ephemeris is sufficiently accurate to yield the true planet motion during the short interval $t_2 - t_1$, where t_1 and t_2 are the times of transit across the inclined and vertical slit respectively (see Figure 2.7.4). The position (α, δ) given in equatorial coordinates corresponds to the intersection of the fiducial slits at O_2' at the time of transit t_2, i.e. when the inclined slit has been translated by an amount corresponding to the calculated displacement $\overrightarrow{C_1 C_2}$.

Together with the position the standard errors $\sigma_{\alpha*} = \sigma_{\alpha \cos\delta}$, σ_δ and the correlation coefficient $\rho^\delta_{\alpha*}$ are given, where small additional error contributions due to the projection on the focal plane are neglected (Figure 2.7.5). The orientation and size of the error ellipse defined by the covariance matrix of the observed equatorial coordinates, as well as the non-zero correlation coefficient, are related to the spatial direction of the slits and to the standard deviations σ_1, σ_2 of the slit abscissae measured along the direction of the slit motion during each observation. The cartesian equation of the ellipse is in the (E, N) frame (see Figure 2.7.5):

$$\frac{(\Delta\alpha*)^2}{\sigma^2_{\alpha*}} + \frac{(\Delta\delta)^2}{\sigma^2_\delta} - \frac{2\,\rho^\delta_{\alpha*}\,\Delta\alpha*\,\Delta\delta}{\sigma_{\alpha*}\,\sigma_\delta} = 1 - (\rho^\delta_{\alpha*})^2 \qquad [2.7.7]$$

The transit epoch, measured at the satellite, is given in Julian date in the TT time scale. In contrast to the astrometric catalogue of the Hipparcos solar system objects

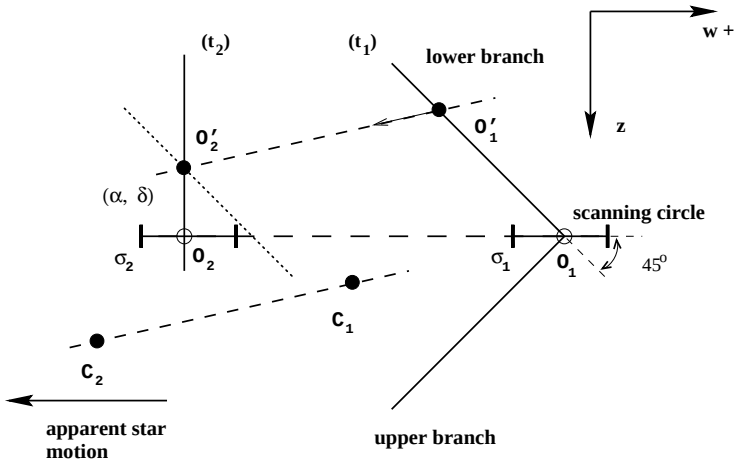

Figure 2.7.4. *A projection on the sky showing how a two-dimensional position of a solar system object is constructed within Tycho. C_1 and C_2 are the calculated positions at times t_1 and t_2. O_1 and O_2 are the observed slits abscissae with error bars σ_1 and σ_2. The published position corresponds to O'_2, i.e. the intersection of the vertical slit at t_2 with the translated inclined slit.*

(Figure 2.7.2), the light-time delay between the satellite and the geocentre is neglected. Thus the position is not corrected for light-time delay, nor is it referred to the geocentre. The position corresponds in first approximation to the astrometric direction, given in equatorial coordinates in the ICRS system (see Section 2.7.1). The apparent magnitudes B_T and V_T are in the Tycho photometric system (see Section 1.3.3).

The Tycho observation principle is to detect transits near the predicted slit crossing time (within a few arcsec on the sky). Some observations were corrupted by the presence, in one of the fields of view, of a parasitic object, i.e. a star near the predicted position. Such observations had to be filtered and rejected. Rejection criteria were based on the observed V_T magnitude, on a comparison between the observed with respect to the calculated position, and on its standard error. Certain ambiguous cases still remain, however, and in these cases the different possible transits are published. These cases are specifically flagged since only one of the published transits can be correct.

Additional information concerning the observations for each transit is also given. These are the standard errors σ_1 and σ_2 (see Figure 2.7.4) related to the observed positions, along the direction **w**, of the inclined and vertical slits. The position angle θ of the direction **w** normal to the vertical slits, and the branch of the inclined slits on which the transit occurred (+1 for the upper and −1 for the lower) are also given (see Figure 2.7.6).

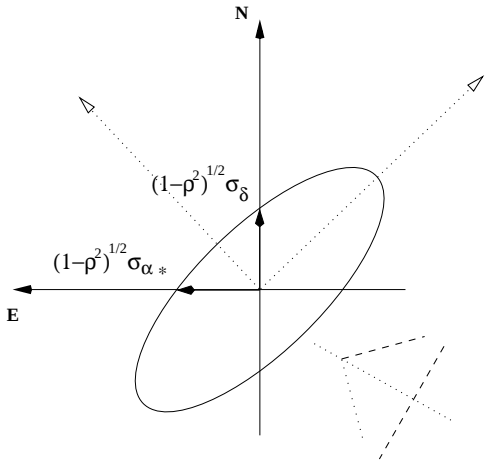

Figure 2.7.5. *Standard errors for Tycho astrometry. In general the published standard errors of the equatorial coordinates do not correspond to the principal components of the ellipse. The published equatorial coordinates are thus correlated. The slit system is shown together with the error ellipse for a realistic observation* ($\sigma_1 = 2\,\sigma_2$) *and a transit in the upper part of the inclined slit.*

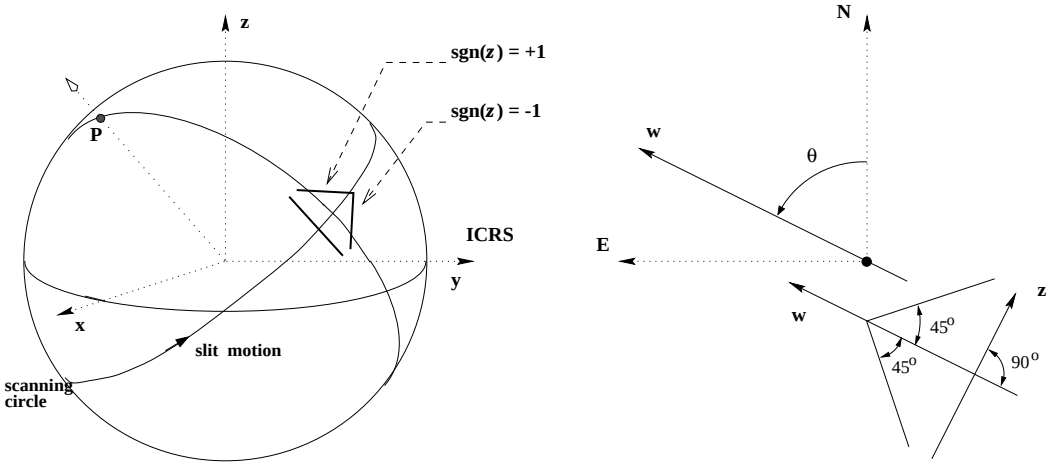

Figure 2.7.6. *Additional information on the slit orientation, on the celestial sphere (left) and in the tangent plane (right). The slit coordinate direction* **w** *is given by the position angle* θ*, from which the directions of the vertical and inclined slits can be reconstructed. The figure in the tangent plane shows the slit coordinate system* (**w**, **z**).

2.7.5. Hipparcos Solar System Objects: Astrometric Catalogue

Field SHA1: Object number

See Table 2.7.1.

Fields SHA2–3: Right ascension and declination of the reference point, (α_0, δ_0)

The reference coordinates are referred to ICRS.

Field SHA4: Measurement epoch, corrected to the geocentre

The measurement epoch is specified in Julian Date with respect to JD(TT) 2 440 000.0 . It is the mean epoch, given with an accuracy of 0.01 s, corrected to the geocentre as described in Section 2.7.2.

Field SHA5: Additional data: light time delay

This gives the applied light time delay in the geocentric direction of the observed object, between the satellite and the geocentre (see Figure 2.7.1), in seconds of TT.

Field SHA6: Position angle θ of the slit coordinate direction **w**

The position angle is referred to the north, reckoned positive from north through east.

Field SHA7: Estimated standard error, $\sigma_{v*} = \sigma_v \cos r^{\mathrm{calc}}$

This provides the standard error of the abscissa v along the direction **w**, in milliarcsec, as described in Section 2.7.2.

Field SHA8: Consortium origin flag

If the transit corresponds to an NDAC record the flag is 1; if it corresponds to a FAST record the flag is 2.

2.7.6. Hipparcos Solar System Objects: Photometric Catalogue

Within the catalogue of solar system objects observed by the Hipparcos main mission, photometry is given only for asteroids.

Field SHP1: Object number

See Table 2.7.1.

Field SHP2: Measurement epoch

The measurement epoch is specified in Julian Date with respect to JD(TT) 2 440 000.0 . In contrast with the Hipparcos astrometric epoch for solar system objects (Field SHA4), the measurement epoch is not corrected to the geocentre (i.e. the light-time delay between the satellite and the geocentre is neglected).

Fields SHP3–4: Magnitude and standard error from unmodulated signal

The magnitude, $Hp_{\rm dc}$, and standard error, $\sigma_{Hp_{\rm dc}}$, are given in the Hipparcos photometric system Hp, as estimated from the unmodulated part of the light signal.

Fields SHP5–6: Magnitude and standard error from modulated signal

The magnitude, $Hp_{\rm ac}$, and standard error, $\sigma_{Hp_{\rm ac}}$, are given in the Hipparcos photometric system Hp, as estimated from the modulated part of the light signal.

Fields SHP7–9: Additional aspect data provided for convenience

The distances Sun-asteroid d and satellite-asteroid Δ are given in AU, the solar phase angle α (the angle between the Sun and the satellite as viewed from the asteroid) is given in degrees.

2.7.7. Tycho Solar System Objects: Astrometric/Photometric Catalogue

Field ST1: Object number

See Table 2.7.1.

Field ST2: Measurement epoch

The measurement epoch is specified in Julian Date with respect to JD(TT) 2 440 000.0 . In contrast with the Hipparcos astrometric epoch for solar system objects (Field SHA4), the measurement epoch is not corrected to the geocentre (i.e. the light-time delay between the satellite and the geocentre is neglected).

Fields ST3–4: Equatorial coordinates (α, δ) in degrees in the ICRS system

Fields ST5–6: Magnitudes in the Tycho system B_T and V_T

Field ST7 Multiple transit flag

If the flag is 1, then only one crossing of the field of view has been detected or retained. If the flag is $n > 1$, generally $n = 2$, then n candidate observed transits have been retained for that particular predicted observation (Fields ST1, ST2, ST7, ST11 and ST12 being identical in those cases).

Fields ST8–10: Standard errors $\sigma_{\alpha *} = \sigma_\alpha \cos\delta$, σ_δ given in milliarcsec, and correlation coefficient $\rho^{\delta}_{\alpha *}$ (see Section 1.2.7)

Fields ST11: Additional data: position angle θ of the slit coordinate direction **w**

Field ST12: Additional data: inclined slit flag, sgn(z)

The flag is +1 if the transit occurred in the upper branch of the inclined slits and −1 if it occurred in the lower half.

Fields ST13–14: Additional data: standard errors of the slit position along the direction **w**, σ_1 and σ_2 for the inclined and vertical slits respectively, given in milliarcsec

Table 2.7.5. Hipparcos solar system objects: astrometric catalogue

Field	Bytes	Format	Description
SHA1	1–4	I3,X	Object number
SHA2	5–16	F11.7,X	Reference point RA α_0 (degrees)
SHA3	17–28	F11.7,X	Reference point Dec δ_0 (degrees)
SHA4	29–42	F13.7,X	Measurement epoch, JD(TT) −2 440 000.0 (days)
SHA5	43–48	F5.2,X	Light time delay satellite–geocentre $\Delta\tau$ (seconds)
SHA6	49–56	F7.3,X	Position angle θ (degrees)
SHA7	57–63	F6.2,X	σ_{v*} (mas)
SHA8	64	I1	NDAC (1) or FAST (2) flag

Table 2.7.6. Hipparcos solar system objects: photometric catalogue

Field	Bytes	Format	Description
SHP1	1–4	I3,X	Object number
SHP2	5–16	F11.5,X	Measurement epoch, JD(TT) −2 440 000.0 (days)
SHP3	17–24	F7.4,X	$Hp_{\rm dc}$ (mag)
SHP4	25–31	F6.4,X	$\sigma_{Hp_{\rm dc}}$
SHP5	32–39	F7.4,X	$Hp_{\rm ac}$ (mag)
SHP6	40–46	F6.4,X	$\sigma_{Hp_{\rm ac}}$
SHP7	47–52	F5.3,X	Distance Sun-asteroid d (AU)
SHP8	53–58	F5.3,X	Distance satellite-asteroid Δ (AU)
SHP9	59–63	F5.2	Solar phase angle α (degrees)

Table 2.7.7. Tycho solar system objects: astrometric and photometric catalogue

Field	Bytes	Format	Description
ST1	1–4	I3,X	Object number
ST2	5–18	F13.7,X	Measurement epoch, JD(TT) −2 440 000.0 (days)
ST3	19–30	F11.7,X	α (degrees)
ST4	31–42	F11.7,X	δ (degrees)
ST5	43–48	F5.2,X	B_T (mag)
ST6	49–54	F5.2,X	V_T (mag)
ST7	55–56	I1,X	Transit flag
ST8	57–62	F5.1,X	$\sigma_{\alpha*}$ (mas)
ST9	63–68	F5.1,X	σ_δ (mas)
ST10	69–74	F5.2,X	$\rho^{\delta}_{\alpha*}$
ST11	75–81	F6.2,X	Position angle θ (degrees)
ST12	82–84	I2,X	sgn(z)
ST13	85–90	F5.1,X	σ_1 (mas)
ST14	91–95	F5.1	σ_2 (mas)

Section 2.8

Hipparcos Catalogue: Intermediate Astrometric Data

2.8. Hipparcos Catalogue: Intermediate Astrometric Data

2.8.1. Introduction

The Hipparcos Intermediate Astrometric Data are the one-dimensional coordinates (abscissae) on reference great circles, obtained by the FAST and NDAC Data Reduction Consortia. The relevance of the data is illustrated in Figure 2.8.1. Details of the data reduction procedures, and the merging of the results from the two consortia, are given in Volume 3.

Since each perigee passage of the satellite forced an interruption of at least a few hours in the observations, it was natural to divide the data into segments corresponding to the intervals between successive perigee passages. Each such interval is referred to as an 'orbit', and is identified by a unique sequential number.

For most orbits each consortium used a single reference great circle. This was always the case for NDAC but, for a few orbits, the FAST consortium split the data into two reference great circles. However, in order to merge the results from the two consortia, a one-to-one correspondence between the observations from each was necessary; in these few cases the FAST results for the two reference great circles in an orbit were averaged.

The data are provided in machine-readable form, in ASCII format, only (see Section 2.11 for further details of the corresponding formats). The first file contains the mid-epochs and poles, referred to ICRS, of the reference great circle adopted for each orbit, by each consortium. The second file gives, for each orbit, the residuals between the observed abscissae for each star and those calculated from the set of reference astrometric parameters which are given in the Hipparcos Catalogue Fields H8–13.

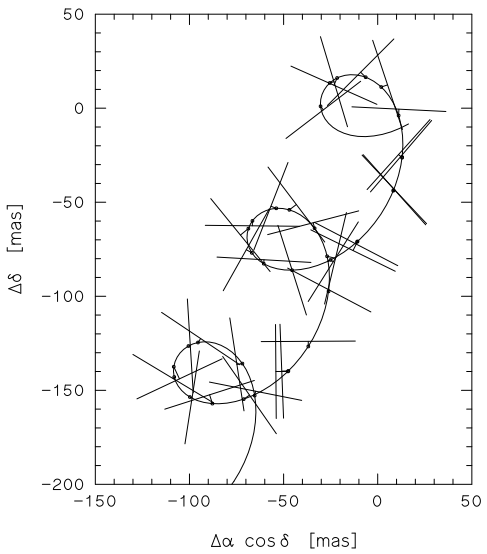

Figure 2.8.1. *The path on the sky of one of the Hipparcos Catalogue objects, over a period of three years. Each straight line indicates the observed position of the star at a particular epoch: because the measurement is one-dimensional, the precise location along this position line is undetermined by the observation. The curve is the modelled stellar path fitted to all the measurements. The inferred position at each epoch is indicated by a dot, and the residual by a short line joining the dot to the corresponding position line. The amplitude of the oscillatory motion gives the star's parallax, with the linear component representing the star's proper motion. The intermediate astrometric data allow the quality of the model fitting to be assessed, and possibly refined.*

2.8.2. Reference Great-Circle Data

This file (see Table 2.8.1) defines the mid-epoch, in years from the catalogue epoch J1991.25(TT) (see Section 1.2.6), for each great circle during the mission, together with the reference pole of these reference great circles. These data may be used for the computation of partial derivatives of abscissae with respect to the astrometric parameters.

The FAST and NDAC mid-epochs for a given orbit were always very close to each other. In some cases, an orbit used by one data reduction consortium was not used by the other one; in this case the relevant fields are blank.

The following formula allows the orbit number o to be derived, using an epoch t expressed in years relative to J1991.25(TT):

$$o = \mathrm{int}(1157.39 + 823.02t + 0.216t^2) \qquad [2.8.1]$$

Fields IR1–7: Reference Great Circle Data

Field IR1: Orbit number

Field IR2: FAST reference great-circle mid-epoch

The mid-epoch of the reference great circle is defined in years, relative to J1991.25(TT).

Field IR3–4: Equatorial position of the FAST reference great-circle pole

This gives the right ascension and declination (in degrees) within ICRS of the FAST reference great-circle pole.

Field IR5: NDAC reference great-circle mid-epoch

The mid-epoch of the reference great circle is defined in years, relative to J1991.25(TT).

Field IR6–7: Equatorial position of the NDAC reference great-circle pole

This gives the right ascension and declination (in degrees) within ICRS of the NDAC reference great-circle pole.

The statistics of the reference great circles are as follows:

Consortium	Number of circles	Minimum orbit number $o_{\min}$	(yr–1991.25)	Maximum orbit number $o_{\max}$	(yr–1991.25)
FAST	2262	48	−1.3478	2763	1.9505
NDAC	2326	1	−1.4049	2768	1.9565

2.8.3. Reference Great-Circle Abscissae

The data are ordered by increasing Hipparcos (HIP) number. For each star, a header record provides the reference astrometric parameters (Fields IH1–9, see Table 2.8.2), followed by a total of N_A individual abscissae records (Fields IA1–10, see Table 2.8.3) providing the results for each observation by each consortium, ordered by increasing orbit number.

Abscissae residuals are given for 118 204 entries. Compared to the main catalogue, 14 entries are missing: 10 entries without astrometry, and 4 double star component solutions obtained by NDAC only. Some entries have abscissae from one consortium only: 6594 entries have FAST data only, 44 entries have NDAC data only.

These discrepencies are due to the fact that the NDAC astrometric reduction of known double stars were not performed using the main NDAC reduction chain. For this reason, the NDAC great circles abscissae of certain double stars were not available for the astrometric merging procedure, and are therefore not available in the intermediate astrometric data file.

Fields IH1–7: Header Data

Field IH1: The Hipparcos Catalogue (HIP) identifier

Field IH2: Provisional *Hp* magnitude used for merging

This is the provisional *Hp* magnitude used for the astrometric data merging. It was not necessarily the final catalogue value derived for *Hp*, and may therefore differ from the final value published in the main Hipparcos Catalogue, Field H44 (such differences, however, having a marginal effect on the final astrometric parameters).

Fields IH3–7: Reference astrometric parameters

These are the Hipparcos astrometric parameters, the same as in Fields H8–9 and H11–13, to which the abscissae residuals refer, in the order position (α, δ), parallax (π), and proper motion ($\mu_{\alpha*}$, μ_δ) respectively.

The right ascension and declination are expressed in degrees, at epoch J1991.25(TT). The trigonometric parallax is given in milliarcsec. The proper motions in right ascension, $\mu_{\alpha*} = \mu_\alpha \cos\delta$, and declination, μ_δ, are expressed in milliarcsec per Julian year and refer to the epoch J1991.25(TT). Coordinates are given within the ICRS system.

A viable astrometric solution could not be found for some entries (flagged '–' in Field IH8). These have no astrometric parameters in Fields H8–13 of the main Hipparcos Catalogue; in these few cases, Fields 3–4 of the Hipparcos Catalogue provide an approximate position. This has been used as the reference position (Fields IH3–4), with Fields IH5–7 set to zero.

Fields IH8: Flag for the adopted astrometric solution

This flag indicates which astrometric solution was finally adopted:
5 : single star solution (5 astrometric parameters)
7 : acceleration solution (DMSA/G), 7 parameters
9 : acceleration solution (DMSA/G), 9 parameters
C : component solution (DMSA/C)
O : orbital solution (DMSA/O)
V : 'VIM' solution (DMSA/V)
X : stochastic solution (DMSA/X)
– : no astrometric solution

Fields IH9: Number of following abscissae records, N_A

Fields IA1–10: Abscissa Data

Field IA1: Orbit number

Field IA2: Source of abscissa

The field has the following meaning:
F : data from FAST;
f : data from FAST rejected in constructing the published astrometric solution;
N : data from NDAC;
n : data from NDAC rejected in constructing the published astrometric solution.

The rejection is indicated only in the case of solutions flagged '5', '7', '9' or 'X' in Field IH8.

Fields IA3–7: Partial derivatives

These are the partial derivatives, $\partial v/\partial a_i$, of the abscissa with respect to the five astrometric parameters $a_i = \alpha* \ (= \alpha \cos\delta)$, δ, π, $\mu_{\alpha*}$, μ_δ, for $i = 1, \ldots, 5$ respectively.

Other derivatives were needed in the case of non-single star solutions. The derivatives with respect to the right ascension and declination components of the second- and third-order motion of the photocentre (Field IH8 = '7' or '9', see Section 2.3.3 for details), may be computed as:

$$\frac{\partial v}{\partial g_i} = \tfrac{1}{2}(t^2 - 0.81)\frac{\partial v}{\partial a_i} \qquad [2.8.2]$$

and:

$$\frac{\partial v}{\partial \dot{g}_i} = \tfrac{1}{6}(t^2 - 1.69)\frac{\partial v}{\partial a_{i+3}} \qquad [2.8.3]$$

where $i = 1, 2$ for $\alpha*$, δ, and the mid-epoch t is given in Fields IR2 or IR5 for the FAST and NDAC data respectively.

The FAST and NDAC partial derivatives differ, partly because of the difference in orientation between the FAST and NDAC reference great circles and, to a lesser extent, because the FAST Consortium used the observation epoch of the star on the given reference great circle whereas the NDAC Consortium used the reference great-circle mid-epoch.

Field IA8: Abscissa residual Δv, in milliarcsec

This is the difference between the observed great-circle abscissa and the great-circle abscissa computed with the reference astrometric parameters. The star abscissa is the angle, as seen from the great-circle pole, from the ascending node of the great circle on the equator to the satellitocentric coordinate direction of the star at the great-circle epoch.

If corrections Δa_i are to be added to the reference astrometric parameters a_i, the abscissae residuals with respect to the new reference astrometric parameters $a_i' = a_i + \Delta a_i$ can be computed as:

$$\Delta v' = \Delta v - \sum_{i=1}^{5} \frac{\partial v}{\partial a_i} \Delta a_i \qquad [2.8.4]$$

The fact that the reference great-circle abscissae are determined modulo the grid period (1.2074 arcsec) means that certain abscissa residuals, in particular some of the residuals related to the entries without astrometric solution (flagged '–' in Field IH8), may be affected by grid-step errors of $\pm 1.2074n$ arcsec. Here n is a small integer, rarely greater than 2, which varies among the abscissa residuals of the entry. In order to enable a consistent astrometric solution, the affected abscissa residuals must be corrected by subtraction of the corresponding grid-step errors. The abscissa residuals of all entries with non-problematic single-star solutions should be free of grid-step errors ($n = 0$).

Field IA9: Standard error of the abscissa

This is the adopted *a priori* standard error of the abscissa measurement, in milliarcsec. Each consortium derived a relative weighting system for its own data reductions. These individual systems were transformed to the adopted self-consistent system during the merging process, as described in Volume 3. The adopted standard error given here does not include the 'cosmic' error added in the stochastic solutions (Field IH8 = 'X').

Field IA10: Correlation coefficient between abscissae

The correlation coefficients between the FAST and NDAC abscissae for a given great circle have been calibrated as a function of magnitude, standard error, and orbit number. Together with the standard error of the FAST and NDAC abscissae, these correlation coefficients provide the necessary information about the covariance matrix of the observations. If abscissa data on a given great circle were obtained by both FAST and NDAC, the correlation coefficient is repeated in the two records to which it refers; otherwise the field is blank.

In the case of stochastic solutions (Field IH8 = 'X'), the correlation coefficients which have been used were computed as a function of the quadratic sum of the abscissae standard errors and the 'cosmic error', and are thus different from those indicated in this field.

Table 2.8.1. Hipparcos Intermediate Astrometric Data: Reference Great Circle Data File

Field	Bytes	Format	Description
IR1	1-5	I4,X	Orbit number
IR2	6-13	F7.4,X	FAST orbit mean epoch (year relative to J1991.25)
IR3	14-26	F12.8,X	Right ascension of the FAST great-circle pole (deg)
IR4	27-39	F12.8,X	Declination of the FAST great-circle pole (deg)
IR5	40-47	F7.4,X	NDAC orbit mean epoch (year relative to J1991.25)
IR6	48-60	F12.8,X	Right ascension of the NDAC great-circle pole (deg)
IR7	61-72	F12.8	Declination of the NDAC great-circle pole (deg)

Table 2.8.2. Hipparcos Intermediate Astrometric Data: Observation File Header Record

Field	Bytes	Format	Description
IH1	1-7	I6,X	Hipparcos Catalogue (HIP) identifier
IH2	8-13	F5.2,X	Provisional Hp magnitude used for the merging (mag)
IH3	14-26	F12.8,X	Right ascension α (deg)
IH4	27-39	F12.8,X	Declination δ (deg)
IH5	40-46	F6.2,X	Trigonometric parallax π (mas)
IH6	47-55	F8.2,X	Proper motion in right ascension $\mu_{\alpha *}$ (mas/yr)
IH7	56-64	F8.2,X	Proper motion in declination μ_δ (mas/yr)
IH8	65-66	A1,X	Code for adopted solution (5, 7, 9, C, O, V, X, –)
IH9	67-69	I3	Number of following abscissae records, N_A

Table 2.8.3. Hipparcos Intermediate Astrometric Data: Observation File Abscissa Record

Field	Bytes	Format	Description
IA1	1-5	I4,X	Orbit number
IA2	6-7	A1,X	‘F’ or ‘f’ if FAST data; ‘N’ or ‘n’ if NDAC data
IA3	8-15	F7.4,X	Abscissa partial derivative with respect to $\alpha *$
IA4	16-23	F7.4,X	Abscissa partial derivative with respect to δ
IA5	24-31	F7.4,X	Abscissa partial derivative with respect to π
IA6	32-39	F7.4,X	Abscissa partial derivative with respect to $\mu_{\alpha *}$
IA7	40-47	F7.4,X	Abscissa partial derivative with respect to μ_δ
IA8	48-56	F8.2,X	Abscissa residual wrt reference astrometric parameters (mas)
IA9	57-64	F7.2,X	Standard error of the abscissa (mas)
IA10	65-69	F5.3	Correlation coefficient between FAST and NDAC abscissae

Section 2.9

Hipparcos Catalogue: Transit Data

2.9. Hipparcos Catalogue: Transit Data

2.9.1. Introduction

The Hipparcos Transit Data file summarises intermediate astrometric and photometric information at the level of individual crossings of targets across the $0.^{\circ}9 \times 0.^{\circ}9$ main grid of the Hipparcos instrument. The data concern a total of 38 535 Hipparcos entries selected mainly on account of their known or suspected multiplicity, or as being parts of two- or three-pointing systems in which the detector signals of the different targets may be intermingled. The Hipparcos Transit Data file was derived from the 'Case History Files' constructed as part of the NDAC double star treatment (see Volume 3) and thus contains exclusively results of the NDAC processing: no merging of FAST and NDAC data at the transit level was deemed practicable in view of the very different approaches taken by the two consortia to the treatment of double stars.

For a specific double or multiple system, the Transit Data file provides a self-contained and globally calibrated compilation of the main detector signal parameters for practically all field transits of the system. For each transit, the five signal parameters (denoted b_1 to b_5 below) describe the detector signal as the sum of a constant component and two harmonics, without any constraints on the amplitudes and phases of the harmonics. Since this is a completely general model applicable to all kinds of objects (whether they are single, multiple, extended, variable, or in rapid orbital motion), the transit data can in principle be used to fit arbitrarily complex object models to the Hipparcos observations. For example, while the NDAC double star treatment was, for practical reasons, limited to the study of double and multiple systems with at most a linear relative motion of the components, the transit data could be used to derive the orbital elements of the resolved components of some short-period binaries with respect to their centre of mass, thus yielding mass ratios in addition to the relative orbits. The transit data may also be used to obtain astrometric results for some Hipparcos objects that were not successfully solved in time for inclusion in the catalogue, or for which the published results are affected by unresolved ambiguities.

The signal parameters given in the Transit Data file are fully calibrated in the sense that the amplitudes are corrected for sensitivity variations across the field of view and as a function of time and colour; similarly the phases are corrected for instrumental variations, and are referred to a specific reference direction in the global celestial reference frame defined by the Hipparcos Catalogue. The signal parameters thus corrected could more properly be called 'rectified', as they correspond to observations by a fictitious, ideal instrument with fixed and known sensitivity and response function. The rectified signal parameters can thus be modelled directly in terms of astrometric data in the ICRS system, and photometric data on the *Hp* magnitude scale, without regard to the actual variations of the instrument properties. Several thousand stars believed to be perfectly ordinary single stars ('*bona fide* singles') have been included in the Transit Data file in order to facilitate future checking of the rectification and for cross-validation of the reference frame and photometric system with respect to the Hipparcos Catalogue. These are not explicitly flagged here, but can be identified with reference to the main Hipparcos Catalogue (suspected) double star flags.

The Transit Data file also contains information on the pointing of the instantaneous field of view for each field transit. This information is essential for interpreting the attenuation effects of the detector's response profile (Table 1.4.1) especially for two- and three-pointing systems and cases where the pointing turned out to be significantly in error compared to the actual star. Note that the pointing data give the target position towards which the instantaneous field of view was aimed during observation. Due to the errors of the real-time satellite attitude determination, the actual pointing in a given transit may have differed by a few arcsec from this intended pointing. Such detailed pointing information, which in principle may be estimated from the difference between the real-time and *a posteriori* attitude determinations, is not contained in the Transit Data file.

In generating the Transit Data file, no screening of the data was applied in order to reject 'unreasonable' observations, e.g. with very small or very large signal strengths. This philosophy was adopted, firstly because it is very difficult to define acceptance limits in view of the variability of many objects, and secondly because the 'strange' values themselves could provide useful clues to some abnormal situation. The definition of a 'bad data point' is moreover a function of the fitted model and is therefore best left to the final user of the data. The user should however be aware that, in any analysis of the data, a few per cent of the transits may have to be rejected—and much more for some specific objects.

2.9.2. Basic Interpretation of the Transit Data

All transits of a particular Hipparcos entry are collected together in a set of consecutive records in the Transit Data file. This set begins with a header record, followed by a pointing record, and finally the transit records. A special index file contains a pointer from the HIP number to the relevant header record in the Transit Data file. For two- and three-pointing systems, data for the different pointings (each corresponding to a separate HIP number) are collected together, and the index file points to the same header record for the two or three different HIP numbers.

In the course of the Hipparcos mission the target positions for some objects (but not the proper motion or parallax of the reference point) were updated as a result of improved ground-based or preliminary space results; these are distinguished in the Transit Data file since the results are associated with the same HIP number but refer to different detector pointings. For simplicity, the set of HIP entries and target positions collected under the same header is here referred to as a 'system'. For most Hipparcos Catalogue entries only a single target position was used.

For a given system the Transit Data file specifies a reference point with astrometric parameters α_0, δ_0, π_0, $\mu_{\alpha*0}$, $\mu_{\delta 0}$ given in the header record. These parameters refer to the epoch J1991.25(TT) and the ICRS system, but they do not correspond to the parameters of any object contained in the Hipparcos Catalogue: usually they were constructed from the Hipparcos Input Catalogue parameters of the dominant target. The phase information in the subsequent transit data is defined relative to this reference point. Note that the reference point may have both a proper motion and a parallax, which must be added to the (relative) proper motion and parallax derived from the transit data in order to represent the absolute quantities on the sky.

The signal parameters b_1 to b_5 describe the fitted and rectified modulation light curve, expressed as photon counts per sample interval of 1/1200 s, according to the general second-order harmonic model:

$$I_k = b_1 + b_2 \cos p_k + b_3 \sin p_k + b_4 \cos 2p_k + b_5 \sin 2p_k \qquad [2.9.1]$$

where the phases p_k are taken relative to the reference point ($k = 1, 2, \ldots$ for successive samples of 1/1200 s). The actual photon counts N_k were modelled as an inhomogeneous Poisson process with a time-dependent expectation (intensity) described roughly as $(1 + g)I_k + B$, where g represents the calibrated sensitivity variations over the field of view and over the mission, and B the similarly calibrated background count rate. The actual calibration and rectification process is much more complicated, involving also the modulation factors and relative phases of the two harmonics, all considered as functions of position in field, time, and colour of the object.

The rectification was made in such a way that the rectified signal expected for a point source of magnitude Hp at the reference point is:

$$I_k = 6200 \times 10^{-0.4Hp} [1 + \bar{M}_1 \cos p_k + \bar{M}_2 \cos 2p_k] \qquad [2.9.2]$$

where $\bar{M}_1 = 0.7100$ and $\bar{M}_2 = 0.2485$ are adopted reference values for the modulation coefficients of the first and second harmonics. An object consisting of n point-like sources is consequently expected to produce the rectified signal:

$$I_k = \sum_{j=1}^{n} K_j [1 + \bar{M}_1 \cos(p_k + \phi_j) + \bar{M}_2 \cos 2(p_k + \phi_j)] \qquad [2.9.3]$$

where $K_j = 6200 \times 10^{-0.4Hp_j}$ are the (instantaneous) intensities of the sources and ϕ_j their phase displacements in the current field transit relative to the reference point. The phase displacements are simply given by the linear expressions:

$$\phi_j = f_x \xi_j + f_y \eta_j + f_p \Delta\pi_j \qquad [2.9.4]$$

where ξ_j, η_j are the positional offsets from the reference point in the directions of $+\alpha$ and $+\delta$, respectively, at the epoch of the transit; $\Delta\pi_j$ is the offset in parallax with respect to the reference point. Numerical values for the factors f_x, f_y, f_p are provided for each transit of a system. They are expressed in radians of phase per radian of angular offset. The factors f_x and f_y are, in effect, the α and δ components of the fundamental spatial frequency of the grid, as projected on the sky for the transit in question. Note that ξ_j and η_j describe the time-dependent offset of the point source including both a difference in position at the reference epoch J1991.25 and its variation due to orbital and proper motion, but excluding the parallactic motion relative to the reference point, which is taken care of by the third term in Equation 2.9.4. ξ_j and η_j are in principle local plane coordinates, tangential to the celestial sphere at the reference point, as defined in Section 1.2.9. Stellar aberration of the reference point has been removed in the rectification process; differential stellar aberration produces a slight stretching or compression of the local apparent scale and has been included as such in the factors f_x, f_y and f_p. Thus stellar aberration does not enter the astrometric modelling of the rectified signal parameters.

The data given for each transit of a target consist of the epoch of the transit (t), the phase factors f_x, f_y, and f_p, and the signal parameters b_1 to b_5 with associated standard errors σ_1 to σ_5. The additional quantities s_1, s_2 and σ_{att} are explained in the next section.

The determination of the signal parameters for a composite object is derived by identifying the fitted I_k in Equation 2.9.1 with the modelled intensity in Equation 2.9.3. In terms of the (generally time-dependent) intensities and positional offsets, this results in the following equations of condition for each transit:

$$\begin{aligned}
b_1 &= \sum_j K_j(t) \\
b_2 &= \bar{M}_1 \sum_j K_j(t) \cos[f_x\xi_j(t) + f_y\eta_j(t) + f_p\Delta\pi_j] \\
b_3 &= -\bar{M}_1 \sum_j K_j(t) \sin[f_x\xi_j(t) + f_y\eta_j(t) + f_p\Delta\pi_j] \\
b_4 &= \bar{M}_2 \sum_j K_j(t) \cos 2[f_x\xi_j(t) + f_y\eta_j(t) + f_p\Delta\pi_j] \\
b_5 &= -\bar{M}_2 \sum_j K_j(t) \sin 2[f_x\xi_j(t) + f_y\eta_j(t) + f_p\Delta\pi_j]
\end{aligned} \qquad [2.9.5]$$

The modelisation is further complicated by possible signal attenuation from the instantaneous field of view profile, which could modify the K_j as a function of the positional offset of each component from the target position; additional corrections may be introduced as a function of the difference in colour index of each component with respect to the colour assumed in the calibrations (see below).

2.9.3. Additional Considerations for the Use of the Data

This section addresses several items that are not essential for a basic understanding of the transit data, but which must nevertheless be considered in order to make optimum use of the data. They concern in particular the interpretation of Fields JT16–19.

Colour effects: All calibrations, especially the photometric calibration of the detector as a function of time and position in the field of view, are colour-dependent, and a specific colour index $(V-I)_{\rm cal}$ had to be assumed for each HIP identifier in order to rectify the signal parameters. The assumed colour index is specified for each HIP identifier in the Transit Data file. (Nominally this colour index should be the same as given in Field H75 — but not necessarily the same as in Field H40; see further details under Field H40.) For double-pointing binaries, where separate colour indices were available for the components, this is fairly non-problematic (assuming the colours to be essentially correct), but for single-pointing doubles there are inevitable problems. The two components generally have different colours, and the (correct) mean of the calibrations is not necessarily equal to the (adopted) calibration for a mean colour. Where the individual colours and intensities are known, a re-derivation of improved transit data would in principle be possible, but the amount of work involved makes that wholly impractical. Also, for most of the close Hipparcos doubles, the individual colours are *not* known, and this 'differential colour problem' had to be left unsolved in the data reduction process.

Even if it were thus necessary to assume that the components have the same colour, two additional quantities s_1 and s_2 have been introduced in the transit records in order to permit the given signal parameters to be approximately corrected, should later observations prove the assumed colour index to be much in error. The corrected parameters are given by:

$$\begin{aligned}
b'_1 &= b_1(1 + s_1\Delta c) \\
b'_k &= b_k(1 + s_2\Delta c)\,, \quad k = 2,\ 3,\ 4,\ 5
\end{aligned} \qquad [2.9.6]$$

where $\Delta c = (V-I)_{\rm true} - (V-I)_{\rm cal}$ is the required correction to the colour index used in the calibration. The need for different corrections of the 'dc' (unmodulated, $k = 1$) and the 'ac' (modulated, $k > 1$) components of the signal reflects the slightly different effective wavelengths of the dc and ac photometric bands (see Section 1.3); that the same correction factor applies to the second harmonic ($k = 4, 5$) as to the first ($k = 2, 3$) is due to the fact that the ratio M_2/M_1 is rather insensitive to the colour.

If the colours of the individual components of a single-pointing system are known, the corrections in Equation 2.9.6 must use the effective colour of the system. An alternative procedure would be to incorporate the inverse correction factors $(1 + s_i \Delta c_j)^{-1}$ separately for each component (j) in the right-hand sides of Equation 2.9.5. This latter procedure seems preferable on theoretical grounds, but has not been tested in practice.

Attitude effects: The given standard errors of the signal parameters include (for σ_2 to σ_5) the uncertainty of the phases of the first and second harmonics. This uncertainty arises primarily from the photon noise of the raw counts, but in the rectification process a contribution from the attitude uncertainty has been added, as determined in the great-circle reductions. However, the attitude errors in successive transits, belonging to the same great-circle reduction, are strongly correlated. Moreover, the formal standard errors in the attitude derived in the great-circle reductions are usually slightly too small. Both effects tend to give an underestimation of the errors in any solution based on the combination of transit data. A satisfactory treatment of these effects is very difficult to achieve and no standard recipe can be given here. The procedure adopted for the NDAC double star treatment is briefly described in Volume 3.

Transits belonging to the same great-circle reduction can be identified as having the same 'orbit number' o calculated from the transit epoch t as in Section 2.8.2, and the expected correlation of the phase data among such transits should be assessed by statistical methods. A further quantity, $\sigma_{\rm att}$, is provided with each transit record. This corresponds to the 'extra abscissa variance' that was added to the formal abscissae variances in the NDAC sphere solution in order to obtain abscissa residuals of unit weight. It is therefore *not* included in the given standard errors of the signal parameters, but should be added (wholly or partially) as phase noise fully correlated among transits sharing the same orbit number.

Pointing noise: A further noise source not included in the transit data standard errors is the photometric modulation caused by time-dependent errors in the piloting of the image dissector instantaneous field of view. This is small as long as a star is well centred in the instantaneous field of view, but may be very dominant for a stellar component at the edge of the response profile (some 15 to 25 arcsec from the centre). The modelling of this effect is quite complex, and may include both an enhancement of the photometric noise within a single transit (due to rapid variations in the actual pointing) and an apparent 'variability' of the component from one transit to the next.

Flagged transits: The standard errors σ_1 to σ_5 were normally computed by inversion of the 5×5 information matrix obtained by summing the information matrices of the individual observation frames (derived from the processing of the image detector tube photon counts), and taking into account the rectification of the frames by the relevant calibration data. For reasons not fully understood, in about 0.4 per cent of the transits, the computed information matrix turned out to be non-positive definite, and no standard errors could be computed as described above. In most of these transits the rectified signal parameters themselves appear to be valid, and it was decided to retain them in the transit data file with a suitable warning and a crude estimate of the standard errors. The affected transits are flagged in Field JT19, and the standard errors are set to the median values of the corresponding standard errors for the remaining transits of the same target position.

2.9.4. The Transit Data File

The Transit Data file contains data for 4 276 420 transits distributed over 37 368 different systems. For each system there is a header record (Table 2.9.1) followed by a pointing record (Table 2.9.2), and finally the transit records for the system (Table 2.9.3). All records are of the same length. The total number of records is 4 351 156.

The Header Record (Fields JH1–13)

Field JH1: The Hipparcos Catalogue (HIP) identifier for the first pointing in the system.

This field always contains an identifier (while Fields JH2–3 only give identifiers for two- or three-pointing systems). For two- and three-pointing systems the selection of the first pointing is to some extent arbitrary (usually it is the brighter component).

Fields JH2–3: Additional Hipparcos Catalogue (HIP) identifiers

These fields contain the additional HIP numbers of two- and three-pointing systems. Unused identifiers are set to zero. Thus, Fields JH2–3 are zero for single-pointing systems and Field JH3 is zero for two-pointing systems.

Field JH4: Number of different target positions in the system, N_P

This is the number of different target positions used to point the instantaneous field of view during observations. Note that a given HIP identifier may correspond to more than one target position, if the latter was updated in the course of the mission. N_P defines the number of significant fields in the subsequent pointing record and is also equal to the maximum pointing index I_P in the following transit records. N_P ranges from 1 to 7.

Field JH5: Number of following transit records, N_T

For 36 205 systems with a single HIP entry, N_T ranges from 6 to 357, with a mean value of 111 (only 25 systems have $N_T < 30$). For 1159 systems with two HIP entries, N_T ranges from 67 to 577 with a mean value of 223. For four systems with three HIP entries, N_T ranges from 259 to 583 with a mean value of 411.

Fields JH6–10: Astrometric parameters for the reference point

The phase information in subsequent transit records are given with respect to a reference point defined by the five astrometric parameters given in the order position (α_0, δ_0), parallax (π_0), and proper motion ($\mu_{\alpha*0}$, $\mu_{\delta 0}$).

The position is expressed in degrees, at epoch J1991.25(TT). The trigonometric parallax is given in milliarcsec (mas). The proper motions in right ascension, $\mu_{\alpha*0} = \mu_{\alpha 0} \cos \delta_0$, and declination, $\mu_{\delta 0}$, are expressed in milliarcsec per Julian year and refer to the epoch J1991.25(TT). Coordinates are given within the ICRS reference system.

Fields JH11–13: Colour indices ($V - I$) assumed in the calibrations

These fields give the values $(V-I)_{\rm cal}$ used to rectify the signal parameters corresponding to the HIP identifiers in Fields JH1–3. Fields JH12–13 are set to zero when the corresponding Fields JH2–3 are zero.

The Pointing Record (Fields JP1–27)

Field JP1: Index (1 to 3) for the HIP identifier of target position 1

This indicates which HIP identifier (Fields JH1–3) and colour index (Fields JH11–13) apply to the transit records with $I_P = 1$ in Field JT1.

Fields JP2–3: Offset in α and δ for target position 1, in arcsec

This is the target position used to point the instantaneous field of view for subsequent transits with $I_P = 1$ in Field JT1. It is given as the offset coordinates in α and δ relative to the reference point defined in the header record (Fields JH6–10) and expressed in arcsec. The offset in α should be interpreted as $\Delta\alpha \cos\delta$.

Fields JP4–27: Information on other target positions

If $N_P > 1$, the corresponding data for target positions 2 to N_P are given in Fields JP4 to JP($3N_P$). Remaining fields in the pointing record are set to zero. The format allows up to nine different target positions, although the actual maximum N_P is seven.

The Transit Record (Fields JT1–19)

Field JT1: Target position index for this transit record, I_P

This index (in the range 1 to N_P) defines the target position of the instantaneous field of view for the observations collected in this transit record. The target position is given in Fields JP($3I_P - 1$) and JP($3I_P$) of the preceding pointing record, and the corresponding HIP identifier and colour index are given, respectively, in Fields JH(JP($3I_P - 2$)) and JH(10+JP($3I_P - 2$)) of the preceding header record.

Field JT2: Epoch of the transit, t, expressed in years from J1991.25(TT)

Fields JT3–5: Phase factors f_x, f_y and f_p

These quantities, defined through Equation 2.9.4, are the partial derivatives of the signal phase (of the fundamental harmonic) with respect to the positional coordinates and parallax, expressed in radians of signal phase per radian of angular displacement.

Field JT6: Signal parameter b_1, given as the natural logarithm $\ln b_1$

b_1 is the 'dc' (unmodulated) component of the detector signal and is always positive. Because of its large range, a logarithmic value is given to preserve space. b_1 is expressed in counts per sample interval of 1/1200 s, normalised to $b_1 = 6200$ at $Hp = 0$ mag.

Fields JT7–10: Normalised signal parameters b_2/b_1 to b_5/b_1

The unit for b_2 to b_5 is the same as for b_1, so the normalised quantities are dimensionless. In practice they range from −1 to +1.

Fields JT11–15: Standard errors σ_i of the signal parameters b_i, given as natural logarithms $\ln \sigma_i$ ($i = 1$ to 5)

The standard errors are expressed in the same unit as the signal parameters.

Fields JT16–17: Colour correction factors, s_1 and s_2

See Section 2.9.3 for an explanation of these quantities. They are expressed in mag^{-1}.

Field JT18: Additional attitude noise, σ_{att}

See Section 2.9.3 for an explanation of this quantity. It is expressed in milliarcsec.

Field JT19: Flag indicating computed (0) or assumed (1) standard errors

This flag is normally set to 0. In some cases when the standard errors in Fields JT11–15 could not be computed in the normal way, this flag is set to 1 and Fields JT11–15 give the median standard errors applicable to the target position. Flagged transits should be treated with caution (see Section 2.9.3).

Table 2.9.1. Hipparcos Transit Data: Header Record

Field	Bytes	Format	Description
JH1	1–7	I6,X	HIP identifier for the first pointing in the system
JH2	8–14	I6,X	Additional HIP identifier (set to 0 if not used)
JH3	15–21	I6,X	Additional HIP identifier (set to 0 if not used)
JH4	22–24	I2,X	Number of different target positions, N_P
JH5	25–28	I3,X	Number of following transit records, N_T
JH6	29–41	F12.8,X	Right ascension of reference point, α_0 (deg)
JH7	42–54	F12.8,X	Declination of reference point, δ_0 (deg)
JH8	55–61	F6.2,X	Parallax of reference point, π_0 (mas)
JH9	62–70	F8.2,X	Proper motion in α of reference point, $\mu_{\alpha*0}$ (mas/yr)
JH10	71–79	F8.2,X	Proper motion in δ of reference point, $\mu_{\delta 0}$ (mas/yr)
JH11	80–87	F7.3,X	Assumed $V - I$ for HIP identifier in Field JH1 (mag)
JH12	88–95	F7.3,X	Assumed $V - I$ for HIP identifier in Field JH2 (mag)
JH13	96–125	F7.3,23X	Assumed $V - I$ for HIP identifier in Field JH3 (mag)

Table 2.9.2. Hipparcos Transit Data: Pointing Record

Field	Bytes	Format	Description
JP1	1–2	I1,X	Index (1 to 3) for the HIP identifier of target position 1
JP2	3–6	I3,X	Offset in α for target position 1 (arcsec)
JP3	7–10	I3,X	Offset in δ for target position 1 (arcsec)
JP4	11–12	I1,X	Index (1 to 3) for the HIP identifier of target position 2
JP5	13–16	I3,X	Offset in α for target position 2 (arcsec)
JP6	17–20	I3,X	Offset in δ for target position 2 (arcsec)
JP7	21–22	I1,X	Index (1 to 3) for the HIP identifier of target position 3
JP8	23–26	I3,X	Offset in α for target position 3 (arcsec)
JP9	27–30	I3,X	Offset in δ for target position 3 (arcsec)
JP10	31–32	I1,X	Index (1 to 3) for the HIP identifier of target position 4
JP11	33–36	I3,X	Offset in α for target position 4 (arcsec)
JP12	37–40	I3,X	Offset in δ for target position 4 (arcsec)
JP13	41–42	I1,X	Index (1 to 3) for the HIP identifier of target position 5
JP14	43–46	I3,X	Offset in α for target position 5 (arcsec)
JP15	47–50	I3,X	Offset in δ for target position 5 (arcsec)
JP16	51–52	I1,X	Index (1 to 3) for the HIP identifier of target position 6
JP17	53–56	I3,X	Offset in α for target position 6 (arcsec)
JP18	57–60	I3,X	Offset in δ for target position 6 (arcsec)
JP19	61–62	I1,X	Index (1 to 3) for the HIP identifier of target position 7
JP20	63–66	I3,X	Offset in α for target position 7 (arcsec)
JP21	67–70	I3,X	Offset in δ for target position 7 (arcsec)
JP22	71–72	I1,X	Index (1 to 3) for the HIP identifier of target position 8
JP23	73–76	I3,X	Offset in α for target position 8 (arcsec)
JP24	77–80	I3,X	Offset in δ for target position 8 (arcsec)
JP25	81–82	I1,X	Index (1 to 3) for the HIP identifier of target position 9
JP26	83–86	I3,X	Offset in α for target position 9 (arcsec)
JP27	87–125	I3,36X	Offset in δ for target position 9 (arcsec)

Table 2.9.3. Hipparcos Transit Data: Transit Record

Field	Bytes	Format	Description
JT1	1–2	I1,X	Target position index (1 to N_P) for this record, I_P
JT2	3–13	F10.7,X	Epoch of the transit, t, in years from J1991.25(TT)
JT3	14–22	I8,X	Spatial frequency f_x (rad/rad)
JT4	23–31	I8,X	Spatial frequency f_y (rad/rad)
JT5	32–40	I8,X	Parallax phase factor f_p (rad/rad)
JT6	41–47	F6.3,X	Natural logarithm of b_1, $\ln b_1$
JT7	48–55	F7.4,X	Normalised signal parameter, b_2/b_1
JT8	56–63	F7.4,X	Normalised signal parameter, b_3/b_1
JT9	64–71	F7.4,X	Normalised signal parameter, b_4/b_1
JT10	72–79	F7.4,X	Normalised signal parameter, b_5/b_1
JT11	80–85	F5.2,X	Natural logarithm of σ_1, $\ln \sigma_1$
JT12	86–91	F5.2,X	Natural logarithm of σ_2, $\ln \sigma_2$
JT13	92–97	F5.2,X	Natural logarithm of σ_3, $\ln \sigma_3$
JT14	98–103	F5.2,X	Natural logarithm of σ_4, $\ln \sigma_4$
JT15	104–109	F5.2,X	Natural logarithm of σ_5, $\ln \sigma_5$
JT16	110–114	F4.2,X	Colour correction factor, s_1 (mag^{-1})
JT17	115–119	F4.2,X	Colour correction factor, s_2 (mag^{-1})
JT18	120–124	F4.1,X	Additional attitude noise, σ_{att} (mas)
JT19	125	I1	Flag for computed (0) or assumed (1) standard errors

Section 2.10

Identification Charts and Tables

2.10.1. Identification Charts

Introduction

Although the Hipparcos mission was dedicated to the astrometry of primarily the brightest stars of the sky, a significant fraction of fainter stars of astrophysical interest were included in the observing programme. Frequently, these stars were originally discovered on objective prism plates, or by blinking plates for proper motion or variability detection. The poor accuracy of many of the original positions sometimes made the candidate identification for the Hipparcos Input Catalogue compilation quite difficult. Frequently it was necessary to investigate individual ESO and Palomar plates, or to use the Astrographic Catalogue and subsequently the Guide Star Catalog (GSC; B.M. Lasker *et al.*, 1990, *Astron. J.*, 99, 2019) in order to verify or obtain suitable positions for the identifications and for the satellite observations.

A complete scientific evaluation of the Hipparcos results will require complementary information on photometry, spectroscopy, and radial velocities. The brightness of most Hipparcos stars allows these observations to be undertaken with small- to medium-sized telescopes. However, the pointing accuracy of such instruments is not always precise enough to ensure an unambiguous identification from accurate coordinates alone, at least for faint stars or stars in crowded areas.

In order to avoid a duplication of identification work by future observers, it was considered useful to produce identification charts for the fainter and more ‘complex’ stars in the Hipparcos Catalogue. The recent availability of the GSC provided an attractive opportunity to produce a compilation of charts with a rather well-defined limiting magnitude and, moreover, a density of faint background stars sufficient to make stellar patterns easy to recognise even in areas of low star density. A few stars in the Hipparcos Catalogue may have been misidentified during the compilation of the Hipparcos Input Catalogue, and therefore will not correspond to the objects considered to have been submitted by the original proposer. The identification charts, and the corresponding positions listed in the main catalogue, will also indicate which stars were actually observed by the satellite.

The identification charts have therefore been constructed on the basis of the positions obtained from the satellite observations accounting, where appropriate, for the object’s proper motion between the catalogue epoch and the epoch of the material used for the identification charts. The charts therefore always identify the object actually observed by the satellite, irrespective of any possible confusion between the position included in the Hipparcos observing programme, and the intended scientific target.

The process of constructing the identification charts also proved to be a useful way of validating certain results of the mission—all targets, for example, were tested to lie within 10 arcsec of their expected position, and within 1 mag of their expected magnitude once V_J from the Hipparcos or ground-based observations was transformed into the V or J magnitudes corresponding to the identification material. For this purpose, the correspondence between the photographic magnitudes and the B and V magnitudes used the following relationships:

$$\begin{aligned} J \text{ plate}: &\quad m = V + 0.72\,(B - V) \\ V \text{ plate}: &\quad m = V - 0.12\,(B - V) \\ E \text{ plate}: &\quad m = V - 0.75\,(B - V) \end{aligned} \qquad [2.10.1]$$

It was consequently straightforward to check coordinate inaccuracies, or the presence of disturbing companions or galaxies, possibly affecting the astrometry or the photometry. It was also a valuable check of the detection and processing of double and multiple stars, and of the presence of nebulosity and veiling-glare effects. Targets confirmed as missed are noted in the catalogue, and no chart was produced for such stars.

In summary, the charts have two goals: to assist the identification of the object at telescope on the one hand, and to provide an indication of the 'cleanliness' in the vicinity of the most complex Hipparcos targets (such as double systems, crowded fields, or objects with surrounding nebulosity) on the other.

Star Selection

Volume 13 contains identification charts for a subset of the objects (a little more than 10 000) contained in the Hipparcos Catalogue: primarily faint objects, and those where there was considered to be some possibility of misidentification. The identification charts have been updated with respect to those presented in the Hipparcos Input Catalogue, ESA SP–1136, Volume 7, in particular by accounting for improved magnitudes provided by the Hipparcos mission, and also by adjusting the limiting magnitude criteria for the chart selection.

The choice of stars needing a chart was guided by the probability of confusing objects of similar magnitudes in an area of about a quarter of a square degree. At high galactic latitudes, stars as faint as 11–12 mag may be located without ambiguity, whereas in the galactic plane stars as bright as 9 mag may require an identification chart if the field is crowded. In order to retain only those stars for which a chart is really useful, a limiting magnitude depending on the galactic latitude was selected. Exceptions were made for stars in open clusters and in the Magellanic Clouds, and for variable stars if these are fainter than the Hipparcos limiting magnitude at minimum luminosity. The threshold adopted for the visual magnitude is given by:

$$V_{\rm lim} = 9.2 + 1.65\,|\sin b\,| \qquad [2.10.2]$$

where b is the galactic latitude (a value of 8.9 rather than 9.2 was adopted in the case of the Hipparcos Input Catalogue identification charts). At galactic latitudes higher than 42° a constant limiting magnitude of $V = 10.5$ mag was adopted (these values were 58° and 10.3 mag respectively in the case of the Hipparcos Input Catalogue).

Material used for the Charts

The charts are all based on material made available by the Space Telescope Science Institute (STScI). The STScI digitized Schmidt survey plates covering the entire sky to obtain the image data necessary for the construction of the Guide Star Catalog (GSC). It subsequently released the digitized plate material on a series of 101 CD-ROMs.

The southern hemisphere material (plate centres $\delta \leq 0°$) was constructed largely from the SERC Southern Sky Survey and the SERC J equatorial extension. These are deep (3600 s) IIIa-J exposures obtained through a GG 395 filter, except for 94 short (1200 s) V-band exposures mostly at low galactic latitudes ($|b| \leq 15°$), two plates covering the Large Magellanic Cloud, and two very short (300 s) V-band exposures each centred on one of the Magellanic Clouds. The northern hemisphere material (plate centres $\delta \geq 6°$) were constructed from the 1950–55 epoch Palomar Sky Survey for the Digitized Sky Survey, and from the Palomar 'Quick V' survey for the Guide Star Catalog.

As indicated by the flag in Field H69 of the main Hipparcos Catalogue, there are two types of chart:

Section D: charts produced directly from the STScI Digitized Sky Survey (DSS);
Section G: charts produced from the Guide Star Catalog (GSC).

It was inappropriate to derive all charts entirely from the DSS, or entirely from the GSC. Thus in crowded regions, or for double systems, the GSC is incomplete, or may include spurious objects arising from the object detection/classification algorithms, or entries added from other sources in order to improve on the GSC completeness. Similarly, the large scale size adopted for the DSS charts (5 arcmin field) is appropriate for the identification of objects in crowded regions, while the smaller scale size adopted for the GSC charts (15 arcmin field) is necessary for the unambiguous identification of objects in less crowded regions.

In practice, GSC charts were initially produced for all candidate identification charts, and superseded by the DSS charts only when necessary. For complex fields the DSS charts were normally preferred while, in cases of a clean stellar vicinity, the chart showing the best stellar pattern allowing a secure identification was retained. For large open clusters, for example, the GSC charts were almost always preferred.

Identification charts were retained for stars located in crowded areas or in front of bright nebulae. In many cases the target star was the secondary component (B, p or C, etc.) close to a bright A component. Since configuration charts are already provided for double and multiple systems (Volume 10), no chart has been given here for faint components when the primary is brighter than the adopted magnitude threshold.

Sections D and G are each ordered according to increasing HIP number, except for the catalogue entries with HIP >120000, which were inserted according to their right ascension. When ranked strictly according to right ascension, HIP numbers are inverted in 54 cases, although the differences in α are always less than 1^s.

Section D: Charts produced directly from the STScI Digitized Sky Survey

The size of each D chart is 5×5 arcmin^2, with north at the top and east to the left. The charts include the HIP number, the (sexagesimal) position identifier (epoch J1991.25, reference system ICRS), and the plate colour.

Each field is centred on the star's position at the Hipparcos catalogue mean epoch, J1991.25, indicated by an open circle of 15.6 arcsec. The star is identified by an open cross at its predicted position at the epoch of the plate, based on the Hipparcos position and proper motion—the reasons for some small discrepancies between the position of the object and the position of the cross are noted below.

Displacements between the crosses and circles thus immediately indicate those cases where the proper motion was significant—with 40 years of epoch difference large proper motions result in non-negligible displacements. However, the range of plate epochs must be taken into account when using visual criteria to establish high proper motion objects.

Identification charts in this category generally apply to the more 'complex' systems, including:

- cluster stars in crowded areas;
- stars in the Large and Small Magellanic Clouds;
- variable stars faint at minimum;
- stars in nebulae;
- multiple systems.

In order to construct the charts, the 101 CD-ROMs of the Digitized Sky Survey were compressed from the original 16 bits (64k intensity levels) to 4 bits, which retains rather satisfactorily the object configuration (whilst, however, strongly degrading any photometric information). The charts were rotated such that north is at the top of each chart.

A mean background over the region corresponding to the (28×28) sub-plates was subtracted, but a low background level was added to the final charts for visual contrast. The background subtraction amplified the contrast between the stars and the background. Uniform contrast was generally achieved, for example, even in areas of high Hα emissivity. Small-scale features are also preserved, such as small bright clouds (e.g. HIP 139), planetary nebula (e.g. HIP 3678, 19395) or more extended nebulae (e.g. HIP 17465).

The plate colour is given at the bottom right of each plate. The original Palomar 'E' plates from the years 1950–55 were used for the northern part of the DSS (nominally for field centres with $\delta \geq 6°$, but with a southern limit oscillating somewhat along the equator). For the southern sky (for both the DSS and the GSC) the V or J plates were used.

The knowledge of the plate epoch was necessary to establish the position of large proper motion stars at the relevant epoch. A mean plate epoch 1952.5 was adopted for the Palomar 'E' Sky Survey. For the southern part, the positions of the relevant plates are given in the GSC, and the epoch of the plates used to produce each individual 'D' chart is given in Table 2.10.1. These epochs allow extrapolation of the position of large proper motion stars from J1991.25 to the epoch of future observations.

Section G: Charts from the Guide Star Catalog (GSC)

The size of each G chart is 15×15 arcmin^2, with north at the top and east to the left. The charts include the HIP number, the (sexagesimal) position identifier (epoch J1991.25, reference system ICRS), and the plate colour.

Stars were selected from the GSC files according to their coordinates given in the Hipparcos Catalogue, and stars within the chart area were retained with information on their coordinates, magnitudes, and plate colour and number. The limiting magnitude of the background stars is around 14.5 mag, but often brighter in the galactic plane.

In case of overlapping plates, and thus multiple entries in the GSC, the data set from the earliest epoch was retained. The spherical coordinates were then transformed into rectangular x, y in units of 0.3 arcsec (to reduce storage requirements). The GSC star having a position closest to the Hipparcos Catalogue object was initially selected by default, and retained only if its position coincided with that of the Hipparcos Catalogue entry. A marker was positioned on the target object, each marker being edited to avoid superposition on field stars thus enhancing readability.

The corresponding epoch of the star positions given in the GSC was also retained for the identification charts. Certain objects were missing from the original GSC, and in these cases the STScI compilation included positions and colours of missing objects from the literature (for example, from the SIMBAD data base). Sometimes the epoch of these additional positions was not available, and not included in the GSC file—if unknown the epoch of the positions of these additional objects was set to 1980.00 for the production of the GSC identification charts. In a few cases, the missing targets had known proper motions, and positions were provided at epoch J2000.0 (for 15 stars in the GSC section, this epoch was given in the GSC as 00 JAN 00).

Similarly, the magnitude of an object in the Guide Star Catalog (which is also included in the GSC file) may not have been derived from the GSC scans. Thus the magnitude of the Hipparcos Catalogue object (or one or more other objects in the area of the chart) may not correspond to the magnitude in the passband of the other objects in the field; this complication has been ignored, and each identification chart lists simply the colour of the plate material used for the basic scan.

Table 2.10.1. Epochs of plates for the DSS charts: epoch = year – 1900

HIP	Epoch	HIP	Epoch	HIP	Epoch	HIP	Epoch
000139	52.50	009429	78.82	022658	52.50	031300	79.97
000172	52.50	009607	52.50	022758	87.07	031361	52.50
000344	52.50	009711	76.66	022794	87.07	031365	52.50
000390	52.50	009867	52.50	022852	52.50	031408	52.50
000523	77.87	010332	52.50	023113	52.50	031481	78.04
000561	52.50	010617	78.82	023177	87.07	031561	52.50
000703	76.66	010687	52.50	023342	79.19	031734	52.50
000731	52.50	010812	79.64	023512	83.85	032159	79.00
000738	77.56	011188	52.50	023519	83.04	032270	84.18
000911	77.84	011350	82.66	023527	79.19	032417	79.90
001006	52.50	011582	79.94	023692	52.50	032592	52.50
001041	52.50	011650	52.50	023894	52.50	032825	76.99
001068	52.50	011792	52.50	023904	52.50	032928	84.18
001182	77.69	011807	52.50	024069	52.50	032940	81.17
001295	52.50	011809	83.69	024347	87.07	033390	78.04
001405	52.50	012101	76.90	024472	84.90	033403	80.20
001511	52.50	012142	52.50	024645	52.50	033963	83.10
001901	52.50	012261	75.69	024728	52.50	033972	83.05
002347	52.50	012456	52.50	024907	87.07	034104	75.00
002354	52.50	012621	52.50	025097	79.19	034115	52.50
002382	52.50	012668	82.78	025101	76.89	034302	82.95
002458	82.85	012695	52.50	025224	52.50	034316	83.10
002499	75.82	012806	52.50	025448	79.19	034541	81.17
003256	52.50	012992	52.50	025578	52.50	034962	80.21
003446	83.85	013198	52.50	025593	52.50	034991	80.21
003460	52.50	013572	83.78	025599	52.50	035023	82.94
003678	82.87	013816	81.76	025615	87.07	035088	81.18
003945	85.96	013948	83.98	025633	52.50	035281	82.98
004004	85.96	014543	52.50	025673	84.90	035305	81.18
004126	85.96	014813	77.78	025815	87.07	035366	81.18
004153	85.96	015312	77.95	026081	82.89	035378	81.18
004189	76.89	015401	52.50	026125	78.09	035755	52.50
004341	85.96	015667	52.50	026135	87.07	035812	52.50
004768	85.96	015726	52.50	026218	87.07	035940	80.21
005267	85.96	015803	77.78	026222	87.07	036369	52.50
005353	52.50	016090	52.50	026322	52.50	036423	75.94
005397	85.96	016227	82.94	026337	52.50	036558	77.94
005658	52.50	016566	77.73	026338	87.07	036596	80.21
005970	52.50	016647	83.70	026675	52.50	036617	83.95
006170	52.50	017278	52.50	026745	79.19	036621	81.18
006171	52.50	017465	52.50	026857	52.50	037018	83.02
006231	52.50	017468	52.50	027286	76.90	037062	83.02
006239	52.50	017648	52.50	027309	83.85	037083	83.02
006818	52.50	018076	52.50	027655	79.19	037217	83.95
007238	52.50	018180	80.94	027784	52.50	037417	79.00
007416	52.50	018253	52.50	027819	79.19	037418	79.00
007454	52.50	018338	52.50	027868	79.19	037433	79.00
007878	52.50	018623	52.50	027894	79.00	037464	83.02
007936	52.50	019245	52.50	028008	76.90	037480	83.02
008125	52.50	019276	52.50	028041	52.50	037507	83.02
008154	52.50	019395	52.50	028116	76.01	037738	80.26
008239	52.50	019532	52.50	028227	82.90	037771	80.26
008305	52.50	019560	52.50	028618	75.03	037780	80.26
008325	52.50	019813	52.50	028754	78.03	037876	77.07
008487	52.50	019833	52.50	029022	52.50	038336	80.06
008691	84.60	019852	52.50	029096	80.04	038384	79.00
008709	52.50	020338	79.00	029121	52.50	038430	80.26
008939	52.50	020777	52.50	029127	52.50	038432	79.00
008946	52.50	021334	52.50	029483	79.00	038441	83.95
009125	52.50	021384	52.50	029861	78.10	038461	79.00
009196	52.50	021492	52.50	029988	52.50	038483	80.26
009221	52.50	022182	52.50	030783	79.08	038534	75.94
009224	52.50	022256	86.97	030992	82.88	038561	52.50
009291	52.50	022466	83.01	030997	52.50	038655	78.03
009410	52.50	022627	52.50	031214	77.05	038683	78.03

Table 2.10.1. (cont.) Epochs of plates for the DSS charts: epoch = year – 1900

HIP	Epoch	HIP	Epoch	HIP	Epoch	HIP	Epoch
038703	80.26	048422	52.50	058987	76.26	067823	75.50
038716	78.03	049139	76.26	058999	87.26	067849	75.50
038721	79.00	049314	77.05	059026	87.26	067906	75.50
038772	76.99	050230	87.19	059069	87.26	068422	80.00
038788	79.00	050610	78.17	059101	87.26	069005	76.27
038798	87.25	050697	81.17	059551	75.00	069084	52.50
038820	76.25	050702	75.00	060488	87.07	069163	74.47
038854	87.25	050704	77.06	060737	87.26	069285	74.47
038915	83.04	050717	75.00	060751	87.07	069292	74.46
038956	52.50	051595	80.07	060814	87.26	069445	87.40
039750	79.24	051612	81.17	060857	87.26	069860	52.50
039987	79.97	051719	78.17	060863	87.07	070079	76.33
040186	82.88	051773	87.19	060875	87.07	070417	75.44
040272	79.97	051857	75.00	060967	76.30	070423	76.19
040351	52.50	051866	87.19	060971	87.26	070730	76.19
040379	76.97	052171	87.19	060974	87.26	070733	76.19
040679	87.25	052444	87.05	061440	76.25	070832	76.19
040717	77.21	052488	87.05	061713	52.50	070870	76.19
040721	77.21	052651	87.08	061874	76.30	070911	76.19
040723	87.25	052839	87.08	061978	87.07	070925	76.19
040730	77.21	052854	80.20	061997	87.26	070975	83.35
040748	87.25	052887	87.08	062115	87.26	071195	80.21
040764	77.21	052988	77.06	062135	76.30	071228	76.19
040769	78.11	053150	79.15	062181	52.50	071389	52.50
041076	52.50	053213	79.31	062374	52.50	071922	75.36
041503	79.99	053491	87.05	062913	75.00	072115	52.50
041661	52.50	053630	75.36	062918	75.00	072287	52.50
041697	76.26	053853	87.08	062931	75.00	072300	52.50
041824	52.50	053867	87.19	062937	75.00	072424	78.35
041936	52.50	053873	78.20	062949	87.07	072444	87.40
042115	84.03	054226	76.26	063040	87.46	072460	78.35
042714	77.28	054365	76.08	063303	52.50	072511	83.29
042787	79.00	054621	87.19	063399	79.16	072605	88.47
042964	52.50	054668	87.05	063488	78.13	072625	52.50
042979	87.19	054744	76.25	063835	87.07	072916	52.50
043465	52.50	054865	79.31	063882	52.50	073205	77.43
043491	52.50	054948	87.19	064438	83.19	073391	78.35
043650	87.19	055031	79.31	064763	75.41	073711	78.35
044232	87.19	055325	78.19	065307	76.25	073732	78.35
044243	87.19	055715	76.33	065344	83.36	073782	78.35
044263	52.50	055753	75.19	065362	83.36	073903	74.46
044605	52.50	055775	77.22	065597	76.25	074397	74.46
044848	77.22	055947	75.19	065618	76.25	074583	75.20
044949	76.08	055955	83.35	065655	76.25	074660	87.65
044968	75.27	056244	77.07	065669	76.41	074721	75.30
045050	76.31	056272	84.39	065782	76.25	074726	87.40
045069	52.50	056432	77.22	065786	76.25	074739	52.50
045205	75.27	056477	52.50	065809	76.49	075155	74.46
045292	83.20	056586	87.19	065818	76.25	075193	52.50
045570	76.31	056592	87.19	066027	76.25	075225	52.50
045880	52.50	056897	80.00	066028	76.25	075745	75.20
046488	84.18	056934	87.51	066054	76.25	075813	76.24
046502	76.31	057009	75.19	066732	77.15	076059	82.55
046610	76.31	057130	87.26	066993	75.27	076172	82.48
046624	79.22	057252	77.07	067164	82.30	076640	76.48
047066	83.13	057294	76.25	067204	76.25	076881	75.52
047085	79.99	057642	77.07	067207	75.50	076896	87.31
047307	52.50	057656	75.41	067227	78.33	076978	88.30
047539	83.36	058107	87.26	067232	75.00	077005	88.43
047626	77.07	058170	78.33	067286	75.19	077157	74.47
047680	77.05	058360	75.41	067626	79.19	077456	76.40
047890	77.05	058411	87.26	067757	76.33	077460	52.50
048159	79.99	058432	87.26	067761	82.52	077663	83.52
048270	52.50	058870	52.50	067798	75.19	077788	52.50
048338	76.31	058909	87.26	067820	75.50	077798	52.50

Table 2.10.1. (cont.) Epochs of plates for the DSS charts: epoch = year – 1900

HIP	Epoch	HIP	Epoch	HIP	Epoch	HIP	Epoch
078053	75.42	088079	52.50	097202	76.34	105261	81.57
078227	76.40	088118	76.33	097673	52.50	105485	52.50
078257	52.50	088333	87.71	097764	52.50	105622	52.50
078307	52.50	088446	76.25	097772	52.50	105638	77.70
078317	75.42	088495	76.34	097785	52.50	105701	52.50
078567	83.52	088786	87.71	097806	52.50	106172	52.50
078771	88.43	088802	76.33	098147	83.68	106175	52.50
078786	80.00	089018	52.50	098265	79.71	106210	52.50
078940	76.24	089278	87.56	098411	52.50	106290	52.50
079440	87.30	089324	76.34	098447	75.66	106417	52.50
079466	88.43	089483	87.56	098793	52.50	106565	82.56
079623	76.24	089535	87.38	098797	52.50	106649	76.66
079743	79.62	089653	86.66	098811	79.71	106905	52.50
079844	75.42	089681	75.00	098884	79.71	107408	52.50
079850	76.24	089743	86.66	098906	52.50	107968	52.50
079891	87.30	089750	86.66	099389	52.50	107983	52.50
079973	87.39	089831	87.56	099438	77.60	108052	52.50
080229	88.45	089842	86.66	099492	83.68	108457	52.50
080290	78.58	089903	76.33	099599	52.50	108523	78.81
080365	87.39	090199	52.50	099635	52.50	108594	75.60
080402	82.54	090249	52.50	099890	82.63	108706	52.50
080817	83.50	090273	52.50	099898	52.50	108768	76.66
080825	75.00	090392	52.50	100137	75.37	108890	77.78
080931	87.30	090658	75.68	100198	52.50	109010	52.50
081182	88.39	090707	83.68	100289	52.50	109020	52.50
081258	76.33	090711	87.38	100818	79.62	109603	52.50
081309	87.30	090983	78.57	101063	78.73	109715	80.48
081463	76.25	091197	78.57	101356	82.63	109756	52.50
082084	76.33	091419	52.50	101453	82.63	110160	78.82
082097	76.33	091420	78.57	101461	79.62	110213	52.50
082318	76.24	091437	52.50	101519	52.50	110280	52.50
082348	87.30	091443	76.63	101527	52.50	110292	82.62
082676	88.29	092009	86.66	101540	52.50	110736	80.77
082691	88.29	092059	87.63	101566	52.50	110964	52.50
082706	75.00	092221	52.50	101574	76.63	111094	52.50
082819	88.29	092486	52.50	101743	52.50	111858	52.50
082876	75.00	092548	52.50	101856	52.50	111932	52.50
082899	76.63	092716	86.67	102190	52.50	111976	52.50
082904	76.63	092811	80.61	102606	52.50	112334	52.50
083008	76.33	092903	52.50	102679	82.56	112558	52.50
083012	76.33	092945	78.58	102682	77.53	112887	52.50
083573	88.29	093030	52.50	102732	52.50	113373	52.50
083582	84.25	093047	52.50	103106	52.50	113652	77.78
083762	52.50	093293	87.59	103180	77.53	113894	52.50
083869	76.24	093477	77.53	103185	52.50	114253	52.50
083944	76.63	093791	76.41	103364	52.50	114469	52.50
084369	76.25	093932	52.50	103393	82.64	114490	52.50
084708	76.26	093987	52.50	103441	52.50	114552	52.50
084752	52.50	094289	52.50	103839	77.53	114791	52.50
084901	87.70	094312	74.56	103992	82.70	114995	52.50
084986	87.70	094419	76.41	104013	52.50	115521	52.50
085245	87.70	095032	52.50	104023	80.52	115566	52.50
085429	52.50	095071	82.56	104078	52.50	116497	52.50
085473	76.26	095444	76.71	104093	52.50	116684	52.50
086011	87.31	095649	52.50	104137	52.50	117728	80.54
086562	78.58	095672	80.53	104170	52.50	118059	52.50
086616	52.50	095676	78.68	104270	52.50	118066	52.50
086714	52.50	095702	52.50	104384	52.50	118163	52.50
086836	77.63	095856	83.68	104623	52.50	118172	52.50
086895	76.25	096515	76.34	104645	76.71	118174	52.50
086897	82.62	096532	52.50	104709	52.50	118188	52.50
087388	87.34	096538	52.50	104777	79.62	118196	52.50
087487	52.50	096581	79.69	104888	52.50	120121	75.34
087938	52.50	096974	75.66	104921	52.50	120132	87.71

2.10.2. Identification Tables

The second part of Volume 13 contains 6 cross-identification tables, organised as follows:

Table 1. HIP Numbers Inconsistent with the HIC Cross-Identifiers

Table 1 gives the HIP number of stars for which the satellite was significantly mispointed because of particularly inaccurate *a priori* coordinates, or for which the identification was erroneous and the star observed by the satellite does not correspond to the identifier(s) or to the component(s) given in the Hipparcos Input Catalogue. Some identification errors (reflected in the Hipparcos Input Catalogue compilation) originated from the literature, where a given variable or high proper motion star was associated with a particular HD or DM number, while the Hipparcos observations showed that the star observed is not variable, or not a high proper motion star.

These inconsistencies are listed for appropriate entries in the corresponding notes of the Hipparcos Catalogue. Resulting corrections to the associated cross-identifications are also reflected in Tables 2 and 5, in Fields H71–74 of the machine-readable version of the Hipparcos Catalogue, and in the updated version of the Hipparcos Input Catalogue included in *Celestia 2000*.

Stars for which a discrepancy was found between the Hipparcos results and the *a priori* information given in the Hipparcos Input Catalogue, but for which a misidentification was not fully evident, are indicated in the corresponding catalogue notes but are not given in this table.

Table 2. HD (Henry Draper) Catalogue Numbers

Table 2 allows the HIP number corresponding to a given HD number to be located. It is ordered according to the running number in the HD Catalogue. Since one HIP number may, in the case of multiple systems, relate to more than one HD number, the same HIP number may be found twice (or, possibly, three times) corresponding to different HD numbers.

Corrections to the cross-identification between HIP and HD numbers, especially (but not only) for multiple systems, for variable stars and for high proper motion stars, have been compiled since the publication of the Hipparcos Input Catalogue. In particular, the lists of errata published by Dommanget & Nys (*Bull. Inf. CDS*, 1995, 46, 13; *Bull. Inf. CDS*, 1996, 48, 19), and identification errors and missed targets indicated in the notes of the Hipparcos Catalogue, have been taken into account. In addition, errors and additions collected when incorporating the HIC identifier into SIMBAD have also been accounted for.

Table 3. HR (Bright Star) Catalogue Numbers

Table 3 allows the HIP number corresponding to a given HR number to be located. It is ordered according to the running number in the HR (Bright Star) Catalogue.

Table 4. Bayer and Flamsteed Names

Table 4 gives the HIP number for stars known under a Bayer and/or Flamsteed name. Constellations are sorted by their full name (not the abbreviated form, thus Cam, Cnc, CVn, CMa, CMi, Cap, Car, etc.). Within each constellation names are sorted either alphabetically (Bayer) or by increasing numbers (Flamsteed), as follows:

- Bayer (Greek letters)
- Bayer (lower case letters)
- Bayer (upper case letters)
- Flamsteed (numbers)

For the machine readable version of Table 4, the equivalence between the phonetic equivalent (and inclusion of the underscore syntax linking the two parts of the star name) follows the convention described under Field P17 of the Variable Star Annex (Section 2.4). A component identification may be given after the star name, thus 59_And_A.

Table 5. Variable Star Names

Table 5 gives the variable star names (i.e. those of the type RR Lyr or V500 Lyr) for all Hipparcos stars properly identified with a variable star name. The table includes stars that were subsequently found to be constant (as indicated in the literature or as found from the Hipparcos data) but excludes those stars that were found to be misidentified in the Hipparcos Input Catalogue (see Table 1). When stars were found to be variable, the variable star name also appears in either Field P17 or Field U17 of Section 2.4. These also include the stars newly discovered as variable from the analysis of Hipparcos epoch photometry, where newly-assigned variable star names were allocated, under the authority of the IAU, by N.N. Samus and colleagues (Moscow).

Variable star names are ordered according to the full name of the constellation (not the abbreviated form, thus Cam, Cnc, CVn, CMa, CMi, Cap, Car, etc.). Within each constellation, they are ordered as follows: Bayer names (Greek letters), Bayer names (lower case), Bayer names (upper case), R, S, ..., Z, RR, RS, ..., ZZ, AA, ..., QZ, V335, V336, ...

For the machine readable version of Table 5, the equivalence between the phonetic equivalent (and inclusion of the underscore syntax linking the two parts of the star name) follows the convention described under Field P17 of the Variable Star Annex (Section 2.4).

Table 6. Common Star Names

Table 6 gives the HIP identifier for a number of stars known under other common or historical designations. The HIP number of the quasar 3C273 is also included.

Section 2.11

Machine-Readable Files and CD-ROMs

2.11. Machine-Readable Files and CD-ROMs

The ASCII CD-ROMs contain the primary products of the mission, as deposited in data centres, and which thus represent the long-term archive of the Hipparcos mission. Users wishing to transfer the Hipparcos and Tycho Catalogues, and their associated annexes, into their own data bases will use these files.

2.11.1. Conventions for the ASCII CD-ROMs

End of records: Records for data and index files in cats/, notes/, and tables/ are terminated by 'carriage return' plus 'line feed' (CR+LF, or \r\n, or decimal ASCII codes [13,10]). Record lengths listed in the file content description tables do not include these two characters.

Retaining CR or LF alone would have satisfied one or more specific systems, but would have left others interpreting the data files as a single record. The penalty for including both is that different systems will interpret the CR+LF as the end of record terminator, plus an additional redundant character (e.g. '^M' appears at the end of line on Unix systems). Nevertheless, the files can be displayed legibly by most Mac word processor applications, by the DOS 'type' command, and by the Unix 'vi' word processor. Files in /src are Unix compatible, and end of record characters must be converted for use on other systems.

Field delimiters: All fields, except for the last one in a record, are followed by the vertical line '|' character, which therefore separates all ASCII file fields. It is indicated in the file content descriptions by the FORTRAN 1X format. The last field in a record is followed by the record terminator.

Alternative choices of spaces, tab characters, or commas, were considered. Avoiding the use of a blank means that blanks can be entered when data are absent, and the files can still be read into editors or spreadsheet-type programmes. The tab character is convenient in some systems, but inconvenient (and invisible) in others.

Integers representing multiple bits: In certain data fields in the annexes a number of 1-bit flags ('binary digits' or 'bits') have been encoded into a single decimal number, for storage efficiency. [A bit-string conversion routine is defined within the file utils.h]

A two-digit decimal number can accommodate up to 6 binary digits (bits), all 6 bits set corresponding to the decimal number 63. The individual bits are to be recovered from the decimal value in the following way: any integer number can uniquely be decomposed into a sum of powers of 2, thus, $45 = 2^0 + 2^2 + 2^3 + 2^5$. The individual bits in such a quantity are numbered from zero (the least-significant bit) upwards. A particular bit is 'set' if the corresponding power of two appears in the decomposition. In this example, bit numbers 0, 2, 3 and 5 are set, while bit numbers 1, 4, and all higher bits are not set.

Missing data: Blanks are used whenever data are absent or when a field is empty. Due caution must be taken to avoid interpreting a blank field as the numerical value 0. [An appropriate interpretation facility is defined within the file utils.h]

2.11.2. Contents and Directory Structure of the ASCII CD-ROMs

The Hipparcos CD-ROMs are formatted for the ISO–9660 Standard, Data Interchange Level 1. Specific details of the data formats are given hereafter.

Directory Structure

Relevant elements of the following directory tree are contained on each CD-ROM:

/			Readme files
	cats/		Catalogue files, index files
	docs/		Documentation (and some figures) in PDF format
	notes/		Notes and references
	tables/		Identification tables (Volume 13)
	charts/		Identification charts
		dss/	DSS identification charts (‘D’ in Field H69)
		gsc/	GSC identification charts (‘G’ in Field H69)
	curves/		Light curves
		a/	Folded light curves (‘A’ in Field H54)
		b/	AAVSO light curves (‘B’ in Field H54)
		c/	Unfolded light curves (‘C’ in Field H54)
	src/		C/Fortran utilities
	fits/		FITS conversion utilities

Data Files and File Names

Details of the index files, file names, formats, and disk organisation are given in Tables 2.11.1–2.11.4. File names follow a DOS-like (ISO–9660 standard) representation: a file name (maximum of 8 characters), followed by an extension of up to 3 letters.

By convention this documentation uses Unix-style directory paths to denote the location of files on the CD-ROMs, with all the paths and file names in lower case. The actual directory path and appearance of the file name on the target computer will depend on the operating system and device driver being used. Thus a UNIX file called temp.ext will appear as follows:

UNIX:	/mycdrom/temp.ext (if the CD-ROM is mounted as mycdrom)
PC:	E:\TEMP.EXT (if the CD-ROM is drive E)
MAC:	DISK1:TEMP.EXT (accessed by double clicking on the DISK1 icon)
VAX/VMS:	MYCDROM:[*]TEMP.EXT;1

The information in each file can be inferred from the extension appended to each file name as follows:

dat:	table data stored as ASCII text
doc:	documentation or other text stored in ASCII format
idx:	index file
eps:	encapsulated PostScript files (for light curves and identification charts)
pdf:	PDF (Portable Document Format) files, viewable with Acrobat/Acroread
f:	Fortran code
c:	C code
h:	C code header

Index Files

Index files are provided for each data file, facilitating the location of records relating to a particular HIP or TYC identifier. As for the machine-readable data files, '|' is used as a field separator, and \r\n at the end of record.

There are four types of 'identifier' which are used to order the relevant data files: HIP identifier; TYC identifier; CCDM identifier; and solar system object identifier. Depending on the specific data file, different structures of the associated index file have been adopted to optimise the search procedure. These search procedures fall into the following categories:

• direct search: hip_main.idx, hip_i.idx, and hip_j.idx contain entries for the complete range of HIP identifier (irrespective of the existence of an associated valid record). The HIP identifier may thus be used as a subscript to directly access the relevant data files, using the corresponding index file;

• binary search: the majority of index files contain entries only for those identifiers existing in the data file. This makes the index file much smaller, but the corresponding data record may only be found indirectly, either by reading the file sequentially, or using a binary search algorithm for more efficient access (see, for example, W.H. Press, S.A. Teukolsky, W.T. Vetterling, B.P. Flannery, *Numerical Recipes in C, 2nd Edition*, Cambridge, 1992);

• mixed search: tyc_main.idx includes direct access for the first component of the TYC identifier (TYC1), and requires a binary search in the data file for the full identifier.

The load and search routines in C described below (and in the readme file) invoke an appropriate search algorithm, based on the index file provided (where appropriate), in a manner fully transparent to the user. Search routines are provided for all files with the exception of curves.idx, charts.idx, and hp_refs.doc for the reasons noted below.

Each index file is summarised hereafter, indicating the applicable search method, and with the detailed structure of each index file given in Table 2.11.1. These will permit users to develop additional access routines, where necessary.

(a) Files ordered by HIP identifier:

hip_main.idx [direct search]: a single-column table provides, as the *n*-th entry, the record number containing the data for HIP *n* (the length of this index table is 120 416). The first record is specified as record 1 (rather than record 0). A value of −1 indicates a non-existing HIP entry.

hip_dm.idx [binary search]: this is a 'combined' index file, which allows the five mutually exclusive parts of the Double and Multiple Systems Annex (C, G, O, V, X) to be accessed using a single index file. The index file has three columns: the HIP identifier; a one-letter column pointing to the relevant annex; and a column providing the record number within the relevant annex. In the case of entries in Part C of the Double and Multiple Systems Annex, the record number corresponds to the *first* record of the solution containing the relevant HIP number: up to eight further records (3 component and 5 correlation records) may follow under the same CCDM identifier. Note that hip_dm_c.dat is also accessible by means of the CCDM identifier (see below).

hip_va.idx [binary search]: this is a 'combined' index file, which allows the two parts of the Variability Annex to be accessed using a single index file. The index file has three columns: the HIP identifier; a one-letter column pointing to the relevant annex; and a column providing the record number within that annex.

hip_ep.idx [direct search]: structured as for hip_main.idx, but with the index giving the *first* record of the relevant HIP identifier.

hip_i.idx [direct search]: structured as for hip_main.idx, but with the index giving the *first* record of the relevant HIP identifier.

hip_j.idx [direct search]: structured as for hip_main.idx, but with the index giving the *first* record of the relevant HIP identifier.

hg_notes.idx [binary search]: the index file has two columns: the HIP identifier; and a column providing the record number of the *first* entry for the given HIP identifier (note that the number of entries for each HIP identifier is stored within each data record).

hd_notes.idx [binary search]: as for hg_notes.idx.

hp_notes.idx [binary search]: as for hg_notes.idx.

hp_auth.idx [binary search]: as for hg_notes.idx. Note that hp_refs.doc provides an alternative (indirect) index associating reference identifiers to a given HIP identifier, particularly convenient for interrogating the printed catalogue. Multiple entries for each HIP identifier are possible. For the machine-readable files, hp_auth.idx circumvents the use of hp_refs.doc (which therefore has no associated index file).

curves.idx: the index file indicates the directory for the corresponding curve. No search routine is provided since the result of the search will be user specific, and since standard UNIX utilities (e.g. grep) are adequate for searching this file.

charts.idx: the index file indicates the directory for the corresponding chart. No search routine is provided since the result of the search will be user specific, and since standard UNIX utilities (e.g. grep) are adequate for searching this file.

Other files (dmsa_o.dat, hip_rgc.dat, ident*.doc) have no associated index files due to their small size, and are interrogated (if required) directly in the relevant search routines.

(b) Files ordered by CCDM identifier:

hip_dm_c.idx [binary search]: this uses a two-column table. The first column gives the CCDM identifier, and the second column gives the record number of the first component record for this system. The lines are sorted on CCDM identifier, in lexical order. hip_dm_c.idx is the CCDM identifier-based index file for Part C of the Double and Multiple Systems Annex only.

Note that all five parts of the Double and Multiple Systems Annex are also indexed on the HIP identifier by means of the combined index file hip_dm.idx. Thus Part C of the Double and Multiple Systems Annex may be accessed either by means of the CCDM or the HIP identifier.

(c) Files ordered by Tycho Catalogue identifier:

Index files for the Tycho Catalogue entries (tyc_main and tyc_ep) are more complex since the TYC identifier comprises three components (e.g. TYC 3512–33–1; see Section 2.2 for details of the numbering scheme). Note that the first two components of the TYC identifier correspond to the GSC identifier, where the first component (TYC1) is in the range 1–9537.

tyc_main.idx [mixed search]: for locating data within the Tycho Catalogue: the Tycho Catalogue comprises one record per entry (i.e. a total of slightly more than 1 million records), ordered by TYC identifier. So, a given entry could be located using a binary-search algorithm in at most 20 steps. In order to speed up this procedure, a one-column table (tyc_main.idx) with 9538 entries provides, as the n-th entry, the record number of the first star in GSC region n. IDX(n+1)–1 gives the last star in the same region. The record related to the relevant entry must be searched for between these limits. The first record is specified as record 1 (rather than record 0).

Example: To find TYC 3512–33–1 within the Tycho Catalogue (on Disk 1), tyc_main.idx is loaded once and held in memory, say in an array I(9538). I(3512) directly gives the record number of the first star in GSC region 3512. I(3512+1)–1 gives the last star in this region. The Tycho Catalogue is then searched for TYC2 = 33, which will fall between records I(3512) and I(3512+1)–1.

tyc_ep.idx [binary search]: for locating data records within the Tycho Epoch Photometry Annex, a table tyc_ep.idx is provided, which contains two columns: the TYC identifier, and the record number of the header record of the corresponding entry in tyc_ep.dat. Note that although the tyc_ep.dat file is larger than tyc_main.dat, a binary search is implemented in the former case because the number of TYC entries (and hence header records) is smaller.

(d) Files ordered by solar system object identifier:

solar.idx [binary search]: this is a combined index file covering the three files containing data on the solar system objects. It has 8 columns. Column 1 gives the solar system object identifier listed in Table 2.7.1 (to be distinguished from a HIP Catalogue number). Column 2 gives a sequential running number (from 1–55) for programming convenience. The remaining 6 columns giving the first record number (–1 if there are no data associated with this object identifier) and the number of records (0 if none) in the three solar system data files, solar_ha.dat, solar_hp.dat, and solar_t.dat.

Data Formats

The formats of data files are included at the end of the section describing the corresponding contents of each relevant catalogue or annex (the relevant section number describing the data is given in Tables 2.11.4/1–6).

Note that 'hip_main' includes the 'extended' Fields H71–77, which are not given in the printed catalogue. Certain data in the Double and Multiple Systems Annex are also contained only in the machine-readable files (as described in Section 2.3).

The formats of the files containing the notes and references are given in Table 2.11.2.

The formats of the 'cross-identification' tables (Volume 13) are given in Table 2.11.3.

Load and Search Routines

Search programs: C code search programs are provided for all data (*.dat) files. Each search program contains a main function which scans the command line for identifiers and applicable search options, then uses the routines summarised below to search for (and print) the relevant data records. The search options are:

- h help
- a apply b, c, s together
- b bit field decoding (applicable to HEPA and TEPA)
- c correlation coefficient extraction (applicable to DMSA/C, G, O, V)
- s sub-record print
- t tabular print

These options may be combined in any order, thus –a ≡ –bcs. The default option prints the main record (verbose), sub-record with no decoding (tabular). Multiple identifiers, and requests for following records, may be given. For certain files (notes/*.doc and solar*.dat) only the tabular print option is likely to be of use.

Naming convention: The C file search programs generally have the same name as the corresponding index file, but with the letter 's' prepended to the name, underscores (_) removed, and with the extension .c (for example, the search routine for hip_main.dat, which makes use of hip_main.idx, is shipmain.c). In the case of hip_ep_e.dat, which utilises the same index file as hip_ep.dat, the search program is named shipepe (i.e. following the name of data file rather than that of the index file). This results in the following search programs: shipmain, stycmain, shipdm, shipdmc, shipva, ssolar, shipep, shipepe, stycep, shipi, shipj.

Additional ('redundant') search programs are provided based on the data file name as follows: shipva1, shipva2, shipdmg, shipdmo, shipdmv, shipdmx, shgnotes, shdnotes, shpnotes, shpauth, sdmsao (indexed on the reference number in Field DO16), shiprgc.

Index code: The C code provided in the src directory loads the index file and locates an entry given an identifier of the appropriate type. It implements a binary or direct search for each index file, as appropriate. The C file has the same name as the corresponding index file, but with the letter 'i' prepended to the name, underscores (_) removed, and with the extention .c (for example, the index interrogation routine accompanying hip_main.idx is ihipmain.c). A header file (.h) accompanies each .c file.

Data code: The src directory contains .c and .h files for every data file (plus some auxilary files in some cases). The source code contains information on the record structure of the corresponding data file (i.e. field names and record length, etc.), as well as routines to perform the following functions:

• search: for a given identifier, the appropriate find routine is used to derive the record number of the requested identifier, and the following routine is used to read it;

• read: for a given record number (not an identifier), the routine reads the record from the data file, including any related data and sub-records (in normal usage, the read routine is invoked by the search request);

• verbose print: for a given record, print the record 'vertically', with a summary description of each field;

• tabular print: for a given record, print the record 'horizontally' (as it would appear in the data file). Field identifiers are given at the top of the record, truncated where necessary to preserve the appropriate layout.

Further details of the load and search routines are given in the readme file in the src/ directory.

Position Propagation Routines

Disk 1 includes Fortran and C implementations of the equations given in Section 1.5.5 for the rigorous epoch transformation of the astrometric parameters and their covariances. The subroutine takes as input the original epoch (in Julian years), the five astrometric parameters (in the units used by the Hipparcos and Tycho Catalogues), the radial velocity parameter ζ (defined by Equation 1.5.24, in mas/yr), and the covariance matrix of the six parameters, all referred to the original epoch, and the required new epoch; the output consists of the corresponding six astrometric parameters and covariance matrix referred to the new epoch. The relevant files are:

- for the Fortran 77 version:
  – src/pos_prop.f (source code with documentation)
- for the C version:
  – src/pos_prop.h (header file containing prototypes and documentation)
  – src/pos_prop.c (source code of the procedure).

It has been verified that the two versions give identical results to within the rounding errors of the double precision arithmetics. No test program is supplied with the routines. The following numerical example should help in validating their application.

Example: Given the Hipparcos astrometric data for Barnard's Star (HIP 87937), propagate its astrometric parameters and covariance matrix to the epoch J1900.0. The five astrometric parameters at epoch J1991.25 are taken from Fields H8–9 and H11–13. Table 1.2.3 gives the radial velocity as −111.0 km/s. The initial values for the parameter vector to be propagated are therefore:

$$\left.\begin{aligned} \alpha_0 &= 269.45402305 \ \text{deg} \\ \delta_0 &= +4.66828815 \ \text{deg} \\ \pi_0 &= 549.01 \ \text{mas} \\ \mu_{\alpha*0} &= -797.84 \ \text{mas/yr} \\ \mu_{\delta 0} &= +10326.93 \ \text{mas/yr} \\ \zeta_0 &= -12855.29 \ \text{mas/yr} \end{aligned}\right\} \ \text{J1991.25}$$

where ζ_0 is calculated from Equation 1.5.24. Using the standard errors in Fields H14–18 and the correlations in Fields H19–28, the initial covariance matrix is found to be:

$$\mathbf{C}_0 = \begin{pmatrix} +1.768900 & +0.143640 & -0.336224 & -0.620977 & -0.017157 & +7.872819 \\ +0.143640 & +1.166400 & -0.324216 & -0.086940 & -0.362232 & +7.591647 \\ -0.336224 & -0.324216 & +2.496400 & +0.381570 & -0.203820 & -58.45420 \\ -0.620977 & -0.086940 & +0.381570 & +2.592100 & +0.436149 & -8.934613 \\ -0.017157 & -0.362232 & -0.203820 & +0.436149 & +1.664100 & +4.772526 \\ +7.872819 & +7.591647 & -58.45420 & -8.934613 & +4.772526 & +4721.914 \end{pmatrix}$$

where Equation 1.5.69 was used to compute the last row and column, assuming a standard error $\sigma_{V_{R0}} = 0.5$ km/s for the radial velocity. Units are mas^2, $\text{mas}^2\text{yr}^{-1}$ and $\text{mas}^2\text{yr}^{-2}$ as appropriate for the different elements.

Propagation of these parameters and covariances from T_0 = J1991.25 to T = J1900.0 by means of pos_prop results in the following parameters (note that the propagation was based on the parameters and covariances calculated in double precision from the catalogue values, not on the rounded values given above):

$$\left.\begin{aligned} \alpha &= 269.47419117 \ \text{deg} \\ \delta &= +4.40801091 \ \text{deg} \\ \pi &= 545.90 \ \text{mas} \\ \mu_{\alpha*} &= -788.54 \ \text{mas/yr} \\ \mu_{\delta} &= +10210.27 \ \text{mas/yr} \\ \zeta &= -12829.25 \ \text{mas/yr} \end{aligned}\right\} \ \text{J1900.0}$$

with covariance matrix:

$$\mathbf{C} = \begin{pmatrix} +21510.98 & +3187.087 & -36.37617 & -234.0989 & -30.28683 & +958.0380 \\ +3187.087 & +14919.00 & +41.45412 & -33.92317 & -172.8802 & -2343.445 \\ -36.37617 & +41.45412 & +2.440553 & +0.412525 & -0.711158 & -56.34087 \\ -234.0990 & -33.92317 & +0.412525 & +2.548358 & +0.314266 & -11.97391 \\ -30.28683 & -172.8802 & -0.711158 & +0.314266 & +2.092324 & +46.58443 \\ +958.0380 & -2343.445 & -56.34087 & -11.97391 & +46.58443 & +4615.337 \end{pmatrix}$$

From ζ and π the radial velocity at J1900.0 is found to be $V_R = -111.406330$ km/s, with a standard error of 0.499986 km/s. Propagation of these parameters and covariance matrix from J1990.0 to J1991.25 should return the original values to within the rounding errors of the arithmetic.

PDF Files

A series of PDF (Portable Document Format) files, viewable with Acrobat/Acroread, are also included on the ASCII CD-ROMs as follows:

- disk 1 includes, in the docs/ directory, four sub-directories, vol1–4, which contain the pdf forms of Volumes 1–4. In each directory the file tocvol*.pdf provides a 'clickable' table of contents. Some figures are low-resolution scans of the printed originals; and some colour images (in particular those from Section 3 of Volume 1, and Appendix F of Volume 2) are not included on disk 1 for reasons of space (see below);

- disk 5 includes, in the docs/ directory, volume*.pdf, which are the pdf forms of Volumes 5–10. The contents of these files follows the sequence of the corresponding printed volumes, as summarised on page xi. The file tocvol.pdf provides a 'clickable' table of contents for these six volumes;

- disk 6 includes, in the docs/ directory, volume11.pdf, which is the pdf form of Volume 11. The contents of this file follows the sequence of the corresponding printed volume, as summarised on page xi. The file tocvol11.pdf provides a 'clickable' table of contents for this volume;

- disk 6 also includes, in the sub-directory docs/figs/, the separate figures from Section 3 of Volume 1. These are included as f3_1_001–007.pdf, f3_2_001–127.pdf, f3_3_001–047.pdf, f3_4_001–042.pdf, and f3_5_001–026.pdf.

The *.pdf files may be viewed (and magnified), searched, printed, and converted to *.ps files, from within Acrobat/Acroread.

Table 2.11.1. Format of the index files.

File	Column	Format	Description of the *n*-th entry (−1 if no information)
hip_main.idx			
	1	I6	Record number of HIP *n* in hip_main.dat
tyc_main.idx			
	1	I7	Record number of first star in GSC region *n*
hip_dm_c.idx			
	1	A10, X	CCDM identifier of HIP *n*
	2	I5	Record number of *first* record for this CCDM identifier in hip_dm_c.dat
hip_dm.idx			
	1	I6, X	HIP identifier
	2	A1, X	Annex identifier (C, G, O, V, X) indicating hip_dm_c/g/o/v/x.dat
	3	I5	Record number of HIP *n* in the given annex (if Field 2 = C, gives the *first* record of the solution)
hip_va.idx			
	1	I6, X	HIP identifier
	2	A1, X	Annex identifier (1, 2) indicating hip_va_1/2.dat
	3	I4	Record number of HIP *n* in the given annex
solar.idx			
	1	I3, X	Solar system object identifier (see Table 2.7.1)
	2	I3, X	Sequential running number of object (from 1–55)
	3	I5, X	Record number of object in solar_ha.dat
	4	I4, X	Corresponding number of records in solar_ha.dat
	5	I5, X	Record number of object in solar_hp.dat
	6	I4, X	Corresponding number of records in solar_hp.dat
	7	I5, X	Record number of object in solar_t.dat
	8	I4	Corresponding number of records in solar_t.dat
hg_notes.idx			
	1	I6, X	HIP identifier
	2	I4	Record number of *first* record for this HIP identifier
hd_notes.idx			
	1	I6, X	HIP identifier
	2	I4	Record number of *first* record for this HIP identifier
hp_notes.idx			
	1	I6, X	HIP identifier
	2	I4	Record number of *first* record for this HIP identifier
hp_auth.idx			
	1	I6, X	HIP identifier
	2	I4	Record number of reference in hp_auth.doc for this HIP identifier Records 1 and 2 may be repeated for a given HIP identifier

...cont

Table 2.11.1. Format of the index files (cont.).

File	Column	Format	Description of the *n*-th entry (−1 if no information)
curves.idx			
	1	I6, X	HIP identifier
	2	A1	A, B, C or J indicating curve for HIP *n* in a/ b/ c/ (J = A and B)
hip_ep.idx			
	1	I8	Record number of *first* record of HIP *n* in hip_ep.dat
charts.idx			
	1	I6, X	HIP identifier
	2	A1	'D' or 'G' indicating chart for HIP *n* in dss/ or gsc/
tyc_ep.idx			
	1	I4, I6, I2, X	TYC identifier
	2	I8	Record number of *first* record of this TYC identifier
hip_i.idx			
	1	I7	Record number of *first* record of HIP *n* in hip_i.dat
hip_j.idx			
	1	I7	Record number of *first* record of HIP *n* in hip_j.dat

Table 2.11.2. Format of the notes and references.

File	Field	Bytes	Format	Description
hg_notes.doc				
	GN1	1–7	I6,X	Hipparcos Catalogue (HIP) identifier
	GN2	8–9	A1,X	If 'D', double and multiple systems note also given
	GN3	10–11	A1,X	If 'P', photometric note also given
	GN4	12–14	I2,X	Number of records *N* for this HIP identifier
	GN5	15–17	I2,X	Sequential number (1 to *N*) of this record
	GN6	18–97	A80	Text of note
hd_notes.doc				
	DN1	1–7	I6,X	Hipparcos Catalogue (HIP) identifier
	DN2	8–9	A1,X	If 'G', general note also given
	DN3	10–11	A1,X	If 'P', photometric note also given
	DN4	12–14	I2,X	Number of records *N* for this HIP identifier
	DN5	15–17	I2,X	Sequential number (1 to *N*) of this record
	DN6	18–97	A80	Text of note
hp_notes.doc				
	PN1	1–7	I6,X	Hipparcos Catalogue (HIP) identifier
	PN2	8–9	A1,X	If 'G', general note also given
	PN3	10–11	A1,X	If 'D', double and multiple systems note also given
	PN4	12–14	I2,X	Number of records *N* for this HIP identifier
	PN5	15–17	I2,X	Sequential number (1 to *N*) of this record
	PN6	18–97	A80	Text of note
hp_auth.doc				
	PA1	1–7	A6	Identifier of this photometric reference (yy.nnn)
	PA2	8–80	A73	Text
hp_refs.doc				
	PR1	1–7	I6,X	Hipparcos Catalogue (HIP) identifier
	PR2	8–10	I2,X	Number of records *N* for this HIP identifier
	PR3	11–13	I2,X	Sequential number (1 to *N*) of this record
	PR4	14–19	A6	Reference identifier (yy.nnn)

(The format of dmsa_o.doc is given in Section 2.3)

Table 2.11.3. Format of Identification Tables

File	Column	Format	Description
ident1.doc			
	1	I6	Hipparcos Catalogue (HIP) identifier
ident2.doc			
	1	I6,X	HD Catalogue identifier
	2	I6	Hipparcos Catalogue (HIP) identifier
ident3.doc			
	1	I6,X	HR (Bright Star Catalogue) identifier
	2	I6	Hipparcos Catalogue (HIP) identifier
ident4.doc			
	1	A11,X	Bayer/Flamsteed name
	2	I6	Hipparcos Catalogue (HIP) identifier
ident5.doc			
	1	A11,X	Variable star name
	2	I6	Hipparcos Catalogue (HIP) identifier
ident6.doc			
	1	A16,X	Common star name
	2	I6	Hipparcos Catalogue (HIP) identifier

Table 2.11.4/1. Directory contents for Disk 1

Directory	File name	Content	File size
	readme.mac	Description file for the CD-ROMs: MAC	
	readme.dos	Description file for the CD-ROMs: PC	
	readme.unx	Description file for the CD-ROMs: Unix	
cats/			
	hip_main.dat	Hipparcos Catalogue [Section 2.1]	53 434 536
	hip_main.idx	Index on HIP	963 328
	tyc_main.dat	Tycho Catalogue [Section 2.2]	372 532 864
	tyc_main.idx	Index on TYC	85 842
	hip_dm_c.dat	DMSA Part C [Section 2.3]	8 922 960
	hip_dm_g.dat	DMSA Part G [Section 2.3]	516 534
	hip_dm_o.dat	DMSA Part O [Section 2.3]	79 665
	hip_dm_v.dat	DMSA Part V [Section 2.3]	42 048
	hip_dm_x.dat	DMSA Part X [Section 2.3]	37 464
	hip_dm_c.idx	Index on CCDM for DMSA Part C	219 510
	hip_dm.idx	Combined index on HIP for DMSA Parts C-X	286 672
	hip_va_1.dat	Variability annex (periodic) [Section 2.4]	390 528
	hip_va_2.dat	Variability annex (unsolved) [Section 2.4]	798 048
	hip_va.idx	Combined index on HIP for hip_va_1/2	123 810
	solar_ha.dat	Solar system objects: HIP astrometry [Section 2.7]	370 194
	solar_hp.dat	Solar system objects: HIP photometry [Section 2.7]	171 535
	solar_t.dat	Solar system objects: TYC data [Section 2.7]	28 227
	solar.idx	Combined index for solar system objects	2310
docs/			
	vol*	Volumes 1–4 (pdf)	~ 70 Mb
	tocvol*.pdf	Table of contents, Volumes 1–4	
notes/			
	hg_notes.doc	Notes (HIP) ordered by HIP	385 902
	hd_notes.doc	Notes (DMSA) ordered by HIP	259 182
	hp_notes.doc	Notes (variability annex) ordered by HIP	241 956
	hp_auth.doc	Author list (variability annex)	355 470
	hp_refs.doc	References (variability annex)	709 149
	dmsa_o.doc	References for DMSA Part O [Section 2.3]	9676
	*.idx	Index file for the associated *.doc file	494 286
tables/			
	ident1.doc	Inconsistencies between HIC/HIP identifiers	728
	ident2.doc	HD Catalogue number to HIP number	1 486 995
	ident3.doc	HR Catalogue number to HIP number	136 155
	ident4.doc	Bayer and Flamsteed names	88 880
	ident5.doc	Variable star names	127 800
	ident6.doc	Common star names	2400
curves/			
	curves.idx	Index on HIP for light curves	35 810
	a/nnnnnn.eps	Folded light curve for HIPnnnnnn	89 297 691
	b/nnnnnn.eps	AAVSO light curve for HIPnnnnnn	8 495 537
	c/nnnnnn.eps	Unfolded light curve for HIPnnnnnn	22 943 559
src/			~ 1 Mb
	pos_prop.c	Position propagation (C)	
	pos_prop.f	Position propagation (Fortran)	
	pos_prop.h	Position propagation (documentation)	
	readme.doc	Description of the C load and search routines	
	s*.c	Search routine for *.dat (without underscore)	
	i*.[ch]	Index routine for *.dat (without underscore)	
	*.[ch]	Data file structure for *.dat	
	utils.[ch]	Utilities invoked by search and read routines	
fits/			
	tofits.doc	Explanation for FITS conversion	
	tofits.dat	FITS conversion files	

Table 2.11.4/2. Directory contents for Disk 2

Directory	File name	Content	File size
	readme.mac	Description file for the CD-ROMs: MAC	
	readme.dos	Description file for the CD-ROMs: PC	
	readme.unx	Description file for the CD-ROMs: Unix	
cats/			
	hip_ep.dat	HIP Epoch Photometry Annex [Section 2.5]	422 367 000
	hip_ep.idx	Index on HIP	1 204 160
charts/			
	charts.idx	Index on HIP for identification charts	116 530
	dss/nnnnnn.eps	DSS identification chart for HIPnnnnnn	109 543 641
	gsc/nnnnnn.eps	GSC identification chart for HIPnnnnnn	98 733 354

Table 2.11.4/3. Directory contents for Disk 3

Directory	File name	Content	File size
	readme.mac	Description file for the CD-ROMs: MAC	
	readme.dos	Description file for the CD-ROMs: PC	
	readme.unx	Description file for the CD-ROMs: Unix	
cats/			
	hip_ep_e.dat	HIP Epoch Photometry Annex Extension [Section 2.5]	647 629 400
	hip_ep_c.dat	HEPA Coincidence file [Section 2.5]	1 894 194
	hip_ep.idx	Index on HIP (identical to index for hip_ep)	1 204 160

Table 2.11.4/4. Directory contents for Disk 4

Directory	File name	Content	File size
	readme.mac	Description file for the CD-ROMs: MAC	
	readme.dos	Description file for the CD-ROMs: PC	
	readme.unx	Description file for the CD-ROMs: Unix	
cats/			
	tyc_ep.dat	TYC Epoch Photometry Annex [Section 2.6]	584 369 054
	tyc_ep.idx	Index on tyc_ep.dat	792 258

Table 2.11.4/5. Directory contents for Disk 5

Directory	File name	Content	File size
	readme.mac	Description file for the CD-ROMs: MAC	
	readme.dos	Description file for the CD-ROMs: PC	
	readme.unx	Description file for the CD-ROMs: Unix	
cats/			
	hip_rgc.dat	Reference great circle data [Section 2.8]	173 234
	hip_i.dat	HIP intermediate astrometry [Section 2.8]	521 438 910
	hip_i.idx	Index on HIP	1 083 744
docs/			
	volume*.pdf	Volumes 5–10 (pdf)	~ 130 Mb
	tocvol.pdf	Table of contents, Volumes 5–10	

Table 2.11.4/6. Directory contents for Disk 6

Directory	File name	Content	File size
	readme.mac	Description file for the CD-ROMs: MAC	
	readme.dos	Description file for the CD-ROMs: PC	
	readme.unx	Description file for the CD-ROMs: Unix	
cats/			
	hip_j.dat	HIP transit data file [Section 2.9]	552 596 812
	hip_j.idx	Index on HIP	1 083 744
docs/			
	volume11.pdf	Volume 11 (pdf)	~ 15 Mb
	tocvol11.pdf	Table of contents, Volume 11	
	figs/f*.pdf	Figures from Section 3 of Volume 1 (pdf)	~ 50 Mb

2.11.3. Checksums for the Printed Catalogue

Astrometric data represents a somewhat specific contribution to astronomical data archives, tending to be only slowly superseded by new observational material. Mindful of its possible historical value, and cautious about the rapid evolution of all forms of machine-readable data archiving, the printed catalogue incorporates a page-by-page checksum in order to facilitate the verification of any form of automated optical character reading of the printed version, should this prove to be necessary or desirable in the future.

For each printed catalogue page, two independent checksums have been computed. All non-blank characters in the table fields (i.e. excluding the headers and page numbers) have been concatenated in normal reading order. For example, for a left-hand page of the main catalogue, the resulting character string starts with the HIP number of the first star (possibly preceded by an asterisk) and ends with the goodness-of-fit of the last star on the page.

At each transition to a new catalogue field, and after the last field on a line, a vertical line symbol, |, is inserted (this field separator, corresponding to the structure of the machine-readable ASCII files, ensures that the correct field association is accounted for). For example, for the first page of the catalogue, the string would begin with:

$$1\,|\,|\,00\,00\,00.22\,|\,+01\,05\,20.4\,|\,9.10\,|\,|\,H\,|\,\ldots$$

and end with:

$$\ldots\,|\,+4\,|\,+16\,|\,+40\,|\,0\,|\,0.26\,|$$

Each character is then replaced by its 8-bit ASCII representation, and a cyclic redundancy check is computed using the CCITT polynomial (see, e.g., W.H. Press, S.A. Teukolsky, W.T. Vetterling, B.P. Flannery, *Numerical Recipes in C, 2nd Edition*, Cambridge, 1992). The resulting checksum is given in decimal representation.

The second checksum has been computed in essentially the same way, but instead of the normal ASCII representation, a bit-reversed representation has been used. For example, the ASCII representation of the character C is 67, or 01000011 in binary representation. For the second checksum, 11000010 is used. The resulting checksum has been bit reversed before being put in decimal form.

The two checksums are appended at the lower right of the tables on each page, in the order: normal checksum, bit-reversed checksum.

The bit pattern corresponding to the character string is considered to represent a polynomial, i.e. the individual bits from the character string are considered as coefficients of a polynomial. If the bits are numbered starting from the least significant bit of the last character, and if the latter bit is numbered 0, then bit n is the coefficient of x^n. This polynomial is then multiplied by x^{16}, and divided in modulo-2 arithmetic by the 'standard CCITT' polynomial $x^{16} + x^{12} + x^5 + 1$. The remainder of this division is a polynomial of degree 15. The (16-)bit pattern representing this polynomial is the checksum.

2.11.4. *Celestia 2000*

The Hipparcos and Tycho Catalogues (main catalogues and some annexes) also appear on one (non-ASCII) CD-ROM which includes software to interrogate the catalogues and annexes, to select samples from the main catalogues, and to draw local and global maps. This product, *Celestia 2000*, includes data from the ASCII disk 1 (see above), including notes and references, identification charts (from disk 2) and variable star light curves, if any. The data related to solar system objects are not included. No other data from disks 2–6 are available on this CD-ROM. The mission results are complemented by additional data taken from an updated version of the Hipparcos Input Catalogue, and by data or cross-identifications taken from the SIMBAD database for Tycho stars.

The data are 'bit-optimised', with an ordering optimised to take account of the requirements of the interrogation software. The CD-ROM follows the ISO-9660 standard. The software offers a wide range of possibilities which are briefly presented below. A complete user's manual and help are included in *Celestia 2000*, as well as technical requirements and instructions for installation and use. At the time of the release of the Hipparcos and Tycho Catalogues the *Celestia 2000* software is only available for IBM-PC compatibles.

Interrogating Facilities

The data are available per star, through eight windows displaying all data available in one catalogue or annex:

(1–5) Satellite data: Hipparcos Catalogue and annexes. These windows provide all data from the main Hipparcos Catalogue, including notes, references, and the identification chart if any; all data from the Double and Multiple Systems Annex, Parts C, G, O, V, and X; tabular data and light curves from Variability Annex, Sections 1 (periodic variables) and 2 (unsolved variable);

(6) Satellite data: Tycho Catalogue. This window provides all data from the main Tycho Catalogue, including notes. These data are complemented by some additional data made available from the SIMBAD data base: cross-identifications and proper motions from the PPM;

(7–8) Ground-based data: updated Hipparcos Input Catalogue and Double and Multiple Star Annex. These windows provide data from the Hipparcos Input Catalogue, with updated radial velocities, spectral types and luminosity classes; and with a few corrections in the cross-identifications. The annex has been updated with the errata provided to the CCDM (J. Dommanget & O. Nys, 1996, *Bull. CDS*, 48, 19).

Sampling Facilities

Samples can be defined using data from the Hipparcos and Tycho Catalogues, or from the Hipparcos Input Catalogue, or using identifiers from the Hipparcos Input Catalogue for HIP stars, or from SIMBAD for TYC stars. Once the source of the data has been selected, three options are available for selecting the subset of stars from which the

sampling will be performed: stars included only in HIP, but not in TYC; stars common to HIP and TYC; and stars included only in TYC, but not in HIP. The chosen subset of stars can also be 'all HIP stars', by selecting the first two options; or 'all TYC stars', by selecting the last two options.

More than 100 parameters can be used to define a criterion. A sample can be selected on the basis of one criterion, or of any logical combination of criteria.

Once a sample has been selected, it is then possible: to list the identifiers of the selected stars (HIP number if the star is in HIP, TYC number *only* if the star is in TYC but not in HIP); to display the HIP or TYC window by clicking on the selected identifier; to switch from any of these windows to any other one, where relevant; to draw a global or a local sky map for the selected sample; to prepare a file for external use, with data and identifiers from HIP and/or TYC and/or HIC.

Mapping Facilities

The global or local sky distribution of HIP and/or TYC stars can be displayed in various ways: draw a local map centred on a given star; draw a local map centred on given coordinates; draw a global sky distribution for a sample previously selected.

The sizes of symbols in local charts are related to the magnitudes of the stars. Different symbols can be used for stars selected by a given criteria, for other HIP stars, or for other TYC stars.

Section 3.1

Statistical Properties: Introduction

3.1. Statistical Properties: Introduction

In the sections of this part a number of statistical properties of the Hipparcos and Tycho Catalogues are presented. For selected fields of both catalogues the variations of the values over the sky are displayed. Histograms give the frequency distributions of the values of the various parameters. The dependence of average values on the value in another field is given for relevant cases. These results can be found in Section 3.2 for the Hipparcos Catalogue, and in Section 3.3 for the Tycho Catalogue.

Furthermore, results from comparisons of the Hipparcos and Tycho Catalogues with other catalogues: the Hipparcos Input Catalogue (HIC), the Fifth Fundamental Catalogue (FK5), and the Catalogue of Positions and Proper Motions (PPM) are presented in Section 3.4.

In Section 3.5 astrophysically related properties of the Hipparcos Catalogue are given, including Hertzsprung-Russell diagrams for different selections of stars.

Section 3.6 gives tables with key data from the Hipparcos Catalogue for selections of stars with a common property: nearby stars, high proper motion stars, stars with high transverse velocity, and the most luminous stars.

In interpreting the results in these sections, the reader should keep in mind that the Hipparcos Catalogue is only partly a survey; more than half of its entries have been selected on the basis of specific proposals for observation. So the distributions cannot always be considered as representative of the real stellar distribution. A much better representation of the latter is given by the Tycho Catalogue, which is a genuine survey of all stars down to its sensitivity limits.

3.1.1. All-Sky Plots

The all-sky plots in Sections 3.2, 3.3, and 3.4 are in Aitoff projection. For spherical coordinates λ ($-180° \le \lambda \le 180°$) and β this projection is defined as:

$$x = -2R \cos\beta \sin(\lambda/2) \Big/ \sqrt{1 + \cos\beta \cos(\lambda/2)}$$

$$y = R \sin\beta \Big/ \sqrt{1 + \cos\beta \cos(\lambda/2)}$$

where R is half the vertical dimension of the projection. The horizontal dimension of the projection is $4R$. The longitudinal coordinate is 0 at the centre, and increases from right to left.

In order to facilitate the interpretation of the sky plots, Figure 3.1.1 gives a coordinate grid for the Aitoff projection, and Figures 3.1.2 to 3.1.7 provide coordinate grids for the various combinations of coordinate systems and projections.

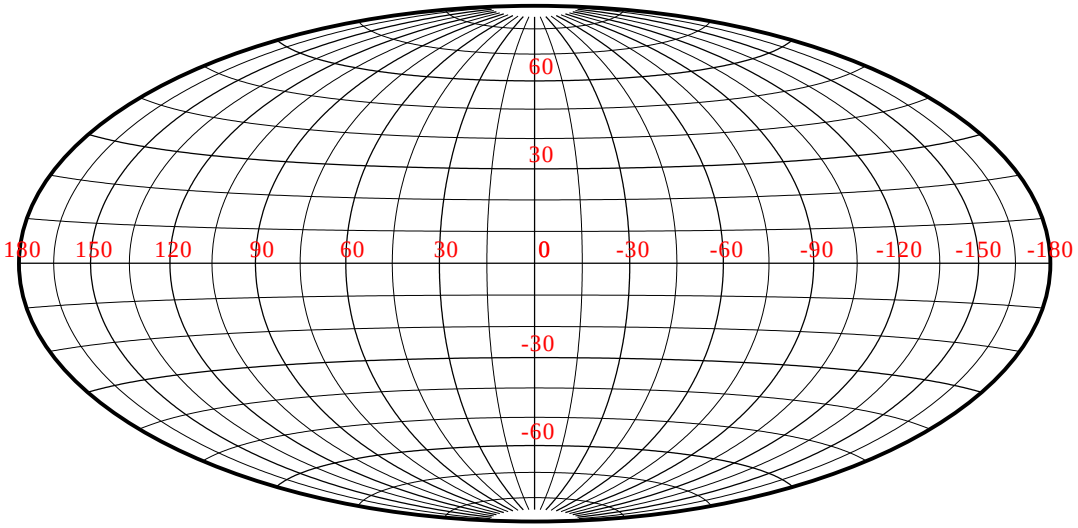

Figure 3.1.1. *Coordinate grid for Aitoff projection.*

In the sky plots, the value in each cell is the median of the values for all participating stars in the cell. The cells have been defined such that for higher latitudes a lower number of cells is chosen in the longitudinal direction, so as to preserve approximately the indicated cell size. In some plots, as indicated in the captions, the cell contents have been smoothed by taking a weighted average of the contents of the cell and its eight closest neighbours, thereby reducing the noise in the image.

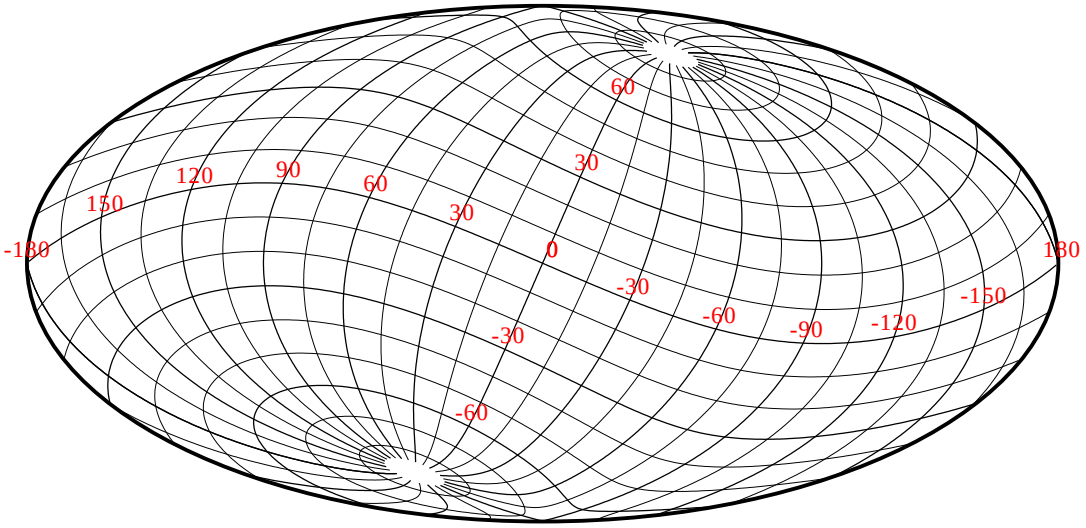

Figure 3.1.2. *Aitoff projection in equatorial coordinates, showing the corresponding grid for ecliptic coordinates.*

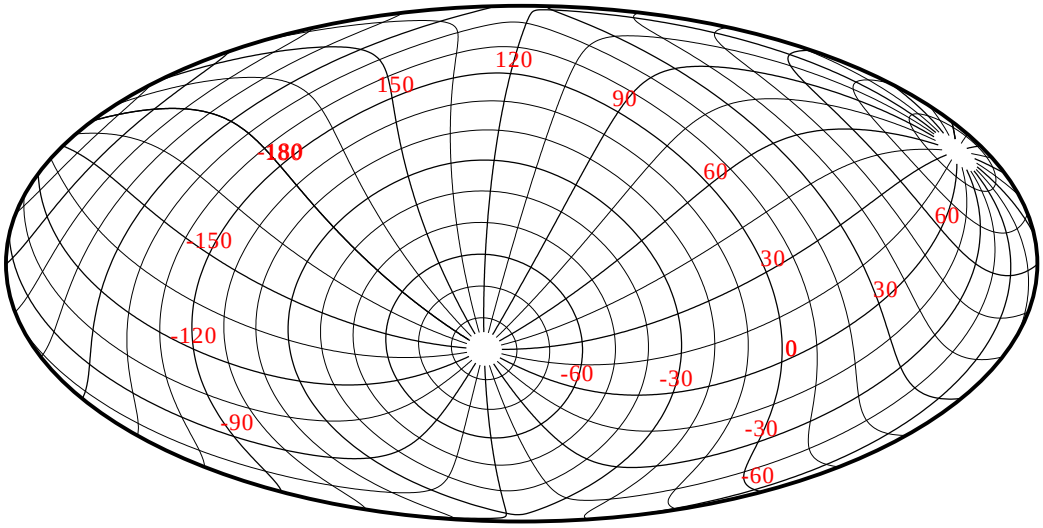

Figure 3.1.3. *Aitoff projection in equatorial coordinates, showing the corresponding grid for galactic coordinates.*

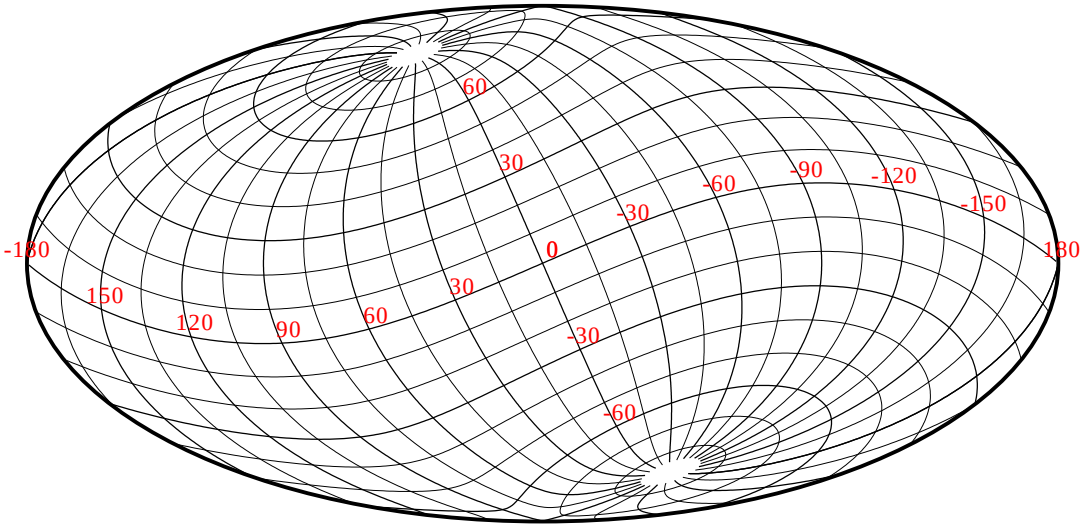

Figure 3.1.4. *Aitoff projection in ecliptic coordinates, showing the corresponding grid for equatorial coordinates.*

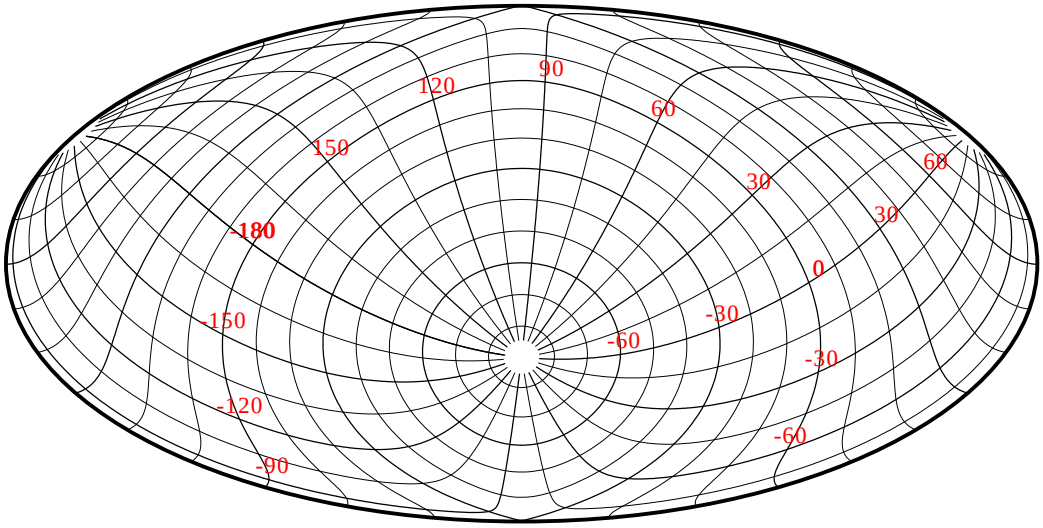

Figure 3.1.5. *Aitoff projection in ecliptic coordinates, showing the corresponding grid for galactic coordinates.*

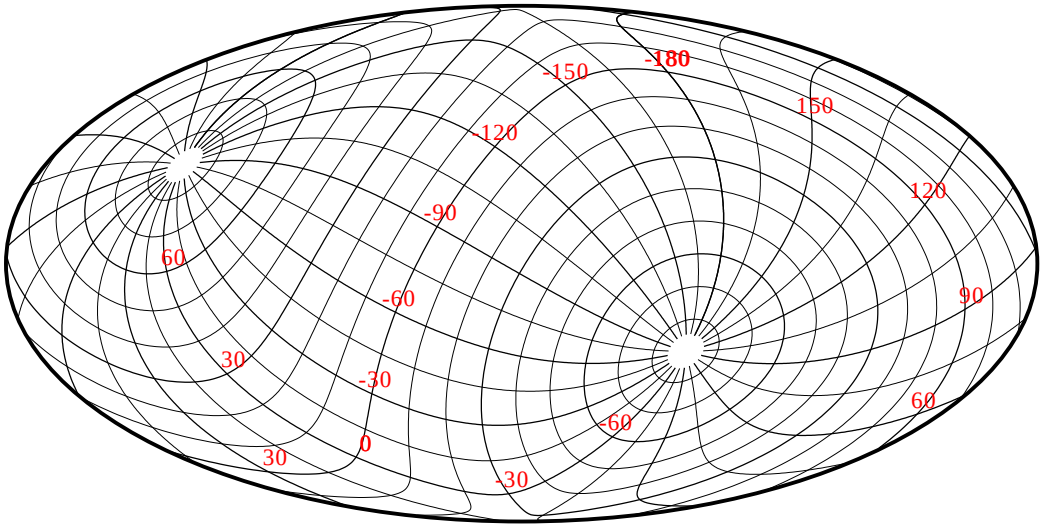

Figure 3.1.6. *Aitoff projection in galactic coordinates, showing the corresponding grid for equatorial coordinates.*

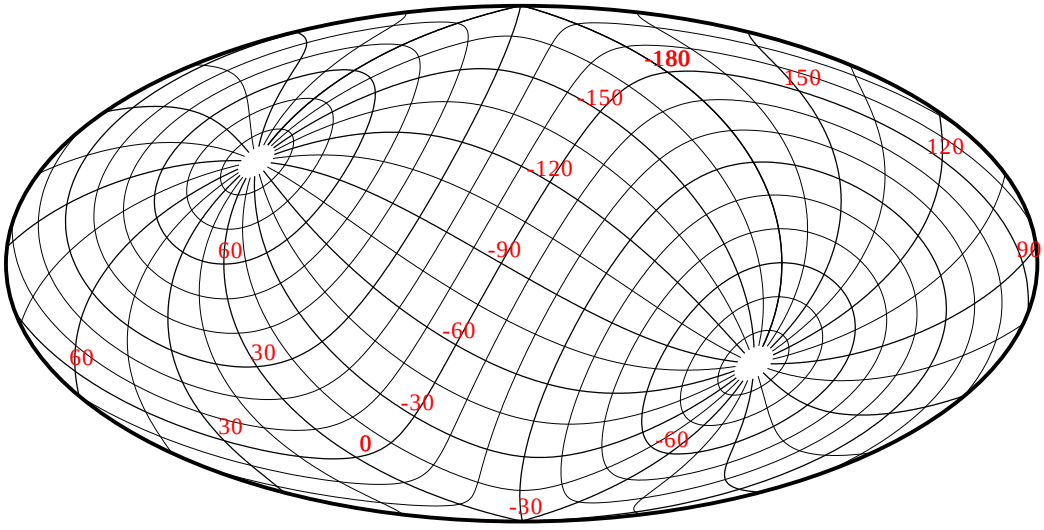

Figure 3.1.7. *Aitoff projection in galactic coordinates, showing the corresponding grid for ecliptic coordinates.*

Section 3.2

Statistical Properties: The Hipparcos Catalogue

3.2. Statistical Properties: The Hipparcos Catalogue

In this section statistical properties of data from the Hipparcos Catalogue are presented, mainly in the form of distributions over the sky, and frequency histograms. In most cases data from the Catalogue have been used directly; in a few cases it was considered appropriate to apply certain transformations in order to demonstrate a physical or astrometric effect. In particular this involves the transformation to the ecliptic and galactic coordinate systems.

3.2.1. Density of Observed Stars

The density of observed stars in the Hipparcos Catalogue depends strongly on the galactic latitude. Within the galactic plane, maxima of the density occur around $l = 100°$ and $l = 300°$, as shown in Figures 3.2.1 and 3.2.2. These maxima are related to the position of the Orion arm of our Galaxy, and the Gould Belt (at $l = 270°$). Noteworthy is also the concentration around $l = 200°$, $b = -20°$, the position of the Orion associations. The area around $l = 15°$, $b = 15°$ with low density corresponds to the dark nebula in Ophiuchus.

The number of observed stars per ecliptic latitude range and per magnitude class is given in Table 3.2.1. The maxima in the range $50° < |\beta| < 60°$ are a direct consequence of the distribution in the galactic plane.

Table 3.2.1. The number of entries in the Hipparcos Catalogue with associated astrometry, divided according to ecliptic latitude (β) and magnitude (median magnitude, Hp, from Field H44).

	Ecliptic latitude ($\|\beta\|$, deg)								
Hp	0–10	10–20	20–30	30–40	40–50	50–60	60–70	70–90	0–90
<2	7	7	6	6	8	6	3	3	46
2–3	21	20	21	11	19	15	8	4	119
3–4	53	45	55	34	40	42	24	22	315
4–5	165	150	152	128	140	121	79	56	991
5–6	490	444	459	420	394	401	281	199	3088
6–7	1434	1365	1457	1345	1241	1156	841	542	9381
7–8	3494	3408	3538	3416	3304	3048	2055	1416	23679
8–9	5895	5842	6015	6006	5909	4814	3566	2682	40729
9–10	4038	4237	4362	4091	4189	3201	2239	1556	27913
10–11	1212	1426	1735	1405	1198	791	460	336	8563
11–12	397	400	407	380	360	294	134	129	2501
≥12	105	120	79	112	76	65	38	35	630
all	17311	17464	18286	17354	16878	13954	9728	6980	117955

3.2.2. Great-Circle Abscissae

The distribution of the median number of great-circle abscissae used for the determination of the astrometric parameters of each catalogue entry is shown in Figure 3.2.3. The numbers used for the construction of this graph are the averages of the number of great-circle abscissae employed by the FAST and NDAC consortia. These numbers are, by nature, closely related to the number of (accepted) photometric transits, for which results are given in Figure 3.2.87. An important difference is that the observations obtained during sun-pointing periods (cf. Volume 3, Chapter 2) are included here. Sun-pointing observations were included in the astrometric adjustments, but the corresponding photometric transits were not considered acceptable (cf. Section 2.5, Field H H5). Traces of the extended sun-pointing period near the end of the mission (around 1 January 1993) are visible at $\lambda \sim 10°$ and $\lambda \sim 190°$; there are also fainter tracks due to shorter sun-pointing episodes in October 1991 ($\lambda \sim 105°$ and $\lambda \sim 285°$) and in August 1992 ($\lambda \sim 60°$ and $\lambda \sim 240°$). The remaining structure in this graph is explained in detail by the definition of the Hipparcos scanning law, the measurement interruptions, and the duration of the mission.

In Section 2.1, under Field H29, an approximate relation is given between the accepted number of transits and the number of great-circle abscissae (quoting a factor of 3.55). This relation is valid for the majority of catalogue entries. In reality, the factor increases for higher numbers of transits. The median number of astrometric abscissae as a function of the number of accepted photometric transits is given in Figure 3.2.4. Note that the higher numbers of transits (> 150) occur only for a small fraction of stars (cf. Figure 3.2.88).

3.2.3. Parallaxes and Proper Motions

The sky distribution of median parallaxes is given in Figure 3.2.5. The frequency histogram is in Figure 3.2.6. The parallaxes are systematically lower in the galactic plane. In a flattened system like the Galaxy, stars are expected to lie further away in the plane. The Hipparcos horizon is well beyond half the thickness of the galactic disk. In Figure 3.2.7 the distributions of parallaxes within and outside the galactic plane are compared.

Systematically larger parallaxes are found in the Hyades region (about 210 members of this open cluster were included in the Hipparcos Input Catalogue), and in the dark nebula region in Ophiuchus where in some places the view beyond 250 pc is obstructed. Distributions of the parallaxes in these two regions can be found in Figure 3.2.8.

The proper motions (Figures 3.2.9 to 3.2.12) show a systematic effect linked to the apex motion of the solar system with respect to the local standard of rest (velocity about 16.5 km/s) towards the point $l = 53°$, $b = 25°$, or $\alpha \sim 270°$, $\delta \sim 30°$. In order to demonstrate this effect more distinctly, Figures 3.2.13 to 3.2.14 give the transverse velocities (cf. Equation 1.2.20) for stars with a parallax greater than 7.5 mas. The systematic trends in these figures again reflect the motion of the solar system with respect to the local standard of rest.

3.2.4. Standard Errors and Correlations

The astrometric standard errors and correlations are given in the Catalogue in the equatorial coordinate system. The Hipparcos scanning strategy was, however, defined with respect to the sun position; as a consequence the error properties of the results are more readily understood in terms of ecliptic coordinates. For this reason the results for these parameters are presented here in both coordinate systems.

Sky distributions of the standard errors of the five astrometric parameters are shown in Figures 3.2.15, 3.2.19, 3.2.23, 3.2.29, and 3.2.33 in the equatorial coordinate system, and in Figures 3.2.16, 3.2.20, 3.2.24, 3.2.30, and 3.2.34 in the ecliptic coordinate system. Frequency distributions of these standard errors are given in Figures 3.2.18, 3.2.22, 3.2.26, 3.2.32, and 3.2.36. The dependence of the standard errors on ecliptic latitude is in Figures 3.2.17, 3.2.21, 3.2.25, 3.2.31, and 3.2.35, and the dependence of the standard errors on the *Hp* magnitude is in Figures 3.2.37, 3.2.38, 3.2.39, 3.2.40, and 3.2.41. The values of the standard errors for each of the five astrometric parameters per ecliptic latitude range and per magnitude class are given in Tables 3.2.2 to 3.2.6.

All these standard errors depend on ecliptic latitude. This is a direct consequence of the Hipparcos scanning strategy, wherein scanning circles must have a minimum angle of 47° with the ecliptic. This had two effects: stars with ecliptic latitude $|\beta| \geq 47°$ were observed more frequently than the stars closer to the ecliptic (with a marked maximum at $|\beta| = 47°$, cf. also Figures 3.2.88 and 3.2.89), and the latter stars were preferentially scanned in directions perpendicular to the ecliptic, thereby leading to a considerably better determination of the latitude components of the parameters. For the longitudinal components of the astrometric parameters these effects cooperate and explain the strong dependence on ecliptic latitude, whereas for the latitudinal components the effects work in opposite directions, so that a less pronounced effect in ecliptic latitude may be expected. In the region around $|\beta| = 47°$ there is an emphasis on longitudinal measurements; minimum values of the standard errors of $\lambda*$ and $\mu_{\lambda*}$ (and consequently $\alpha*$ and $\mu_{\alpha*}$) are found there.

Sky distributions for the relative precision of the distance σ_π/π are given in Figures 3.2.27 and 3.2.28. The structure is mainly related to the precision of the parallax. There is a conspicuous systematic effect of less precise distances around the galactic meridians $l = 0°$ and $l = 180°$. This systematic effect is the direct consequence of the decision to include extra F and G stars near the galactic meridian plane through the galactic centre and anticentre in the Hipparcos Input Catalogue (cf. ESA SP-1111, Vol. 2, Section 7.3). A related effect appears in a number of photometric results.

The distributions over the sky of the various correlations, in ecliptic and equatorial coordinates, are shown in Figures 3.2.42 to 3.2.61. Frequency histograms for the ten correlations in the equatorial coordinate system are in Figure 3.2.66.

One of the consequences of using the equatorial coordinate system is the introduction of certain systematic effects in some of the astrometric correlations. For example, the axes of the error ellipses of λ versus β tend to be parallel to the ecliptic latitude circles, i.e. the connected correlations are low. Transforming to the equatorial system introduces a rotation over an angle dependent on the position on the sky, and therefore a position-dependent correlation. The size of this correlation depends on the rotation angle between the local plane coordinate systems (cf. Sections 1.2.9 and 1.5.3) in equatorial and ecliptic coordinates, respectively, and on the eccentricity of the error ellipse, in other words, the difference between $\sigma_{\lambda*}$ and σ_β. In the region around the

Table 3.2.2. Median standard errors in right ascension, $\sigma_{\alpha*}$, for the entries in the Hipparcos Catalogue with associated astrometry, divided according to ecliptic latitude and magnitude as in Table 3.2.1, and expressed in milliarcsec (mas) for the catalogue epoch J1991.25.

	Ecliptic latitude ($\|\beta\|$, deg)								
Hp	0–10	10–20	20–30	30–40	40–50	50–60	60–70	70–90	0–90
<2	0.80	0.90	0.71	0.60	0.43	0.46	0.48	0.50	0.69
2–3	0.87	0.73	0.69	0.58	0.39	0.41	0.42	0.44	0.65
3–4	0.81	0.75	0.69	0.58	0.42	0.42	0.44	0.47	0.63
4–5	0.80	0.75	0.68	0.59	0.41	0.42	0.44	0.48	0.63
5–6	0.80	0.75	0.68	0.57	0.41	0.42	0.44	0.46	0.62
6–7	0.83	0.79	0.72	0.61	0.45	0.45	0.47	0.49	0.65
7–8	0.92	0.89	0.82	0.70	0.53	0.52	0.54	0.55	0.73
8–9	1.08	1.04	0.97	0.83	0.65	0.64	0.65	0.66	0.86
9–10	1.33	1.28	1.19	1.02	0.82	0.79	0.80	0.79	1.07
10–11	1.80	1.73	1.60	1.37	1.14	1.10	1.05	1.04	1.51
11–12	2.64	2.54	2.39	2.04	1.70	1.61	1.62	1.58	2.22
≥12	3.92	3.64	3.50	3.32	3.12	2.52	3.27	2.39	3.45
all	1.11	1.08	1.01	0.86	0.67	0.65	0.66	0.66	0.87

Table 3.2.3. Median standard errors in declination, σ_δ, for the entries in the Hipparcos Catalogue with associated astrometry, divided according to ecliptic latitude and magnitude as in Table 3.2.1, and expressed in milliarcsec (mas) for the catalogue epoch J1991.25.

	Ecliptic latitude ($\|\beta\|$, deg)								
Hp	0–10	10–20	20–30	30–40	40–50	50–60	60–70	70–90	0–90
<2	0.53	0.60	0.46	0.49	0.45	0.47	0.42	0.46	0.49
2–3	0.59	0.52	0.51	0.49	0.46	0.44	0.44	0.45	0.50
3–4	0.55	0.53	0.53	0.52	0.44	0.44	0.42	0.45	0.48
4–5	0.54	0.52	0.52	0.50	0.44	0.44	0.43	0.44	0.48
5–6	0.53	0.52	0.51	0.48	0.45	0.44	0.43	0.45	0.48
6–7	0.55	0.55	0.54	0.52	0.49	0.48	0.47	0.48	0.51
7–8	0.61	0.61	0.60	0.59	0.57	0.56	0.54	0.54	0.58
8–9	0.72	0.72	0.72	0.71	0.71	0.69	0.66	0.65	0.70
9–10	0.89	0.89	0.89	0.88	0.90	0.85	0.81	0.80	0.87
10–11	1.21	1.21	1.20	1.17	1.21	1.17	1.07	1.06	1.18
11–12	1.82	1.82	1.80	1.77	1.85	1.71	1.58	1.60	1.78
≥12	2.73	2.61	2.66	2.72	3.04	2.86	3.11	2.37	2.69
all	0.74	0.75	0.75	0.73	0.74	0.69	0.66	0.66	0.72

Table 3.2.4. Median standard errors in parallax, σ_π, for the entries in the Hipparcos Catalogue with associated astrometry, divided according to ecliptic latitude and magnitude as in Table 3.2.1, and expressed in milliarcsec (mas).

	Ecliptic latitude ($\|\beta\|$, deg)								
Hp	0–10	10–20	20–30	30–40	40–50	50–60	60–70	70–90	0–90
<2	0.88	0.98	0.90	0.78	0.64	0.60	0.53	0.49	0.79
2–3	0.88	0.81	0.77	0.76	0.68	0.56	0.49	0.48	0.76
3–4	0.91	0.82	0.79	0.74	0.65	0.55	0.52	0.49	0.74
4–5	0.88	0.86	0.81	0.76	0.66	0.55	0.51	0.48	0.75
5–6	0.88	0.85	0.82	0.75	0.67	0.56	0.52	0.49	0.75
6–7	0.92	0.90	0.86	0.81	0.73	0.61	0.55	0.52	0.80
7–8	1.02	1.01	0.97	0.92	0.86	0.72	0.63	0.59	0.91
8–9	1.21	1.19	1.16	1.12	1.07	0.89	0.77	0.71	1.09
9–10	1.49	1.47	1.43	1.37	1.35	1.11	0.94	0.86	1.36
10–11	2.01	1.97	1.93	1.82	1.84	1.54	1.24	1.13	1.85
11–12	2.98	2.96	2.81	2.74	2.73	2.26	1.88	1.73	2.72
≥12	4.35	4.19	4.11	4.10	4.00	3.67	3.49	2.51	4.11
all	1.23	1.24	1.20	1.15	1.11	0.89	0.77	0.71	1.10

ecliptic equator, $\sigma_{\lambda*} > \sigma_\beta$, and a sinusoidal variation along the ecliptic is expected. Around $|\beta| = 47°$, $\sigma_{\lambda*}$ becomes rather abruptly smaller than σ_β, leading to an inversion in the sign of the transformed correlation. In the ecliptic pole region, $\sigma_{\lambda*} \sim \sigma_\beta$; no systematic effect is expected. All these features are clearly discernible in Figure 3.2.42.

Other systematic features can be ascribed to non-uniform coverage due to the effects of the measurement interruptions (see Volume 2, Section 7.3). Measurements on stars that are asymmetrically distributed with respect to the epoch of the catalogue are expected to exhibit correlations between position and proper motion components ($\alpha*$, $\mu_{\alpha*}$) and (δ, μ_δ) and their analogues in ecliptic coordinates. Figure 3.2.62 gives the results for the mean epoch of observation computed from individual measurement epochs, and agrees very well with the results for the relevant correlations. In Section 1.2.7 the definition of an effective mean epoch computed from the correlation coefficients is given (Equation 1.2.10). Its sky distribution is given for comparison in Figure 3.2.63. In the same section (Equations 1.2.6 and 1.2.8) a definition of the effective mean epochs for right ascension and declination is given. The distribution of the difference between these epochs is shown in Figure 3.2.65. The time span over which observations were made also varies considerably over the sky (Figure 3.2.64). This explains the larger standard errors obtained in some unfavourably covered regions.

There are two more systematic effects to be discussed: one is an asymmetry in the distribution of the correlation between parallax and declination, visible mainly in the histogram (Figure 3.2.66), but also in the sky distribution (Figure 3.2.46). The negative mean value for this correlation is a consequence of the scanning law. The nominal scanning law is defined such that the speed of the nominal z-axis relative to the stars is roughly constant. Because the revolving motion about the sun was chosen in the clockwise direction, as seen from the satellite, this means that the z-axis must spend more time south of the ecliptic than on the north side. When the z-axis is directly below the sun ($\nu = 270°$, see Chapter 8 of Volume 2), the latitude component of the

Table 3.2.5. Median standard errors of proper motion in right ascension, $\sigma_{\mu_{\alpha*}}$, for the entries in the Hipparcos Catalogue with associated astrometry, divided according to ecliptic latitude and magnitude as in Table 3.2.1, and expressed in milliarcsec per year (mas/yr).

	Ecliptic latitude ($\|\beta\|$, deg)								
Hp	0–10	10–20	20–30	30–40	40–50	50–60	60–70	70–90	0–90
<2	1.02	0.99	0.76	0.59	0.53	0.54	0.54	0.53	0.72
2–3	1.02	0.84	0.78	0.64	0.48	0.44	0.46	0.46	0.74
3–4	1.02	0.88	0.81	0.64	0.46	0.49	0.48	0.52	0.67
4–5	0.94	0.90	0.80	0.66	0.47	0.48	0.49	0.50	0.69
5–6	0.95	0.89	0.80	0.67	0.47	0.48	0.51	0.51	0.68
6–7	1.00	0.95	0.84	0.72	0.53	0.52	0.54	0.54	0.73
7–8	1.10	1.07	0.96	0.82	0.62	0.60	0.62	0.61	0.83
8–9	1.31	1.26	1.16	0.99	0.77	0.74	0.75	0.73	0.99
9–10	1.63	1.56	1.45	1.22	0.98	0.94	0.93	0.90	1.26
10–11	2.23	2.16	1.96	1.66	1.36	1.31	1.25	1.19	1.80
11–12	3.29	3.19	2.91	2.46	2.05	1.98	1.92	1.72	2.67
≥12	5.02	4.63	4.23	4.05	3.22	3.04	3.72	2.72	4.25
all	1.34	1.31	1.20	1.02	0.79	0.75	0.75	0.74	1.02

Table 3.2.6. Median standard errors of proper motion in declination, σ_{μ_δ}, for the entries in the Hipparcos Catalogue with associated astrometry, divided according to ecliptic latitude and magnitude as in Table 3.2.1, and expressed in milliarcsec per year (mas/yr).

	Ecliptic latitude ($\|\beta\|$, deg)								
Hp	0–10	10–20	20–30	30–40	40–50	50–60	60–70	70–90	0–90
<2	0.57	0.62	0.47	0.53	0.49	0.55	0.43	0.45	0.54
2–3	0.68	0.61	0.62	0.56	0.56	0.49	0.47	0.52	0.59
3–4	0.70	0.62	0.63	0.61	0.50	0.51	0.47	0.54	0.58
4–5	0.64	0.64	0.62	0.57	0.51	0.48	0.49	0.51	0.56
5–6	0.66	0.62	0.60	0.56	0.52	0.50	0.49	0.53	0.56
6–7	0.67	0.66	0.63	0.61	0.56	0.54	0.53	0.56	0.60
7–8	0.75	0.75	0.72	0.69	0.66	0.64	0.61	0.64	0.68
8–9	0.89	0.88	0.87	0.83	0.82	0.78	0.75	0.77	0.83
9–10	1.10	1.10	1.08	1.02	1.04	0.99	0.94	0.96	1.03
10–11	1.54	1.51	1.44	1.36	1.44	1.37	1.23	1.28	1.42
11–12	2.28	2.27	2.11	2.12	2.13	1.98	1.86	1.90	2.12
≥12	3.53	3.34	3.12	3.11	3.44	3.58	3.83	3.05	3.33
all	0.90	0.91	0.89	0.86	0.85	0.79	0.75	0.78	0.85

parallactic displacement on the scanning circle is negative for all stars along the circle. Conversely, when the z-axis is above the sun ($\nu = 90°$), the parallax has a positive latitude component. Since the former situation occurs during a longer time interval than the latter, it follows that the parallax on average has a negative latitude component, and therefore that the mean correlation between the parallax and the latitude is negative. A nominal scanning law chosen such that the revolving motion was counterclockwise as seen from the satellite would have resulted in a positive mean correlation. (Of the 2328 reference great circles in the N37.05 solution, cf. Chapter 16 of Volume 3, 1273, or 55 per cent, have poles with a negative declination.)

The other systematic effect is the global variation of the correlations between right ascension and parallax (and to a lesser extent, those between proper motion in right ascension and parallax). In order to obtain a low correlation between ecliptic longitude and parallax, the measurements should be symmetrically distributed over the ellipse described by the parallactic motion. In particular, for a star on the ecliptic, equal numbers of measurements should be obtained on both sides of the sun. In the case of Hipparcos, this condition is not fulfilled: for the actual mission interval, observations were made in all four years between January and March, whereas the period from September to November was covered only twice. This explains a global systematic effect ranging from +0.4 to −0.4; within this global variation, much faster variations are seen, related to the presence or absence of particular scanning circles during these periods. The traces of these scanning circles are clearly visible in the plot, Figure 3.2.45.

Figures 3.2.67 to 3.2.70 give results for the indicators of solution quality F1 and F2. Occasional higher rejection rates are mainly found in the region around the ecliptic; the rejection percentages appear to be slightly higher systematically in the ecliptic pole regions. These patterns are essentially a quantisation effect: for, say, 30 abscissae the rejection of one abscissa gives a rejection percentage of 3 without the possibility for values between 0 and 3. The values for F2, the goodness-of-fit indicator, are systematically higher in the region of the ecliptic than in the ecliptic pole regions, indicating a slightly less satisfactory adjustment in general.

3.2.5. Photometric Data

Figures 3.2.71 to 3.2.74 give frequency distributions for the Tycho B_T and V_T magnitudes and their associated standard errors.

The distribution of colours over the sky is shown in Figure 3.2.75 for the $B - V$ colour index and in Figure 3.2.77 for the $V - I$ colour index. In the galactic plane more early-type stars are observed than elsewhere. The young stars in the Orion associations stand out at $l = 200°$, $b = -20°$. The bands of slightly bluer stars at $l = 0°$ and $l = 180°$ are a consequence of the already mentioned selection of extra F and G stars near the galactic meridian plane through the galactic centre and anticentre for the Hipparcos Input Catalogue.

The frequency distribution of both colour indices are given in Figures 3.2.76 and 3.2.78 and show similar features. The peak around $B - V = 0$ mag is due to the inclusion, in the Hipparcos Input Catalogue, of a large number of early-type stars for galactic structure studies. The high peak near $B - V = 0.5$ mag is due to the survey stars near the turn-off (cf. also the Hertzsprung-Russell diagrams in Section 3.5), indicating that the mean age of the galactic disk is about $5\,10^9$ yr. The maximum around $B - V = 1$ mag is due to

the G8–K0 giants in the core helium burning phase. The small bump in the interval $B - V = 1.3 - 1.7$ mag is due to nearby dK–dM dwarfs.

Frequency distributions of the standard errors for the colour indices are given in Figures 3.2.79 and 3.2.80.

The sky distribution of the magnitude in the Hipparcos photometric system *Hp* is displayed in Figure 3.2.81. The special selection for $l = 0°$ and $l = 180°$ mentioned before manifests itself here as the presence of fainter stars in these areas. There are further global variations over the sky. The frequency distribution is given in Figure 3.2.82. The associated standard error is found in Figures 3.2.83 and 3.2.84.

The scatter in the photometric observations (cf. Section 1.3, Appendix 1) is shown in Figures 3.2.85 and 3.2.86. There is a clear enhancement in the regions around $|\beta| = 47°$, where the number of observation is greatest (see below). It can be shown that the value of the scatter is correlated with the number of observations in the Hipparcos Catalogue.

The distributions of the number of accepted photometric transits (also a measure of the number of astrometric measurements, see Section 3.2.2) are shown in three different representations in Figures 3.2.87, 3.2.88, and 3.2.89. The structure of these plots follows accurately from the Hipparcos scanning law and the limited duration of the mission. Note that the periods of sun pointing leave no trace in these diagrams because they do not yield any accepted photometric transits. The two peaks in the histogram correspond to observations in the regions $|\beta| < 47°$ and $|\beta| > 47°$, respectively.

The sky distribution of the median amplitude of luminosity variations is given in Figure 3.2.90. As was the case for the scatter, enhanced values are found around $|\beta| = 47°$. In the Hipparcos Catalogue, there is a correlation between the number of photometric transits and the amplitude. This has not been studied in detail, but evidently the probability of detecting variability increases with the number of observations.

Frequency distributions for various other results from the photometric analysis are presented in Figures 3.2.91 to 3.2.97. Figure 3.2.97 deserves some explanation (cf. Volume 3, Section 21.4). The broad peak below 10 days corresponds to the region where the spacing of Hipparcos observations is optimally suited to determine periods. It is in this region that most newly-discovered periods are found. The other peak around 250 days indicates the period range where Hipparcos can confirm and possibly improve already known periods (the distribution of longer gaps between observations peaks between 85 and 140 days at lower ecliptic latitudes, cf. Volume 3, Figure 14.16).

3.2.6. Multiple-Star Data

Results for the multiple-star data as given in the main catalogue are presented in Figures 3.2.98 to 3.2.106, mostly in the form of frequency histograms. These plots illustrate the absence of significant systematic effects in the detection and characterisation of double systems. There appears to be a slight preference for larger magnitude differences in the galactic plane, perhaps related to the brighter stars in that region (Figure 3.2.102). The diagram of separation versus magnitude difference (Figure 3.2.106) shows, not unexpectedly, that for the detection of larger differences in magnitude larger separations are needed. The upper limit at 10 arcsec corresponds to the typical changeover to

two-pointing systems for *a priori* known doubles (cf. Section 1.4.2). Components were sometimes detected beyond this separation limit, especially for larger differences in magnitude.

Results from the Double and Multiple Systems Annex (DMSA) are organised according to the various solution types.

Results from the DMSA, Acceleration Solutions (DMSA/G) are given in Figures 3.2.107 to 3.2.112. The cut-offs in Figures 3.2.109 and 3.2.112 for values below 3.44 are a consequence of the choice of the limit for significance of the acceleration solutions (Section 2.3.1). The entries present below this limit for F_g have a significant $F_{\dot{g}}$.

Results from the DMSA, Orbital Solutions (DMSA/O) are presented in Figures 3.2.113 to 3.2.119. Not unexpectedly, Hipparcos measurements are optimal for the determination of orbital periods of a few years (Figure 3.2.113). In the absence of spectroscopic information there is an ambiguity of $\pm 180°$ in the position angle of the ascending node, in which case the catalogue gives the value between $0°$ and $180°$. This explains why in Figure 3.2.119 there are more entries in the first two quadrants than in the other two.

Results from the DMSA, Variability-Induced Mover (VIM) Solutions (DMSA/V) are in Figures 3.2.120 to 3.2.125. The distributions for the parameters from the DMSA, Stochastic Solutions (DMSA/X) are in Figures 3.2.126 and 3.2.127.

Figure 3.2.1. *Hipparcos Catalogue: number of observed stars per square degree, in galactic coordinates (cell size $2^\circ \times 2^\circ$). On the average there are 2.8 stars per square degree in the Hipparcos Catalogue.*

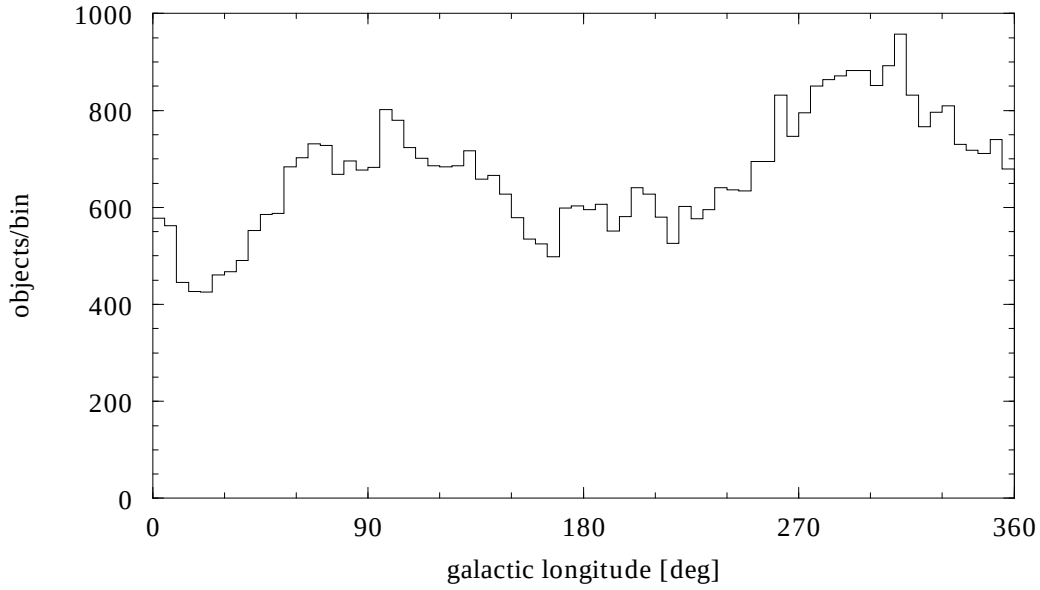

Figure 3.2.2. *Distribution of number of stars near the galactic equator ($|b| < 10^\circ$, bin size 5°).*

Figure 3.2.3. *Hipparcos Catalogue: median number of great-circle abscissae used for astrometry, in ecliptic coordinates (cell size $2° \times 2°$).*

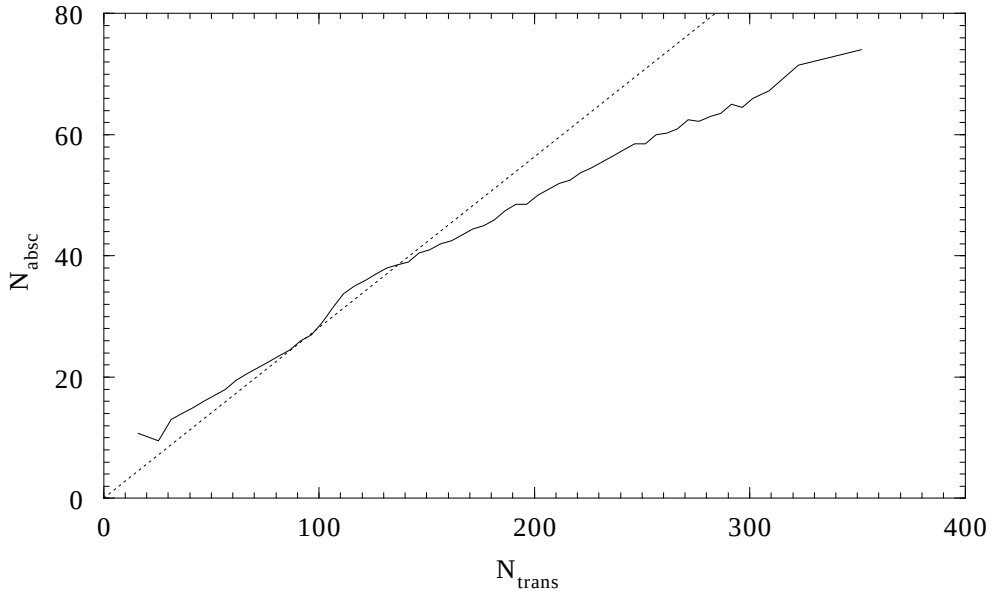

Figure 3.2.4. *Hipparcos Catalogue: median number of abscissae used for astrometry versus number of accepted photometric transits. The dotted line represents the approximate relation valid for most entries, as given in Section 2.1, under Field H29.*

Figure 3.2.5. *Hipparcos Catalogue, Field H11: median parallax π, in galactic coordinates (cell size $2° \times 2°$). On the average the stars of the Hipparcos Catalogue are more distant in the galactic plane than outside this plane.*

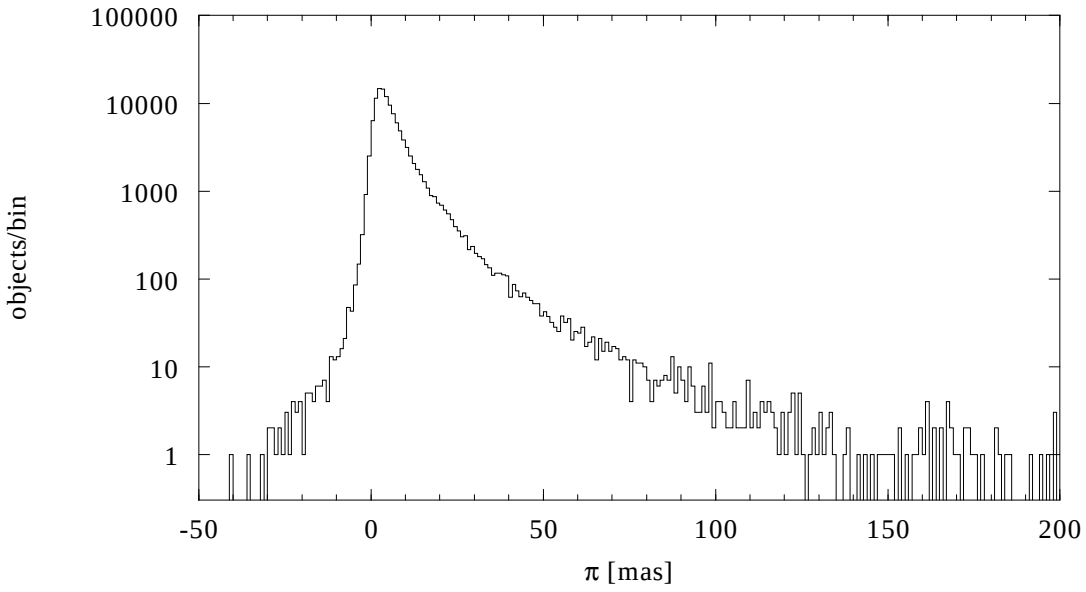

Figure 3.2.6. *Hipparcos Catalogue, Field H11: parallax π (bin size 1 mas).*

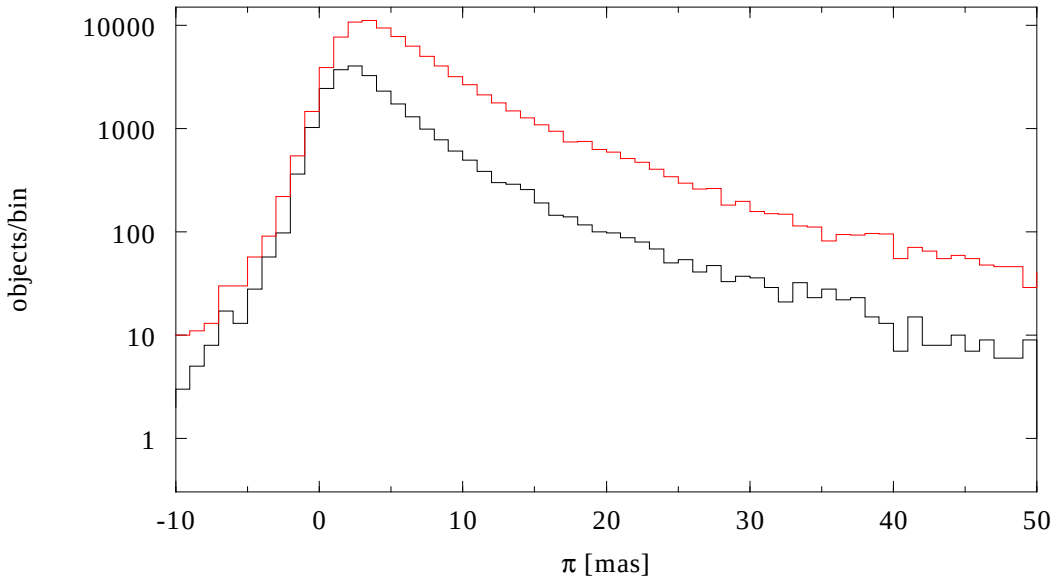

Figure 3.2.7. *Distribution of parallaxes within and outside the galactic plane (bin size 1 mas). Black line: stars with* $|b| < 10°$. *Red line: stars with* $|b| \geq 10°$.

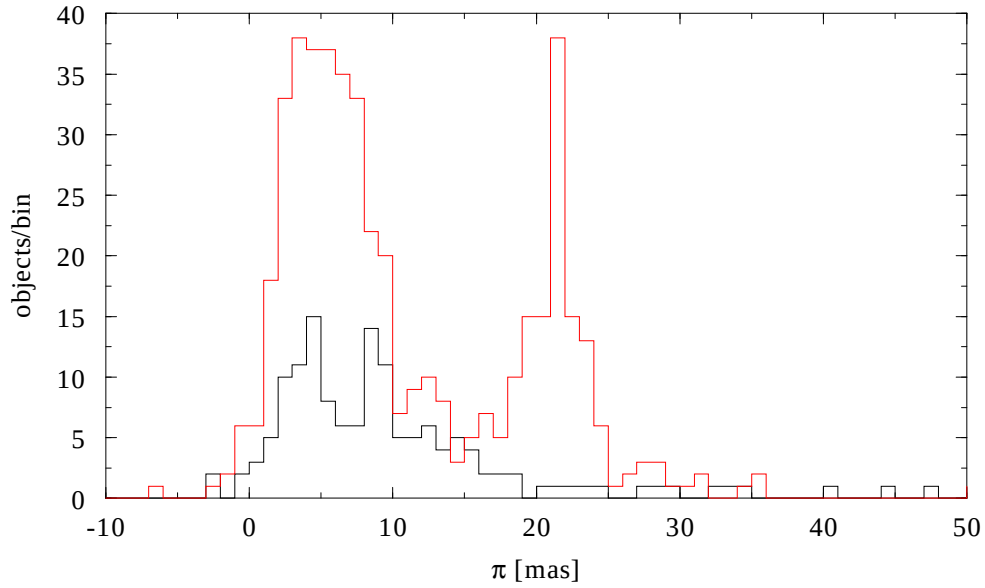

Figure 3.2.8. *Distribution of parallaxes in two selected regions of the sky (bin size 1 mas). Black line: stars with* $10° < l < 20°$, $13° < b < 23°$ *(including the Ophiuchus dark nebula). Red line: stars with* $170° < l < 195°$, $-25° < b < -18°$ *(including most Hyades cluster members).*

Figure 3.2.9. *Hipparcos Catalogue, Field H12: median proper motion in galactic longitude, in galactic coordinates (cell size $2^\circ \times 2^\circ$). The bipolar structure of the plot results from the motion of the solar system towards the apex (see text).*

Figure 3.2.10. *Hipparcos Catalogue, Field H12: median proper motion in right ascension, in equatorial coordinates (cell size $2^\circ \times 2^\circ$). The solar motion accounts for the preferentially positive proper motions at $\alpha = 0^\circ$ and negative values at $\alpha = 180^\circ$.*

Figure 3.2.11. *Hipparcos Catalogue, Field H13: median proper motion in galactic latitude, in galactic coordinates (cell size $2^\circ \times 2^\circ$).*

Figure 3.2.12. *Hipparcos Catalogue, Field H13: median proper motion in declination, in equatorial coordinates (cell size $2^\circ \times 2^\circ$).*

Figure 3.2.13. *Hipparcos Catalogue, Field H12: median component of transverse velocity in galactic longitude for stars with parallax $\pi > 7.5$ mas, in galactic coordinates (cell size $2^\circ \times 2^\circ$). The distribution has been smoothed over the eight closest neighbours of each cell. The bipolar structure of the plot results from the motion of the solar system towards the apex.*

Figure 3.2.14. *Hipparcos Catalogue, Field H13: median component of transverse velocity in galactic latitude for stars with parallax $\pi > 7.5$ mas, in galactic coordinates (cell size $2^\circ \times 2^\circ$). The distribution has been smoothed over the eight closest neighbours of each cell. The structure of the plot results from the motion of the solar system towards the apex.*

Figure 3.2.15. *Hipparcos Catalogue, Field H14: median standard error of $\alpha*$, in equatorial coordinates (cell size $2^\circ \times 2^\circ$).*

Figure 3.2.16. *Hipparcos Catalogue, Field H14: median standard error of $\lambda*$, in ecliptic coordinates (cell size $2^\circ \times 2^\circ$).*

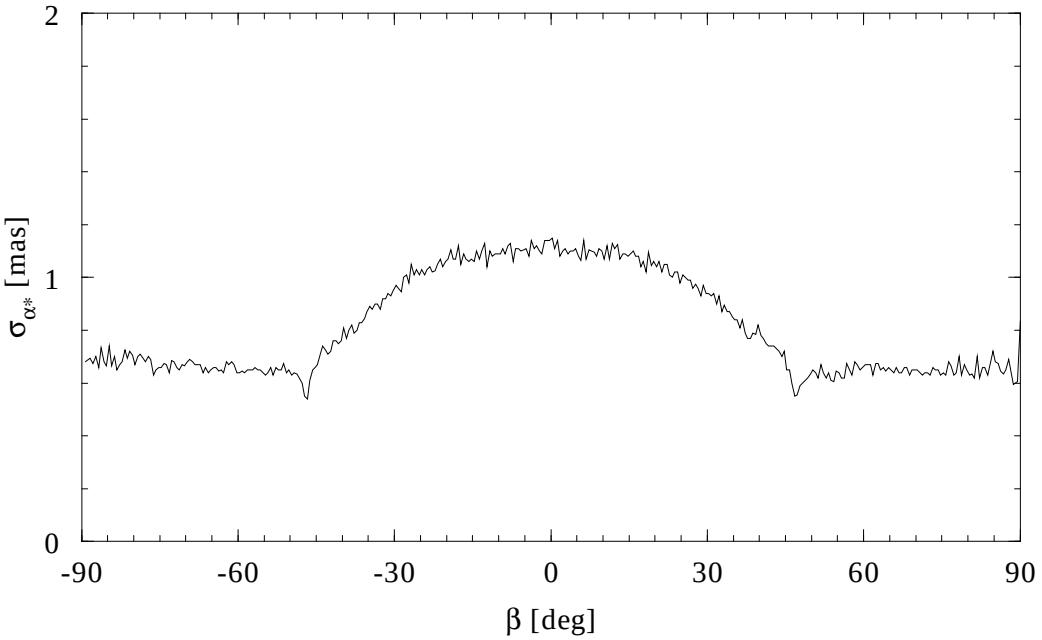

Figure 3.2.17. *Hipparcos Catalogue, Field H14: median standard error of $\alpha*$ versus ecliptic latitude (bin size 0.5°).*

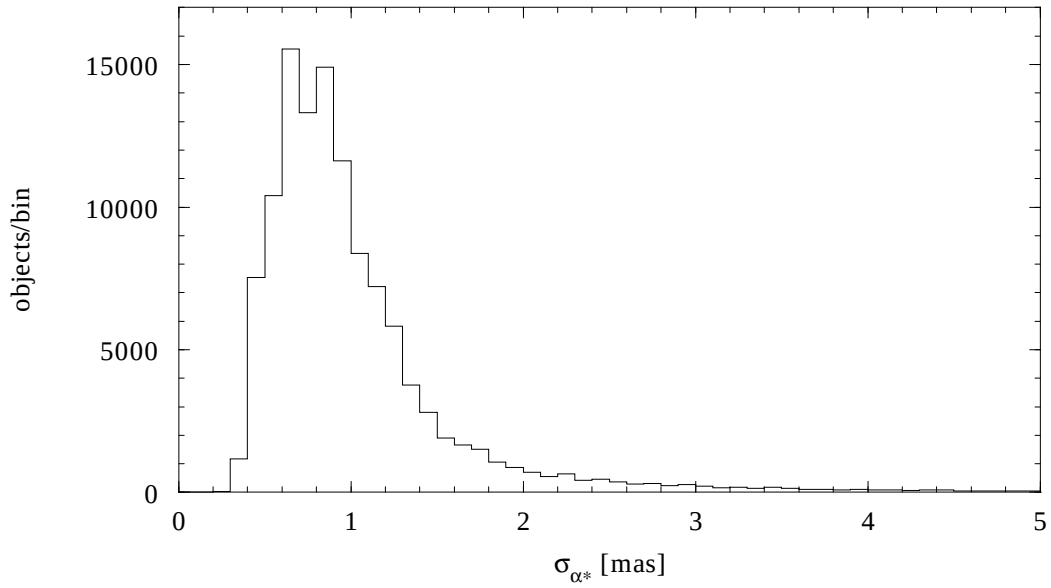

Figure 3.2.18. *Hipparcos Catalogue, Field H14: standard error of $\alpha*$ (bin size 0.1 mas).*

Figure 3.2.19. *Hipparcos Catalogue, Field H15: median standard error of δ, in equatorial coordinates (cell size $2^\circ \times 2^\circ$).*

Figure 3.2.20. *Hipparcos Catalogue, Field H15: median standard error of β, in ecliptic coordinates (cell size $2^\circ \times 2^\circ$).*

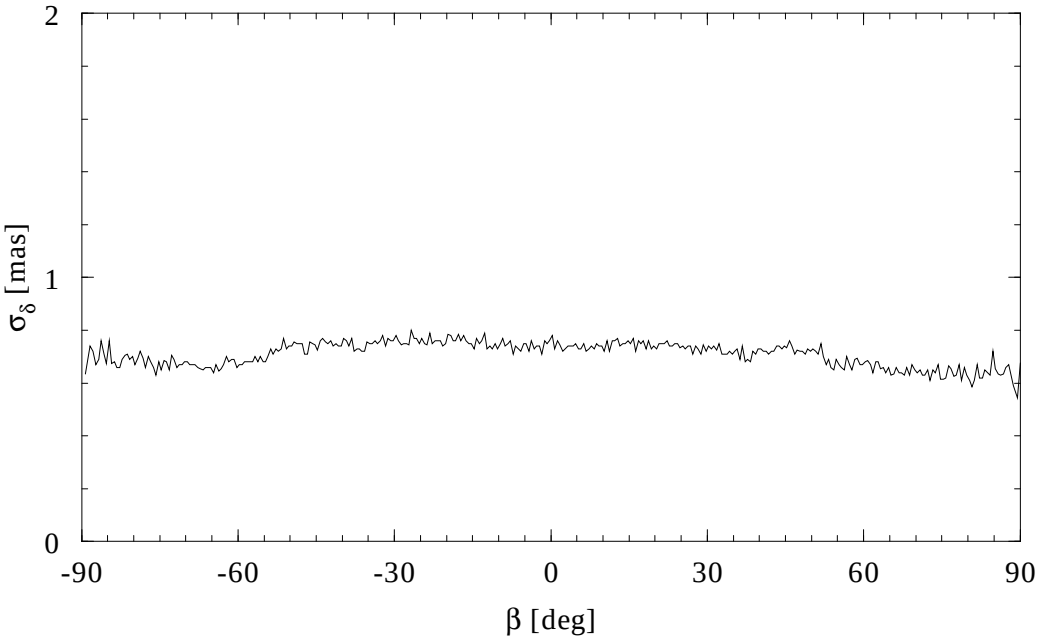

Figure 3.2.21. *Hipparcos Catalogue, Field H15: median standard error of δ versus ecliptic latitude (bin size 0.5°).*

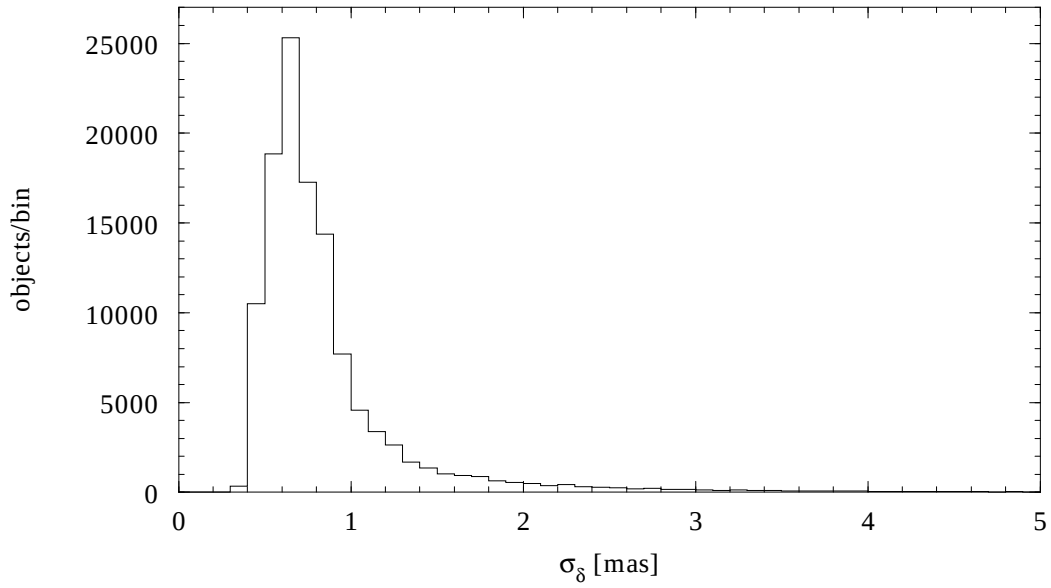

Figure 3.2.22. *Hipparcos Catalogue, Field H15: standard error of δ (bin size 0.1 mas).*

Figure 3.2.23. *Hipparcos Catalogue, Field H16: median standard error of π, in equatorial coordinates (cell size $2^\circ \times 2^\circ$).*

Figure 3.2.24. *Hipparcos Catalogue, Field H16: median standard error of π, in ecliptic coordinates (cell size $2^\circ \times 2^\circ$).*

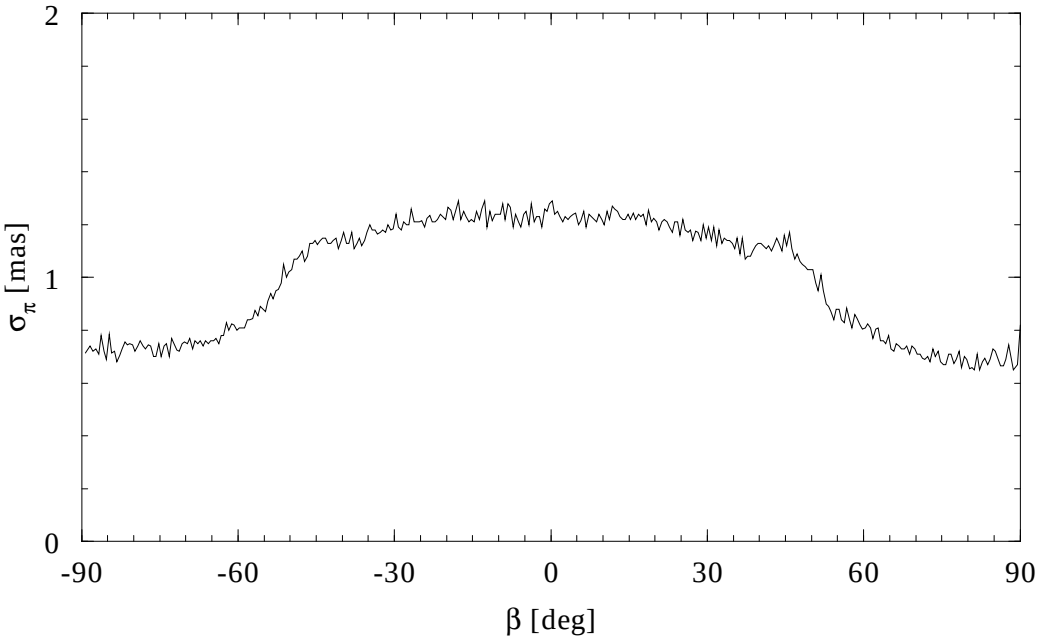

Figure 3.2.25. *Hipparcos Catalogue, Field H16: median standard error of π versus ecliptic latitude (bin size 0.5°).*

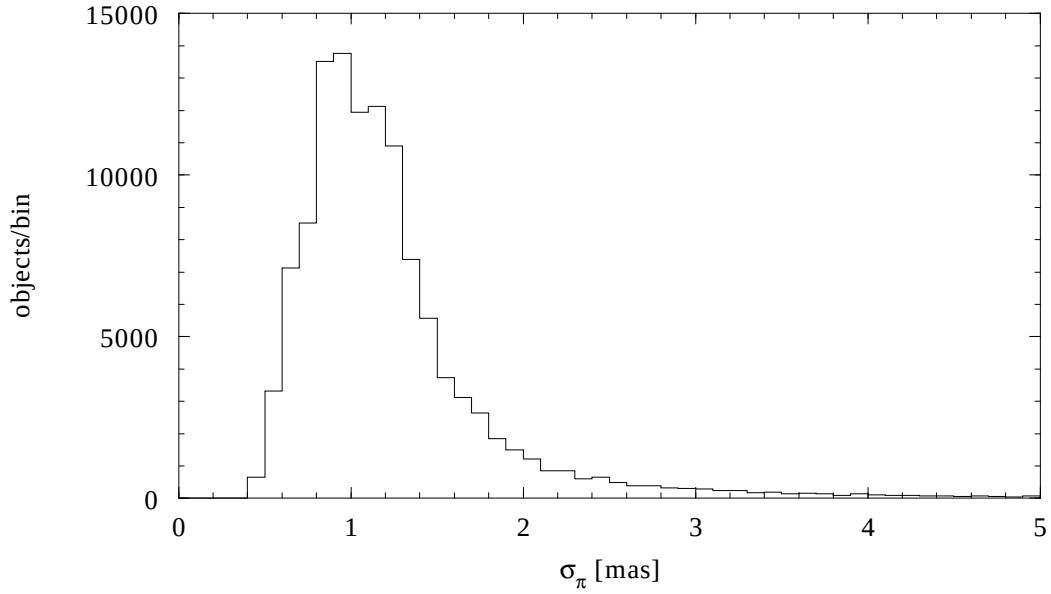

Figure 3.2.26. *Hipparcos Catalogue, Field H16: standard error of π (bin size 0.1 mas).*

Figure 3.2.27. *Hipparcos Catalogue, Field H11/H16: median relative precision of distance σ_π/π for stars with a parallax $\pi > 2$ mas, in ecliptic coordinates (cell size $2^\circ \times 2^\circ$).*

Figure 3.2.28. *Hipparcos Catalogue, Field H11/H16: median relative precision of distance σ_π/π for stars with a parallax $\pi > 7.5$ mas, in galactic coordinates (cell size $2^\circ \times 2^\circ$).*

Figure 3.2.29. *Hipparcos Catalogue, Field H17: median standard error of $\mu_{\alpha*}$, in equatorial coordinates (cell size $2^\circ \times 2^\circ$).*

Figure 3.2.30. *Hipparcos Catalogue, Field H17: median standard error of $\mu_{\lambda*}$, in ecliptic coordinates (cell size $2^\circ \times 2^\circ$).*

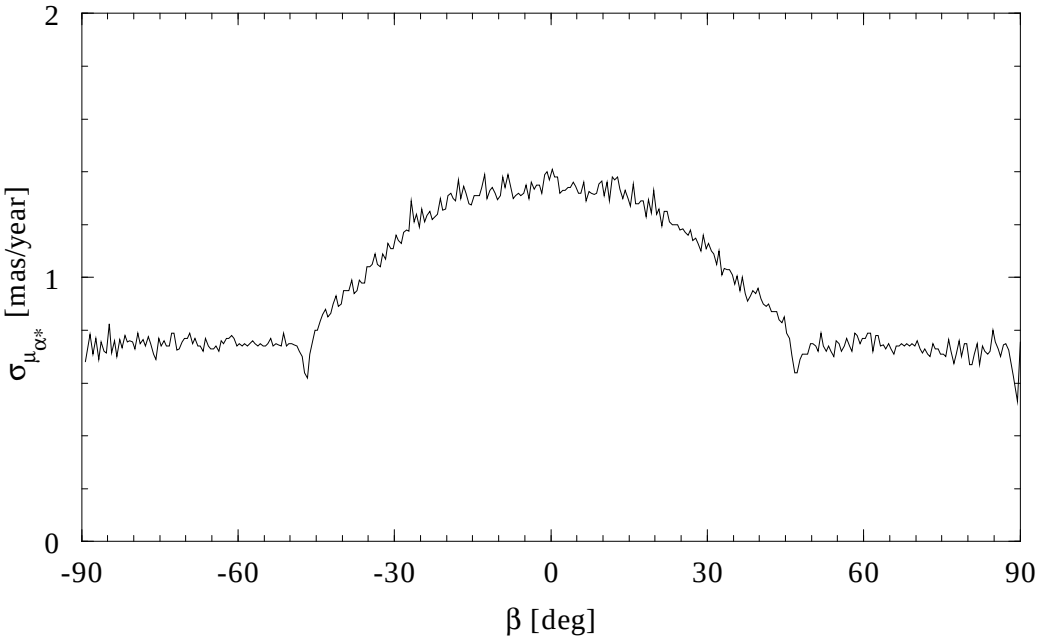

Figure 3.2.31. *Hipparcos Catalogue, Field H17: median standard error of $\mu_{\alpha*}$ versus ecliptic latitude (bin size 0.5°).*

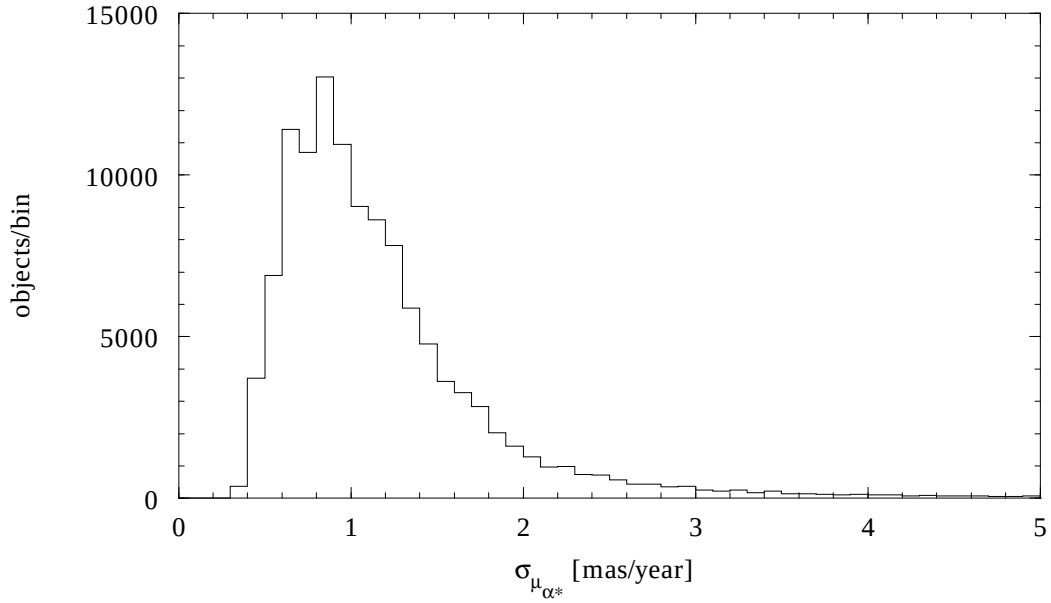

Figure 3.2.32. *Hipparcos Catalogue, Field H17: standard error of $\mu_{\alpha*}$ (bin size 0.1 mas/year).*

Figure 3.2.33. *Hipparcos Catalogue, Field H18: median standard error of μ_δ, in equatorial coordinates (cell size $2^\circ \times 2^\circ$).*

Figure 3.2.34. *Hipparcos Catalogue, Field H18: median standard error of μ_β, in ecliptic coordinates (cell size $2^\circ \times 2^\circ$). The distribution is almost independent of the latitude for the same reasons as for the standard error of the ecliptic latitude. The remaining effect in longitude is due to the time distribution of the observations.*

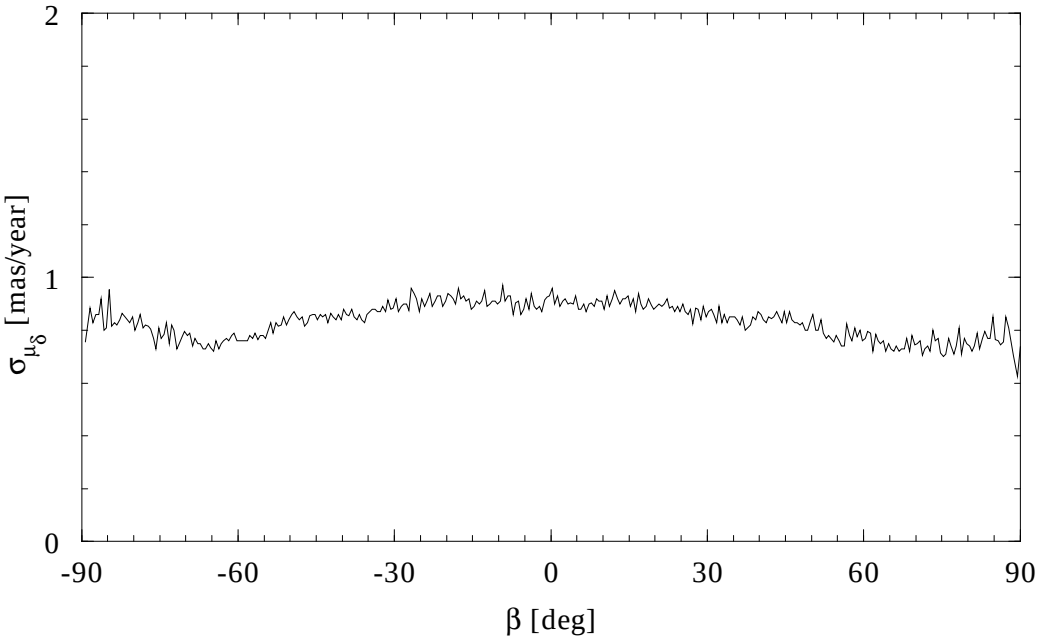

Figure 3.2.35. *Hipparcos Catalogue, Field H18: median standard error of μ_δ versus ecliptic latitude (bin size 0.5°).*

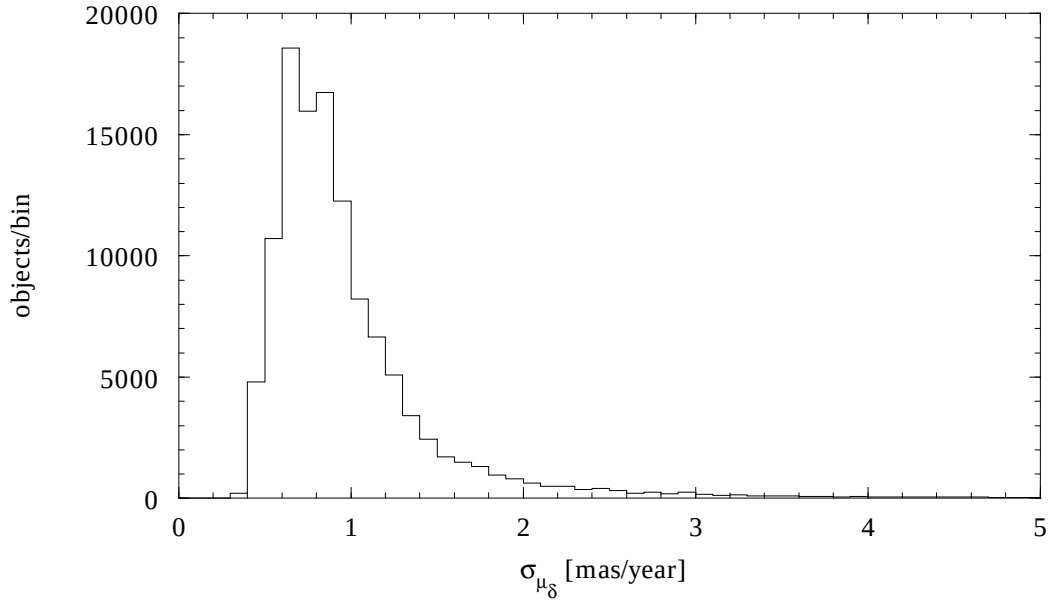

Figure 3.2.36. *Hipparcos Catalogue, Field H18: standard error of μ_δ (bin size 0.1 mas/year).*

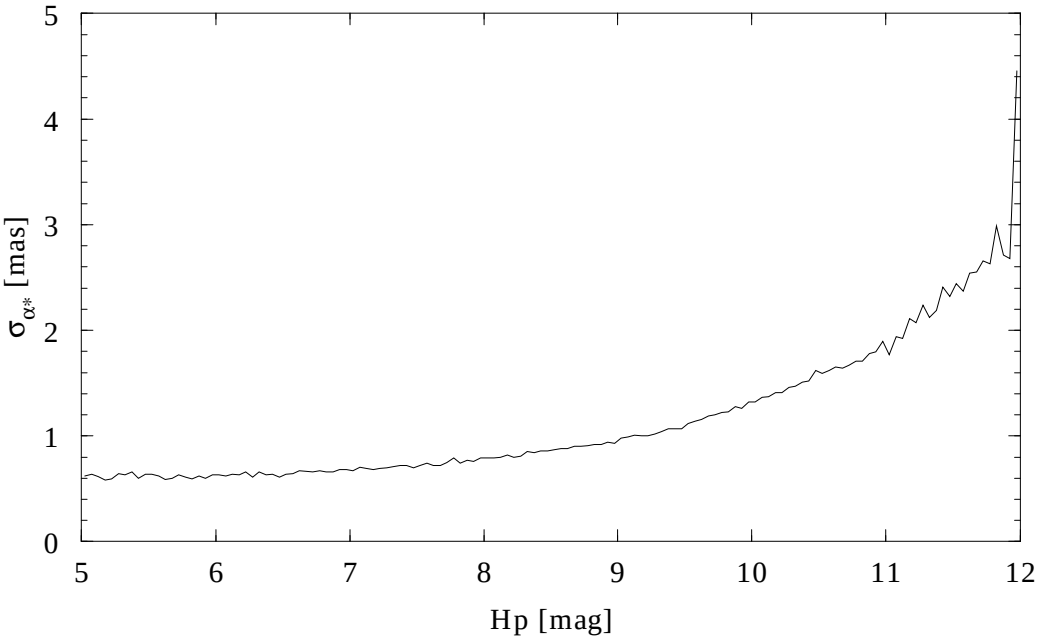

Figure 3.2.37. *Hipparcos Catalogue, Field H14: median standard error of $\alpha*$ versus Hp (bin size 0.05 mag).*

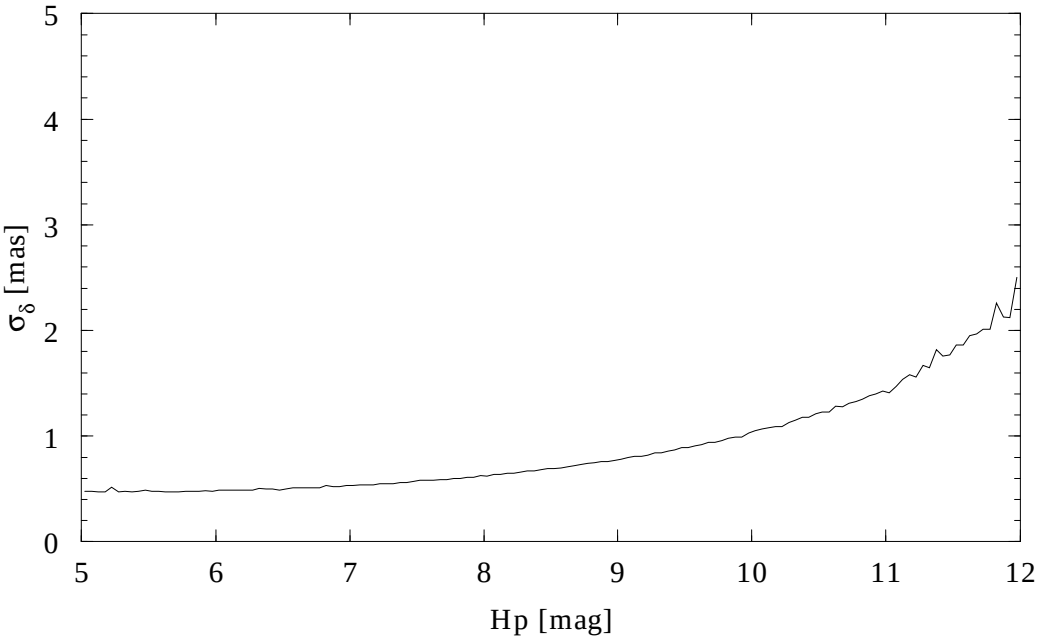

Figure 3.2.38. *Hipparcos Catalogue, Field H15: median standard error of δ versus Hp (bin size 0.05 mag).*

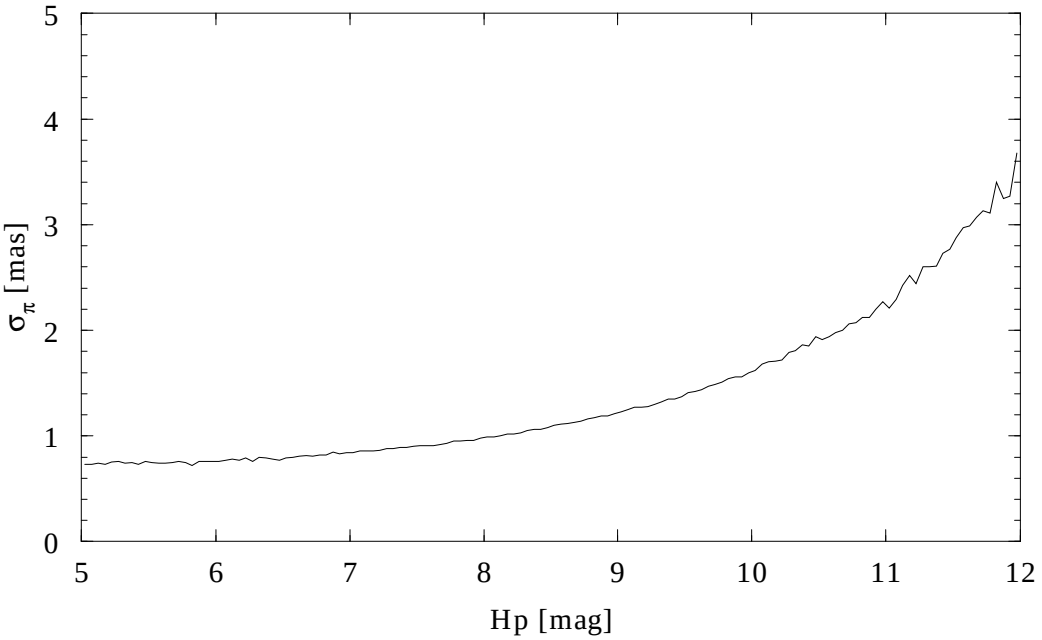

Figure 3.2.39. *Hipparcos Catalogue, Field H16: median standard error of π versus Hp (bin size 0.05 mag).*

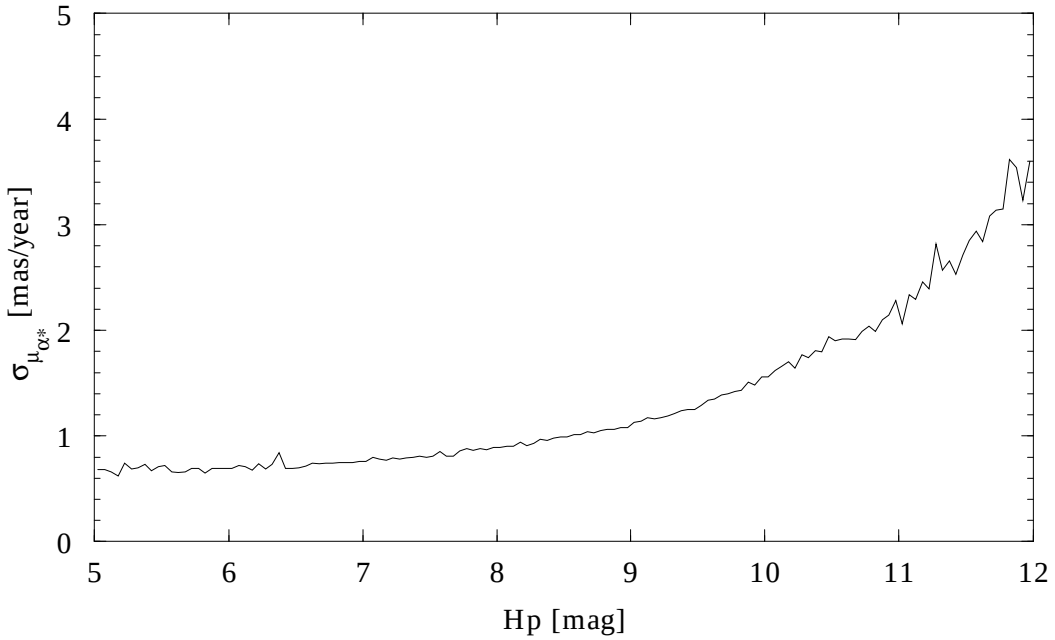

Figure 3.2.40. *Hipparcos Catalogue, Field H17: median standard error of $\mu_{\alpha*}$ versus Hp (bin size 0.05 mag).*

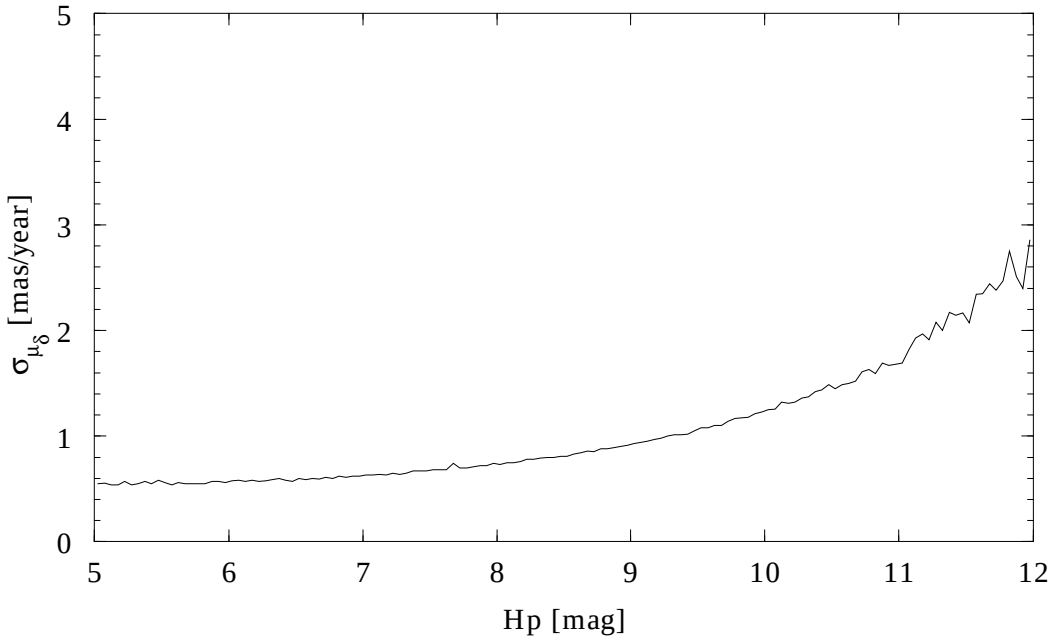

Figure 3.2.41. *Hipparcos Catalogue, Field H18: median standard error of μ_δ versus Hp (bin size 0.05 mag).*

Figure 3.2.42. *Hipparcos Catalogue, Field H19: median correlation between $\alpha*$ and δ in equatorial coordinates (cell size $2^\circ \times 2^\circ$). The systematic strucure is caused by the transformation from ecliptic to equatorial coordinates, see text.*

Figure 3.2.43. *Hipparcos Catalogue, Field H19: median correlation between $\lambda*$ and β in ecliptic coordinates (cell size $2^\circ \times 2^\circ$). Features are clearly connected to the scanning law.*

Figure 3.2.44. *Hipparcos Catalogue, Field H20: median correlation between $\alpha*$ and π in equatorial coordinates (cell size $2^\circ \times 2^\circ$).*

Figure 3.2.45. *Hipparcos Catalogue, Field H20: median correlation between $\lambda*$ and π in ecliptic coordinates (cell size $2^\circ \times 2^\circ$). The variations are very large over the sky with much structure. The strong asymmetry with the ecliptic longitude is due to a lack of symmetry in the distribution of the observations with respect to the position of the sun (see text).*

Figure 3.2.46. *Hipparcos Catalogue, Field H21: median correlation between δ and π in equatorial coordinates (cell size $2^\circ \times 2^\circ$).*

Figure 3.2.47. *Hipparcos Catalogue, Field H21: median correlation between β and π in ecliptic coordinates (cell size $2^\circ \times 2^\circ$). The variations are not prominent over the sky and show little structure. The bias towards negative values is explained in the text.*

Figure 3.2.48. *Hipparcos Catalogue, Field H22: median correlation between $\alpha*$ and $\mu_{\alpha*}$ in equatorial coordinates (cell size $2^\circ \times 2^\circ$).*

Figure 3.2.49. *Hipparcos Catalogue, Field H22: median correlation between $\lambda*$ and $\mu_{\lambda*}$ in ecliptic coordinates (cell size $2^\circ \times 2^\circ$). This correlation coefficient should be zero whenever the observations are distributed symmetrically with respect to the Catalogue epoch. The plot reflects the distribution of the mean epoch of each star (cf. Figure 3.2.62) combined with the latitude effect in the standard error of the longitude.*

Figure 3.2.50. *Hipparcos Catalogue, Field H23: median correlation between δ and $\mu_{\alpha*}$ in equatorial coordinates (cell size $2^\circ \times 2^\circ$).*

Figure 3.2.51. *Hipparcos Catalogue, Field H23: median correlation between β and $\mu_{\lambda*}$ in ecliptic coordinates (cell size $2^\circ \times 2^\circ$). All the features in this plot are linked to the scanning law.*

Figure 3.2.52. *Hipparcos Catalogue, Field H24: median correlation between π and $\mu_{\alpha*}$ in equatorial coordinates (cell size $2^\circ \times 2^\circ$).*

Figure 3.2.53. *Hipparcos Catalogue, Field H24: median correlation between π and $\mu_{\lambda*}$ in ecliptic coordinates (cell size $2^\circ \times 2^\circ$). The global bipolar structure has the same cause as the strong effect observed in the correlation between the parallax and the ecliptic longitude.*

Figure 3.2.54. *Hipparcos Catalogue, Field H25: median correlation between $\alpha*$ and μ_δ in equatorial coordinates (cell size $2^\circ \times 2^\circ$).*

Figure 3.2.55. *Hipparcos Catalogue, Field H25: median correlation between $\lambda*$ and μ_β in ecliptic coordinates (cell size $2^\circ \times 2^\circ$). The thread-like features are linked to the scanning law.*

Figure 3.2.56. *Hipparcos Catalogue, Field H26: median correlation between δ and μ_δ in equatorial coordinates (cell size $2^\circ \times 2^\circ$).*

Figure 3.2.57. *Hipparcos Catalogue, Field H26: median correlation between β and μ_β in ecliptic coordinates (cell size $2^\circ \times 2^\circ$). This correlation coefficient should be zero whenever the observations are distributed symmetrically with respect to the Catalogue epoch. The plot reflects the distribution of the mean epoch of each star (cf. Figure 3.2.62) combined with the (very small) latitude effect in the standard error of the longitude. The observations performed in the sun-pointing mode show up as a narrow strip close to $\lambda = 0^\circ$ and $\lambda = 180^\circ$.*

Figure 3.2.58. *Hipparcos Catalogue, Field H27: median correlation between π and μ_δ in equatorial coordinates (cell size $2^\circ \times 2^\circ$).*

Figure 3.2.59. *Hipparcos Catalogue, Field H27: median correlation between π and μ_β in ecliptic coordinates (cell size $2^\circ \times 2^\circ$). The features are connected to the time distribution of the observations.*

Figure 3.2.60. *Hipparcos Catalogue, Field H28: median correlation between $\mu_{\alpha*}$ and μ_δ in equatorial coordinates (cell size $2^\circ \times 2^\circ$). The variations over the sky are due to the transformation from ecliptic to equatorial coordinates, see text.*

Figure 3.2.61. *Hipparcos Catalogue, Field H28: median correlation between $\mu_{\lambda*}$ and μ_β in ecliptic coordinates (cell size $2^\circ \times 2^\circ$). The features are related to the time distribution of the observations, with a global variation over the sky.*

Figure 3.2.62. *Hipparcos Catalogue: median of the mean observation epoch relative to J1991.25, in ecliptic coordinates (cell size $2^\circ \times 2^\circ$). The loop structure in the range of latitude $\pm 47^\circ$ is a consequence of the scanning law and of the limited duration of the mission. The meridian strip at the centre of the plot corresponds to the region of the sky observed during the sun-pointing period at the end of the mission. The rest of this circle is visible at $\lambda \sim -170^\circ$.*

Figure 3.2.63. *Hipparcos Catalogue: median effective observation epoch relative to J1991.25, as defined in Equation 1.2.10, in ecliptic coordinates (cell size $2^\circ \times 2^\circ$).*

Figure 3.2.64. *Hipparcos Catalogue: median duration between first and last observation, in ecliptic coordinates (cell size $2^\circ \times 2^\circ$). The features are a direct consequence of the scanning law, the mission duration, and the observation interruptions.*

Figure 3.2.65. *Hipparcos Catalogue: median difference between mean observational epoch in right ascension and in declination, in ecliptic coordinates (cell size $2^\circ \times 2^\circ$).*

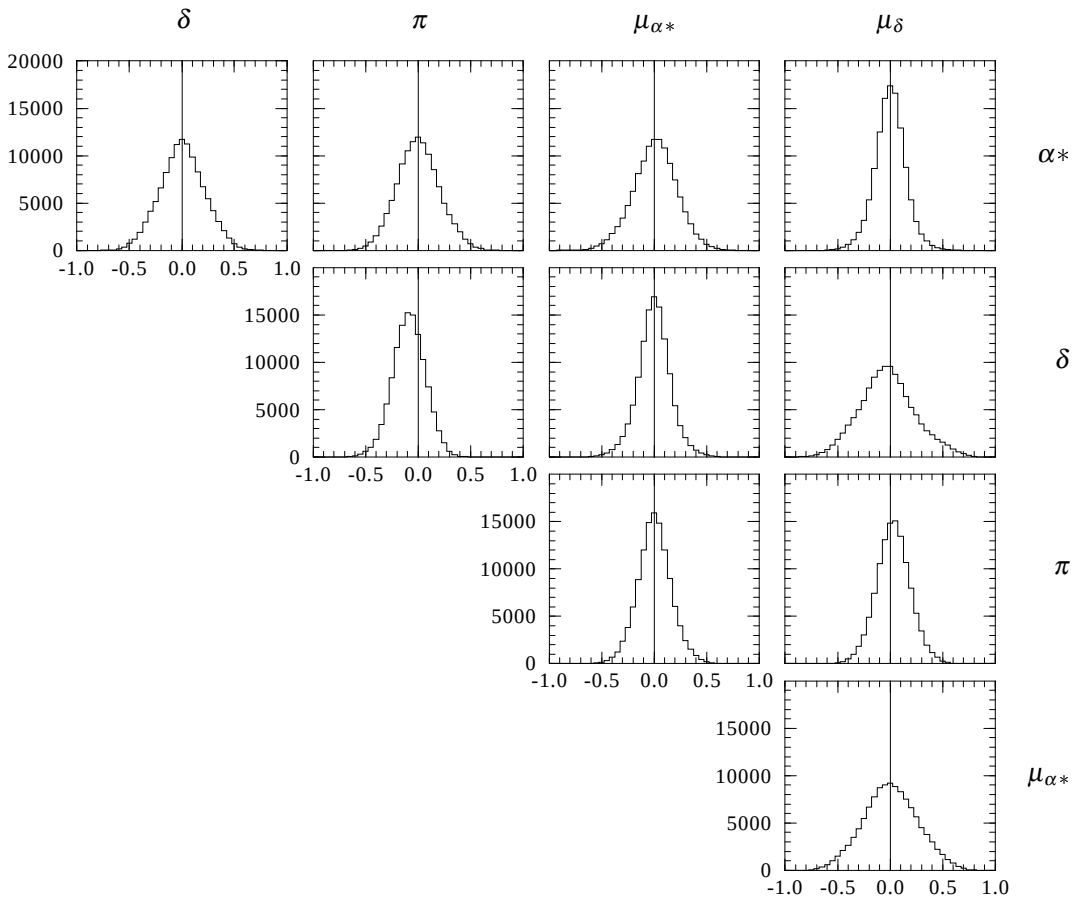

Figure 3.2.66. *Hipparcos Catalogue, Field H19–H28: correlations between astrometric parameters (bin size 0.05). The main features of these correlations, in particular the asymmetry in the π versus δ correlation, are described in the text.*

Figure 3.2.67. *Hipparcos Catalogue, Field H29: median percentage of rejected observations, F1, in ecliptic coordinates (cell size $2^\circ \times 2^\circ$).*

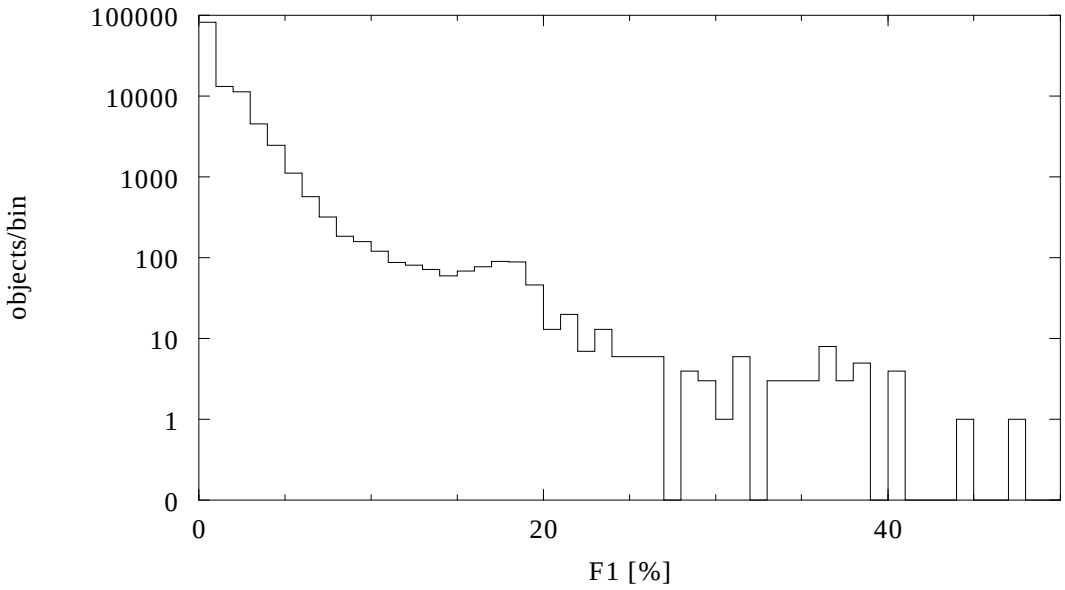

Figure 3.2.68. *Hipparcos Catalogue, Field H29: percentage of rejected observations, F1 (bin size 1%).*

Figure 3.2.69. *Hipparcos Catalogue, Field H30: median goodness-of-fit, F2, in ecliptic coordinates (cell size $2^\circ \times 2^\circ$). The structure indicates that the adjustment is slightly less satisfactory around the ecliptic than around the ecliptic poles.*

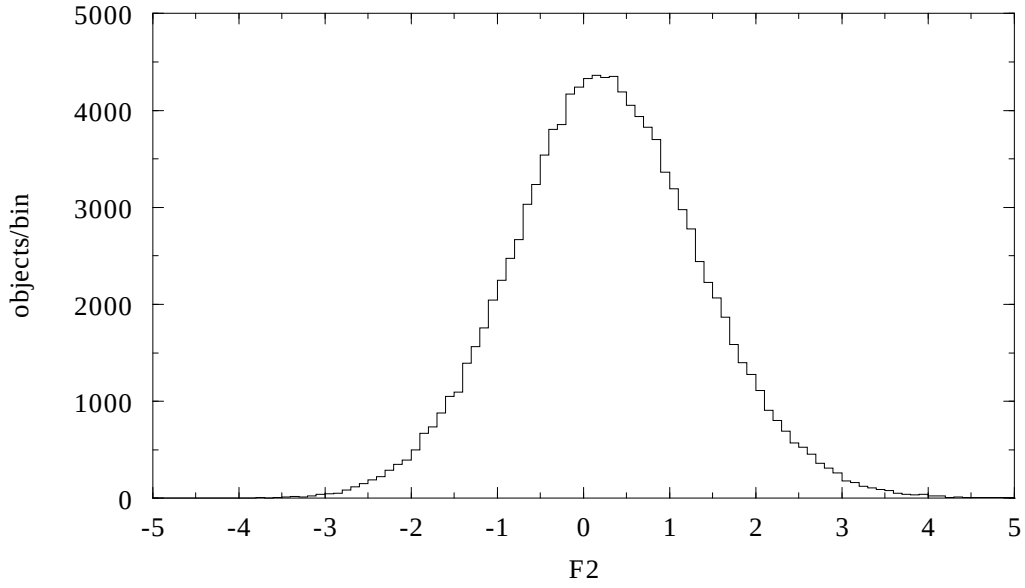

Figure 3.2.70. *Hipparcos Catalogue, Field H30: goodness-of-fit, F2 (bin size 0.1).*

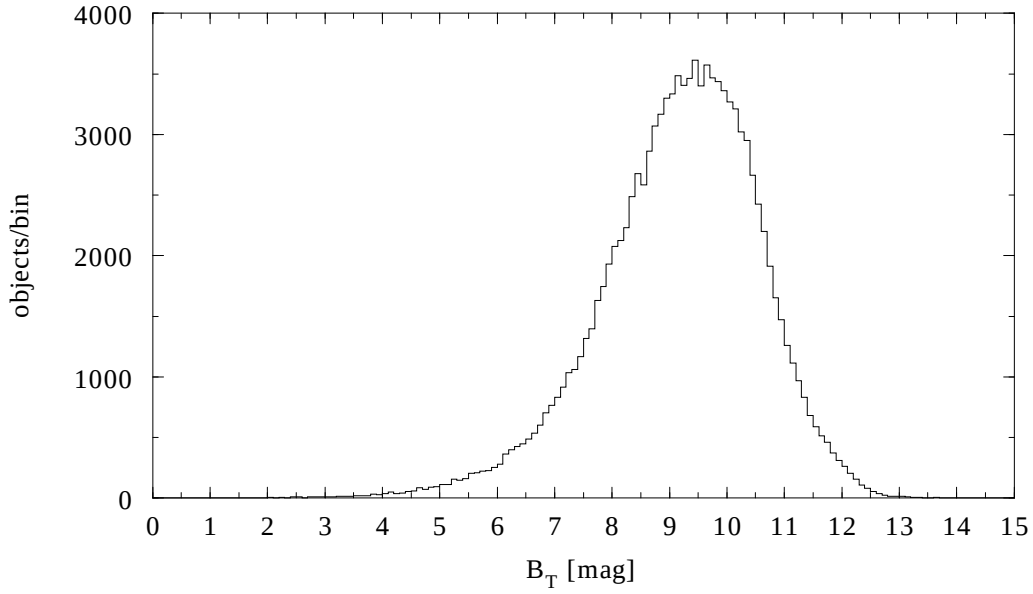

Figure 3.2.71. *Hipparcos Catalogue, Field H32: B_T magnitude (bin size 0.1 mag).*

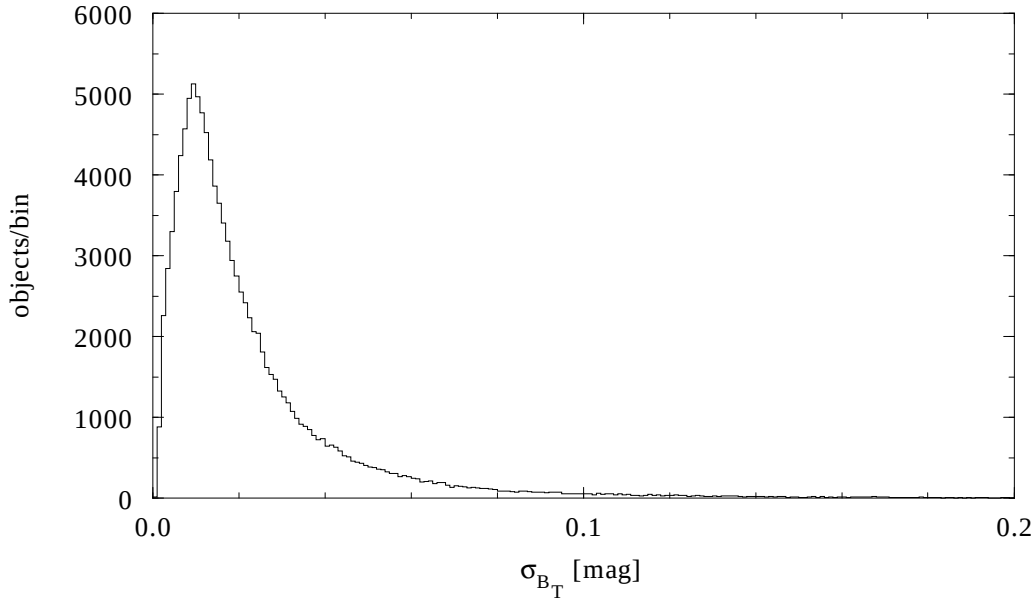

Figure 3.2.72. *Hipparcos Catalogue, Field H33: standard error in B_T magnitude (bin size 0.001 mag).*

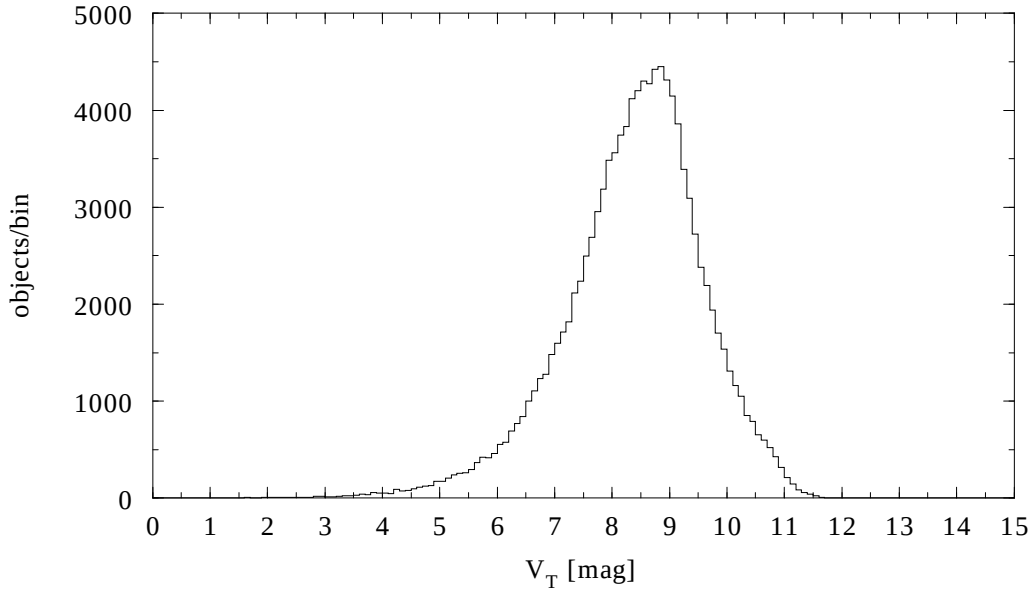

Figure 3.2.73. *Hipparcos Catalogue, Field H34: V_T magnitude (bin size 0.1 mag).*

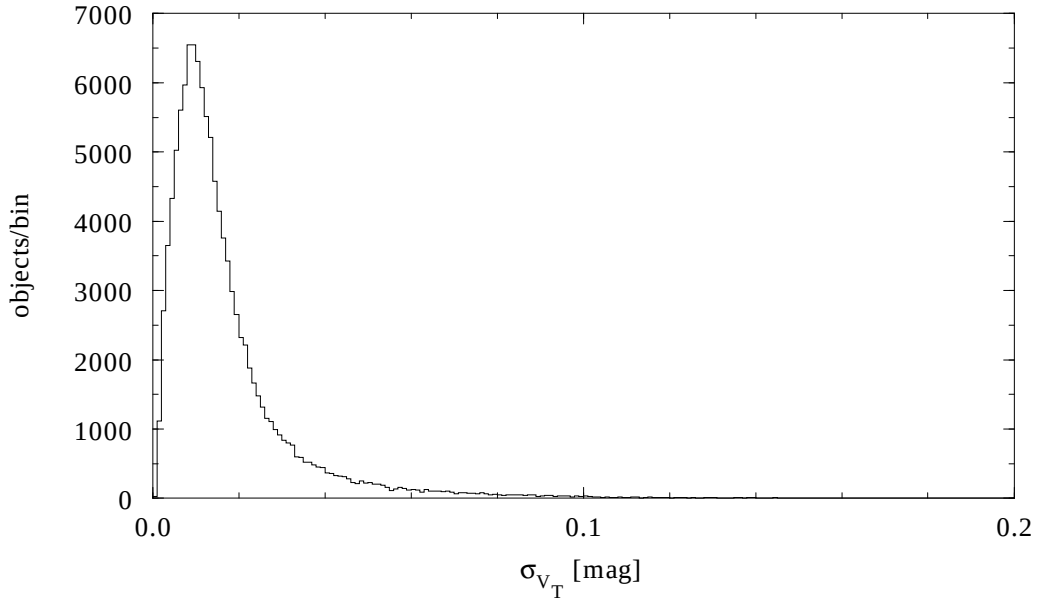

Figure 3.2.74. *Hipparcos Catalogue, Field H35: standard error in V_T magnitude (bin size 0.001 mag).*

Figure 3.2.75. *Hipparcos Catalogue, Field H37: median colour index $B-V$, in galactic coordinates (cell size $2^\circ \times 2^\circ$). As expected most of the early-type stars are in the galactic plane while on the average those outside this plane are redder.*

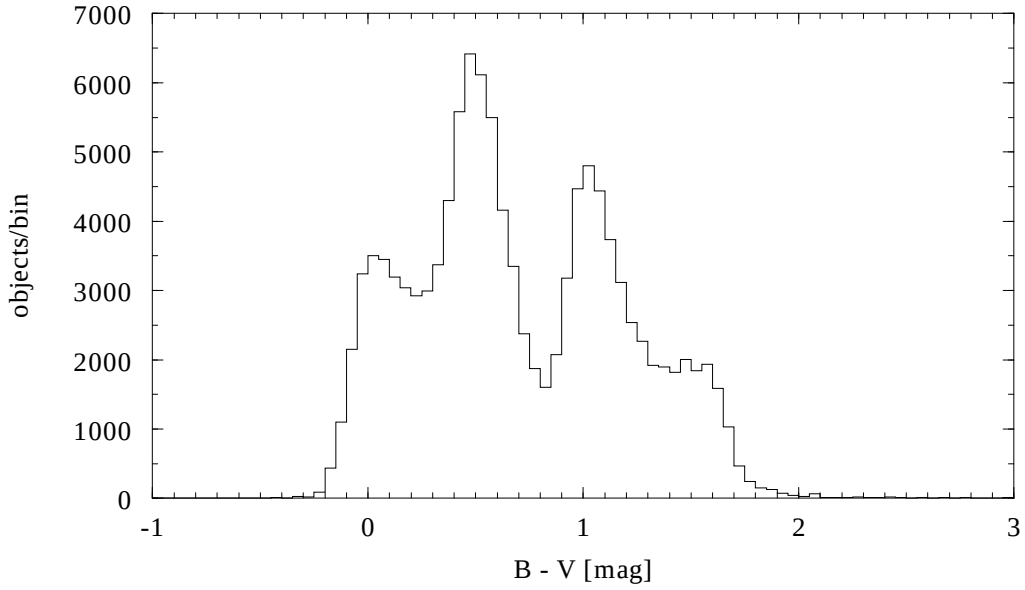

Figure 3.2.76. *Hipparcos Catalogue, Field H37: colour index $B-V$ (bin size 0.05 mag).*

Figure 3.2.77. *Hipparcos Catalogue, Field H40: median colour index $V - I$, in galactic coordinates (cell size $2^\circ \times 2^\circ$). Most of the early-type stars are in the galactic plane while on the average those outside this plane are redder.*

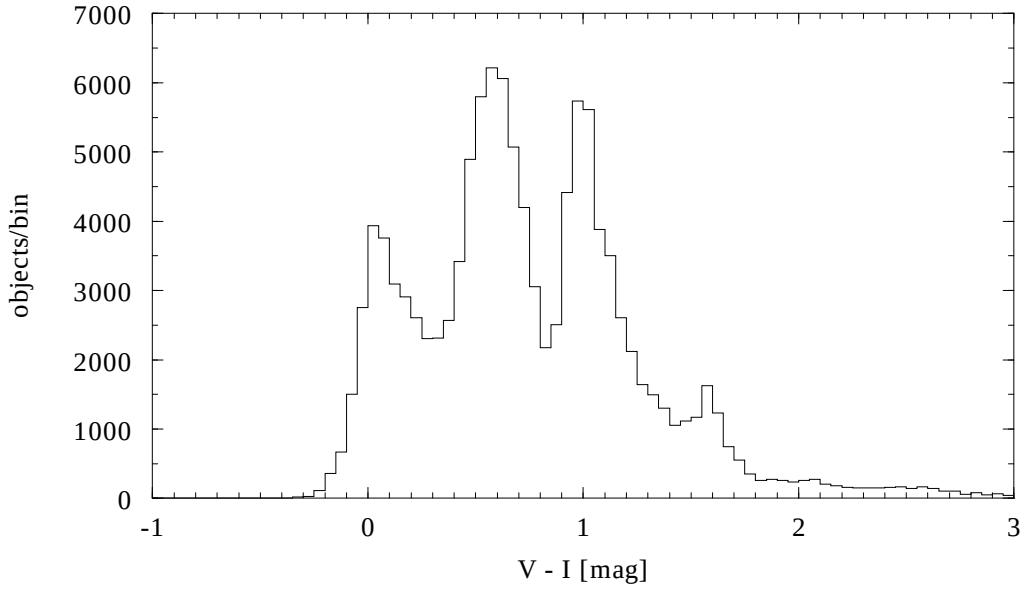

Figure 3.2.78. *Hipparcos Catalogue, Field H40: colour index $V - I$ (bin size 0.05 mag).*

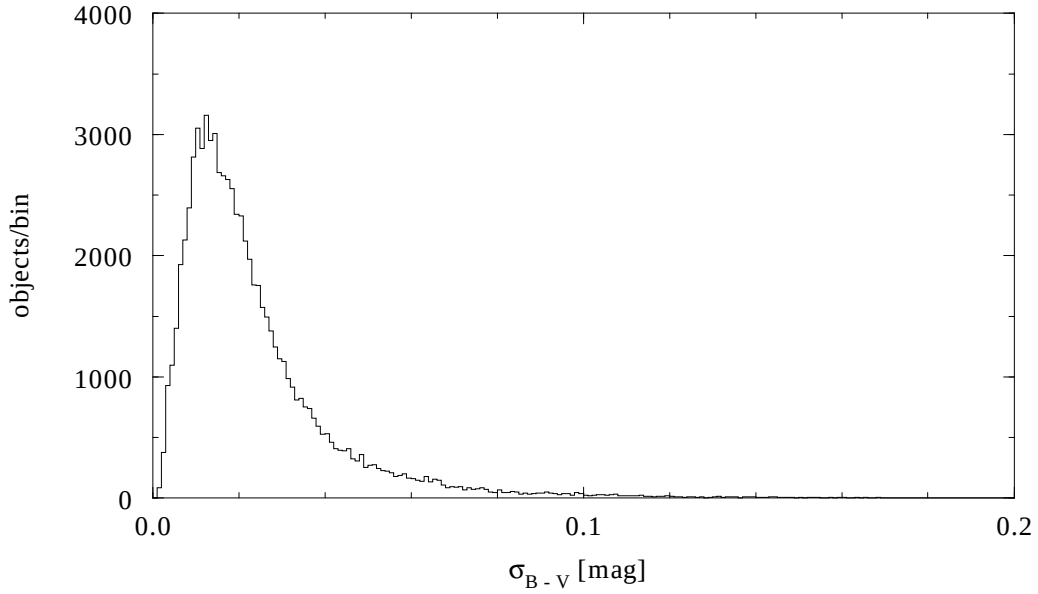

Figure 3.2.79. *Hipparcos Catalogue, Field H38: standard error in colour index $B - V$ for objects with Field H39 = 'T' (bin size 0.001 mag).*

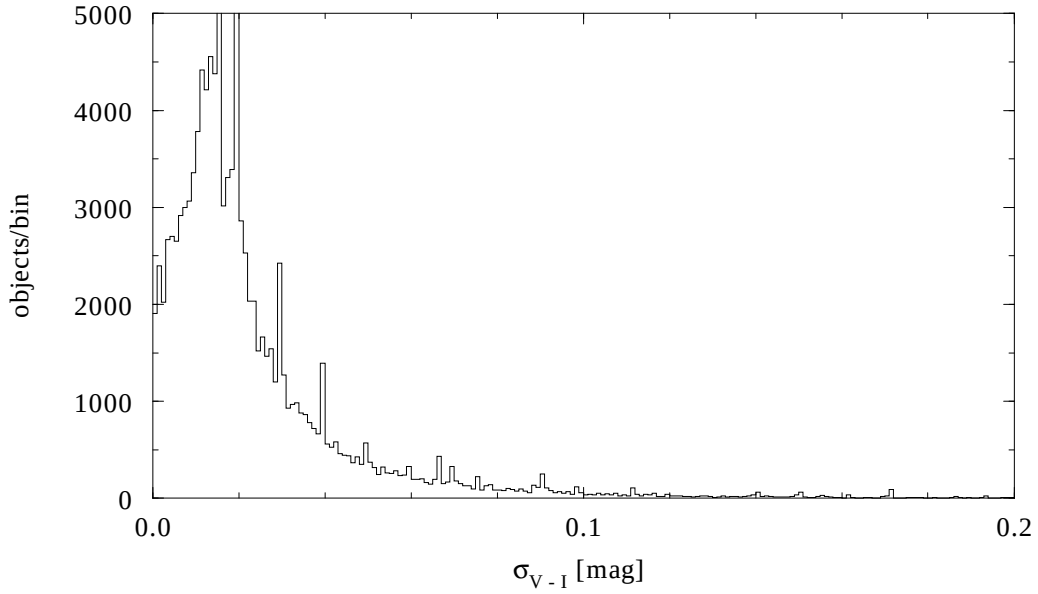

Figure 3.2.80. *Hipparcos Catalogue, Field H41: standard error in colour index $V - I$ (bin size 0.001 mag).*

Figure 3.2.81. *Hipparcos Catalogue, Field H44: median Hp magnitude, in galactic coordinates (cell size $2^\circ \times 2^\circ$). The average of the Catalogue is Hp ~ 8.5 mag with significant variations with galactic latitude.*

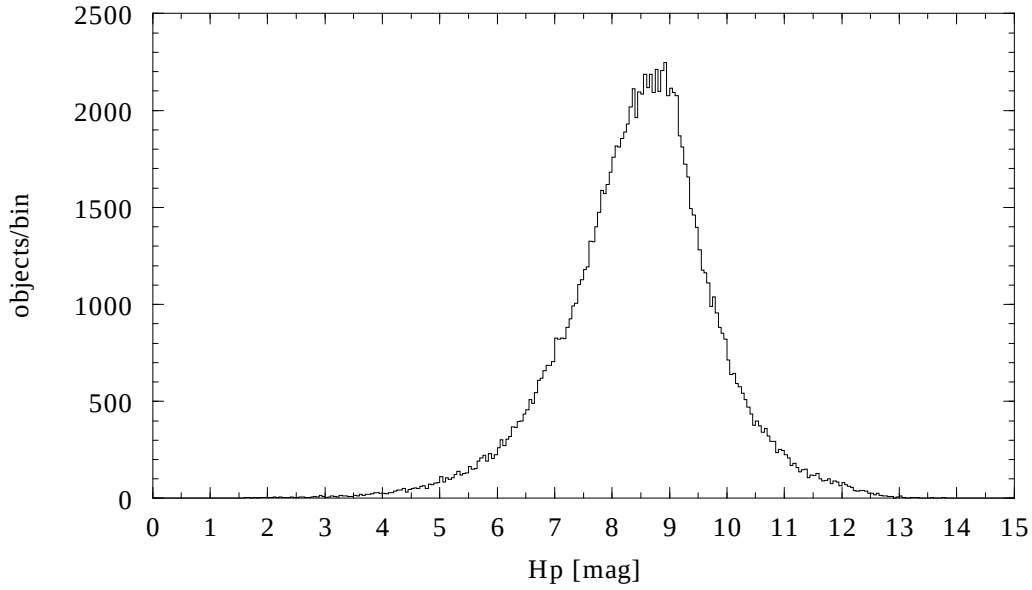

Figure 3.2.82. *Hipparcos Catalogue, Field H44: median Hp magnitude (bin size 0.05 mag).*

Figure 3.2.83. *Hipparcos Catalogue, Field H45: median standard error in Hp magnitude, in galactic coordinates (cell size $2° \times 2°$). The main structure is connected to the magnitude distribution.*

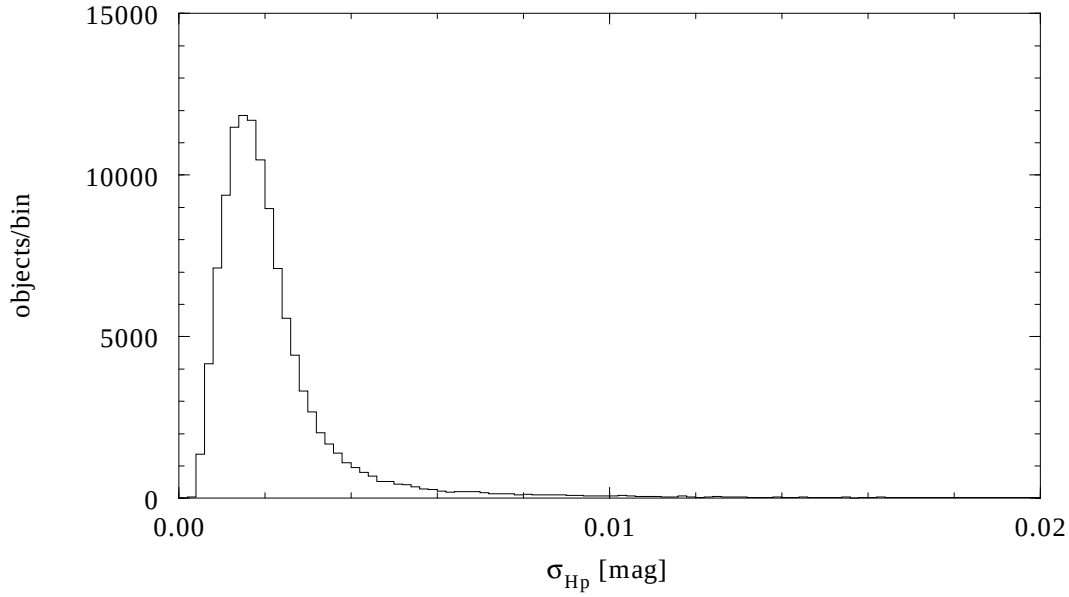

Figure 3.2.84. *Hipparcos Catalogue, Field H45: standard error in Hp magnitude (bin size 0.0002 mag).*

Figure 3.2.85. *Hipparcos Catalogue, Field H46: median scatter in Hp magnitude, in ecliptic coordinates (cell size $2^\circ \times 2^\circ$).*

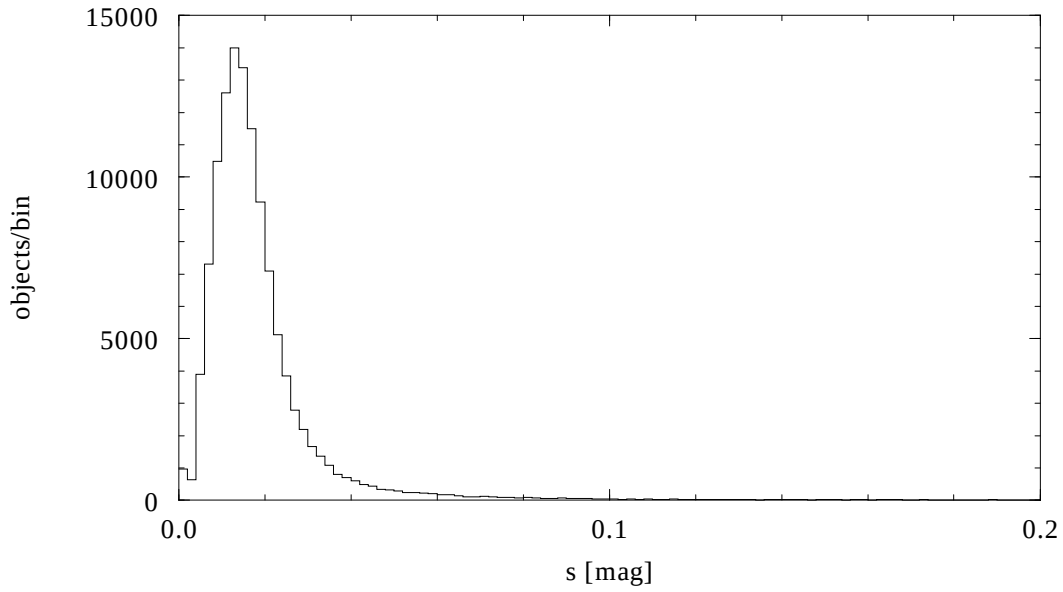

Figure 3.2.86. *Hipparcos Catalogue, Field H46: scatter in Hp magnitude (bin size 0.002 mag).*

Figure 3.2.87. *Hipparcos Catalogue, Field H47: median number of accepted photometric transits, in ecliptic coordinates (cell size $2^\circ \times 2^\circ$). The structure reflects the properties of the scanning law and the limited duration of the mission.*

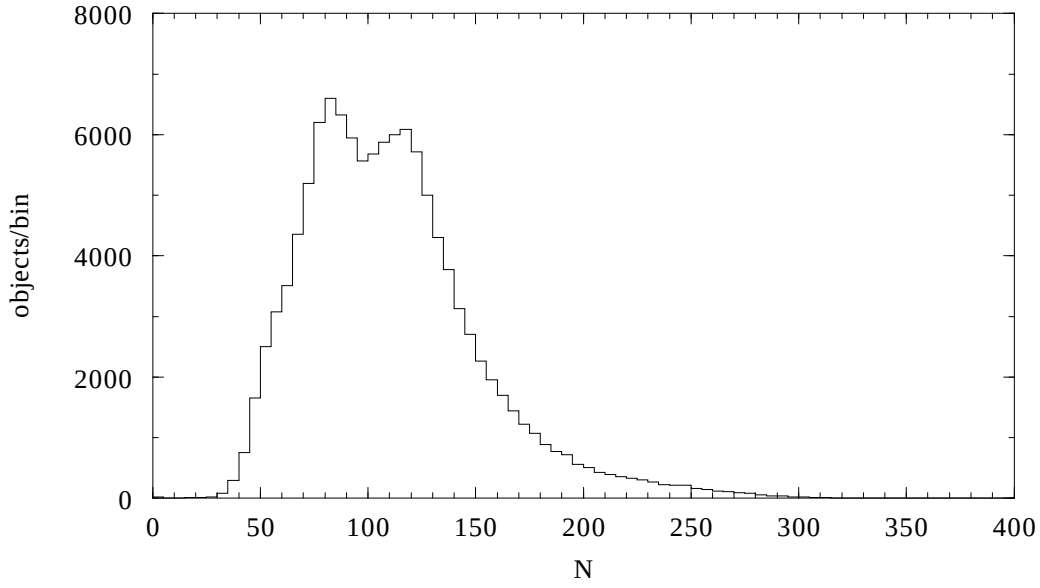

Figure 3.2.88. *Hipparcos Catalogue, Field H47: number of accepted photometric transits, N (bin size 5).*

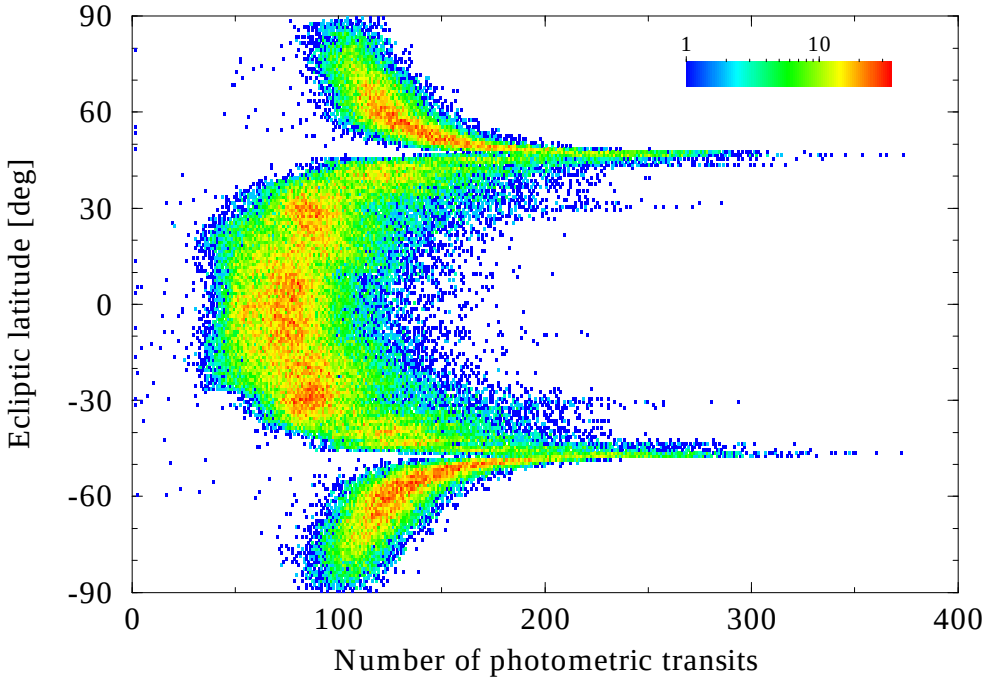

Figure 3.2.89. *Hipparcos Catalogue, Field H47: number of accepted photometric transits versus ecliptic latitude, as a density plot. Scale indicates number of stars per bin of 1 transit $\times 1^\circ$.*

Available on disk 6

Figure 3.2.90. *Hipparcos Catalogue, Fields H49/H50: median difference between the observed magnitude Hp at minimum and maximum luminosities, in ecliptic coordinates (cell size $2^\circ \times 2^\circ$). The pattern is similar to that seen in the sky distribution of the scatter.*

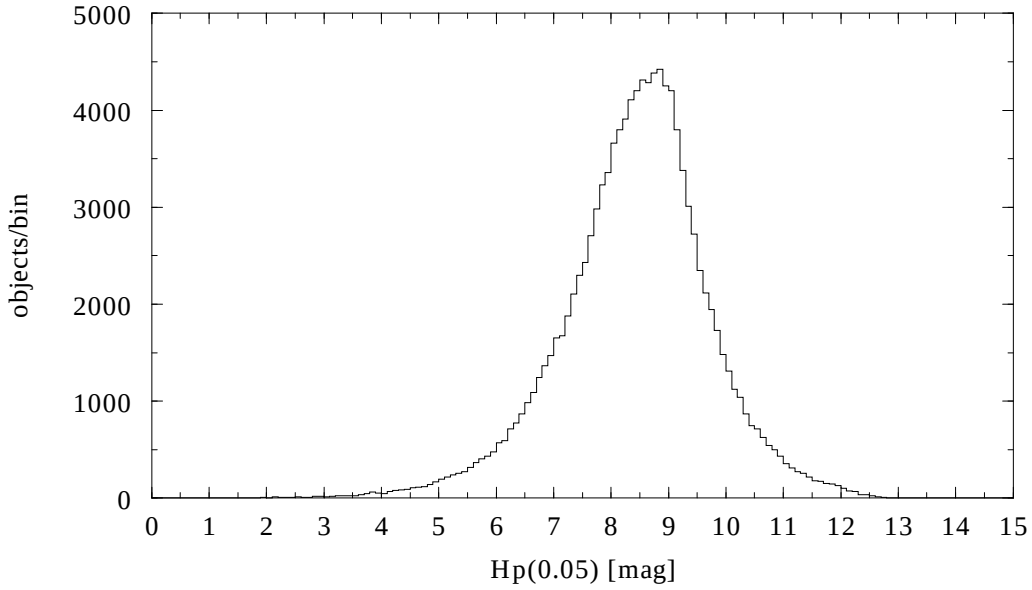

Figure 3.2.91. *Hipparcos Catalogue, Field H49: Hp magnitude, 5th percentile (bin size 0.1 mag).*

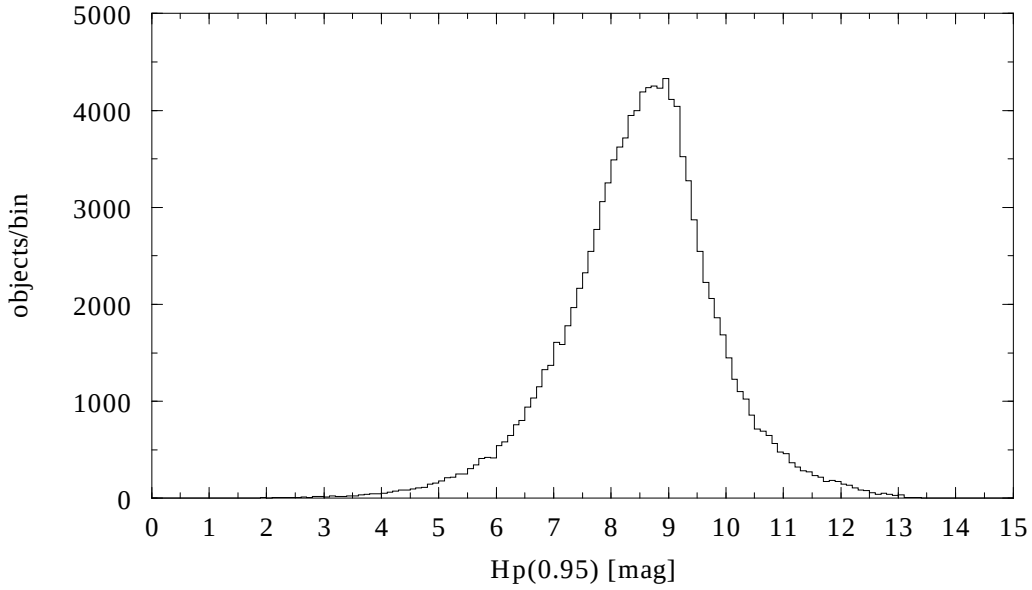

Figure 3.2.92. *Hipparcos Catalogue, Field H50: Hp magnitude, 95th percentile (bin size 0.1 mag).*

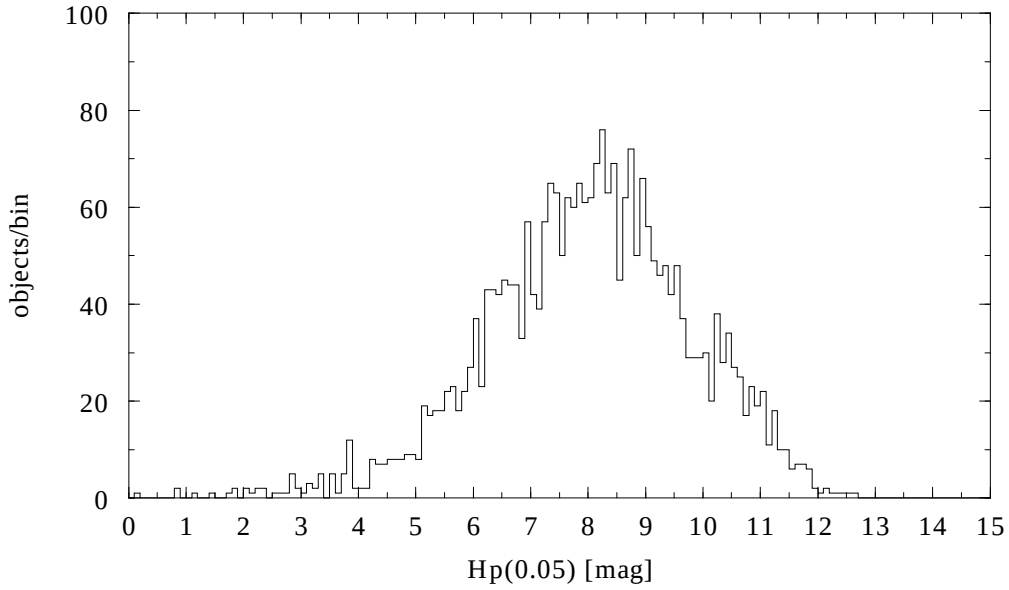

Figure 3.2.93. *Hipparcos Catalogue, Field H49: Hp magnitude, 5th percentile for objects in Section 1 of the Variability Annex (Periodic Variables) (bin size 0.1 mag).*

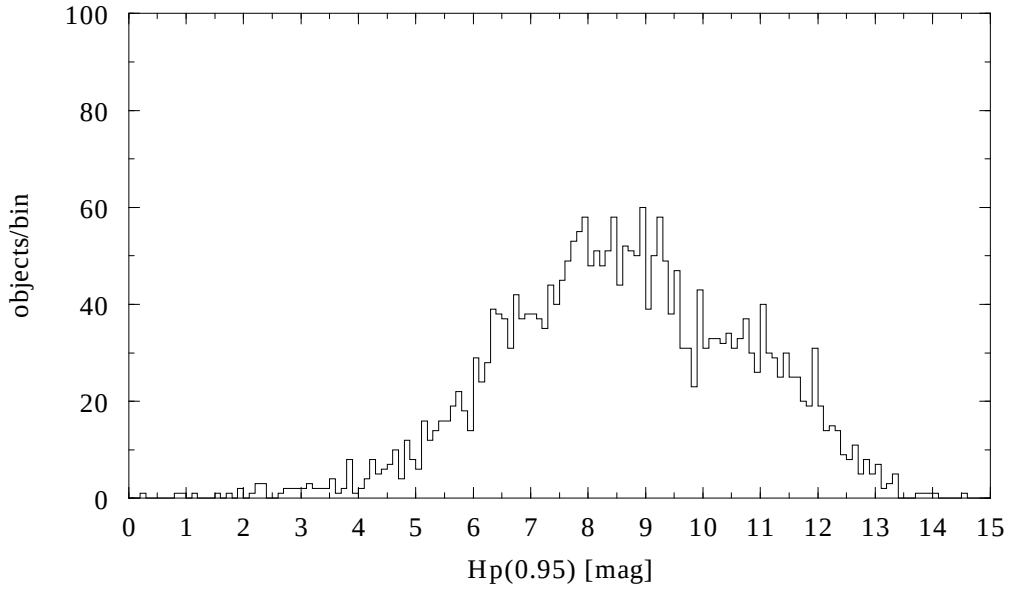

Figure 3.2.94. *Hipparcos Catalogue, Field H50: Hp magnitude, 95th percentile for objects in Section 1 of the Variability Annex (Periodic Variables) (bin size 0.1 mag).*

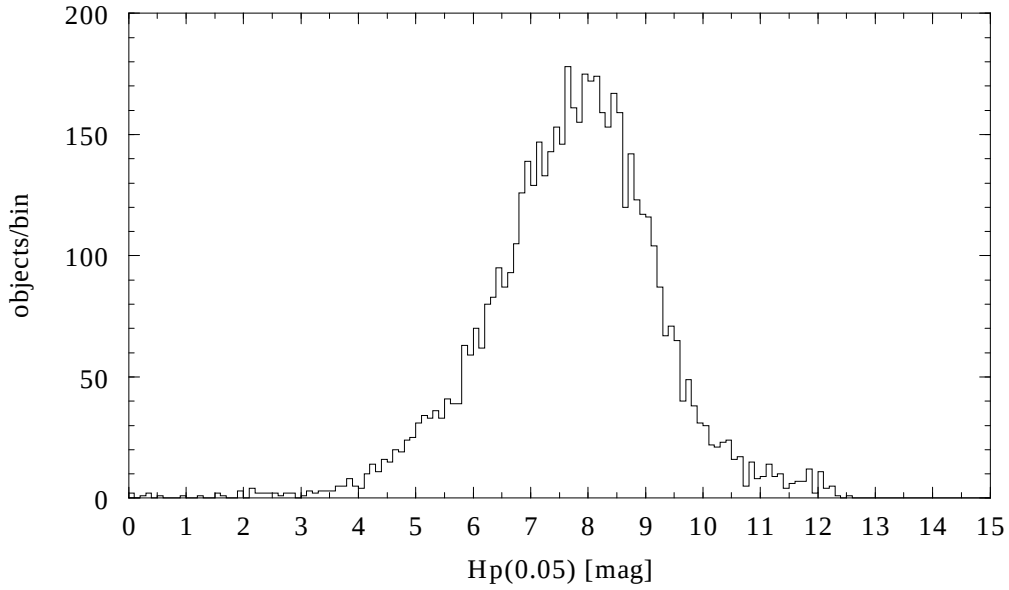

Figure 3.2.95. *Hipparcos Catalogue, Field H49: Hp magnitude, 5th percentile for objects in Section 2 of the Variability Annex (Unsolved Variables) (bin size 0.1 mag).*

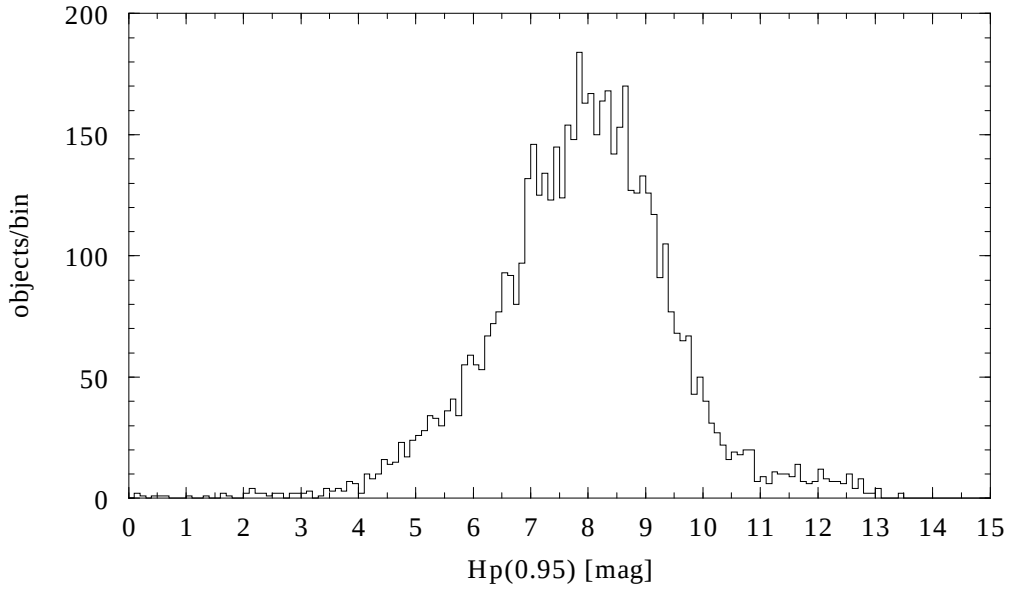

Figure 3.2.96. *Hipparcos Catalogue, Field H50: Hp magnitude, 95th percentile for objects in Section 2 of the Variability Annex (Unsolved Variables) (bin size 0.1 mag).*

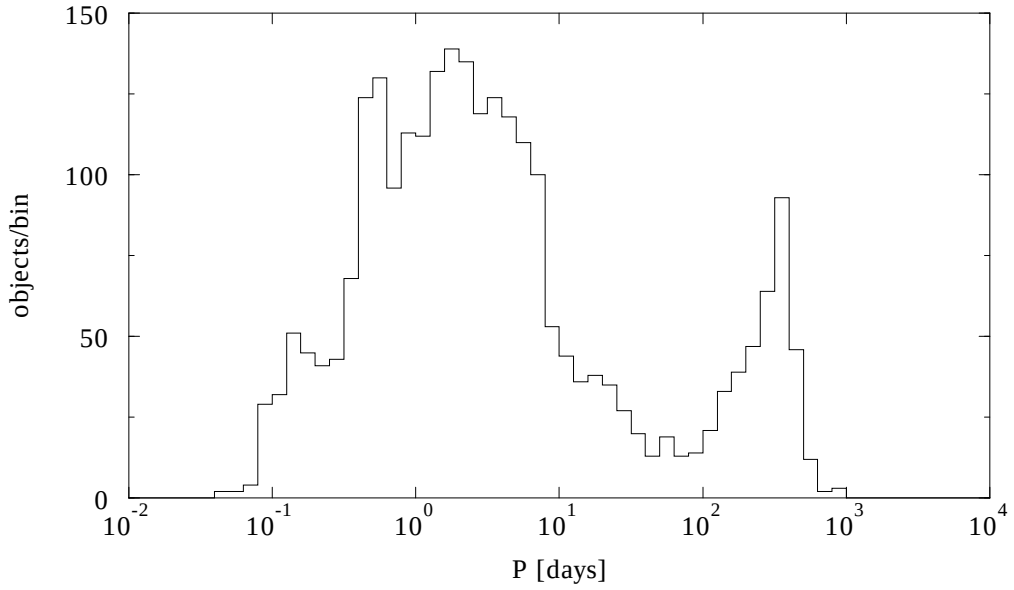

Figure 3.2.97. *Hipparcos Catalogue, Field H51: variability period, P (bin size $10^{0.1}$).*

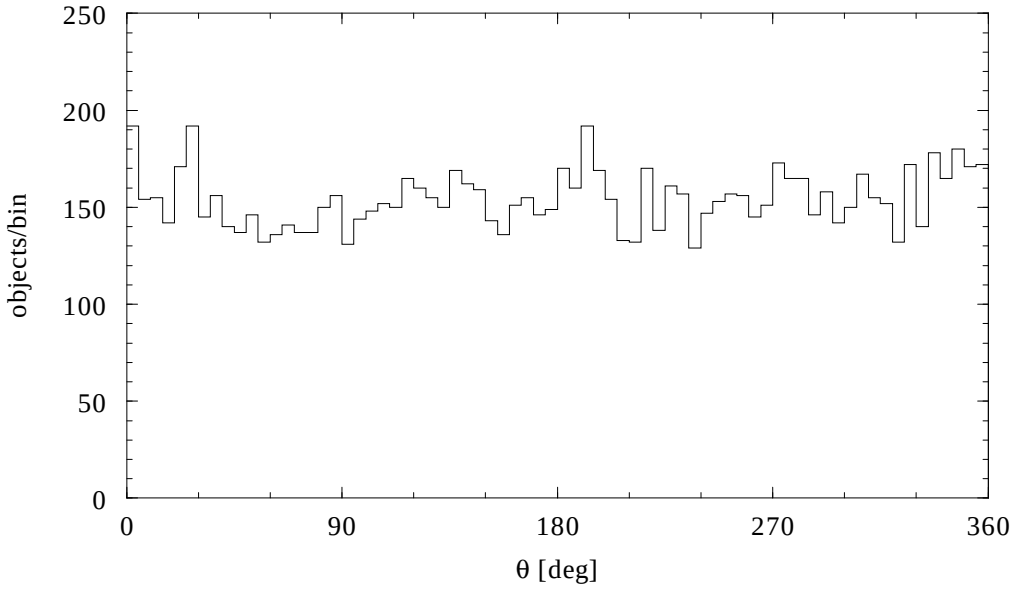

Figure 3.2.98. *Hipparcos Catalogue, Field H63: position angle, θ (bin size 5°).*

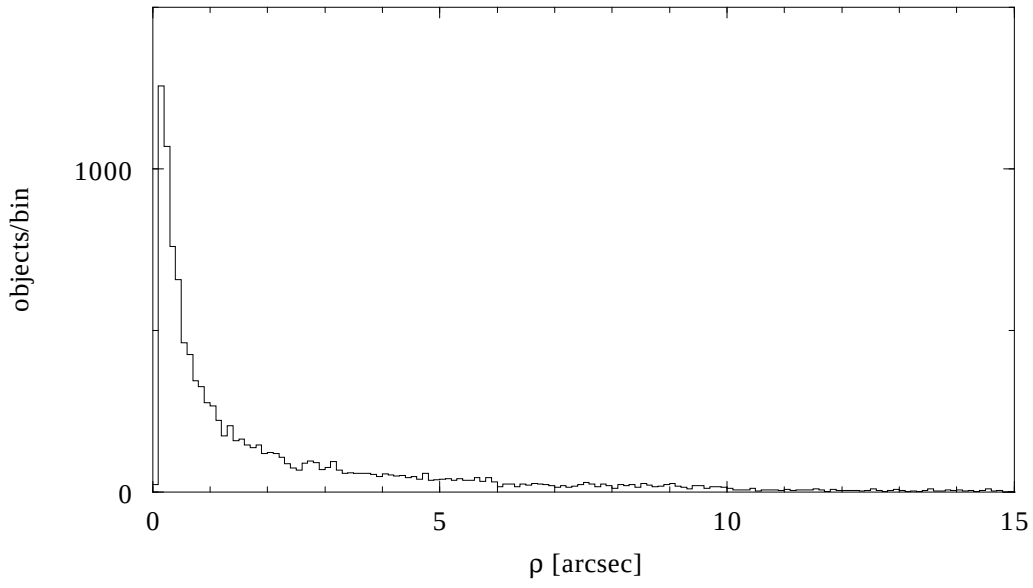

Figure 3.2.99. *Hipparcos Catalogue, Field H64: angular separation, ϱ (bin size 0.1 arcsec).*

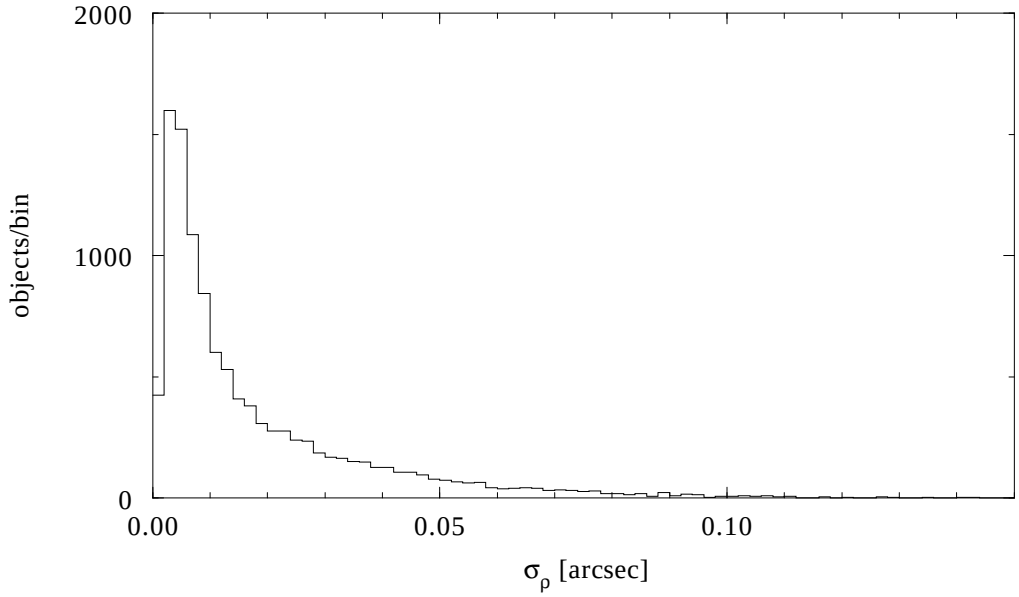

Figure 3.2.100. *Hipparcos Catalogue, Field H65: standard error in angular separation, ϱ (bin size 0.02 arcsec).*

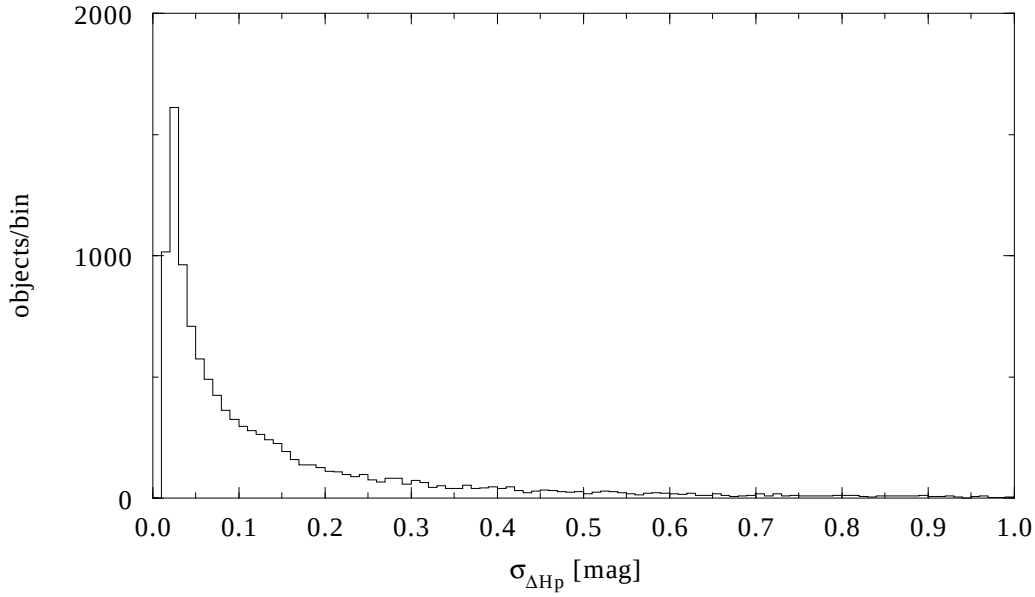

Figure 3.2.101. *Hipparcos Catalogue, Field H67: standard error in magnitude difference, ΔHp (bin size 0.01 mag).*

Figure 3.2.102. *Hipparcos Catalogue, Field H66: median magnitude difference, ΔHp, in galactic coordinates (cell size $2^\circ \times 2^\circ$). The distribution has been smoothed over the eight closest neighbours of each cell.*

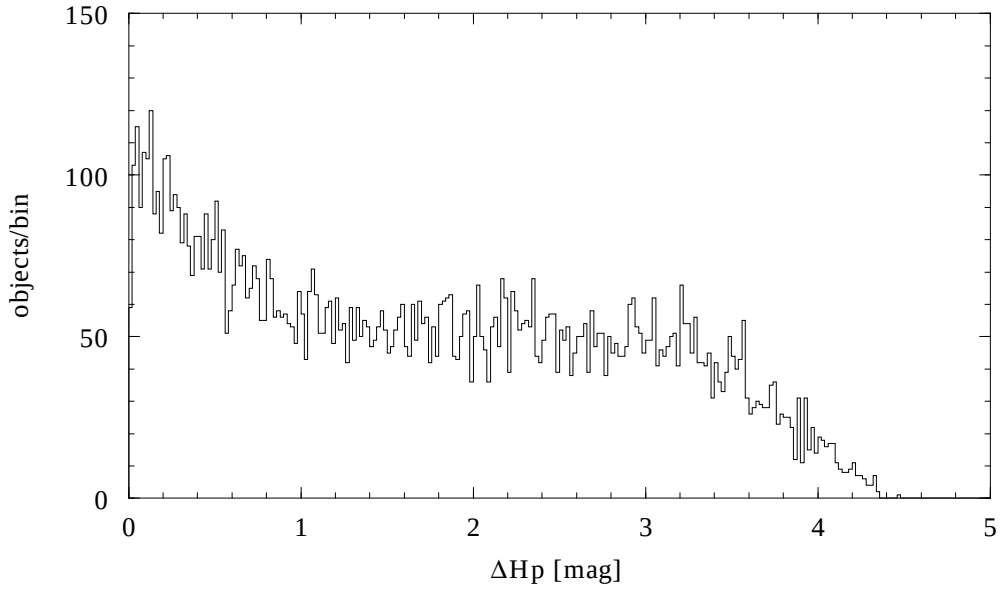

Figure 3.2.103. *Hipparcos Catalogue, Field H66: magnitude difference, ΔHp (bin size 0.02 mag).*

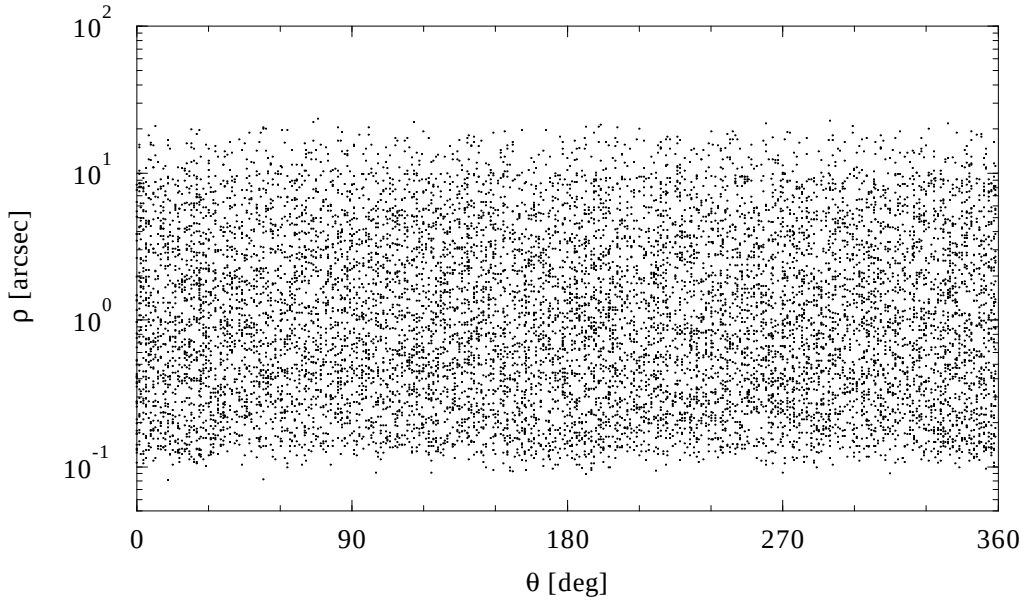

Figure 3.2.104. *Hipparcos Catalogue, Fields H63/H64: angular separation, ϱ versus position angle, θ.*

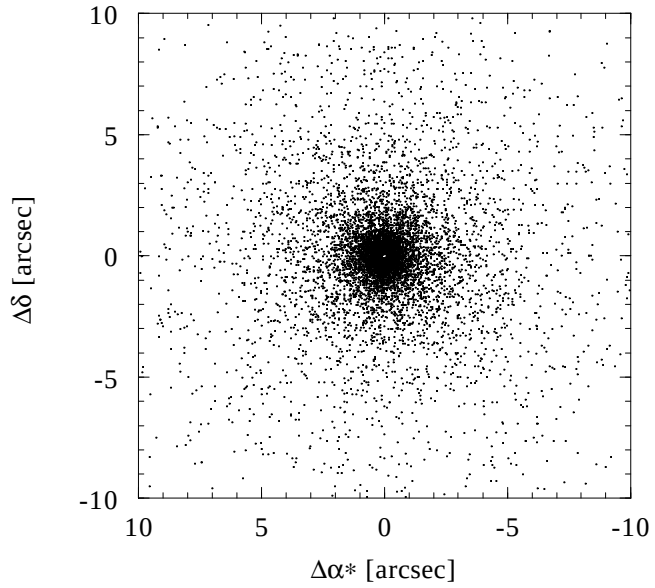

Figure 3.2.105. *Hipparcos Catalogue, Fields H63/H64: double star relative position from angular separation, ϱ, and position angle, θ.*

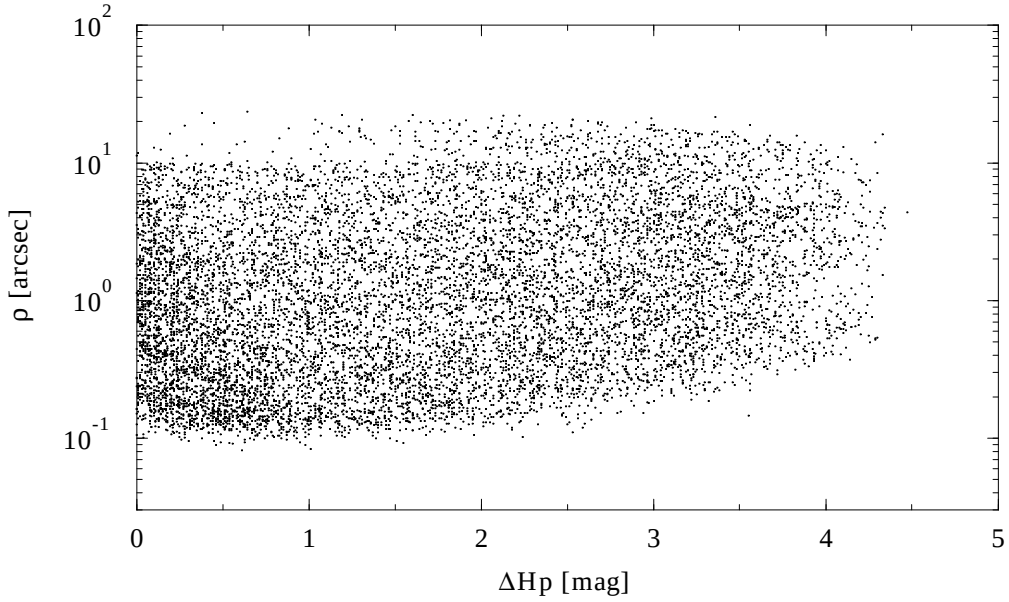

Figure 3.2.106. *Hipparcos Catalogue, Fields H63/H64: angular separation, ϱ versus magnitude difference, ΔHp.*

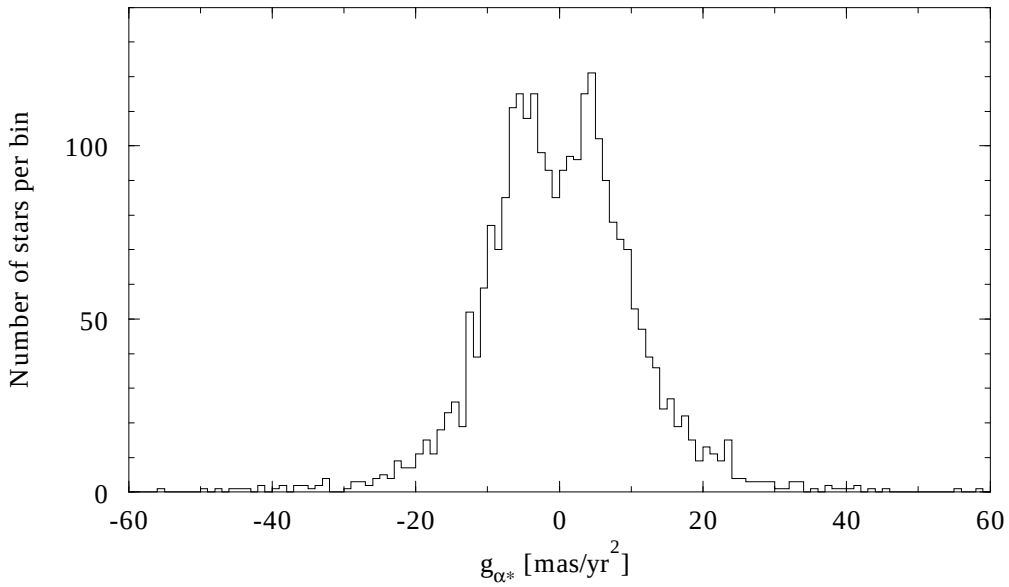

Figure 3.2.107. *Hipparcos Catalogue, DMSA/G, Field DG2: acceleration in right ascension at epoch J1991.25, $g_{\alpha*} = d\mu_{\alpha*}/dt$ (bin size 1 mas/yr^2).*

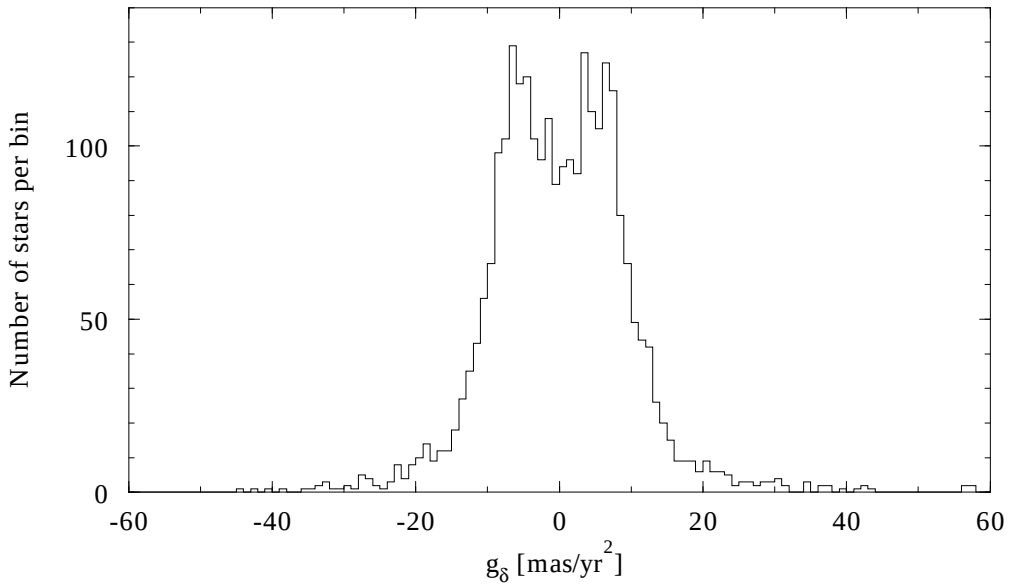

Figure 3.2.108. *Hipparcos Catalogue, DMSA/G, Field DG3: acceleration in declination at epoch J1991.25, $g_{\delta} = d\mu_{\delta}/dt$ (bin size 1 mas/yr^2).*

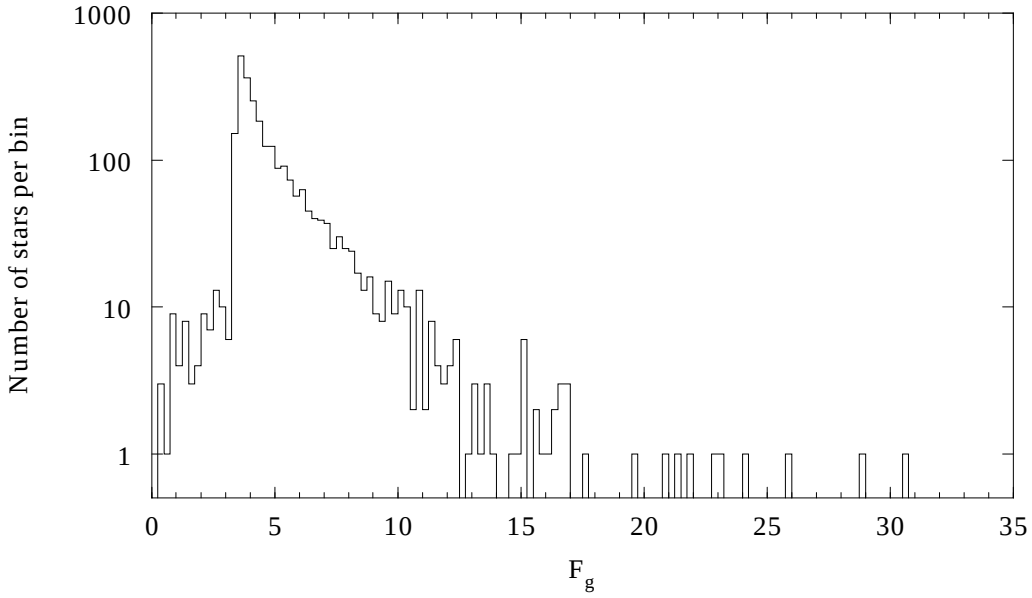

Figure 3.2.109. *Hipparcos Catalogue, DMSA/G, Field DG6: statistic for the significance of the accelerations, F_g (bin size 0.25).*

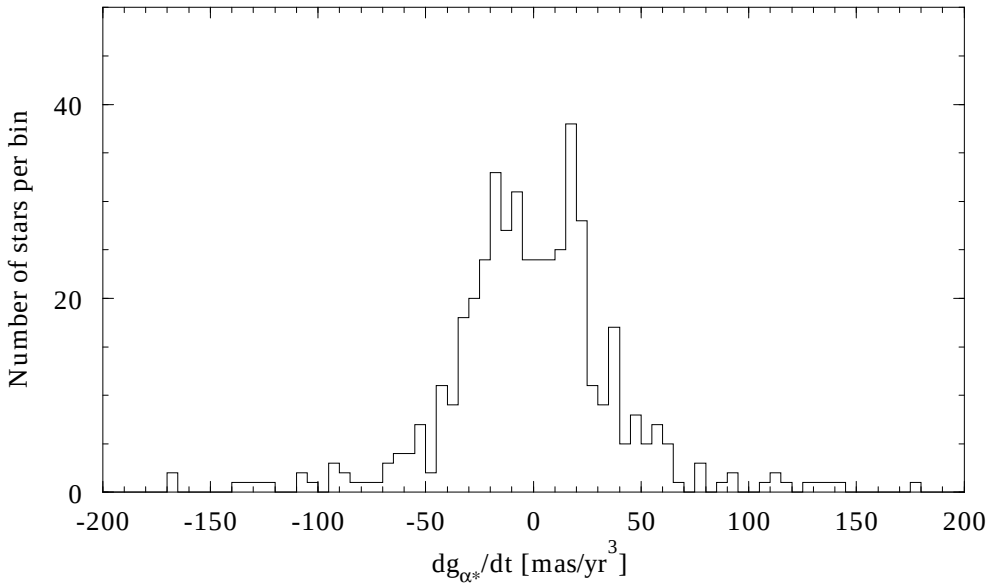

Figure 3.2.110. *Hipparcos Catalogue, DMSA/G, Field DG7: rate of change of $g_{\alpha*}$ at epoch J1991.25, $\dot{g}_{\alpha*} = d^2\mu_{\alpha*}/dt^2$ (bin size 5 mas/yr^3).*

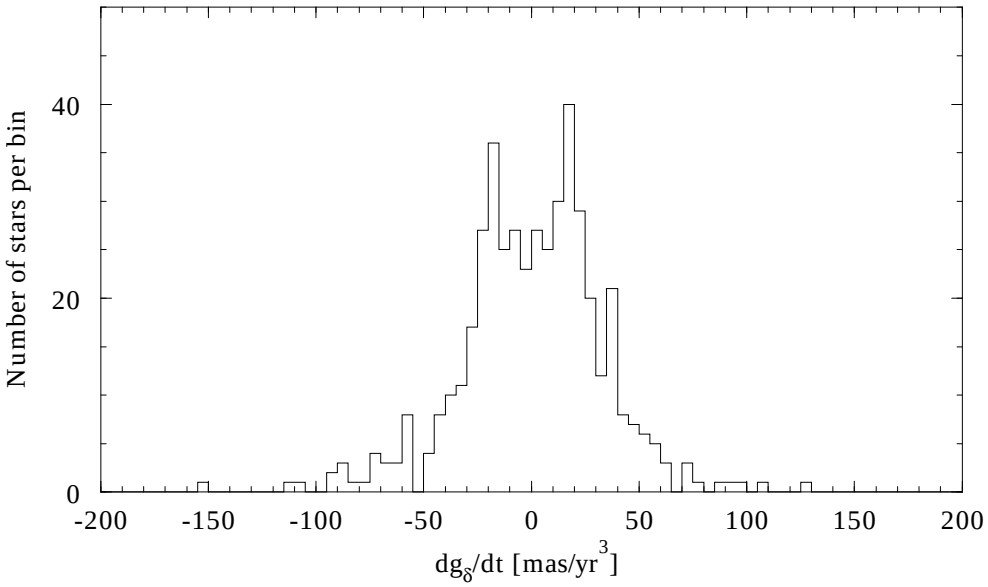

Figure 3.2.111. *Hipparcos Catalogue, DMSA/G, Field DG8: rate of change of g_δ at epoch J1991.25, $\dot{g}_\delta = d^2\mu_\delta/dt^2$ (bin size 5 mas/yr^3).*

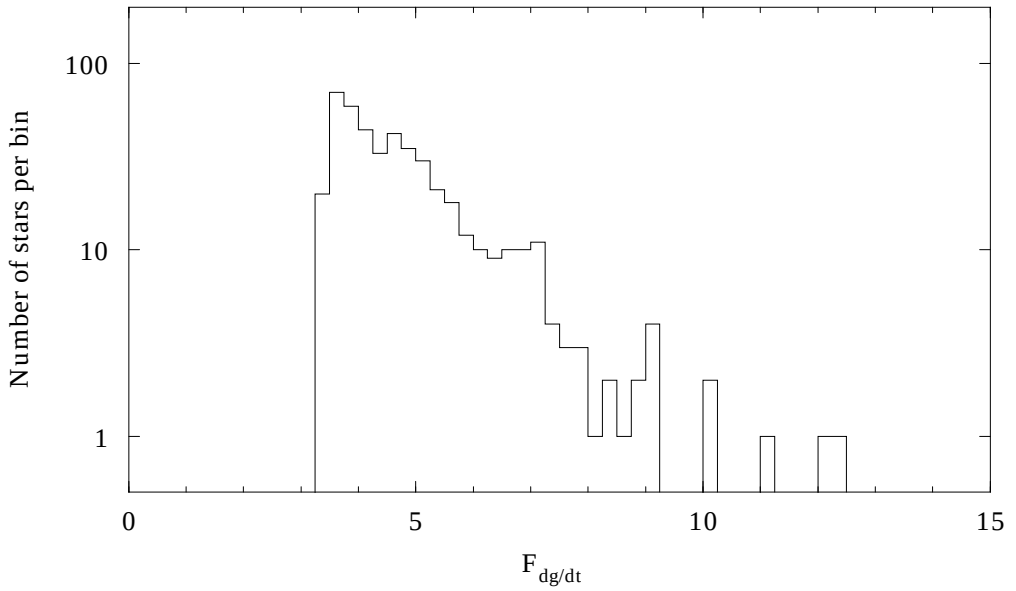

Figure 3.2.112. *Hipparcos Catalogue, DMSA/G, Field DG11: statistic for the significance of the rate of change of accelerations, $F_{\dot{g}}$ (bin size 0.25).*

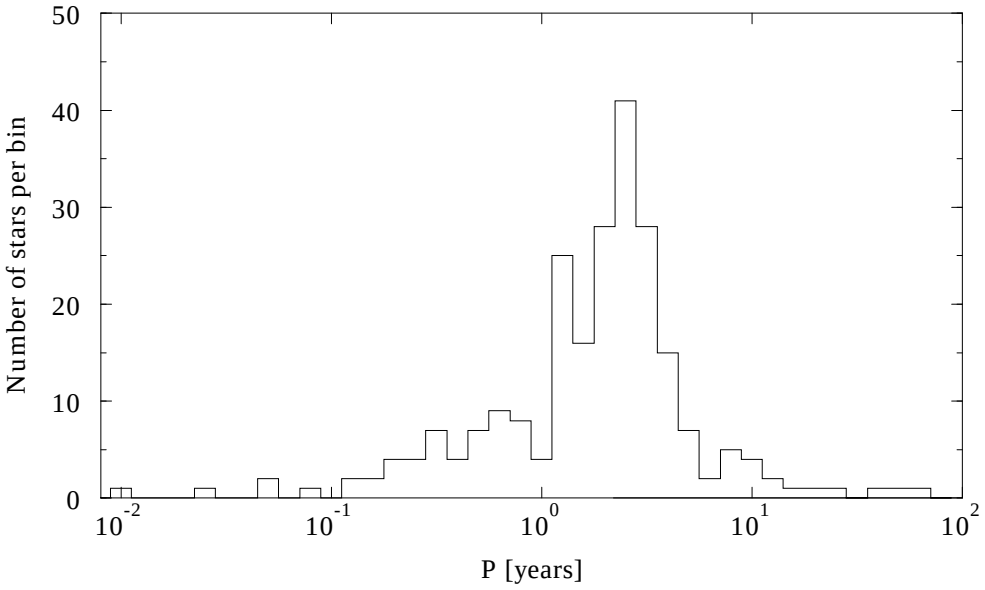

Figure 3.2.113. *Hipparcos Catalogue, DMSA/O, Field DO2: orbital period, P (bin size 0.1 dex).*

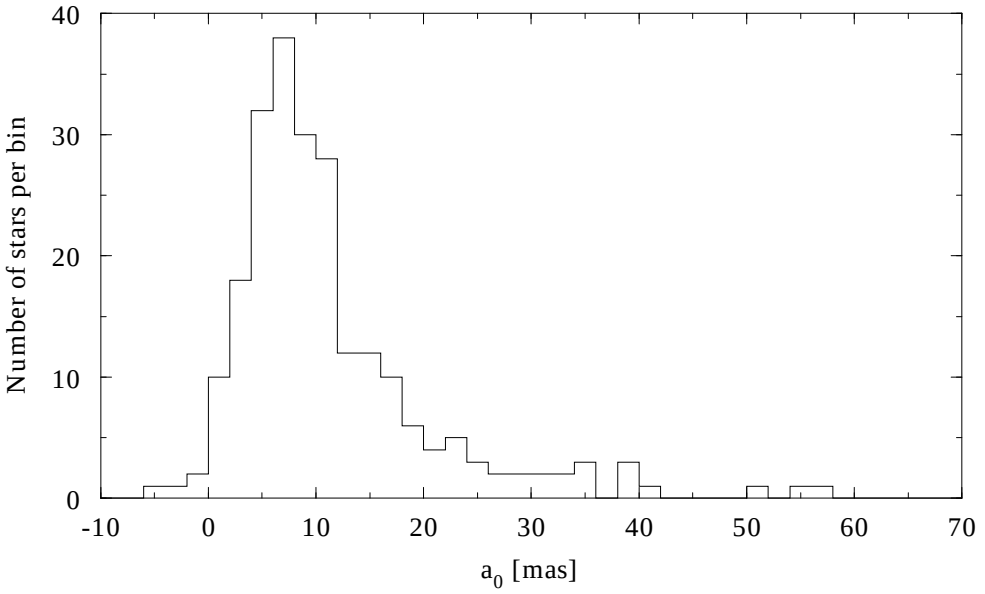

Figure 3.2.114. *Hipparcos Catalogue, DMSA/O, Field DO3: semi-major axis of the photocentre orbit, a_0 (bin size 2 mas).*

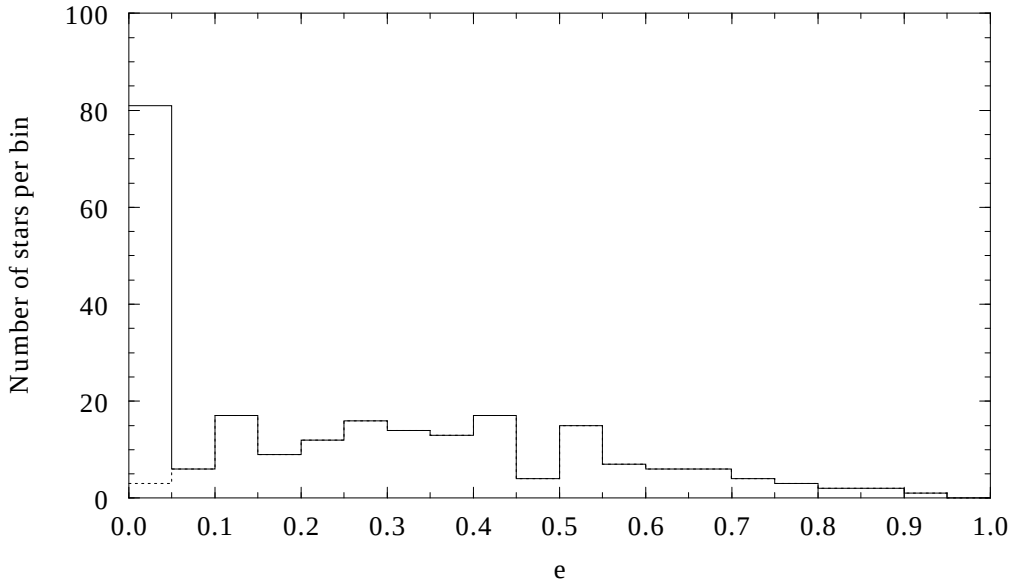

Figure 3.2.115. *Hipparcos Catalogue, DMSA/O, Field DO4: eccentricity, e (bin size 0.05). Solid line: all systems; dotted line: systems with assumed e = 0 and ω = 0 excluded.*

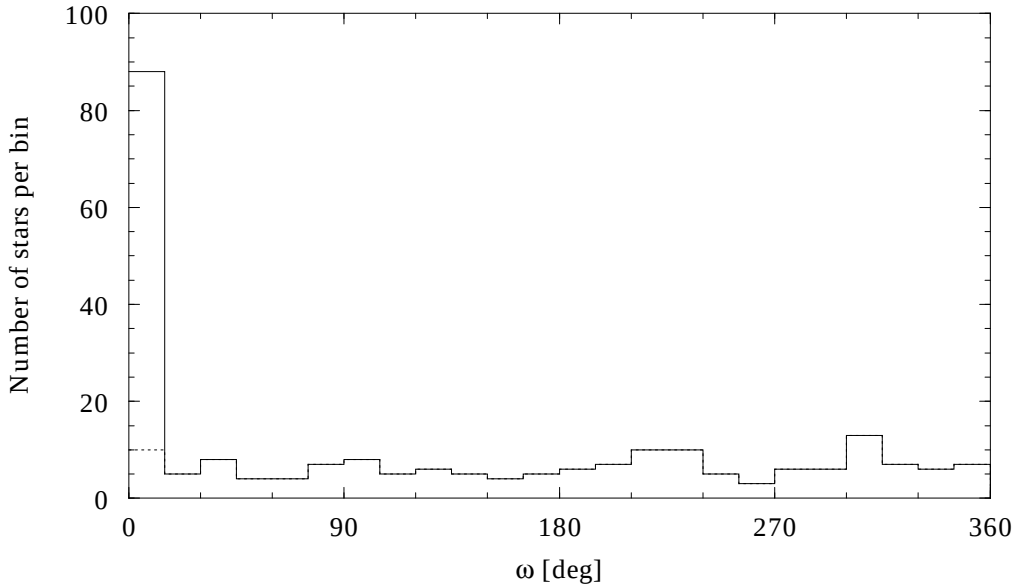

Figure 3.2.116. *Hipparcos Catalogue, DMSA/O, Field DO5: argument of periastron, ω (bin size 15°). Solid line: all systems; dotted line: systems with assumed e = 0 and ω = 0 excluded.*

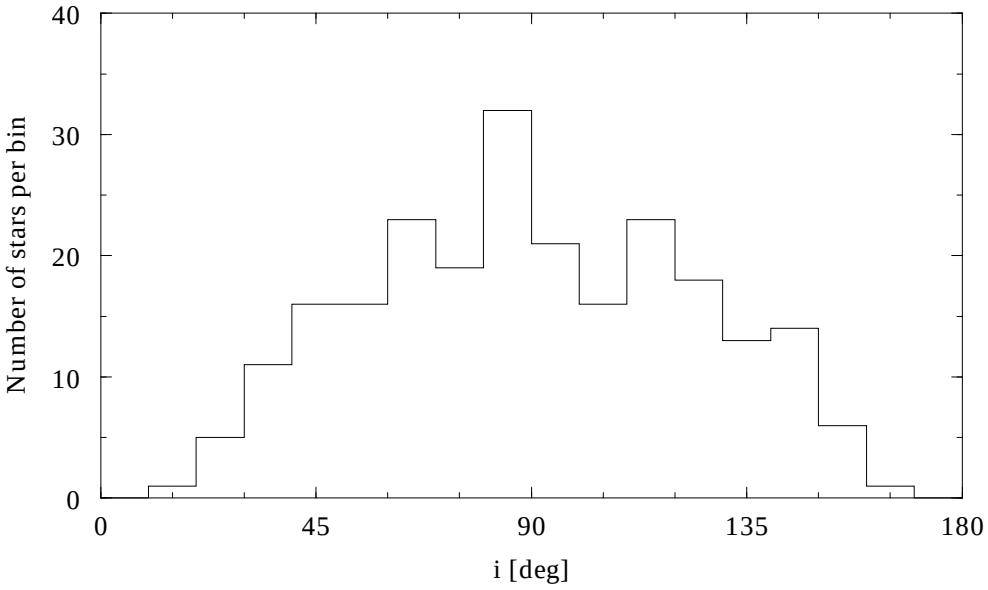

Figure 3.2.117. *Hipparcos Catalogue, DMSA/O, Field DO6: inclination, i (bin size 10°).*

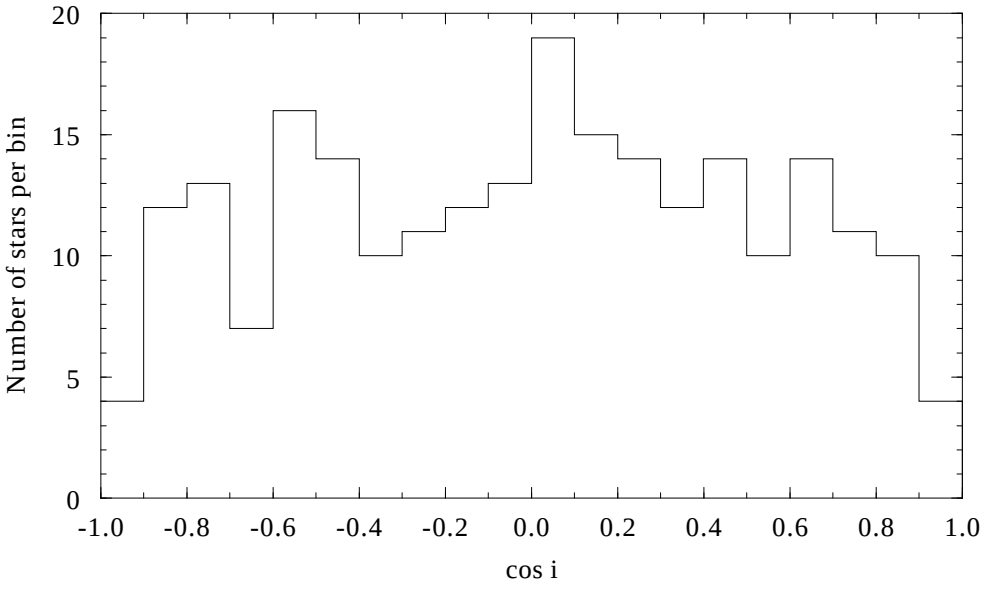

Figure 3.2.118. *Hipparcos Catalogue, DMSA/O, Field DO6: cosine of inclination, $\cos i$ (bin size 0.1).*

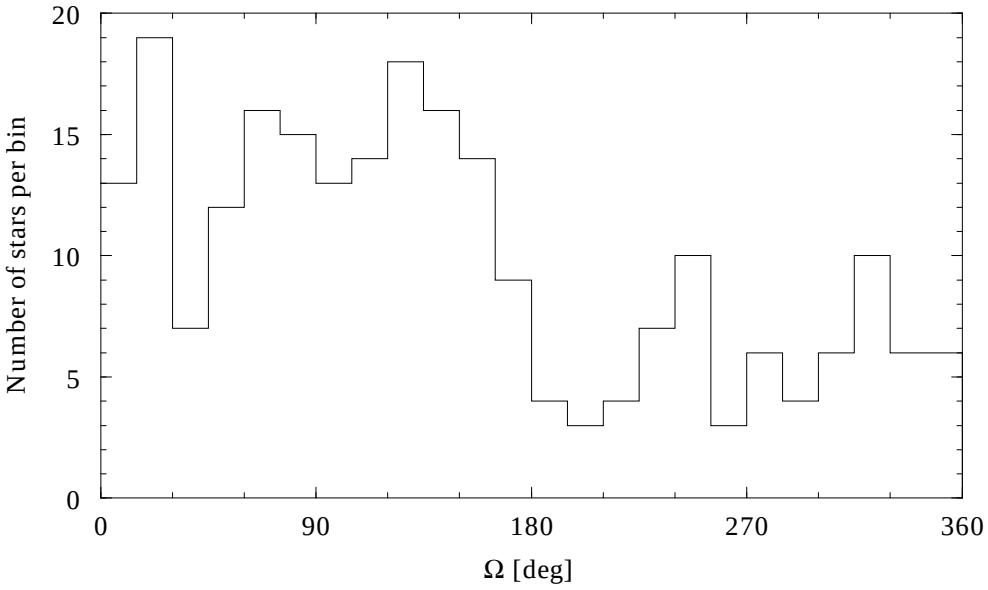

Figure 3.2.119. *Hipparcos Catalogue, DMSA/O, Field DO7: position angle of the node, Ω (bin size 15°).*

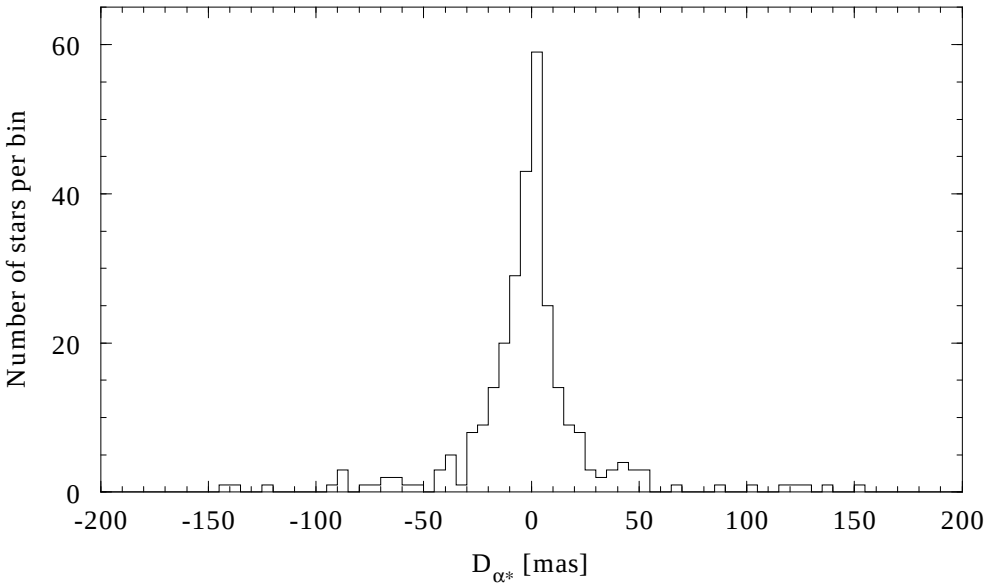

Figure 3.2.120. *Hipparcos Catalogue, DMSA/V, Field DV3: element of the variability-induced motion in right ascension, $D_{\alpha*}$ (bin size 5 mas).*

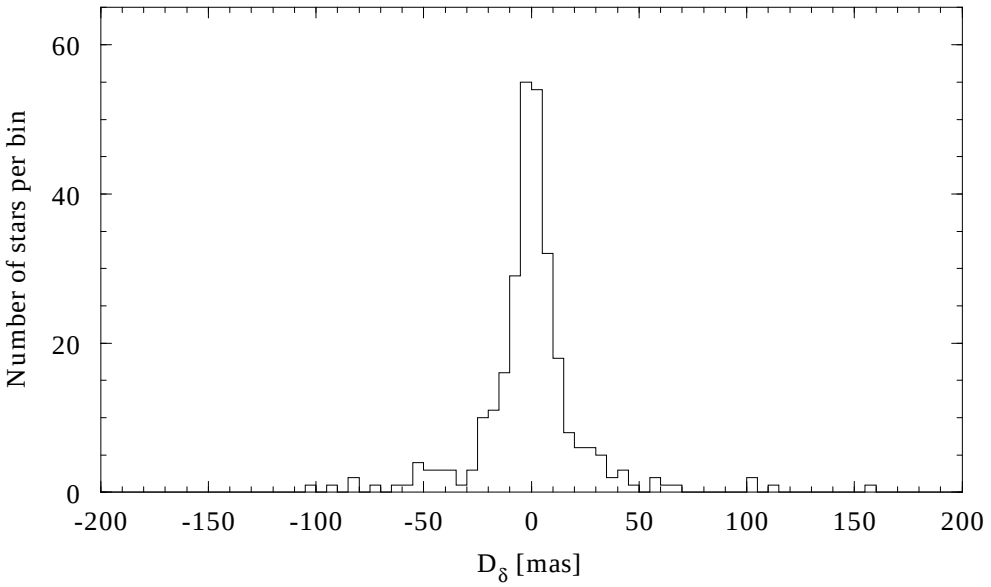

Figure 3.2.121. *Hipparcos Catalogue, DMSA/V, Field DV4: element of the variability-induced motion in declination, D_{δ} (bin size 5 mas).*

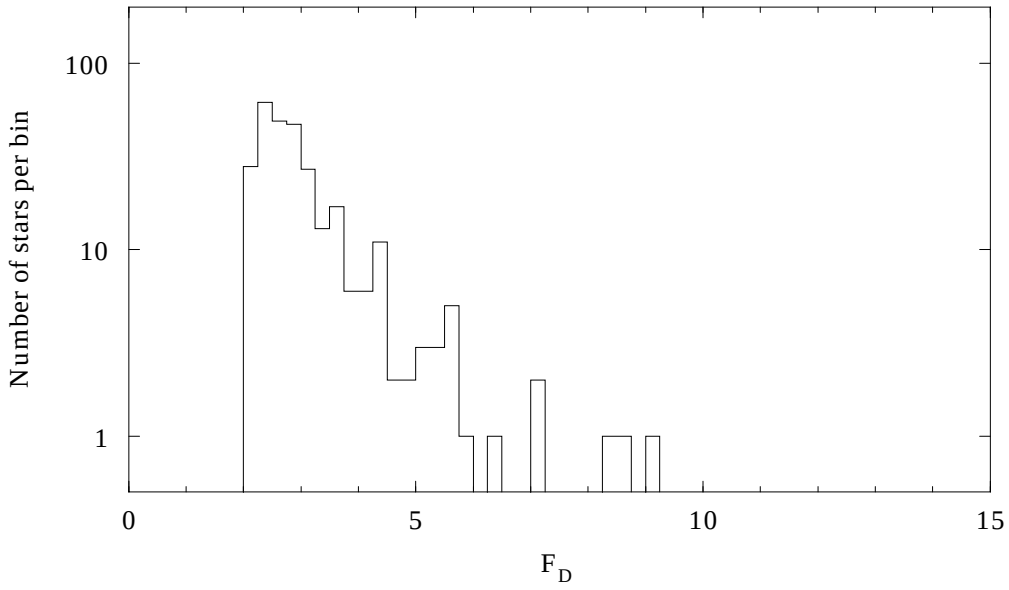

Figure 3.2.122. *Hipparcos Catalogue, DMSA/V, Field DV7: statistic for the significance of the variability-induced motion, F_D (bin size 0.25).*

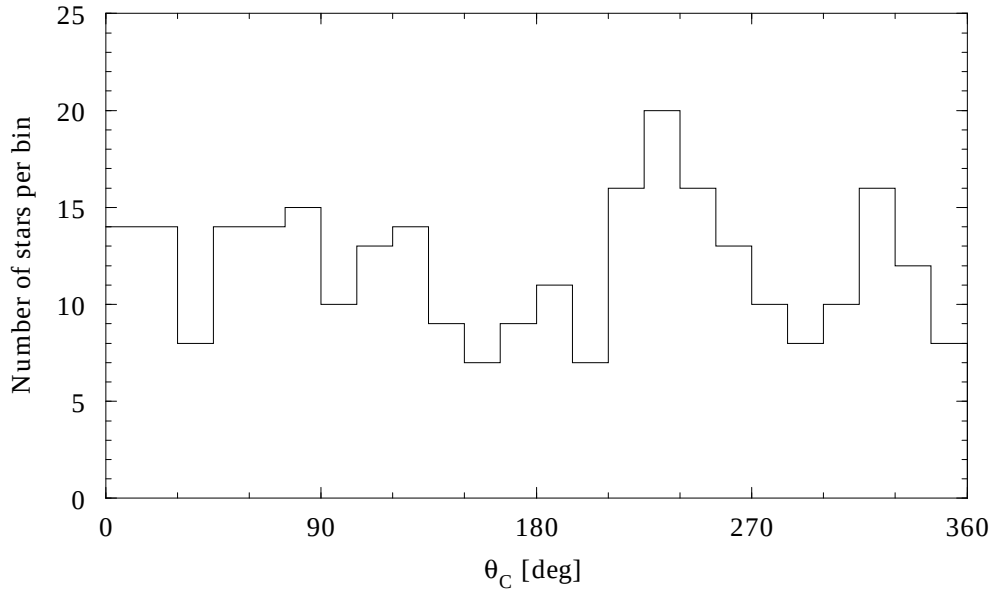

Figure 3.2.123. *Hipparcos Catalogue, DMSA/V, Field DV8: position angle of the constant component, θ_C (bin size 15°).*

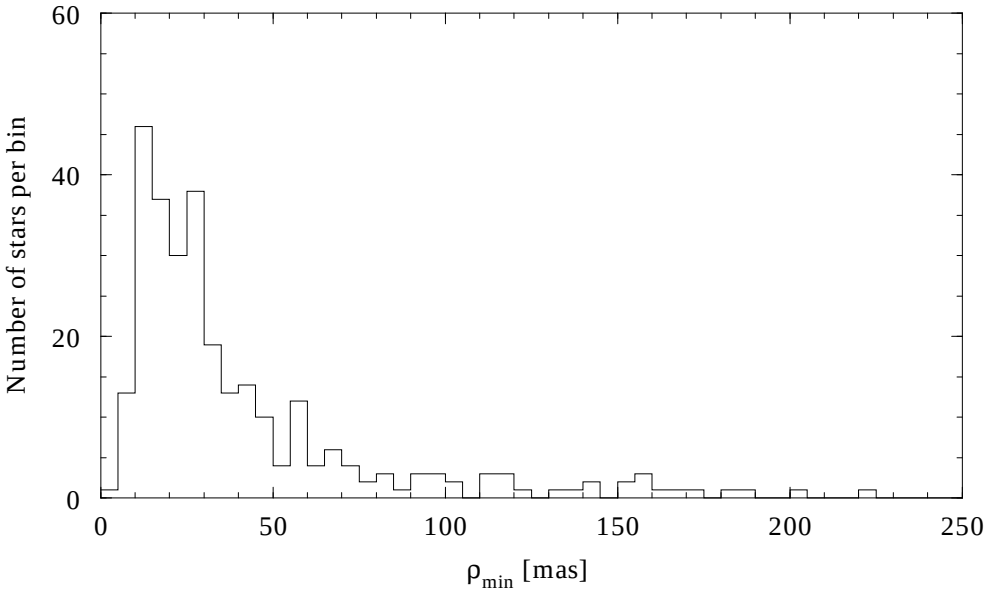

Figure 3.2.124. *Hipparcos Catalogue, DMSA/V, Field DV10: lower limit for the separation, ϱ_{min} (bin size 5 mas).*

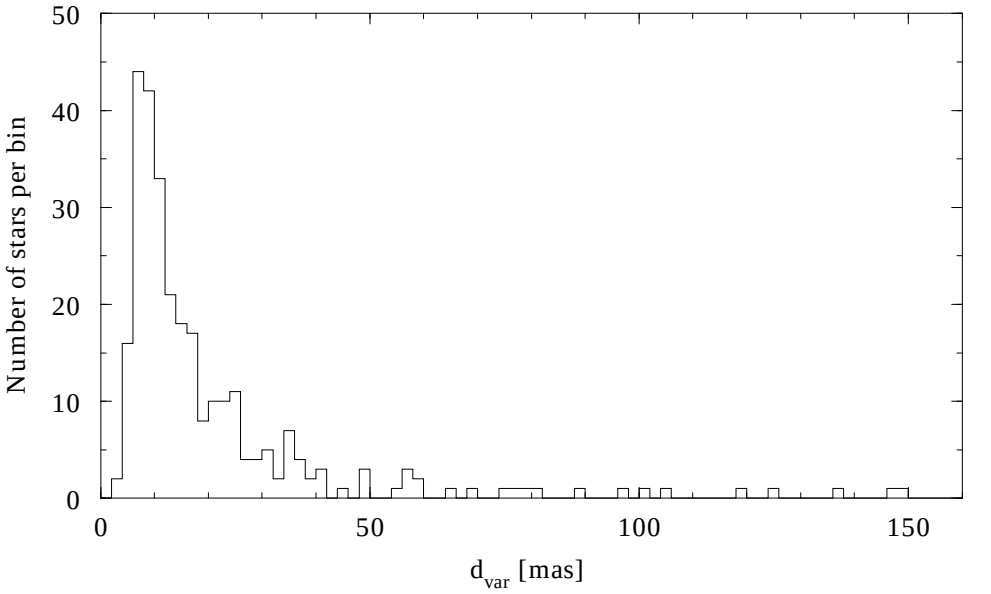

Figure 3.2.125. *Hipparcos Catalogue, DMSA/V, Field DV11: displacement of the photocentre between maximum and minimum luminosity, d_{var} (bin size 2 mas).*

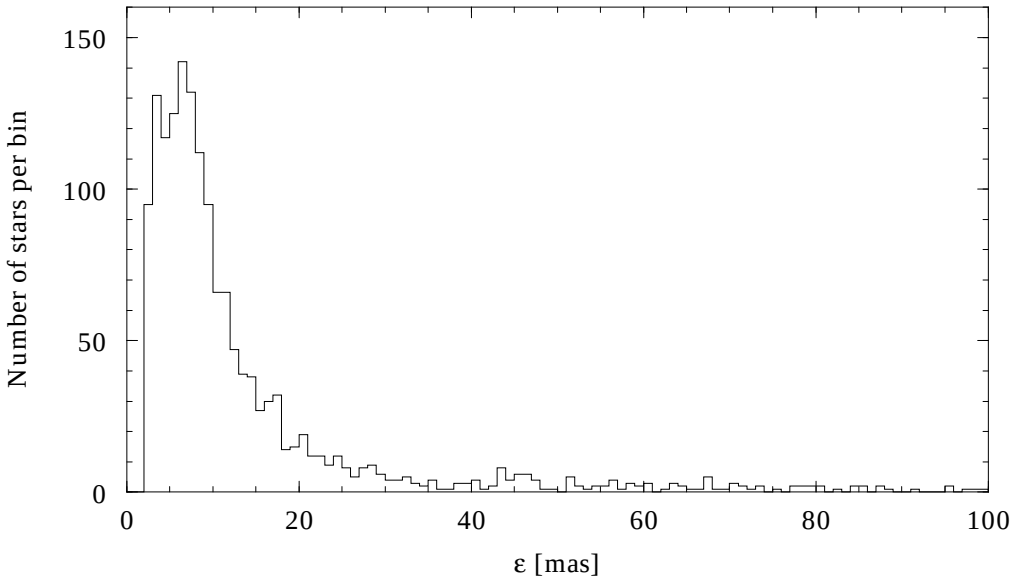

Figure 3.2.126. *Hipparcos Catalogue, DMSA/X, Field DX2: cosmic error, ϵ (bin size 1 mas).*

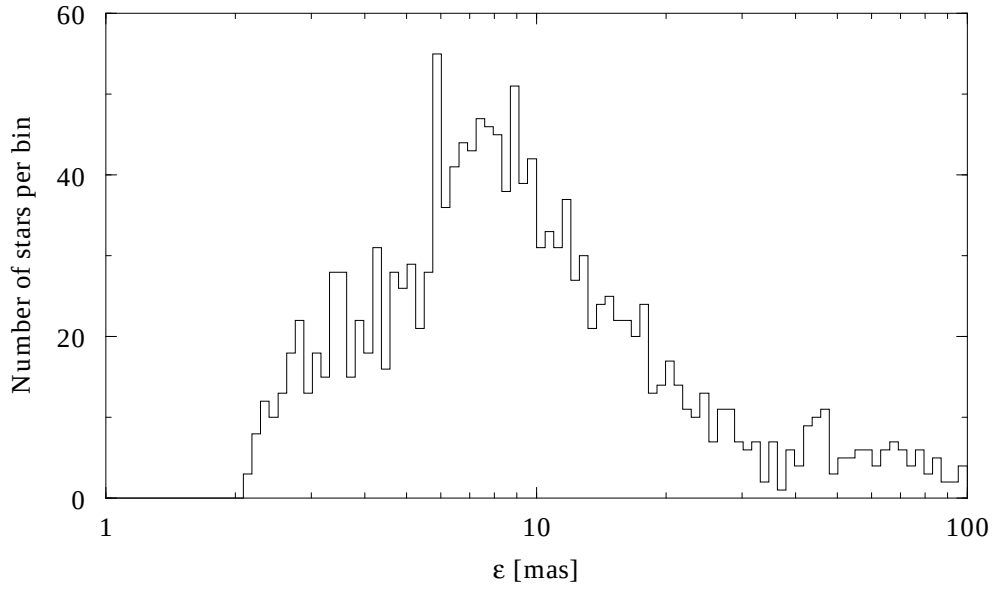

Figure 3.2.127. *Hipparcos Catalogue, DMSA/X, Field DX3: standard error in the cosmic error, σ_ϵ (bin size 0.02 dex).*

Section 3.3

Statistical Properties: The Tycho Catalogue

3.3. Statistical Properties: The Tycho Catalogue

In this section some statistical properties of the data in the Tycho Catalogue are presented. As in the previous section, for a number of parameters distributions over the entire sky, and frequency histograms are given.

Many features of the data shown here are similar to those from the Hipparcos Catalogue; for a general description, the reader is referred to Section 3.2. Here, in general, only differences will be emphasized. Such differences result mainly from two causes: (i) the Hipparcos measurements were based on the selection of stars in the Hipparcos Input Catalogue, and therefore cannot be considered a survey; its overall statistical properties are strictly properties of the selection, and not those of a random, or complete, sample of stars. On the other hand, the entries in the Tycho Catalogue come much closer to a survey down to a certain apparent magnitude, although the limiting magnitude depends somewhat on the location on the sky (cf. Volume 4, Chapter 16); (ii) the difference in measurement geometry: while Hipparcos performed one-dimensional abscissa measurements in the direction along the scanning great circle, Tycho added information about the perpendicular direction, albeit with lower weight.

Certain of the results shown in this section are also given in Chapter 16 of Volume 4, and discussed in more detail there.

3.3.1. Density of Observed Stars and Number of Observations

The density of observed stars in the Tycho Catalogue is shown in Figure 3.3.1. Comparison with the corresponding figure for the Hipparcos Catalogue illustrates strikingly the difference in character of the two catalogues. For example, the emphasis on the Orion region present in the Hipparcos Catalogue is not present in the Tycho Catalogue. On the other hand, the difference in star density between the galactic equator and pole regions, and the low star densities in some regions (e.g. the Ophiuchus area), are emphasized in the Tycho Catalogue.

Figure 3.3.3 gives the distribution of the median number number of astrometric observations per star. This figure is very similar to that for the Hipparcos Catalogue. The features related to the sun-pointing periods visible in the Hipparcos case are absent here, since the measurements made during those periods were not used in the construction of the Tycho Catalogue. Figure 3.3.4 shows the frequency distribution of this number.

3.3.2. Standard Errors and Correlations

Sky distributions of the standard errors of the five astrometric parameters are given in Figures 3.3.5, 3.3.9, 3.3.13, 3.3.17, and 3.3.21. Frequency distributions of these standard errors are shown in Figures 3.3.6, 3.3.10, 3.3.14, 3.3.18, and 3.3.22. The

dependence of the standard errors on ecliptic latitude and on the V_T magnitude is shown in Figures 3.3.7, 3.3.11, 3.3.15, 3.3.19, and 3.3.23, and in Figures 3.3.8, 3.3.12, 3.3.16, 3.3.20, and 3.3.24, respectively. It is interesting to note the differences between the ecliptic latitude dependence shown here and the corresponding dependencies for the Hipparcos Catalogue. The overall shape of the curves is similar, but details differ: for example, the marked minimum near $\beta \sim \pm 47°$ is present for all five parameters, whereas in the Hipparcos case it was only visible for the longitudinal ones. This illustrates the difference in measurement geometry between the two cases. Also, the curve for σ_π is much smoother for the Tycho than for the Hipparcos case, probably for the same reason.

The astrometric correlations are distributed over the sky as shown in Figures 3.3.25 to 3.3.34. For a general discussion on these correlations, see Section 3.2.3. Frequency histograms for the correlations are combined in Figure 3.3.35.

Differences with respect to the Hipparcos Catalogue are present in the histograms. There is a marked asymmetry in the correlations between $\alpha*$ and $\mu_{\alpha*}$, and δ and μ_δ. These asymmetries indicate that the mean effective epoch of the Tycho Catalogue is somewhat later than that of the Hipparcos Catalogue, in accordance with Equations 1.2.6 and 1.2.8, due to a different weighting of the two types of observation towards the end of the mission. On the other hand, the asymmetry in the correlation between declination and parallax present in the Hipparcos Catalogue is much smaller in the case of the Tycho Catalogue, due to the measurement geometry of Tycho. There is an additional magnitude-related effect: for stars fainter than $V_T = 10$ mag, there is no asymmetry; for brighter stars, there is an effect, but always smaller than in the case of the Hipparcos Catalogue measurements.

Figures 3.3.36 and 3.3.37 give the results for the goodness-of-fit indicator F2. The distribution over the sky turns out to be much less uniform than that shown for the Hipparcos Catalogue. Note that F2 was not considered a reliable parameter for use in the construction of the Tycho Catalogue, and the values should be used with great care (see Section 16.2 of Volume 4).

3.3.3. Photometric Data

Results for the B_T and V_T magnitudes and their standard errors are shown in Figures 3.3.38 to 3.3.43. The sky distributions of the median B_T and V_T magnitudes show a strong relationship with the scanning pattern, but the heavily scanned regions at $\beta \sim \pm 47°$ are not particularly visible here.

The sky distribution of the median (Johnson) colour index $B - V$ is presented in Figure 3.3.44. Differences with the corresponding figure for the Hipparcos Catalogue again show clearly the marked difference in character of the two catalogues. The present figure represents the statistical properties of the galactic solar neighbourhood to 100–250 pc. North of the galactic centre the dust complexes in Ophiuchus and Scorpius cause red and reddened stars to dominate. In the galactic plane, intrinsically brighter stars are over-represented, as expected for a magnitude-limited catalogue, leading to extra early-type stars. This is particularly true in the region $180° < l < 270°$ where there is less interstellar absorption. The emphasis of the Hipparcos Catalogue on the Orion region and the galactic meridians $l = 0°$ and $l = 180°$ is absent, as expected.

The frequency histogram, Figure 3.3.45, of the $B - V$ colour index shows two maxima, the one near $B - V = 0.5$ mag corresponding to the high concentration of stars near the turn-off point in the Hertzsprung-Russell diagram, and the other near $B - V = 1$ mag being due to the G8–K0 giants in the core helium-burning phase. The two other peaks present in the corresponding figure for the Hipparcos Catalogue were due to selection effects of that catalogue, and are therefore much less prominent here.

Figure 3.3.46 shows the distribution of the standard error of the $B - V$ colour index. Figure 3.3.47 gives the distribution for the scatter s in the V_T magnitudes.

Figure 3.3.1. *Tycho Catalogue: number of observed stars per square degree, in galactic coordinates (cell size $2^\circ \times 2^\circ$).*

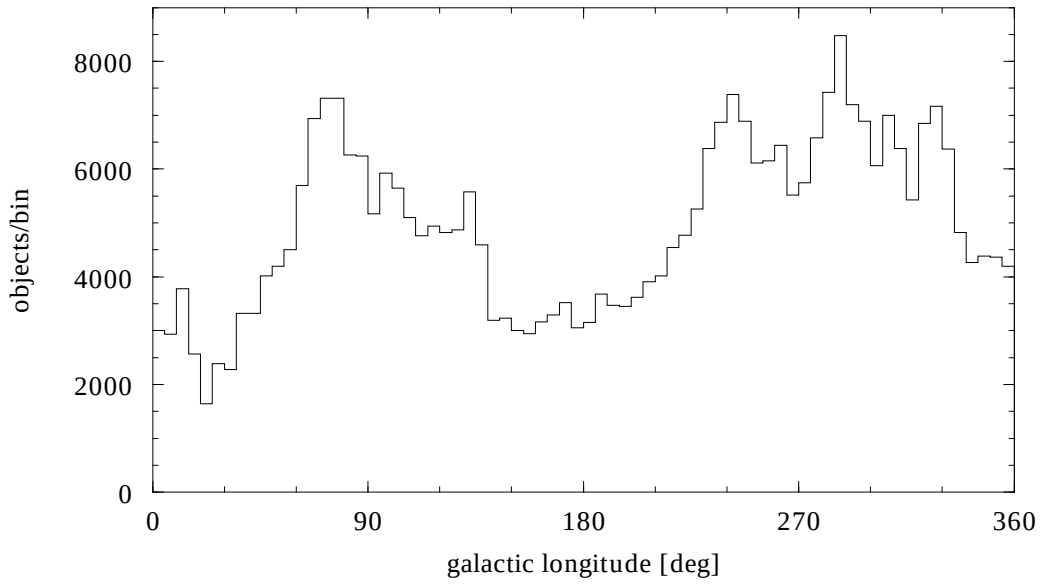

Figure 3.3.2. *Tycho Catalogue: distribution of number of stars near the galactic equator ($b < 10^\circ$, bin size 5°).*

Figure 3.3.3. *Tycho Catalogue: mean number of observations per star, in ecliptic coordinates (cell size $3° \times 3°$).*

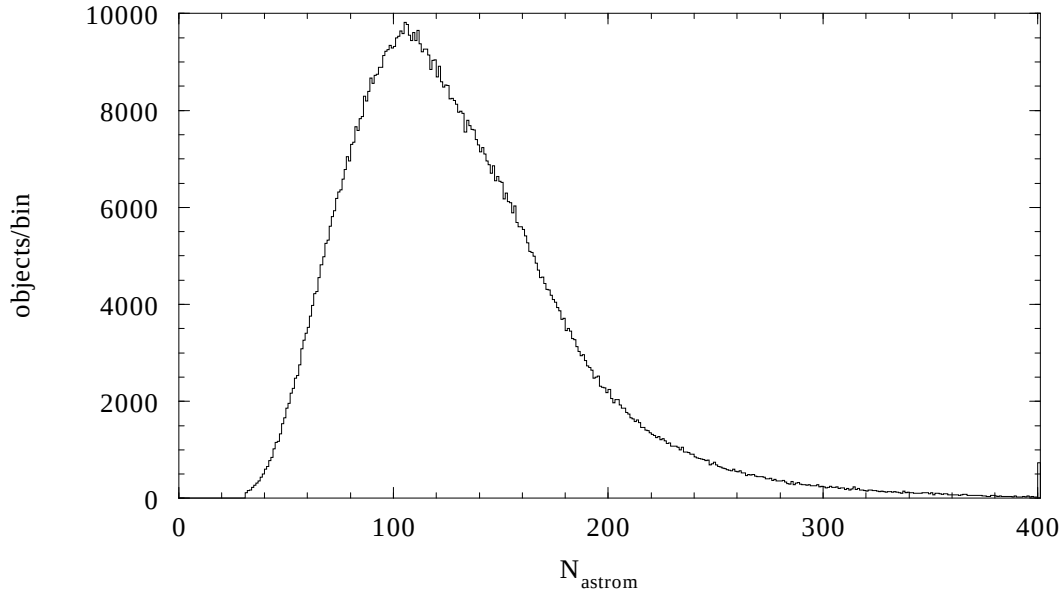

Figure 3.3.4. *Tycho Catalogue, Field T29: number of transits retained in the astrometric adjustment (bin size 1). The rightmost bin contains all values above 400.*

Figure 3.3.5. *Tycho Catalogue, Field T14: median standard error of $\alpha*$, in ecliptic coordinates (cell size $3^\circ \times 3^\circ$).*

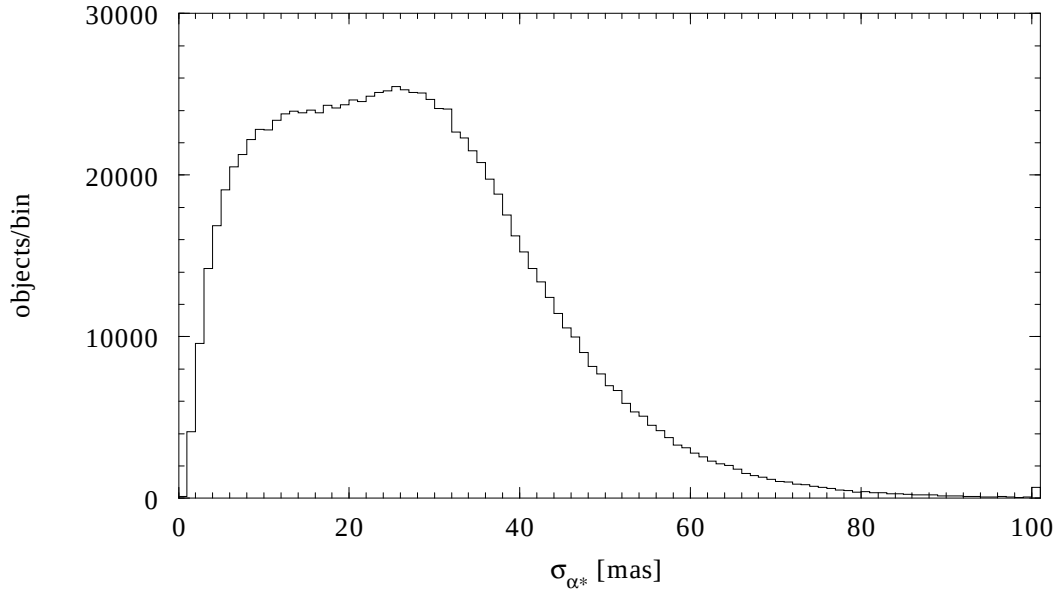

Figure 3.3.6. *Tycho Catalogue, Field T14: standard error of $\alpha*$ (bin size 1 mas). The rightmost bin contains all values above 100 mas.*

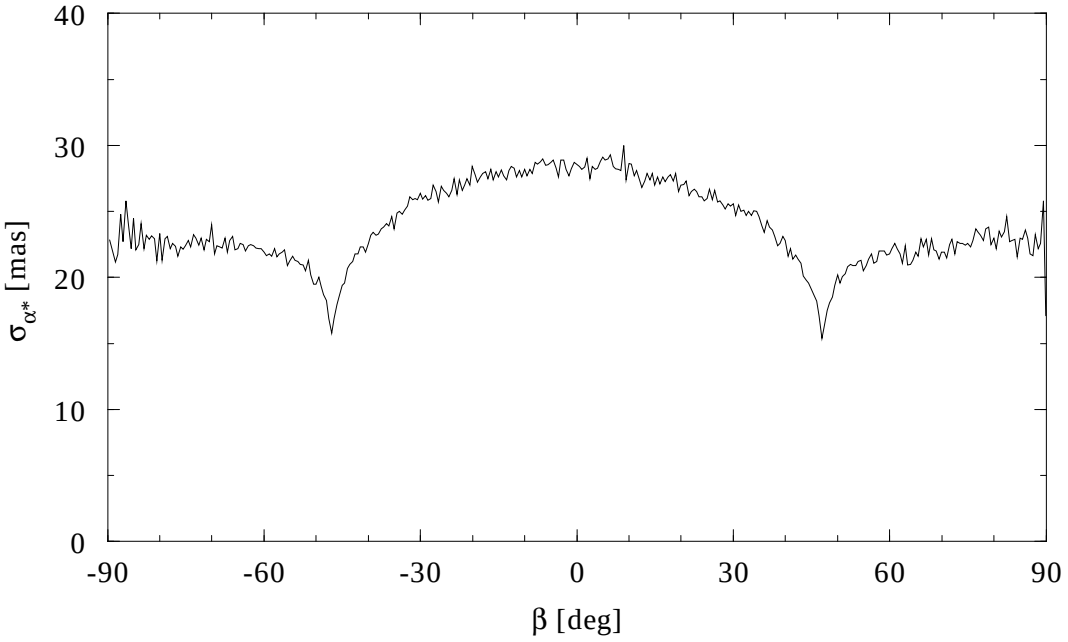

Figure 3.3.7. *Tycho Catalogue, Field T14: median standard error of $\alpha*$ versus ecliptic latitude (bin size 0.5°).*

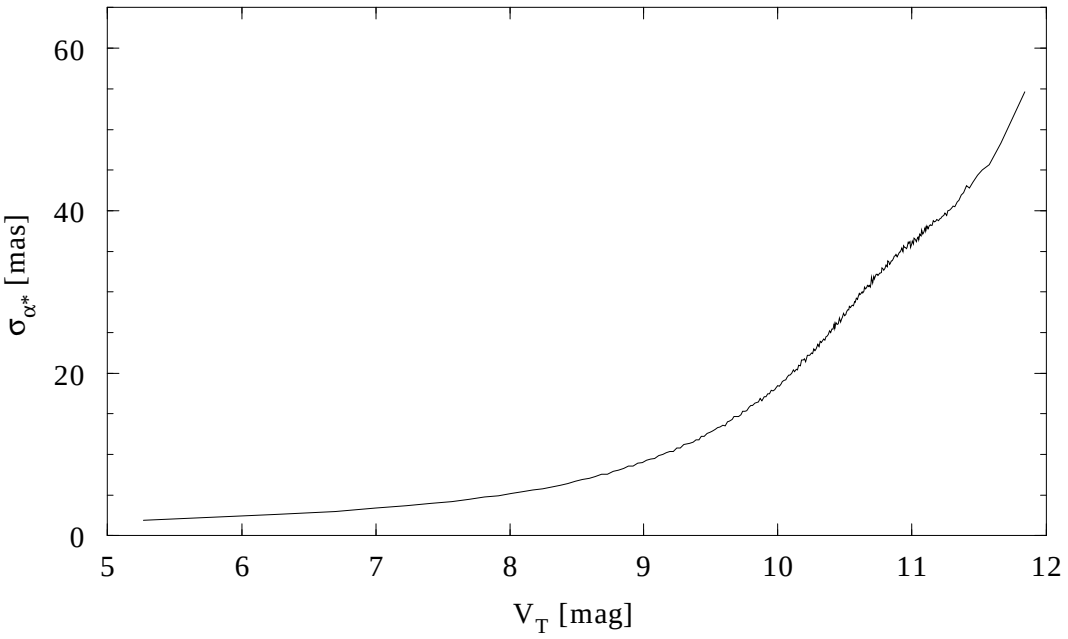

Figure 3.3.8. *Tycho Catalogue, Field T14: median standard error of $\alpha*$ versus V_T (bin size 0.05 mag).*

Figure 3.3.9. *Tycho Catalogue, Field T15: median standard error of δ, in ecliptic coordinates (cell size $3^\circ \times 3^\circ$).*

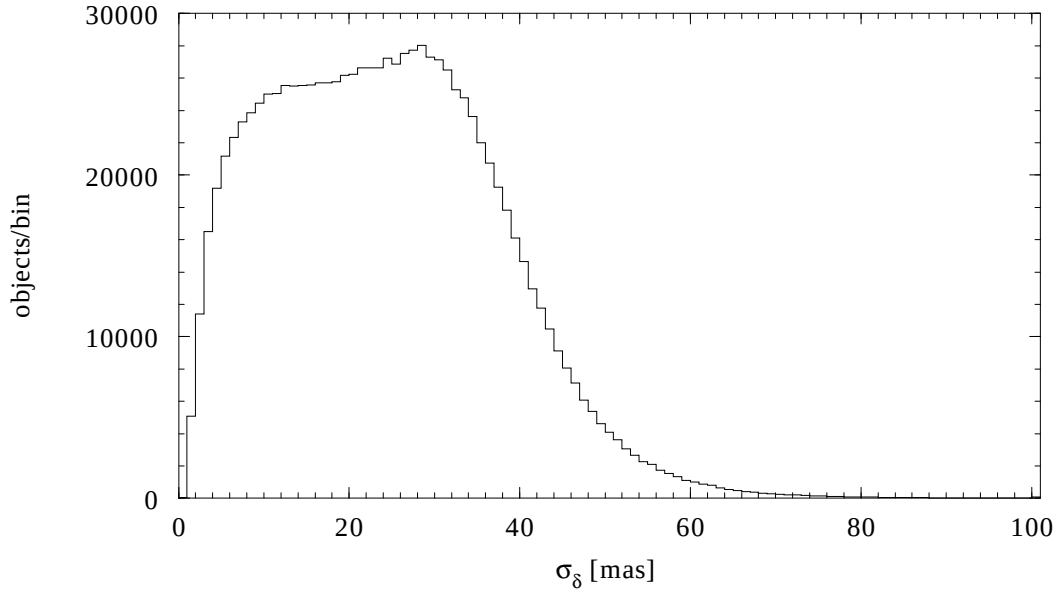

Figure 3.3.10. *Tycho Catalogue, Field T15: standard error of δ (bin size 1 mas). The rightmost bin contains all values above 100 mas.*

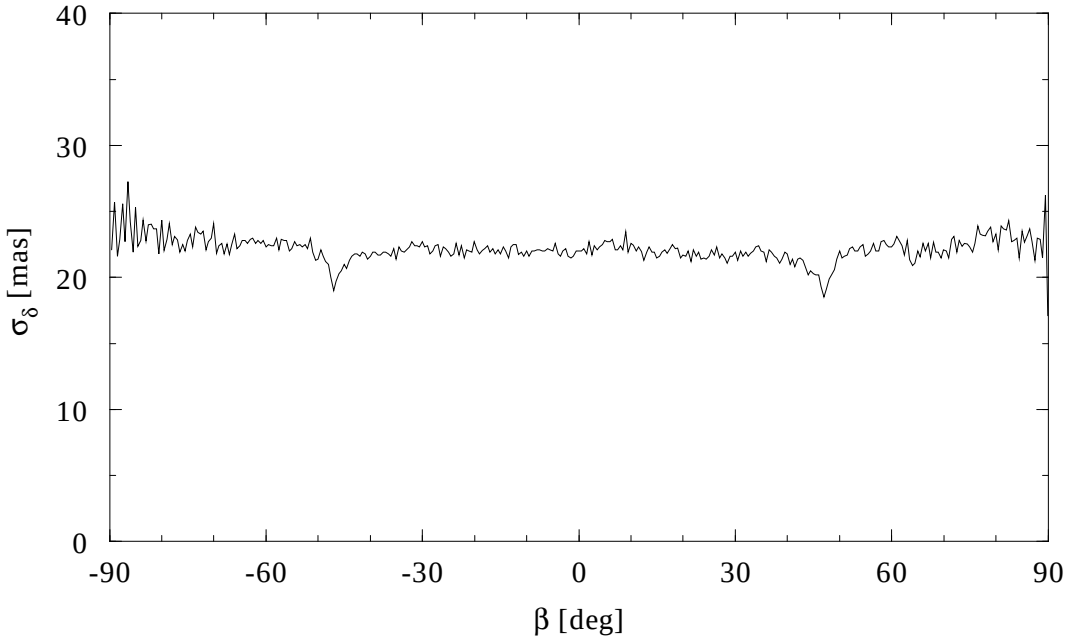

Figure 3.3.11. *Tycho Catalogue, Field T15: median standard error of δ versus ecliptic latitude (bin size 0.5°).*

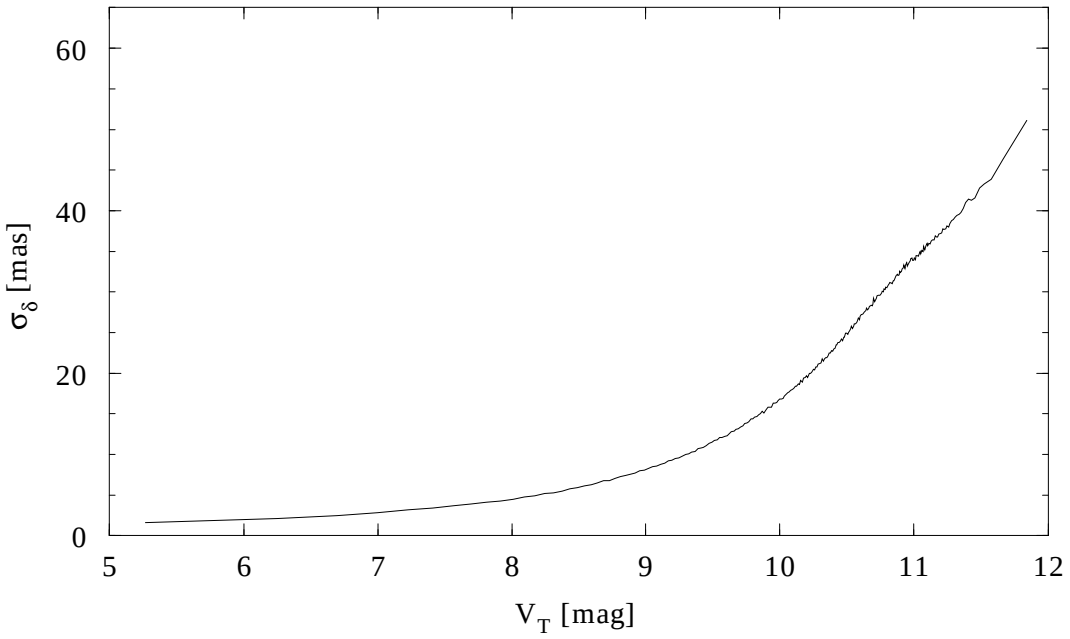

Figure 3.3.12. *Tycho Catalogue, Field T15: median standard error of δ versus V_T (bin size 0.05 mag).*

Figure 3.3.13. *Tycho Catalogue, Field T16: median standard error of π, in ecliptic coordinates (cell size $3^\circ \times 3^\circ$).*

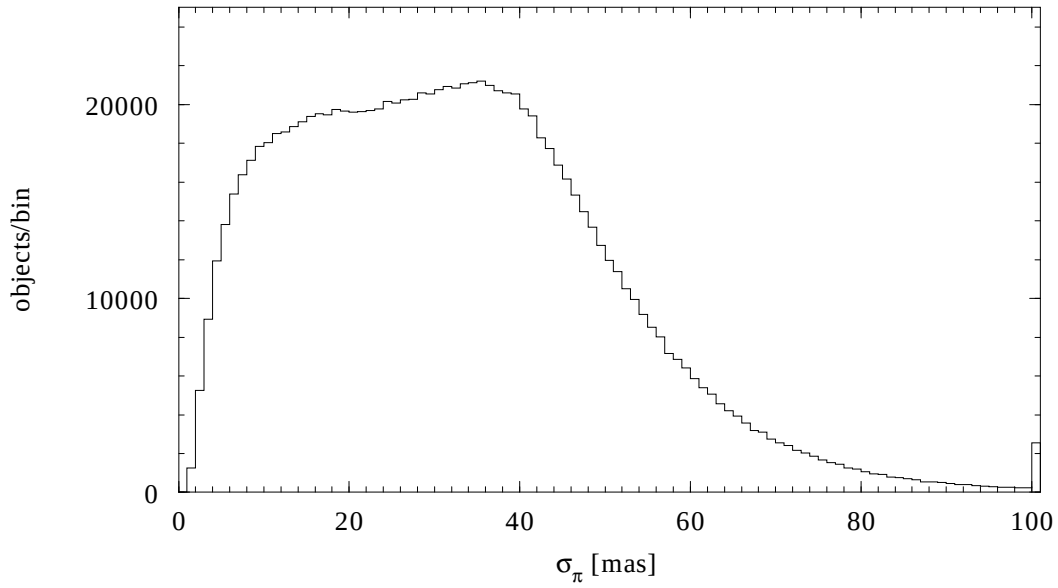

Figure 3.3.14. *Tycho Catalogue, Field T16: standard error of π (bin size 1 mas). The rightmost bin contains all values above 100 mas.*

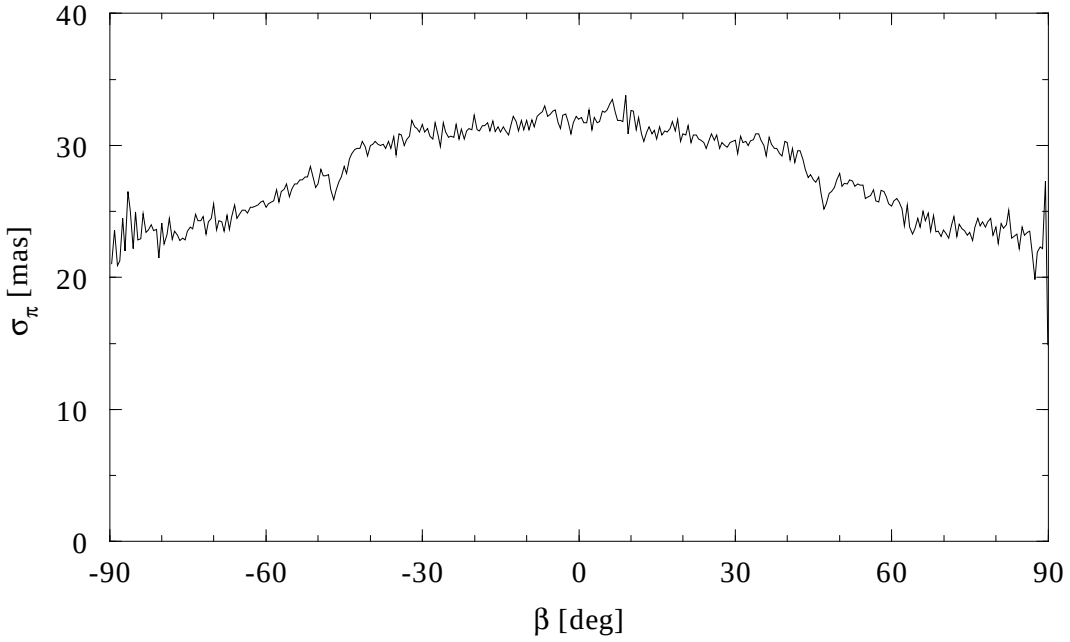

Figure 3.3.15. *Tycho Catalogue, Field T16: median standard error of π versus ecliptic latitude (bin size 0.5°).*

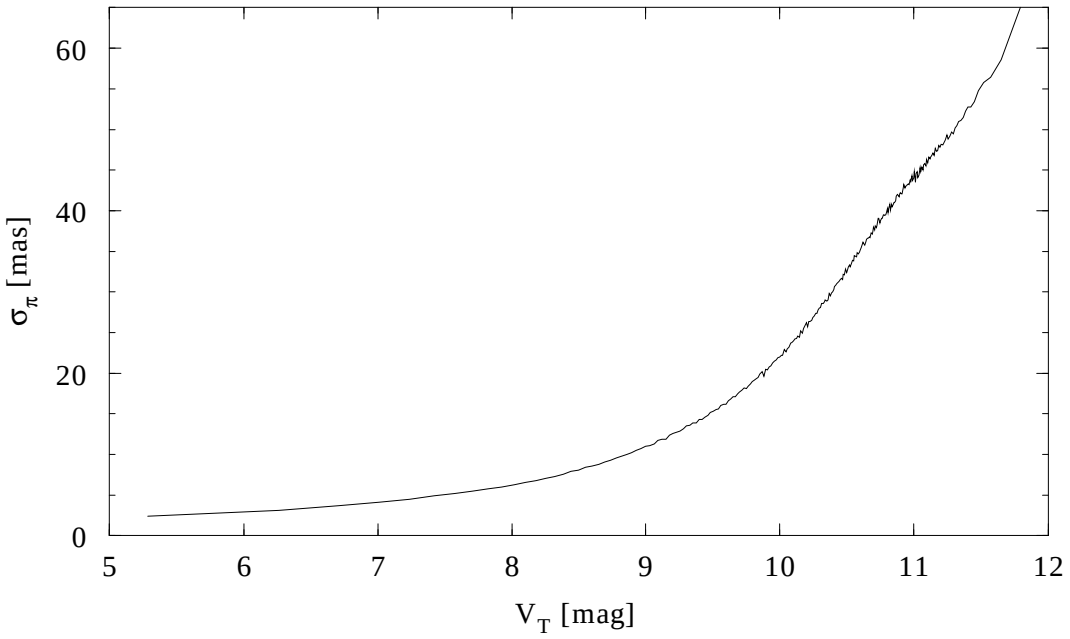

Figure 3.3.16. *Tycho Catalogue, Field T16: median standard error of π versus V_T (bin size 0.05 mag).*

Figure 3.3.17. *Tycho Catalogue, Field T17: median standard error of $\mu_{\alpha*}$, in ecliptic coordinates (cell size $3^\circ \times 3^\circ$).*

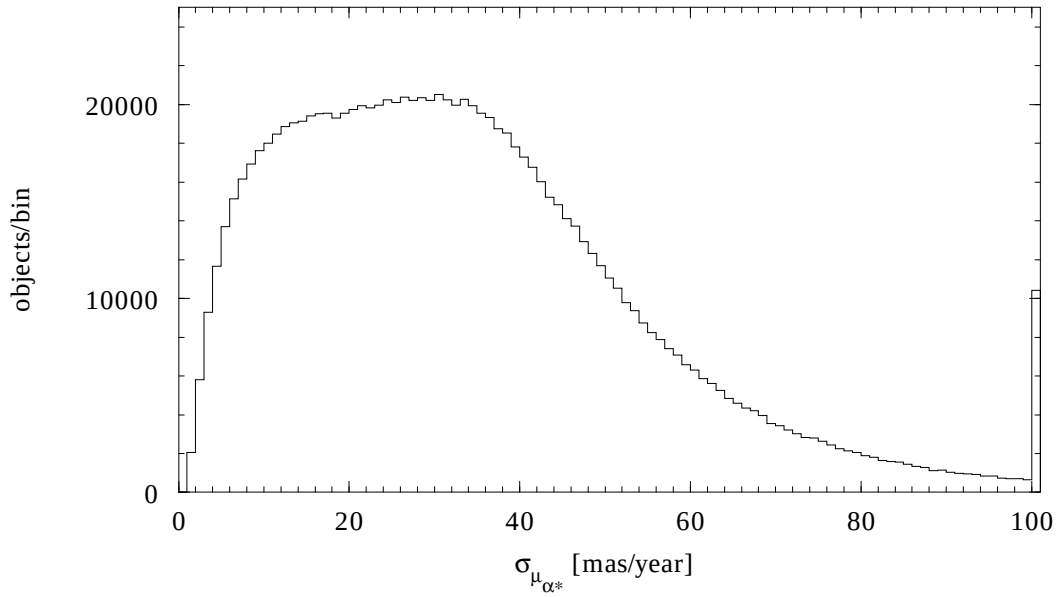

Figure 3.3.18. *Tycho Catalogue, Field T17: standard error of $\mu_{\alpha*}$ (bin size 1 mas/year). The rightmost bin contains all values above 100 mas/year.*

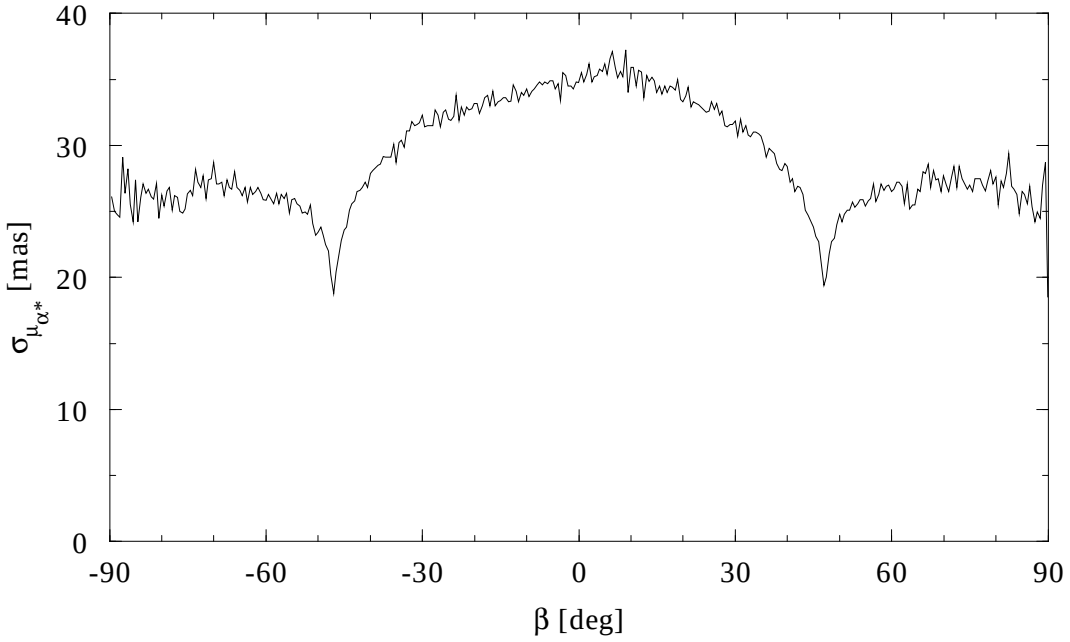

Figure 3.3.19. *Tycho Catalogue, Field T17: median standard error of $\mu_{\alpha *}$ versus ecliptic latitude (bin size 0.5°).*

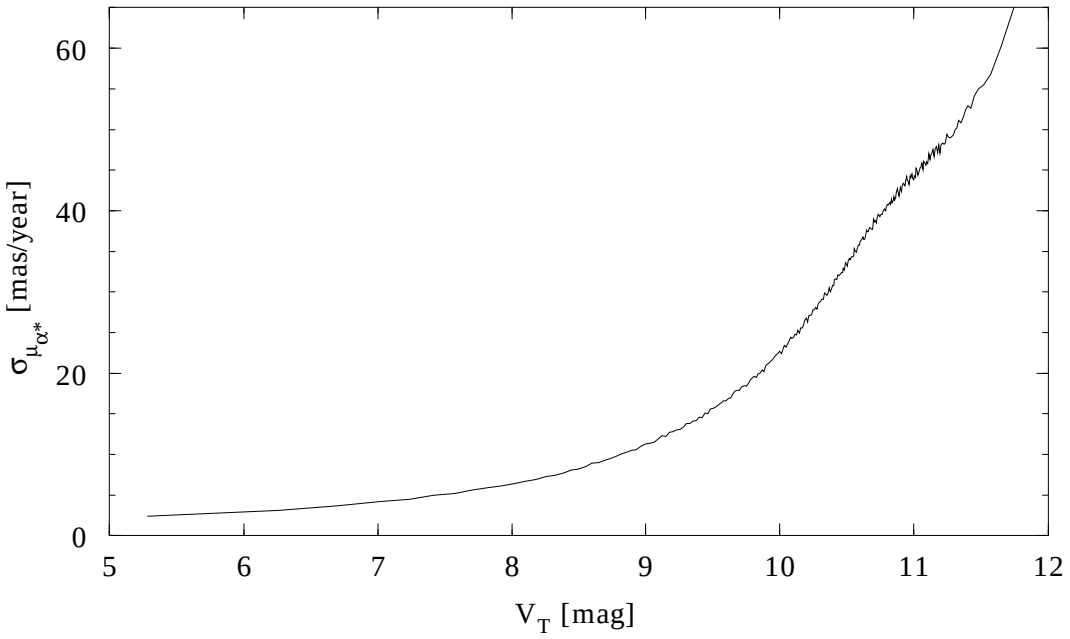

Figure 3.3.20. *Tycho Catalogue, Field T17: median standard error of $\mu_{\alpha *}$ versus V_T (bin size 0.05 mag).*

Figure 3.3.21. *Tycho Catalogue, Field T18: median standard error of μ_δ, in ecliptic coordinates (cell size $3^\circ \times 3^\circ$).*

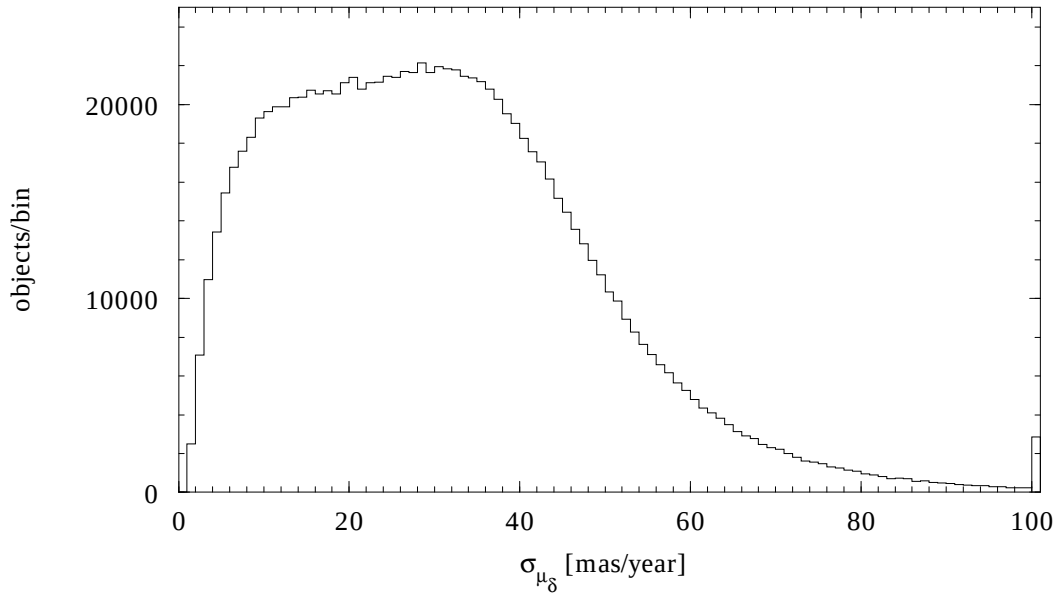

Figure 3.3.22. *Tycho Catalogue, Field T18: standard error of μ_δ (bin size 1 mas/year). The rightmost bin contains all values above 100 mas/year.*

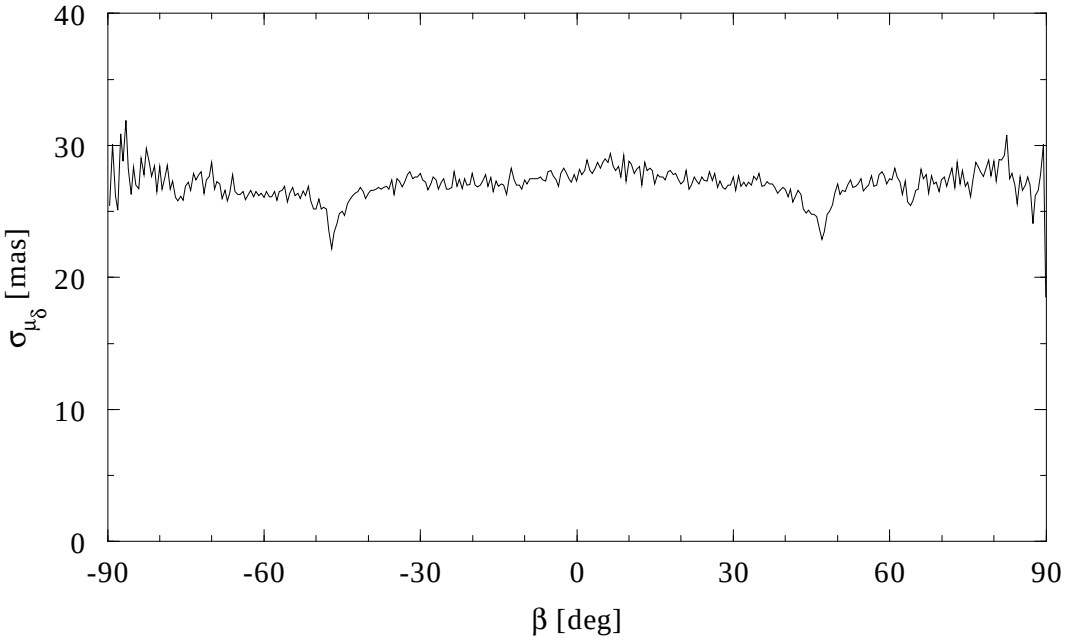

Figure 3.3.23. *Tycho Catalogue, Field T18: median standard error of μ_δ versus ecliptic latitude (bin size 0.5°).*

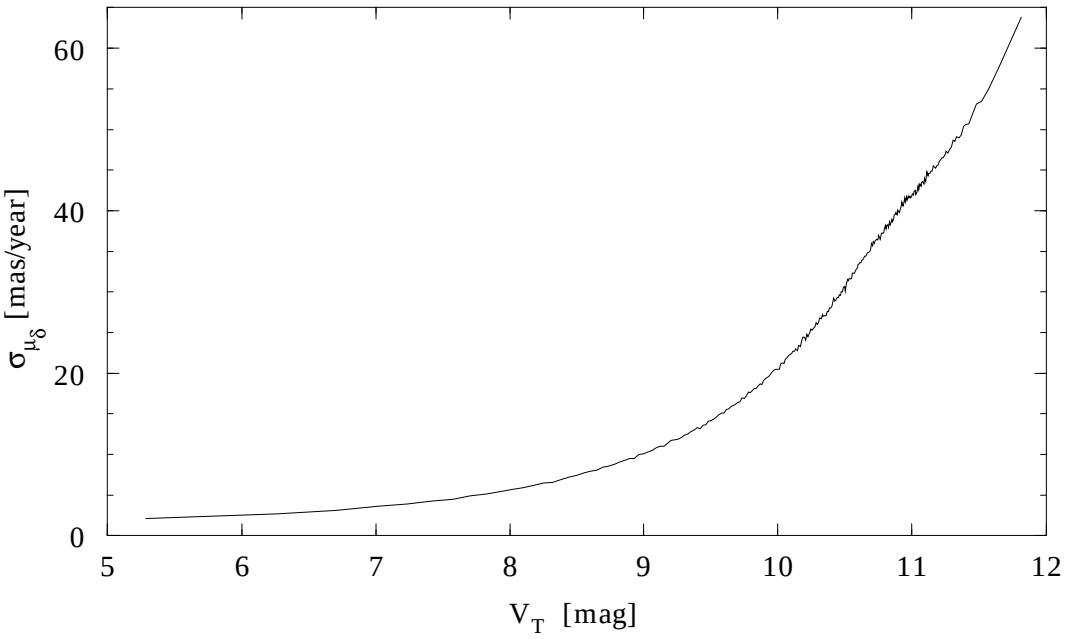

Figure 3.3.24. *Tycho Catalogue, Field T18: median standard error of μ_δ versus V_T (bin size 0.05 mag).*

Figure 3.3.25. *Tycho Catalogue, Field T19: median correlation between $\alpha*$ and δ in equatorial coordinates (cell size $2^\circ \times 2^\circ$).*

Figure 3.3.26. *Tycho Catalogue, Field T20: median correlation between $\alpha*$ and π in equatorial coordinates (cell size $2^\circ \times 2^\circ$).*

Figure 3.3.27. *Tycho Catalogue, Field T21: median correlation between δ and π in equatorial coordinates (cell size $2^\circ \times 2^\circ$).*

Figure 3.3.28. *Tycho Catalogue, Field T22: median correlation between $\alpha*$ and $\mu_{\alpha*}$ in equatorial coordinates (cell size $2^\circ \times 2^\circ$).*

Figure 3.3.29. *Tycho Catalogue, Field T23: median correlation between δ and $\mu_{\alpha *}$ in equatorial coordinates (cell size $2^\circ \times 2^\circ$).*

Figure 3.3.30. *Tycho Catalogue, Field T24: median correlation between π and $\mu_{\alpha *}$ in equatorial coordinates (cell size $2^\circ \times 2^\circ$).*

Figure 3.3.31. *Tycho Catalogue, Field T25: median correlation between $\alpha*$ and μ_δ in equatorial coordinates (cell size $2^\circ \times 2^\circ$).*

Figure 3.3.32. *Tycho Catalogue, Field T26: median correlation between δ and μ_δ in equatorial coordinates (cell size $2^\circ \times 2^\circ$).*

Figure 3.3.33. *Tycho Catalogue, Field T27: median correlation between π and μ_δ in equatorial coordinates (cell size $2^\circ \times 2^\circ$).*

Figure 3.3.34. *Tycho Catalogue, Field T28: median correlation between $\mu_{\alpha *}$ and μ_δ in equatorial coordinates (cell size $2^\circ \times 2^\circ$).*

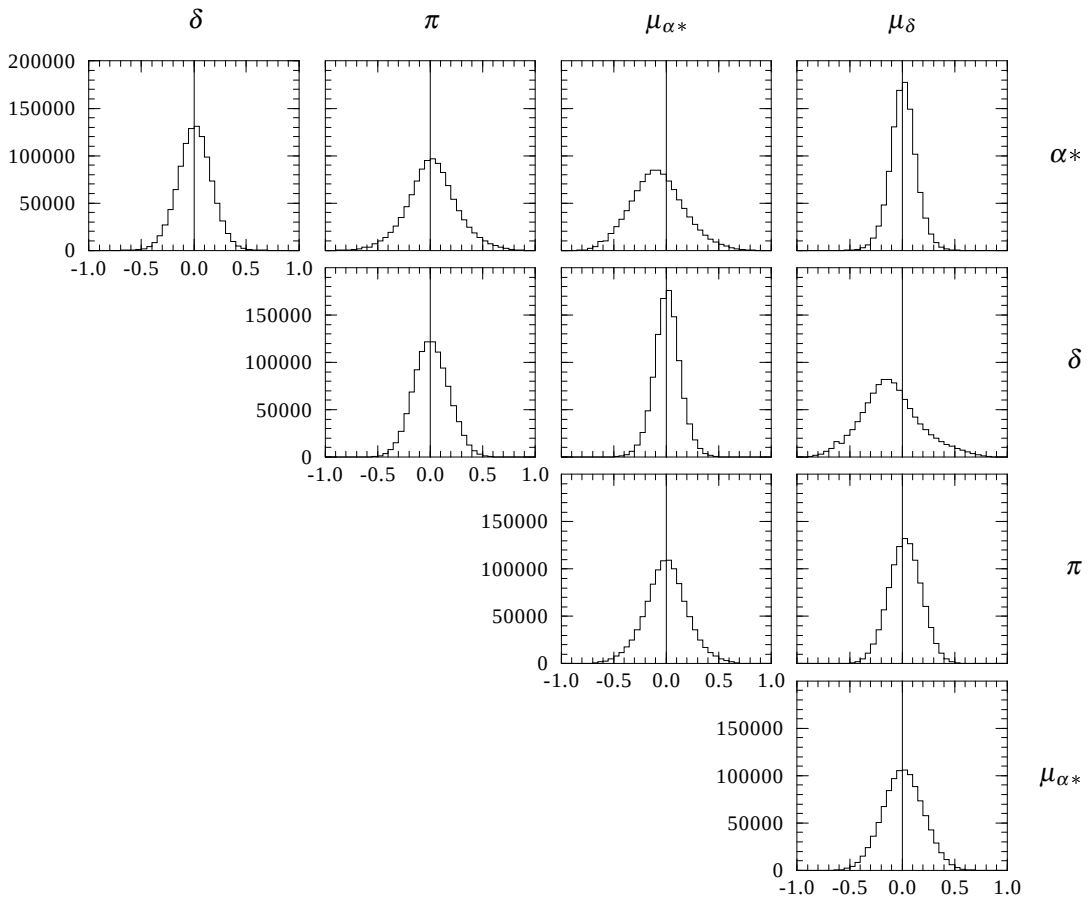

Figure 3.3.35. *Tycho Catalogue, Field T19–T28: correlations between astrometric parameters (bin size 0.05).*

Figure 3.3.36. *Tycho Catalogue, Field T30: median goodness-of-fit parameter, F2, in ecliptic coordinates (cell size $3^\circ \times 3^\circ$).*

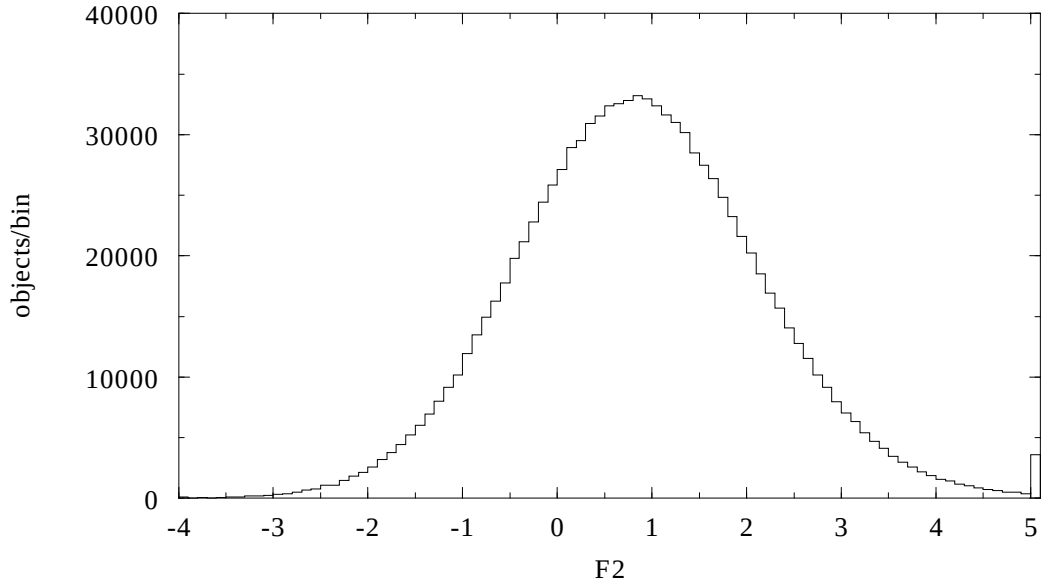

Figure 3.3.37. *Tycho Catalogue, Field T30: goodness-of-fit parameter, F2 (bin size 0.1). The rightmost bin contains all values above 5.*

Figure 3.3.38. *Tycho Catalogue, Field T33: median B_T mean magnitude, in equatorial coordinates (cell size $2^\circ \times 2^\circ$).*

Figure 3.3.39. *Tycho Catalogue, Field T35: median V_T mean magnitude, in equatorial coordinates (cell size $2^\circ \times 2^\circ$).*

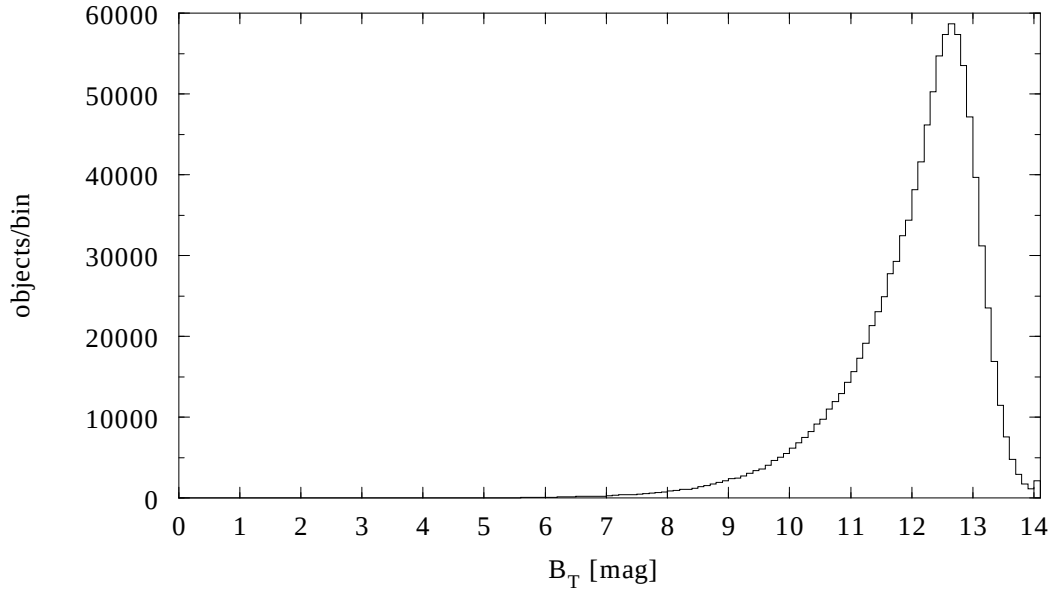

Figure 3.3.40. *Tycho Catalogue, Field T33: B_T mean magnitude (bin size 0.1 mag). The rightmost bin contains all values above 14 mag.*

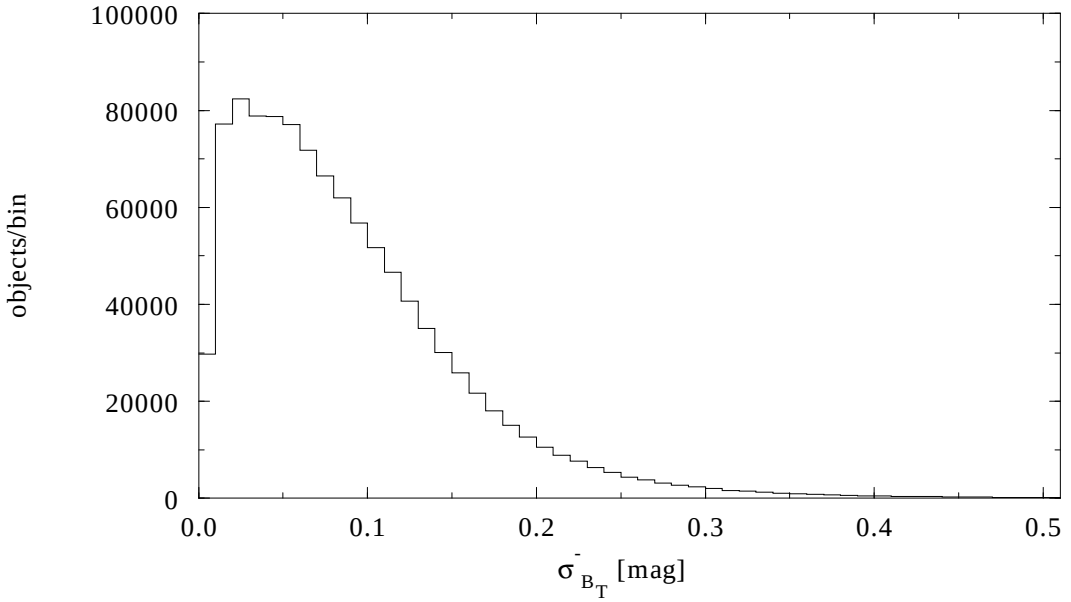

Figure 3.3.41. *Tycho Catalogue, Field T34: standard error in B_T mean magnitude (bin size 0.01 mag). The rightmost bin contains all values above 0.5 mag.*

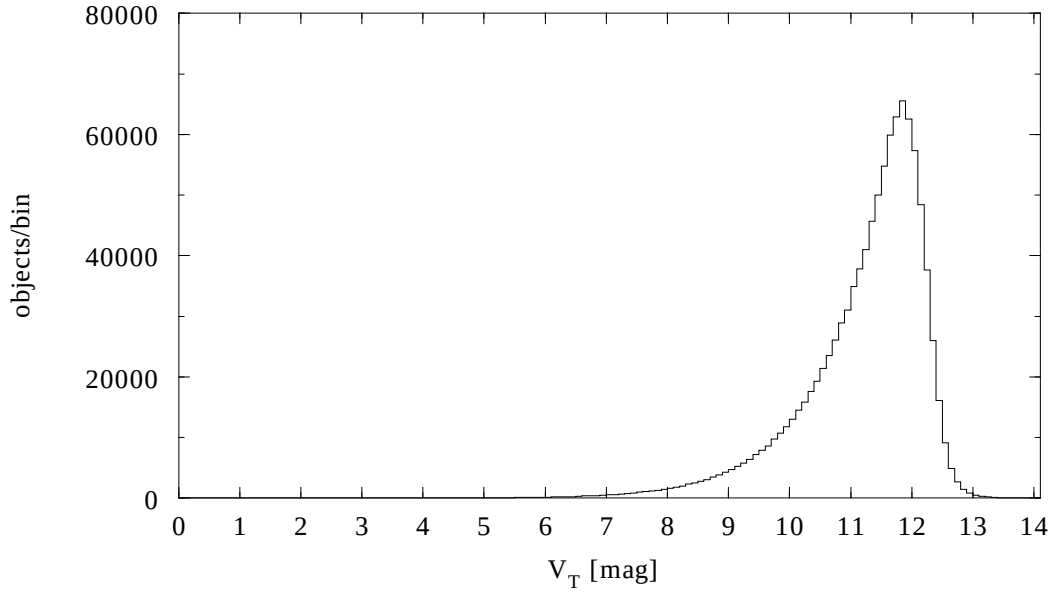

Figure 3.3.42. *Tycho Catalogue, Field T35: V_T mean magnitude (bin size 0.1 mag). The rightmost bin contains all values above 14 mag.*

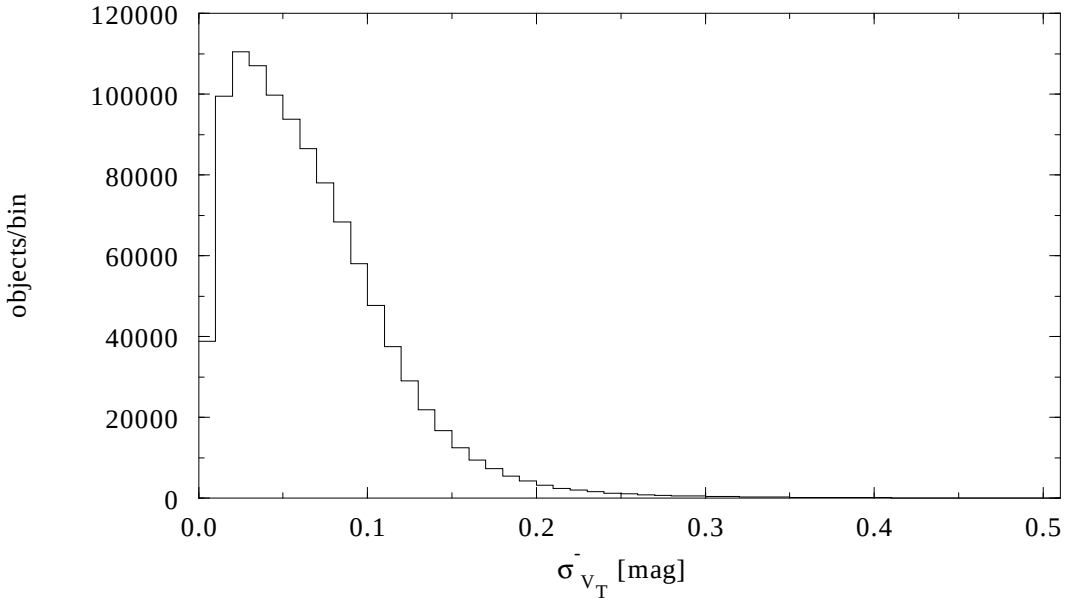

Figure 3.3.43. *Tycho Catalogue, Field T36: standard error in V_T mean magnitude (bin size 0.01 mag). The rightmost bin contains all values above 0.5 mag.*

Figure 3.3.44. *Tycho Catalogue, Field T37: median colour index $B-V$, in galactic coordinates (cell size $3^\circ \times 3^\circ$).*

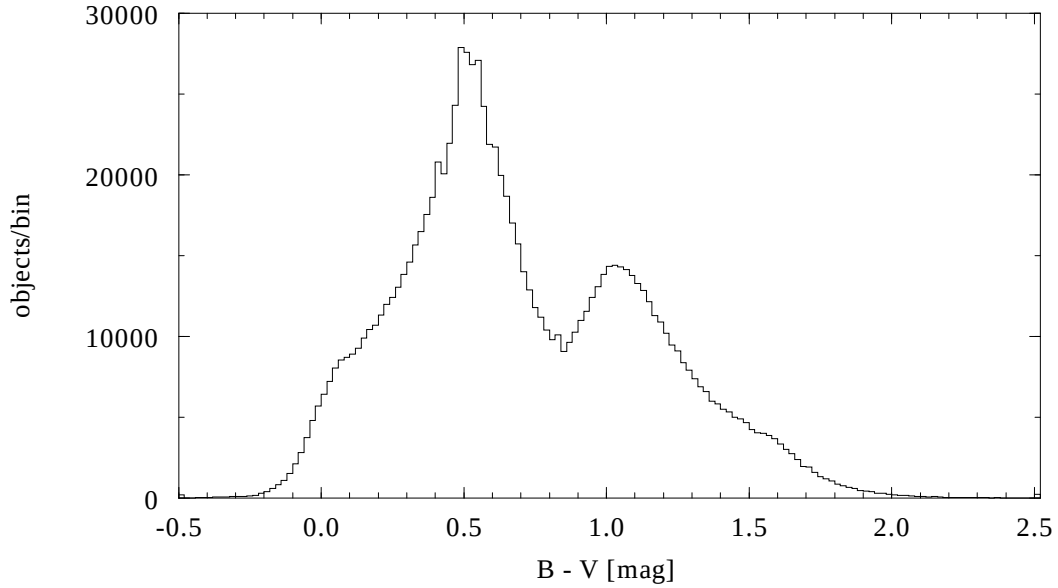

Figure 3.3.45. *Tycho Catalogue, Field T37: colour index $B-V$ (bin size 0.02 mag). The rightmost bin contains all values above 2.5 mag.*

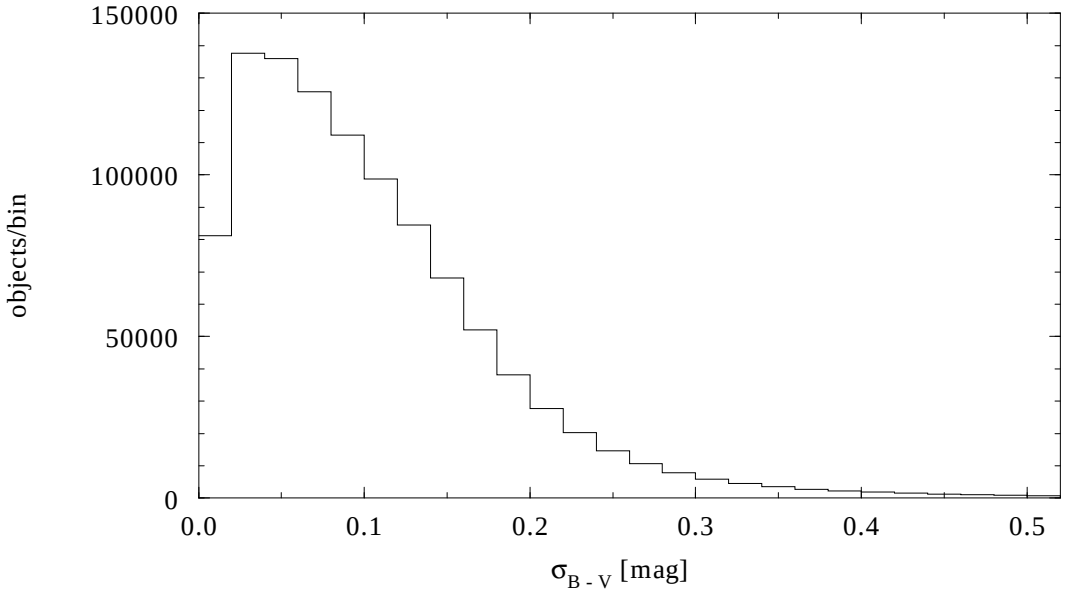

Figure 3.3.46. *Tycho Catalogue, Field T38: standard error in colour index $B - V$ (bin size 0.02 mag). The rightmost bin contains all values above 0.5 mag.*

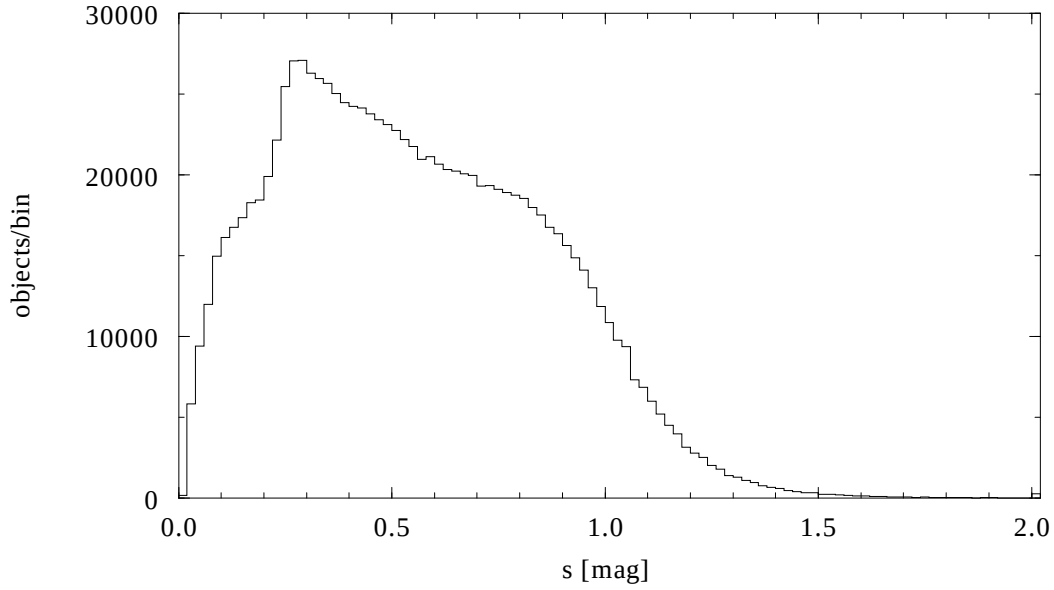

Figure 3.3.47. *Tycho Catalogue, Field T44: V_T scatter (bin size 0.02 mag). The rightmost bin contains all values above 2 mag.*

Section 3.4

Statistical Properties: Catalogue Comparisons

3.4. Statistical Properties: Catalogue Comparisons

In this section results from comparisons of the Hipparcos and Tycho Catalogues with each other, and with certain other catalogues, are presented.

Figures 3.4.1 to 3.4.10 give sky distributions and frequency histograms for the differences in the five astrometric parameters between the Hipparcos stars in the Tycho Catalogue and the same stars in the Hipparcos Catalogue. Excluded from the comparison are the 'Hipparcos only' stars from the Tycho Catalogue (Field T42 = 'H'), and the entries with Field T51 non-blank (in order to avoid situations where one Hipparcos Catalogue entry corresponds to two Tycho Catalogue entries, and vice versa). There is little residual structure, and, for the longitudinal parameters, a slightly higher scatter in the ecliptic region. The widths of the histograms reflect the precision of the Tycho results for the Hipparcos stars, which is better than the overall precision of the Tycho results, because the Hipparcos selection emphasizes the brighter stars (cf. Figure 1.1.1).

Figures 3.4.11 to 3.4.18 illustrate the differences of $\alpha*$, δ, $\mu_{\alpha*}$, and μ_δ between the Hipparcos Input Catalogue and the Hipparcos Catalogue. The dramatic improvement, particularly in the position, is evident. The presence of zonal (especially declination-dependent) structure in the Hipparcos Input Catalogue may also be seen.

Figures 3.4.19 to 3.4.26 compare the results of the Hipparcos Catalogue with those in the Fifth Fundamental Catalogue (FK5) (W. Fricke, H. Schwan, T. Lederle, 1988, *Fifth Fundamental Catalogue*, Veröff. Astron. Rechen-Inst. Heidelberg). A running median over 50 stars has been computed. Again, the large corrections made by Hipparcos, especially in the southern hemisphere, are clearly depicted. Further details of the relationship between ICRS(Hipparcos) and J2000(FK5) are given in Section 1.5.7.

Figures 3.4.27 to 3.4.42 give a similar comparison of the results of the Tycho Catalogue with those from the PPM, the Catalogue of Positions and Proper Motions (S. Röser, U. Bastian, 1991, *PPM Star Catalogue, Vol. I–II*; U. Bastian, S. Röser, 1993, *PPM Star Catalogue, Vol. III–IV*, Astron. Rechen-Inst. Heidelberg). In view of the large number of stars, the results are presented as density plots, and a median over a fixed range is computed (see captions for details). Only Tycho 'recommended stars' (blank in Field T10) have been used, and separate comparisons are presented for brighter and fainter stars, for the reasons explained in Volume 4, Section 18.3. Indeed some of the comparisons differ considerably, especially in the northern hemisphere. The sudden change in scatter at $\delta = -2.5°$ is due to the different statistical properties of the northern and southern parts of the PPM. The northern part is based on older catalogues, so that the present day accuracy is modest (0.27 arcsec and 4 mas/year for the positions and proper motions respectively, according to the authors). The southern part is based on more recent catalogues; the authors quote accuracies of 0.11 arcsec and 3 mas/year for the positions and proper motions respectively.

Figure 3.4.1. *Median difference between $\alpha*$ from the Tycho Catalogue and $\alpha*$ from the Hipparcos Catalogue, in equatorial coordinates (cell size $2^\circ \times 2^\circ$).*

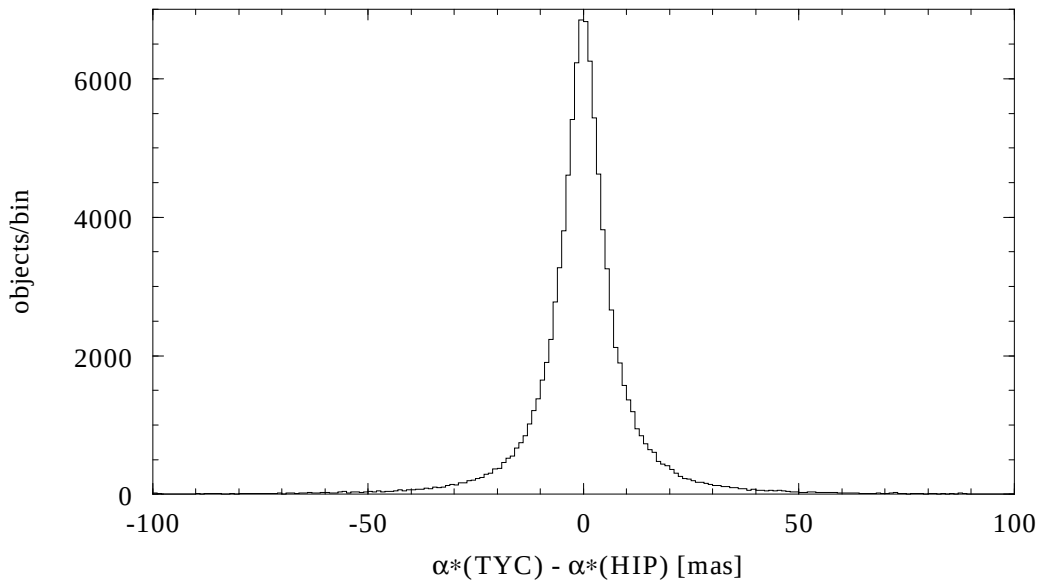

Figure 3.4.2. *Difference between $\alpha*$ from the Tycho Catalogue and $\alpha*$ from the Hipparcos Catalogue.*

Figure 3.4.3. *Median difference between δ from the Tycho Catalogue and δ from the Hipparcos Catalogue, in equatorial coordinates (cell size $2° \times 2°$).*

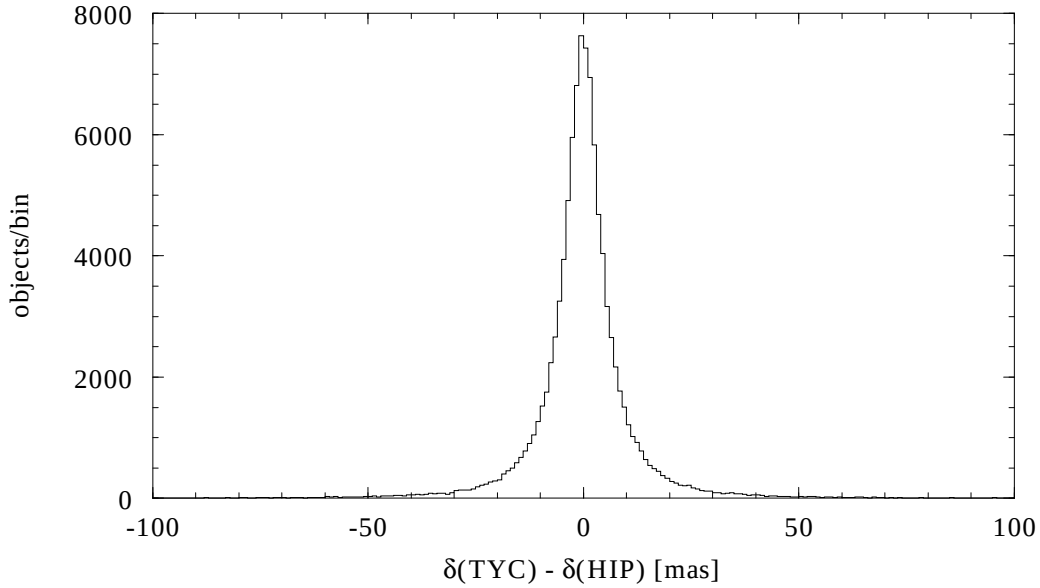

Figure 3.4.4. *Difference between δ from the Tycho Catalogue and δ from the Hipparcos Catalogue.*

Figure 3.4.5. *Median difference between $\mu_{\alpha*}$ from the Tycho Catalogue and $\mu_{\alpha*}$ from the Hipparcos Catalogue, in equatorial coordinates (cell size $2^\circ \times 2^\circ$).*

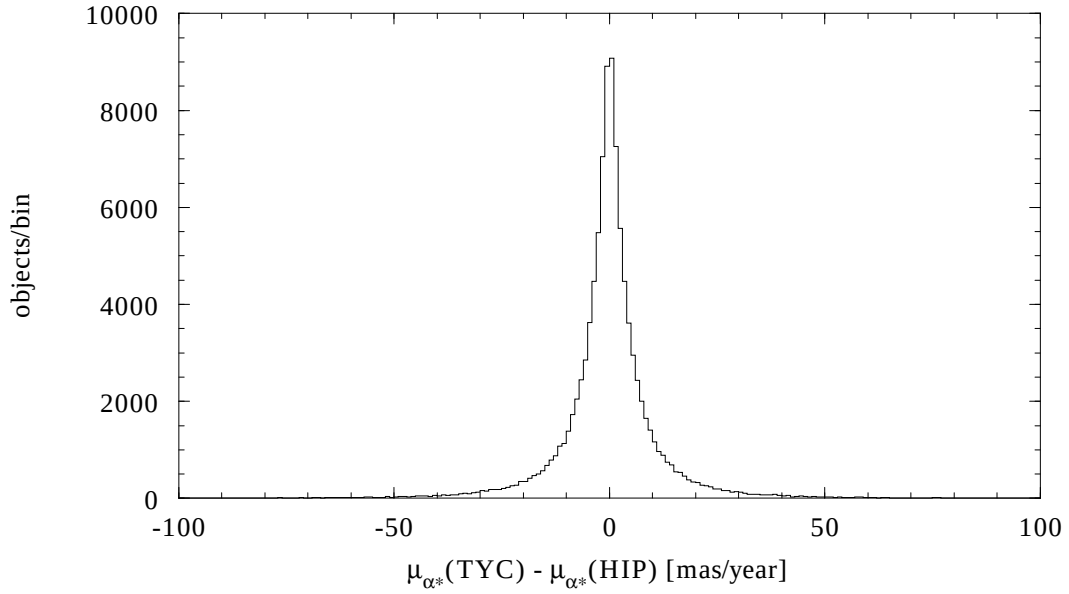

Figure 3.4.6. *Difference between $\mu_{\alpha*}$ from the Tycho Catalogue and $\mu_{\alpha*}$ from the Hipparcos Catalogue.*

Figure 3.4.7. *Median difference between μ_δ from the Tycho Catalogue and μ_δ from the Hipparcos Catalogue, in equatorial coordinates (cell size $2^\circ \times 2^\circ$).*

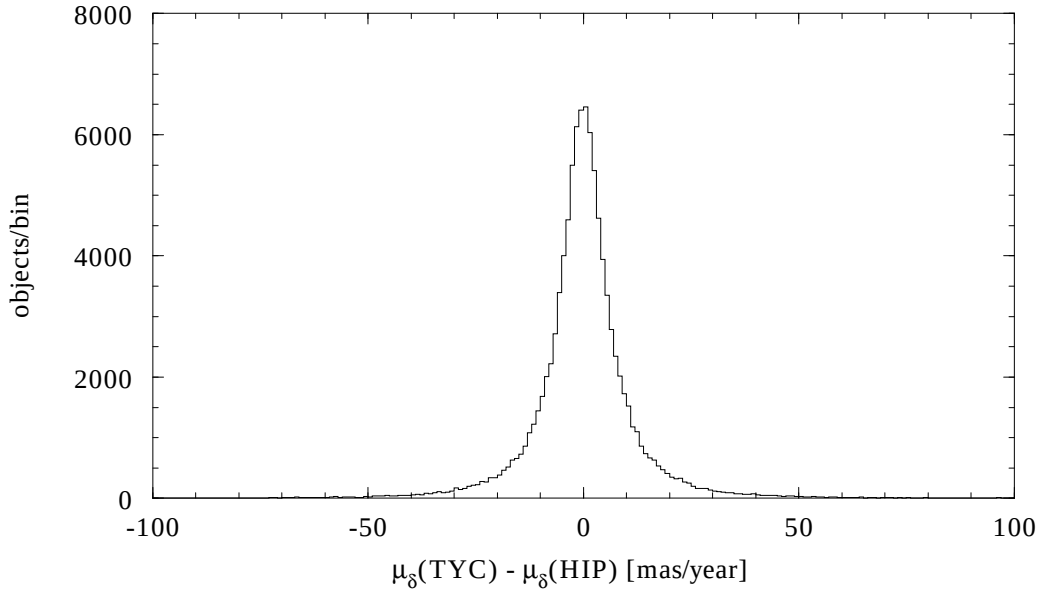

Figure 3.4.8. *Difference between μ_δ from the Tycho Catalogue and μ_δ from the Hipparcos Catalogue.*

Figure 3.4.9. *Median difference between π from the Tycho Catalogue and π from the Hipparcos Catalogue, in equatorial coordinates (cell size $2^\circ \times 2^\circ$).*

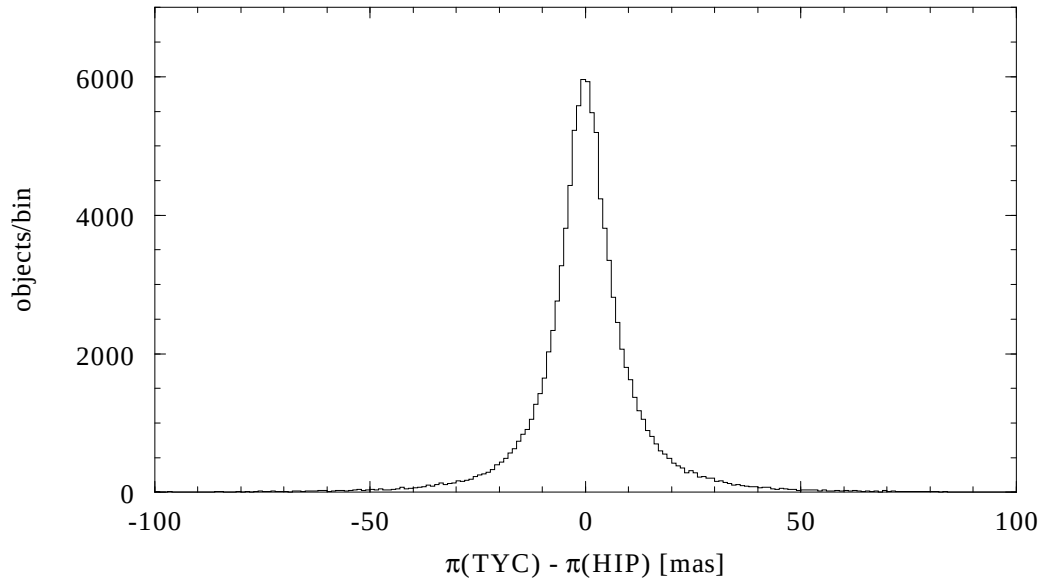

Figure 3.4.10. *Difference between π from the Tycho Catalogue and π from the Hipparcos Catalogue.*

Figure 3.4.11. *Median difference between $\alpha*$ from the Hipparcos Input Catalogue (after rotation to the Hipparcos reference frame) and $\alpha*$ from the Hipparcos Catalogue, in equatorial coordinates (cell size $2^\circ \times 2^\circ$).*

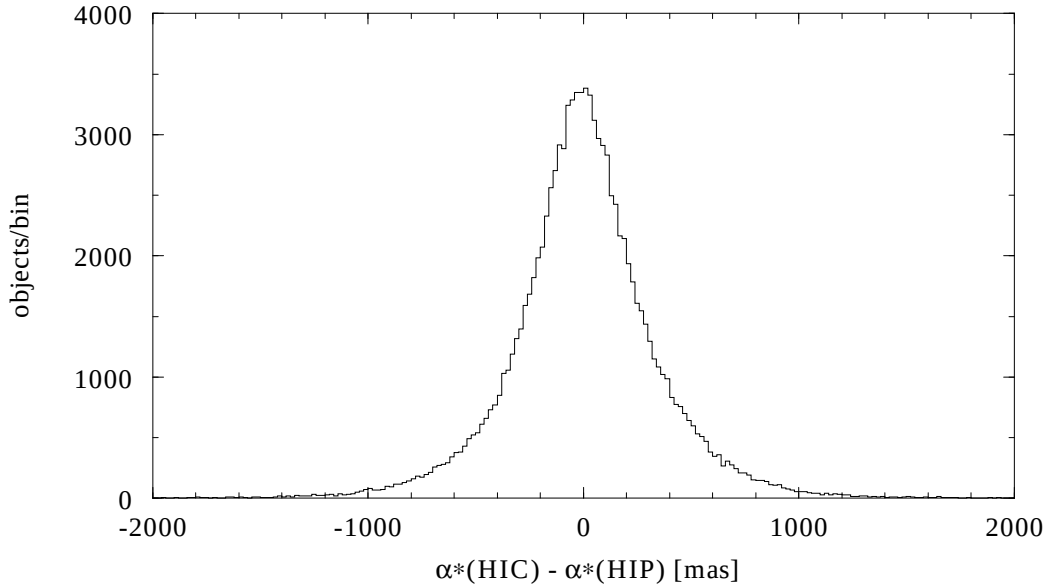

Figure 3.4.12. *Difference between $\alpha*$ from the Hipparcos Input Catalogue (after rotation to the Hipparcos reference frame) and $\alpha*$ from the Hipparcos Catalogue.*

Figure 3.4.13. *Median difference between δ from the Hipparcos Input Catalogue (after rotation to the Hipparcos reference frame) and δ from the Hipparcos Catalogue, in equatorial coordinates (cell size $2^\circ \times 2^\circ$).*

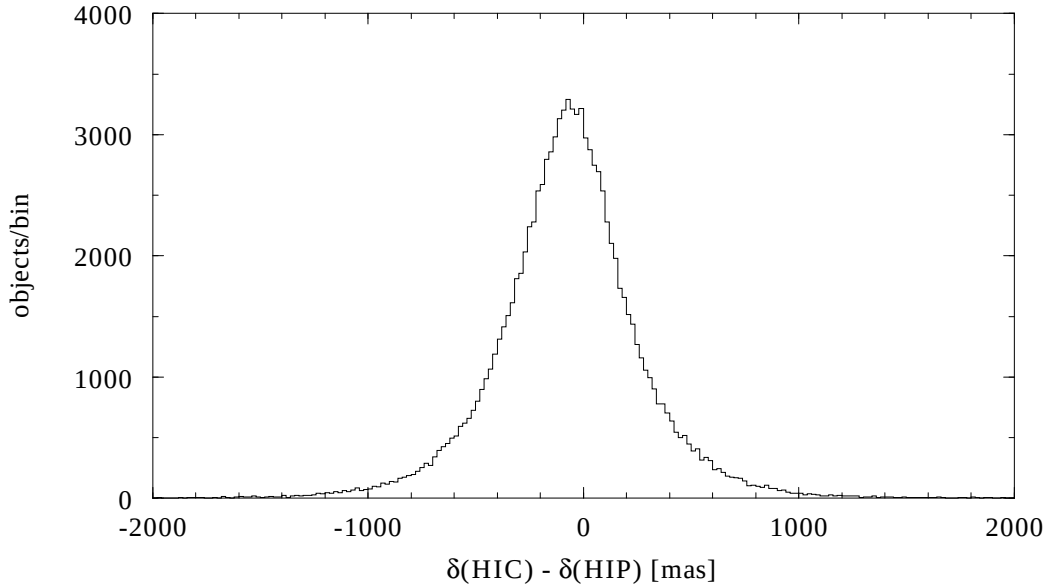

Figure 3.4.14. *Difference between δ from the Hipparcos Input Catalogue (after rotation to the Hipparcos reference frame) and δ from the Hipparcos Catalogue.*

Figure 3.4.15. *Median difference between $\mu_{\alpha*}$ from the Hipparcos Input Catalogue (after rotation to the Hipparcos reference frame) and $\mu_{\alpha*}$ from the Hipparcos Catalogue, in equatorial coordinates (cell size $2^\circ \times 2^\circ$).*

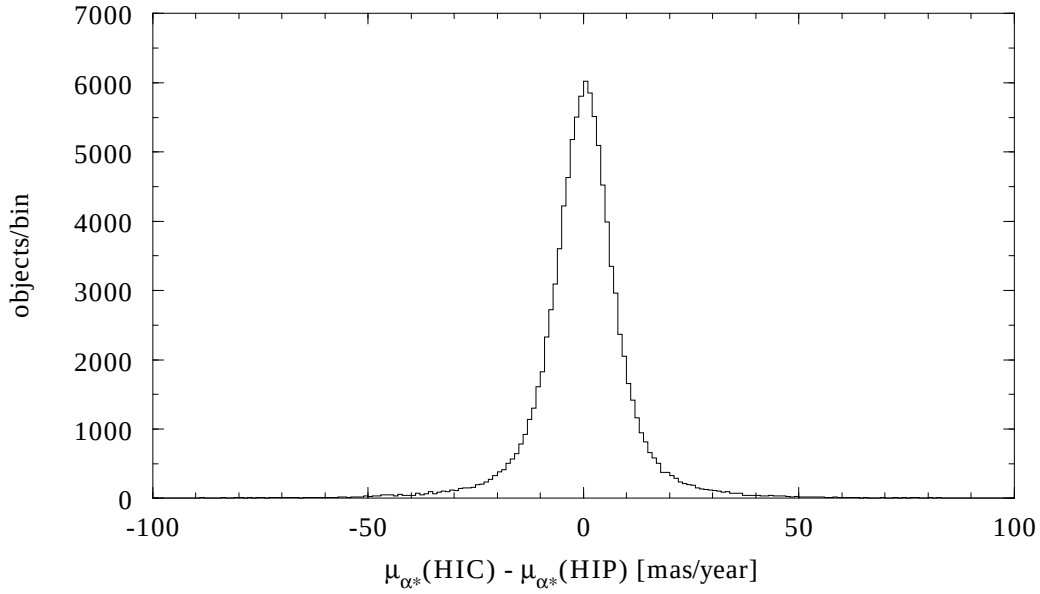

Figure 3.4.16. *Difference between $\mu_{\alpha*}$ from the Hipparcos Input Catalogue (after rotation to the Hipparcos reference frame) and $\mu_{\alpha*}$ from the Hipparcos Catalogue.*

Figure 3.4.17. *Median difference between μ_δ from the Hipparcos Input Catalogue (after rotation to the Hipparcos reference frame) and μ_δ from the Hipparcos Catalogue, in equatorial coordinates (cell size $2^\circ \times 2^\circ$).*

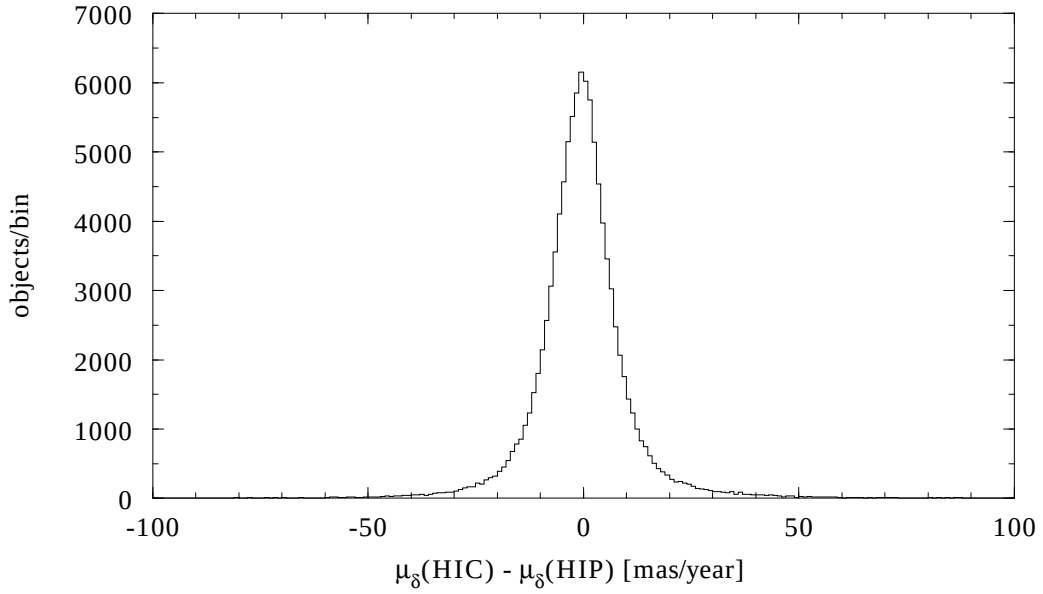

Figure 3.4.18. *Difference between μ_δ from the Hipparcos Input Catalogue (after rotation to the Hipparcos reference frame) and μ_δ from the Hipparcos Catalogue.*

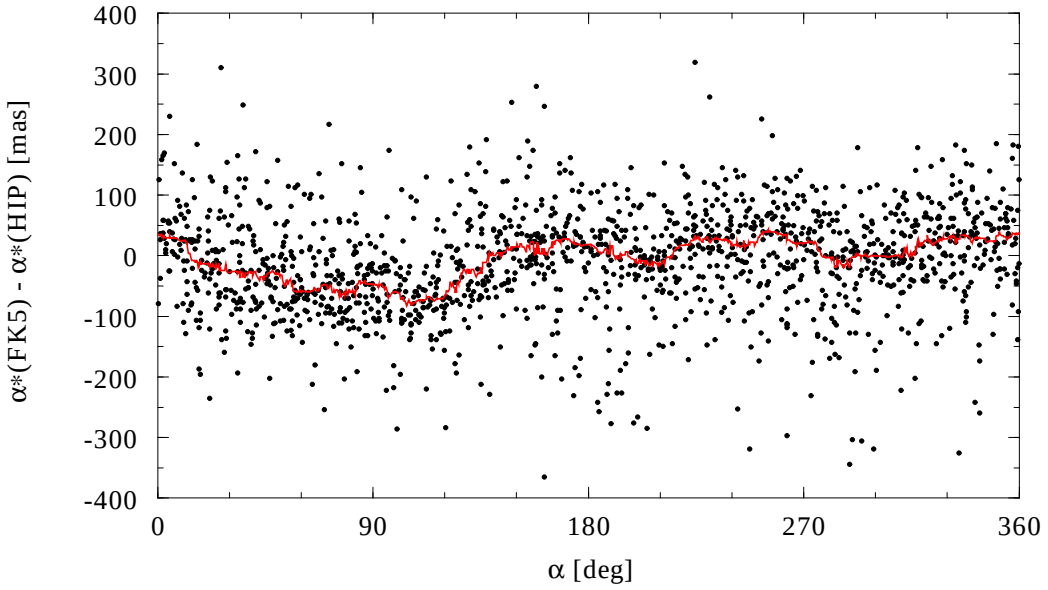

Figure 3.4.19. *Difference between $\alpha*$ from FK5 (after rotation to the Hipparcos reference frame) and $\alpha*$ from the Hipparcos Catalogue, versus α. The red curve is the running median over 50 points.*

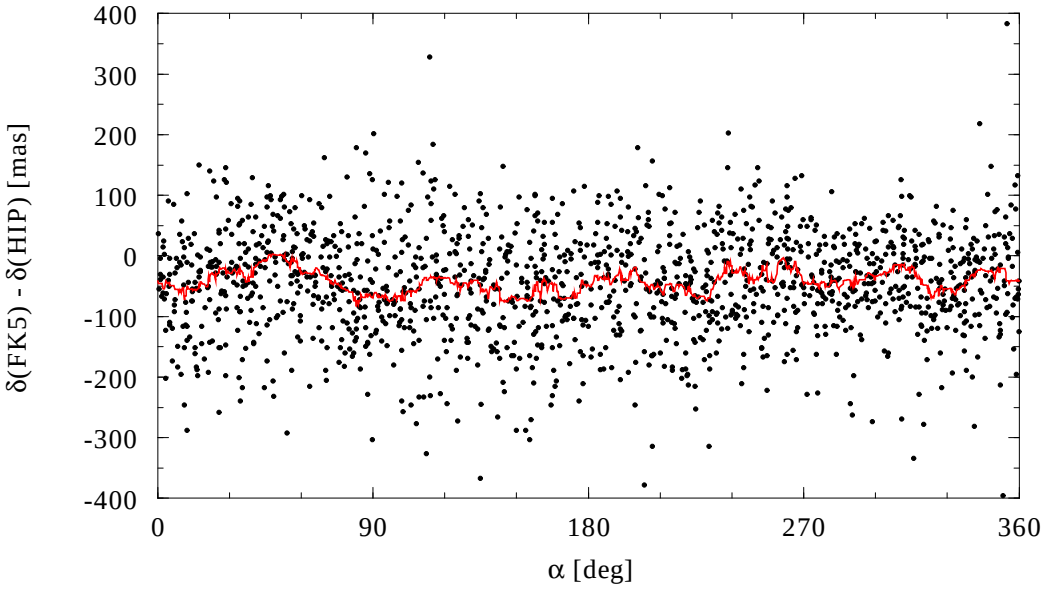

Figure 3.4.20. *Difference between δ from FK5 (after rotation to the Hipparcos reference frame) and δ from the Hipparcos Catalogue, versus α. The red curve is the running median over 50 points.*

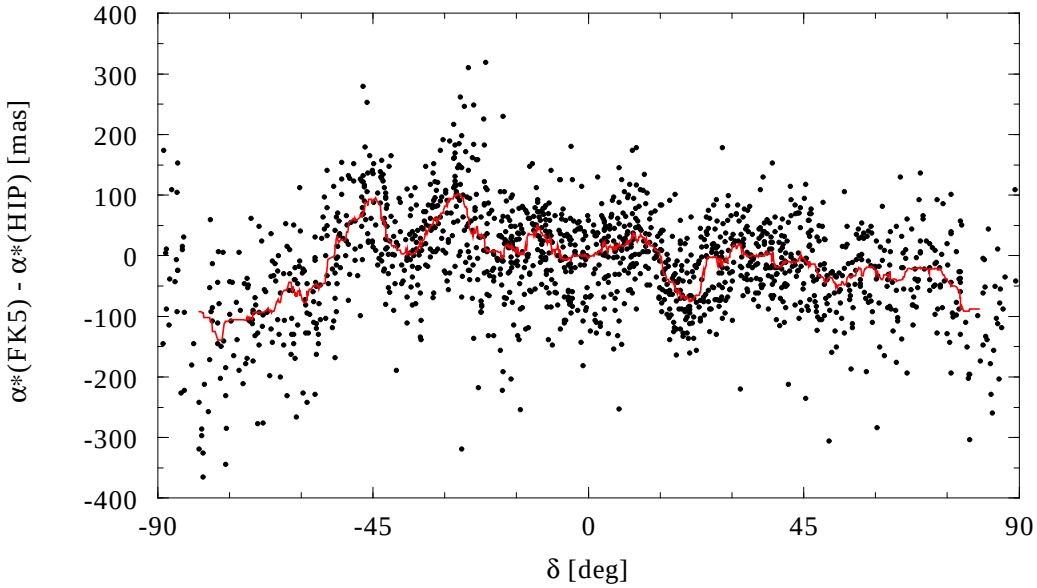

Figure 3.4.21. *Difference between $\alpha*$ from FK5 (after rotation to the Hipparcos reference frame) and $\alpha*$ from the Hipparcos Catalogue, versus δ. The red curve is the running median over 50 points.*

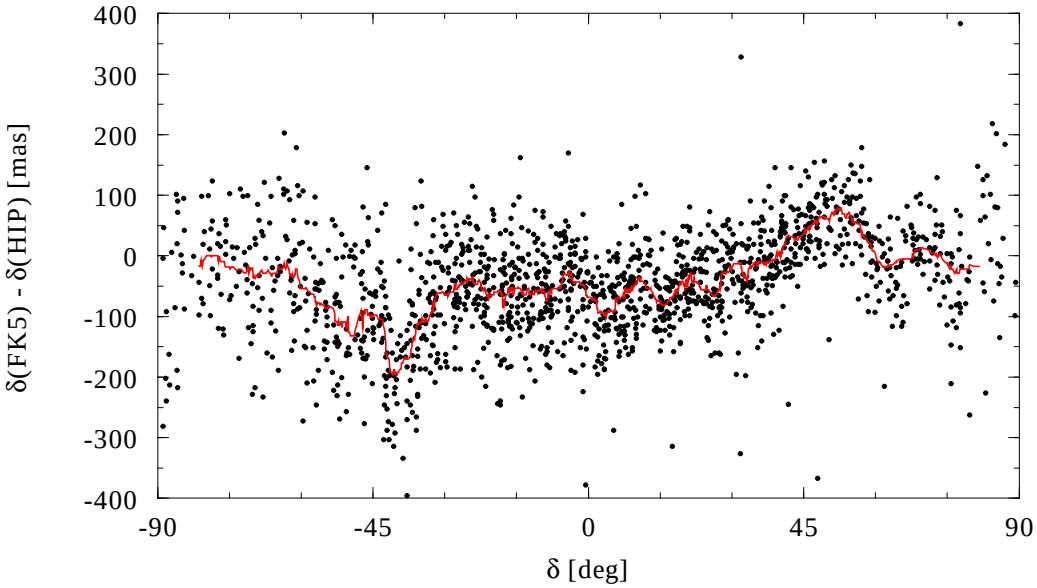

Figure 3.4.22. *Difference between δ from FK5 (after rotation to the Hipparcos reference frame) and δ from the Hipparcos Catalogue, versus δ. The red curve is the running median over 50 points.*

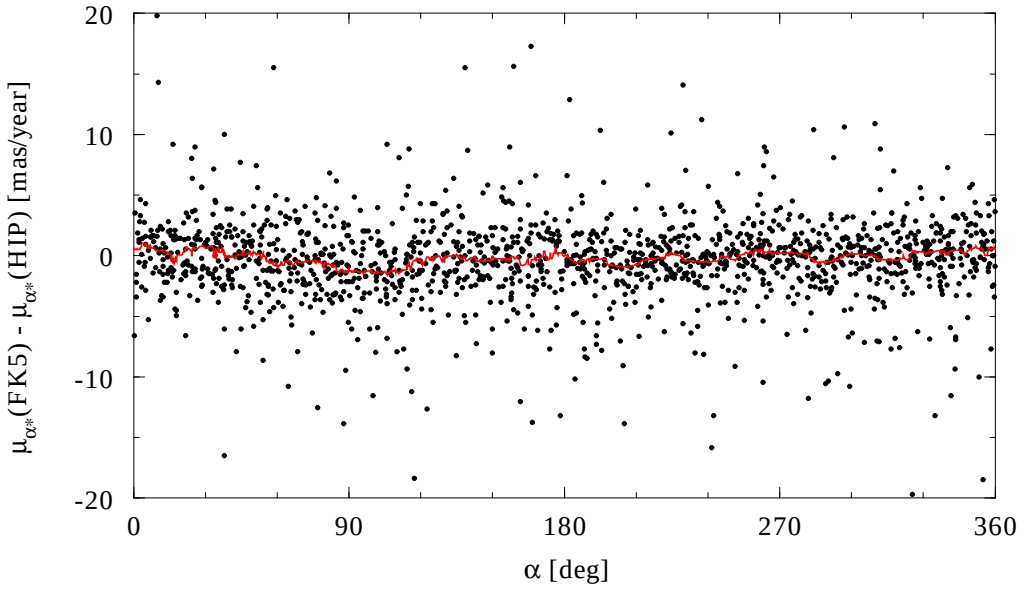

Figure 3.4.23. *Difference between $\mu_{\alpha *}$ from FK5 (after rotation to the Hipparcos reference frame) and $\mu_{\alpha *}$ from the Hipparcos Catalogue, versus α. The red curve is the running median over 50 points.*

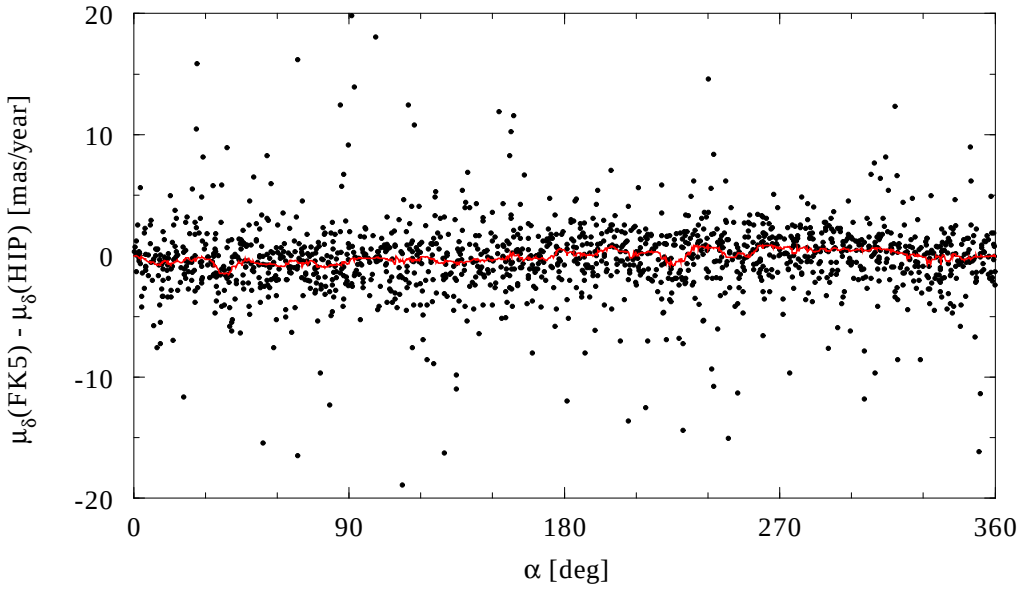

Figure 3.4.24. *Difference between μ_{δ} from FK5 (after rotation to the Hipparcos reference frame) and μ_{δ} from the Hipparcos Catalogue, versus α. The red curve is the running median over 50 points.*

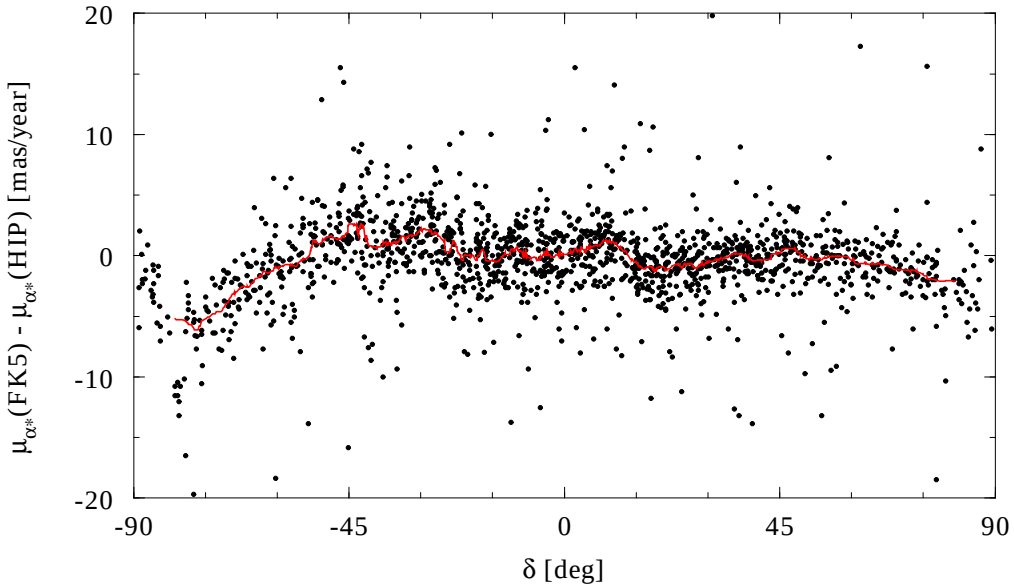

Figure 3.4.25. *Difference between $\mu_{\alpha*}$ from FK5 (after rotation to the Hipparcos reference frame) and $\mu_{\alpha*}$ from the Hipparcos Catalogue, versus δ. The red curve is the running median over 50 points.*

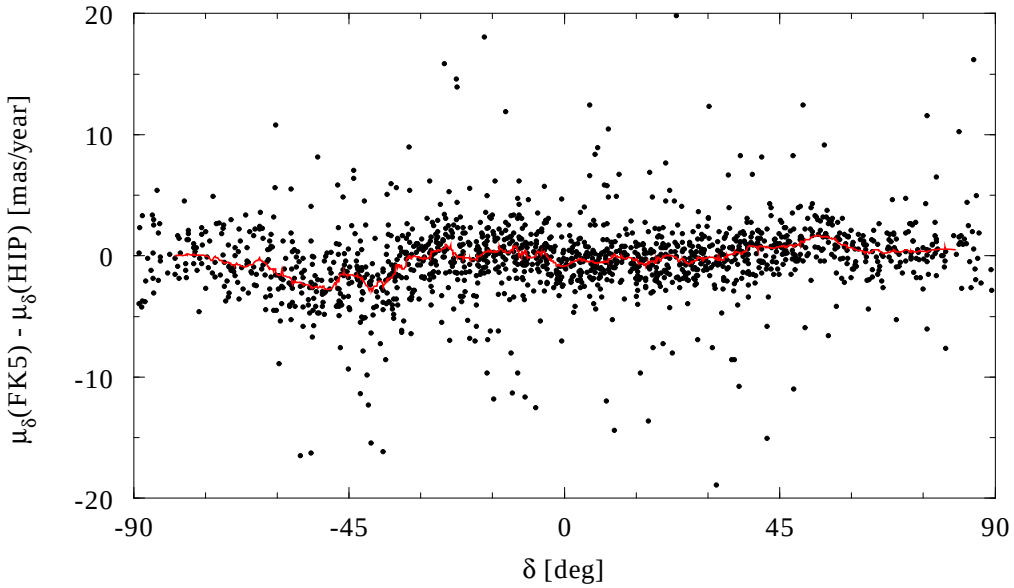

Figure 3.4.26. *Difference between μ_{δ} from FK5 (after rotation to the Hipparcos reference frame) and μ_{δ} from the Hipparcos Catalogue, versus δ. The red curve is the running median over 50 points.*

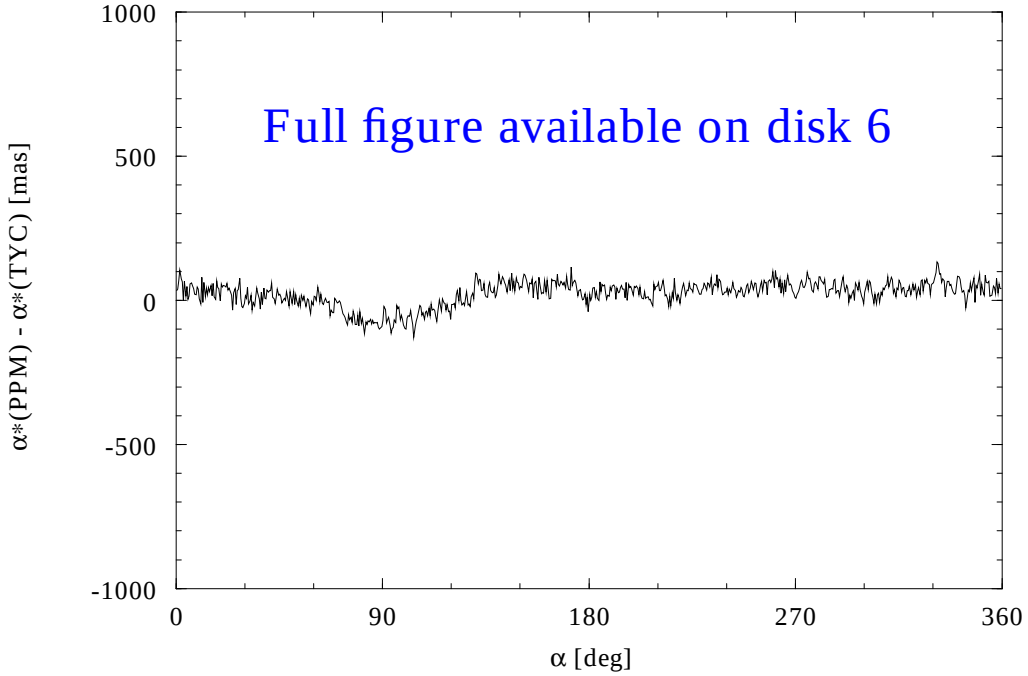

Figure 3.4.27. *Difference between $\alpha*$ from PPM (after rotation to the Hipparcos reference frame) and $\alpha*$ from the Tycho Catalogue, versus α, as a density plot, for recommended Tycho Catalogue stars brighter than $B_T = 10$ mag. The colour scale indicates the number of stars in a cell of $1^\circ \times 8$ mas. The curve is the median difference over intervals of 0.5°.*

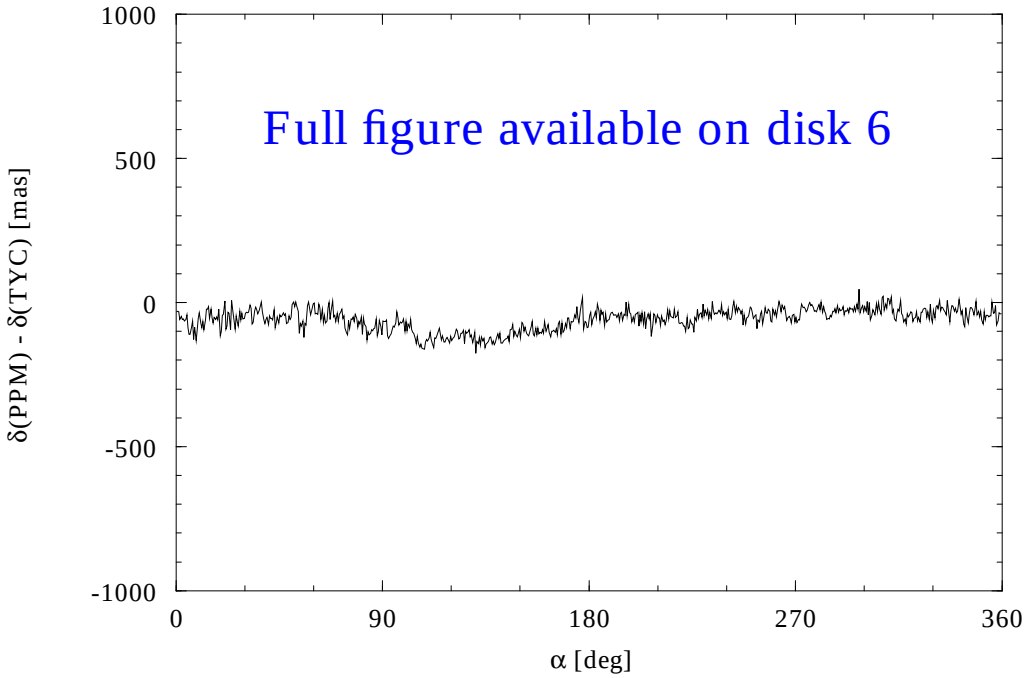

Figure 3.4.28. *Difference between δ from PPM (after rotation to the Hipparcos reference frame) and δ from the Tycho Catalogue, versus α, as a density plot, for recommended Tycho Catalogue stars brighter than $B_T = 10$ mag. The colour scale indicates the number of stars in a cell of $1^\circ \times 8$ mas. The curve is the median difference over intervals of 0.5°.*

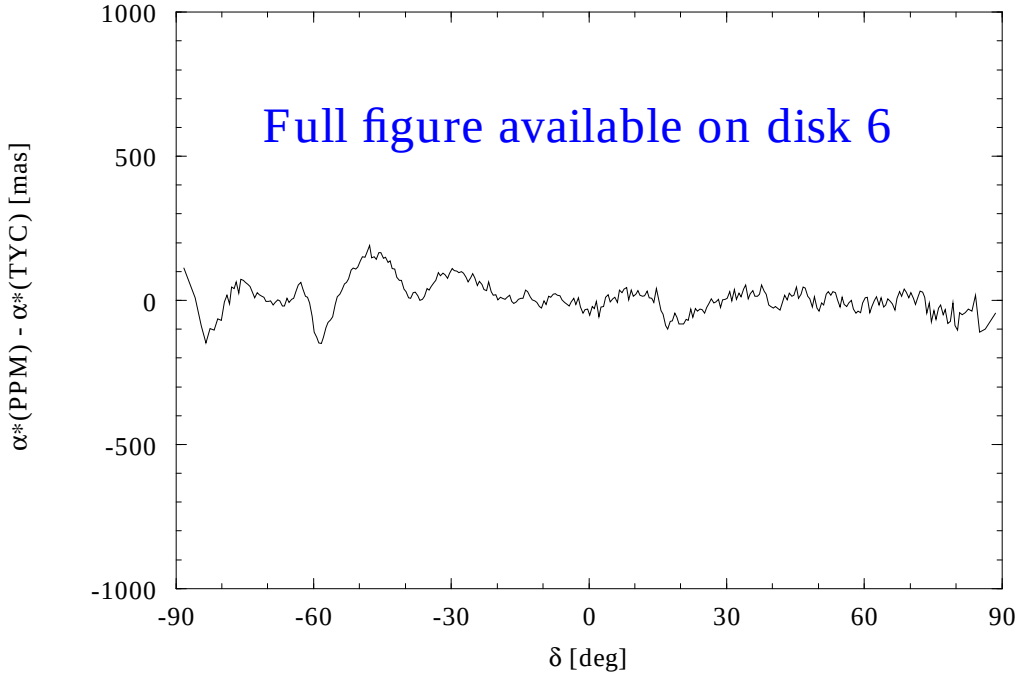

Figure 3.4.29. *Difference between $\alpha*$ from PPM (after rotation to the Hipparcos reference frame) and $\alpha*$ from the Tycho Catalogue, versus δ, as a density plot, for recommended Tycho Catalogue stars brighter than $B_T = 10$ mag. The colour scale indicates the number of stars in a cell of $0.5^\circ \times 8$ mas. The curve is the median difference over intervals of 0.5°.*

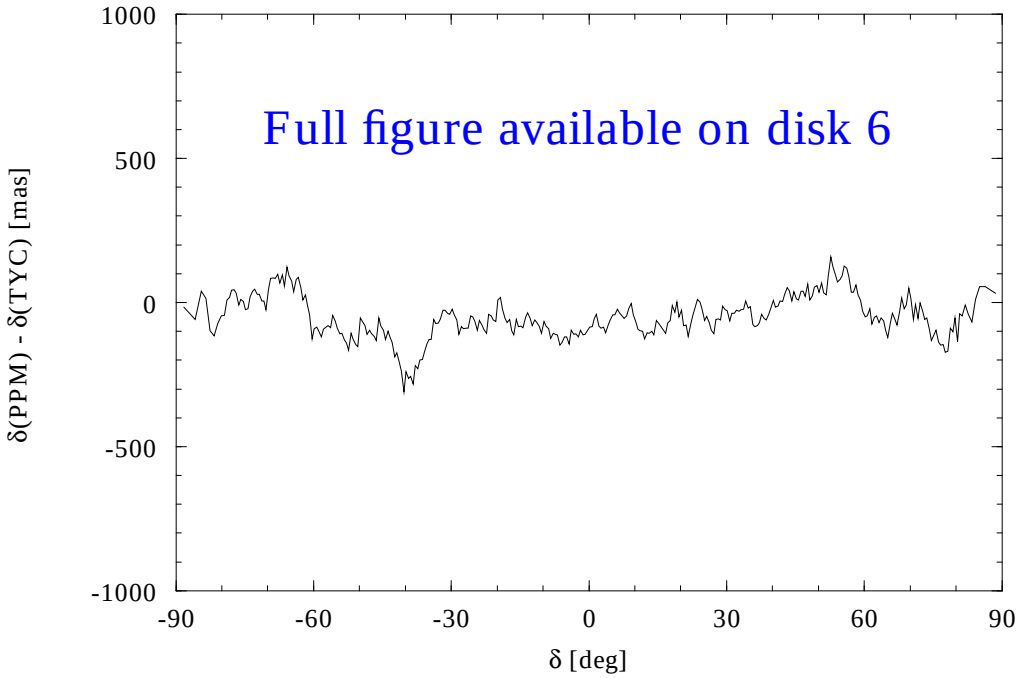

Figure 3.4.30. *Difference between δ from PPM (after rotation to the Hipparcos reference frame) and δ from the Tycho Catalogue, versus δ, as a density plot, for recommended Tycho Catalogue stars brighter than $B_T = 10$ mag. The colour scale indicates the number of stars in a cell of $0.5^\circ \times 8$ mas. The curve is the median difference over intervals of 0.5°.*

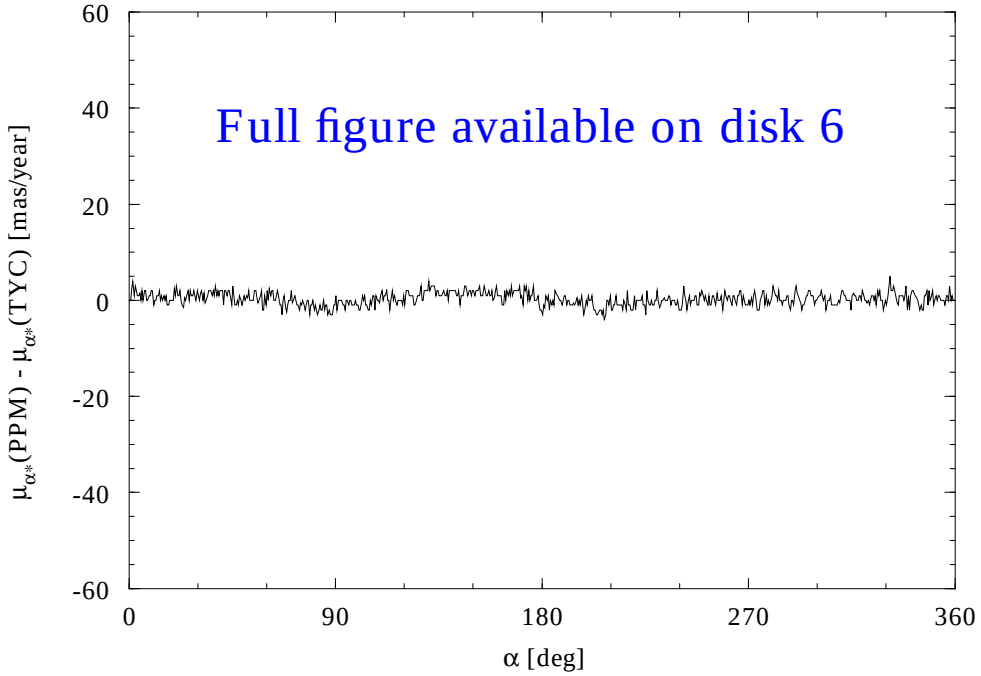

Figure 3.4.31. *Difference between $\mu_{\alpha *}$ from PPM (after rotation to the Hipparcos reference frame) and $\mu_{\alpha *}$ from the Tycho Catalogue, versus α, as a density plot, for recommended Tycho Catalogue stars brighter than $B_T = 10$ mag. The colour scale indicates the number of stars in a cell of $1^\circ \times 1$ mas/yr. The curve is the median difference over intervals of 0.5°.*

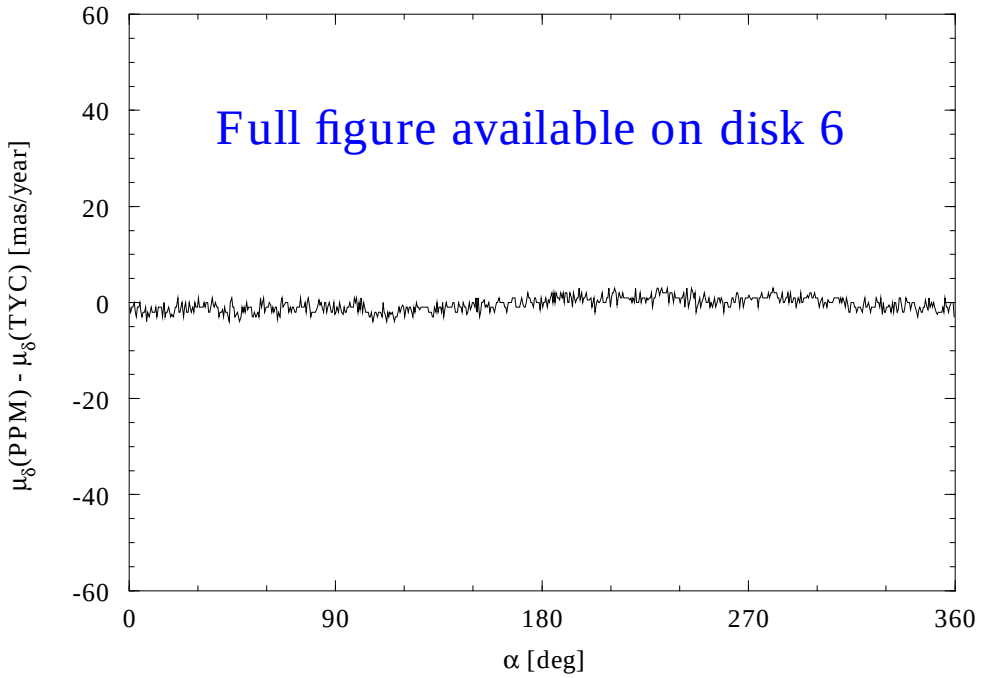

Figure 3.4.32. *Difference between μ_δ from PPM (after rotation to the Hipparcos reference frame) and μ_δ from the Tycho Catalogue, versus α, as a density plot, for recommended Tycho Catalogue stars brighter than $B_T = 10$ mag. The colour scale indicates the number of stars in a cell of $1^\circ \times 1$ mas/yr. The curve is the median difference over intervals of 0.5°.*

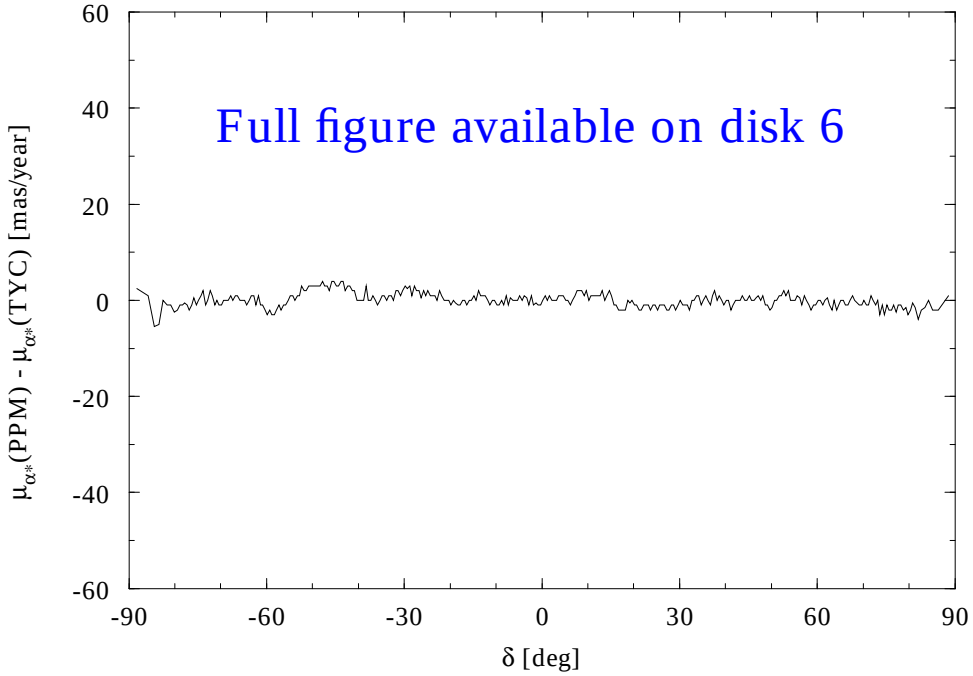

Figure 3.4.33. *Difference between $\mu_{\alpha *}$ from PPM (after rotation to the Hipparcos reference frame) and $\mu_{\alpha *}$ from the Tycho Catalogue, versus δ, as a density plot, for recommended Tycho Catalogue stars brighter than $B_T = 10$ mag. The colour scale indicates the number of stars in a cell of $0.5° \times 1$ mas/yr. The curve is the median difference over intervals of $0.5°$.*

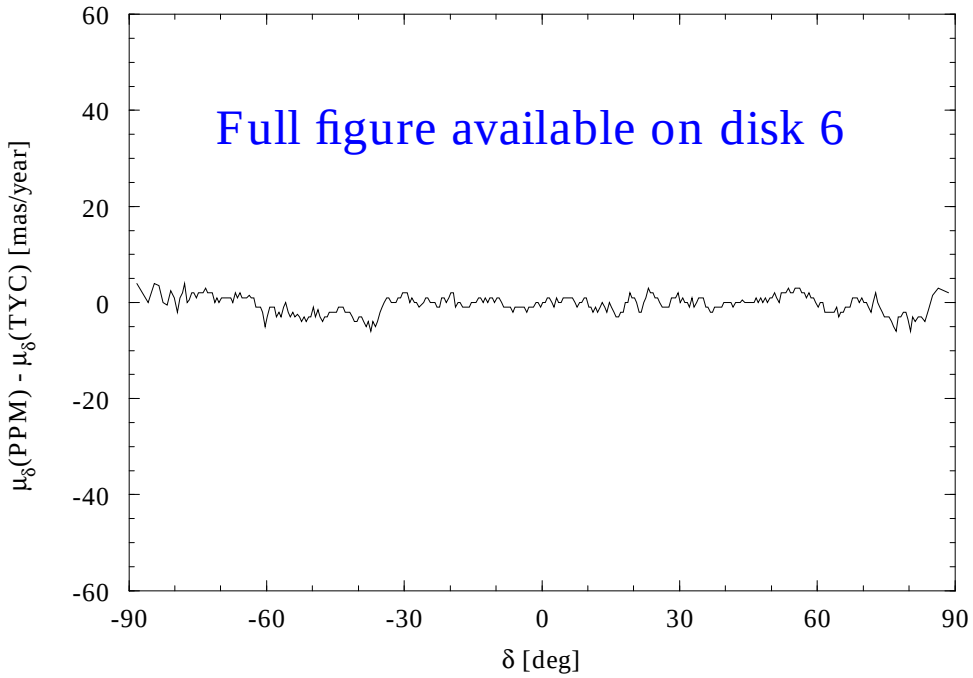

Figure 3.4.34. *Difference between μ_δ from PPM (after rotation to the Hipparcos reference frame) and μ_δ from the Tycho Catalogue, versus δ, as a density plot, for recommended Tycho Catalogue stars brighter than $B_T = 10$ mag. The colour scale indicates the number of stars in a cell of $0.5° \times 1$ mas/yr. The curve is the median difference over intervals of $0.5°$.*

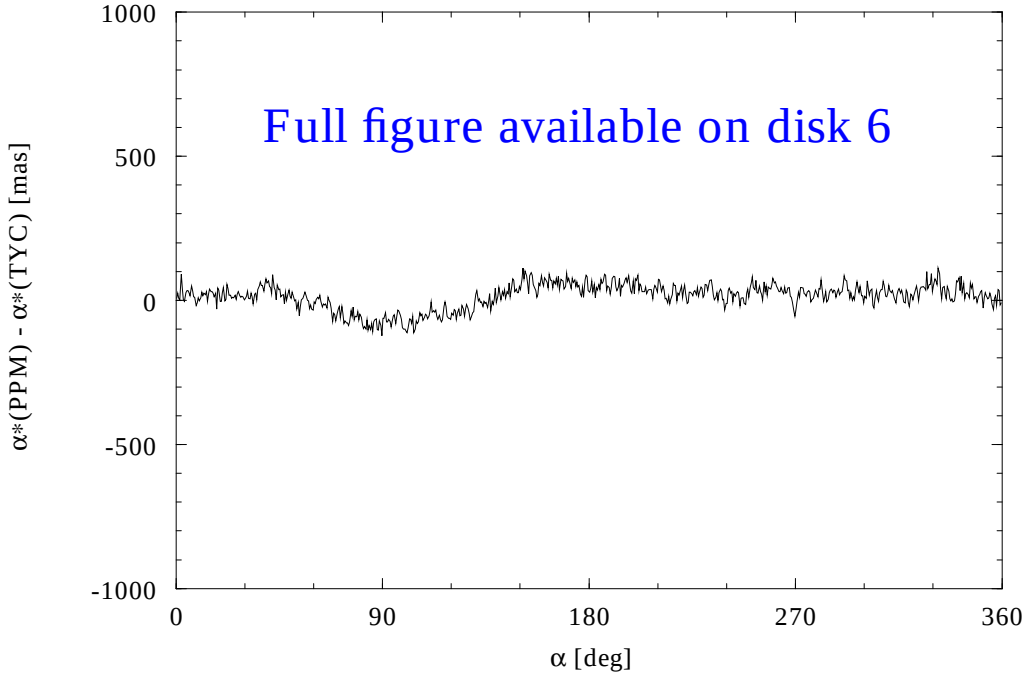

Figure 3.4.35. *Difference between $\alpha*$ from PPM (after rotation to the Hipparcos reference frame) and $\alpha*$ from the Tycho Catalogue, versus α, as a density plot, for recommended Tycho Catalogue stars fainter than $B_T = 10$ mag. The colour scale indicates the number of stars in a cell of $1° \times 8$ mas. The curve is the median difference over intervals of $0.5°$.*

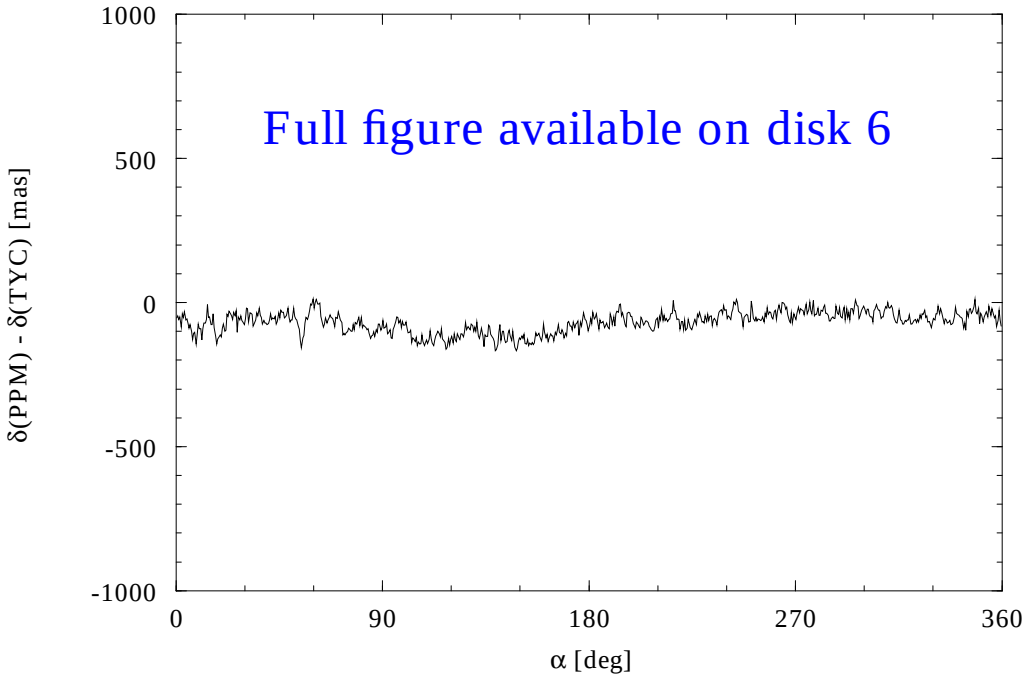

Figure 3.4.36. *Difference between δ from PPM (after rotation to the Hipparcos reference frame) and δ from the Tycho Catalogue, versus α, as a density plot, for recommended Tycho Catalogue stars fainter than $B_T = 10$ mag. The colour scale indicates the number of stars in a cell of $1° \times 8$ mas. The curve is the median difference over intervals of $0.5°$.*

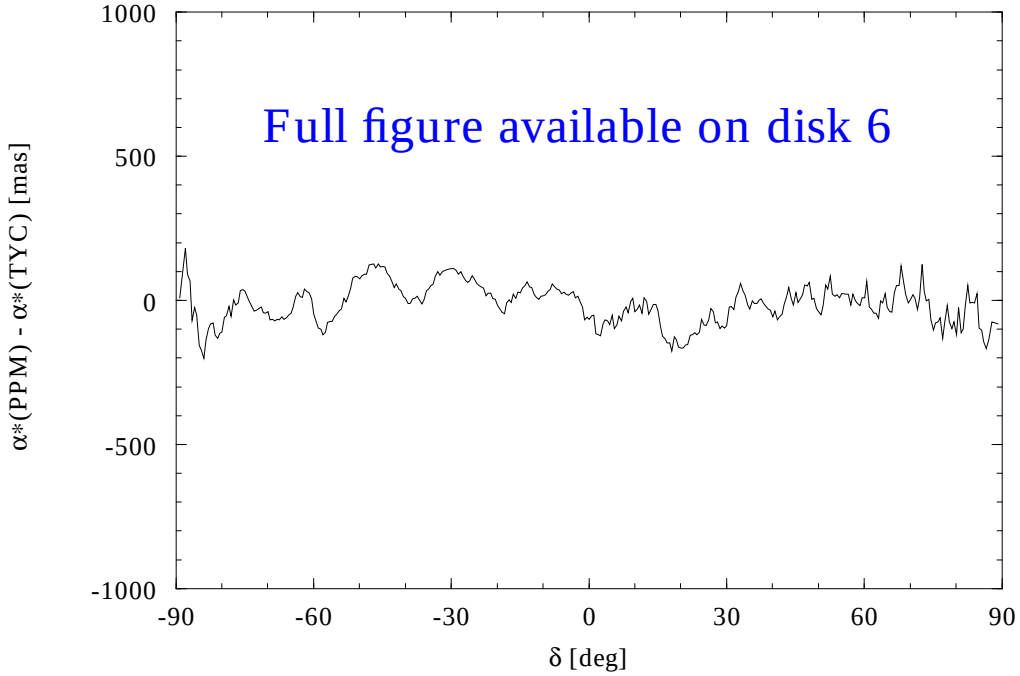

Figure 3.4.37. *Difference between $\alpha*$ from PPM (after rotation to the Hipparcos reference frame) and $\alpha*$ from the Tycho Catalogue, versus δ, as a density plot, for recommended Tycho Catalogue stars fainter than $B_T = 10$ mag. The colour scale indicates the number of stars in a cell of $0.5^\circ \times 8$ mas. The curve is the median difference over intervals of 0.5°.*

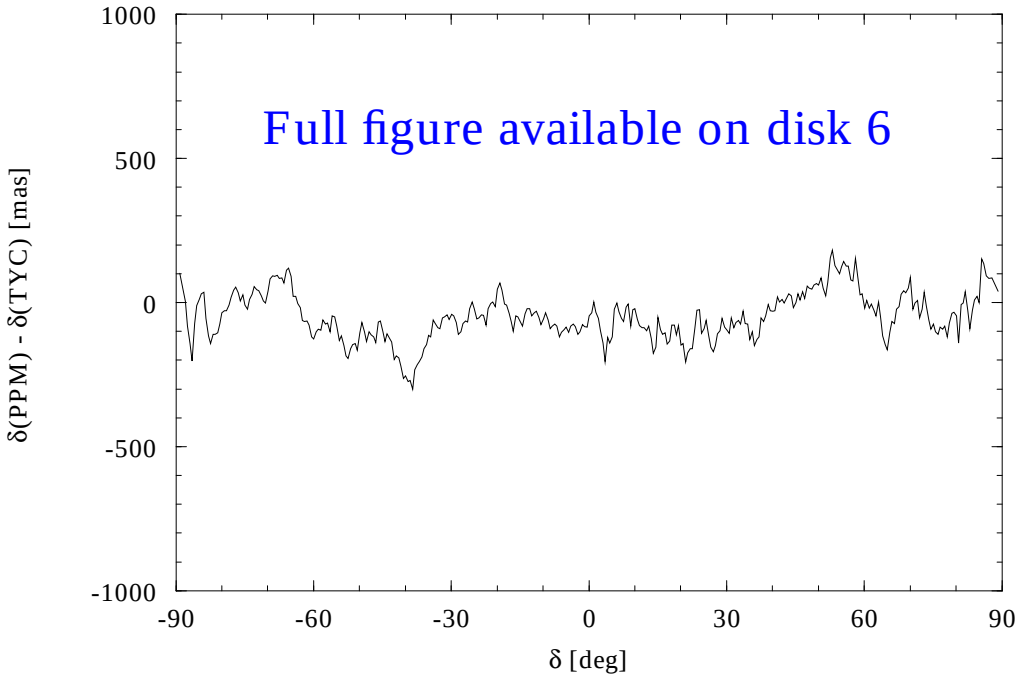

Figure 3.4.38. *Difference between δ from PPM (after rotation to the Hipparcos reference frame) and δ from the Tycho Catalogue, versus δ, as a density plot, for recommended Tycho Catalogue stars fainter than $B_T = 10$ mag. The colour scale indicates the number of stars in a cell of $0.5^\circ \times 8$ mas. The curve is the median difference over intervals of 0.5°.*

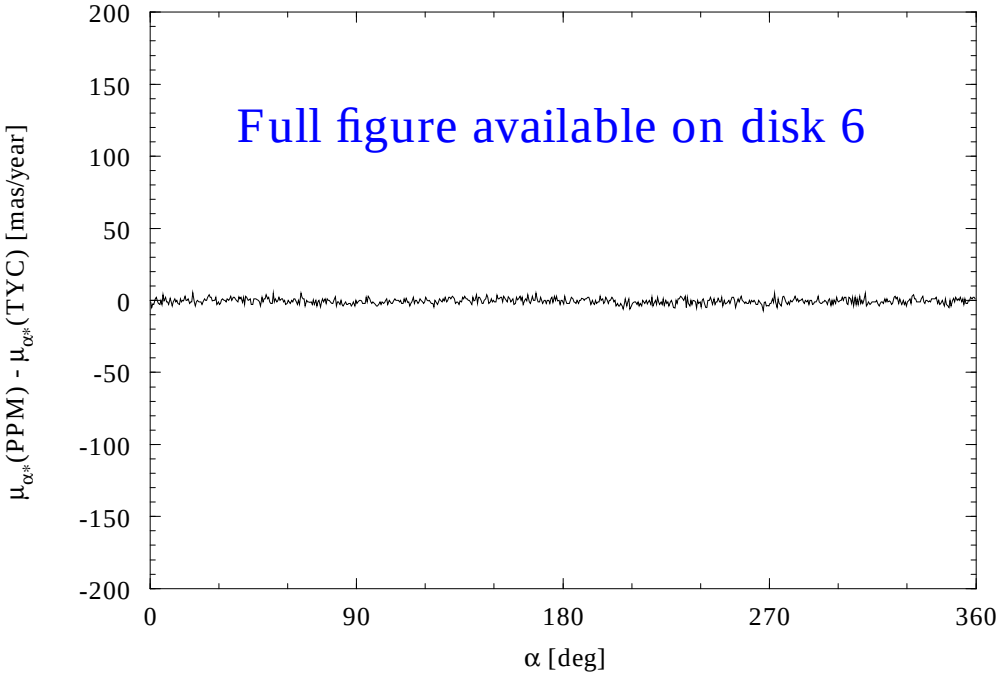

Figure 3.4.39. *Difference between $\mu_{\alpha *}$ from PPM (after rotation to the Hipparcos reference frame) and $\mu_{\alpha *}$ from the Tycho Catalogue, versus α, as a density plot, for recommended Tycho Catalogue stars fainter than $B_T = 10$ mag. The colour scale indicates the number of stars in a cell of $1^\circ \times 2$ mas/yr. The curve is the median difference over intervals of 0.5°.*

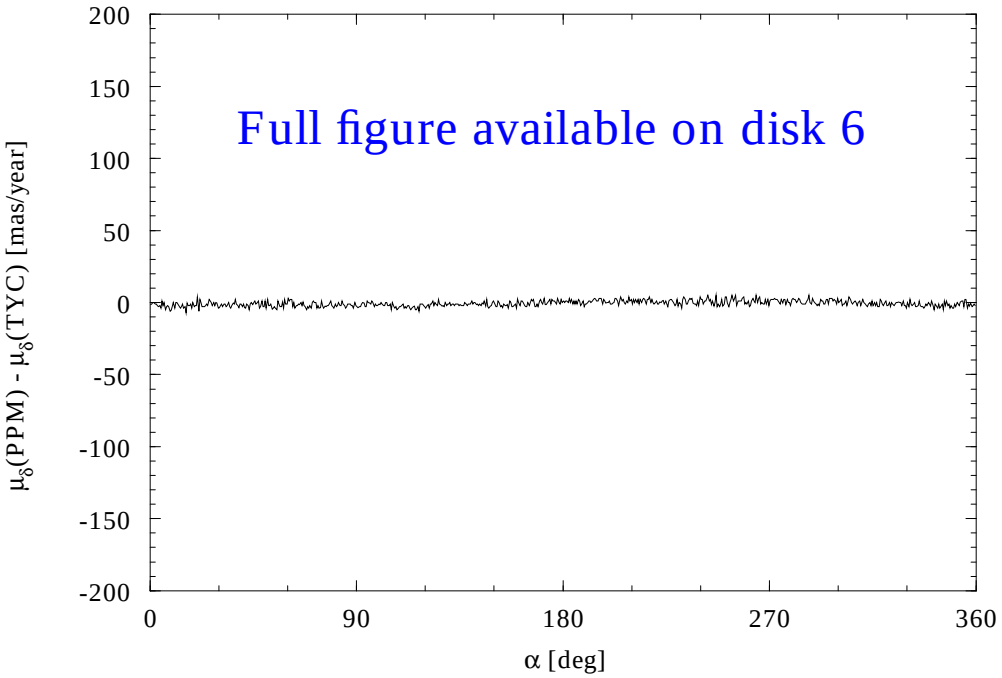

Figure 3.4.40. *Difference between μ_δ from PPM (after rotation to the Hipparcos reference frame) and μ_δ from the Tycho Catalogue, versus α, as a density plot, for recommended Tycho Catalogue stars fainter than $B_T = 10$ mag. The colour scale indicates the number of stars in a cell of $1^\circ \times 2$ mas/yr. The curve is the median difference over intervals of 0.5°.*

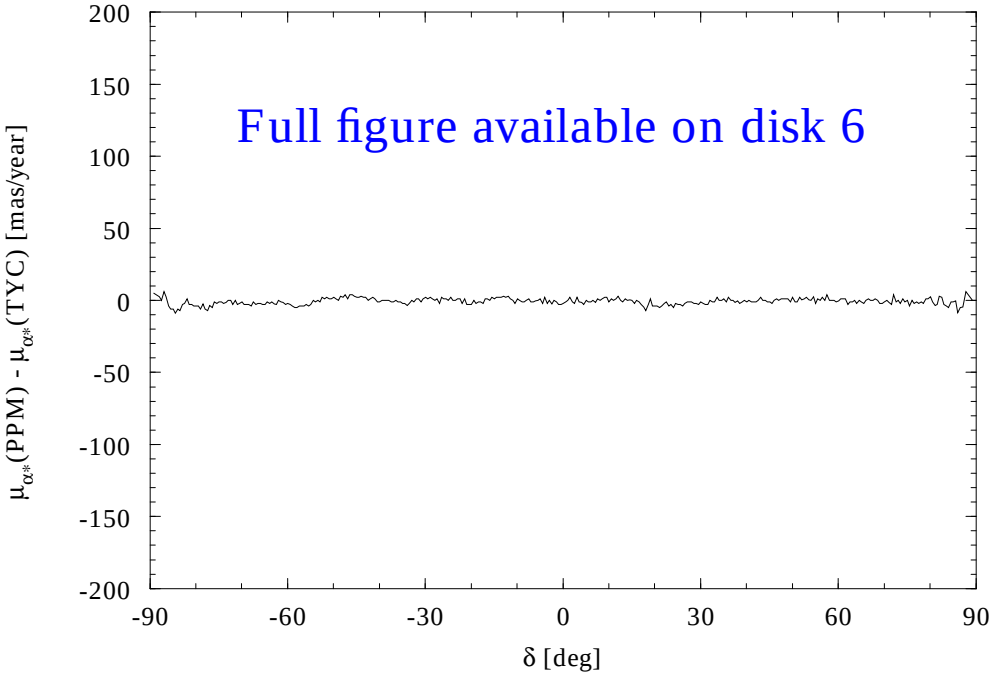

Figure 3.4.41. *Difference between $\mu_{\alpha *}$ from PPM (after rotation to the Hipparcos reference frame) and $\mu_{\alpha *}$ from the Tycho Catalogue, versus δ, as a density plot, for recommended Tycho Catalogue stars fainter than $B_T = 10$ mag. The colour scale indicates the number of stars in a cell of $0.5^\circ \times 2$ mas/yr. The curve is the median difference over intervals of 0.5°.*

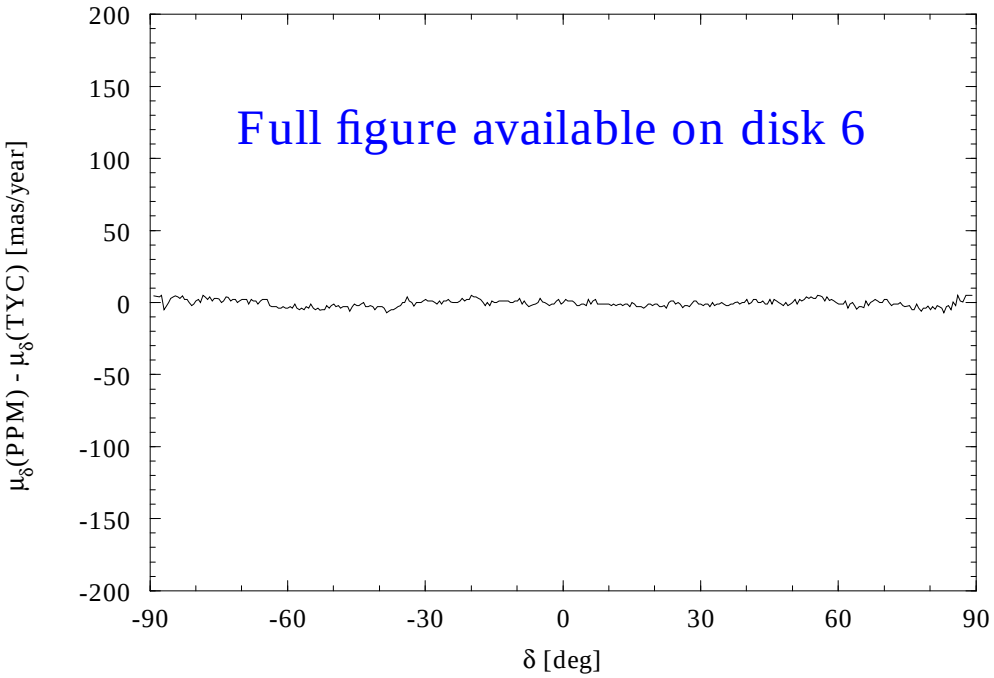

Figure 3.4.42. *Difference between μ_δ from PPM (after rotation to the Hipparcos reference frame) and μ_δ from the Tycho Catalogue, versus δ, as a density plot, for recommended Tycho Catalogue stars fainter than $B_T = 10$ mag. The colour scale indicates the number of stars in a cell of $0.5^\circ \times 2$ mas/yr. The curve is the median difference over intervals of 0.5°.*

Section 3.5

Statistical Properties: Astrophysical Relationships

3.5. Statistical Properties: Astrophysical Relationships

In this section a number of astrophysical relationships in the Hipparcos Catalogue are illustrated. Most prominent of these are a set of Hertzsprung-Russell diagrams using two different systems of colour/magnitude representation, and for different selections of stars, based on their precision or other properties.

3.5.1. Hertzsprung-Russell Diagrams

Hertzsprung-Russell (HR) diagrams are presented in the form of (observational) luminosity-colour diagrams, with two choices for the photometric parameters: (i) M_V versus $B-V$, and (ii) M_{Hp} versus $V-I$. For a definition of these quantities, refer to Section 1.3. The absolute luminosities were computed as:

$$M_V = V + 5\log\pi - 10$$
$$M_{Hp} = Hp + 5\log\pi - 10$$

where the parallax, π, is in milliarcsec. Interpretation of the detailed astrophysical features of the observational HR diagram must take into account effects such as the *a priori* selection of stars in the catalogue, Lutz-Kelker bias (T.E. Lutz, D.H. Kelker, 1973, *Mon. Not. R. Astron. Soc.* 85, 573), and the fact that the expectation of the stellar distance can differ from that of the inverse of the parallax (H. Smith, H. Eichhorn, 1996, *Mon. Not. R. Astron. Soc.* 281, 211), effects which are ignored in the presentation of the observational properties of the catalogue in this section.

For the general HR diagrams three different sets of stars were selected according to the precision of their parallax and colour index:

(i) $\sigma_\pi/\pi < 0.05$ (corresponding to an error in the absolute magnitudes σ_M of about 0.1 mag), and standard error of the colour index $\sigma_{\rm CI} \le 0.025$;

(ii) $\sigma_\pi/\pi < 0.1$ (corresponding to $\sigma_M \simeq 0.2$ mag), and $\sigma_{\rm CI} \le 0.025$;

(iii) $\sigma_\pi/\pi < 0.2$ (corresponding to $\sigma_M \simeq 0.4$ mag), and $\sigma_{\rm CI} \le 0.05$.

where the subscript CI refers to the colour index ($B - V$ or $V - I$, as appropriate). Double stars have been excluded from most diagrams, as indicated in the captions. In the Hipparcos main catalogue, Hp magnitudes are often given for such systems for a combination of components (as indicated in Field H48, or in the Notes). Use of these magnitudes leads to a systematic over-estimation of the absolute magnitudes compared with those of single stars. For the diagrams where the caption indicates the inclusion of single stars only, catalogue entries included in any of the parts of the Double and Multiple Star Annex have been excluded.

Since the global Hipparcos Catalogue is not a complete catalogue in any sense, caution must be exercised in drawing conclusions of a statistical nature from the present diagrams; in general there will be a strong bias towards stars with a higher apparent

luminosity (cf. Figure 1.1.1), in particular for stars with less precisely determined distances (since the relative parallax precision is correlated with the parallax, cf. Figure 3.5.19).

Some of the most prominent features of the Hipparcos HR diagram have been discussed, for a preliminary version of the catalogue, by M.A.C. Perryman *et al.*, 1995, *Astron. Astrophys.* 304, 69.

Figures 3.5.1, 3.5.3, and 3.5.5 give $M_V, B-V$ diagrams for the three star selections. In these, and most of the following diagrams, the number of stars in a cell of size 0.01 mag in $B-V$ and 0.05 mag in M_V has been colour coded according to the (logarithmic) scale given in the figure. Figures 3.5.2, 3.5.4, and 3.5.6 give $M_{Hp}, V-I$ diagrams for the same three star selections.

Figure 3.5.7 illustrates the relative contributions from stars of the three precision classes to the diagram in Figure 3.5.6: i.e. the stars in set (i), the stars in set (ii) not occurring in (i), and the stars in set (iii) not in sets (i) and (ii). The lower end of the HR diagram, largely populated by nearby stars with well-determined distances, is dominated by stars in the highest precision class. The presence of a distinct 'spine' shows that the broadening of the diagram when including less precise data is not only due to the statistical effect of including more stars, but is also a consequence of the progressively degrading measurement accuracy. In general the 'wings' are mostly extended towards the brighter stars, a consequence of the selection effects intrinsic in the Hipparcos Catalogue.

Figure 3.5.8 illustrates that the fraction of stars that have a non-blank coarse variability flag (Field H6) is quite variable over the Hertzsprung-Russell diagram. Figures 3.5.9 and 3.5.10 give the position in the $M_{Hp}, V-I$ diagram for single and double stars with the coarse variability indicator (Field H6) set. Almost all very red giants are variable in the category 2 (i.e. variability amplitude in the range 0.06–0.6 mag). Stars with variability amplitude larger than 0.6 mag are almost all on the main sequence. Mira variables could be expected to appear on the giant branch; only one such variable in the Hipparcos Catalogue meets both criteria on precision, however.

The subsequent diagrams show the position of stars of different variability categories in the $M_{Hp}, V-I$ diagram: eclipsing binaries in Figure 3.5.11; pulsating variables in Figure 3.5.12; rotating variables in Figure 3.5.13; and eruptive variables in Figure 3.5.14. All categories present in variability annexes 1 and 2 (periodic and unsolved variables, respectively) having more than 5 members with the quoted relative distance and colour index precision have been included.

The Hertzsprung-Russell diagram for stars in Part C of the Double and Multiple Systems Annex (i.e. the 'component solutions' of DMSA/C) is shown in Figure 3.5.15. All values have been taken from the main catalogue, so that in the cases where the components are not separated ('*' or '-' in Field H48) the total magnitude has been used, with the consequence that such systems are displaced higher in the diagram compared with single stars. The average value of this offset is expected to be 0.3 mag for components of equal colour index. This is further illustrated in Figure 3.5.16, which shows the ratio of the numbers of double and multiple stars (as in the previous figure) compared with the union of double and multiple stars and the single stars (as in Figure 3.5.6). The distribution is as expected for the ratio of two distributions of which one is slightly offset: for reasonable distributions the maximum ratio is expected near the boundary.

3.5.2. Other Diagrams

Figure 3.5.17 shows the distribution of the relative distance precision σ_π/π as a function of the *Hp* magnitude. The distribution follows rather closely the distribution of *Hp*, as shown in Section 3.2, but somewhat shifted to fainter stars, an effect caused by the fact that the fainter stars tend to lie at larger distances, and consequently have a higher (numerical) value of the precision. Figure 3.5.18 relates the parallax to the *Hp* magnitude for stars with $\sigma_\pi/\pi < 0.2$. The sharp edge at the bottom of the diagram is directly related to this limit, and follows the distribution of σ_π as a function of *Hp*. Nearby stars are found for all magnitudes, but there is a slight increase in concentration for the faintest stars, due to the selection made for the Hipparcos Input Catalogue. Figure 3.5.19 shows the correlation between σ_π/π and π; the main features of this diagram reflect the fact that the parallax standard error is $\sigma_\pi \simeq 1$ mas for most stars in the catalogue. The relationship between the transverse velocity, computed as in Equation 1.2.20, and the parallax is shown in Figure 3.5.20.

Figure 3.5.21 shows the parallax as a function of the $B-V$ colour index, essentially reflecting the features of the histogram of the $B-V$ colour index. The rising feature near $B-V = 1.5$ mag corresponds to the lower part of the main sequence; these intrinsically faint stars could only be observed by Hipparcos if they are relatively nearby.

The relation between the parallax and the total proper motion $|\mu|$ is shown in Figure 3.5.22. The relationship between the total proper motion and the *Hp* magnitude is shown in Figure 3.5.23. For fainter stars there are two groups: the nearby faint stars with high proper motion, and the intrinsically bright, distant stars. The relationship between the total proper motion and the $B-V$ colour index (Figure 3.5.24) follows closely the distribution of stars with this colour index.

The features of the relationship between $Hp-V$ versus $B-V$ (Figure 3.5.25) and between $Hp-V_T$ versus B_T-V_T (Figure 3.5.26) are described in Section 1.3, Appendix 4.

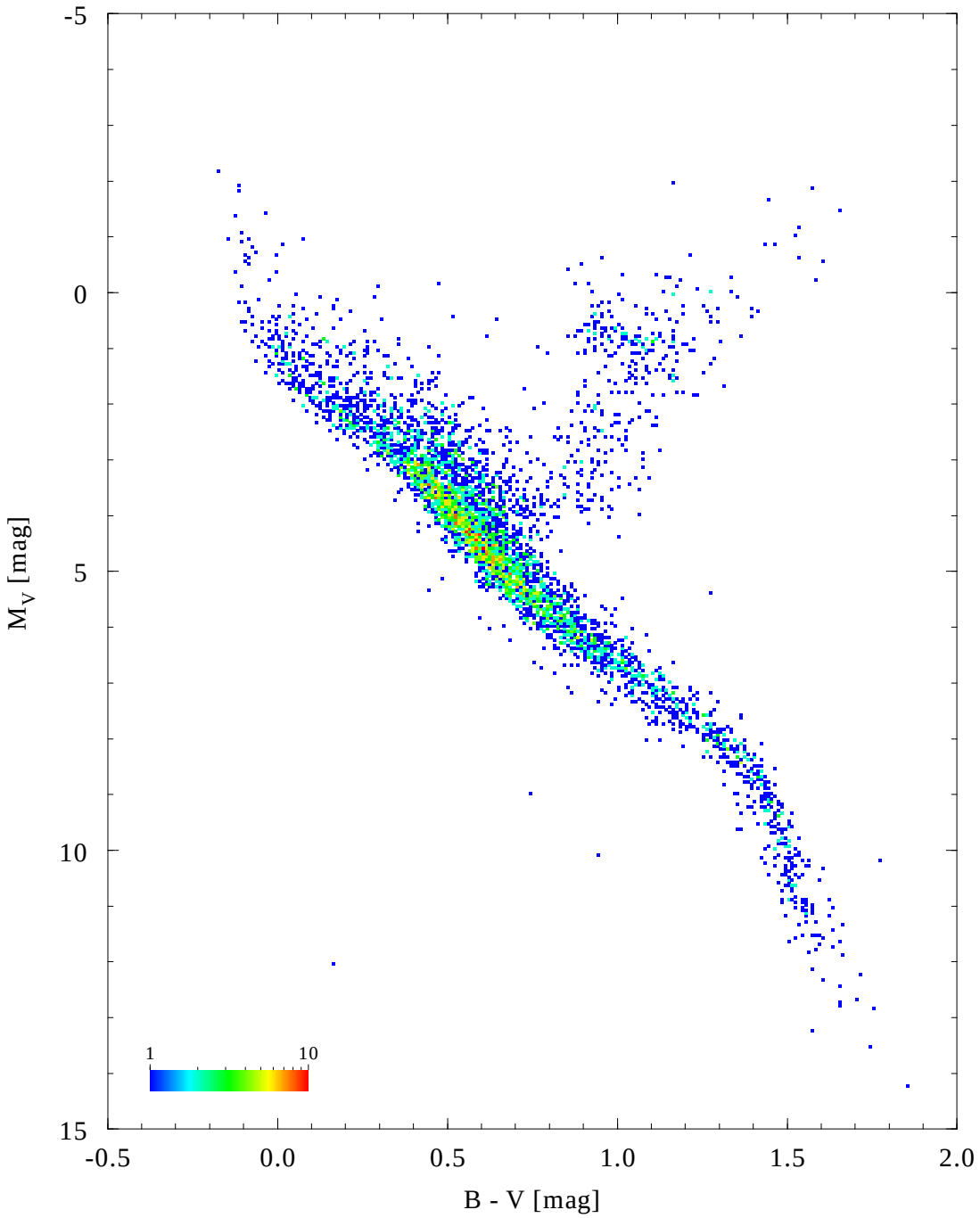

Figure 3.5.1. *$(M_V, B-V)$ diagram for the 4902 single stars from the Hipparcos Catalogue with relative distance precision $\sigma_\pi/\pi < 0.05$ and $\sigma_{B-V} \leq 0.025$ mag. Colours indicate number of stars in a cell of 0.01 mag in $B-V$ and 0.05 mag in M_V.*

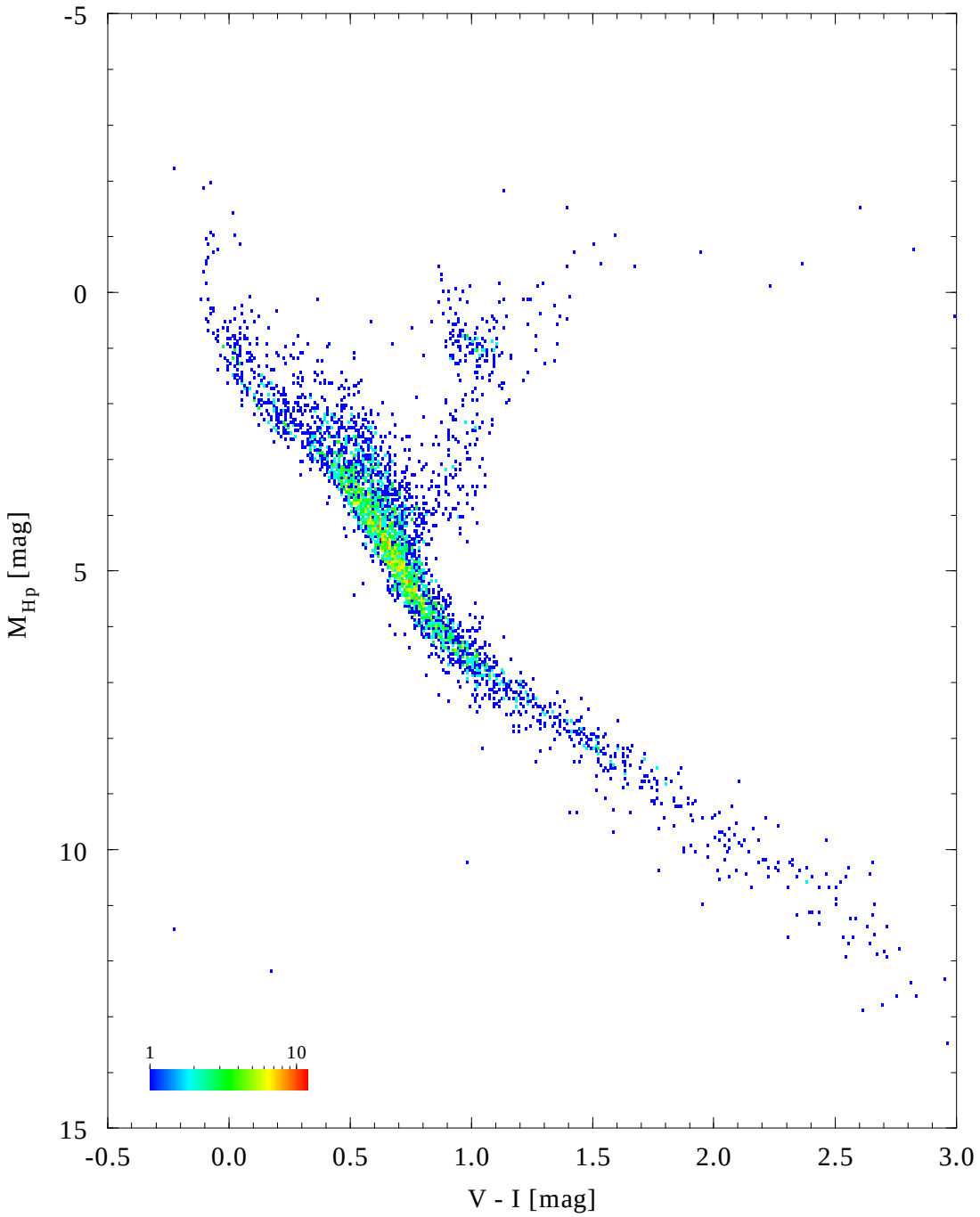

Figure 3.5.2. *$(M_{Hp}, V-I)$ diagram for the 4477 single stars from the Hipparcos Catalogue with relative distance precision $\sigma_\pi/\pi < 0.05$ and $\sigma_{V-I} \leq 0.025$ mag. Colours indicate number of stars in a cell of 0.01 mag in $V-I$ and 0.05 mag in M_{Hp}.*

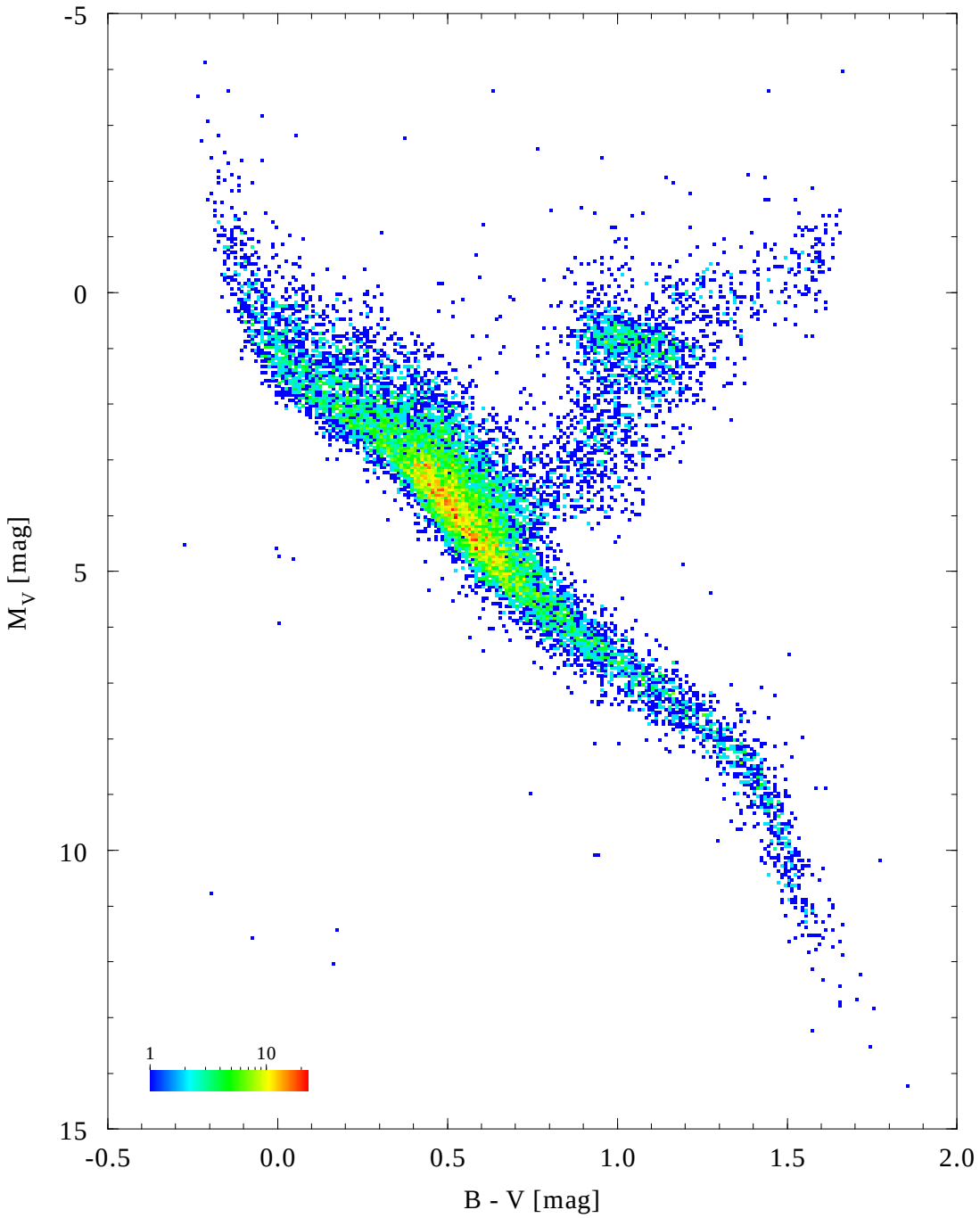

Figure 3.5.3. *$(M_V, B-V)$ diagram for the 16 631 single stars from the Hipparcos Catalogue with relative distance precision $\sigma_\pi/\pi < 0.1$ and $\sigma_{B-V} \leq 0.025$ mag. Colours indicate number of stars in a cell of 0.01 mag in $B-V$ and 0.05 mag in M_V.*

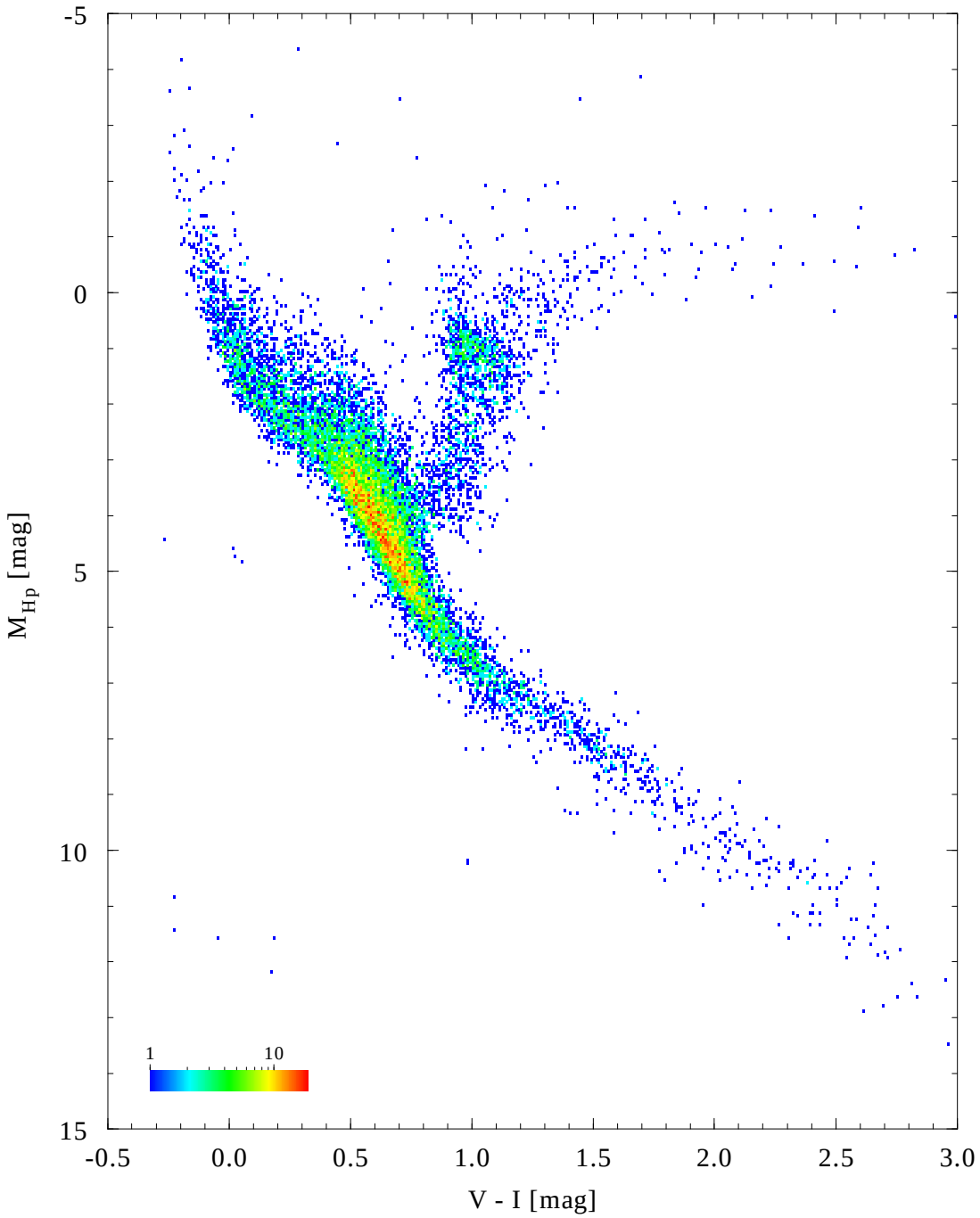

Figure 3.5.4. *$(M_{Hp}, V-I)$ diagram for the 15 727 single stars from the Hipparcos Catalogue with relative distance precision $\sigma_\pi/\pi < 0.1$ and $\sigma_{V-I} \leq 0.025$ mag. Colours indicate number of stars in a cell of 0.01 mag in $V-I$ and 0.05 mag in M_{Hp}.*

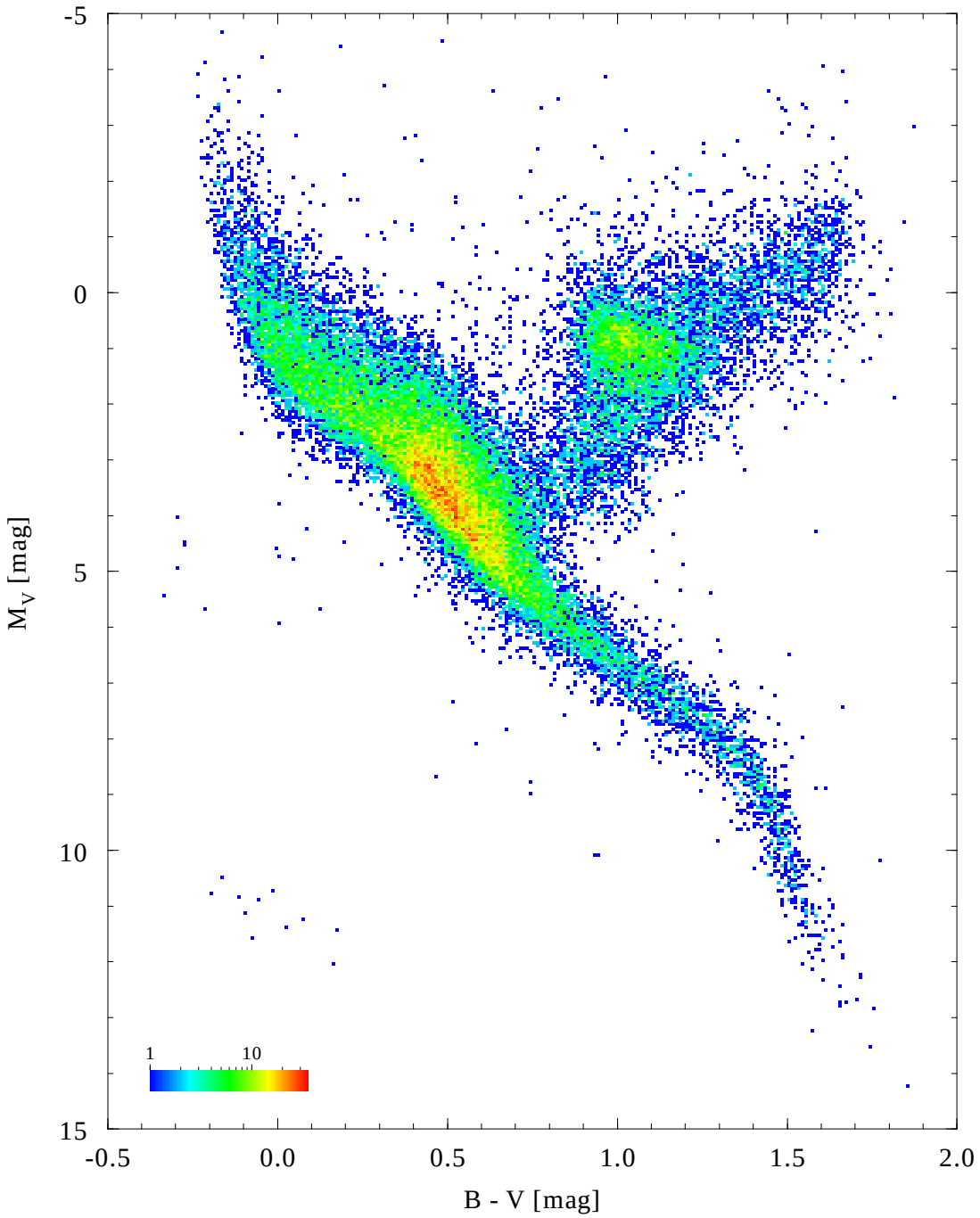

Figure 3.5.5. *$(M_V, B-V)$ diagram for the 41 704 single stars from the Hipparcos Catalogue with relative distance precision $\sigma_\pi/\pi < 0.2$ and $\sigma_{B-V} \leq 0.05$ mag. Colours indicate number of stars in a cell of 0.01 mag in $B-V$ and 0.05 mag in M_V.*

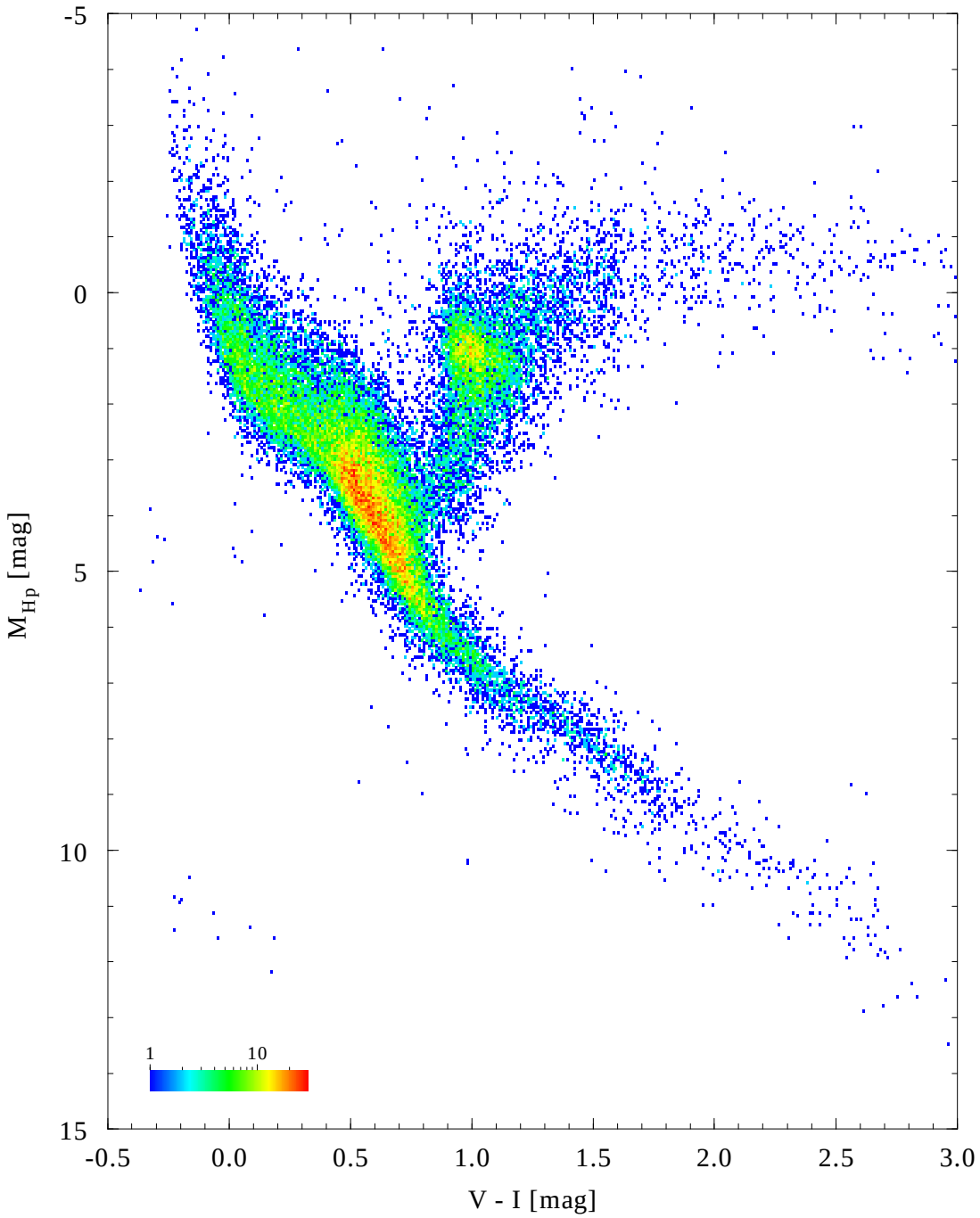

Figure 3.5.6. *$(M_{Hp}, V-I)$ diagram for the 41 453 single stars from the Hipparcos Catalogue with relative distance precision $\sigma_\pi/\pi < 0.2$ and $\sigma_{V-I} \leq 0.05$ mag. Colours indicate number of stars in a cell of 0.01 mag in $V-I$ and 0.05 mag in M_{Hp}.*

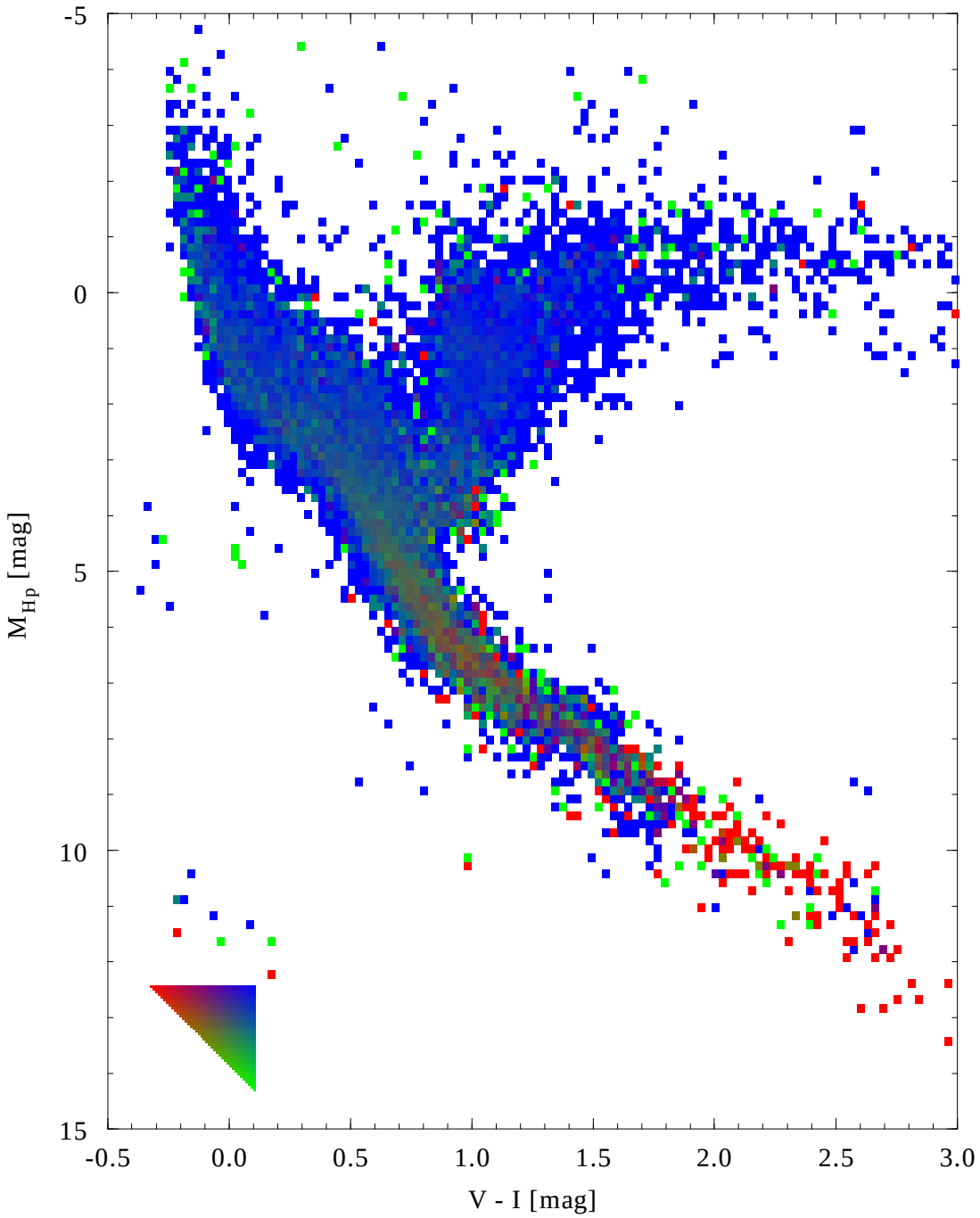

Figure 3.5.7. *Relative contribution of single stars with relative distance precision $\sigma_\pi/\pi < 0.05$ (red), $0.05 \leq \sigma_\pi/\pi < 0.1$ (green), and $0.1 \leq \sigma_\pi/\pi < 0.2$ (blue) to the $(M_{Hp}, V-I)$ diagram. The cell size is 0.03 mag in $V-I$ and 0.15 mag in M_{Hp}. The triangular colour scale covers all possibilities (the contribution from the 'red' category decreases from 100 per cent to 0 per cent from left to right, the contribution from the 'green' category decreases from 100 per cent to 0 per cent from bottom to top, and the 'blue' category comprises the remaining stars, and is therefore 100 per cent at top right).*

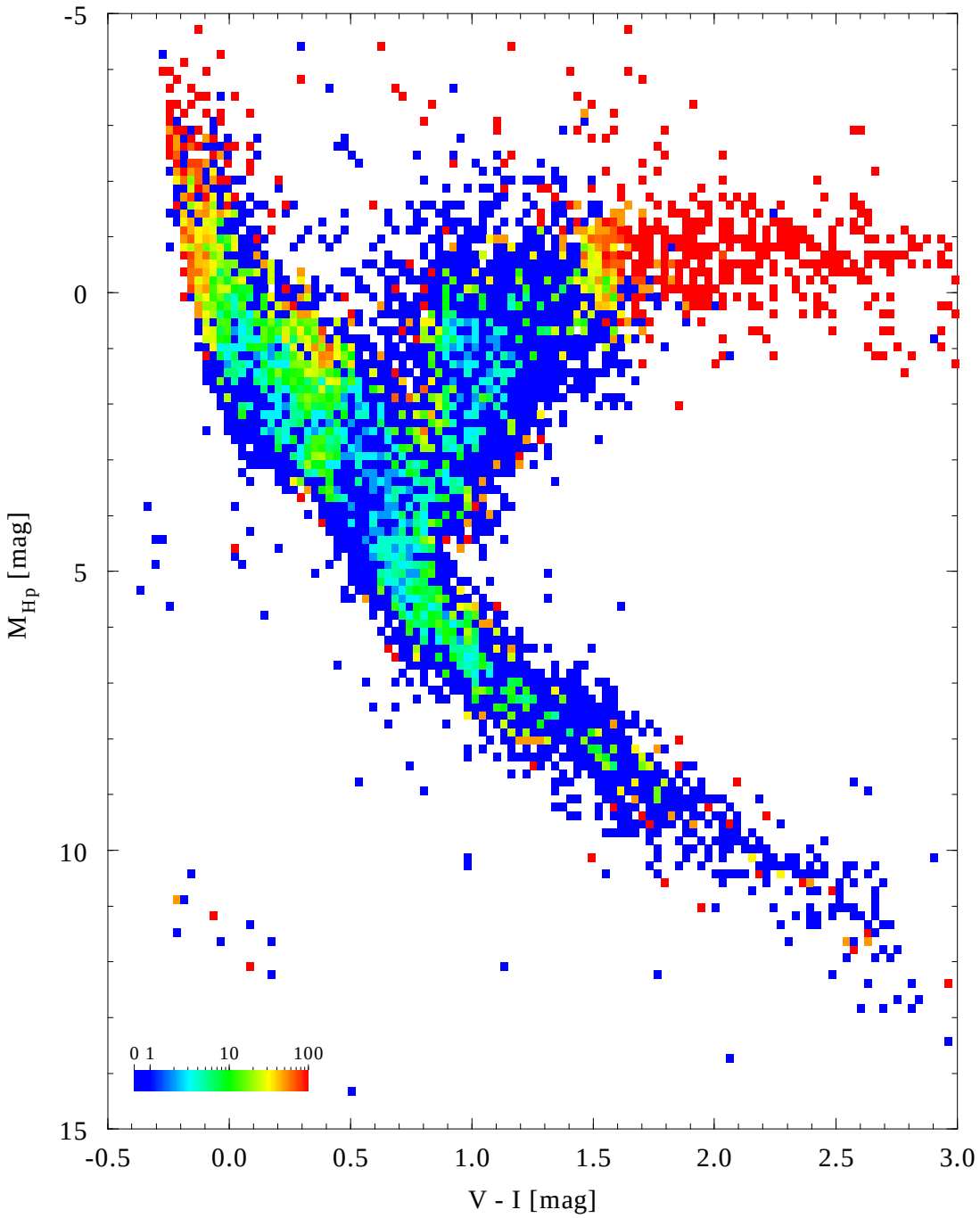

Figure 3.5.8. *Fraction of stars that are variable (Field H6 non-blank) in a $(M_{Hp}, V-I)$ diagram. In each cell of 0.03 mag in $V-I$ and 0.15 mag in M_{Hp}, the percentage of variable stars is coded according to the colour scale.*

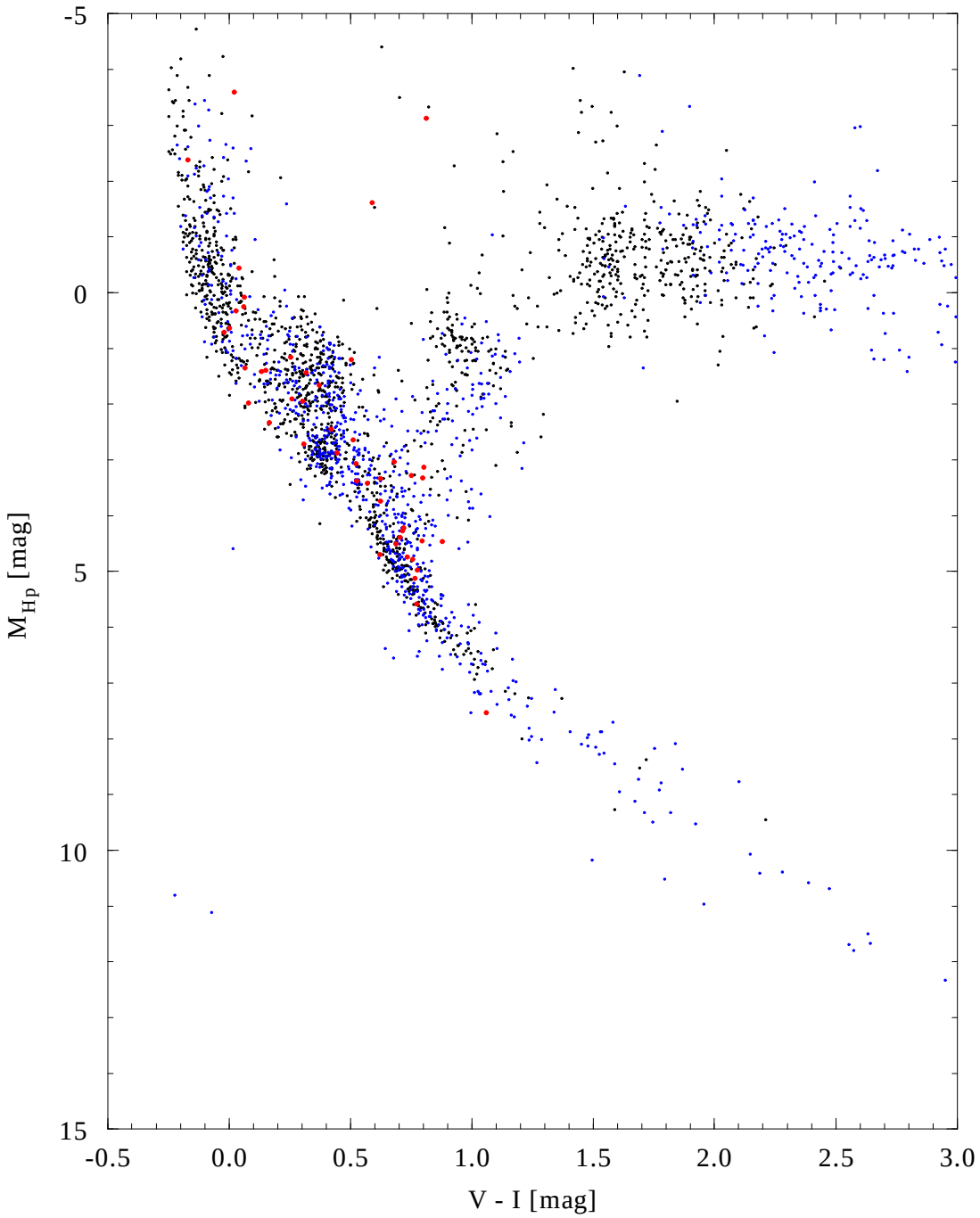

Figure 3.5.9. *($M_{Hp}, V-I$) diagram for single stars from the Hipparcos Catalogue with coarse variability indicator (Field H6) non-blank, and with relative distance precision $\sigma_\pi/\pi < 0.2$ and $\sigma_{V-I} \leq 0.05$. The values of the coarse variability flag are coded by different colours: 1 (< 0.06 mag, 1512 stars) = black, 2 (0.06 – 0.6 mag, 977 stars) = blue, and 3 (> 0.6 mag, 48 stars) = red.*

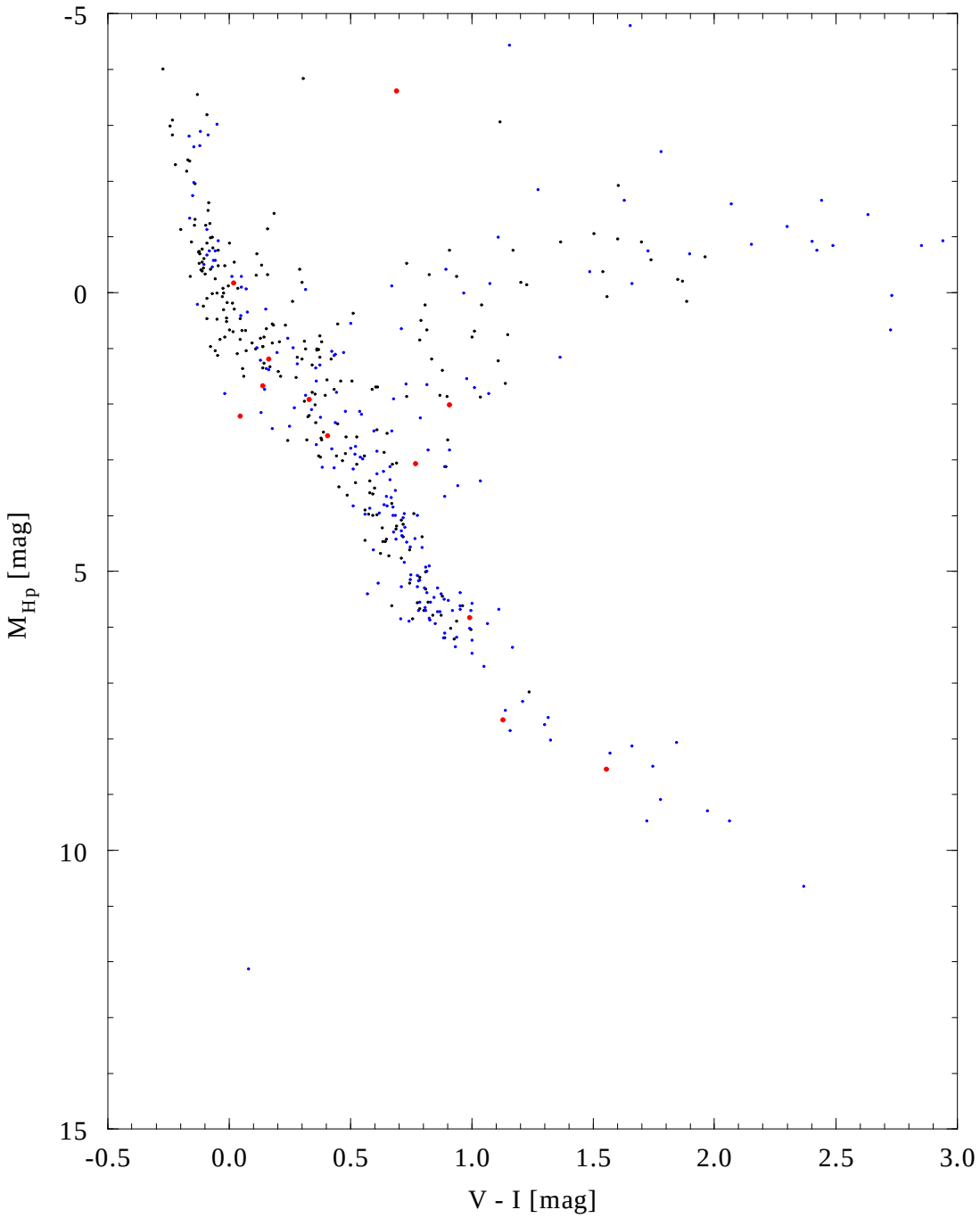

Figure 3.5.10. *$(M_{Hp}, V-I)$ diagram for stars from all parts of the DMSA with coarse variability indicator (Field H6) non-blank, and with relative distance precision $\sigma_\pi/\pi < 0.2$ and $\sigma_{V-I} \leq 0.05$. The values of the coarse variability flag are coded by different colours: 1 (< 0.06 mag, 238 stars) = black, 2 (0.06 – 0.6 mag, 206 stars) = blue, and 3 (> 0.6 mag, 16 stars) = red.*

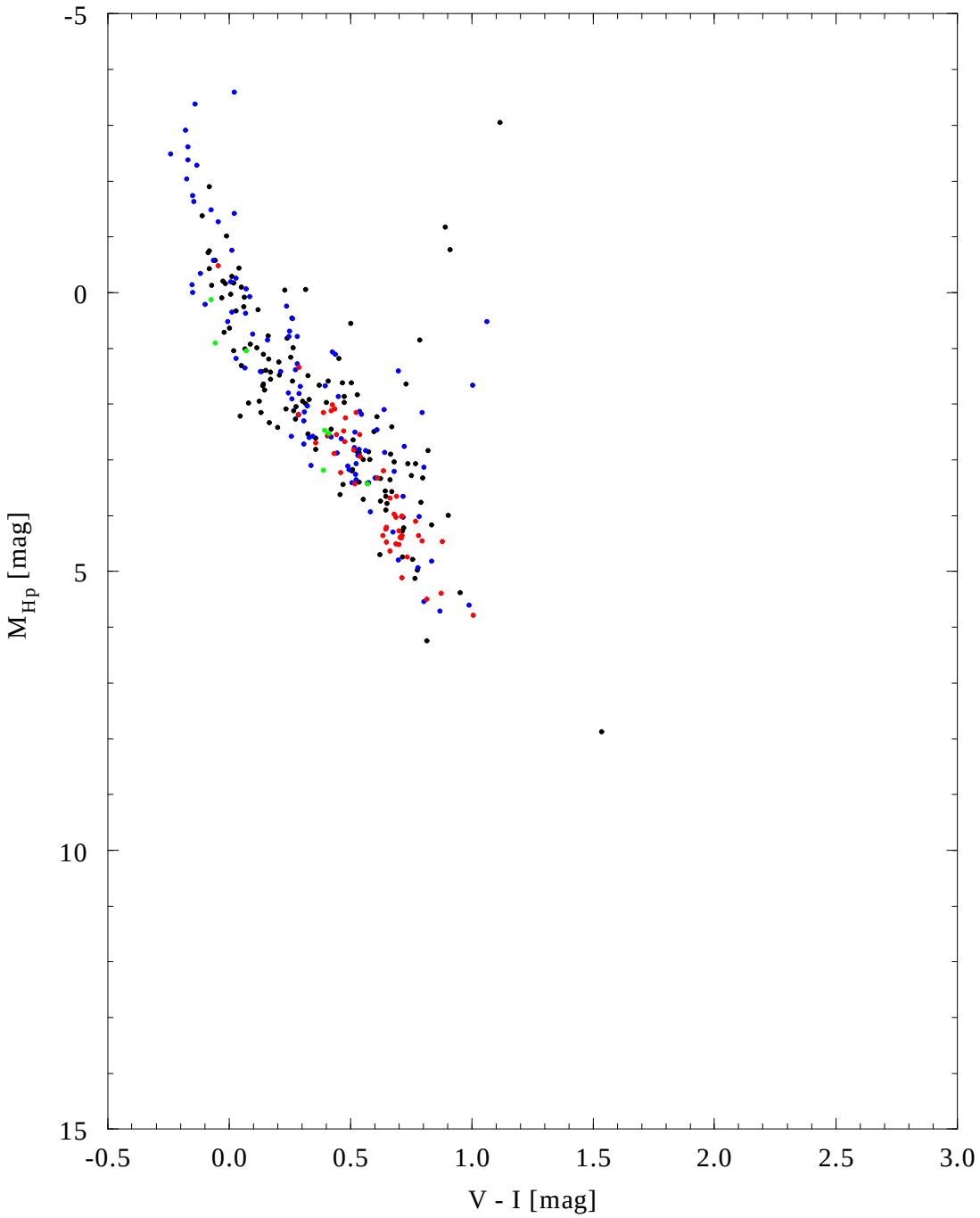

Figure 3.5.11. *($M_{Hp}, V-I$) diagram for eclipsing binary stars in the Variability Annex, Part 1 (Periodic Variables) with relative distance precision $\sigma_\pi/\pi < 0.2$ and $\sigma_{V-I} \leq 0.05$ mag. ●: Algol type (EA, 125 stars), ●: β Lyrae type (EB, 95 stars), ●: W Ursae Majoris type (EW, 48 stars), ●: other E (7 stars).*

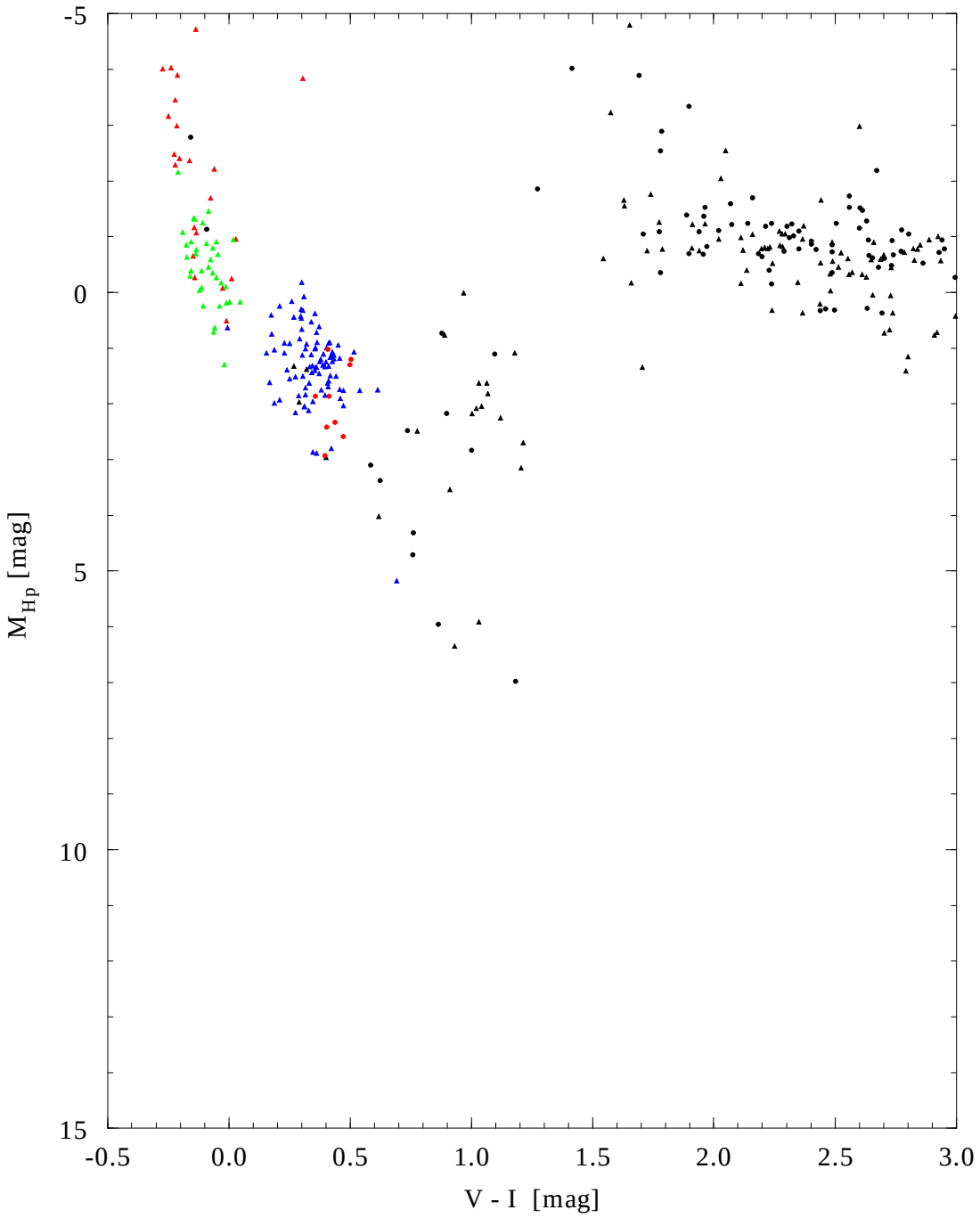

Figure 3.5.12. *(M_{Hp}, $V-I$) diagram for pulsating types of variable stars in the Variability Annexes, Part 1 (Periodic Variables) and Part 2 (Unsolved Variables) with relative distance precision $\sigma_\pi/\pi < 0.2$ and $\sigma_{V-I} \leq 0.05$ mag. ▲: semi-regular (SR..., 116 stars), ▲: δ Scuti type (DSCT, 89 stars), ▲: β Cephei type (BCEP..., 24 stars), ▲: small-amplitude multi-period pulsating stars (SPB, 35 stars), ●: slow irregular (L..., 93 stars), ●: RR Lyrae type (RR..., 9 stars).*

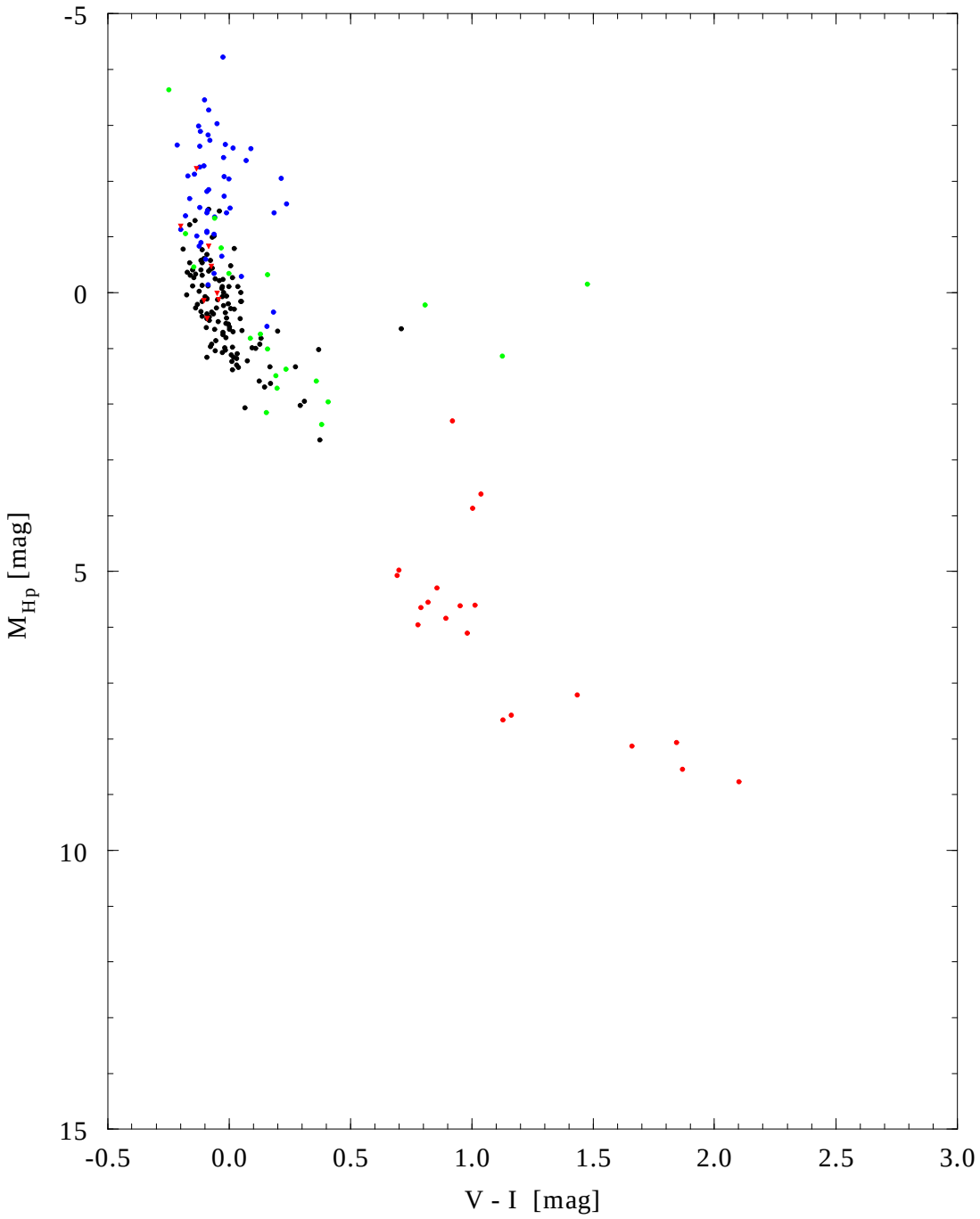

Figure 3.5.13. *($M_{Hp}, V-I$) diagram for rotating types of variable stars in the Variability Annexes, Part 1 (Periodic Variables) and Part 2 (Unsolved Variables) with relative distance precision $\sigma_\pi/\pi < 0.2$ and $\sigma_{V-I} \leq 0.05$ mag. ●: α^2 Canum Venaticorum type (ACV, 114 stars), ●: γ Cassiopeiae type (GCAS, 49), ●: BY Draconis type (BY, 20 stars), ●: rotating ellipsoidal type (ELL..., 20 stars), ▼: SX Arietis type (SXARI, 8 stars).*

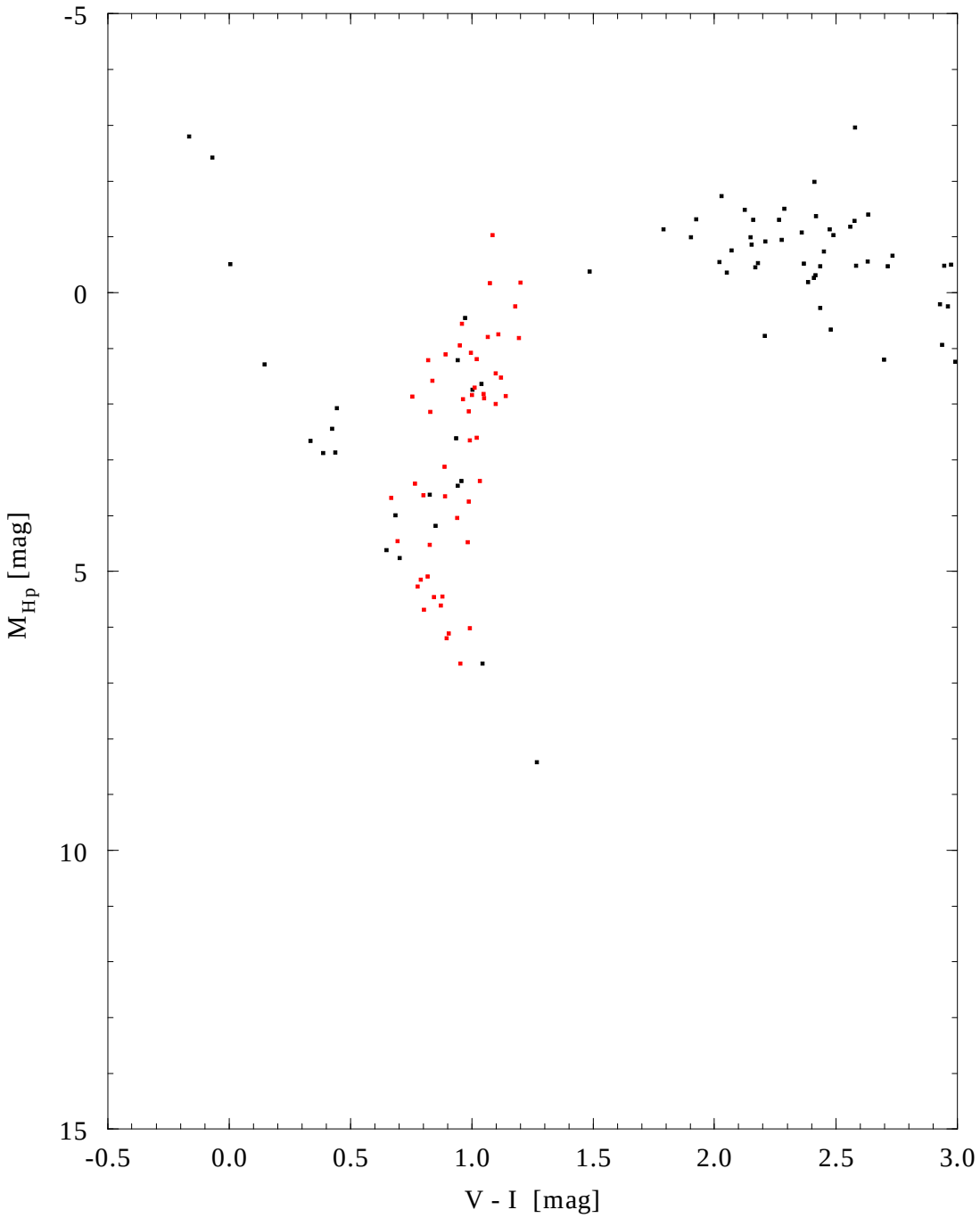

Figure 3.5.14. *$(M_{Hp}, V-I)$ diagram for eruptive types of variable stars in the Variability Annexes, Part 1 (Periodic Variables) and Part 2 (Unsolved Variables) with relative distance precision $\sigma_\pi/\pi < 0.2$ and $\sigma_{V-I} \leq 0.05$. ■: irregular (I..., 76 stars), ■: RS Canum Venaticorum type (RS, 50 stars).*

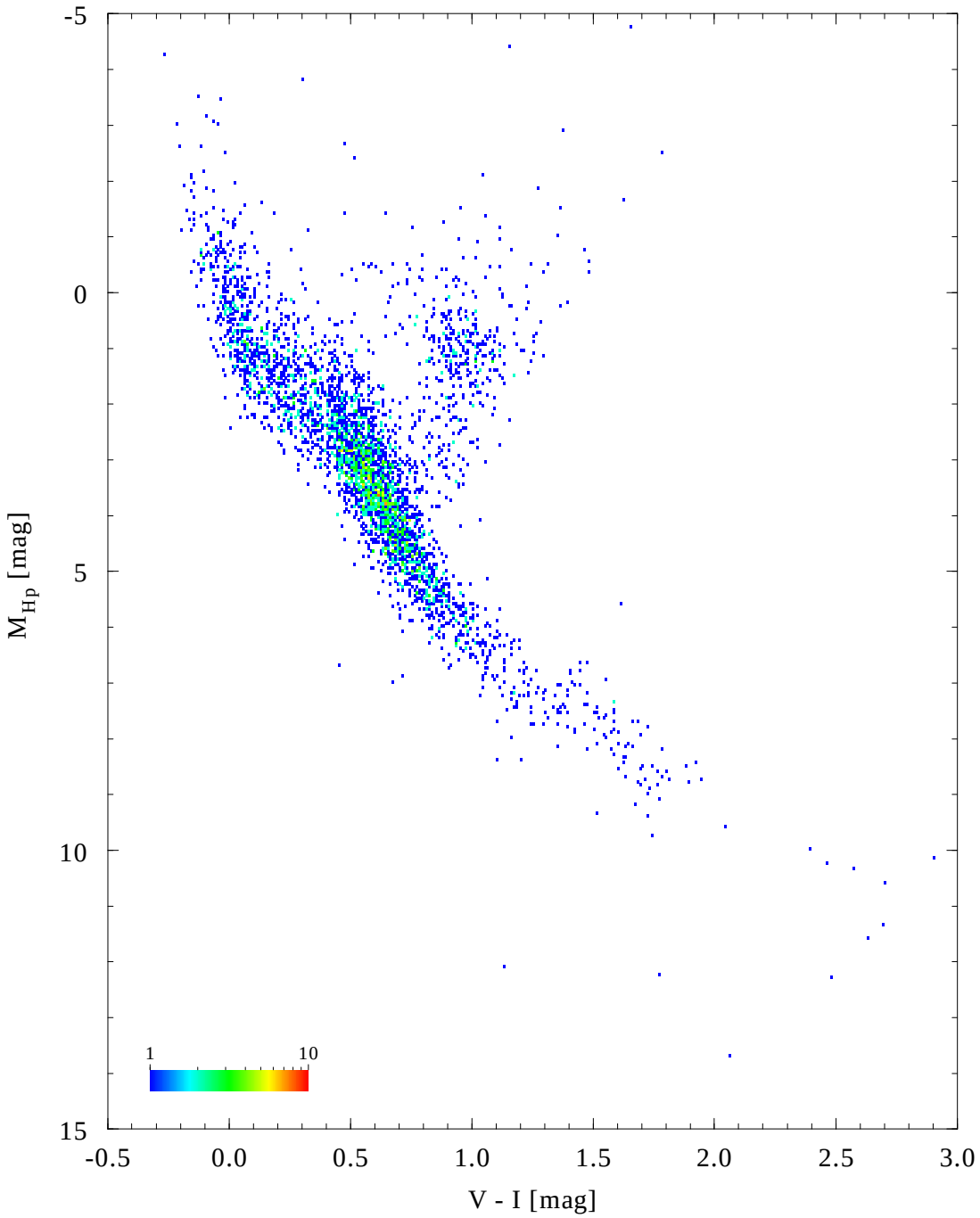

Figure 3.5.15. *$(M_{Hp}, V-I)$ diagram for 3926 stars in the Double and Multiple Systems Annex, Component Solutions (DMSA/C) with relative distance precision $\sigma_\pi/\pi < 0.2$ and $\sigma_{V-I} \leq 0.05$ mag. All parameters are taken from the main Hipparcos Catalogue. Colours indicate the number of stars in a cell of 0.01 mag in $V-I$ and 0.05 mag in M_{Hp}.*

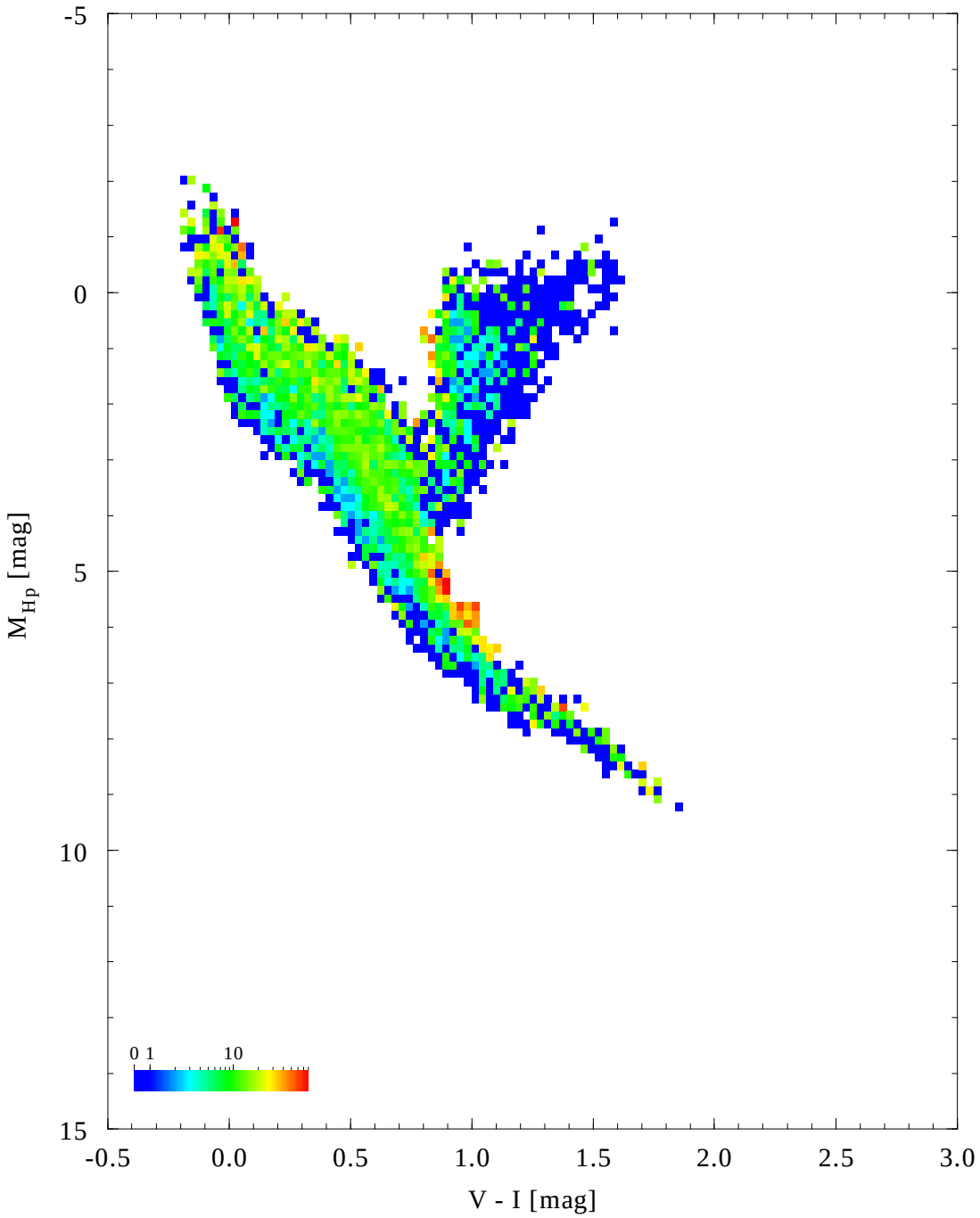

Figure 3.5.16. *Fraction of stars that are double or multiple (Field H59 = 'C') in the $(M_{Hp}, V-I)$ diagram. In each cell of 0.03 mag in $V-I$ and 0.15 mag in M_{Hp} with at least 5 stars, the relevant percentage is coded according to the colour scale.*

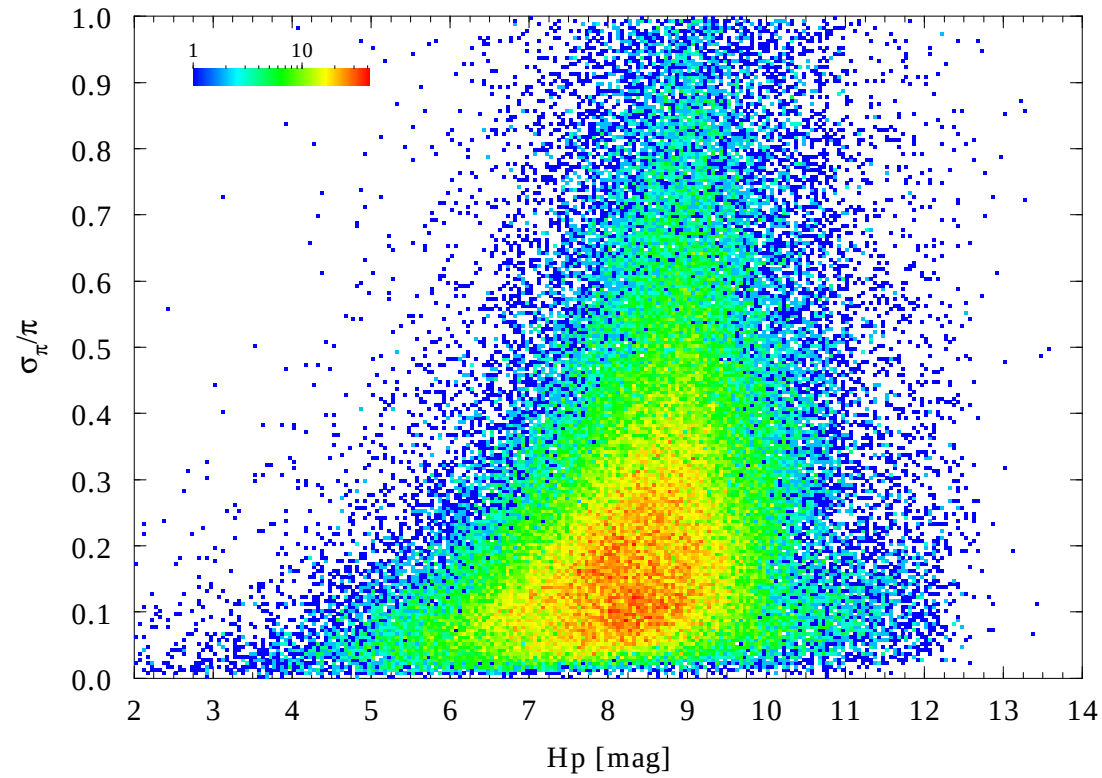

Figure 3.5.17. *Hipparcos Catalogue: relative distance precision σ_π/π versus Hp magnitude (bin size 0.05 mag in Hp and 0.005 in σ_π/π).*

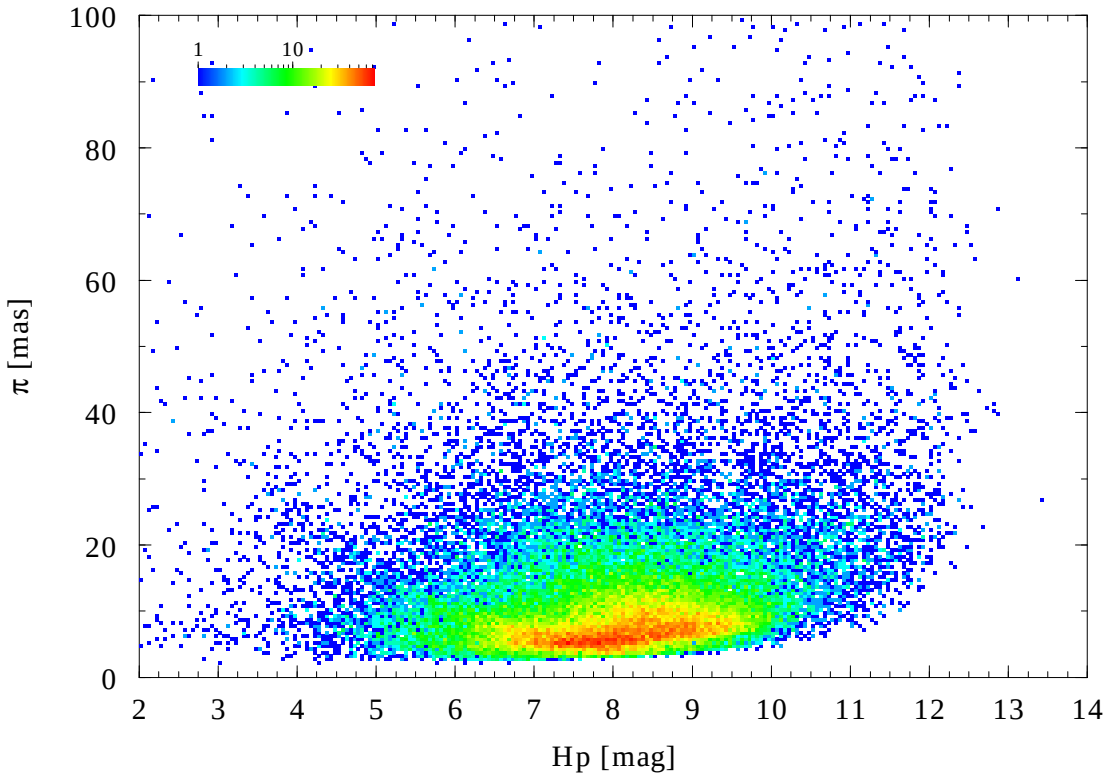

Figure 3.5.18. *Hipparcos Catalogue: parallax π versus Hp magnitude for all objects with $\sigma_\pi/\pi \leq 0.2$ (bin size 0.05 mag in Hp and 0.5 mas in π).*

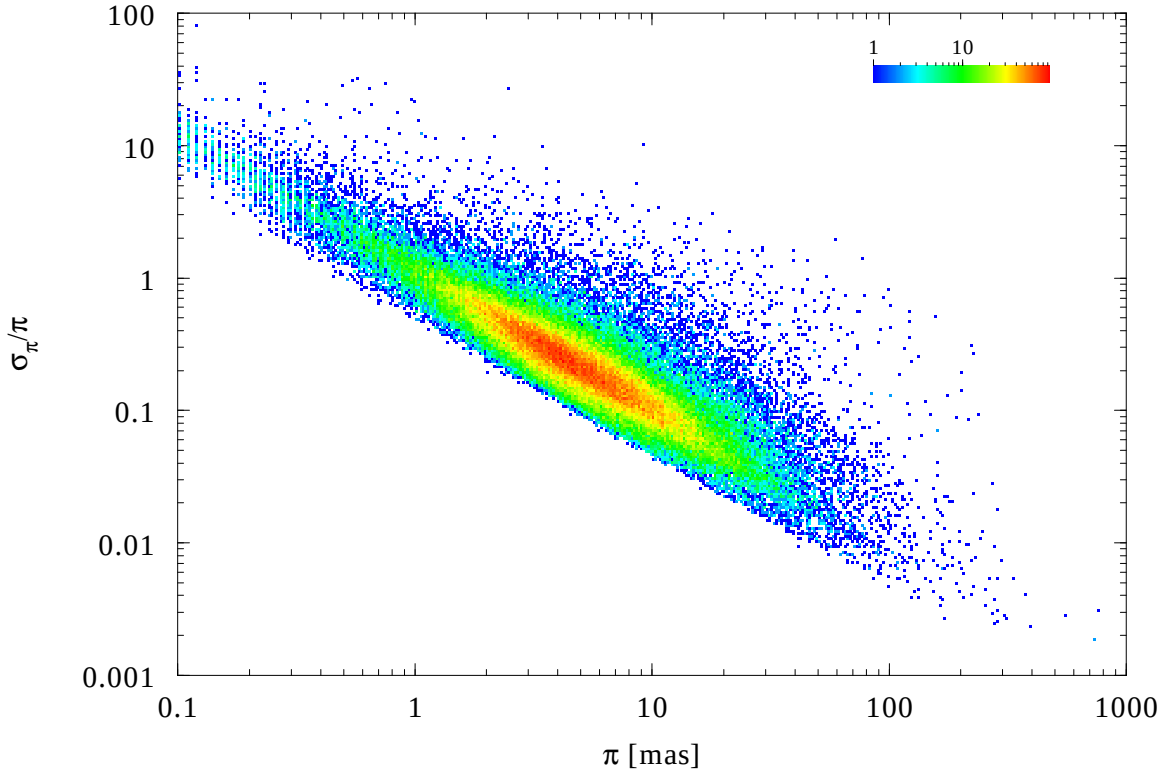

Figure 3.5.19. *Hipparcos Catalogue: relative distance precision σ_π/π versus parallax π (bin size 0.01 dex in π and 0.02 dex in σ_π/π).*

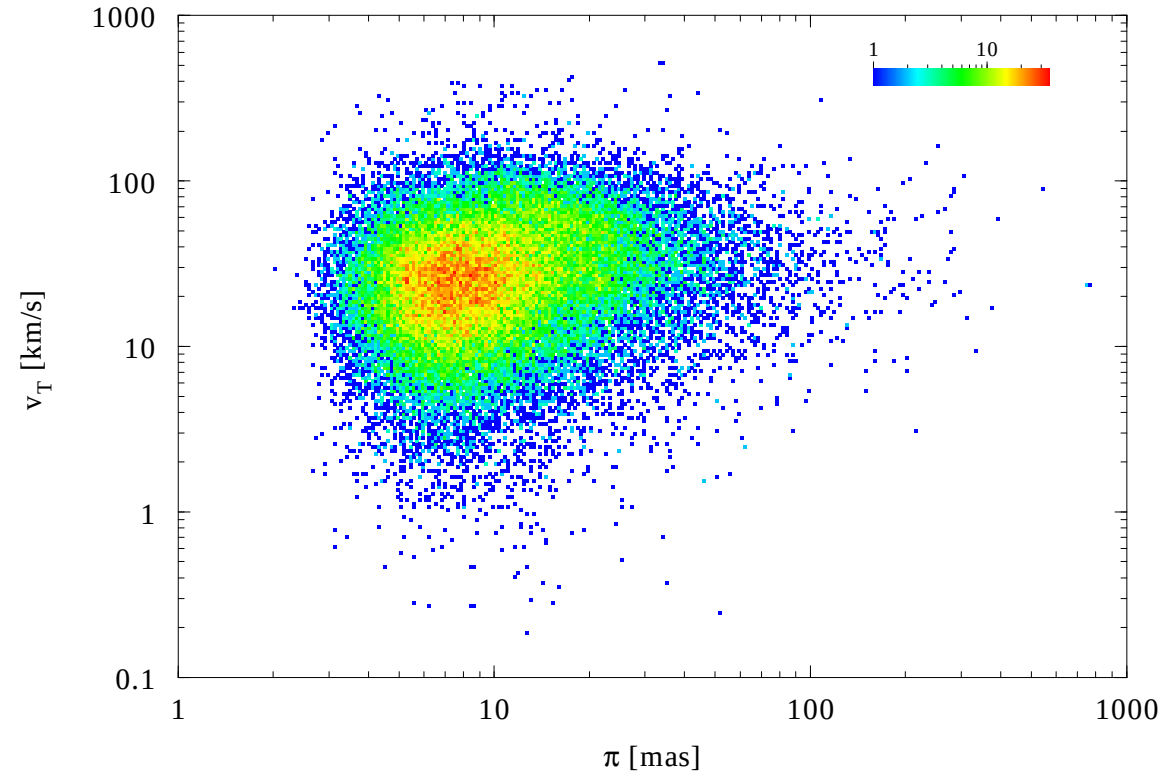

Figure 3.5.20. *Hipparcos Catalogue: tranverse velocity v_T versus parallax π (bin size 0.01 dex in π and 0.02 dex in v_T).*

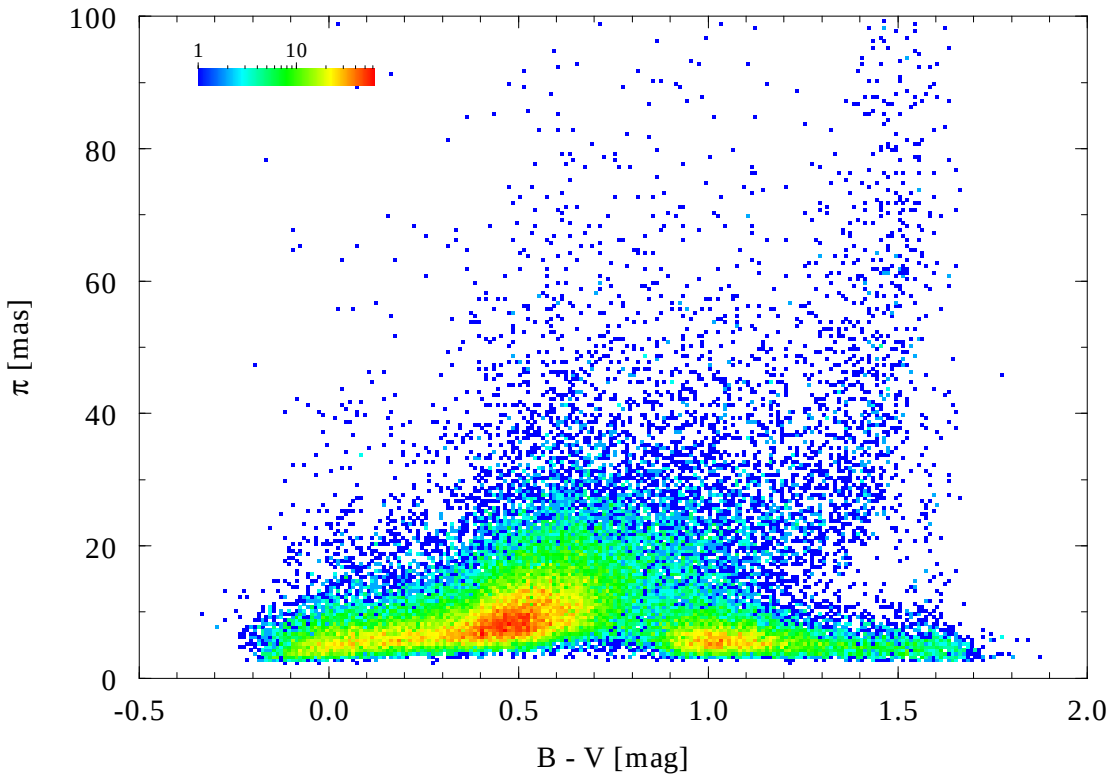

Figure 3.5.21. *Hipparcos Catalogue: parallax π versus $B-V$ colour index for all objects with $\sigma_\pi/\pi \leq 0.2$ and $\sigma_{B-V} \leq 0.1$ (bin size 0.01 mag in $B-V$ and 0.5 mas in π).*

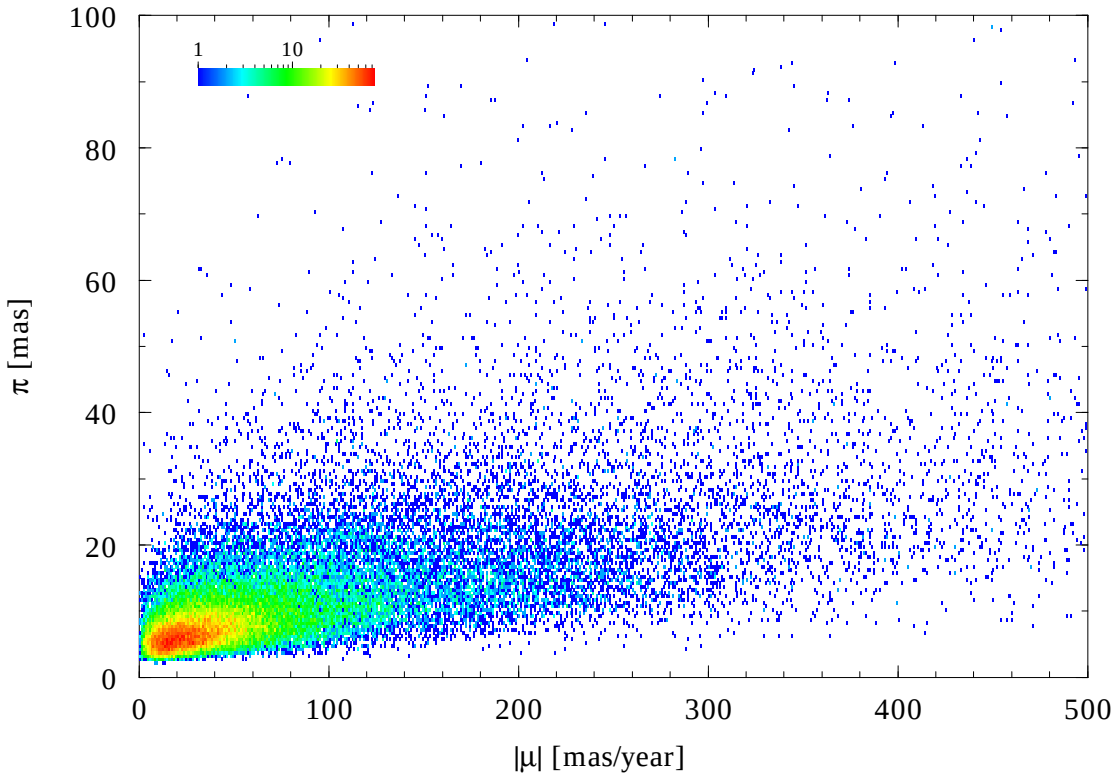

Figure 3.5.22. *Hipparcos Catalogue: parallax π versus total proper motion $|\boldsymbol{\mu}|$ for all objects with $\sigma_\pi/\pi \leq 0.2$ (bin size 1 mas/year in $|\boldsymbol{\mu}|$ and 0.5 mas in π).*

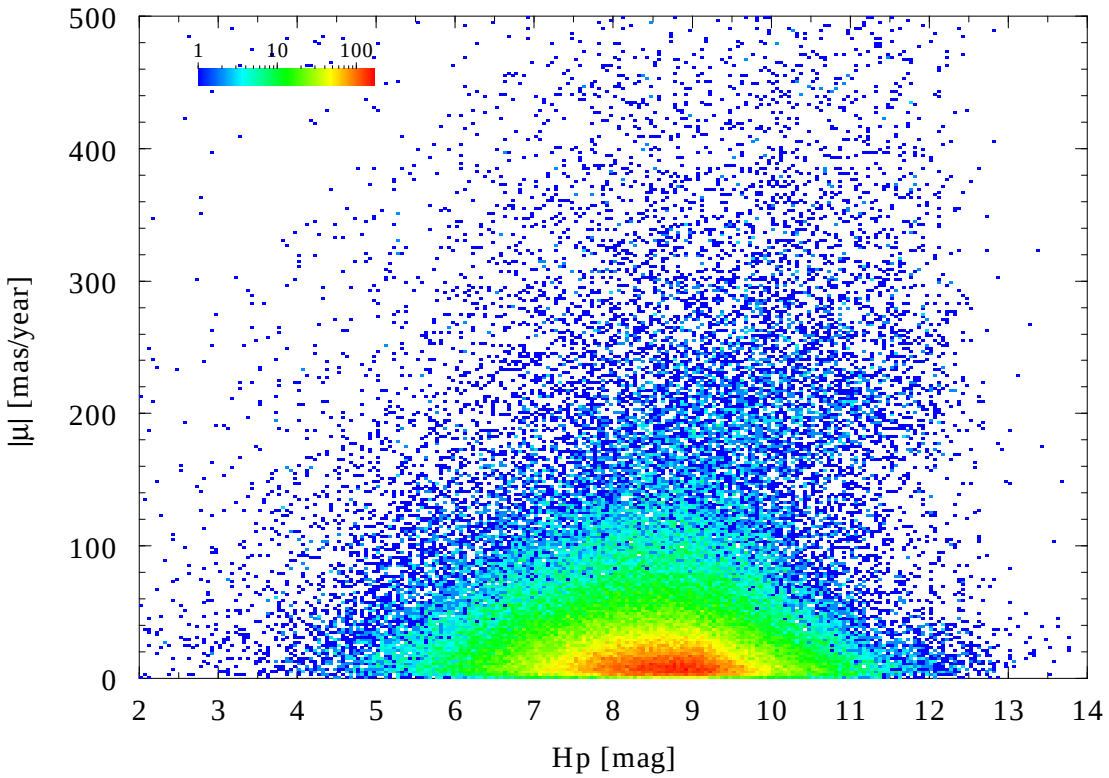

Figure 3.5.23. *Hipparcos Catalogue: total proper motion $|\boldsymbol{\mu}|$ versus Hp magnitude (bin size 0.05 mag in Hp and 2 mas/year in $|\boldsymbol{\mu}|$).*

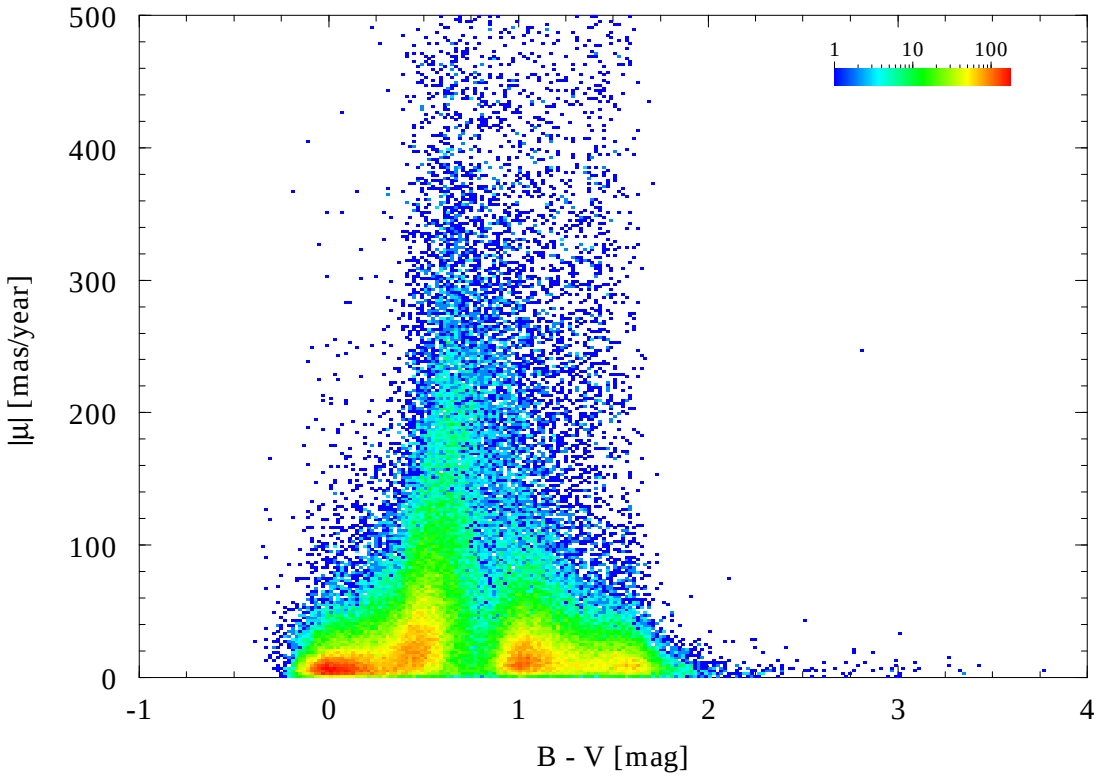

Figure 3.5.24. *Hipparcos Catalogue: total proper motion $|\boldsymbol{\mu}|$ versus $B-V$ colour index for all objects with $\sigma_{B-V} \leq 0.1$ mag (bin size 0.02 mag in $B-V$ and 2 mas/year in $|\boldsymbol{\mu}|$).*

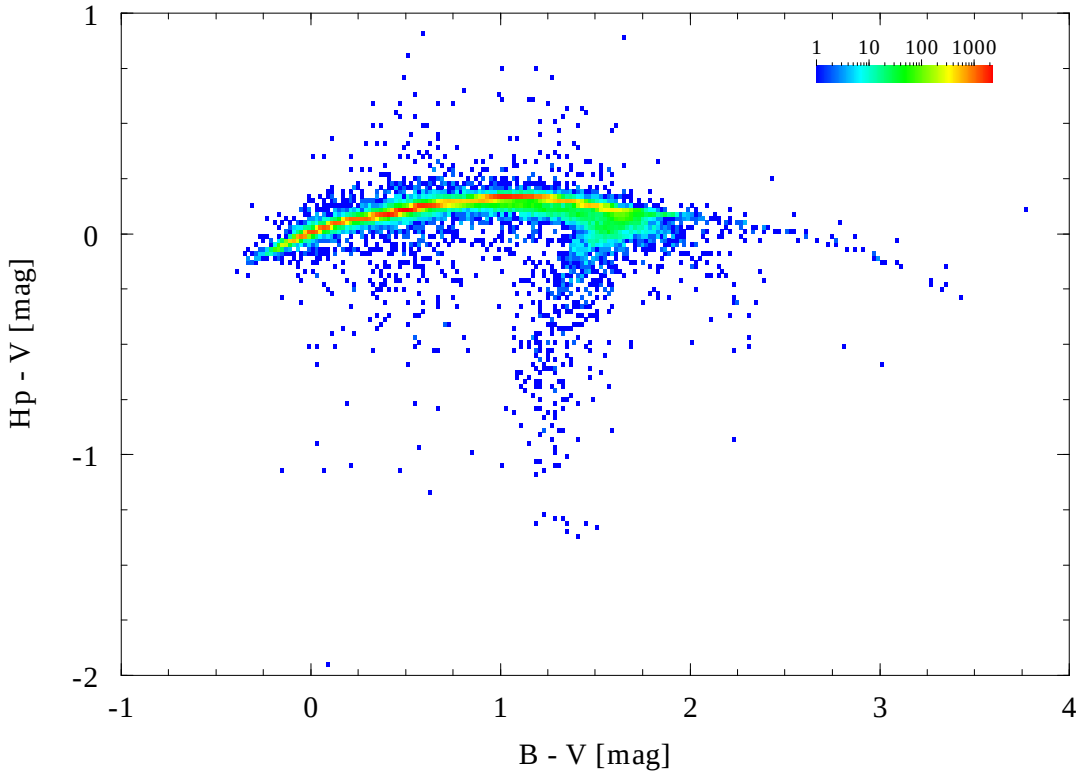

Figure 3.5.25. *Hipparcos Catalogue: $Hp - V$ versus $B - V$ colour index for all objects with $\sigma_{B-V} \leq 0.1$ mag (bin size 0.02 mag in both axes).*

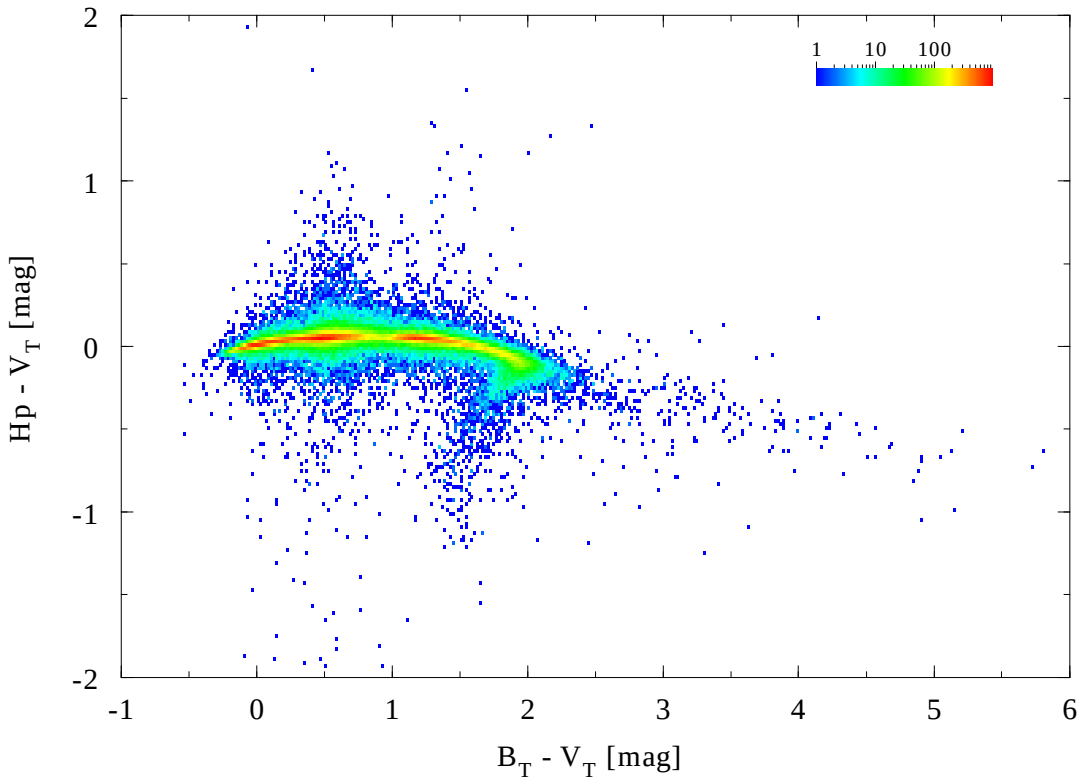

Figure 3.5.26. *Hipparcos Catalogue: $Hp - V_T$ versus $B_T - V_T$ colour index (bin size 0.02 mag in both axes).*

Section 3.6

Selected Stars from the Hipparcos Catalogue

3.6. Selected Stars from the Hipparcos Catalogue

In this section certain key results from the Hipparcos Catalogue are presented for various sets of stars selected according to a number of criteria.

Table 3.6.1 lists results for the 150 stars closest to the Sun, as deduced from the Hipparcos parallaxes. No criterion was applied to the precision of the individual parallax determinations. The entries in the table are sorted by decreasing parallax (increasing distance).

Table 3.6.2 gives the results for the 150 stars with the largest total proper motions in the Hipparcos Catalogue, again without further selection on precision. Table 3.6.3 gives the results for the 150 stars with the largest total transverse velocity, as deduced from the Hipparcos proper motions and parallaxes. In the latter table, only stars with relative distance precision $\sigma_\pi/\pi < 0.1$ were included. The entries in these tables are sorted by decreasing total proper motion and total transverse velocity, respectively.

For Table 3.6.4, the table with 150 stars with the highest absolute luminosity, the selection was more delicate. Although Hipparcos has determined for each entry at least a lower limit for the distance, and consequently for the luminosity, the inclusion of stars with only such a lower limit in the table was not considered meaningful. The stars in the table meet the two following criteria: (i) relative distance precision $\sigma_\pi/\pi < 0.3$; (ii) absolute magnitude M_V when computed with the 2-σ lower distance limit $1/(\pi + 2\sigma_\pi)$ smaller than -2 mag. The entries are sorted by increasing M_V, i.e. decreasing luminosity.

All four tables give results for the same series of quantities. The successive fields contain:

(1) the identifier in the Hipparcos Catalogue (the HIP number, Field H1);
(2) if available, the identifier in the HD Catalogue (the HD number, Field H71);
(3) the (truncated) right ascension α, in degrees (Field H8);
(4) the (truncated) declination δ, in degrees (Field H9);
(5) the visual magnitude V (Field H5);
(6) the absolute visual magnitude, computed as $M_V = V + 5\log\pi - 10$, with π in milliarcsec;
(7) the trigonometric parallax π, in milliarcsec (Field H11);
(8) the standard error in the trigonometric parallax σ_π, in milliarcsec (Field H16);
(9) the relative precision of the distance σ_π/π;
(10) the total proper motion $|\boldsymbol{\mu}|$ in milliarcsec per year;
(11) the proper motion in right ascension $\mu_{\alpha*}$ in milliarcsec per year (Field H12);
(12) the proper motion in declination μ_δ in milliarcsec per year (Field H13);
(13) the transverse velocity, computed as $V_\mathrm{T} = A_V|\boldsymbol{\mu}|/\pi$, in km/s (cf. Equation 1.2.20);
(14) an asterisk indicating that the star is in the Catalogue of Nearby Stars, 3rd version (CNS3);
(15) the Bayer/Flamsteed name of the star (as in Volume 13); if not available, a common name (as in Volume 13); if not available, blank.

For the star with a negative parallax value, for which the proper motion value is nevertheless significant, the computed fields using the parallax (absolute magnitude, distance precision, and transverse velocity) are left blank.

Table 3.6.1. The 150 stars in the Hipparcos Catalogue closest to the Sun.

HIP	HD	α	δ	V	M_V	π	σ_π	σ_π/π	$\lvert\mu\rvert$	$\mu_{\alpha*}$	μ_δ	V_T	C	Name
70890		217.449	−62.681	11.01	15.45	772.33	2.42	0.003	3852.99	−3775.64	768.16	23.65	*	α Cen C
71681	128621	219.914	−60.839	1.35	5.70	742.12	1.40	0.002	3724.12	−3600.35	952.11	23.79	*	α^2 Cen
71683	128620	219.920	−60.835	−0.01	4.34	742.12	1.40	0.002	3709.62	−3678.19	481.84	23.70	*	α^1 Cen
87937		269.454	+04.668	9.54	13.24	549.01	1.58	0.003	10357.70	−797.84	10326.93	89.43	*	Barnard's star
54035	95735	165.836	+35.981	7.49	10.46	392.40	0.91	0.002	4802.27	−580.20	−4767.09	58.01	*	
32349	48915	101.289	−16.713	−1.44	1.45	379.21	1.58	0.004	1339.42	−546.01	−1223.08	16.74	*	α CMa
92403		282.454	−23.836	10.37	13.00	336.48	1.82	0.005	665.97	637.55	−192.47	9.38	*	
16537	22049	53.235	−09.458	3.72	6.18	310.75	0.85	0.003	976.61	−976.44	17.97	14.90	*	ϵ Eri
114046	217987	346.447	−35.856	7.35	9.76	303.90	0.87	0.003	6896.07	6767.26	1326.66	107.57	*	
57548		176.934	+00.808	11.12	13.50	299.58	2.20	0.007	1361.36	605.62	−1219.23	21.54	*	
104214	201091	316.712	+38.741	5.20	7.49	287.13	1.51	0.005	5280.65	4155.10	3258.90	87.18	*	61 Cyg A
37279	61421	114.827	+05.228	0.40	2.68	285.93	0.88	0.003	1258.50	−716.57	−1034.58	20.86	*	α CMi
104217	201092	316.717	+38.734	6.05	8.33	285.42	0.72	0.003	5172.40	4107.40	3143.72	85.91	*	61 Cyg B
91772	173740	280.702	+59.622	9.70	11.97	284.48	5.01	0.018	2312.51	−1393.20	1845.73	38.53	*	
91768	173739	280.701	+59.626	8.94	11.18	280.28	2.57	0.009	2237.91	−1326.88	1802.12	37.85	*	
1475	1326	4.586	+44.022	8.09	10.33	280.27	1.05	0.004	2917.95	2888.92	410.58	49.35	*	
108870	209100	330.823	−56.780	4.69	6.89	275.76	0.69	0.003	4703.94	3959.97	−2538.84	80.86	*	ϵ Ind
8102	10700	26.021	−15.940	3.49	5.68	274.17	0.80	0.003	1922.00	−1721.82	854.07	33.23	*	τ Cet
5643		18.125	−17.001	12.10	14.25	269.05	7.57	0.028	1372.17	1210.09	646.95	24.18	*	
36208		111.851	+05.235	9.84	11.94	263.26	1.43	0.005	3738.16	571.27	−3694.25	67.31	*	Luyten's star
24186	33793	77.897	−45.004	8.86	10.89	255.26	0.86	0.003	8670.50	6506.05	−5731.39	161.02	*	Kapteyn's star
105090	202560	319.324	−38.865	6.69	8.71	253.37	1.13	0.004	3454.95	−3259.00	−1146.99	64.64	*	
110893	239960	337.002	+57.697	9.59	11.58	249.52	3.03	0.012	989.56	−870.23	−471.10	18.80	*	Kruger 60
30920		97.346	−02.812	11.12	13.05	242.89	2.64	0.011	930.24	694.73	−618.62	18.16	*	
72511		222.390	−26.106	11.72	13.58	235.24	22.43	0.095	1396.32	−1389.70	135.76	28.14	*	
80824		247.575	−12.660	10.10	11.95	234.51	1.82	0.008	1188.59	−93.61	−1184.90	24.03	*	
439	225213	1.335	−37.352	8.56	10.36	229.33	1.08	0.005	6099.89	5634.07	−2337.94	126.09	*	
15689		50.523	−13.278	12.16	13.94	227.45	61.79	0.272	319.66	−112.94	−299.04	6.66		
3829		12.288	+05.395	12.37	14.15	226.95	5.35	0.024	2977.84	1233.05	−2710.56	62.20	*	Van Maanen 2
72509		222.386	−26.111	12.07	13.80	221.80	69.07	0.311	1436.11	−1421.60	−203.60	30.69	*	
86162		264.110	+68.342	9.15	10.87	220.85	0.92	0.004	1309.37	−320.47	−1269.55	28.11	*	
85523		262.164	−46.893	9.38	11.10	220.43	1.63	0.007	1050.15	573.32	−879.84	22.58	*	
114110		346.662	−14.872	12.24	13.92	216.52	18.28	0.084	139.76	112.27	83.24	3.06		
57367		176.414	−64.841	11.50	13.18	216.40	2.11	0.010	2687.64	2665.17	−346.83	58.88	*	
113020		343.317	−14.262	10.16	11.80	212.69	2.10	0.010	1174.19	960.33	−675.64	26.17	*	
54211		166.384	+43.524	8.82	10.40	206.94	1.19	0.006	4510.53	−4410.79	943.32	103.32	*	
49908	88230	152.847	+49.455	6.60	8.16	205.22	0.81	0.004	1452.19	−1361.55	−505.00	33.54	*	
82725		253.634	−62.404	11.72	13.26	203.01	29.27	0.144	308.29	254.79	173.56	7.20		
85605		262.401	+24.653	11.39	12.92	202.69	39.48	0.195	362.24	97.33	348.92	8.47		
106440	204961	323.392	−49.007	8.66	10.19	202.53	1.33	0.007	819.31	−46.18	−818.01	19.18	*	
86214		264.268	−44.317	10.94	12.43	198.32	2.43	0.012	1176.47	−710.11	−937.99	28.12	*	
19849	26965	63.823	−07.645	4.43	5.92	198.24	0.84	0.004	4087.79	−2239.33	−3419.86	97.75	*	o^2 Eri
112460		341.710	+44.335	10.29	11.77	198.07	2.05	0.010	841.18	−704.66	−459.39	20.13	*	
88601	165341	271.363	+02.502	4.03	5.50	196.62	1.38	0.007	970.68	124.56	−962.66	23.40	*	70 Oph
97649	187642	297.695	+08.867	0.76	2.20	194.44	0.94	0.005	660.92	536.82	385.54	16.11	*	α Aql
1242		3.865	−16.132	11.49	12.90	191.86	17.24	0.090	954.74	728.18	−617.48	23.59	*	
57544		176.913	+78.690	10.80	12.14	185.48	1.43	0.008	884.95	743.21	480.40	22.62	*	
67155	119850	206.428	+14.895	8.46	9.79	184.13	1.27	0.007	2298.14	1778.46	−1455.52	59.17	*	
103039		313.138	−16.975	11.41	12.71	182.15	3.68	0.020	308.24	−306.70	30.78	8.02		
21088		67.792	+58.982	10.82	12.11	181.36	3.67	0.020	2426.71	1300.21	−2048.99	63.43	*	
33226	265866	103.706	+33.269	9.89	11.18	181.32	1.87	0.010	831.49	−729.33	−399.31	21.74	*	
53020		162.719	+06.810	11.64	12.89	177.46	23.00	0.130	1141.28	−804.40	−809.60	30.49	*	
25878	36395	82.862	−03.672	7.97	9.19	175.72	1.20	0.007	2227.65	763.05	−2092.89	60.10	*	
82817	152751	253.872	−08.334	9.02	10.23	174.23	3.90	0.022	1208.35	−829.34	−878.81	32.88	*	
96100	185144	293.086	+69.665	4.67	5.87	173.41	0.46	0.003	1838.91	598.43	−1738.81	50.27	*	σ Dra
29295	42581	92.645	−21.863	8.15	9.34	173.19	1.12	0.006	727.09	−137.01	−714.06	19.90	*	
26857		85.534	+12.493	11.56	12.75	172.78	3.88	0.022	2542.26	1999.05	−1570.64	69.75	*	
86990		266.648	−57.316	10.75	11.93	172.08	2.22	0.013	1755.97	−1119.87	−1352.52	48.37	*	
94761	180617	289.232	+05.172	9.12	10.28	170.26	1.37	0.008	1452.07	−578.86	−1331.70	40.43	*	
73184	131977	224.364	−21.411	5.72	6.86	169.32	1.67	0.010	2011.77	1034.18	−1725.60	56.32	*	
37766		116.168	+03.554	11.19	12.32	168.59	2.67	0.016	567.62	−344.87	−450.84	15.96	*	
76074		233.058	−41.273	9.31	10.44	168.52	1.42	0.008	1563.65	−1177.47	−1028.86	43.99	*	
3821	4614	12.271	+57.817	3.46	4.59	167.99	0.62	0.004	1222.71	1087.11	−559.65	34.50	*	η Cas
84478	156026	259.057	−26.543	6.33	7.45	167.56	1.06	0.006	1221.51	−479.71	−1123.37	34.56	*	
117473		357.300	+02.404	8.98	10.10	167.51	1.49	0.009	1388.44	995.12	−968.25	39.29	*	
84405	155885	258.839	−26.600	4.33	5.44	167.08	1.07	0.006	1238.13	−473.69	−1143.93	35.13	*	36 Oph
99461	191408	302.798	−36.097	5.32	6.41	165.24	0.90	0.005	1639.84	456.89	−1574.91	47.04	*	
15510	20794	49.972	−43.072	4.26	5.35	165.02	0.55	0.003	3123.70	3038.08	726.34	89.73	*	e Eri
99240	190248	302.174	−66.179	3.55	4.62	163.73	0.65	0.004	1656.04	1210.29	−1130.34	47.95	*	δ Pav
71253		218.571	−12.521	11.32	12.39	163.51	2.77	0.017	694.24	−357.50	595.12	20.13	*	
86961		266.553	−32.103	10.49	11.53	161.77	11.29	0.070	323.68	−49.82	−319.82	9.48		
86963		266.560	−32.102	11.39	12.43	161.77	11.29	0.070	281.05	−77.62	−270.12	8.24		
45343	79210	138.601	+52.688	7.64	8.68	161.59	5.23	0.032	1633.59	−1533.58	−562.80	47.92	*	
99701	191849	303.470	−45.164	7.97	9.01	161.17	1.08	0.007	794.37	778.18	−159.55	23.36	*	
116132		352.966	+19.937	10.05	11.07	160.06	2.81	0.018	557.92	554.40	−62.61	16.52	*	

Table 3.6.1. The 150 stars in the Hipparcos Catalogue closest to the Sun (continued).

HIP	HD	α	δ	V	M_V	π	σ_π	σ_π/π	$\lvert\mu\rvert$	$\mu_{\alpha*}$	μ_δ	V_T	C	Name
74995		229.865	−07.722	10.57	11.58	159.52	2.27	0.014	1228.59	−1224.55	−99.52	36.51	*	
120005	79211	138.609	+52.688	7.70	8.71	159.48	6.61	0.041	1684.40	−1551.30	−656.25	50.07	*	
84140	155876	258.032	+45.670	9.31	10.31	158.17	3.26	0.021	1624.76	325.96	−1591.73	48.70	*	
34603		107.509	+38.532	11.65	12.63	157.24	3.32	0.021	1045.33	−439.68	−948.36	31.51	*	
54298		166.628	−53.269	11.69	12.65	155.28	78.30	0.504	275.63	−39.50	272.78	8.41		
82809		253.857	−08.320	11.73	12.67	153.96	4.04	0.026	1209.62	−813.47	−895.23	37.24	*	
114622	219134	348.311	+57.168	5.57	6.50	153.24	0.65	0.004	2095.24	2074.37	294.97	64.82	*	
80459		246.351	+54.305	10.13	11.04	151.93	1.11	0.007	464.78	432.29	−170.71	14.50	*	
53767		165.019	+22.834	10.03	10.92	150.96	1.59	0.011	510.01	−426.31	−279.94	16.02	*	
72659	131156	222.847	+19.101	4.54	5.41	149.26	0.76	0.005	168.62	152.81	−71.28	5.36	*	ξ Boo
106106		322.401	+17.642	10.33	11.19	148.29	1.85	0.012	1076.00	1008.09	376.21	34.40	*	
114176		346.831	−32.268	12.28	13.13	147.95	13.76	0.093	225.64	−223.58	−30.45	7.23		
113296	216899	344.148	+16.554	8.68	9.49	145.27	1.22	0.008	1071.35	−1033.21	−283.33	34.96	*	
84709	156384	259.735	−34.990	5.91	6.69	143.45	17.12	0.119	1152.82	1149.24	−90.80	38.10	*	
103096	199305	313.332	+62.156	8.55	9.31	141.95	0.77	0.005	774.24	1.08	−774.24	25.86	*	
12114	16160	39.016	+06.883	5.79	6.50	138.72	1.04	0.007	2311.58	1806.27	1442.50	78.99	*	
51317		157.233	+00.843	9.65	10.35	138.29	2.13	0.015	947.85	−602.32	−731.87	32.49	*	
83945		257.380	+43.682	11.77	12.47	137.84	8.95	0.065	434.51	333.92	−278.02	14.94	*	
3765	4628	12.094	+05.283	5.74	6.38	134.04	0.86	0.006	1370.04	758.04	−1141.22	48.45	*	
7981	10476	25.625	+20.270	5.24	5.87	133.91	0.91	0.007	741.72	−302.12	−677.40	26.26	*	107 Psc
2021	2151	6.413	−77.255	2.82	3.45	133.78	0.51	0.004	2243.69	2220.12	324.37	79.50	*	β Hyi
73182	131976	224.358	−21.407	8.01	8.64	133.63	33.56	0.251	1937.14	987.05	−1666.81	68.72	*	
12781		41.062	+25.524	10.55	11.16	132.42	2.48	0.019	939.49	864.77	−367.17	33.63	*	
5336	6582	17.054	+54.924	5.17	5.78	132.40	0.60	0.005	3776.76	3421.44	−1599.27	135.22	*	μ Cas
65859		202.496	+10.380	9.05	9.64	131.12	1.29	0.010	1557.72	1128.00	−1074.30	56.32	*	
113283	216803	344.099	−31.565	6.48	7.07	130.94	0.92	0.007	367.16	330.53	−159.86	13.29	*	
61874		190.195	−43.568	12.24	12.82	130.52	3.87	0.030	1045.23	−782.02	693.51	37.96	*	
113368	216956	344.412	−29.622	1.17	1.74	130.08	0.92	0.007	367.90	329.22	−164.22	13.41	*	α PsA
85295	157881	261.440	+02.114	7.54	8.10	129.54	0.95	0.007	1319.36	−580.47	−1184.81	48.28	*	
91262	172167	279.234	+38.783	0.03	0.58	128.93	0.55	0.004	350.77	201.02	287.46	12.90	*	α Lyr
88574	165222	271.280	−03.031	9.37	9.91	128.28	1.44	0.011	660.06	570.14	−332.59	24.39	*	
49986		153.074	−03.745	9.26	9.80	127.99	1.53	0.012	287.03	−152.93	−242.90	10.63	*	
101180		307.631	+65.449	10.54	11.04	125.62	1.11	0.009	526.46	443.25	284.06	19.87	*	
106255		322.825	−09.791	11.96	12.44	124.82	28.85	0.231	1163.06	1161.80	−54.19	44.17	*	
33499		104.448	−44.291	10.81	11.29	124.62	2.64	0.021	1103.07	−1102.25	−42.57	41.96	*	
22449	30652	72.459	+06.961	3.19	3.67	124.60	0.95	0.008	463.59	463.44	11.62	17.64	*	π^3 Ori
80346		246.035	+48.354	10.27	10.74	124.34	1.16	0.009	1231.40	1145.33	−452.28	46.95	*	
89937	170153	275.260	+72.734	3.55	4.02	124.11	0.48	0.004	636.92	531.08	−351.59	24.33	*	χ Dra
86287		264.470	+18.589	9.62	10.07	123.02	1.62	0.013	1351.18	926.83	983.19	52.07	*	
5496		17.593	−67.446	9.80	10.25	122.86	7.53	0.061	691.84	389.20	571.98	26.69	*	
113576	217357	345.070	−22.524	7.88	8.33	122.80	0.94	0.008	906.07	−904.21	58.09	34.98	*	
4856		15.621	+71.681	9.98	10.43	122.77	1.23	0.010	1786.66	1745.69	−380.43	68.99	*	
7751	10360	24.947	−56.196	5.76	6.21	122.75	1.41	0.011	286.58	286.10	16.66	11.07	*	p Eri
38956		119.552	+41.305	12.02	12.46	122.53	11.52	0.094	717.25	212.35	−685.10	27.75	*	
76901		235.532	−19.469	11.83	12.26	121.86	43.95	0.361	2282.67	−2032.22	−1039.54	88.80	*	
62452		191.988	+09.753	11.39	11.82	121.78	2.90	0.024	1108.17	−1007.72	−461.01	43.14	*	
93449		285.474	−36.952	11.57	12.00	121.75	68.24	0.560	61.14	−34.36	50.57	2.38		
20968		67.437	−29.026	11.42	11.83	120.70	56.47	0.468	289.06	−58.31	−283.12	11.35		
31292		98.448	−75.626	11.41	11.80	119.54	13.42	0.112	401.45	−308.79	256.54	15.92		
61317	109358	188.438	+41.357	4.24	4.63	119.46	0.83	0.007	763.49	−705.06	292.93	30.30	*	β CVn
86974	161797	266.615	+27.722	3.42	3.80	119.05	0.62	0.005	804.63	−291.42	−750.00	32.04	*	μ Her
80018		245.017	−37.531	10.56	10.92	118.03	2.28	0.019	1230.59	−729.36	991.16	49.42	*	
23452	32450	75.619	−21.256	8.31	8.66	117.38	1.81	0.015	263.07	−141.55	−221.74	10.62	*	
64924	115617	199.604	−18.309	4.74	5.09	117.30	0.71	0.006	1508.75	−1069.90	−1063.78	60.97	*	61 Vir
57802		177.781	+35.271	9.76	10.10	116.92	1.38	0.012	372.77	−271.97	254.93	15.11	*	
1599	1581	5.008	−64.878	4.23	4.56	116.38	0.64	0.005	2067.32	1707.56	1165.36	84.21	*	ζ Tuc
113229		343.950	−75.456	10.42	10.74	116.02	1.33	0.011	1477.26	−1027.28	−1061.60	60.36	*	
93873		286.774	+20.889	10.77	11.09	115.91	2.47	0.021	592.14	−480.82	−345.60	24.22	*	
111802	214479	339.689	−20.621	9.06	9.38	115.71	1.50	0.013	457.60	450.58	−79.86	18.75	*	
27913	39587	88.596	+20.276	4.39	4.70	115.43	1.08	0.009	190.81	−163.17	−98.92	7.84	*	χ^1 Ori
25578		82.001	+09.646	12.48	12.78	115.04	5.22	0.045	783.92	−194.06	−759.52	32.30	*	
32984	50281	103.077	−05.174	6.58	6.88	114.94	0.86	0.007	544.42	−544.41	−3.30	22.45	*	
14559		46.991	−28.221	11.72	12.02	114.73	33.98	0.296	214.04	−156.07	−146.48	8.84		
31293		98.433	−75.631	10.35	10.64	114.18	3.18	0.028	402.39	−290.42	278.52	16.71		
109388		332.415	−04.641	10.41	10.69	113.97	2.10	0.018	1135.07	1134.90	−19.71	47.21	*	
84720	156274	259.762	−46.637	5.47	5.75	113.81	1.36	0.012	1041.00	1035.25	109.22	43.36	*	
23311	32147	75.203	−05.751	6.22	6.49	113.46	0.82	0.007	1238.49	550.74	−1109.30	51.75	*	
99825	192310	303.819	−27.033	5.73	6.00	113.33	0.89	0.008	1254.54	1241.35	−181.46	52.48	*	
93899	349726	286.806	+20.878	10.76	11.02	112.82	2.41	0.021	585.28	−481.05	−333.38	24.59	*	
60559		186.216	−18.237	11.28	11.54	112.52	2.51	0.022	2554.50	1095.90	−2307.48	107.62	*	
108706		330.304	+28.307	11.99	12.23	111.57	3.19	0.029	373.89	372.11	36.48	15.89	*	
27072	38393	86.117	−22.447	3.59	3.83	111.49	0.60	0.005	470.39	−292.42	−368.45	20.00	*	γ Lep
47103		144.006	−21.658	10.91	11.14	111.41	1.99	0.018	999.00	137.17	−989.54	42.51	*	
56528		173.862	−32.538	9.81	10.03	110.65	1.81	0.016	855.40	−69.85	−852.54	36.65	*	
17378	23249	55.812	−09.765	3.52	3.74	110.58	0.88	0.008	747.87	−91.71	742.23	32.06	*	δ Eri

Table 3.6.2. The 150 stars in the Hipparcos Catalogue with largest proper motions.

HIP	HD	α	δ	V	M_V	π	σ_π	σ_π/π	$\lvert\mu\rvert$	$\mu_{\alpha*}$	μ_δ	V_T	C	Name
87937		269.454	+04.668	9.54	13.24	549.01	1.58	0.003	10357.70	−797.84	10326.93	89.43	*	Barnard's star
24186	33793	77.897	−45.004	8.86	10.89	255.26	0.86	0.003	8670.50	6506.05	−5731.39	161.02	*	Kapteyn's star
57939	103095	178.233	+37.733	6.42	6.61	109.21	0.78	0.007	7058.36	4003.69	−5813.00	306.38	*	Groombr. 1830
114046	217987	346.447	−35.856	7.35	9.76	303.90	0.87	0.003	6896.07	6767.26	1326.66	107.57	*	
439	225213	1.335	−37.352	8.56	10.36	229.33	1.08	0.005	6099.89	5634.07	−2337.94	126.09	*	
67593		207.756	+23.764	13.31	12.72	76.20	107.46	1.410	5834.20	2281.92	5369.43	362.95		
104214	201091	316.712	+38.741	5.20	7.49	287.13	1.51	0.005	5280.65	4155.10	3258.90	87.18	*	61 Cyg A
104217	201092	316.717	+38.734	6.05	8.33	285.42	0.72	0.003	5172.40	4107.40	3143.72	85.91	*	61 Cyg B
54035	95735	165.836	+35.981	7.49	10.46	392.40	0.91	0.002	4802.27	−580.20	−4767.09	58.01	*	
108870	209100	330.823	−56.780	4.69	6.89	275.76	0.69	0.003	4703.94	3959.97	−2538.84	80.86	*	ϵ Ind
54211		166.384	+43.524	8.82	10.40	206.94	1.19	0.006	4510.53	−4410.79	943.32	103.32	*	
19849	26965	63.823	−07.645	4.43	5.92	198.24	0.84	0.004	4087.79	−2239.33	−3419.86	97.75	*	o^2 Eri
70890		217.449	−62.681	11.01	15.45	772.33	2.42	0.003	3852.99	−3775.64	768.16	23.65	*	α Cen C
5336	6582	17.054	+54.924	5.17	5.78	132.40	0.60	0.005	3776.76	3421.44	−1599.27	135.22	*	μ Cas
36208		111.851	+05.235	9.84	11.94	263.26	1.43	0.005	3738.16	571.27	−3694.25	67.31	*	Luyten's star
71681	128621	219.914	−60.839	1.35	5.70	742.12	1.40	0.002	3724.12	−3600.35	952.11	23.79	*	α^2 Cen
71683	128620	219.920	−60.835	−0.01	4.34	742.12	1.40	0.002	3709.62	−3678.19	481.84	23.70	*	α^1 Cen
74234	134440	227.557	−16.454	9.44	7.08	33.68	1.67	0.050	3681.49	−1001.47	−3542.66	518.17	*	
74235	134439	227.557	−16.371	9.07	6.74	34.14	1.36	0.040	3681.02	−998.86	−3542.91	511.12	*	
105090	202560	319.324	−38.865	6.69	8.71	253.37	1.13	0.004	3454.95	−3259.00	−1146.99	64.64	*	
56936		175.083	+67.267	12.20	10.43	44.28	2.83	0.064	3168.11	262.62	−3157.21	339.17		
15510	20794	49.972	−43.072	4.26	5.35	165.02	0.55	0.003	3123.70	3038.08	726.34	89.73	*	e Eri
3829		12.288	+05.395	12.37	14.15	226.95	5.35	0.024	2977.84	1233.05	−2710.56	62.20	*	Van Maanen 2
55360		170.038	+65.846	9.31	9.52	109.95	1.11	0.010	2952.47	−2946.70	184.52	127.30	*	
1475	1326	4.586	+44.022	8.09	10.33	280.27	1.05	0.004	2917.95	2888.92	410.58	49.35	*	
55042		169.012	−57.551	11.66	11.17	79.71	2.80	0.035	2732.50	−2465.03	1179.06	162.51	*	
57367		176.414	−64.841	11.50	13.18	216.40	2.11	0.010	2687.64	2665.17	−346.83	58.88	*	
10279		33.092	+03.580	10.04	9.96	96.28	1.80	0.019	2556.23	−1761.07	−1852.82	125.86	*	
60559		186.216	−18.237	11.28	11.54	112.52	2.51	0.022	2554.50	1095.90	−2307.48	107.62	*	
26857		85.534	+12.493	11.56	12.75	172.78	3.88	0.022	2542.26	1999.05	−1570.64	69.75	*	
9560		30.712	+05.708	12.26	10.05	36.17	4.30	0.119	2442.54	2338.67	−704.72	320.12		
21088		67.792	+58.982	10.82	12.11	181.36	3.67	0.020	2426.71	1300.21	−2048.99	63.43	*	
91772	173740	280.702	+59.622	9.70	11.97	284.48	5.01	0.018	2312.51	−1393.20	1845.73	38.53	*	
12114	16160	39.016	+06.883	5.79	6.50	138.72	1.04	0.007	2311.58	1806.27	1442.50	78.99	*	
67155	119850	206.428	+14.895	8.46	9.79	184.13	1.27	0.007	2298.14	1778.46	−1455.52	59.17	*	
76901		235.532	−19.469	11.83	12.26	121.86	43.95	0.361	2282.67	−2032.22	−1039.54	88.80	*	
69673	124897	213.918	+19.187	−0.05	−0.31	88.85	0.74	0.008	2278.87	−1093.45	−1999.40	121.59	*	α Boo
2021	2151	6.413	−77.255	2.82	3.45	133.78	0.51	0.004	2243.69	2220.12	324.37	79.50	*	β Hyi
91768	173739	280.701	+59.626	8.94	11.18	280.28	2.57	0.009	2237.91	−1326.88	1802.12	37.85	*	
104059		316.225	−16.954	11.45	10.04	52.26	3.06	0.059	2231.65	−914.54	−2035.65	202.43	*	
25878	36395	82.862	−03.672	7.97	9.19	175.72	1.20	0.007	2227.65	763.05	−2092.89	60.10	*	
18915	25329	60.807	+35.277	8.51	7.18	54.14	1.08	0.020	2205.93	1732.49	−1365.50	193.15	*	
10138	13445	32.600	−50.825	6.12	5.93	91.63	0.61	0.007	2192.74	2092.84	654.32	113.44	*	
104432		317.321	−13.298	10.87	10.45	82.33	2.40	0.029	2117.88	710.44	−1995.17	121.95	*	
114622	219134	348.311	+57.168	5.57	6.50	153.24	0.65	0.004	2095.24	2074.37	294.97	64.82	*	
1599	1581	5.008	−64.878	4.23	4.56	116.38	0.64	0.005	2067.32	1707.56	1165.36	84.21	*	ζ Tuc
23518		75.844	+53.132	9.96	9.23	71.35	1.76	0.025	2015.94	1304.13	−1537.29	133.94	*	
73184	131977	224.364	−21.411	5.72	6.86	169.32	1.67	0.010	2011.77	1034.18	−1725.60	56.32	*	
91668		280.401	+00.925	12.23	9.30	25.98	3.65	0.140	1980.77	50.43	−1980.13	361.42		
38541	64090	118.386	+30.610	8.27	6.01	35.29	1.04	0.029	1965.35	705.00	−1834.55	264.00	*	
73182	131976	224.358	−21.407	8.01	8.64	133.63	33.56	0.251	1937.14	987.05	−1666.81	68.72	*	
8102	10700	26.021	−15.940	3.49	5.68	274.17	0.80	0.003	1922.00	−1721.82	854.07	33.23	*	τ Cet
52621		161.418	−19.113	11.03		−7.21	25.22		1900.14	−1804.68	−594.70		*	
67090		206.270	+17.790	9.79	9.21	76.70	1.46	0.019	1886.31	451.03	−1831.59	116.58	*	
94349		288.056	+02.888	11.09	11.06	98.56	2.66	0.027	1863.20	1789.15	−520.07	89.62	*	
48336		147.787	−12.326	10.04	9.36	73.10	22.31	0.305	1848.68	1137.36	−1457.41	119.89	*	
96100	185144	293.086	+69.665	4.67	5.87	173.41	0.46	0.003	1838.91	598.43	−1738.81	50.27	*	σ Dra
67487	120467	207.441	−22.110	8.16	7.40	70.49	1.01	0.014	1817.22	−1748.63	−494.56	122.21	*	
4856		15.621	+71.681	9.98	10.43	122.77	1.23	0.010	1786.66	1745.69	−380.43	68.99	*	
38082		117.065	+20.371	11.46	10.71	70.74	2.66	0.038	1756.65	1451.22	−989.83	117.72	*	
86990		266.648	−57.316	10.75	11.93	172.08	2.22	0.013	1755.97	−1119.87	−1352.52	48.37	*	
2552		8.112	+67.236	10.27	10.24	98.74	3.37	0.034	1753.52	1739.07	−224.63	84.19	*	
37853	63077	116.397	−34.177	5.36	4.45	65.79	0.56	0.009	1736.98	−220.83	1722.89	125.16	*	
4964		15.913	−45.788	11.62	6.54	9.66	17.61	1.823	1734.13	−261.65	−1714.28	850.99		
120005	79211	138.609	+52.688	7.70	8.71	159.48	6.61	0.041	1684.40	−1551.30	−656.25	50.07	*	
70865		217.376	+15.529	10.67	9.90	70.06	2.25	0.032	1673.20	−1053.37	1300.01	113.21	*	
99240	190248	302.174	−66.179	3.55	4.62	163.73	0.65	0.004	1656.04	1210.29	−1130.34	47.95	*	δ Pav
79537	145417	243.456	−57.567	7.53	6.84	72.75	0.82	0.011	1649.13	−853.99	−1410.79	107.46	*	
75181	136352	230.457	−48.317	5.65	4.83	68.70	0.79	0.011	1645.86	−1622.71	−275.10	113.57	*	ν^2 Lup
82588	152391	253.247	−00.023	6.65	5.51	59.04	0.87	0.015	1645.54	−711.75	−1483.65	132.12	*	
99461	191408	302.798	−36.097	5.32	6.41	165.24	0.90	0.005	1639.84	456.89	−1574.91	47.04	*	
45343	79210	138.601	+52.688	7.64	8.68	161.59	5.23	0.032	1633.59	−1533.58	−562.80	47.92	*	
84140	155876	258.032	+45.670	9.31	10.31	158.17	3.26	0.021	1624.76	325.96	−1591.73	48.70	*	
4012		12.867	+58.301	10.66	9.33	54.23	2.12	0.039	1618.38	1566.84	405.19	141.47	*	
49189		150.593	+48.092	10.03	9.16	67.14	1.66	0.025	1604.99	−637.32	−1473.03	113.32	*	

Table 3.6.2. The 150 stars in the Hipparcos Catalogue with largest proper motions (continued).

HIP	HD	α	δ	V	M_V	π	σ_π	σ_π/π	$\lvert\mu\rvert$	$\mu_{\alpha*}$	μ_δ	V_T	C	Name
16404		52.815	+66.733	9.91	6.14	17.58	1.53	0.087	1598.39	1190.86	−1066.16	431.01		
57443	102365	176.634	−40.501	4.89	5.06	108.23	0.70	0.006	1583.92	−1531.69	403.41	69.38	*	
5247		16.776	+63.941	9.00	8.11	66.46	1.27	0.019	1580.79	1548.21	319.28	112.75	*	
76074		233.058	−41.273	9.31	10.44	168.52	1.42	0.008	1563.65	−1177.47	−1028.86	43.99	*	
65859		202.496	+10.380	9.05	9.64	131.12	1.29	0.010	1557.72	1128.00	−1074.30	56.32	*	
16209		52.218	+37.385	11.10	9.07	39.19	2.52	0.064	1546.25	1120.24	−1065.81	187.04		
64924	115617	199.604	−18.309	4.74	5.09	117.30	0.71	0.006	1508.75	−1069.90	−1063.78	60.97	*	61 Vir
10812		34.788	−36.779	11.59	10.86	71.56	2.99	0.042	1498.69	1394.12	549.99	99.28	*	
23932		77.145	−18.169	10.28	10.43	107.30	2.00	0.019	1488.03	503.75	−1400.17	65.74	*	
15330	20766	49.435	−62.577	5.53	5.11	82.51	0.54	0.007	1486.81	1337.83	648.71	85.42	*	ζ^1 Ret
115332		350.407	+17.294	11.70	11.55	93.50	3.58	0.038	1485.52	−536.53	−1385.25	75.32	*	
15371	20807	49.546	−62.508	5.24	4.83	82.79	0.53	0.006	1479.94	1331.10	646.84	84.74	*	ζ^2 Ret
113229		343.950	−75.456	10.42	10.74	116.02	1.33	0.011	1477.26	−1027.28	−1061.60	60.36	*	
98906		301.264	+54.436	11.98	10.98	63.23	6.44	0.102	1472.40	−1165.35	−899.95	110.39	*	
110618	211998	336.143	−72.254	5.28	2.98	34.60	0.60	0.017	1466.57	1302.45	−674.12	200.93	*	ν Ind
83591	154363	256.266	−05.064	7.70	7.54	92.98	1.04	0.011	1461.33	−916.86	−1137.91	74.50	*	
80837	148816	247.620	+04.182	7.27	4.20	24.34	0.90	0.037	1458.03	−432.73	−1392.34	283.97		
83599		256.310	−05.091	10.08	9.84	89.70	28.71	0.320	1456.53	−921.19	−1128.23	76.98	*	
49908	88230	152.847	+49.455	6.60	8.16	205.22	0.81	0.004	1452.19	−1361.55	−505.00	33.54	*	
94761	180617	289.232	+05.172	9.12	10.28	170.26	1.37	0.008	1452.07	−578.86	−1331.70	40.43	*	
21609	29907	69.589	−65.419	9.85	6.00	17.00	0.98	0.058	1448.49	732.93	1249.38	403.91		
72509		222.386	−26.111	12.07	13.80	221.80	69.07	0.311	1436.11	−1421.60	−203.60	30.69	*	
2941	3443	9.332	−24.767	5.57	4.61	64.38	1.40	0.022	1422.19	1422.09	−17.15	104.72	*	
13375		43.027	+34.392	9.60	8.83	70.19	1.68	0.024	1402.58	994.66	−988.88	94.73	*	
72511		222.390	−26.106	11.72	13.58	235.24	22.43	0.095	1396.32	−1389.70	135.76	28.14	*	
117473		357.300	+02.404	8.98	10.10	167.51	1.49	0.009	1388.44	995.12	−968.25	39.29	*	
17666	23439	56.757	+41.430	7.67	5.72	40.83	2.24	0.055	1377.03	598.96	−1239.94	159.88	*	
70536		216.442	+23.623	9.98	8.99	63.35	1.81	0.029	1372.91	795.23	−1119.15	102.73	*	
5643		18.125	−17.001	12.10	14.25	269.05	7.57	0.028	1372.17	1210.09	646.95	24.18	*	
3765	4628	12.094	+05.283	5.74	6.38	134.04	0.86	0.006	1370.04	758.04	−1141.22	48.45	*	
70529		216.429	+23.620	9.77	8.64	59.54	1.73	0.029	1369.53	794.49	−1115.53	109.04	*	
116317		353.516	+00.182	11.16	10.43	71.56	4.77	0.067	1367.70	−997.02	−936.24	90.60	*	
74537	135204	228.465	−01.350	6.58	5.39	57.80	0.85	0.015	1365.71	−1269.65	−503.15	112.01	*	
57548		176.934	+00.808	11.12	13.50	299.58	2.20	0.007	1361.36	605.62	−1219.23	21.54	*	
98792	190404	300.970	+23.343	7.28	6.32	64.17	0.85	0.013	1355.89	−1002.84	−912.55	100.16	*	
73192		224.387	+31.399	11.08	8.03	24.56	5.24	0.213	1351.90	−694.60	−1159.81	260.94	*	
86287		264.470	+18.589	9.62	10.07	123.02	1.62	0.013	1351.18	926.83	983.19	52.07	*	
41926	72673	128.218	−31.503	6.38	5.95	82.15	0.66	0.008	1349.23	−1113.64	761.73	77.86	*	
32349	48915	101.289	−16.713	−1.44	1.45	379.21	1.58	0.004	1339.42	−546.01	−1223.08	16.74	*	α CMa
29277		92.582	+82.110	10.48	10.62	106.43	1.44	0.014	1337.80	50.26	−1336.86	59.59	*	
9724		31.267	−17.614	10.19	10.32	105.94	2.04	0.019	1328.96	1317.53	−173.94	59.47	*	
4569		14.613	−27.856	11.77	11.18	76.32	2.88	0.038	1327.47	1293.37	−298.93	82.45	*	
6351		20.390	−41.655	10.15	9.01	59.29	1.59	0.027	1320.17	1238.97	−455.84	105.55	*	
78072	142860	239.112	+15.665	3.85	3.62	89.92	0.72	0.008	1319.40	311.20	−1282.17	69.56	*	γ Ser
85295	157881	261.440	+02.114	7.54	8.10	129.54	0.95	0.007	1319.36	−580.47	−1184.81	48.28	*	
86162		264.110	+68.342	9.15	10.87	220.85	0.92	0.004	1309.37	−320.47	−1269.55	28.11	*	
15234		49.109	+38.101	10.67	8.10	30.63	2.36	0.077	1295.70	739.73	−1063.79	200.53		
21932	285968	70.731	+18.961	9.95	10.08	106.16	2.51	0.024	1295.37	659.83	−1114.72	57.84	*	
70956	127339	217.702	−08.646	9.40	8.31	60.53	1.57	0.026	1292.08	−1269.37	−241.19	101.19	*	
114962	219617	349.272	−13.848	8.16	3.56	12.04	2.41	0.200	1291.87	−502.28	−1190.23	508.64		
27080	39194	86.135	−70.147	8.09	6.05	39.08	0.75	0.019	1277.10	−309.03	1239.15	154.91	*	
49091		150.298	−30.392	11.43	10.40	62.33	2.35	0.038	1274.15	−1098.13	646.19	96.90	*	
14632	19373	47.262	+49.614	4.05	3.94	94.93	0.67	0.007	1265.60	1262.29	−91.53	63.20	*	ι Per
37279	61421	114.827	+05.228	0.40	2.68	285.93	0.88	0.003	1258.50	−716.57	−1034.58	20.86	*	α CMi
99825	192310	303.819	−27.033	5.73	6.00	113.33	0.89	0.008	1254.54	1241.35	−181.46	52.48	*	
46120		141.084	−80.526	10.11	6.19	16.46	0.99	0.060	1253.64	202.13	1237.24	361.05		
55988		172.116	+07.520	10.21	8.12	38.23	1.76	0.046	1248.89	−272.87	−1218.72	154.86		
58345	103932	179.487	−27.706	6.99	6.95	98.16	0.88	0.009	1244.99	−1079.64	−619.99	60.12	*	
23311	32147	75.203	−05.751	6.22	6.49	113.46	0.82	0.007	1238.49	550.74	−1109.30	51.75	*	
84405	155885	258.839	−26.600	4.33	5.44	167.08	1.07	0.006	1238.13	−473.69	−1143.93	35.13	*	36 Oph
93101	176029	284.501	+05.911	9.22	8.99	90.02	1.46	0.016	1237.16	−194.47	−1221.78	65.15	*	
80346		246.035	+48.354	10.27	10.74	124.34	1.16	0.009	1231.40	1145.33	−452.28	46.95	*	
80018		245.017	−37.531	10.56	10.92	118.03	2.28	0.019	1230.59	−729.36	991.16	49.42	*	
74995		229.865	−07.722	10.57	11.58	159.52	2.27	0.014	1228.59	−1224.55	−99.52	36.51	*	
3821	4614	12.271	+57.817	3.46	4.59	167.99	0.62	0.004	1222.71	1087.11	−559.65	34.50	*	η Cas
84478	156026	259.057	−26.543	6.33	7.45	167.56	1.06	0.006	1221.51	−479.71	−1123.37	34.56	*	
112120		340.659	+17.668	11.78	10.15	47.13	2.96	0.063	1220.71	1106.85	514.80	122.78	*	
57087		175.544	+26.709	10.67	10.62	97.73	2.27	0.023	1210.61	896.37	−813.70	58.72	*	
82809		253.857	−08.320	11.73	12.67	153.96	4.04	0.026	1209.62	−813.47	−895.23	37.24	*	
82817	152751	253.872	−08.334	9.02	10.23	174.23	3.90	0.022	1208.35	−829.34	−878.81	32.88	*	
49066		150.187	+32.311	11.93	9.83	38.09	3.31	0.087	1207.13	−1008.34	−663.64	150.23		
65877		202.560	−08.574	12.31	11.03	55.50	3.77	0.068	1204.93	−1107.17	−475.43	102.92	*	
171	224930	0.540	+27.084	5.80	5.33	80.63	3.03	0.038	1204.26	778.59	−918.72	70.80	*	85 Peg
19394		62.311	−53.375	11.79	10.91	66.82	2.01	0.030	1194.99	1043.71	581.95	84.78	*	
64394	114710	197.971	+27.876	4.23	4.42	109.23	0.72	0.007	1192.59	−801.94	882.70	51.76	*	β Com

Table 3.6.3. The 150 stars in the Hipparcos Catalogue with largest transverse velocities.

HIP	HD	α	δ	V	M_V	π	σ_π	σ_π/π	$\lvert\mu\rvert$	$\mu_{\alpha*}$	μ_δ	V_T	C	Name
74234	134440	227.557	−16.454	9.44	7.08	33.68	1.67	0.050	3681.49	−1001.47	−3542.66	518.17	*	
74235	134439	227.557	−16.371	9.07	6.74	34.14	1.36	0.040	3681.02	−998.86	−3542.91	511.12	*	
16404		52.815	+66.733	9.91	6.14	17.58	1.53	0.087	1598.39	1190.86	−1066.16	431.01		
21609	29907	69.589	−65.419	9.85	6.00	17.00	0.98	0.058	1448.49	732.93	1249.38	403.91		
49616	89499	151.889	−85.077	8.66	3.41	8.93	0.73	0.082	687.53	−563.56	393.83	364.98		
46120		141.084	−80.526	10.11	6.19	16.46	0.99	0.060	1253.64	202.13	1237.24	361.05		
24316	34328	78.267	−59.647	9.43	5.24	14.55	1.01	0.069	1068.00	935.43	515.36	347.96		
56936		175.083	+67.267	12.20	10.43	44.28	2.83	0.064	3168.11	262.62	−3157.21	339.17		
117254	223065	356.636	−41.580	7.33	2.88	12.91	0.78	0.060	894.11	255.64	−856.78	328.31		
48152	84937	147.233	+13.746	8.33	3.80	12.44	1.06	0.085	860.22	373.81	−774.75	327.80		
76976	140283	235.766	−10.933	7.20	3.41	17.44	0.97	0.056	1155.90	−1115.54	−302.77	314.19	*	
34285		106.621	−57.460	9.53	4.67	10.68	0.91	0.085	697.55	−93.65	691.23	309.62		
57939	103095	178.233	+37.733	6.42	6.61	109.21	0.78	0.007	7058.36	4003.69	−5813.00	306.38	*	Groombr. 1830
10449		33.665	−01.201	9.08	5.12	16.17	1.34	0.083	997.90	994.65	−80.42	292.55		
80837	148816	247.620	+04.182	7.27	4.20	24.34	0.90	0.037	1458.03	−432.73	−1392.34	283.97		
38541	64090	118.386	+30.610	8.27	6.01	35.29	1.04	0.029	1965.35	705.00	−1834.55	264.00	*	
92167	175305	281.774	+74.725	7.18	1.13	6.18	0.56	0.091	329.08	319.24	79.89	252.43		
86431	160693	264.905	+37.186	8.39	4.70	18.32	0.78	0.043	959.03	−497.69	−819.78	248.16		
100568	193901	305.898	−21.368	8.65	5.45	22.88	1.24	0.054	1185.87	539.73	−1055.93	245.70		
65201	116064	200.435	−39.311	8.80	4.76	15.54	1.44	0.093	761.32	−754.20	103.90	232.24		
33582	51754	104.660	−00.479	9.02	4.85	14.63	1.39	0.095	693.04	336.15	−606.06	224.56		
72726		223.038	+71.663	10.85	7.54	21.76	1.50	0.069	959.67	−868.01	−409.29	209.07		
104059		316.225	−16.954	11.45	10.04	52.26	3.06	0.059	2231.65	−914.54	−2035.65	202.43	*	
110618	211998	336.143	−72.254	5.28	2.98	34.60	0.60	0.017	1466.57	1302.45	−674.12	200.93	*	ν Ind
15234		49.109	+38.101	10.67	8.10	30.63	2.36	0.077	1295.70	739.73	−1063.79	200.53		
14759		47.653	−84.544	10.25	6.17	15.27	1.10	0.072	628.19	592.38	209.06	195.02		
59785	106572	183.878	−41.913	6.24	1.10	9.39	0.81	0.086	383.03	−337.63	−180.89	193.37		
18915	25329	60.807	+35.277	8.51	7.18	54.14	1.08	0.020	2205.93	1732.49	−1365.50	193.15	*	
117702	223713	358.059	−61.423	9.43	6.01	20.70	1.20	0.058	835.17	178.75	−815.82	191.26		
60417	107773	185.813	−67.632	6.36	2.83	19.69	0.59	0.030	793.89	−751.13	257.04	191.13		
7869	10607	25.309	−67.676	8.33	4.06	14.01	0.74	0.053	554.34	320.78	−452.10	187.57		
16209		52.218	+37.385	11.10	9.07	39.19	2.52	0.064	1546.25	1120.24	−1065.81	187.04		
19143	281540	61.547	+32.953	10.00	7.21	27.68	1.77	0.064	1075.63	682.14	−831.67	184.21		
84164	155185	258.091	−46.561	9.19	5.43	17.74	1.51	0.085	688.40	−60.63	−685.72	183.95		
3086	3628	9.803	+03.133	7.34	4.03	21.79	0.88	0.040	835.80	781.34	296.76	181.83		
93623	177095	285.987	−20.459	9.62	5.70	16.45	1.41	0.086	628.77	−227.10	−586.32	181.19		
89523		274.016	+68.648	10.13	5.53	12.04	1.07	0.089	459.53	127.76	441.41	180.93		
30514		96.214	−32.123	9.43	4.74	11.55	1.08	0.094	440.02	150.56	413.46	180.60		
69201	123505	212.514	−61.520	9.68	6.29	20.95	1.65	0.079	792.09	−460.09	−644.77	179.23	*	
111783		339.629	+10.541	9.50	5.54	16.15	1.49	0.092	603.09	−277.76	−535.32	177.02		
96062	184400	292.983	+48.592	8.51	3.31	9.13	0.73	0.080	337.37	67.17	330.62	175.17		
12483	16784	40.160	−30.136	8.01	3.99	15.67	1.00	0.064	574.87	569.90	75.41	173.91	*	
80850	150275	247.663	+77.446	6.35	0.87	8.00	0.58	0.072	291.99	−103.74	272.94	173.02		
58843	104800	181.023	+03.342	9.21	5.23	15.97	1.26	0.079	578.47	58.76	−575.48	171.71		
53169		163.152	−02.109	9.79	6.69	23.94	1.71	0.071	867.15	−402.25	−768.21	171.71		
64345	114606	197.840	+09.625	8.72	4.79	16.36	1.15	0.070	585.15	−520.57	267.23	169.55		
53523		164.253	+41.885	9.72	6.33	21.01	1.28	0.061	743.72	−686.26	−286.64	167.80		
36818		113.579	−45.280	10.49	6.42	15.32	1.38	0.090	539.23	−311.93	439.85	166.85		
81170	149414	248.677	−04.227	9.60	6.18	20.71	1.50	0.072	716.47	−133.09	−704.00	164.00	*	
6159	7983	19.751	−08.938	8.90	4.77	14.91	1.23	0.082	513.54	−230.33	−458.99	163.27		
57349	102158	176.379	+47.668	8.06	4.47	19.17	0.87	0.045	659.33	−591.50	−291.29	163.04		
55042		169.012	−57.551	11.66	11.17	79.71	2.80	0.035	2732.50	−2465.03	1179.06	162.51	*	
58708	104556	180.622	+43.085	6.64	2.92	18.05	0.84	0.047	618.06	−347.02	−511.45	162.32		
24186	33793	77.897	−45.004	8.86	10.89	255.26	0.86	0.003	8670.50	6506.05	−5731.39	161.02	*	Kapteyn's star
60956	108754	187.429	−03.332	8.99	5.41	19.20	1.13	0.059	651.28	−328.02	−562.64	160.80	*	
74033	134113	226.945	+08.880	8.26	4.20	15.40	1.37	0.089	522.11	−518.99	−57.02	160.72		
17666	23439	56.757	+41.430	7.67	5.72	40.83	2.24	0.055	1377.03	598.96	−1239.94	159.88	*	
10652	14056	34.279	+21.567	9.06	4.86	14.43	1.33	0.092	481.44	474.18	83.29	158.16		
14594	19445	47.107	+26.333	8.04	5.10	25.85	1.14	0.044	856.36	−209.55	−830.33	157.04		
7007	9138	22.546	+06.144	4.84	−0.38	9.05	0.73	0.081	296.87	293.23	−46.36	155.50		μ Psc
21131	29029	67.946	−49.321	9.26	4.27	10.06	0.79	0.079	329.21	36.00	327.24	155.13		
27080	39194	86.135	−70.147	8.09	6.05	39.08	0.75	0.019	1277.10	−309.03	1239.15	154.91	*	
62809	111777	193.052	−56.574	8.48	5.20	22.09	1.07	0.048	721.69	−687.39	−219.85	154.87		
55988		172.116	+07.520	10.21	8.12	38.23	1.76	0.046	1248.89	−272.87	−1218.72	154.86		
98532	189558	300.252	−12.255	7.72	3.57	14.76	1.10	0.075	478.56	−309.16	−365.29	153.70		
64972	115346	199.747	−74.840	8.38	3.60	11.07	0.79	0.071	358.44	−346.94	−90.08	153.50		
46191	81408	141.271	−12.965	9.64	6.60	24.63	1.53	0.062	795.55	555.69	−569.31	153.12		
104659	201891	317.996	+17.730	7.37	4.63	28.26	1.01	0.036	907.03	−121.58	−898.84	152.15		
15495	278543	49.915	+33.600	9.67	6.34	21.57	1.60	0.074	687.89	404.73	−556.22	151.18		
49066		150.187	+32.311	11.93	9.83	38.09	3.31	0.087	1207.13	−1008.34	−663.64	150.23		
61563		189.213	−76.955	10.98	8.20	27.80	1.60	0.058	877.94	−873.35	−89.61	149.71	*	
71469	128429	219.251	−12.306	6.20	3.58	29.97	0.95	0.032	944.23	−870.88	364.89	149.35		
3456	4211	11.050	−38.422	5.90	0.61	8.76	0.72	0.082	274.92	247.02	120.68	148.77		λ^2 Scl
100792	194598	306.549	+09.451	8.33	4.60	17.94	1.24	0.069	562.21	117.90	−549.71	148.56		
17671	24049	56.775	−56.042	9.48	4.81	11.65	0.92	0.079	364.58	363.03	33.53	148.35		

Table 3.6.3. The 150 stars in the Hipparcos Catalogue with largest transverse velocities (continued).

HIP	HD	α	δ	V	M_V	π	σ_π	σ_π/π	$\lvert\mu\rvert$	$\mu_{\alpha*}$	μ_δ	V_T	C	Name
55806	233832	171.525	+50.375	10.15	6.14	15.74	1.57	0.100	489.78	−473.50	125.21	147.51		
67534	120329	207.569	−57.261	8.34	4.11	14.24	1.05	0.074	438.03	−297.76	−321.26	145.82		
149		0.479	+26.006	11.26	8.06	22.92	2.17	0.095	700.73	−309.64	−628.61	144.93	*	
114971	219615	349.290	+03.282	3.70	0.68	24.92	0.89	0.036	760.56	760.35	17.96	144.68		γ Psc
110468	212038	335.649	−50.805	8.75	6.48	35.14	1.30	0.037	1071.14	165.19	−1058.33	144.50		
109680	210368	333.271	−71.145	9.67	5.52	14.79	1.18	0.080	449.56	323.47	−312.20	144.09		
2743	3222	8.757	−63.694	8.55	6.21	34.04	0.86	0.025	1031.09	881.63	−534.68	143.59		
115610		351.298	+34.289	9.35	6.34	25.02	1.34	0.054	756.17	−297.94	−695.00	143.27		
64125	114076	197.143	−41.644	9.39	5.79	19.08	1.28	0.067	572.64	−568.09	−72.02	142.27		
99267		302.255	+42.864	10.11	5.51	12.04	1.13	0.094	360.88	119.35	340.57	142.09		
55415	98732	170.231	−58.704	7.02	2.05	10.16	0.78	0.077	303.65	−302.57	25.61	141.68		
4012		12.867	+58.301	10.66	9.33	54.23	2.12	0.039	1618.38	1566.84	405.19	141.47	*	
35633		110.300	−15.357	9.78	6.02	17.74	1.32	0.074	527.21	336.88	−405.54	140.88		
109368		332.362	−78.926	10.87	7.30	19.32	1.53	0.079	572.47	309.08	−481.86	140.46		
57888	103112	178.088	+09.948	7.61	3.08	12.39	0.97	0.078	364.85	−347.87	110.01	139.59	*	
63090	112300	193.902	+03.398	3.39	−0.57	16.11	0.88	0.055	474.39	−471.44	−52.81	139.59		δ Vir
39911	68089	122.272	−42.075	9.60	5.48	14.99	0.99	0.066	441.30	−396.81	193.11	139.56		
99792	351759	303.708	+18.466	10.46	7.35	23.91	1.78	0.074	703.50	−120.84	−693.04	139.48		
106924		324.819	+60.283	10.36	6.27	15.20	1.21	0.080	447.16	−381.55	233.17	139.46		
18180		58.333	−37.064	12.13	10.11	39.48	2.69	0.068	1159.32	−408.80	−1084.85	139.20	*	
70791	127243	217.159	+49.845	5.58	0.70	10.59	0.61	0.058	308.04	−304.53	−46.36	137.89		g Boo
52104	93118	159.689	−83.109	8.84	4.11	11.32	0.82	0.072	329.02	−265.89	193.79	137.78		
86013	159482	263.681	+06.013	8.37	4.97	20.90	1.18	0.056	607.26	−478.64	373.73	137.74		
45593		139.389	+77.245	10.12	7.95	36.74	3.39	0.092	1067.29	−1067.29	−0.91	137.71	*	
13366	17820	42.993	+11.371	8.38	4.31	15.38	1.39	0.090	446.27	37.33	−444.71	137.55		
43393	75530	132.588	−05.535	9.18	5.55	18.78	1.48	0.079	544.46	−181.54	−513.30	137.43		
67863	121004	208.494	−46.539	9.02	5.14	16.73	1.35	0.081	482.18	−482.10	8.87	136.63		
5122	5256	16.407	+87.319	8.77	4.01	11.19	0.83	0.074	320.33	310.23	79.80	135.70		
93968	179141	287.000	+58.144	7.95	1.97	6.37	0.63	0.099	182.08	−11.39	181.72	135.50		
8558	11569	27.601	−71.949	9.01	3.89	9.47	0.77	0.081	270.58	268.97	−29.45	135.45		
5336	6582	17.054	+54.924	5.17	5.78	132.40	0.60	0.005	3776.76	3421.44	−1599.27	135.22	*	μ Cas
18802	25704	60.434	−57.208	8.11	4.51	19.02	0.87	0.046	539.99	347.27	413.51	134.58		
67285		206.849	−06.135	10.27	7.13	23.52	1.70	0.072	667.67	−338.90	−575.27	134.57		
18235	24616	58.497	−23.136	6.68	2.68	15.87	0.81	0.051	449.15	336.31	−297.71	134.16		
23518		75.844	+53.132	9.96	9.23	71.35	1.76	0.025	2015.94	1304.13	−1537.29	133.94	*	
117029	222794	355.861	+58.079	7.14	3.85	22.01	0.65	0.030	619.42	390.05	481.19	133.41		
71819	129290	220.371	+13.602	8.37	4.11	14.04	1.19	0.085	394.74	−387.65	−74.47	133.28		
53311	94518	163.551	−31.159	8.33	3.85	12.72	1.00	0.079	357.54	−113.91	−338.91	133.25	*	
3114	4229	9.909	−85.701	6.81	0.76	6.18	0.52	0.084	173.68	173.24	−12.36	133.22		
90393	170357	276.658	+46.083	8.27	4.06	14.37	0.73	0.051	402.02	−348.79	199.92	132.62		
59198		182.095	−00.482	11.25	8.95	34.60	2.58	0.075	967.52	−963.32	−90.07	132.56	*	
70520	126512	216.375	+20.592	7.27	3.91	21.32	0.83	0.039	596.05	132.60	−581.11	132.53		
63559	113083	195.361	−27.374	8.04	4.38	18.51	1.12	0.061	517.34	−476.18	−202.22	132.49		
41269		126.298	+32.611	10.10	7.02	24.18	1.83	0.076	674.97	13.71	−674.83	132.33	*	
82588	152391	253.247	−00.023	6.65	5.51	59.04	0.87	0.015	1645.54	−711.75	−1483.65	132.12	*	
2293		7.322	+80.913	11.37	7.60	17.58	1.75	0.100	489.22	300.75	385.86	131.92		
107314		326.043	+25.333	9.48	6.23	22.39	1.41	0.063	620.93	−359.01	−506.62	131.46		
64444	114692	198.134	−34.747	7.76	3.38	13.30	1.24	0.093	368.61	−250.44	−270.47	131.38		
102237		310.750	+35.498	11.41	8.11	21.86	2.18	0.100	605.44	−205.32	−569.56	131.29		
65982	117635	202.918	−02.318	7.32	4.87	32.35	1.77	0.055	895.47	−854.52	267.70	131.22	*	
89587	167768	274.221	−03.007	5.99	0.97	9.91	0.83	0.084	273.87	18.11	−273.27	131.01		
84988	155918	260.562	−75.348	7.00	4.77	35.85	0.70	0.020	990.21	−957.24	−253.38	130.94	*	
50713	89777	155.321	−17.049	9.35	5.54	17.30	1.26	0.073	474.27	−459.09	119.03	129.96		
80	224817	0.242	−11.824	8.40	4.36	15.59	1.43	0.092	427.15	419.04	−82.83	129.88		
53070	94028	162.868	+20.279	8.21	4.63	19.23	1.13	0.059	526.13	−261.86	−456.33	129.70		
102046	196892	310.206	−18.792	8.24	4.23	15.78	1.22	0.077	430.84	44.38	−428.55	129.43		
115359	220197	350.492	+16.633	8.92	4.80	14.97	1.23	0.082	408.35	405.37	−49.22	129.31		
88166		270.102	+14.716	9.23	5.72	19.84	1.40	0.071	540.57	−469.66	−267.64	129.16		
117159	222935	356.289	+29.562	8.40	6.11	34.85	1.02	0.029	948.86	948.85	−3.41	129.07		
66413		204.238	+07.768	10.00	7.49	31.52	1.66	0.053	856.33	−776.59	−360.85	128.79	*	
7902	10145	25.403	+66.911	7.70	4.88	27.28	0.96	0.035	740.89	692.05	−264.55	128.75	*	
88033	316899	269.722	−30.170	9.34	6.33	25.06	1.91	0.076	680.24	173.92	−657.63	128.68	*	
102862	198245	312.594	−40.607	8.94	5.06	16.78	1.30	0.077	455.19	−75.09	−448.95	128.59		
113477		344.720	+69.030	8.76	5.71	24.52	0.77	0.031	664.38	593.24	299.10	128.44		
67755	120764	208.208	−54.579	7.20	2.33	10.64	0.96	0.090	287.89	−265.77	−110.66	128.26		
103392	199580	314.199	+42.895	7.21	2.54	11.64	0.68	0.058	313.92	218.84	225.06	127.84		
55360		170.038	+65.846	9.31	9.52	109.95	1.11	0.010	2952.47	−2946.70	184.52	127.30	*	
7961	10519	25.561	−17.889	7.45	4.00	20.45	0.99	0.048	548.93	548.81	11.38	127.25		
439	225213	1.335	−37.352	8.56	10.36	229.33	1.08	0.005	6099.89	5634.07	−2337.94	126.09	*	
10279		33.092	+03.580	10.04	9.96	96.28	1.80	0.019	2556.23	−1761.07	−1852.82	125.86	*	
34082		106.012	+71.196	9.34	5.31	15.64	1.44	0.092	415.08	−61.23	−410.54	125.81		
40841	68744	125.012	+73.337	8.44	3.48	10.18	0.91	0.089	270.01	−100.39	−250.65	125.73		
110035	211476	334.311	+12.898	7.04	4.60	32.55	0.95	0.029	863.26	857.66	98.18	125.72		
72407		222.079	+58.910	9.74	4.84	10.49	0.93	0.089	277.52	−269.10	67.83	125.41		
106356	205027	323.120	+01.013	8.31	4.39	16.43	1.23	0.075	433.99	−278.88	−332.52	125.22		

Table 3.6.4. The 150 most luminous stars in the Hipparcos Catalogue.

HIP	HD	α	δ	V	M_V	π	σ_π	σ_π/π	$\lvert\mu\rvert$	$\mu_{\alpha*}$	μ_δ	V_T	C	Name
24436	34085	78.634	−08.202	0.18	−6.69	4.22	0.81	0.192	1.95	1.87	−0.56	2.19		β Ori
100453	194093	305.557	+40.257	2.23	−6.12	2.14	0.51	0.238	2.60	2.43	−0.93	5.76		γ Cyg
39429	66811	120.896	−40.003	2.21	−5.95	2.33	0.51	0.219	35.09	−30.82	16.77	71.39		ζ Pup
48002	85123	146.776	−65.072	2.92	−5.56	2.01	0.40	0.199	12.57	−11.55	4.97	29.65		υ Car
30438	45348	95.988	−52.696	−0.62	−5.53	10.43	0.53	0.051	30.98	19.99	23.67	14.08		α Car
68702	122451	210.956	−60.373	0.61	−5.42	6.21	0.56	0.090	42.21	−33.96	−25.06	32.22		β Cen
25985	36673	83.183	−17.822	2.58	−5.40	2.54	0.72	0.283	3.61	3.27	1.54	6.75		α Lep
48774	86440	149.216	−54.568	3.52	−5.34	1.69	0.50	0.296	13.43	−13.13	2.83	37.68		ϕ Vel
39953	68273	122.383	−47.337	1.75	−5.31	3.88	0.53	0.137	11.54	−5.93	9.90	14.10		γ Vel
26727	37742	85.190	−01.943	1.74	−5.26	3.99	0.79	0.198	4.73	3.99	2.54	5.62		ζ Ori
27989	39801	88.793	+07.407	0.45	−5.14	7.63	1.64	0.215	29.41	27.33	10.86	18.27		α Ori
85927	158926	263.402	−37.104	1.62	−5.05	4.64	0.90	0.194	31.24	−8.90	−29.95	31.92		λ Sco
25930	36486	83.002	−00.299	2.25	−4.99	3.56	0.83	0.233	1.76	1.67	0.56	2.35		δ Ori
35264	56855	109.286	−37.097	2.71	−4.92	2.98	0.55	0.185	12.68	−10.57	7.00	20.17		π Pup
46974	83183	143.611	−59.230	4.08	−4.83	1.65	0.49	0.297	12.74	−11.23	6.02	36.61		h Car
27366	38771	86.939	−09.670	2.07	−4.65	4.52	0.77	0.170	1.96	1.55	−1.20	2.06		κ Ori
38518	64760	118.326	−48.103	4.22	−4.65	1.68	0.50	0.298	7.66	−4.90	5.89	21.62		J Pup
47854	84810	146.312	−62.508	3.69	−4.64	2.16	0.47	0.218	15.31	−12.88	8.28	33.60		l Car
41037	71129	125.629	−59.510	1.86	−4.58	5.16	0.49	0.095	34.03	−25.34	22.72	31.27		ϵ Car
18246	24398	58.533	+31.884	2.84	−4.55	3.32	0.75	0.226	10.16	4.41	−9.15	14.50		ζ Per
37819	63032	116.314	−37.969	3.62	−4.52	2.35	0.55	0.234	12.31	−10.77	5.97	24.84		c Pup
43023	75063	131.507	−46.042	3.87	−4.52	2.10	0.53	0.252	13.15	−12.23	4.82	29.67		a Vel
15863	20902	51.081	+49.861	1.79	−4.50	5.51	0.66	0.120	35.47	24.11	−26.01	30.51		α Per
45556	80404	139.273	−59.275	2.21	−4.42	4.71	0.46	0.098	23.11	−19.03	13.11	23.26		ι Car
85267	157246	261.349	−56.378	3.31	−4.40	2.87	0.75	0.261	15.87	−0.77	−15.85	26.21		γ Ara
33856	52877	105.430	−27.935	3.49	−4.37	2.68	0.59	0.220	7.59	−6.01	4.64	13.43		σ CMa
40091	68553	122.840	−39.619	4.44	−4.36	1.74	0.52	0.299	9.43	−8.91	3.10	25.70		h^1 Pup
31407	47306	98.744	−52.976	4.35	−4.31	1.85	0.51	0.276	13.67	−7.65	11.33	35.03		
99675	192577	303.408	+46.741	3.80	−4.29	2.41	0.57	0.237	4.60	4.20	1.87	9.04		o^1 Cyg
4427	5394	14.177	+60.717	2.15	−4.22	5.32	0.56	0.105	25.93	25.65	−3.82	23.11		γ Cas
60718	108248	186.650	−63.099	0.77	−4.19	10.17	0.67	0.066	38.31	−35.37	−14.73	17.86		α^1 Cru
107315	206778	326.046	+09.875	2.38	−4.19	4.85	0.84	0.173	30.05	30.02	1.38	29.37		ϵ Peg
26207	36861	83.784	+09.934	3.39	−4.16	3.09	0.78	0.252	2.13	−1.03	−1.86	3.26		λ Ori
32246	48329	100.983	+25.131	3.06	−4.15	3.61	0.91	0.252	14.12	−5.93	−12.81	18.54		ϵ Gem
42312	73634	129.411	−42.989	4.11	−4.11	2.27	0.50	0.220	14.05	−10.38	9.47	29.34		e Vel
33579	52089	104.656	−28.972	1.50	−4.10	7.57	0.57	0.075	3.49	2.63	2.29	2.18		ϵCMa
42624	74272	130.305	−47.317	4.74	−4.08	1.72	0.46	0.267	12.57	−10.53	6.87	34.65		n Vel
104060	200905	316.233	+43.928	3.72	−4.07	2.77	0.52	0.188	8.61	8.60	0.35	14.73		ξ Cyg
65936	117440	202.761	−39.407	3.90	−4.03	2.60	0.75	0.288	19.27	−15.65	−11.25	35.14		d Cen
36514	59890	112.678	−30.962	4.65	−4.00	1.86	0.53	0.285	11.77	−11.74	0.84	30.00		
34981	56014	108.563	−26.353	4.42	−4.00	2.07	0.59	0.285	7.64	−6.58	3.89	17.51		27 CMa
44816	78647	136.999	−43.433	2.23	−3.99	5.69	0.53	0.093	27.25	−23.21	14.28	22.70		λ Vel
88886	166182	272.190	+20.815	4.37	−3.98	2.14	0.63	0.294	6.77	−2.71	−6.20	14.99		102 Her
30324	44743	95.675	−17.956	1.98	−3.95	6.53	0.66	0.101	3.48	−3.45	−0.47	2.53		β CMa
62434	111123	191.930	−59.689	1.25	−3.92	9.25	0.61	0.066	49.91	−48.24	−12.82	25.58		β Cru
109074	209750	331.446	−00.320	2.95	−3.88	4.30	0.83	0.193	20.47	17.90	−9.93	22.57		α Aqr
42568	74375	130.154	−59.761	4.31	−3.87	2.31	0.46	0.199	8.45	−6.87	4.92	17.34		d Car
107136	206672	325.524	+51.190	4.69	−3.87	1.94	0.53	0.273	5.66	5.25	−2.11	13.83		π^1 Cyg
80112	147165	245.297	−25.593	2.90	−3.86	4.44	0.81	0.182	20.63	−10.03	−18.03	22.03		σ Sco
25281	35411	81.119	−02.397	3.35	−3.86	3.62	0.88	0.243	3.26	−0.54	−3.21	4.26		η Ori
71860	129056	220.482	−47.388	2.30	−3.83	5.95	0.76	0.128	32.15	−21.15	−24.22	25.62		α Lup
88714	165024	271.658	−50.091	3.65	−3.81	3.22	0.71	0.220	12.52	−8.43	−9.26	18.44		θ Ara
29276	42933	92.575	−54.969	4.72	−3.81	1.97	0.50	0.254	7.72	−4.11	6.53	18.57		δ Pic
34088	52973	106.027	+20.570	4.01	−3.76	2.79	0.81	0.290	5.80	−5.72	−0.96	9.85		ζ Gem
26069	37350	83.406	−62.490	3.76	−3.76	3.14	0.59	0.188	12.60	1.06	12.56	19.03		β Dor
51232	90853	156.970	−58.739	3.81	−3.71	3.13	0.53	0.169	13.43	−13.25	2.21	20.34		s Car
50555	89682	154.903	−55.029	4.59	−3.71	2.19	0.48	0.219	15.33	−14.79	4.03	33.18		
99848	192909	303.868	+47.714	3.96	−3.70	2.94	0.60	0.204	4.06	3.88	1.20	6.55		o^2 Cyg
51849	91942	158.897	−57.558	4.45	−3.68	2.37	0.52	0.219	15.43	−15.43	−0.16	30.86		r Car
50676	89890	155.228	−56.043	4.50	−3.65	2.34	0.49	0.209	18.21	−18.15	1.49	36.89		J Vel
92420	174638	282.520	+33.363	3.52	−3.64	3.70	0.52	0.141	4.59	1.10	−4.46	5.89		β Lyr
11767	8890	37.946	+89.264	1.97	−3.64	7.56	0.48	0.063	45.75	44.22	−11.74	28.69		α UMi
45941	81188	140.528	−55.011	2.47	−3.62	6.05	0.48	0.079	15.53	−10.72	11.24	12.17		κ Vel
82273	150798	252.166	−69.028	1.91	−3.62	7.85	0.63	0.080	37.45	17.85	−32.92	22.61		α TrA
111104	213420	337.622	+43.123	4.52	−3.60	2.38	0.64	0.269	6.11	−2.05	−5.76	12.18		6 Lac
65474	116658	201.298	−11.161	0.98	−3.55	12.44	0.86	0.069	53.04	−42.50	−31.73	20.21		α Vir
41039	70930	125.632	−48.490	4.79	−3.54	2.16	0.57	0.264	9.26	−6.28	6.81	20.33		B Vel
107533	207330	326.698	+49.310	4.23	−3.52	2.82	0.52	0.184	4.06	3.61	−1.86	6.83		π^2 Cyg
70069	125288	215.081	−56.386	4.30	−3.50	2.75	0.59	0.215	11.98	−9.29	−7.57	20.66		v Cen
78820	144217	241.359	−19.805	2.56	−3.50	6.15	1.12	0.182	25.79	−6.75	−24.89	19.88		β^1 Sco
85258	157244	261.325	−55.530	2.84	−3.49	5.41	0.76	0.140	26.04	−8.23	−24.71	22.82		β Ara
38901	65456	119.417	−30.335	4.76	−3.47	2.26	0.58	0.257	10.81	−8.11	7.14	22.66		
109556	210839	332.877	+59.415	5.05	−3.47	1.98	0.46	0.232	13.21	−7.22	−11.06	31.62		λ Cep
106278	204867	322.890	−05.571	2.90	−3.47	5.33	0.94	0.176	23.75	22.79	−6.70	21.13		β Aqr
93279	176670	285.003	+32.145	4.94	−3.43	2.12	0.55	0.259	11.52	6.13	9.75	25.75		λ Lyr

Table 3.6.4. The 150 most luminous stars in the Hipparcos Catalogue (continued).

HIP	HD	α	δ	V	M_V	π	σ_π	σ_π/π	$\lvert\mu\rvert$	$\mu_{\alpha*}$	μ_δ	V_T	C	Name
111022	213310	337.383	+47.707	4.34	−3.42	2.80	0.50	0.179	3.42	−0.60	−3.37	5.80		5 Lac
32759	50013	102.460	−32.508	3.50	−3.42	4.13	0.50	0.121	10.03	−9.18	4.04	11.51		κ CMa
76297	138690	233.785	−41.167	2.80	−3.40	5.75	1.24	0.216	30.15	−16.05	−25.52	24.85		γ Lup
23522	31910	75.855	+60.442	4.03	−3.40	3.27	0.74	0.226	15.99	−6.11	−14.78	23.19		β Cam
42828	74575	130.898	−33.186	3.68	−3.39	3.86	0.53	0.137	17.78	−14.28	10.60	21.84		α Pyx
50371	89388	154.271	−61.332	3.39	−3.38	4.43	0.49	0.111	25.08	−24.25	6.38	26.83		q Car
86670	160578	265.622	−39.030	2.39	−3.38	7.03	0.73	0.104	26.36	−6.49	−25.55	17.78		κ Sco
109492	210745	332.714	+58.201	3.39	−3.35	4.49	0.50	0.111	14.08	13.35	4.49	14.87		ζ Cep
73273	132058	224.633	−43.134	2.68	−3.35	6.23	0.71	0.114	51.25	−34.06	−38.30	39.00		β Lup
38020	63578	116.881	−46.609	5.22	−3.33	1.95	0.47	0.241	8.71	−3.57	7.95	21.19		
110991	213306	337.293	+58.415	4.07	−3.32	3.32	0.58	0.175	16.85	16.47	3.55	24.06		δ Cep
40943	70556	125.338	−36.484	5.18	−3.31	2.00	0.56	0.280	10.65	−8.04	6.98	25.24		
47193	81817	144.272	+81.326	4.28	−3.31	3.03	0.54	0.178	23.14	−16.77	−15.95	36.21		
85696	158408	262.691	−37.296	2.70	−3.31	6.29	0.81	0.129	29.44	−4.19	−29.14	22.19		υ Sco
98162	188603	299.237	−27.170	4.54	−3.30	2.70	0.75	0.278	17.77	9.60	−14.95	31.19		b Sgr
24845	34816	79.894	−13.177	4.29	−3.30	3.03	0.77	0.254	5.35	−2.49	−4.74	8.38		λ Lep
38957	65818	119.560	−49.245	4.47	−3.29	2.80	0.51	0.182	10.18	−7.48	6.91	17.24		
23015	31398	74.248	+33.166	2.69	−3.29	6.37	0.96	0.151	18.89	3.63	−18.54	14.06		ι Aur
98425	189687	299.980	+37.043	5.15	−3.27	2.07	0.50	0.242	0.48	0.41	−0.24	1.09		25 Cyg
57696	102839	177.486	−70.226	4.98	−3.27	2.24	0.58	0.259	7.86	−7.61	−1.96	16.63		
25044	35039	80.441	−00.382	4.72	−3.26	2.53	0.74	0.292	1.73	0.45	1.67	3.24		o Ori
35037	56139	108.703	−26.773	4.01	−3.25	3.53	0.58	0.164	13.82	−11.50	7.67	18.56		ω CMa
80079	147084	245.159	−24.169	4.55	−3.24	2.77	0.76	0.274	15.31	−4.23	−14.71	26.19		o Sco
23453	32068	75.620	+41.076	3.69	−3.22	4.14	0.81	0.196	23.20	8.88	−21.43	26.56		ζ Aur
81377	149757	249.290	−10.567	2.54	−3.20	7.12	0.71	0.100	28.60	13.07	25.44	19.04		ζ Oph
93194	176437	284.736	+32.690	3.25	−3.20	5.14	0.51	0.099	3.28	−2.76	1.77	3.02		γ Lyr
42834	74753	130.918	−49.823	5.15	−3.19	2.15	0.57	0.265	5.10	−3.56	3.65	11.24		D Vel
18532	24760	59.463	+40.010	2.90	−3.19	6.06	0.82	0.135	27.16	12.61	−24.06	21.25		ϵ Per
55831	99556	171.648	−61.115	5.22	−3.17	2.10	0.55	0.262	13.94	−13.83	1.78	31.48		
78401	143275	240.083	−22.622	2.29	−3.16	8.12	0.88	0.108	37.90	−8.67	−36.90	22.13		δ Sco
83081	152786	254.655	−55.990	3.12	−3.11	5.68	0.91	0.160	39.76	−18.31	−35.29	33.18	*	ζ Ara
94481	180163	288.440	+39.146	4.43	−3.09	3.13	0.51	0.163	1.70	−1.59	−0.61	2.58		η Lyr
42712	74455	130.567	−48.099	5.48	−3.09	1.93	0.57	0.295	6.04	−4.92	3.51	14.84		
9640	12533	30.975	+42.330	2.10	−3.08	9.19	0.73	0.079	66.65	43.08	−50.85	34.38		γ^1 And
106032	205021	322.165	+70.561	3.23	−3.08	5.48	0.47	0.086	15.33	12.60	8.73	13.26		β Cep
61136	108968	187.918	−59.424	5.49	−3.07	1.94	0.57	0.294	13.64	−13.19	−3.47	33.33		35 Cru
99824	192685	303.816	+25.592	4.79	−3.04	2.72	0.77	0.283	8.53	6.90	−5.02	14.87		
17358	22928	55.731	+47.788	3.01	−3.04	6.18	0.85	0.138	48.23	23.83	−41.93	36.99		δ Per
97278	186791	296.565	+10.613	2.72	−3.03	7.08	0.75	0.106	16.02	15.72	−3.08	10.73		γ Aql
48374	85622	147.920	−46.548	4.58	−3.03	3.01	0.56	0.186	26.30	−24.41	9.80	41.43		m Vel
66657	118716	204.972	−53.466	2.29	−3.02	8.68	0.77	0.089	19.41	−14.60	−12.79	10.60		ϵ Cen
113726	217675	345.480	+42.326	3.62	−3.01	4.71	0.67	0.142	22.47	22.47	0.24	22.62		o And
107374	207198	326.222	+62.461	5.94	−3.01	1.62	0.48	0.296	4.09	−2.98	−2.80	11.97		
26176	36822	83.705	+09.490	4.39	−3.01	3.31	0.77	0.233	2.78	−1.24	−2.49	3.98		ϕ^1 Ori
99120	190421	301.847	−52.881	4.93	−3.00	2.60	0.72	0.277	14.46	−12.72	6.88	26.37		ξ Tel
52468	93070	160.885	−60.567	4.58	−2.99	3.06	0.50	0.163	15.54	−15.22	3.12	24.07		w Car
92791	175588	283.626	+36.899	4.22	−2.98	3.63	0.56	0.154	7.48	−6.73	3.26	9.77		δ^2 Lyr
73771	131246	226.196	−83.038	5.65	−2.98	1.88	0.52	0.277	19.66	−8.65	−17.65	49.56		π^2 Oct
43325	75630	132.413	−40.320	5.47	−2.97	2.05	0.52	0.254	9.79	−9.76	−0.76	22.64		
17884	23475	57.380	+65.526	4.39	−2.97	3.38	0.63	0.186	14.20	−2.50	−13.98	19.92		
73334	132200	224.790	−42.104	3.13	−2.96	6.05	0.73	0.121	27.76	−17.76	−21.33	21.75		κ Cen
70574	126341	216.534	−45.221	4.56	−2.95	3.15	0.69	0.219	19.47	−13.51	−14.02	29.30		τ^1 Lup
103632	200120	314.956	+47.521	4.74	−2.95	2.90	0.64	0.221	7.66	7.25	2.47	12.52		f^1 Cyg
64820	115211	199.304	−66.783	4.86	−2.94	2.75	0.62	0.225	16.53	−15.27	−6.34	28.50		
44626	78764	136.410	−70.539	4.66	−2.94	3.02	0.53	0.175	10.81	−4.36	9.89	16.97		
84970	157056	260.502	−24.999	3.27	−2.92	5.79	0.69	0.119	25.24	−8.84	−23.64	20.66		θ Oph
52154	92449	159.827	−55.603	4.29	−2.92	3.62	0.53	0.146	19.36	−18.87	4.31	25.35		x Vel
52419	93030	160.739	−64.394	2.74	−2.91	7.43	0.50	0.067	22.39	−18.87	12.06	14.29		θ Car
98194	189178	299.308	+40.368	5.46	−2.90	2.13	0.54	0.254	7.10	7.08	−0.47	15.79		
38872	65551	119.327	−44.110	5.08	−2.90	2.54	0.50	0.197	13.40	−11.48	6.92	25.02		N Pup
98068	188892	298.966	+38.487	4.95	−2.89	2.71	0.54	0.199	1.58	1.46	0.60	2.76		22 Cyg
51140	90677	156.704	−54.877	5.58	−2.87	2.04	0.50	0.245	14.60	−13.71	5.01	33.92		
30867	45725	97.204	−07.033	3.76	−2.87	4.72	1.10	0.233	8.58	−7.00	−4.97	8.62		β Mon
107348	206859	326.128	+17.350	4.34	−2.87	3.62	0.74	0.204	13.34	7.90	−10.75	17.47		9 Peg
39690	67582	121.668	−45.266	5.04	−2.86	2.63	0.51	0.194	12.20	−5.28	11.00	21.99		
78265	143018	239.713	−26.114	2.89	−2.85	7.10	0.84	0.118	28.37	−12.00	−25.71	18.94		π Sco
75097	137422	230.182	+71.834	3.00	−2.84	6.79	0.46	0.068	25.25	−18.03	17.68	17.63		γ UMi
59196	105435	182.090	−50.722	2.58	−2.84	8.25	0.79	0.096	47.96	−47.53	−6.42	27.56		δ Cen
104194	201251	316.650	+47.648	4.56	−2.83	3.32	0.55	0.166	6.58	6.51	−0.99	9.40		f^2 Cyg
38010	63465	116.854	−38.511	5.07	−2.83	2.63	0.53	0.202	10.99	−9.94	4.69	19.81		
101076	195295	307.349	+30.369	4.01	−2.82	4.30	0.52	0.121	6.90	6.87	−0.64	7.61		41 Cyg
31978	47839	100.244	+09.896	4.66	−2.82	3.19	0.73	0.229	2.60	−0.66	−2.51	3.86		15 Mon
27204	38666	86.500	−32.306	5.18	−2.81	2.52	0.55	0.218	22.82	3.01	−22.62	42.93		μ Col
114104	218376	346.653	+59.420	4.84	−2.81	2.95	0.53	0.180	7.05	6.77	−1.97	11.33		1 Cas
68002	121263	208.885	−47.288	2.55	−2.81	8.48	0.74	0.087	72.58	−57.14	−44.75	40.57		ζ Cen

APPENDIX A

GLOSSARY

Appendix A. Glossary

AAVSO: the American Association of Variable Star Observers. The AAVSO provided data for the construction of pre-launch ephemerides of large-amplitude variable stars, and provided data for the construction of the Hipparcos light curves (Volume 12) for these objects.

Abscissa: the angular coordinate of a star measured from an arbitrary origin on the reference great-circle to the normal projection of the star on that circle. The perpendicular coordinate is known as the ordinate of the star. The collection of abscissa measurements were used to derive the astrometric parameters of each star. The individual abscissa measurements are retained as useful intermediate astrometric data on the ASCII CD-ROMs. See also great-circle reduction.

ac magnitude: the magnitude derived from measurements of the modulation amplitude of the image dissector tube (IDT) signal. See also dc magnitude, IDT signal, and main grid.

Accuracy: the uncertainty of a measured quantity, including accidental and systematic errors. The term is often used synonymously with 'external standard error' (cf. precision).

Astrometric binary: a physical stellar system not observed as a visual double because of its small separation and/or large magnitude difference, but evidently non-single because of the detectable non-linear proper motion of the photocentre. A large residual from a model with five astrometric parameters may also indicate that the actual motion may deviate from the assumed rectilinear motion of the centre of mass.

Astrometric parameter determination: the final step of the 'three-step' method, which allowed the calculation of astrometric parameters for any (single) star from its observed abscissae on (typically) 50 different reference great-circles.

Attitude determination: the name given to the process by which the data from the satellite (the star mapper transits and the gyro data) were used to derive a description of the three-axis attitude of the viewing directions of the payload at any instant in time. On-board, this process (referred to as real-time attitude determination) used the brighter star transit information from the star mapper to yield a three-axis attitude accurate to about 1 arcsec rms. On the ground, this was improved to some 0.1 arcsec for the direction of the spin axis, and to a few milliarcsec for the spin phase.

Barycentric Julian Date: see Section 1.2.3 on time scales. The epochs in the Hipparcos and Tycho Epoch Photometry Annexes (the compilations of epoch photometry) have been corrected to the solar system barycentre by the application of light-time corresponding to the projected coordinate distance from the satellite to the barycentre, and are expressed in terms of Barycentric Julian Date, BJD(TT).

Basic angle: the fixed angle, approximately 58°, between the two viewing directions of the Hipparcos telescope. The exact value of the basic angle was determined during commissioning to a precision of about 1 arcsec, sufficient for the piloting of the image dissector tube to the transiting programme stars. During the great-circle reductions, the basic angle was determined, as part of the geometrical transformation parameters, to much better than a milliarcsec. The stability of the basic angle during the calibration period (of one reference great-circle, or about 10.7 hours) was ensured by the payload thermal control.

BJD: see Barycentric Julian Date

B_T magnitude: see Tycho magnitudes.

Catalogue entry: the term 'entry', rather than object or star, is used in those contexts where it is appropriate to draw attention to the fact that a given HIP number may refer not necessarily to a single star, but either to the photocentre, or to a component, or to the centre of mass of a double or multiple system. An entry can represent the whole (double or multiple) system; it may be one of two or three entries processed together

(referred to as a 'two-pointing' or 'three-pointing' system); or it may have been processed independently of any other entry of the system.

Catalogue epoch: J1991.25. Positions are given at the catalogue epoch.

CCDM Catalogue: the Catalogue of Components of Double and Multiple Stars, compiled at the Observatoire Royal de Belgique for the purposes of the collection and unification of double and multiple star data (see Section 1.4.4).

CCDM number: the data in Part C of the Double and Multiple Systems Annex (see Section 2.3) are identified by their numbers in the CCDM Catalogue. These numbers are based upon the approximate equatorial coordinates of the system at epoch and equinox J2000.0, in the format hhmm.m±ddmm.

CDS: the Centre de Données astronomiques de Strasbourg (the astronomical data centre at Strasbourg).

Celestia 2000: the CD-ROM package containing the primary parts of the Hipparcos and Tycho Catalogues, in a bit-optimised format, and supplied with interrogation software for use on specific computer platforms.

Censoring: see de-censoring.

Complementary field of view: during the observation of a programme star in one of the two fields of view, the region of the sky covered by the other field of view is referred to as the complementary field of view.

Cosmic error: see stochastic solutions.

Cramér-Rao limit (or Minimum Variance Bound): in statistical estimation a lower bound to the variance of an unbiased estimator of a parameter. The practical importance of the limit is that it is often much easier to calculate than the actual variance of a given estimator, and is independent of the choice of estimator: it is given by the negative inverse of the expected curvature (or Hessian matrix) of the log-likelihood function. The realism of the Cramér-Rao limit as an estimator of the variance of a given parameter must be investigated e.g. by Monte Carlo simulations.

Data analysis consortia (or data reduction consortia): the scientific groups responsible for the parallel treatment of the main mission data (FAST and NDAC) and the star mapper (or Tycho) data (TDAC). Their composition is given in the introduction to this volume. FAST and NDAC each delivered their own astrometric, double star, and photometric catalogues and annexes, which were merged to provide the unique Hipparcos Catalogue products.

dc magnitude: the magnitude derived from measurements of the zero-level of the image dissector tube (IDT) signal. See also ac magnitude, IDT signal, and main grid.

De-censoring: Because of photon noise, a star close to the magnitude limit of the Tycho observations will not be detected at every transit across the star mapper. Those transits not giving a detection are referred to as 'censored'. If only the detected transits were used to derive a mean magnitude for such a star, this would be strongly biased towards higher brightness. De-censoring is the mathematical process taking the censored transits into account in order to derive a bias-free mean magnitude (see Volume 4 for further details).

Detection: in the context of the Tycho Catalogue, this refers to a significant peak in the stream of photon count samples from the star mapper. The transit of a star may or may not produce a detection, depending on the star's brightness, the level of background counts and photon noise. Conversely, a detection does not necessarily correspond to a transit of a star, but may also be produced by random photon noise.

Detector's response profile: the response of the main detector as a function of the distance to its centre. It is tabulated in Section 1.4.

Double and multiple stars: an introduction to the complexities of the analysis and presentation of double and multiple systems in the context of the Hipparcos Catalogue is given in Section 1.4. Systems may be classified as 'double' or 'multiple', with between one to four entries with a common system identifier (CCDM number). An individual *entry* may also be classified as 'double' or 'multiple'. Systems may be further considered as 'single-pointing', 'two-pointing', or 'three-pointing', depending upon the number of entries considered together during the data analysis (the term 'pointing' referring to the way in which the sensitive area of the image dissector tube detector was directed to receive the light from a catalogue entry). Thus a double system may be 'single-pointing' or 'two-pointing', or may have two completely 'independent' entries.

Similarly, a multiple system may be 'single-pointing', 'two-pointing', or 'three-pointing', or may have two to four independent entries (with a common CCDM number). The term 'multiple' is to be considered as specifically referring to a number of components equal to or larger than three. There is not always a clear distinction between independent entries and multiple entries considered as a multiple system.

Double and Multiple Systems Annex: all of the Hipparcos Catalogue data on double and multiple systems is collected into the Double and Multiple Systems Annex, divided into five parts (C, G, O, V, and X), each comprising data on specific types of double or multiple system. Flags in the main catalogue indicate the way in which the system was processed (Fields H10, 48, 55–61). Summary data are given in Fields H62–67 of the main catalogue for entries resolved into exactly two components. See Section 2.3 for details.

Double star processing: the specific treatment of the Hipparcos data aimed at discovering and determining the astrometric parameters of double and multiple star systems. The Hipparcos instrument could resolve doubles down to about 0.1 arcsec separation with a magnitude difference below about 4 magnitudes. Some 10 000 systems were known in the Hipparcos Input Catalogue to need this special treatment. An additional 3000 new double or multiple systems have been discovered by Hipparcos, and due to its many complexities, the double-star processing has been a major problem area in the reductions. Not only the implementation but also the basic principles of the double-star reductions were different in the two reduction-consortia.

Ephemeris: the barycentric motion of the Earth was taken from the ephemerides VSOP 82 and ELP 2000 constructed by the Bureau des Longitudes. For the purposes of calculating stellar aberration and parallax this is equivalent, to within 0.01 mas, with the use of the Jet Propulsion Laboratory DE200 ephemeris.

Epoch photometry: the data contained in the Hipparcos or Tycho Epoch Photometry Annex, being the calibrated photometric data acquired at each epoch of observation. Observation times are given in Julian Date (TT), and corrected for arrival time at the solar system barycentre.

Equinox: see J2000, and ICRS.

FAST Consortium (Fundamental Astrometry by Space Techniques): one of the two data analysis consortia for the main mission data. See also data analysis consortia.

Field of view: one of the regions of sky, $0\overset{\circ}{.}9 \times 0\overset{\circ}{.}9$ in size, visible at any given instant to the Hipparcos payload. The two fields of view (preceding and following), separated by the basic angle of about 58°, were brought to a common focal surface by means of the 'beam-combining' mirror.

Five-parameter model: the basic model describing the modulated image dissector tube signal in terms of a general two-harmonic trigonometric function, with five unknown parameters. The phases determined from the model fitting were used as inputs to the great-circle reductions. The term may also refer to the standard astrometric model, whereby the apparent motion of a (single, unperturbed) star is described by the five astrometric parameters.

Great circle: one revolution of the satellite, roughly corresponding to a great circle projected on the sky, corresponded to a period of approximately 2.1 hours. Data from several great circles, comprising a reference great-circle set, were reduced together as part of the great-circle reductions.

Great-circle reduction: the first step in the 'three-step' reduction method, whereby phases determined by the image dissector tube data processing were brought together (over about 5 satellite rotations or revolutions, or about 10.7 hours), to derive the along-scan abscissae of the stars, with respect to an adopted 'reference great-circle' by the method of least-squares.

Grid period (or grid step): the period of the main modulating grid. From the great-circle reductions the mean grid period was found to be 1.207 366 arcsec, with extreme values (depending on position in the field of view) of 1.207 348 and 1.207 371 arcsec. Where only an approximate value of the grid period is relevant, the nominal pre-launch value of 1.208 arcsec is frequently used. Where a more accurate value was appropriate (for example, to correct slit errors in the sphere solution), a value of 1.2074 arcsec has been adopted.

Grid-step ambiguity: the along-scan phase measurements were made modulo one grid period (approximately 1.208 arcsec), so that stars with relatively poor *a priori* knowledge in their positions (or as a consequence of the poor instantaneous knowledge of the satellite attitude) suffered a corresponding uncertainty in the determination of their grid coordinates. If different measurements differ within a reference great-circle, this

fact can be recognised in the great-circle processing and duly corrected—the effect is then referred to as a grid-step inconsistency. Once made consistent at the level of the great-circle reductions, the grid coordinate may still be incorrect by a multiple of the grid step. This problem is referred to as that of grid-step errors. Such errors do not generally affect the validity of the great-circle abscissae derivations: they are recognised and corrected during the sphere solution process, and updated values are used in iterations of the great-circle reductions to improve the attitude knowledge.

Grid-step error: see also grid-step ambiguity. In the double-star reductions, a grid-step error may occur for any (or several) stars in a system with poorly known *a priori* positions, and especially for new doubles with a large magnitude difference, the separation may be in error by one or more times 1.2 arcsec (due to differences in the scanning geometry, the unit is not exactly that of the nominal grid period).

GSC: the Guide Star Catalog for the Hubble Space Telescope. Used as an element of the Tycho Input Catalogue, and for the construction of identification charts (Volume 13).

HIC: catalogue identifier with associated running numbers, identifying entries and corresponding data in the Hipparcos Input Catalogue.

HIP: catalogue identifier with associated running numbers, identifying entries and corresponding data in the (final) Hipparcos Catalogue and associated annexes. HIP is also the 'official' concise name for the Hipparcos Catalogue, assigned by the CDS.

Hipparcos Input Catalogue: the catalogue of about 120 000 programme stars, constructed by the Input Catalogue Consortium as the basis for the scientific observations and satellite attitude reference. It contained all the information necessary for the scientific satellite operations, as well as the compilation of available data necessary for the data reductions. It was published in printed form as ESA SP–1136 (1992), and on CD-ROM. It is also available, in machine-readable form, from the CDS.

Hipparcos magnitude: the magnitude, designated by *Hp*, sensed by the (broad-band) main detection system of the Hipparcos payload. The payload response was calibrated as a function of wavelength before launch, and photometric calibration was carried out throughout the mission by means of the reductions to an adopted system defined by standard stars.

Hp: see Hipparcos magnitude.

ICRF: the International Celestial Reference Frame is the realisation of the International Celestial Reference System, of which the Hipparcos and Tycho Catalogues represent extensions to optical wavelengths (see Section 1.2.2 for further details).

ICRS: the International Celestial Reference System, in which the Hipparcos and Tycho Catalogue positions and proper motions are given. This is consistent with the conventional equatorial system for the mean equator and equinox of J2000, previously realised by the FK5 Catalogue (see Section 1.2.2 for further details).

IDT detector: see image dissector tube.

IDT signal: the signal of an image passing over the grid as recorded by the image dissector tube (IDT) detector. The signal consisted of a zero-level (dc component) and a first and second harmonic modulation (ac component). See also main grid, ac magnitudes and dc magnitudes.

IFOV: abbreviation for 'Instantaneous Field of View'. See image dissector tube.

IFOV attenuation: a double-star component at a certain distance from the target position was observed with a reduced intensity that can be expressed in magnitudes. The double-star photometry has to take this attenuation into account.

IFOV profile: see detector's response profile.

Image dissector tube: the main detector used for the Hipparcos payload. A standard ITT 4012 RP tube, the detector had a sensitive area, or instantaneous field of view, of about 38 arcsec diameter, pointed towards the programme stars as they crossed the main field of view by adjusting the detector's coil currents. The instantaneous field of view was not sharp-edged: its profile is given in Section 1.4. The sloping wings resulted in considerable problems with double and multiple stars at around 20 arcsec separation, and the non-zero response at even larger distances resulted in the so-called 'veiling-glare' effect near bright stars.

INCA Consortium: the scientific consortium responsible for the construction of the Hipparcos Input Catalogue.

Inclined slits: part of the star mapper grid consisting of four $\vee$-shaped slits, and used for the determination of the transverse coordinate of star images. The apex of the inclined is located in the viewing plane. See also vertical slits.

Instantaneous field of view: see image dissector tube.

J2000: the relevance of the standard epoch J2000 is described in Section 1.2.6. The conventional equatorial system for the mean equator and equinox of J2000, and its relationship with the International Celestial Reference System (ICRS) in which the Hipparcos and Tycho Catalogue positions and proper motions are given, is described in Sections 1.2.1 and 1.2.2.

Julian Date: see Section 1.2.3 on time scales.

Main grid: the main modulating grid of 2688 parallel slits, each of width 3.13 μm, and separated by 8.2 μm, or approximately 1.208 arcsec on the sky. The grid, engraved on the spherical surface of a piece of glass matching the telescope's focal plane curvature, was built up from 168 by 46 elements (each containing 16 lines), referred to as 'scan fields'. With the scanning of the telescopes, stellar images moved across the focal plane roughly perpendicular to the grid lines, resulting in a very regular modulation of the light observed from behind the grid. See also IDT signal.

Main mission/main experiment/main grid: sometimes used to refer to the Hipparcos Catalogue related aspects of the satellite or mission, in contrast to the 'star mapper' or Tycho Catalogue related aspects.

mas: milliarcsec (0.001 seconds of arc).

Mission duration: before launch, the nominal mission duration had been set as 2.5 years, in addition to the 4–6 weeks required for the satellite and payload commissioning, although consumables on-board (principally the cold gas necessary for the attitude control) were sized for a period of approximately 5 years. A proposed mission duration of 2.5 years was determined as a result of simulations demonstrating the extent to which the astrometric parameters of the programme stars can be decoupled as a function of the mission lifetime. A longer mission would theoretically provide an improvement in positions and parallaxes by a factor $T^{1/2}$, where T is the mission lifetime, while proper motions would improve by a factor of $T^{3/2}$, the additional factor of T improvement being due to the larger time baseline. The actual mission duration, between launch and formal termination of operations, was just over four years, with high-quality scientific data being accumulated during a period of about 37 months.

Modulating grid: see main grid.

Multiple stars: see double and multiple stars.

NDAC Consortium (Northern Data Analysis Consortium): one of the two data analysis consortia for the main mission data. See also data analysis consortia.

Nominal scanning law: see scanning law.

Observational frame: the basic time unit of 32/15 s, also referred to as T4, used to fit the photon counts to the five-parameter model.

Orbital period (of the Hipparcos satellite): the interval between perigee passages. In its geostationary transfer orbit, the orbital period of the Hipparcos satellite was approximately 10.7 hours.

Parallax: the Hipparcos and Tycho Catalogues provide the annual parallax, π, from which the coordinate distance is $(\sin\pi)^{-1}$ astronomical units, or with sufficient approximation, π^{-1} parsec if π is expressed in arcsec. The parallax determinations are trigonometric, absolute (in the sense that the parallax determination of a given star is not dependent upon either the parallaxes, or assumptions concerning the parallaxes, of other stars—including stars close by on the sky), and independent of any previous distance determinations. Analyses place a limit on the global parallax zero-point offset of less than 0.1 milliarcsec, and give confidence that the published standard errors are a reliable indication of their true external errors.

Position: the Hipparcos and Tycho Catalogues provide the barycentric coordinate direction, specified as right ascension, α, and declination, δ.

Precision: the uncertainty of a measured quantity due to accidental errors. The term 'precision' is often used synonymously with 'internal (or formal) standard error' as derived e.g. from a least-squares solution (cf. accuracy).

Programme star: one of the stars (approximately 120 000) contained in the Hipparcos Input Catalogue, and observed by the main detector. The observing programme was defined before launch and remained essentially fixed for the entire mission duration.

Proper motion: the Hipparcos and Tycho Catalogues provide the rate of change of the barycentric coordinate direction expressed as proper motion components $\mu_{\alpha *} = \mu_\alpha \cos\delta$ and μ_δ, in angular measure per unit time (milliarcsec per Julian year).

Quantile: the term 'quantile' is used synonymously with the term 'fractile', the latter defined in *A Dictionary of Statistical Terms* (M.G. Kendall & W.R. Buckland 1957) as 'A term introduced ... to denote the variate value below which lies a given fraction of the cumulative frequency. This term is synonymous with the more generally used term quantile (q.v.), and the necessity for its coining is not clear.' The corresponding definition of 'quantile' implies that its use strictly relates only to rational fractiles.

Reference frame/reference system: the terminology used in the 1991 IAU resolution on reference frames and reference systems advocates the use of the term 'reference system' for conceptual matters, and 'reference frame' for the practical realisation of such a reference system in the form of a catalogue. The relationship between the Hipparcos reference frame, the International Celestial Reference System (ICRS), and the International Celestial Reference Frame (ICRF) are described in Section 1.2.2.

Reference great-circle: a reference plane chosen to correspond to the mean scanning motion of the satellite during several hours, and signifying also the collection of observations during this time-interval. In practice the maximum duration of observations constituting the reference great-circle was limited by the satellite's orbital period, corresponding to about 5 great-circle scans, or about 10.67 hours—typical lengths of the reference great-circles were somewhat shorter. Star abscissae were projected onto the reference great-circle (through a knowledge of the three-axis attitude of the satellite) and solved for during the great-circle reductions.

Scanning law: the three-axis attitude of the satellite, determining where the two fields of view of the satellite were directed, at any instant of time. The nominal scanning law is a deterministic scanning motion which defined the required satellite attitude. By comparing the target and actual attitude on-board, by means of the star mapper transits, corrections to the actual attitude were effected by means of regular (roughly every 400 s) three-axis gas jet actuations, which brought the attitude back to its target one. In this way, deviations between the actual and nominal scanning law were kept to within about 10 arcmin throughout the mission.

Scientific Selection Committee: the ESA-appointed selection committee responsible for independently allocating scientific priorities to the stars proposed for observation by Hipparcos, and generally monitoring the scientific contents of the Hipparcos Input Catalogue.

SIMBAD Data Base: the data base set up by the Centre de Données astronomiques de Strasbourg.

Single-pointing systems: double or multiple systems comprising two or more stars within a single catalogue entry. They were observed as a unique target by pointing the detector to the direction assigned to them in the Hipparcos Input Catalogue. As a rule, multiple systems with no relative distance larger than about 10 arcsec were observed as a single entry.

Sphere solution: the second step of the 'three-step method', which combined the great-circle data for a number of reference stars and determined the 'great-circle zero-points'. These zero-points defined the interconnection between the reference great-circle reference systems leading to the global Hipparcos reference system.

Standard error: estimated errors are given following the recommendations of the *'ISO Standards Handbook 3: Statistical Methods'*, where the standard error is defined as: 'the standard deviation of an estimator; the standard error provides an estimation of the random part of the total estimation error involved in estimating a population parameter from a sample.'

Star mapper: the detection chain (including aperiodic vertical and inclined grids, relay optics and detectors) located on each side of the main grid (two were provided for redundancy reasons). The prime purpose of the star mapper was to provide three-axis (hence, the inclined slits) attitude information to the satellite, in

real-time, on the basis of the time of transits of some 40 000 bright reference stars distributed over the sphere. It was also used for the Tycho experiment, and included, for this reason, two photometric channels (B_T and V_T), each sampled by their own photomultiplier tube detectors. In contrast to the detector used for the main field of view, the star mapper detectors sampled the entire signal generated simultaneously by star transits over the entire star mapper grid.

Star mapper grid: the arrangement of four vertical and four inclined grids, arranged aperiodically at one side of the main grid, used for the satellite real-time attitude determination and the Tycho measurements.

Star observing strategy: the on-board algorithm which determined the cycle of star observations on the main grid, on the basis of the satellite attitude, and the information contained in the programme star file.

Stochastic solutions: in the Hipparcos Catalogue context this refers to cases where astrometric solutions could not be found in reasonable agreement with the standard errors of the Hipparcos observations. The solutions postulate the presence of a non-zero physical scatter in excess of the measurement noise, referred to as the 'cosmic error'. They may be double or multiple systems of unknown characteristics, or short-period astrometric binaries (see Part X of the Double and Multiple Systems Annex).

Survey: the magnitude-limited set of stars (dependent on the galactic latitude and spectral type) that were included in the Hipparcos Input Catalogue. Some objects in very crowded regions (and thus suffering from an excessive demand for observing time) or subject to severe veiling glare had to be excluded from the survey, and its completeness was also influenced by the uncertainties on magnitudes and/or spectral types.

Target: any direction defined by an entry of the Hipparcos Input Catalogue used to direct the sensitive area of the image dissector tube during the mission.

TDAC Consortium: see Tycho Consortium

Terrestrial Time (TT): see Section 1.2.3 on time scales.

Three-pointing system: an extension of the two-pointing system, where three consecutive pointings of the detector system were reduced together.

Three-step method: the break-down of the (directly) intractably large Hipparcos reduction problem (to estimate simultaneously more than 600 000 astrometric parameters along with large numbers of additional satellite attitude unknowns and time-dependent geometrical calibration terms) in three partial steps. The first step is the 'great-circle reduction', the second step the 'sphere solution' and the last step the 'astrometric parameter determination'.

Transit: the crossing of a star's image across the modulating grid assembly. In the context of the Hipparcos Catalogue this term refers to a crossing of the main grid; in the context of the Tycho Catalogue it refers to the crossing of one of the star mapper slit systems (either vertical or inclined; see star mapper).

Transit file: a compilation of the calibrated 5-parameter model data from the image dissector tube for a subset of the Hipparcos Catalogue entries, including also the detailed scanning geometry. The transit files were originally used in the NDAC double-star reductions, and were constructed for all systems recognised as double or multiple, or suspected as such during the early phases of the data reductions. As a result, the transit data are available for all double and multiple systems, plus a few thousand catalogue entries finally considered as either suspected or single stars. See Section 2.9.

Two-pointing system: a double or multiple system with two catalogue entries sufficiently separated on the sky that they could not be observed within a single detector pointing, yet sufficiently nearby on the sky that the consecutive pointings of the detector were influenced by light from the other component, demanding that the two consecutive pointings had to be reduced together, taking into account the influence of the signals from each possibly affecting the other due to their proximity (typical separations of such systems are around 20 arcsec). A two-pointing double is a specific case of a two-pointing system, where the system comprises a total of two components, each corresponding to an individual catalogue entry. A two-pointing system may be a triple star, with two components contained within one detector pointing (or catalogue entry) and the third within a second pointing. Similarly a two-pointing system may embrace a quadruple system.

TYC: catalogue identifier with associated running numbers, identifying stars in the (final) Tycho Catalogue and associated annexes. TYC is also the 'official' concise name for the Tycho Catalogue, assigned by the CDS.

Tycho Consortium: the data analysis consortium responsible for the star mapper (or Tycho) data.

Tycho experiment: the exploitation of the star mapper data measurements (needed for a real-time determination of the satellite attitude) to provide astrometric and two-colour photometric data for all stars recognised as crossing the star mapper grid.

Tycho Input Catalogue: the catalogue, derived from the Guide Star Catalog and the INCA data base, in collaboration with members of the Guide Star Selection team at the Space Telescope Science Institute and of the INCA Consortium, used as an input to the Tycho data reductions.

Tycho Input Catalogue Revision (TICR): an intermediate catalogue produced in the Tycho data reductions. It was derived from the first year of Tycho observations.

Tycho magnitudes (B_T, V_T): the magnitude system defined by the Tycho instrument, in reasonable correspondence with the usual Johnson B and V magnitude system. Transformation equations between the various systems are provided.

Veiling glare: phase perturbations on the measurements of programme stars on the main grid in the presence of nearby bright stars, from either field of view, caused by the profile of the image dissector tube response (see also image dissector tube).

Vertical slits: part of the star mapper grid consisting of four slits perpendicular to the scanning motion of the satellite, used for the determination of the along-scan attitude angle. See also inclined slits and attitude determination.

VIM (Variability Induced Mover): a close binary, astrometrically observed by its photocentre, in which one (or both) of the components is variable (see R. Wielen, 1996, *Astronomy & Astrophysics*, 314, 679). The duplicity of such an object can be discovered from the fact that the photocentre oscillates along the arc joining the two components in relation to the total brightness of the system. This effect appears to be significant for a few hundred stars in the Hipparcos Catalogue, for which special solutions are given in Part V of the Double and Multiple Systems Annex. See Section 2.3.5 for details.

V_T: see Tycho magnitudes.

WDS: the Washington Catalogue of Visual Double Stars (see Section 1.4.4).

APPENDIX B

ACKNOWLEDGEMENTS

Appendix B. Acknowledgements

Acknowledgements by the Hipparcos Science Team

The Hipparcos project developed over a period of some 20 years. During this period, some two hundred or more scientists, and several hundred engineers, managers, computer system managers, secretaries, administrative assistants, politicians, and others have contributed directly or indirectly to the gradual, and sometimes very difficult, progress towards the final Hipparcos and Tycho Catalogues. Most main participants owe a debt of gratitude to many individuals who supported their work during this period, and they are offered a warm, if generally anonymous, expression of gratitude.

ESA's involvement with the hardware development began with the project's acceptance in 1980, but even before then, many scientists and engineers had been involved in the preparations for the mission. The earliest concept for a space astrometry mission was put forward in 1966 by P. Lacroute, who retained an active interest in the project's evolution throughout its development, and launch, until his death in 1993.

The work of industry and the work of the scientific study team, during the course of the ESA Phase A studies was essential to the acceptance of the Hipparcos project. This work laid the foundations for a mission both technically feasible and scientifically justifiable. The contributions of those individuals and companies, as well as the ESA technical staff, involved in those early studies, are acknowledged.

The contributions of the members of the ESA Project Team in ESTEC are acknowledged. The technical foundations of the satellite construction owes particular acknowledgement to the first Hipparcos Project Manager in ESTEC, L. Emiliani (1980–84). H. Hassan thereafter supervised the engineering aspects of the satellite development through integration, testing and calibration, to satellite launch in 1989.

The Hipparcos Project found in its prime contractor, Matra (now Matra Marconi Space), in the co-prime contractor Aeritalia (now Alenia Spazio), and in their many industrial subcontractors, great competence, and dedication to a successful mission. The technical difficulties that had to be overcome were considerable, and it is a great tribute to the work of industry that the satellite development was completed largely on schedule (a one year delay of the programme was introduced by launcher problems), and within 10 per cent of the originally approved cost-to-completion.

Noteworthy in this context was Matra's emphasis on developing a global error budget for the mission. A system analysis team in industry, supported by software consultants, identified those areas having the most fundamental effect on the final accuracy. The effort undertaken by Matra to interface with scientific advisors, and hence to appreciate the scientific goals, illustrated this approach. Many innovations, ranging from the predicted performance of the attitude control system and the outstanding quality of the modulating grid, to the introduction of the Tycho experiment and the thorough on-ground calibration of the scientific payload, benefited from this commitment.

Some 1800 persons in Europe were involved in developing the Hipparcos satellite. The Matra (now Matra Marconi Space) Project Managers, C. Guionnet and M. Bouffard, and Aeritalia (now Alenia Spazio) Project Manager B. Strim, as representatives of this major industrial effort, are thanked for their dedicated work over a number of years. With dual burdens of financial and schedule considerations, they were nevertheless receptive to the advice and aspirations of the scientific community.

During the course of the Phase B and Phase C/D activities, the scientific advisory team, the Hipparcos Science Team, was fully involved in the industrial design and the corresponding project reviews, aside from its involvement in the more scientific aspects of the project as a whole. The parallel activities of the scientific consortia during the evolution of the satellite design greatly strengthened the overall project development. The work of many consortia members who participated directly and indirectly in the optimisation of the satellite, payload, and operations is acknowledged.

Even in the present days of frequent satellite launches, the successful launch of the Hipparcos satellite was a noteworthy achievement, a remarkable event that will be remembered with awe by those that witnessed it. The contributions to the mission by the large number of people involved in the Ariane Flight V33 launch activities are gratefully acknowledged. As representatives of the enormous launch commitment undertaken by Arianespace and CSG we thank in particular the Mission Director, Roger Solari, and the Deputy Mission Director, Yves Guerin.

Preparations for launch, early orbit operations and routine mission operations, was an extensive programme lasting for several years and involving hundreds of individuals. The ESOC Ground Segment Manager, J. van der Ha, was an efficient and highly appreciated interface between the ESTEC Project Team and the Hipparcos Science Team. A. Schütz is also acknowledged for his important contributions to the implementation of the scientific observing programme at ESOC.

With the failure of the apogee boost motor, the mission was in jeopardy. The remarkable efforts of many individuals, under the direction of the Satellite Operations Managers, H. Nye and D. Heger, and the Ground Segment Manager, J. van der Ha, allowed the mission to continue. The entire missions operations team engaged itself in a prolonged and strenuous effort to maintain satellite operations for the four years necessary to the bring the mission to a successful scientific conclusion. All individuals and teams involved in this effort (cited in Volume 2) are acknowledged with gratitude. The Satellite Operations Manager, D. Heger, and the operations team at ESOC, are particularly thanked for the enthusiasm and tenacity with which they maintained efficient satellite operations under conditions which were extremely difficult after launch, and became more problematic as the mission proceeded, and as the complexity of operations increased. In ESTEC, M.F. McCaig, M.R. Weinberger, R.L. Crabb, E.J. Daly, G. Dudley, H. Fiebrich, and A. Errington provided significant post-launch support in the areas of attitude control, solar array degradation, power supply, and on-board data handling.

During operations, industrial support was provided with considerable ingenuity: for their contributions to maintaining satellite operations in the face of radiation degradation of the satellite in its geostationary transfer orbit, and associated gyroscope and thermal control failures, the dedicated support of D. Pawlak, P. Peyrot, J. Degremont, A. Benoit, S. Val Serra, P. Delagnes, and J.M. Oberto of Matra Marconi Space is acknowledged. Matra Marconi Space also supported the in-orbit performance monitoring of the satellite.

The efforts of staff at the four ground stations (at Odenwald, Perth, Goldstone, and Kourou) in maintaining the efficient collection of satellite data throughout the operational phase is acknowledged. NASA's collaboration, through the rapid provision and continual and efficient support of the Goldstone station to the Hipparcos operational network, is noted with appreciation.

P. Lantos (Observatoire de Paris-Meudon) is acknowledged for regularly supplying the Meudon Solar Warning reports, which allowed satellite operations to take account of solar activity events throughout the mission.

During the satellite development, before launch, and during mission operations, numerous scientific advisory groups of ESA were called upon to make sometimes difficult decisions: the members of the Astronomy Working Group, and in particular its then Chairman, J.P. Swings, gave the mission, and the Project Scientist, unqualified support, especially at the time that such support was in greatest need. The Hipparcos Project expresses gratitude to members of the ESA Space Science Advisory Committee, and the ESA Science Programme Committee, for their crucial support through the various phases of the project development, launch

and operations, and especially their support given to the extension of satellite operations to further the scientific goals of the mission. The scientific teams acknowledge the contribution made by K. Mattila during these deliberations. That this support was given in times of financial pressures on the ESA science programme budget is fully acknowledged. In this context contingency financing of the satellite operations was supported by the ESA Director General and the ESA Council.

The various ESA advisory groups also gave their support to the scientific teams in allowing proper and adequate time for completion of the Hipparcos and Tycho Catalogues before distribution of the final data. The Hipparcos Science Team advocated that the release of preliminary data would not be in the long term interests of the Hipparcos mission: that this advice was heeded has been appreciated. The ESA Director of Science, R.M. Bonnet, supported the Hipparcos Project in various tangible ways; in particular the Hipparcos Science Team wishes to extend its appreciation for his support during the recovery mission implementation, operations and, subsequently, of the final publication strategy.

The Hipparcos Science Team acknowledges the support and commitment given to the project elsewhere within the ESA Scientific Directorate, in particular by H. Olthof, S. Volonté, and G. Cavallo in ESA, Paris. The Head of the Scientific Projects Department in ESTEC, D. Dale, is thanked for various interventions during mission operations leading to the rapid resolution of potential ground-station utilisation conflicts, and proper contingency operational support. F. Jagtman of the Project Management Support and Coordination Office greatly assisted the financial control of the project, especially during the operational phase.

The Hipparcos project is very grateful for the support and participation of a number of institutes not directly involved in astronomical research—in particular the geodetic and space research institutes. The Danish Space Research Institute (DK) and the Geodetic Institute (DK) supported NDAC; the Centre National d'Etudes Spatiales (F), the Delft University of Technology (NL), the Istituto di Topografia, Fotogrametria e Geofisica, Milano (I), Dipartimento di Matematica, Bologna (I), CSATA, Bari (I), CSS, Torino (I), and the Istituto Nazionale di Ottica, Firenze (I) gave support to FAST.

The entire data reduction process was a complex exercise. Maintaining projected schedules in the face of continuous unexpected developments, and insisting on convergence in the activities of nearly a hundred active scientific participants, was a continuous challenge. The commitment, skill, ingenuity, and energy devoted by the members of the four scientific consortia has been essential to the healthy progress of the scientific aspects of the mission, and to its successful conclusion.

J. Chapront, G. Francou and the late B. Morando are acknowledged for preparing a dedicated compact representation of the position and velocity of the Earth, to the precision required by the data analysis.

The scientific teams, and especially the Double Star Working Group, gratefully acknowledges the contributions of C.E. Worley (of the U.S. Naval Observatory) for supplying, in December 1994, a pre-release version of the WDS Catalogue, which allowed the double star reductions to take account of previous knowledge of identified double systems to the maximum extent possible. Supplying a catalogue in advance of publication is a difficult decision, and we are grateful for his confidence and collaboration.

The Hipparcos Science Team acknowledges the important contributions brought by the many institutes and organisations not otherwise involved in one of the four Hipparcos consortia which have participated in the realisation of the link of the Hipparcos Catalogue to the extragalactic reference system ICRS. These are: the Associated Universities operating the VLBA and VLA arrays; the Astronomical Institute of the Czech Academy of Sciences in Prague; AURA Inc. operating the Hubble Space Telescope; the International Earth Rotation Service in Paris; the Main Astronomical Observatory of the Ukraine Academy of Sciences in Kiev; the NASA Deep Space Network; Potsdam University (WIP); the University of Manchester, operating the MERLIN network; the University of Texas, Austin; the US and European VLBI networks; the US Naval Observatory; and Yale University Observatory.

The American Association of Variable Star Observers, under the direction of J.A. Mattei, supported the Hipparcos mission enthusiastically before launch and during satellite operations through their contribution of information on variable stars. Their contribution is gratefully acknowledged.

The Hipparcos Project is very grateful to Dr N.N. Samus and colleagues of the Institute of Astronomy (Russian Academy of Science, Moscow) and the Sternberg Astronomical Institute (Moscow University), for their rapid and efficient support in the allocation of GCVS official names to new variables discovered with Hipparcos in advance of the catalogue publication.

R.T. Fienberg was a driving force in the collaboration between ESA and Sky Publishing Corporation leading to the production of *Sky & Telescope*'s 'Millennium Star Atlas', from which Volumes 14–16 have been constructed.

P.T. Wallace, M. Feissel, and F. Arias are thanked for comments on the catalogue introduction.

The ESA Publications Division, under the direction of N. Longdon and subsequently B. Battrick, has supported the preparation of the Hipparcos scientific products with care and enthusiasm. These individuals, and also H. Wapstra and C. Haakman, are thanked for their very significant contributions to the quality of the final mission products.

M.A.C. Perryman acknowledges with great appreciation the support provided to him by B. Fitton in ESTEC during the early phases of the Hipparcos project, and subsequently the valuable and unfailing support, advice, and assistance of the Head of the Astrophysics Division within the ESA Space Science Department, B.G. Taylor. G. Thörner is acknowledged for support of the Astrophysics Division computer facilities over many years. J. Kostelnyk is acknowledged for administrative assistance, advice, and profound support throughout the entire duration of the project.

Acknowledgements by the NDAC Consortium

Thanks are due to the UK Science and Engineering Research Council (now PPARC) for supporting the team at the Royal Greenwich Observatory. Support from University College, London, for work carried out at the Mullard Space Science Laboratory, and from University College, Cardiff, are also gratefully acknowledged.

The work performed at Lund Observatory has been generously supported by the Swedish National Space Board through yearly grants to L. Lindegren and co-workers. Support from the University of Lund and the Royal Physiographic Society, Lund, is also gratefully acknowledged.

The work at Copenhagen was performed under grants from the Danish Space Board to E. Høg, Copenhagen University Observatory, and was supported by the Danish Space Research Institute.

Acknowledgements by the FAST Consortium

The involvement of the Centre National d'Etudes Spatiales (CNES) in preliminary studies of the space astrometry proposal made by P. Lacroute in 1968–71, and the support given by CNES before it became an ESA mission, are recognised as important steps towards the realisation of the Hipparcos programme.

During the fifteen years of activity of FAST in France, the work of the consortium was made possible by the major involvement of the staff and the computing centre of the Centre Spatial de Toulouse of CNES, and the considerable support provided by CNES to the Hipparcos project as a whole.

The Centre National de la Recherche Scientifique (CNRS) was another very important contributor through the provision of scientific and technical staff, and through its support within the 'Groupement de Recherche Hipparcos'. The Ministry in charge of the Universities has similarly provided scientific and technical staff working in the various teams. In addition, the Bureau des Longitudes, CERGA (included since 1988 in the Observatoire de la Côte d'Azur) and the Laboratoire d'Astronomie Spatiale of the CNRS have also contributed from their own funds and provided the necessary facilities.

The work at the Faculty of Geodesy of the Delft University of Technology was supported by the Netherlands Organisation for Scientific Research (NWO) in the form of a four-year research fellowship. The Faculty of Geodesy also financed several short-term contracts for (student) assistants from its own resources. The support by staff members and students is also gratefully acknowledged. Travel was supported by funds from the Faculty of Geodesy, the NWO, SRON, CSS, CNRS and CERGA. The work in Utrecht was supported by the Space Research Organisation of the Netherlands, SRON.

The Italian participation in the FAST Consortium, which comprises the Italian institutes and individuals participating in the FAST Consortium, was formed in 1981 by P.L. Bernacca (University of Padova), V. Castellani (IAS–CNR, now at the University of Pisa), the late M.G. Fracastoro (University of Torino) and I. Galligani (University of Bologna). Its precursor was the involvement of P.L. Bernacca as System and Mission Analysis Leader during the Phase A study of the satellite performed by Aeritalia (Torino) under contract to ESA.

In the pre-launch phase, the Italian contribution to the FAST work was sponsored by the Piano Spaziale Nazionale of the Consiglio Nazionale delle Ricerche (CNR–PSN), which monitored and supervised the work, independently from, but in coordination with, the FAST management, by means of a CNR–PSN project team, which comprised G. Cecchini (Project Manager), G. Rossetti (Contract Officer) and P.L. Bernacca (Project Scientist).

Every year from 1982 until 1988, CNR–PSN entrusted contracts to the Department of Astronomy of Padova (for missions and computer time of the scientific institutes involved), and to the Centro di Studi sui Sistemi in Torino and to Tecnopolis–CSATA in Bari (for manpower and computer time).

During the data reduction phase (1989–94), the sponsor of the Italian participation to the FAST work was the Italian Space Agency (ASI), instigated by Parliament in May 1988, which formed a similar organisation for funding with the CISAS 'G. Colombo' of the University of Padova replacing the Department of Astronomy, and provided the same supervising structure, as that given before launch.

At the origin of the Italian participation in the Hipparcos project, in 1977, was the initiative provided by the late F. Scandone, former Chairman of the Space Research Committee of the Italian CNR, and by U. Sacerdote, former Director of the old Aeritalia Space Sector.

The efforts of the staff of the National Radio Astronomy's Very Large Array and Greenbank facilities, of Owens Valley Radio Observatory, of Haystack Observatory, of the Max Planck Institute for Radio Astronomy, and of the Deep Space Network, which were directly involved in the VLBI observations of the radio stars related to the link to an extragalactic reference frame, are gratefully acknowledged. All the Mark III VLBI radio observations were correlated at the Haystack Observatory. Associated research was carried out, in part, by the Jet Propulsion Laboratory, California Institute of Technology, under contract with the National Aeronautics and Space Administration.

The work of the Astronomisches Rechen-Institut, Heidelberg, for the Hipparcos mission was mainly financed by the Ministerium für Wissenschaft und Forschung (MWF), Stuttgart, of the State of Baden-Württemberg (Kapitel 1497). Additional support was provided by the Bundesministerium für Bildung, Wissenschaft, Forschung und Technologie (BMBF), Bonn, of the Federal Republic of Germany, through the Deutsche Agentur für Raumfahrtangelegenheiten (DARA), Köln, Project Nos. 01 OO 0421 and 50 OO 9002 0.

Acknowledgements by the Tycho Consortium

The work in Copenhagen was performed under grants from the Danish Space Board to E. Høg, Copenhagen University Observatory, and was supported by the Danish Space Research Institute.

The work performed at Lund Observatory has been generously supported by the Swedish National Space Board through yearly grants to L. Lindegren and co-workers. Support from the University of Lund and the Royal Physiographic Society, Lund, is also gratefully acknowledged.

The work of the Astronomisches Rechen-Institut, Heidelberg, for the Hipparcos mission was mainly financed by the Ministerium für Wissenschaft und Forschung (MWF), Stuttgart, of the State of Baden-Württemberg (Kapitel 1497). Additional support was provided by the Bundesministerium für Bildung, Wissenschaft, Forschung und Technologie (BMBF), Bonn, of the Federal Republic of Germany, through the Deutsche Agentur für Raumfahrtangelegenheiten (DARA), Köln, Project Nos. 01 OO 0421 and 50 OO 9002 0.

The work in Tübingen was supported under grant No. 01 OO 8502 9 by the Bundesministerium für Bildung, Wissenschaft, Forschung und Technologie (BMBF), and under grant No. 01 OO 9106 0 by the Deutsche Agentur für Raumfahrtangelegenheiten (DARA).

The work in Groningen was supported by the Space Research Organisation of the Netherlands, SRON.

The work in Padova and Torino has been supported by the Piano Spaziale Nazionale of the Consiglio Nazionale delle Ricerche (CNR–PSN).

The work in Geneva was supported by the University and the Observatory of Geneva.

The work at Royal Greenwich Observatory was supported by grants from the Science and Engineering Research Council.

The work at CERGA was supported by the Centre National d'Etudes Spatiales (CNES), the Observatoire de la Côte d'Azur, and the Centre National de la Recherche Scientifique (CNRS).

The work in Strasbourg was supported by grants from the Centre National d'Etudes Spatiales (CNES), the Centre National de la Recherche Scientifique (CNRS), and the Institut National des Sciences de l'Univers (INSU).

The support of the Space Telescope Science Institute (Catalogs and Surveys Branch), and in particular B. Lasker and H. Jenkner, in providing early access to the Guide Star Catalog for the Tycho Input Catalogue production is acknowledged. The Space Telescope Science Institute at Baltimore is operated by the Association of Universities for Research in Astronomy, Inc., under contract to the National Aeronautics and Space Administration. The support of the INCA Consortium in aspects of the Tycho Input Catalogue production is also acknowledged.

The Tycho Catalogue validation and double star reductions were supported by observing time at the European Southern Observatory (ESO).

Acknowledgements by the INCA Consortium

The work of the participants of the INCA Consortium was supported and funded individually by each participating country. A complete list of the participants, of their institutes and funding authorities is given, for each country, in the printed version of Hipparcos Input Catalogue, ESA SP-1136, 1992.

The work performed in Australia, dealing with radio stars and the Hipparcos/Hubble Space Telescope link, was supported by the Australia Telescope National Facility of CSIRO.

The work performed in Belgium dealt mainly with double and multiple star systems during the preparation of the mission, and with the cross-identification of systems newly discovered by Hipparcos. J. Dommanget is particularly indebted for financial support to the Fonds de la Recherche Fondamentale Collective (Bruxelles) under convention 2.9009.79 for the period 1979-87, and the Fonds National de la Recherche Scientifique, Crédits aux Chercheurs, under conventions No. 1.5.388.88F for the period 1988-90, 1.5.179.91F for the period 1991-93, and 1.5.160.94F for the period 1994-96. The Commission des Communautés Européennes provided a grant (No. SC1-0057) for the period 1989-90. P. Melchior and P. Paquet, successive directors of the Observatoire Royal de Belgique have conceded to J. Dommanget, Chef de Département Honoraire, although retired since 1 July 1989, to pursue his researches as previously with all necessary means in staff and equipment.

The work performed in Denmark, dealing with new astrometric and photometric observations, and the participation in the operation of the Carlsberg Automatic Meridian Circle, was supported by the Danish Space Board, the Danish Natural Science Research Council and the Carlsberg Foundation.

The work performed in France dealt mainly with the coordination of the Consortium, the production and publication of the Hipparcos Input Catalogue, new astrometric observations and measurements, work on variable stars, minor planets and satellites, and mission simulations, during the Hipparcos Input Catalogue construction; merging of the two astrometric catalogues from FAST and NDAC, processing of some categories of double stars, and production of *Celestia 2000*. It was supported by the Centre National de la Recherche Scientifique (CNRS) and Ministère de l'Education Nationale, de l'Enseignement Supérieur et de la Recherche (MENESR) by providing scientific and technical staff dedicated to the project for up to fifteen years, and by funding through the 'Groupement de Recherche Hipparcos' and each contributing URA for CNRS and through each Observatory for MENESR. It was also constantly and unfailingly supported by the Centre National d'Etudes Spatiales (CNES), the Institut National des Sciences de l'Univers (INSU), by Observatories of Besançon, Bordeaux, Marseille, Paris-Meudon and Strasbourg, by University of Montpellier and by the Bureau des Longitudes. The SIMBAD project is supported by INSU. The Centre National d'Etudes Spatiales is also acknowledged for grants for operating the two data bases: SIMBAD, and INCA. The host of the two data bases was the Computer Centre of Paris-Sud University (Paris-Sud Informatique) from 1985 to 1990, and its director, J.B. Johannin, is especially acknowledged for his constant support.

The work performed in Germany dealt mainly with astrometric compilation and analysis, measurement of cluster stars and double star positions and the preparations for the linking of the Hipparcos reference frame to the radio/extragalactic frame. The work of the Astronomisches Rechen-Institut, Heidelberg, was mainly financed by the Ministerium für Wissenschaft und Kunst (MWK), Stuttgart, of the Land Baden-Württemberg (Kapitel 1497). Additional support was provided by the Bundesministerium für Bildung, Wissenschaft, Forschung und Technologie (BMBF), Bonn, of the Federal Republic of Germany, through the Deutsche Forschungs- und Versuchsanstalt für Luft-und Raumfahrt (DFVLR), Köln, under Project No. 01 OO 0421 (Project Leader: R. Wielen). The work at Hamburg Observatory was financed by BMFB under Project No. 50 OO 8810 4 (Project Leader: C. de Vegt). The work at the University of Bonn was financed by BMFB under Project No. 01 OO 023-6 (Project Leader: P. Brosche).

The work performed in The Netherlands at Sterrewacht Leiden, dealing with new astrometric measurements and photometric observations, was supported by Leiden University, in turn supported by the Ministerie voor Onderwijs en Wetenschappen.

The work performed in Spain by the Real Instituto y Observatorio de la Armada and by the Universitat de Barcelona, dealing with new astrometric and photometric observations, variable stars and minor planets, and the participation in the operation of the Carlsberg Automatic Meridian Circle, were funded by the Comisión Interministerial de Ciencia y Tecnología (CICYT), Dirección General de Investigación Científica y Técnica (DGICYT) and Estado Mayor de la Armada. For the period 1981-85, financial support was provided by the Comisión Nacional de Investigación del Espacio (CONIE). The Comissió Interdepartamental de Recerca i Innovació Tecnològica (CIRIT) is also acknowledged.

The work performed in Switzerland, dealing with new photometric observations, photometric data compilation, and mission simulations, during the construction of the Hipparcos Input Catalogue; with Hipparcos and Tycho pass-bands calibration as a function of the optics ageing, photometric standard stars compilation, and variability studies, was financed by the Universités de Genève and Lausanne, and the Fonds National Suisse de la Recherche Scientifique.

The work performed in the United Kingdom, dealing with new astrometric measurements and observations, the linking of the Hipparcos reference frame to the radio/extragalactic reference frame and double star observations, the participation in the operation of the Carlsberg Automatic Meridian Circle, and travel funds, was supported and funded by the United Kingdom Science and Engineering Research Council (SERC). The support of the Royal Greenwich Observatory for the measurements of positions of faint stars in the Cape Zone, and of Cambridge University for the work on double stars and the reference frame link, is also acknowledged.

The work performed in the United States of America by the Hubble Space Telescope Astrometry Team in preparation of the link of the Hipparcos reference frame to the radio/extragalactic reference frame, through the use of the Hubble Space Telescope Fine Guidance Sensors, was supported by the Astronomy Department of the University of Texas and NASA (NASA contract NAS 8-32906 and NASA grant NAGW-233).

The support of the Centre National d'Etudes Spatiales (CNES) in mission simulations, through the assistance of personnel and the use of the Toulouse computer, the host of the complete simulation chain, is gratefully acknowledged.

Acknowledgements are particularly due to the staff of the Centre de Données astronomiques de Strasbourg (CDS), Observatoire de Strasbourg, for their constant and efficient help in the creation and operation of the INCA Data Base, stemming from the SIMBAD Data Base and mainly operated using its basic software.

Many observers, in various observatories, undertook extensive measurement programmes related to the Hipparcos Input Catalogue preparation (astrometric observations and measurements, photoelectric observations, special observations of double and multiple systems). The work performed and the support they received from their respective institutions is gratefully acknowledged. The support of the management and staff of the European Southern Observatory (ESO), of the Carlsberg Automatic Meridian Circle (operated jointly by the Copenhagen University Observatory, the Royal Greenwich Observatory and the Real Instituto y Observatorio de la Armada en San Fernando) and of the Bordeaux automatic meridian circle, is especially acknowledged.

The Guide Star Catalog Team of the Space Telescope Science Institute (STScI), Baltimore, and particularly B. McLean, is gratefully acknowledged for the efficiency with which they answered requests about those stars left without measurements at the end of the ground-based observing programmes.

The Royal Greenwich Observatory and the Hamburg Observatory are acknowledged for the use of the CPC2 Catalogue prior to publication, as a joint contribution from these observatories.

For the work on variable stars, and especially large-amplitude variable stars requiring the use of ephemerides for their efficient observation by Hipparcos, the work performed by the world-wide network of observers and the American Association of Variable Star Observers (AAVSO), under the direction of Dr J.A. Mattei, before and during the Hipparcos mission, and the support of this work by NASA (NASA grant NAGW-1493), is acknowledged. Acknowledgements also are due to the AFOEV staff and observers, to O. Gascuel and J. Quinqueton of CRIM (Centre de Recherches en Informatique de Montpellier), to E. Diday of INRIA (Institut National de Recherche en Informatique et Automatique), and especially to A. Schütz, P.E. Davies and A.J.C. McDonald of ESOC.

For the preparation of the link of the Hipparcos reference frame to the radio/extragalactic reference frame, supporting activities were carried out by many observers in various observatories. The work performed and the support they received from their respective institutions is gratefully acknowledged. Two groups provided speckle interferometry observations for candidate Hipparcos stars to be observed by Hubble Space Telescope: O. Franz (Flagstaff) and H. McAlister (Atlanta), using the Georgia State University Speckle Camera provided northern hemisphere observations; A.N. Argue (Cambridge, UK), in collaboration with B. Morgan and H. Vine (London), provided southern hemisphere observations. The group is also grateful to M. Feissel, Director of the Central Bureau of IERS, to O. Sovers of JPL, and to D. Robertson of the National Geodetic Survey for their kind cooperation.

For the preparatory work on minor planets and satellites, and also for the ephemerides of major planets, the Bureau des Longitudes (Paris) is particularly acknowledged.

The INCA Consortium acknowledges the careful work of reviewing the astronomical proposals submitted to ESA by the Scientific Proposals Selection Committee and especially to the Committee's Chairman, A. Blaauw, for his enthusiastic involvement in the work of the Consortium. The time and effort expended by proposers around 1982, many of whom had no intention of exploiting the final Hipparcos Catalogue data, but submitted proposals in order to ensure the lasting scientific quality of the Hipparcos Catalogue, has also been gratefully appreciated.

The members of the ESTEC Hipparcos Project Team, in particular M. Schuyer, R.D. Wills, S. Vaghi and R. Bonnefoy, are thanked for the many helpful exchanges throughout the preparation of the Hipparcos Input Catalogue. The staff of the ESA Operations Centre (ESOC), and in particular A. Schütz, were responsible for the implementation of the Hipparcos Input Catalogue, and their work under the Ground Segment Manager, J. van der Ha, and the Spacecraft Operations Manager, D. Heger, was an important contribution to the proper functioning of the Hipparcos Input Catalogue after the satellite launch.

The INCA Steering Committee, on behalf of the entire INCA Consortium, would like to use this opportunity to give recognition to the impetus given to the project in its early phases by the late W. Fricke, and to the effective support he brought to the preparation of the Hipparcos Input Catalogue.

The INCA Team Leader wants to highlight her deep appreciation for the dedication shown by the Hipparcos Project Scientist in ESA, M.A.C. Perryman, and in particular for his unremitting and stimulating interest in all parts of the work performed in the INCA Consortium and of all its connections with other parts of the Hipparcos work.

APPENDIX C

CONTRIBUTORS BY NAME

Appendix C. Contributors by Name

This section lists scientific involvement during the data analysis preparation, observing programme preparation, data reduction, and catalogue production (principal contributors to the Hipparcos Input Catalogue, a full listing of which is given in the printed Hipparcos Input Catalogue, SP–1136, are also included). Evidently, the level of contributions differed greatly, between those who were involved for a short period for a particular contribution, to those whose involvement has extended, essentially full time, for almost 20 years. Bold type indicates leading contributor to the task. Institutes correspond to locations where the activities were undertaken. ESA/ESOC and industrial contributions are not listed here, nor are those of the Scientific Proposals Selection Committee (see introductory pages).

J.R. Allington-Smith *Mullard Space Science Laboratory, Holmbury St Mary, U.K.* Early developments for data simulation.

M. Amoretti *Istituto di Astrofisica Spaziale, CNR, Frascati, Italy.* Initial studies of optical modelling in FAST.

G.K. Andreasen *Copenhagen University Observatory, Denmark.* Development of photometric data analysis algorithms for NDAC. Development of photometric data analysis algorithms for Tycho.

S.V. Antipin *Sternberg Astronomical Institute, Moscow University, Russia.* Checks of identifications of Hipparcos variables with catalogues of variable and suspected variable stars, PPM catalogue, etc.

F. Arenou *Observatoire de Paris-Meudon, URA CNRS 335, France.* Construction of the Hipparcos Input Catalogue. **Merging of the FAST and NDAC single star data.** Astrometric results merging group. **Parts G and X of the Double and Multiple Systems Annex.** Production of Hipparcos Catalogue intermediate astrometry.

A.N. Argue *Institute of Astronomy, Cambridge, England.* **Selection of reference frame link stars for the Hipparcos Input Catalogue. Coordination of the observations of pre-launch data for reference frame link stars.** Speckle interferometry of southern link stars observed by Hubble Space Telescope.

J.E. Arlot *Bureau des Longitudes, URA CNRS 707, Paris, France.* **Pre-launch ephemerides of satellites of major planets.**

M. Badiali *Istituto di Astrofisica Spaziale, CNR, Frascati, Italy.* Optical modelling for FAST calibration. **Double star reductions in FAST.** Double star working group.

A. Baglin *Observatoire de Paris-Meudon, URA CNRS 335, France.* Compilation of pre-launch data for variable stars.

D. Barthès *Université de Montpellier II, URA CNRS 1368, France.* Pre-launch ephemerides of large-amplitude variable stars, and updates throughout mission.

G. Bässgen *Astronomisches Institut, Tübingen, Germany.* **Tycho data reductions.**

U. Bastian *Astronomisches Rechen-Institut, Heidelberg, Germany.* Tycho data reductions. **Prediction of Tycho transits for stars and solar system objects. Compilation of Volume 4.** Astrometric parameter determination for FAST. **Hipparcos Science Team.** Development of *Celestia 2000*.

M.O. Baylac *Observatoire de Paris-Meudon, URA CNRS 335, France.* Reliability of the Hipparcos Input Catalogue data.

A. Bec-Borsenberger *Bureau des Longitudes, URA CNRS 707, Paris, France.* **Pre-launch ephemerides of minor planets.**

P. Belforte *Centro di Studi sui Sistemi, Torino, Italy.* Pre-launch studies for first steps of the data reduction in FAST.

P.L. Bernacca *Osservatorio Astrofisico di Asiago and Centro di Studi e Attività Spaziali (CISAS) 'G.Colombo', Università di Padova, Italy.* **Leader of system and mission analysis during industrial feasibility study, 1977. Promotion of mission approval by ESA/SPC (1979–80). Scientific supervision and control of the Italian contributions and tasks in FAST:** optical modelling, main grid and star mapper data reduction, attitude determination, sphere solution, double star reduction; **and to the Hipparcos Project:** comparison of attitude determinations by FAST and NDAC. Preparation of double star reductions in FAST. **Hipparcos Science Team.** FAST Steering Committee.

H.H. Bernstein *Astronomisches Rechen-Institut, Heidelberg, Germany.* Absolute astrometry of double stars in FAST. Double star working group. Part O of the Double and Multiple Systems Annex.

D. Bertani *Istituto Nazionale di Ottica, Firenze, Italy.* Optical modelling for FAST calibrations.

B. Betti *Dipartimento di Topografia e Rilevamento, Politecnico di Milano, Italy.* Pre-launch studies of sphere solution methods in FAST.

A. Blaauw *Kapteyn Laboratory, Groningen, The Netherlands.* **Chairman of Scientific Proposals Selection Committee. Coordination of external review of Hipparcos Input Catalogue preparation.**

E. Bois *Observatoire de la Côte d'Azur/CERGA, URA CNRS 1360, Grasse, France.* Theoretical studies of satellite rotation.

L. Borriello *Tecnopolis-CSATA, Bari, Italy.* **Double star recognition and preparation of reductions in FAST.**

P. Brosche *Sternwarte der Universitaet Bonn, Germany.* Measurement of pre-launch astrometric data. Reference frame working group (photographic method). Former member of Hipparcos Science Team (1982).

W.N. Brouw *CSIRO, Epping, Australia.* FAST Steering Committee.

B. Bucciarelli *Osservatorio Astronomico di Torino, Italy.* Baseline sphere solution method and software implementation in FAST. **Validation of the sphere solution by alternative methods.** Assessment of residual systematic errors between FAST and NDAC catalogues.

A. Budowski *CNES, Toulouse, France.* Integration and test of sphere and astrometric parameter software for FAST.

M. Burnet *Observatoire de Genève, Switzerland.* Observation of photometric data pre-launch and during the mission.

A. Butchins *University of London Observatory, London, U.K.* Development of data analysis algorithms for Tycho.

E. Canuto *Politecnico di Torino & Centro di Studi sui Sistemi, Torino, Italy.* **Image dissector and star mapper reductions. Attitude determination in FAST.**

D. Cardini *Istituto di Astrofisica Spaziale, CNR, Frascati, Italy.* Optical modelling for FAST calibration. Double star reductions in FAST.

D. Carlucci *Centro di Studi sui Sistemi, Torino, Italy.* Pre-launch studies for first steps of the data reduction in FAST.

M. Cetica *Istituto Nazionale di Ottica, Firenze, Italy.* Optical modelling for FAST calibration.

M. Chareton *Observatoire de Besançon, France.* Pre-launch simulations of satellite observations. Global observing programme optimisation.

B. Chausserie-Laprée *CNES, Toulouse, France.* Sphere software support for FAST.

C. Coleman *University College, London, U.K.* Former member of Hipparcos Science Team (1981–82).

S.A. Cowling *Department of Applied Mathematics and Astronomy, University College, Cardiff, Wales.* General relativistic metric studies in NDAC.

M. Crézé *Observatoire Astronomique de Strasbourg, URA CNRS 1280, France.* **Construction of the Hipparcos Input Catalogue: pre-launch simulations. Global observing programme optimisation. Hipparcos Science Team.**

F. Crifo *Observatoire de Paris-Meudon, URA CNRS 335, France.* Construction of the Hipparcos Input Catalogue. **Survey definition. Reliability of the Hipparcos Input Catalogue data.**

A.M. Cruise *Mullard Space Science Laboratory, Holmbury St Mary, U.K.* Organisation of NDAC Consortium. Early developments of star mapper reduction software. Former member of Hipparcos Science Team (1983–86).

D.T. van Daalen *Faculty of Geodetic Engineering, Delft University of Technology, The Netherlands.* **Great-circle reduction for FAST.** Former member of Hipparcos Science Team (1986).

S. Daillet *CNES, Toulouse, France.* Attitude determination software support and integration for FAST.

W. Delaney *Istituto di Scienze dell'Informazione, Università di Bari, Italy.* Pre-launch studies for double star reductions in FAST.

J. Delhaye *Observatoire de Paris-Meudon, URA CNRS 335, France.* Construction of the Hipparcos Input Catalogue.

C. Dettbarn *Astronomisches Rechen-Institut, Heidelberg, Germany.* Pre-launch measurements of astrometric data for cluster stars. Astrometric parameter determination in FAST.

P. Didelon *Observatoire Astronomique de Strasbourg, URA CNRS 1280, France.* Production of the Tycho Input Catalogue.

G. Dinderman *Sky Publishing Corporation, Cambridge, Massachusetts, U.S.A.* Technical illustrator for the Millennium Star Atlas.

J. Dommanget *Observatoire Royal de Belgique, Bruxelles, Belgium.* **Coordination of the compilation and observations of pre-launch double/multiple star data. Construction of the Catalogue of the Components of Double and Multiple Stars (CCDM) used for the double/multiple star annexes.** Double star working group. Chairman of the INCA Steering Committee (from 1988).

F. Donati *Politecnico di Torino & Centro di Studi sui Sistemi, Torino, Italy.* **Attitude determination in FAST. Image dissector tube and star mapper data reductions in FAST. Comparison of attitude between FAST and NDAC. Hipparcos Science Team.**

M.T. Dumoulin† *Observatoire de la Côte d'Azur/CERGA, URA CNRS 1360, Grasse, France.* Satellite data modelling and data calibration.

J. Dupic *CNES, Toulouse, France.* **Data simulation software design and development for FAST.**

O.V. Durlevich *Sternberg Astronomical Institute, Moscow University, Russia.* Computer processing of the lists of GCVS names allocated to new variables discovered with Hipparcos.

D. Egret *Observatoire Astronomique de Strasbourg, URA CNRS 1280, France.* **Compilation of complementary data for the Hipparcos Input Catalogue. Construction of the Tycho Input Catalogue.**

N. Elton *Mullard Space Science Laboratory, Holmbury St Mary, U.K.* Development of image dissector tube data analysis algorithms in NDAC.

A. Emanuele *Istituto di Astrofisica Spaziale, CNR, Frascati, Italy.* Optical modelling for FAST calibrations. Double star reductions in FAST. **Orbital double star solutions in FAST.**

M. Erbach *Astronomisches Rechen-Institut, Heidelberg, Germany.* Compilation of pre-launch astrometric data.

D.W. Evans *Royal Greenwich Observatory, Cambridge, U.K.* **Photometric reductions in NDAC. Merging of FAST and NDAC photometric data. Production of the Hipparcos Catalogue Epoch Photometry Annex. Leader of photometry working group.**

L. Eyer *Observatoire de Genève, Switzerland.* **Variable star analysis. Construction of light curves.** Variable star working group.

C. Fabricius *Copenhagen University Observatory, Denmark.* **Tycho Catalogue verification.**

J. Falin *Observatoire de la Côte d'Azur/CERGA, URA CNRS 1360, Grasse, France.* Scientific secretary for FAST-France.

J.L. Falin *Observatoire de la Côte d'Azur/CERGA, URA CNRS 1360, Grasse, France.* **FAST data reductions. Coordination of the software developed in FAST institutes. FAST consortium interface document. Coordination of the FAST data reductions.**

B. Fassino *Centro di Studi sui Sistemi, Torino, Italy.* Image dissector tube and star mapper data reduction in FAST. Attitude determination in FAST.

R.T. Fienberg *Sky Publishing Corporation, Cambridge, Massachusetts, U.S.A.* Publisher and overall coordinator for the Millennium Star Atlas.

F. Figueras *Universitat de Barcelona, Spain.* Observation of pre-launch photometric data.

G. Foster *AAVSO, Cambridge, U.S.A.* Construction of light curves.

W. Fricke† *Astronomisches Rechen-Institut, Heidelberg, Germany.* Chairman of the INCA Steering Committee (1982–88). FAST Steering Committee.

M. Frœschlé *Observatoire de la Côte d'Azur/CERGA, URA CNRS 1360, Grasse, France.* **Pre-launch simulations of satellite and intermediate data. FAST data reductions. Sphere solution and astrometric parameter determination in FAST.** Astrometric results merging group.

M.S. Frolov *Institute of Astronomy (Russian Academy of Science), Moscow, Russia.* Preparing the list of new variables discovered with Hipparcos and satisfying the requirements for GCVS name lists.

J.Y. Le Gall *Laboratoire d'Astronomie Spatiale du CNRS, Marseille, France.* Modelling of the instrument optics.

I. Galligani *Instituto di Matematica, Bologna, Italy.* **Baseline FAST sphere solution.**

F. Gazengel *Observatoire de la Côte d'Azur/CERGA, URA CNRS 1360, Grasse, France.* **Triple star solutions.**

F. Genova *CNES, Paris, France.* FAST Steering Committee.

A. Gòmez *Observatoire de Paris-Meudon, URA CNRS 335, France.* **Construction of the Hipparcos Input Catalogue. Coordination of the production of successive versions of the Hipparcos Input Catalogue. Reliability of the Hipparcos Input Catalogue data.** Interface with proposers. Publication of the Hipparcos Input Catalogue.

M.H. Gomez *CNES, Toulouse, France.* Management of the software documentation for FAST.

M. Gonano *Observatoire de la Côte d'Azur/CERGA, URA CNRS 1360, Grasse, France.* Preparation of data calibrations.

M. Grenon *Observatoire de Genève, Switzerland.* **Construction of the Hipparcos Input Catalogue: coordination of acquisition and compilation of pre-launch photometric data. Photometric standard stars. Calibration of the Hipparcos and Tycho photometric systems. Variable star analysis. Construction of light curves. Construction of identification charts. Joint leader of variable star working group. Photometry working group. Hipparcos Catalogue photometry. Hipparcos Science Team.**

M. Grewing *Astronomisches Institut, Tübingen, Germany.* Organisation of the Tycho Consortium. **Hipparcos Science Team.**

V. Großmann *Astronomisches Institut, Tübingen, Germany.* **Tycho photometric calibrations and reductions. Production of the Tycho Catalogue Epoch Photometry Annex. Preparation of ASCII data files and index files for Tycho Catalogue Epoch Photometry Annex.** Photometry working group.

A. Guerry *CNES, Toulouse, France.* Integration of the global software system for FAST. **Exploitation of the data reduction software.**

J.L. Halbwachs *Observatoire Astronomique de Strasbourg, URA CNRS 1280, France.* **Production of Tycho Input Catalogue Revision. Tycho double star reductions. Tycho photometric reductions.**

P.C. Hansen *Copenhagen University Observatory, Denmark.* Development of algorithms for the Tycho Input Catalogue Revision and for Tycho astrometric processing. Development of algorithms for dynamical smoothing in NDAC.

L. Helmer *Astronomisk Observatorium, Brorfelde, Denmark.* Carlsberg Meridian Circle pre-launch observations.

P. Hemenway *University of Texas, Austin, U.S.A.* **Selection of Hipparcos-Hubble link stars.** Reference frame working group (Hubble Space Telescope observations).

R. Hering *Astronomisches Rechen-Institut, Heidelberg, Germany.* **Astrometric parameter determination in FAST.**

M. Hernandez *Royal Greenwich Observatory, Cambridge, U.K.* On-board clock calibrations.

D. Hestroffer *Bureau des Longitudes, URA CNRS 707, Paris, France/Astrophysics Division, ESA-ESTEC, The Netherlands.* **Solar system objects: reduction of FAST data; comparison of FAST/NDAC/TDAC data. Preparation of solar system object data for publication.**

F.A. van den Heuvel *Faculty of Geodetic Engineering, Delft University of Technology, The Netherlands.* Great-circle reductions for FAST.

E. Høg *Copenhagen University Observatory, Denmark.* **Satellite and payload design: Option A (1975), Tycho (1981). Leader of Tycho Consortium. Theoretical development of Tycho data reduction principles. Organisation of the Tycho Consortium. Development of the Hipparcos data reduction principles. Leader of NDAC Consortium (1982–90). Organisation of the NDAC Consortium. Compilation of Volume 4. Hipparcos Science Team. Preparation of Tycho data for the Millennium Star Atlas charts.** Documentation working group. Development of *Celestia 2000*.

C. Huc *CNES, Toulouse, France.* **Data Management and Command System. FAST Consortium software interface document. Integration of the institute-developed software in CNES.** Support of the great-circle reductions.

D. Iorio-Fili *Istituto Nazionale di Ottica, Firenze, Italy.* **Optical modelling for FAST calibrations.**

H. Jahreiß *Astronomisches Rechen-Institut, Heidelberg, Germany.* **Construction of the Hipparcos Input Catalogue: compilation of pre-launch astrometric data.**

C. Jaschek *Observatoire Astronomique de Strasbourg, URA CNRS 1280, France.* Former member of Hipparcos Science Team (1981).

K.J. Johnston *U.S. Naval Observatory, Washington, U.S.A.* Reference frame working group (radio stars: VLA observations).

D.L. Jones *Jet Propulsion Laboratory, Pasadena, U.S.A.* VLBI observations of radio stars for the reference frame link.

P.J. de Jonge *Faculty of Geodetic Engineering, Delft University of Technology, The Netherlands.* Great-circle reductions for FAST.

C. Jordi *Universitat de Barcelona, Spain.* Observation of pre-launch photometric data.

T.M. Kamperman *SRON, Utrecht, The Netherlands.* Pre-launch initial hardware studies.

E.V. Kazarovets *Institute of Astronomy (Russian Academy of Science), Moscow, Russia.* Checks of identifications of Hipparcos new variables with stars of the recent, still unpublished, GCVS name lists.

N.N. Kireeva *Institute of Astronomy (Russian Academy of Science), Moscow, Russia.* Selection of NSV catalogue stars confirmed with Hipparcos for allocating official GCVS names.

V. Kislyuk *Main Astronomical Observatory, Kiev, Ukraine.* Reference frame working group.

J.J. Kok† *Faculty of Geodetic Engineering, Delft University of Technology, The Netherlands.* Great-circle reductions for FAST.

J. Kovalevsky *Observatoire de la Côte d'Azur/CERGA, URA CNRS 1360, Grasse, France.* **Leader of FAST Consortium. Coordination of FAST data reductions. Pre-launch data simulation. Theoretical development of Hipparcos data reduction principles. In-flight instrument calibration. Joint leader of reference frame working group.** Double and multiple star analysis. **Hipparcos Science Team.** Documentation working group.

P. Lacroute† *Strasbourg, France.* **Initiator of satellite astrometry concepts. Studies of satellite options, instrumentation, and reduction methods.** FAST Steering Committee.

P. Lampens *Koninklijke Sterrewacht van België, Brussels, Belgium.* Compilation of data for variable components in double/multiple systems. **Double star results: links with ground-based observations.** Double star working group.

M.G. Lattanzi *Osservatorio Astronomico di Torino, Italy.* Baseline sphere solution in FAST. **Formulation of alternative sphere solution method using real data in FAST.** Assessment of residual systematic errors between FAST and NDAC catalogues.

T. Lederle *Astronomisches Rechen-Institut, Heidelberg, Germany.* **Construction of the Hipparcos Input Catalogue: compilation of pre-launch astrometric data.**

F. van Leeuwen *Royal Greenwich Observatory, Cambridge, U.K.* **Attitude determination in NDAC. Image dissector tube and star mapper data reductions in NDAC. Instrument calibration. Satellite attitude control and torque calibration. Hipparcos Catalogue Epoch Photometry Annex. Variability analysis. Variability Annex. Joint leader of variable star working group. Photometric notes and references. Photometry working group. Compilation of Volume 3. Hipparcos Science Team. Documentation working group.**

M.B. van Leeuwen-Toczko *Cambridge, U.K.* Literature search for period determination methods for variability analysis.

H. Lenhardt *Astronomisches Rechen-Institut, Heidelberg, Germany.* Astrometric parameter determination in FAST.

J.F. Lestrade *Observatoire de Paris, URA CNRS 1757, Meudon, France.* **VLBI observations of radio stars for the reference frame link.** Reference frame working group.

L. Lindegren *Lund Observatory, Sweden.* **Leader of NDAC Consortium. Theoretical development of the Hipparcos data reduction principles. Satellite and payload design and optimisation. Theory and implementation of sphere solution and astrometric parameter determination. Double and multiple star reductions in NDAC.** Double star working group. **Production of Double and Multiple Systems Annex. Astrometric results merging group. Joint leader of reference frame working group. Documentation working group. Production of final Hipparcos Catalogue. Production of Hipparcos Catalogue intermediate astrometry. Production of the Hipparcos Transit Data. Transformation of astrometric data (Section 1.5). Compilation of Volume 3. Hipparcos Science Team.** Development of *Celestia 2000*.

J. Lub *Sterrewacht, Leiden, The Netherlands.* Observation of pre-launch photometric data.

N. Lund *Danish Space Research Institute, Copenhagen, Denmark.* Great-circle and sphere solution studies in NDAC. Organisation of NDAC Consortium. Organisation of Tycho Consortium.

S.M. MacGillivray *Sky Publishing Corporation, Cambridge, Massachusetts, U.S.A.* Publication manager for the Millennium Star Atlas.

V.V. Makarov *Copenhagen University Observatory, Denmark.* **Tycho data reductions. Tycho double star reductions. Tycho Catalogue production. Preparation of Tycho data for the Millennium Star Atlas charts.**

J. Manfroid *Institut d'Astronomie, Liège, Belgium.* Observation of pre-launch photometric data.

H. van der Marel *Faculty of Geodetic Engineering, Delft University of Technology, The Netherlands.* **Great-circle reductions in FAST. Comparison of great-circle abscissae between NDAC and FAST.** Instrument calibration. **Hipparcos Science Team.**

C. Martin *Observatoire de la Côte d'Azur/CERGA, URA CNRS 1360, Grasse, France.* **Double star photometry.**

J.A. Mattei *AAVSO, Cambridge, U.S.A.* **Compilation of AAVSO data for variable stars prelaunch and during the mission. Ephemerides for large-amplitude variable stars.** Variable star analysis. Variable star working group. Construction of light curves.

H. Mauder *Astronomisches Institut, Tübingen, Germany.* Tycho photometric data reductions.

J.M. Mazurier *Observatoire de Bordeaux, URA CNRS 352, France.* Bordeaux Meridian Circle pre-launch observations.

B. McLean *Space Telescope Science Institute, Baltimore, U.S.A.* Connection between the Tycho Catalogue and the Guide Star Catalog.

D. McNally *University of London Observatory, London, U.K.* Organisation of Tycho Consortium. Development of data analysis algorithms for Tycho.

S. Meara *Royal Greenwich Observatory, Cambridge, U.K.* Literature search for variability analysis.

D. Mégevand *Observatoire de Genève, Switzerland.* Construction of identification charts. Construction of light curves. **Preparation of identification charts and light curves for publication.**

M.O. Mennessier *Université de Montpellier II, URA CNRS 1368, France.* **Compilation of pre-launch data for variable stars. Pre-launch ephemerides of large-amplitude variable stars, and updates throughout mission. Evaluation of ESOC real-time monitoring of red variable stars.** Improvement of photometric calibrations for red stars.

E.T. Mentall *Sky Publishing Corporation, Cambridge, Massachusetts, U.S.A.* Shapes of nebulae and orientations of galaxies for the Millennium Star Atlas.

J.C. Mermilliod *Institut d'Astronomie de l'Université de Lausanne, Switzerland.* **Selection and compilation of pre-launch data for stars in open clusters.** Compilation of pre-launch photometric data.

M. Mermilliod *Institut d'Astronomie de l'Université de Lausanne, Switzerland.* Compilation of pre-launch photometric data.

F. Migliaccio *Dipartimento di Topografia e Rilevamento, Politecnico di Milano, Italy.* Pre-launch studies of sphere solution methods in FAST.

F. Mignard *Observatoire de la Côte d'Azur/CERGA, URA CNRS 1360, Grasse, France.* **FAST data reductions: astrometry and photometry. Theoretical development of Hipparcos data reduction principles. Photometry working group. Leader of double star working group.** Astrometric results merging group. **Hipparcos Science Team. Documentation working group. Production of Hipparcos Catalogue intermediate astrometry. Compilation of Volume 3.**

B. Morando† *Bureau des Longitudes, URA CNRS 707, Paris, France.* **Solar system objects.**

D. Morin *Observatoire de Paris-Meudon, URA CNRS 335, France.* **Construction of the Hipparcos Input Catalogue. Distribution of Hipparcos Catalogue data. Hipparcos Input Catalogue updates.** Development of *Celestia 2000*.

L.V. Morrison *Royal Greenwich Observatory, Cambridge, U.K.* **Carlsberg Meridian Circle pre-launch observations.** Reference frame working group (radio stars: Merlin observations).

F.P. Murgolo *Tecnopolis-CSATA, Bari, Italy.* **Software finalisation and engineering for baseline sphere solution in FAST.** Preparation of double star reductions in FAST.

C.A. Murray *Royal Greenwich Observatory, Herstmonceux, U.K.* Measurement of pre-launch astrometric data. Astrometric reductions in NDAC. **Hipparcos Science Team. Astrometric results merging group.** Intermediate astrometric results.

B. Nicolet *Observatoire de Genève, Switzerland.* Pre-launch simulations of satellite observing programme. Pre-launch optimisation of global observing programme.

O. Nys *Observatoire Royal de Belgique, Bruxelles, Belgium.* **Compilation of pre-launch double and multiple star data. Construction of the Catalogue of the Components of Double and Multiple Stars (CCDM) used for the double/multiple star annexes.**

E. Oblak *Observatoire de Besançon, France.* Observation and compilation of pre-launch photometric data, in particular for double and multiple stars. Global observing programme optimisation.

F. Ochsenbein *Observatoire Astronomique de Strasbourg, URA CNRS 1280, France.* FITS interfaces.

K.S. O'Flaherty *Astrophysics Division, European Space Agency, ESTEC, The Netherlands.* **Preparation of ASCII CD-ROMs. FITS interfaces. Compilation of Volume 2.**

W. O'Mullane *Astrophysics Division, European Space Agency, ESTEC, The Netherlands.* **Preparation of ASCII CD-ROMs. Load and search routines for ASCII data files.**

R. Pannunzio *Osservatorio Astronomico di Torino, Italy.* **Double and triple star reductions in FAST.** Double star working group.

E.N. Pastukhova *Institute of Astronomy (Russian Academy of Science), Moscow, Russia.* Computer determination of constellations for the GCVS names of new variables discovered with Hipparcos, checks of border cases, GSC identifications.

H. Pedersen *Copenhagen University Observatory, Denmark.* **Tycho astrometric catalogue production.**

M.J. Penston *Royal Greenwich Observatory, Cambridge, U.K.* Pre-launch astrometric measurements. **ESOC–RGO and internal NDAC interface software. Variable star period determinations. Control of data reduction software within NDAC/RGO.** Image dissector tube and star mapper data reductions in NDAC. Satellite torque analysis and on-board clock analysis. Variability annex. Variable star working group.

J.P. Périé *Observatoire de Bordeaux, URA CNRS 352, France.* Measurement of pre-launch astrometric data.

B. Pernier *Observatoire de Genève, Switzerland.* Observation of pre-launch photometric data.

M.A.C. Perryman *Astrophysics Division, European Space Agency, ESTEC, The Netherlands.* **ESA Project Scientist for Hipparcos. Scientific coordination of the Hipparcos project. Hipparcos Science Team (Chairman). Interface between scientific teams, industry, ESOC, and ESA advisory groups. Coordination of scientific inputs to satellite design, calibration and operation. Project manager during satellite operations. Interface with INCA, NDAC, FAST and TDAC Consortia, and working groups. Leader of documentation working group. Compilation of Volumes 1 and 2. Coordination of final mission products.**

C.S. Petersen *Copenhagen University Observatory, Denmark.* **Great-circle reductions in NDAC.** Instrument calibration.

R.B. Phillips *Haystack Observatory, Westford, U.S.A.* VLBI observations of radio stars for the reference frame link.

J.L. Pieplu *CNES, Toulouse, France.* **Coordination of the CNES operational software development, integration and test in FAST.** Astrometric parameter determination software support and integration. FAST data reductions. FAST Steering Committee.

I. Platais *Yale University Observatory, New Haven, U.S.A.* Reference frame working group (Lick and Yale proper motion stars).

K. Poder *Geodetic Institute, Copenhagen, Denmark.* Great-circle and sphere solution studies in NDAC.

R.S. Le Poole *Sterrewacht, Leiden, The Netherlands.* Construction of the Hipparcos Input Catalogue: observations related to pre-launch astrometric data. Instrument evolution and analysis. Optimisation of data reductions and error evaluation. **Hipparcos Science Team.** FAST Steering Committee. Verification of double and multiple systems annex data by ground-based observations.

R.A. Preston *Jet Propulsion Laboratory, Pasadena, U.S.A.* **Organisation of VLBI observations of radio stars for the reference frame link.**

L. Prévot *Observatoire de Marseille, URA CNRS 237, France.* **Measurement of pre-launch astrometric data.**

G. Prezioso *Tecnopolis-CSATA, Bari, Italy.* **Preparation of double star reductions in FAST.**

D. Priou *IGN, Paris, France.* **Development of HICIS software for the Hipparcos Input Catalogue CD-ROM. Development of *Celestia 2000*.**

L. Quijano *Real Instituto y Observatorio de la Armada, San Fernando, Spain.* Observation of pre-launch astrometric data.

C.F. Quist *Lund Observatory, Sweden.* Preparation of the Hipparcos Transit Data file.

N. Ramamani *Royal Greenwich Observatory, Cambridge, U.K.* Image dissector tube and star mapper data reductions in NDAC.

M. Rapaport *Observatoire de Bordeaux, URA CNRS 352, France.* Pre-lauch ephemerides of minor planets.

Y. Réquième *Observatoire de Bordeaux, URA CNRS 352, France.* **Construction of the Hipparcos Input Catalogue. Coordination of the observations of pre-launch astrometric data. Bordeaux Meridian Circle pre-launch observations.**

L.J. Robinson *Sky Publishing Corporation, Cambridge, Massachusetts, U.S.A.* Chief consultant on the Millennium Star Atlas.

V. Roman *CNES, Toulouse, France.* Software configuration control in CNES for FAST.

S. Röser *Astronomisches Rechen-Institut, Heidelberg, Germany.* Reference frame working group. Prediction of Tycho transits for solar system objects.

M. Rousseau *Observatoire de Bordeaux, URA CNRS 352, France.* **Measurement of pre-launch astrometric data.**

J.L. Russell *Space Telescope Science Institute, Baltimore, U.S.A.* Application of the Guide Star Catalog to the Tycho Input Catalogue.

M. Saisse *Laboratoire d'Astronomie Spatiale du CNRS, Marseille, France.* Former member of Hipparcos Science Team (1981).

N.N. Samus *Institute of Astronomy (Russian Academy of Science), Moscow, Russia.* **Allocation of GCVS official names to new variables discovered with Hipparcos.**

F. Sansò *Dipartimento di Topografia e Rilevamento, Politecnico di Milano, Italy.* Pre-launch studies of sphere solution methods in FAST.

A.B. Saust *Copenhagen University Observatory, Denmark.* Development of data analysis algorithms for Tycho astrometry.

D. Scales *Astronomisches Institut, Tübingen, Germany.* Tycho photometric data reductions.

E. Schilbach *Sternwarte Babelsberg, Potsdam, Germany.* Reference frame working group (Schmidt plate observations).

M.G. Schirone *Tecnopolis-CSATA, Bari, Italy.* Preparation of double star reductions in FAST. Implementation of baseline sphere solution in FAST.

H. Schrijver *SRON, Utrecht, The Netherlands.* **First-Look analysis and instrument calibration in FAST. Satellite payload geometrical calibration. Construction and development of the final results data base. Coordination of inputs to the final results data base. Final results compilation and verification. Hipparcos Science Team.** Documentation working group. **Production of printed and machine-readable Hipparcos Catalogue and Annexes. Preparation of Hipparcos data for the Millennium Star Atlas charts. Preparation of ASCII CD-ROMs.** Development of *Celestia 2000*.

P. Schwekendiek *Astronomisches Rechen-Institut, Heidelberg, Germany.* Prediction of Tycho transits. **Tycho transit prediction updating.**

G. Sechi *Centro di Studi sui Sistemi, Torino, Italy.* Comparison of attitudes determined by FAST and NDAC.

A. Sellier *Observatoire de Paris-Meudon, URA CNRS 335, France*. Compilation of pre-launch data for double and multiple stars. **Preparation of open cluster charts.**

G. Serieys *CNES, Toulouse, France*. **Exploitation of the data reduction software for FAST.**

R.W. Sinnott *Sky Publishing Corporation, Cambridge, Massachusetts, U.S.A.* **Programming and plotting of the Millennium Star Atlas charts.**

M.A.J. Snijders *Royal Greenwich Observatory, Cambridge, U.K. & Astronomisches Institut, Tübingen, Germany.* Preparation of NDAC data reductions. Tycho photometric error analysis.

S. Söderhjelm *Lund Observatory, Sweden*. Software for sphere solution and astrometric parameter determination in NDAC. Simulations of determination of general relativistic metric. **Double and multiple star reductions in NDAC. Construction of the Hipparcos Transit Data. Double star working group.**

A. Spagna *Osservatorio Astronomico di Torino, Italy.* Double and multiple star reductions in FAST.

B. Stewart *Rutherford Appleton Laboratory, Chilton, U.K.* Development of star mapper data processing algorithms for Tycho.

J. Storm *Copenhagen University Observatory, Denmark*. Development of data analysis algorithms for Tycho astrometry.

C. Taieb *Laboratoire d'Astronomie Spatiale du CNRS, Marseille, France*. Modelling of the instrument.

T. Tommasini *Dipartimento di Matematica, Università di Bologna, Italy.* **Baseline sphere solution numerical methods in FAST.**

J. Torra *Universitat de Barcelona, Spain*. Observation of pre-launch photometric data.

H.-J. Tucholke *Sternwarte der Universitaet Bonn, Germany.* Measurement of pre-launch astrometric data for stars in open clusters. Reference frame working group (photographic method).

C. Turon *Observatoire de Paris-Meudon, URA CNRS 335, France*. **Leader of INCA Consortium. Production of the Hipparcos Input Catalogue. Updating of observing programme throughout the mission. Interface with proposers. Interface with Scientific Selection Committee. Development of *Celestia 2000*. Verification of final catalogue formats. Hipparcos Science Team.** Documentation working group.

M. Vadel *CNES, Toulouse, France*. Exploitation of the data reduction software for FAST.

A. Vargas *CNES, Toulouse, France*. **Design of the Data Management and Command System.** Support and integration of the grid coordinate software in FAST.

C. de Vegt *Hamburg Observatory, Germany.* Measurement of pre-launch astrometric data. Reference frame working group (photographic and CCD observations).

M. Villenave *CNES, Toulouse, France*. **Data preparation software in FAST.**

J. Vondrak *Astronomical Institute, Prague, Czech Republic*. Reference frame working group (Earth rotation observations).

C. Waelkens *Instituut voor Sterrenkunde, Leuven, Belgium*. Classification of A- and B-type small-amplitude variables.

K. Wagner *Astronomisches Institut, Tübingen, Germany.* **Tycho transit identifications.**

H.G. Walter *Astronomisches Rechen-Institut, Heidelberg, Germany.* Pre-launch compilation of data for radio stars. **Astrometric parameter determination in FAST.** Former member of Hipparcos Science Team (1981).

L. Weber *Observatoire de Genève, Switzerland.* Construction of identification charts.

P.R. Wesselius *Department of Space Research, Groningen, The Netherlands.* Organisation of Tycho Consortium. Development of data analysis algorithms for Tycho.

G. Whitfield *Royal Greenwich Observatory, Cambridge, U.K.* Development of attitude reconstruction software.

A. Wicenec *Astronomisches Institut, Tübingen, Germany.* **Detection of star signal and sky background with Tycho. Tycho Epoch Photometry Annex production. Tycho Catalogue verification.**

R. Wielen *Astronomisches Rechen-Institut, Heidelberg, Germany.* **Parts G, O, V and X of the Double and Multiple Systems Annex.** FAST Steering Committee.

G.J. Wiersma *SRON, Utrecht, The Netherlands.* First-Look analysis and instrument calibration.

C.G. Wynne *Royal Greenwich Observatory, Cambridge, U.K.* Former member of Hipparcos Science Team (1981–84).

M. Yoshizawa *Copenhagen University Observatory, Denmark*. Development of star mapper data processing algorithms for Tycho.

V. Zappalà *Osservatorio Astronomico di Torino, Italy.* Modelling of minor planets in FAST.

I. Zegelaar *Sterrewacht, Leiden, The Netherlands.* Variability analysis of RR Lyrae variables.

INDEX

Index